U.S. DEPARTMENT OF COMMERCE
National Technical Information Service

PB-253 736

THE TRANSPORT OF OXIDANT BEYOND URBAN AREAS

Battelle Columbus Laboratories

prepared for
Environmental Sciences Research Laboratory

February 1976

173187

EPA-600/3-76-018 a
February 1976

PB 253 736

Ecological Research Series

UNITED STATES · ENVIRONMENTAL PROTECTION AGENCY

REPRODUCED BY
NATIONAL TECHNICAL
INFORMATION SERVICE
U. S. DEPARTMENT OF COMMERCE
SPRINGFIELD, VA. 22161

RESEARCH REPORTING SERIES

Research reports of the Office of Research and Development, U.S. Environmental Protection Agency, have been grouped into five series. These five broad categories were established to facilitate further development and application of environmental technology. Elimination of traditional grouping was consciously planned to foster technology transfer and a maximum interface in related fields. The five series are:

1. Environmental Health Effects Research
2. Environmental Protection Technology
3. Ecological Research
4. Environmental Monitoring
5. Socioeconomic Environmental Studies

This report has been assigned to the ECOLOGICAL RESEARCH series. This series describes research on the effects of pollution on humans, plant and animal species, and materials. Problems are assessed for their long- and short-term influences. Investigations include formation, transport, and pathway studies to determine the fate of pollutants and their effects. This work provides the technical basis for setting standards to minimize undesirable changes in living organisms in the aquatic, terrestrial, and atmospheric environments.

This document is available to the public through the National Technical Information Service, Springfield, Virginia 22161.

EPA-600/3-76-018-a
February 1976

THE TRANSPORT OF OXIDANT BEYOND URBAN AREAS

by

Chester W. Spicer, James L. Gemma, Darrell W. Joseph
Philip R. Stricksel, and Gerald F. Ward
BATTELLE - Columbus Laboratories
Columbus, Ohio 43201

Contract No. 68-02-1714

Joseph J. Bufalini
Gas Kinetics and Photochemistry Branch
Environmental Sciences Research Laboratory
Research Triangle Park, North Carolina 27711

U.S. ENVIRONMENTAL PROTECTION AGENCY
OFFICE OF RESEARCH AND DEVELOPMENT
ENVIRONMENTAL SCIENCES RESEARCH LABORATORY
RESEARCH TRIANGLE PARK, NORTH CAROLINA 27711

ia

DISCLAIMER

This report has been reviewed by the Environmental Sciences Research Laboratory, U.S. Environmental Protection Agency, and approved for publication. Approval does not signify that the contents necessarily reflect the views and policies of the U. S. Environmental Protection Agency, nor does mention of trade names or commercial products constitute endorsement or recommendation for use.

CONTENTS

Page

TABLES. vi

FIGURES viii

ACKNOWLEDGMENTS xii

INTRODUCTION. 1

SCOPE AND SUMMARY OF PROGRAM. 2

SITING. 4

  Location and Topography. 4

  Population 4

  Meteorology. 8

  Study Sites. 8

EXPERIMENTAL METHODS. 9

  Meteorological Measurements. 15

  Air Quality Measurements 18

    Methane/Non-Methane Hydrocarbons. 18

    Acetylene, Ethylene, Ethane 20

    Carbon Monoxide 20

    Sulfur Dioxide. 20

  Aerosol Collections. 21

  Aerosol Analysis 22

  Dustfall Analysis. 22

  Aircraft Measurements. 23

RESULTS 27

DISCUSSION. 54

  Overview of the Dayton Field-Study Results 54

    Air-Quality Data. 55

      Downtown Dayton (Site No. 1) 55

CONTENTS (Continued)

Page

Huber Heights (Site No. 2). 56

New Carlisle (Site No. 3) 58

Aerosol Composition. 59

Pollutant Directionality and Frequency 66

A Statistical View of the Dayton Field-Study Results. 85

Linear Regression Analysis 85

Interpretation of Maximum Ozone Concentration by Means of Regression Integrals 92

Graphical Analysis of Ozone Directionality 100

Analysis of the Dayton Ozone Data by an Interaction Method 124

The Effect of Meteorological Variables on Dayton Ozone. 131

Ozone-Meteorology Relationships. 134

Ozone and Haze 136

Haze and Trajectories. 137

Vertical Temperature Structure and Surface Ozone. 139

Airplane and Balloon Soundings 141

July 18, 1974 150

Other Soundings 151

Contribution of Upper Atmospheric Ozone on August 5 and 6, 1974 152

Description of Selected Study Days. 154

Model of Urban and Rural Ozone Patterns. 154

July 18, 1974. 179

July 25, 1974. 190

July 30 and 31, 1974 196

CONTENTS (Continued)

Page

August 1, 1974. 203

August 5, 1974. 206

August 6, 1974. 212

August 7 and 9, 1974. 223

Intercomparability of Data 228

CONCLUSION. 232

REFERENCES. 235

TABLES

Page

Table 1. Major Population Centers in RAPCA Area (1970 Census). 6

Table 2. Chemical and Meteorological Determinations by Site. . 16

Table 3. Meteorological Measurements 17

Table 4. Air Monitoring Instrumentation. 19

Table 5. Summary of Air Quality Data - Dayton Site No. 1 . . . 29

Table 6. Summary of Air Quality Data - Dayton Site No. 2 . . . 32

Table 7. Summary of Air Quality Data - Dayton Site No. 2 . . . 33

Table 8. Summary of Air Quality Data - Dayton Site No. 3 . . . 40

Tables 9 A-B. Ozone (ppm) Miamisburg, Ohio. 43-44

Tables 10 A-B. Ozone (ppm) Timber Lane - Dayton, Ohio. 44-46

Tables 11 A-B. Ozone (ppm) Wayne Township - Huber Heights, Ohio. . . 47-48

Table 12. Average of 3-Hour Integrated Data 49

Table 13. Dayton Aerosol Data 51

Table 14. Large Particle (>2.5 μm) Composition. 52

Table 15. Dayton Meteorological Factors 53

Table 16. Dayton Aerosol Composition (Weight Percent) 61

Table 17. Aerosol Composition (Weight Percent 61

Table 18. Dayton Filter Nitrogen Balance. 64

Table 19. Aerosol Nitrogen Balance. 65

Table 20. Dayton Area Ozone Levels. 83

Table 21. Six Site Ozone Correlations 86

Table 22. Site 1 Regressions (3-Hour Average Except as Marked). 87

Table 23. Site 2 Regressions (Hourly Averages). 88

Table 24. Site 3 Regressions (3-Hour Averages Except as Marked). 89

TABLES (Continued)

Page

Table 25. Stepwise Regression Integrals 95

Table 26. Multiple Stepwise Regression Integral Maximum Ozone vs Wind Direction, NO, NO_2, and Non-Methane Hydrocarbons. 101

Table 27. Variables Used in Aid Analysis. 127

Table 28. Weather Frequency During Dayton Study 132

Table 29. Airplane Bag Sample Results July 18, 1974 185

Table 30. Airplane Bag Sample Results July 30, 1974 199

Table 31. Airplane Bag Sample Results July 31, 1974 200

Table 32. Airplane Bag Sample Results August 5, 1974 Afternoon 213

Table 33. Airplane Bag Sample Results August 6, 1974. 220

Table 34. Battelle-EPA Cross Calibration. 233

FIGURES

			Page
Figure	1.	Location of the Study Region	5
Figure	2.	Population Centers in the Vicinity of Dayton, Ohio	7
Figure	3.	Siting Arrangement	10
Figure	4.	Battelle Mobile Air Quality Laboratory	11
Figure	5 A.	Interior of Air Quality Laboratory	12
Figure	5 B.	Mobile Air Quality Laboratory.	13
Figure	6.	Aircraft with Door Removed	24
Figure	7.	Monitoring Instrumentation within Aircraft	25
Figure	8.	Aircraft Sampling Probe.	26
Figures	9 A-B.	Site 1 Composite Profiles.	30-31
Figures	10 A-F.	Site 2 Composite Profiles.	34-39
Figures	11 A-B.	Site 3 Composite Profiles.	41-42
Figure	12.	Dayton Regression: Sulfate Versus Ammonium. . . .	62
Figure	13.	Wind Rose - Dayton - 2	67
Figure	14.	Pollutant Rose - Dayton - 2 - Sulfur Dioxide . . .	69
Figure	15.	Pollutant Rose - Dayton - 2 - Nitrogen Oxides. . .	70
Figure	16.	Pollutant Rose - Dayton - 2 - Ammonia.	71
Figure	17.	Pollutant Rose - Dayton - 2 - Methane.	73
Figure	18.	Pollutant Rose - Dayton - 2 - Non-Methane Hydrocarbon.	74
Figure	19.	Pollutant Rose - Dayton - 2 - Carbon Monoxide. . .	75
Figure	20.	Pollutant Rose - Dayton - 2 - Ozone.	76
Figure	21.	Wind Rose - New Carlisle/Dayton - 3.	78
Figure	22.	Pollutant Rose - New Carlisle/Dayton - 3 - Sulfur Dioxide	79

FIGURES (Continued)

Page

Figure 23. Pollutant Rose - New Carlisle/Dayton - 3 - Nitrogen Oxides. 80

Figure 24. Pollutant Rose - New Carlisle/Dayton - 3 - Ozone . 81

Figure 25. Impact Functions - Wind Direction on Maximum Hourly Ozone 97

Figure 26. Impact Functions - Precursors on Maximum Hourly Ozone 99

Figure 27. Measured vs Predicted Maximum Hourly Ozone 102

Figure 28. Maximum Hourly Ozone vs Wind Direction 103

Figure 29. Study Area Divided into Wind Sectors 106

Figures 30 A-E. Ozone Profiles by Wind Direction 107-111

Figures 31 A-D. Site-to-Site Ozone Profiles by Wind Sector 114-117

Figures 32 A-D. Site-to-Site Ozone Profiles by Wind Sector 120-123

Figure 33. Automatic Interaction Detector - Dayton Ozone Study - Site 3 125

Figure 34. Aid Partition of Ozone Results by Wind Vector. . . 130

Figure 35. Variations of Peak Ozone and Selected Meteorological Parameters During the Dayton Study Period. 135

Figure 36. Examples of Dayton NWS Soundings of Temperature and Dewpoint 140

Figure 37. Afternoon Soundings for July 18 - Airplane, 4 p.m.; NWS Balloon, 8 p.m. 142

Figure 38. Morning Soundings for July 30 - Airplane, 11 a.m.; NWS Balloon, 8 a.m. 143

Figure 39. Afternoon Soundings for July 30 - Airplane, 4 p.m.; NWS Balloon, 8 p.m. 144

Figure 40. Morning Soundings for July 31 - Airplane, 11 a.m.; NWS Balloon, 8 a.m. 145

Figure 41. Afternoon Soundings for July 31 - Airplane, 4 p.m.; NWS Balloon, 8 p.m. 146

FIGURES (Continued)

Page

Figure 42. Afternoon Soundings for August 5 - Airplane, 4 p.m.; NWS Balloon, 8 p.m. 147

Figure 43. Morning Soundings for August 6 - Airplane, 11 a.m.; NWS Balloon, 8 a.m. 148

Figure 44. Afternoon Soundings for August 6 - Airplane, 4 p.m.; NWS Balloon, 8 p.m. 149

Figures 45 A-U. Six Site Profiles of Ozone (in ppm). 155-175

Figure 46. 20-Day Average Dayton Area Ozone Profiles. 180

Figure 47. Dayton Area Ozone Profiles - July 18, 1974 182

Figures 48 A-B. Aircraft Ozone Results 183-184

Figure 49. Vertical Temperature Profiles. 188

Figure 50. Vertical Ozone Profiles, Downtown Dayton 189

Figure 51. Dayton Area Ozone Profiles - July 25, 1974 192

Figures 52 A-B. Aircraft Ozone Results 193-194

Figures 53 A-B. Aircraft Ozone Results 197-198

Figures 54 A-B. Aircraft Ozone Results 201-202

Figure 55. Dayton Area Ozone Profiles - August 1, 1974. . . . 205

Figure 56 A. Morning Ozone Concentration in ppb - August 5, 1974 209

Figure 56 B. Afternoon Ozone Concentration in ppb - August 5, 1974 210

Figure 57 A. Dayton Area Ozone and Solar Intensity Profile - August 6, 1974 215

Figure 57 B. "Predicted" Dayton Area Ozone - August 6, 1974 . . 215

Figure 58 A. August 6, 1974 - 9-12 a.m. Ozone Concentration in ppb 218

Figure 58 B. August 6, 1974 - 1-4 p.m. Ozone Concentration in ppb 219

Figure 59. Ozone at 1000 Feet Between Dayton Airport and Columbus 222

FIGURES (Continued)

Page

Figure 60. Aborted Comparison Flight - August 7, 1974 Ozone Concentration in ppb 225

Figure 61 A. First Loop - Comparison Flight - August 9, 1974 Ozone Concentration in ppb 226

Figure 61 B. Second Loop - Comparison Flight - August 9, 1974 Ozone Concentration in ppb 227

Figure 62. Battelle-RTI Comparison Flight Pattern 229

Figure 63. Data from RTI/Battelle Comparison Flight 230

Figure 64. Data from RTI/Battelle Comparison Flight 231

ACKNOWLEDGMENTS

The authors would like to acknowledge the interest and assistance of the Regional Air Pollution Control Agency (RAPCA) and especially Mr. Paul D. Buffington. Other Battelle-Columbus staff members who made major contributions to this program include Fred Blakeslee, G. W. Keigley, and John Kouyoumjian.

THE TRANSPORT OF OXIDANT
BEYOND URBAN AREAS

by

Chester W. Spicer, James L. Gemma, Darrell W. Joseph,
Philip R. Sticksel, and Gerald F. Ward

INTRODUCTION

In recent years it has become increasingly clear that the hypothesis that ozone formation in polluted atmospheres is parochial in nature, and therefore confined to urban areas, is inadequate. As our monitoring capability has increased and data from more rural monitoring stations have become available it has become obvious that ozone is not simply an urban phenomenon but can be found in some of the remotest areas of the country. Several mechanisms have been suggested to account for the unusual patterns of ozone behavior in rural and urban areas. Included among these explanations are the transport of ozone downward from the stratosphere, ozone formation from natural precursors, transport of urban-generated ozone to areas downwind of cities, and the trapping of urban ozone within stable inversion strata with subsequent transport and fumigation when the inversion breaks.

Obviously, the mechanism of ozone formation and transport has major policy implications in terms of control strategies. It is therefore the general objective of this study to investigate patterns of ozone formation and movement. The specific objective of the program is to determine the propensity of urban air masses to generate and transport ozone downwind of urban areas.

SCOPE AND SUMMARY OF PROGRAM

The 1974 investigation of oxidants in the midwestern United States involved several research groups positioned throughout the Ohio Valley. The geographical region selected for Battelle-Columbus' study was the Dayton, Ohio, area.

In order to investigate oxidant formation and movement into and beyond the Dayton area, a number of ground stations were set up for horizontal monitoring, and an aircraft was outfitted for vertical sampling. Three heavily instrumented ground stations were set up in (1) downtown Dayton, (2) Huber Heights (about 10 miles northeast of downtown Dayton), and (3) New Carlisle (about 20 miles northeast of downtown Dayton). These stations were established to determine either continuously or on an integrated basis O_3, NO, NO_2, NO_x, NH_3, CH_4, C_2H_6, C_2H_4, C_2H_2, NMHC, CO, SO_2, PAN, HNO_3, aerosol mass loading, NH_4^+ , NO_3^-, $SO_4^=$, total CHN, light scattering, wind direction, wind speed, temperature, relative humidity, and solar intensity. Ozone data from three additional ground stations in the Dayton area were also acquired and integrated with the data from our three main stations, providing a total of six ground-level ozone monitoring sites.

The aircraft was outfitted for continuous ozone monitoring and collection of Teflon bag samples. The bag samples were returned to the central laboratory for determination of CH_4, C_2H_6, C_2H_4, C_2H_2, NMHC, CO, and PAN.

Data collection was carried out over a 20-day period between July 17 and August 12, 1974. The large volume of data collected during the field study is summarized in this report. Interpretations of the results of the program are then discussed in terms of statistical, graphical, chemical, and meteorological analyses of the data. Based on the results of the data analysis effort, an empirical model of ozone behavior is presented which emphasizes the need to include several different ozone sources in any complete explanation of ozone behavior. Of the several potential ozone sources mentioned in the introduction to this report, none can be totally rejected and indeed each can be important under certain conditions of meteorology, topography, etc. The important point is that no one particular ozone source, be it urban transport, natural emissions, stratospheric transport, etc., can account for the ozone patterns observed in this and other studies. We suggest that only the interaction and superposition of these various sources can fully explain rural and urban ozone patterns. A more detailed discussion of the various sources of ozone and their potential impact on urban and rural areas is presented in a separate section toward the end of this report.

SITING

Location and Topography

The general location selected for this study was the Dayton, Ohio, area. Dayton was chosen as one of the key study sites in EPA's major investigation of oxidant and precursor transport in the Ohio Valley. Other EPA groups and contractors were located in Wilmington and Canton, Ohio, and the total O_3 monitoring network extended as far east as Pittsburgh. Aircraft monitoring efforts were undertaken in the Canton area and the Columbus vicinity, in addition to our flights in and around Dayton. The location of the study region relative to major industrial and population centers is indicated in Figure 1.

The topography of the Dayton area consists mainly of gently rolling hills which outline the Miami River Valley. The Miami River flows southwestward to join the Ohio River, so the Miami Valley is oriented in a generally southwest-to-northeast direction. The Valley consists of a flat plain approximately 50-200 feet below the mean elevation of the surrounding area, which rises to slightly more than 100 feet. Since the elevation differentials are minimal, topography generally does not play a major role in determining wind direction or pollution dispersion conditions. Local drainage winds do develop but are normally insignificant in comparison to regional meteorological factors.

Population

Although Dayton is the major city within our immediate study area, there are a number of large communities located throughout the area. Communities with populations greater than 10,000 in the 1970 census are listed in Table 1 along with their population totals. The locations of these communities within the five-county area served by the Regional Air Pollution Control Agency (RAPCA) are displayed in Figure 2.

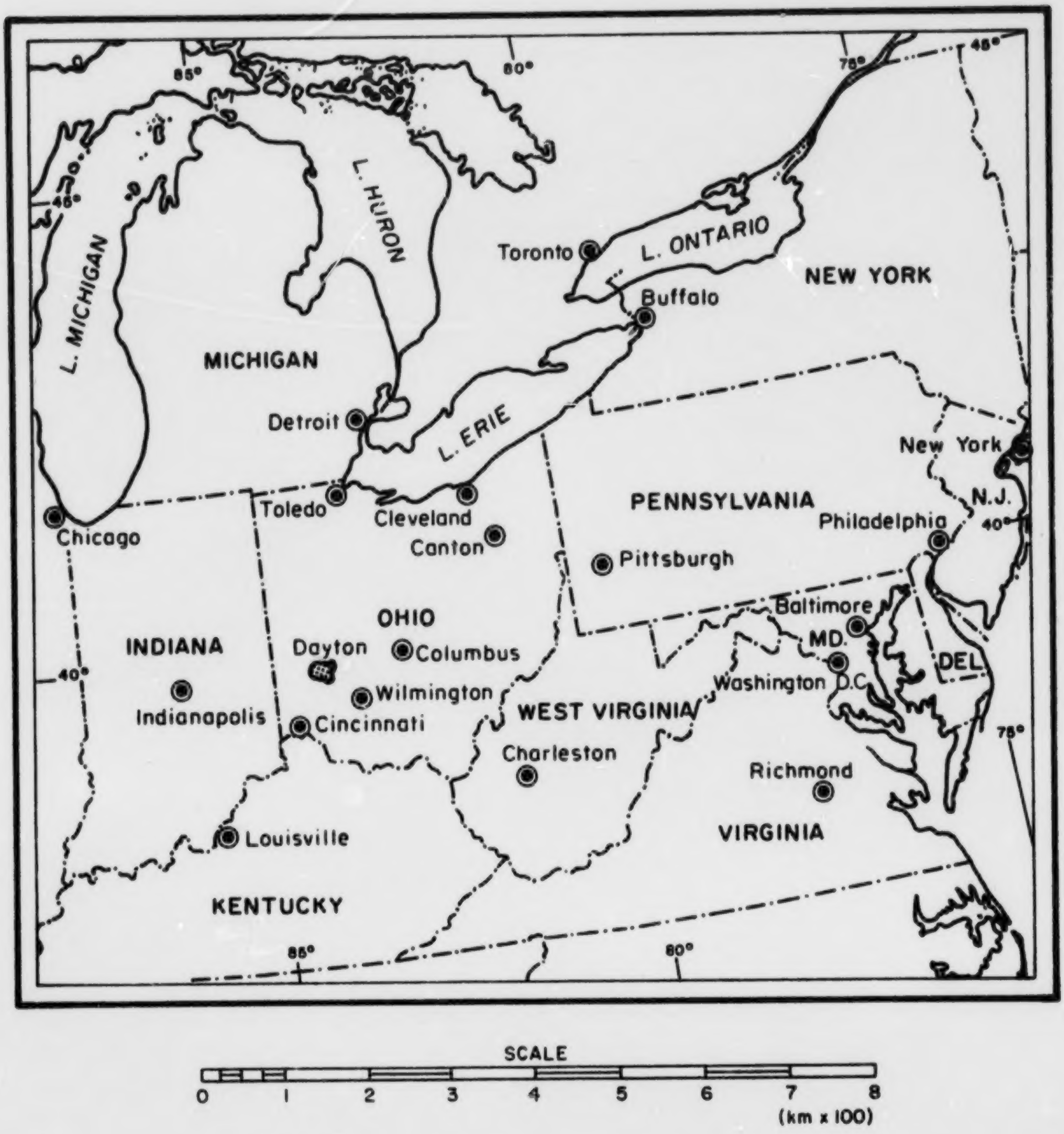
L. MICHIGAN
L. HURON
L. ONTARIO
L. ERIE
MICHIGAN
NEW YORK
PENNSYLVANIA
OHIO
INDIANA
WEST VIRGINIA
VIRGINIA
KENTUCKY
MD.
DEL
N.J.
Toronto
Buffalo
Detroit
Toledo
Cleveland
Canton
Chicago
Pittsburgh
New York
Philadelphia
Baltimore
Washington D.C.
Dayton
Columbus
Wilmington
Cincinnati
Indianapolis
Charleston
Richmond
Louisville
85°
80°
75°
45°
40°
SCALE
0
1
2
3
4
5
6
7
8
(km x 100)

FIGURE 1. LOCATION OF THE STUDY REGION

TABLE 1. MAJOR POPULATION CENTERS IN RAPCA AREA (1970 CENSUS)

Community	Population
Dayton	243,601
Springfield	81,926
Kettering	69,599
Fairborn	32,267
Xenia	25,373
Piqua	20,741
Huber Heights	18,943
Troy	17,186
Miamisburg	14,797
Greenville	12,380
West Carollton	10,748
Centerville	10,333
Wright-Patterson AFB	10,151

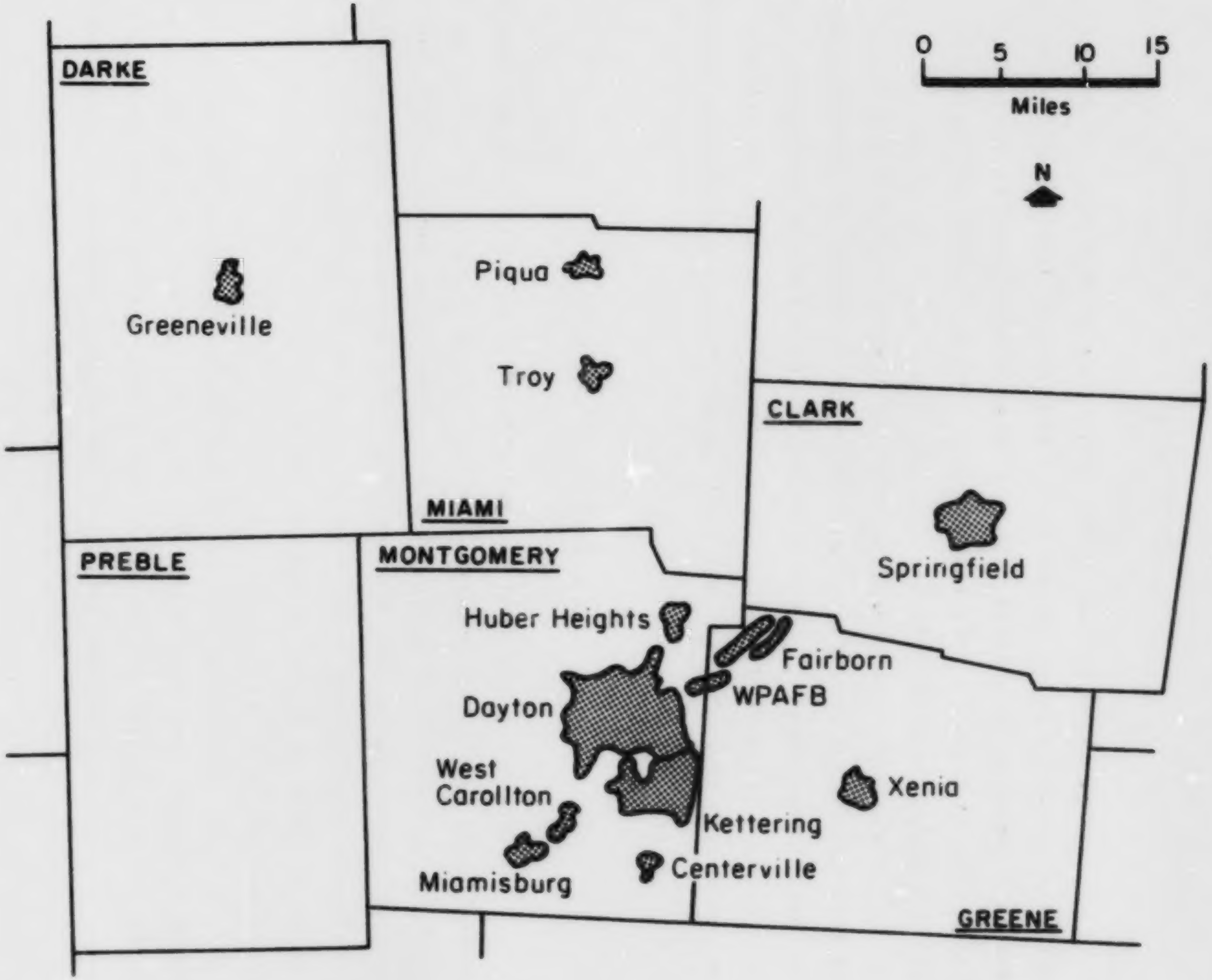
0
5
10
15
Miles
N
DARKE
Greeneville
Piqua
Troy
MIAMI
CLARK
Springfield
PREBLE
MONTGOMERY
Huber Heights
Fairborn
WPAFB
Dayton
West Carollton
Xenia
Kettering
Centerville
Miamisburg
GREENE

FIGURE 2. POPULATION CENTERS IN THE VICINITY OF DAYTON, OHIO

Meteorology

Temperature in the Dayton region can be described as moderate, with precipitation being rather evenly distributed throughout the year. Relative humidity is usually high. Average temperatures in July and August are 75.0 and 73.3 F, respectively. Precipitation averages 3.4 and 2.8 inches in those months.

The mean wind speeds in July and August are 8.0 and 7.5 mph. On both months the resultant prevailing wind direction is from the south southwest. Holtzworth(1)* has reported the mean morning mixing depth in Dayton to be 370 meters in July and 350 meters in August. Afternoon mixing depths average 1,720 and 1,600 meters in July and August, respectively.

Study Sites

In keeping with the program objective of monitoring air masses as they pass through and beyond Dayton, three main sites were selected parallel to the prevailing wind vector. These sites were in downtown Dayton, Huber Heights, and New Carlisle. The downtown Dayton site (Site 1) was located at 451 West Third Street and is one of the RAPCA's monitoring stations. This is a typical urban station in close proximity (100 meters) to major city streets.

The Huber Heights site (Site 2) was situated in the parking lot of a new community fire hall which was not yet occupied. It was surrounded on three sides by unused fields and on the fourth side by a two-lane highway and a housing development. The site was slightly less than 1 mile south of the Interstate 70 highway. The Huber Heights site was approximately 9 miles northeast of the downtown Dayton site.

The New Carlisle mobile laboratory (Site 3) was situated in the parking lot of the local police station in the northeast corner of this small Ohio town. The site was approximately 50 meters from a two-lane highway. The town of New Carlisle is surrounded for many miles by farm land. It is located approximately 18 miles northeast of our downtown Dayton site and 9 miles northeast of the Huber Heights station.

---

*References are listed on page 235.

In addition to these three stations, we have also acquired ozone data from three additional points in the Dayton region from monitoring stations operated by the RAPCA. These stations are located in Miamisburg (approximately 10 miles southwest of Dayton), at Timberlane Road (approximately 4 miles north of downtown), and at the Huber Heights site. The ozone monitor at the Huber Heights site was located within 20 meters of our central laboratory and should therefore serve as a good cross-check on ozone calibration factors.

These six monitoring sites all fall roughly on a line running southwest to northeast (220° southwest to 40° northeast) through Dayton. Thus they are aligned along the prevailing wind vector according to the historical meteorological data mentioned earlier. The distance between the extreme southwest and northeast sites is approximately 30 miles. The siting arrangement and the relationship of the sites to nearby population centers is shown in Figure 3.

EXPERIMENTAL METHODS

Two mobile air quality laboratories and a third, fixed, instrumental ground station were employed in this study to monitor meteorological conditions, solar irradiation intensity, and gas-phase composition, while simultaneously collecting aerosol samples for subsequent chemical analysis. Battelle-Columbus' Mobile Air Quality Laboratory, which served as the main laboratory facility and headquarters during this investigation, is pictured in Figure 4. The TETCO Mobile Laboratory shown in Figure 5 was used as a remote monitoring laboratory during this study. Our third ground station consisted of the downtown Dayton monitoring station of the Regional Air Pollution Control Agency (RAPCA), to which we added instruments pertinent to our investigation.

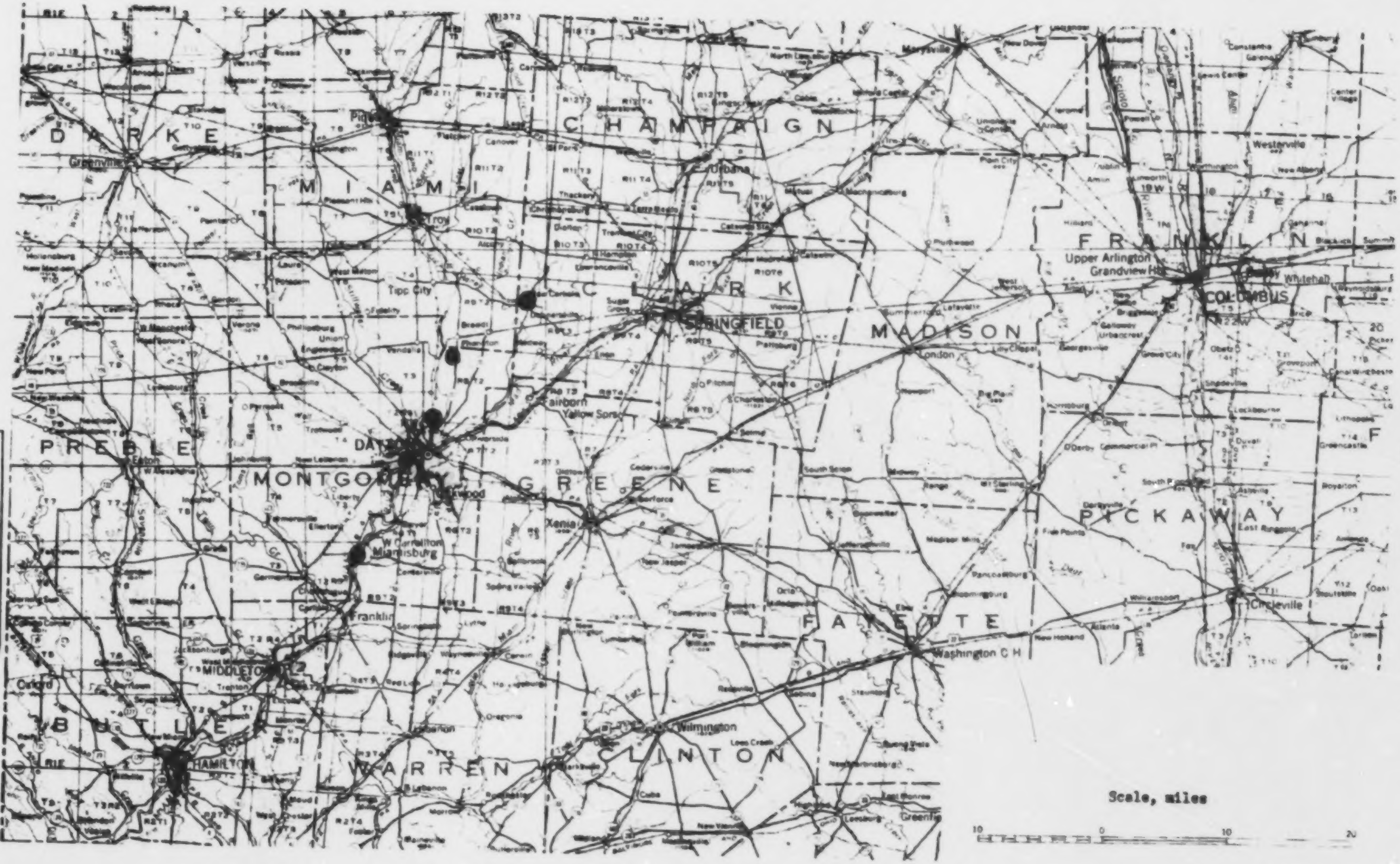
DARKE
Greenville
MIAMI
Piqua
Troy
Tipp City
CHAMPAIGN
Urbana
CLARK
SPRINGFIELD
MADISON
London
FRANKLIN
Upper Arlington
Grandview Hts
COLUMBUS
Whitehall
PREBLE
Eaton
MONTGOMERY
DAYTON
GREENE
Fairborn
Yellow Sprs
Xenia
W Carrollton
Miamisburg
Franklin
PICKAWAY
Circleville
FAYETTE
Washington C H
BUTLER
MIDDLETOWN
HAMILTON
Oxford
WARREN
Lebanon
CLINTON
Wilmington
Scale, miles
10
0
10
20

FIGURE 3. SITING ARRANGEMENT

Reproduced from best available copy.

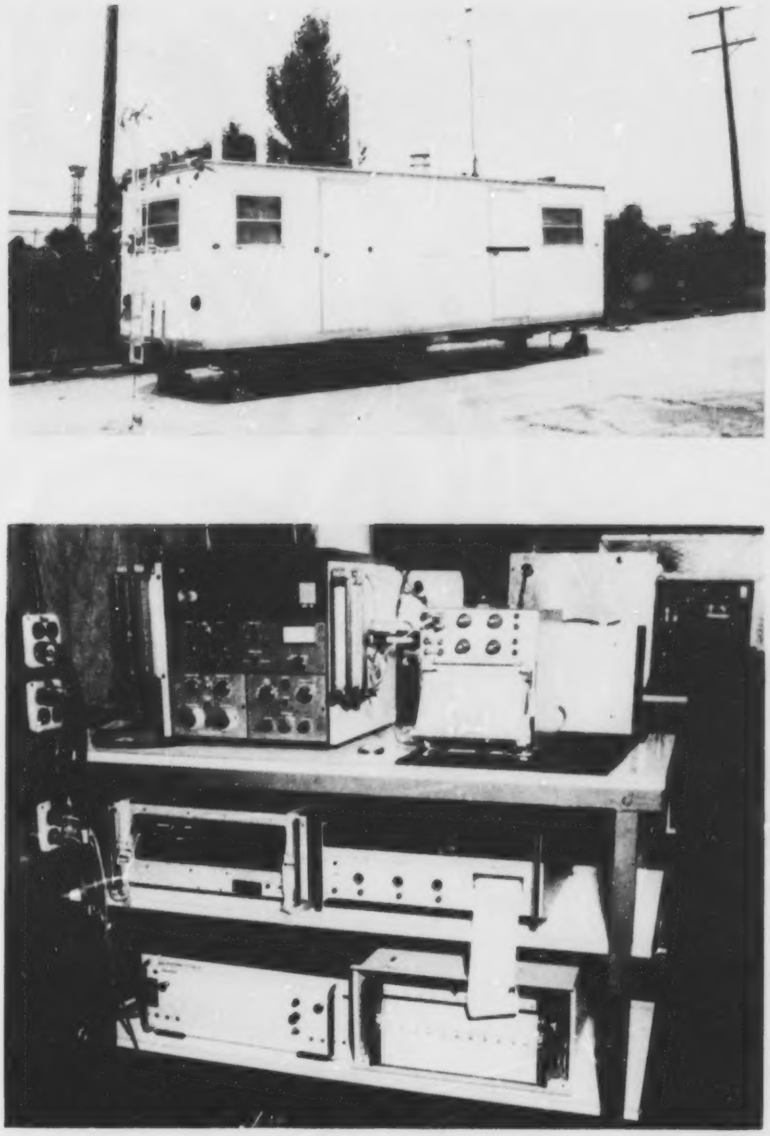

FIGURE 4. BATTELLE MOBILE AIR QUALITY LABORATORY

FIGURE 5A. INTERIOR OF AIR QUALITY LABORATORY

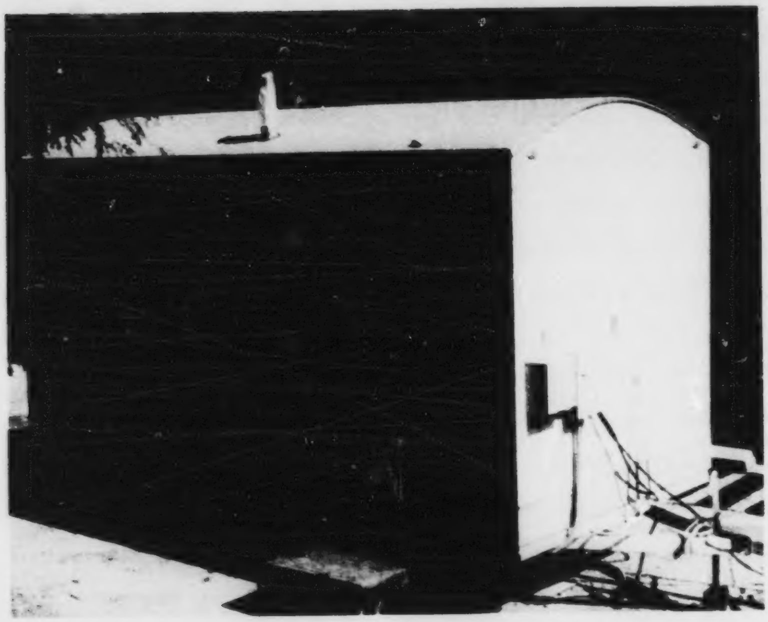

FIGURE 5B. MOBILE AIR QUALITY LABORATORY

During this study, both continuous and integrated analysis of air samples were employed. We will first discuss the procedures used in continuous monitoring and then review our integrated sample collection techniques.

The continuous data from the downtown Dayton site were collected on strip-chart recorders and reduced manually. The data were subsequently placed on cards and read into the Battelle CDC-6400 computer where they were conditioned and permanently stored on magnetic tape. The outputs from all instruments (except the gas chromatographs) from the Huber Heights Site were fed to a Digi-Tem data acquisition system where the analog input is converted to digital form, serialized by bit, and presented in ASCII code on paper tape. Each instrument channel was interrogated every 10 minutes for 24 hours each day. The information on paper tape was read into Battelle's CDC-6400 computer, conditioned, and permanently stored on magnetic tape. The instrument outputs from our third site, the TETCO Mobile Laboratory, were recorded on magnetic tape cartridges after conditioning by a Westinghouse data acquisition system. The magnetic tapes were sent to Westinghouse for translation to engineering units and transfer to a computer-compatible 7-track tape. This tape was read into Battelle's computer, where the data are permanently stored on magnetic tape.

The gas chromatographic and nitric acid instrument outputs, in addition to all Teflon sampling bag data, were manually reduced and fed to the computer on cards. These data were also conditioned and permanently stored on magnetic tape.

A computer program was used to average all analyses (except wind direction) from all sites and plot all analyses as 24-hour profiles.

Integrated samples were collected three times each day at the urban station and the remote site. Three-hour integrated samples were collected in 50-liter Teflon bags between 6-9 a.m., 9 a.m.-12 noon, and 12 noon-3 p.m. After collection, the bag samples were returned to the central laboratory (Site 2) for analysis. Most samples were analyzed within 1 hour of their collection. However, on days when airplane bag samples were being analyzed, delays up to 2 or 3 hours were sometimes experienced.

The bag samples were collected by pumping sample air from the sample manifold through Teflon tubing, through a contamination-free stainless steel diaphragm pump, and into the large Teflon sampling bags. A jeweled orifice was used to maintain the desired constant flow over the 3-hour collection periods. The pumps were wired to electrical timers which started and stopped the bag filling at the appropriate times. Even after extended use, the stainless steel diaphragm pumps showed no contamination with respect to the species we monitored, as determined by pumping "zero" air into Teflon bags and analyzing the samples thus collected. After each bag was analyzed it was exhausted through a diaphragm pump, backfilled with "zero" nitrogen, exhausted again, backfilled again, and finally exhausted and sealed for future use. We were able to detect no bag carry-over from sample to sample of any of the substances we were monitoring during the study.

The chemical and meteorological variables which were determined during this study are broken down in Table 2 by site. The techniques used for these determinations are discussed in the next sections.

Meteorological Measurements

The Battelle Mobile Laboratory makes use of an automated MRI, Inc., Model 1071 weather station. The instruments listed in Table 3 provide a continuous readout of temperature, relative humidity, wind speed, and wind direction. The laboratory also employs an Eppley Laboratory, Inc., 180° pyrheliometer to determine global radiation (total sun and sky). The remote station also employed MRI, Inc., instrumentation to determine wind speed and direction.

Laboratory and newspaper records were kept of general weather conditions such as cloud cover and intervals during which rain occurred.

TABLE 2. CHEMICAL AND METEOROLOGICAL DETERMINATIONS BY SITE

Urban Station (Dayton)	Main Laboratory (Huber Heights)	Remote Station (New Carlisle)	RAPCA Station (Miamisburg)	RAPCA Station (Timberlane)	EPA Station (Huber Heights)	Airplane
O_3	O_3	O_3	O_3	O_3	O_3	O_3
NO	NO	NO				Temperature (Vertical)
NO_2	NO_2	NO_2				CH_4 (a)
NO_x	NO_x	NO_x				C_2H_2 (a)
HNO_3	HNO_3	HNO_3				C_2H_4 (a)
SO_2	SO_2	SO_2				C_2H_6 (a)
CH_4 (a)	NH_3	CH_4 (a)				NMHC (a)
C_2H_4 (a)	PAN	C_2H_2 (a)				CO (a)
C_2H_6 (a)	CH_4	C_2H_4 (a)				PAN (a)
PAN (a)	C_2H_2	C_2H_6 (a)				
CO (a)	C_2H_4	NMHC (a)				
	C_2H_6	CO (a)				
	NMHC	PAN (a)				
	CO	Wind Speed				
	Mass Loading	Wind Direction				
	Light Scattering					
	NH_4^+					
	NO_3^-					
	$SO_4^=$					
	CHN					
	Solar Intensity					
	Wind Speed					
	Wind Direction					
	Temperature					
	Relative Humidity					

(a) Integrated Bag Samples

TABLE 3. METEOROLOGICAL MEASUREMENTS

Analysis	Instrument
Wind Speed and Direction	MRI, Model 1074-2 sensor
Temperature	MRI, Model 802 sensor
Relative Humidity	MRI, Model 907 sensor
Global Radiation Intensity	Eppley Lab, 180° pyrheliometer

Air Quality Measurements

The instruments used for air quality monitoring are listed in Table 4. Air samples are pulled into the main laboratory (Site 2) through an aluminum stack used for high-volume aerosol sampling. The top of the stack is about 15 feet above the trailer roof or roughly 25 feet above the ground. Flow rate through the stack is at least 30 cubic feet per minute, so that the residence time is no more than about 6 seconds in the stack. From the stack the samples are transported through short lengths of 1/4-inch Teflon tubing to the appropriate instrument. At the other sites, air samples were pulled into the stations by high capacity blowers through Pyrex manifolds which extended above the sampling station. Short lengths of Teflon tubing connect the instruments to the sampling manifold.

A detailed discussion of the principles, sensitivity, and calibration procedures used in this program for monitoring ozone and the nitrogen-containing species may be found in an earlier report(2). A discussion of the remaining analytical procedures follows.

Methane/Non-Methane Hydrocarbons

Methane and NMHC determination is based on the analysis of total hydrocarbons by a flame ionization detector and methane by a second FID. The difference in the signals from the two continuously operating FID's is a measure of non-methane hydrocarbons (NMHC). A heated Hopcalite catalyst is used prior to the second FID to destroy all hydrocarbons except CH_4, thus providing the selectivity required. The instrument is calibrated with "CH_4/C_3H_8 in air" calibration gas referenced to a NBS "propane in air" standard.

TABLE 4. AIR MONITORING INSTRUMENTATION

Analysis	Instrument
O_3	REM, Model 612 chemiluminescence monitor
NO NO_x NO_2 (by difference)	Bendix, Model 8101-B chemiluminescence analyzer, carbon catalytic converter
NH_3	Bendix, Model 8101-B chemiluminescence analyzer, dual stainless steel and carbon catalytic converters
Peroxyacetyl Nitrate (PAN)	Varian Series 1200 gas chromatograph with electron-capture detection
HNO_3	Modified acid-detecting Mast coulometric analyzer
CH_4 NMHC	MSA, Model 11-2 Methane/THC analyzer
C_2H_2 C_2H_4 C_2H_6	Varian Series 1200 gas chromatograph with flame ionization detection
CO	MSA, Carbon Monoxide Air Quality Monitor
SO_2	Phillips SO_2 Monitor System

Acetylene, Ethylene, Ethane

A flame ionization gas chromatograph equipped with a Porapak Q/ Porapak N packed column was used to separate and quantitate the C_2 hydrocarbons. The instrument was operated isothermally at 50 C using high-purity nitrogen and hydrogen and ultra-high purity air. The sample volume was 5 ml. Span gases prepared from the actual C_2 hydrocarbons and referenced to an NBS hydrocarbon standard were employed for daily calibration. An analysis was run every 15 minutes with the data being quantitated and averaged manually on site.

Carbon Monoxide

Carbon monoxide was determined by monitoring the heat of combustion of CO over a Hopcalite catalyst. The instrument consists of a dual tower sample drier to reduce water vapor interferences, and a detector and reference cell enclosed in a very rigidly temperature-controlled oven. The detector cell contains the catalyst and a thermistor while the reference cell is packed with an inert material and a second thermistor. The thermistors are arranged electrically in a Wheatstone bridge to detect temperature differences between the reference and detector cells. The instrument is provided with 0-10 ppm and 0-50 ppm ranges. Calibration was accomplished with cylinders of known concentrations of CO in air in the range of 0-10 ppm and 0-50 ppm.

Sulfur Dioxide

Sulfur dioxide was monitored potentiometrically by its reaction with bromine in a redox system. The Phillips instrument employs two filters to remove particulate matter from the air sample and a heated silver catalyst to destroy ozone. Sulfur dioxide in the air sample reacts with Br_2 to change the cell redox potential as follows:

$$SO_2 + Br_2 + 2H_2O \longrightarrow H_2SO_4 + 2H^+ + 2Br^- .$$

At constant temperature, this change in potential is a measure of the SO_2 concentration. The detection limit of the technique is 0.003 ppm SO_2.

Aerosol Collections

Aerosol samples were collected on a 24-hour-per-day basis at the central laboratory (Site 2). Samples were collected from 25 feet above ground through two 6-inch-diameter aluminum stacks. High-volume blowers were used to maintain an average flow rate of 30 cfm. Pressure-drop measurements were made at the beginning and end of each day's sampling in order to correct for day-to-day fluctuations in flow rate. Initial calibration of the blowers was done with a calibrated venturi.

Aerosol samples were collected on 6-inch-diameter high-purity quartz mat filters (Pallflex Product Corporation) backed by a stainless steel fritted disk. Each filter was cut and preweighed in the laboratory at 40 percent relative humidity and then stored in an individual glassine envelope enclosed in a sealed polyethylene bag. After sampling, the filter was returned to its glassine envelope in its plastic bag, purged with and then sealed under argon. On return to the Columbus Laboratories, the filters were equilibrated at 40 percent relative humidity and reweighed. The filters were then partitioned for analysis.

A third high-volume sampler incorporated a specially designed cyclone which served as a collector for particles > 2.5 μm in diameter. The cyclone was operated for 24 hours per day for the entire sampling period. The total particulate collected by the cyclone was analyzed as a representative average "dustfall" sample.

Aerosol Analysis

Filters from the field study were analyzed at Battelle's Columbus Laboratories for NH_4^+, $SO_4^=$, NO_3^-, and total carbon, hydrogen, and nitrogen. A brief description of the varous methods follows:

- *Ammonium* was determined by dissolving soluble ammonium salts in water, adding NaOH, and measuring the resulting NH_3 with an ammonia gas sensing electrode
- *Sulfate* was determined on an aliquot of the filter wash by the barium perchlorate colorimetric procedure
- *Nitrate* analysis made use of an aliquot of the water extract from the filter and the brucine sulfate method, ASTM D992
- *Total C, H, N* were determined with a Perkin Elmer Model 240 Elemental Analyzer which employs pyrolysis and thermal conductivity detection for elemental analysis.

Dustfall Analysis

Particles larger than 2.5 μm were collected 24 hours per day by a special cyclone sampler connected to a high-volume blower. Air was delivered to the cyclone from 25 feet above ground through a 6-inch-diameter aluminum stack. At the end of sample collections, the composite "dustfall" sample was returned to Battelle's Columbus Laboratories, weighed, and analyzed for NH_4^+, $SO_4^=$, NO_3^-, and total C, H, N. The results of these analyses are reported in percent by weight of the total dust sample.

Aircraft Measurements

A Cessna 172 single-engine aircraft and the services of a pilot were rented for this study from a local aviation firm in Columbus, Ohio. The aircraft is pictured in Figure 6. The rear seats of the plane were removed and an instrument rack erected in their place. The front passenger seat was reversed so that it faced the instrument rack, and the steering device on that side of the plane was removed for additional room. A picture of the instruments and rack positioned within the plane is shown in Figure 7.

Ram air was supplied to the instruments through a stainless steel sampling probe located under the wing and well outside of the prop and engine backwash. The sampling probe, shown in Figure 8, was connected to an all-Teflon manifold by flexible Teflon tubing passing within the wing shell and into the plane. The residence time within the sample tubing was less than 6 seconds. Most of the ram air was exhausted from the Teflon mainfold through a vent at the rear of the plane. A small fraction of the flow was provided to an REM, Inc., chemiluminescent instrument for continuous ozone monitoring. The manifold was also connected through stopcocks to three 50-liter Teflon bags mounted in the rear luggage section of the plane. These bags could be filled by opening the appropriate stopcock.

An inverter and Variac were used to supply power for the chemiluminescent instrument and dual pen recorder through the airplane's alternator and battery system. An electrical switch was arranged for instantaneously changing from aircraft to ground power (via an extension cord) so that it was never necessary to shut the instrumentation down either at night or before or after takeoff and landing. Records of time, position, weather conditions, etc., were kept on the strip-chart recorder along with the ozone signal output. Temperature was also read manually and marked on the recorder chart along with altitude.

A typical flight consisted of the pilot and technician flying from Columbus, Ohio to Dayton, reaching the Dayton area at approximately

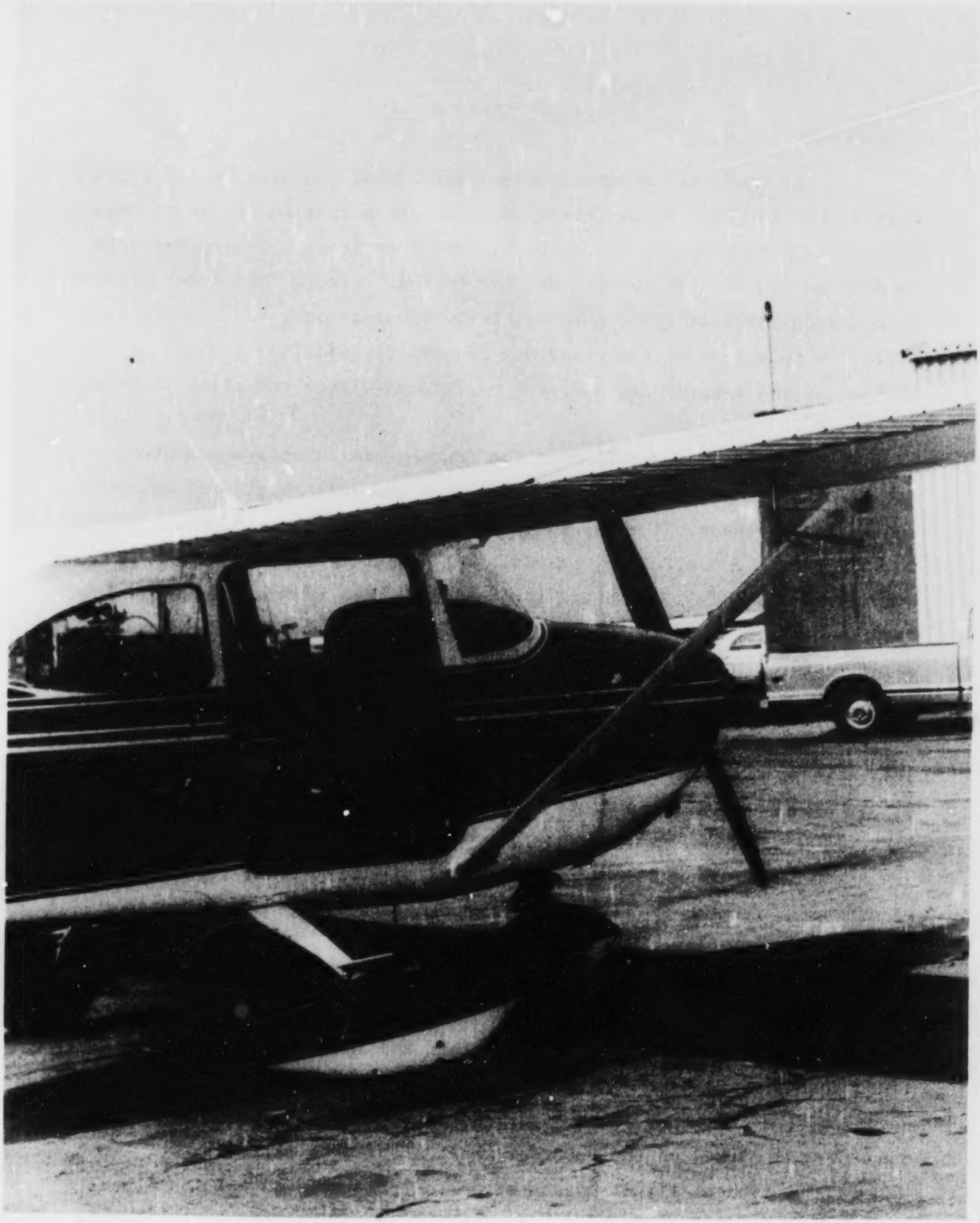

FIGURE 6. AIRCRAFT WITH DOOR REMOVED

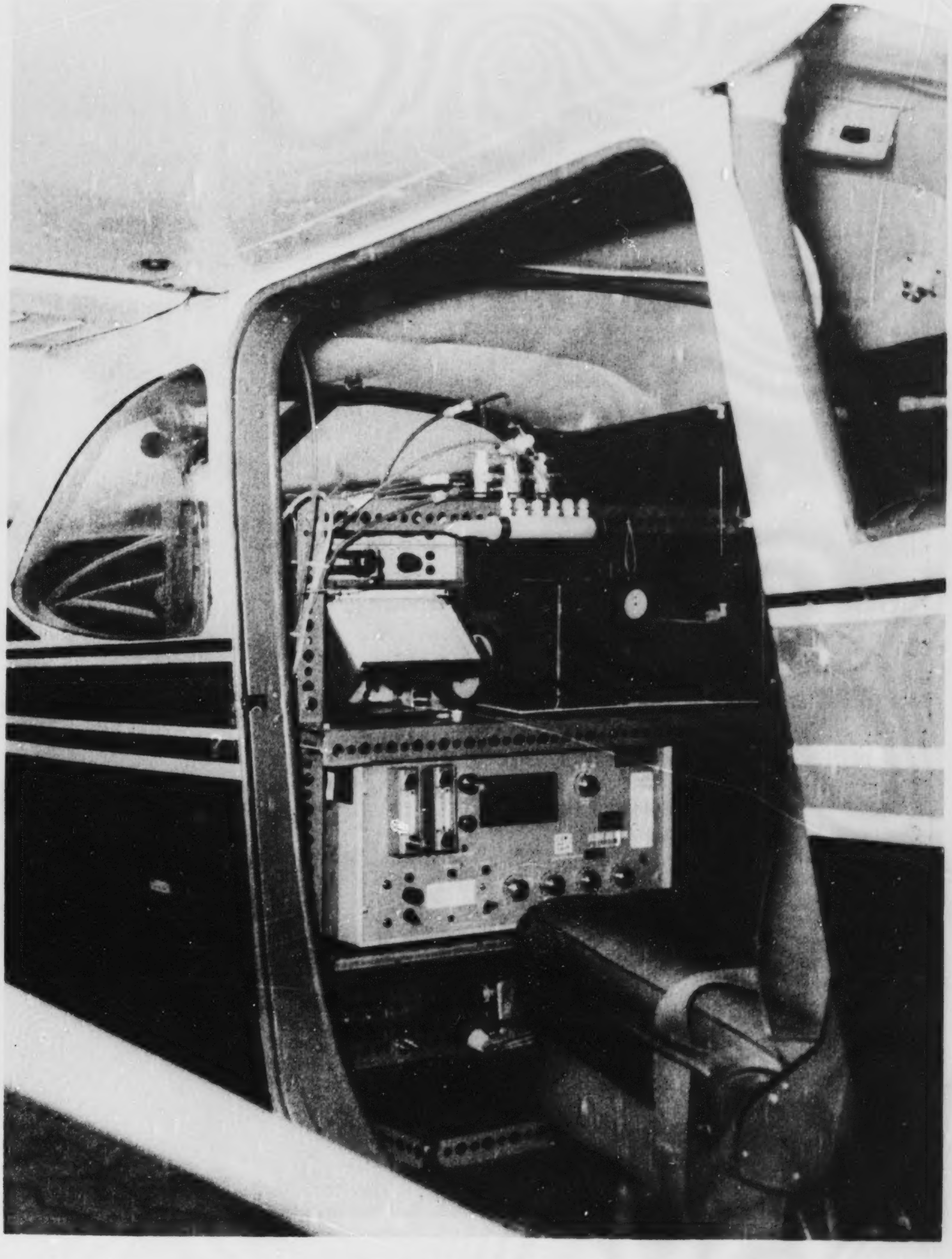

FIGURE 7. MONITORING INSTRUMENTATION WITHIN AIRCRAFT

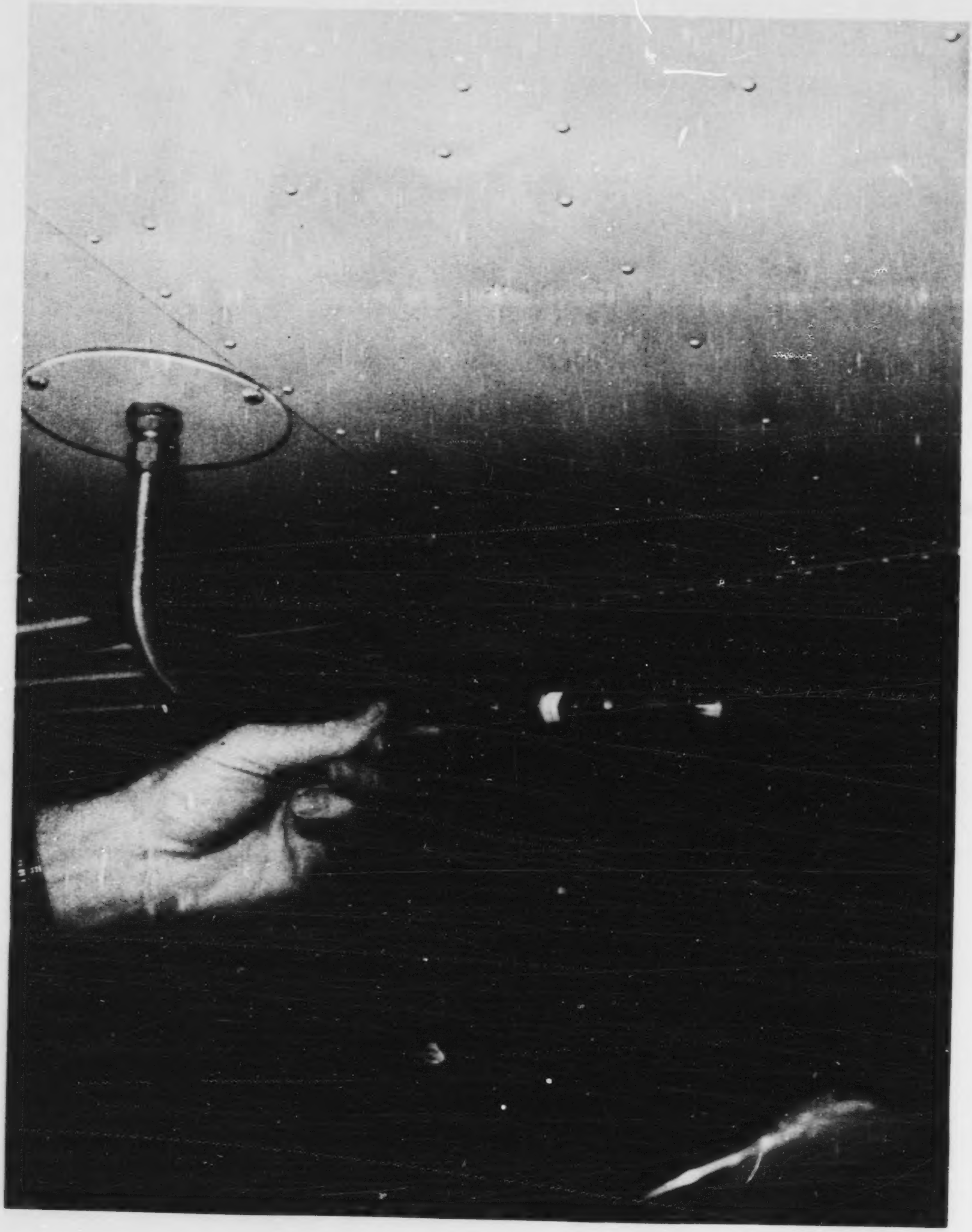

FIGURE 8. AIRCRAFT SAMPLING PROBE

9 a.m. The flight pattern would commence with a loop being flown from downtown Dayton to a point 20 miles in the upwind direction. The plane would then be flown in a 20-mile loop downwind of Dayton, and finally in a 60-mile loop downwind of the city. The distance across the loops at their extremes was 15-20 miles. This entire pattern was always flown at 1000 feet above mean ground level. Ozone was monitored continuously and Teflon bag samples were collected at the extremes of each of the three loops. In this manner it was possible to characterize the air mass entering Dayton (20-mile upwind loop) and the air mass after passing through Dayton (20- and 60-mile downwind loops). Upon completion of the three loops, the aircraft returned to Dayton and carried out a spiral maneuver to an altitude of 5000 feet. Ozone and temperature were monitored continuously during this spiral to determine the vertical temperature and ozone profiles. The aircraft would then land (at approximately 12 noon) for servicing. The bag samples were transferred to the main laboratory at this time and the analysis of the bags was carried out for the species indicated in Table 2. During the afternoon (1:00-4:00 p.m.) the same patterns were flown as in the morning. After landing to transfer the afternoon bag collections, the plane was flown back to Columbus. Ozone was monitored during this return flight.

RESULTS

In this section of the report we will summarize the field monitoring data collected in Dayton. The large volume of data requires that all of the results be summarized in one place for ease in referencing. The plots of the airplane flight patterns and associated ozone concentrations will be included in a later section of the report. Daily meteorological maps and trajectory plots will be included in appendices to this report.

A detailed summary of the air-quality data for the 20 days of field monitoring in the Dayton area in July and August, 1974, will be presented in subsequent tables. For the New Carlisle site, 27 days' worth of data were collected during the July and August period.

The summary of air-quality data for the downtown Dayton station (Site No. 1) is shown in Table 5. The gas-phase data are presented as both 24-hour averages and as maximum 1-hour averages. Measurements of HNO_3 at this site were discontinued in the latter half of the study when it was discovered that the ethylene reagent used with the nitric acid instrument was occasionally backflushing and contaminating our bag samples.

Figure 9 profiles the average diurnal air quality at the downtown Dayton site during the field program. The individual daily profiles are included in the appendix of this report.

The air-quality data and meteorology at the Huber Heights site (Site No. 2) are summarized in Tables 6 and 7. The 24-hour averages are given in Table 6, while Table 7 shows the maximum 1-hour averages. Profiles of the average gas-phase and meteorology results from Site 2 are presented as Figure 10. The individual daily profiles are included in the appendix.

Table 8 summarizes the 24-hour averages and maximum 1-hour averages of the New Carlisle (Site No. 3) data during 27 days in July and August. The profiles of the average Site 3 data are shown as Figure 11.

Ozone data from three additional locations have been made available to us courtesy of the RAPCA. The three stations were located in Miamisburg, Timberlane (north of downtown Dayton), and at Huber Heights. Tabulations of hourly average ozone concentrations at these three locations during the study period are given in Tables 9, 10, and 11.

Three-hour integrated bag samples were collected and analyzed three times each day at Site Nos. 1 and 3. The bags were collected from 6-9 a.m., 9 a.m.-12 noon, and 12 noon-3 p.m. each sampling day. The same species that were determined in the bag samples at Sites 1 and 3 were monitored continuously at Site 2. For purposes of comparison the Site 2 data have been averaged over the same 3-hour time intervals as the integrated bag data. The average concentrations of the gases determined from the bag collections are shown for Sites 1-3 in Table 12. The individual daily concentrations are tabulated in the appendix.

TABLE 5. SUMMARY OF AIR QUALITY DATA - DAYTON SITE NO. 1

Date	Day	Pollutants									
		24-Hour Average, ppm					1-Hour Max., ppm				
		O_3	NO	NO_x	SO_2	HNO_3	O_3	NO	NO_x	SO_2	HNO_3
7-17	W	0.042	0.007	0.031	0.022	0.036	0.088	0.080	0.128	0.046	0.054
7-18	Th	0.035	0.020	0.051	0.020	0.011	0.068	0.154	0.206	0.032	0.016
7-19	F	0.034	0.007	0.034	0.015	0.010	0.079	0.039	0.079	0.037	0.017
7-23	T	0.017	0.020	0.048	0.015	0.000	0.029	0.093	0.133	0.015	0.000
7-24	W	0.034	0.010	0.030	0.008	0.001	0.073	0.048	0.082	0.012	0.004
7-25	Th	0.043	0.020	0.047	0.017	0.001	0.079	0.111	0.157	0.037	0.004
7-26	F	0.041	0.041	0.085	0.019	0.003	0.098	0.257	0.304	0.032	0.009
7-29	M	0.024	0.022	0.046	0.015	0.001	0.055	0.162	0.162	0.201	0.030
7-30	T	0.017	0.031	0.049	0.019	0.000	0.039	0.099	0.111	0.025	0.002
7-31	W	0.019	0.049	0.078	0.011	0.002	0.054	0.178	0.195	0.012	0.007
8-1	Th	0.045	0.049	0.077	0.019	0.000	0.120	0.408	0.451	0.037	0.000
8-2	F	0.035	0.009	0.034	0.013	--	0.083	0.021	0.074	0.042	--
8-5	M	0.012	0.029	0.052	0.022	--	0.032	0.101	0.135	0.032	--
8-6	T	0.034	0.020	0.044	0.026	--	0.071	0.117	0.152	0.034	--
8-7	W	0.029	0.015	0.033	0.023	--	0.068	0.094	0.116	0.034	--
8-8	Th	0.016	0.020	0.056	0.018	--	0.051	0.062	0.104	0.039	--
8-9	F	0.038	--	0.042	0.018	--	0.093	0.025	0.133	0.025	--
8-10	Sat.	0.038	0.007	0.018	0.034	--	0.061	0.012	0.034	0.046	--
8-11	Sun.	0.015	0.010	0.024	0.050	--	0.029	0.018	0.040	0.061	--
8-12	M	0.020	0.029	0.059	0.013	--	0.037	0.079	0.111	0.039	--

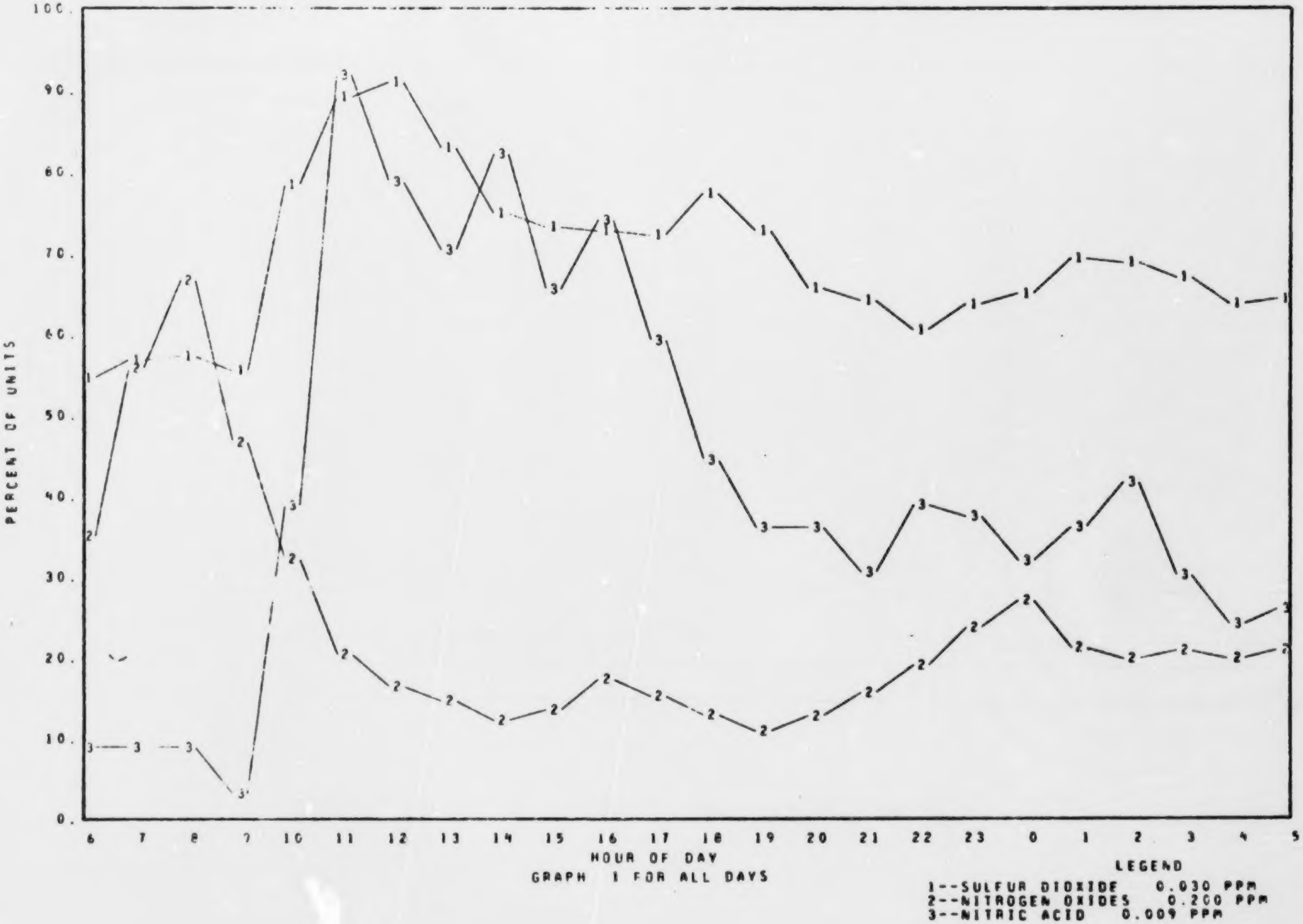
PERCENT OF UNITS
100.
90.
80.
70.
60.
50.
40.
30.
20.
10.
0.
6
7
8
9
10
11
12
13
14
15
16
17
18
19
20
21
22
23
0
1
2
3
4
5
HOUR OF DAY
GRAPH 1 FOR ALL DAYS
LEGEND
1--SULFUR DIOXIDE 0.030 PPM
2--NITROGEN OXIDES 0.200 PPM
3--NITRIC ACID 0.009 PPM

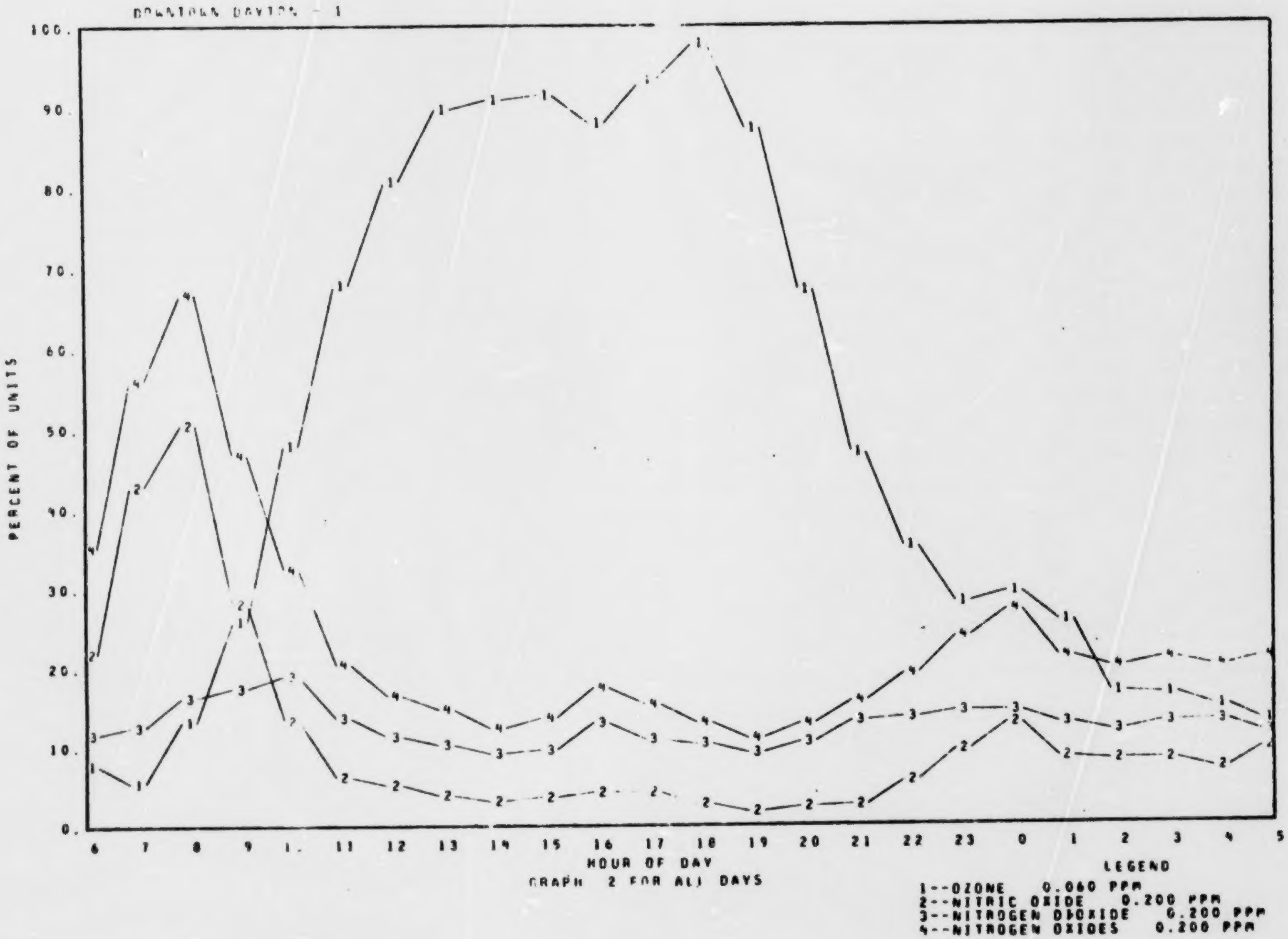

FIGURE 9 B. SITE 1 COMPOSITE PROFILES

TABLE 6. SUMMARY OF AIR QUALITY DATA – DAYTON SITE NO. 2

Date	Day	Weather Conditions			Aerosol Mass Loading, g/m^3	Light Scattering, 10^{-4} M^{-1}	Pollutants												
												Pollutants – 24-Hour Average, ppm							
		Temp, C	RH %	G.I.(a)			O_3	NO	NO_x	SO_2	NH_3	CH_4	NMHC	CO	C_2H_4	C_2H_2	C_2H_6	PAN	HNO_3
7-17	W	24.0	53.0	0.35	79.1	1.6	0.050	0.007	0.030	0.056	0.001	1.68	0.59	1.22	–	–	–	0.002	0.003
7-18	Th	25.8	59.2	0.30	136.8	5.5	0.068	0.004	0.021	0.061	0.002	1.74	0.51	1.31	–	–	–	0.002	0.005
7-19	F	26.4	66.3	0.22	74.9	4.5	0.049	0.003	0.020	0.055	0.005	1.71	0.77	1.02	–	–	–	0.001	0.001
7-23	T	19.4	88.4	0.14	69.6	7.0	0.038	0.003	0.020	0.022	0.003	1.56	0.38	0.95	–	–	–	0.000	0.000
7-24	W	21.6	66.0	0.34	57.8	3.2	0.041	0.007	0.028	0.007	0.000	1.50	0.29	0.84	0.012	0.004	–	0.000	0.000
7-25	Th	22.8	61.6	0.30	106.8	4.8	0.053	0.009	0.029	0.034	0.000	1.52	0.40	1.02	0.011	0.004	0.006	0.000	0.004
7-26	F	24.9	63.0	0.25	141.4	7.8	0.041	0.013	0.041	0.013	0.000	1.58	0.61	1.44	0.016	0.004	0.011	0.001	0.001
7-29	M	23.0	64.1	0.34	132.5	2.5	0.043	0.008	0.026	0.009	0.000	1.50	0.42	0.85	0.009	0.003	0.006	0.000	0.000
7-30	T	20.9	58.6	0.35	117.6	1.1	0.025	0.013	0.032	0.008	0.000	1.49	0.49	0.68	0.007	0.003	0.006	0.000	0.000
7-31	W	22.0	59.9	0.31	101.0	1.5	0.023	0.018	0.043	0.022	0.000	1.55	0.58	1.15	0.011	0.004	0.007	0.001	0.000
8-1	Th	23.7	59.9	0.30	88.3	2.7	0.064	0.015	0.035	0.018	0.000	1.47	0.46	0.91	0.006	0.003	0.004	0.000	0.000
8-2	F	22.0	77.7	0.23	72.0	2.5	0.042	0.006	0.023	0.015	0.000	1.39	0.43	1.09	0.005	0.003	0.004	0.000	0.000
8-5	M	19.4	62.7	0.30	30.7	1.3	0.031	0.007	0.022	0.009	0.000	1.48	0.38	0.46	0.003	0.002	0.002	0.001	0.000
8-6	T	20.5	60.0	0.35	75.1	2.5	0.042	0.003	0.006	–	0.000	1.43	0.37	0.89	0.006	0.003	0.006	0.000	0.000
8-7	W	21.5	75.9	0.24	66.9	3.6	0.034	0.008	0.024	–	0.000	1.51	0.37	0.89	0.006	0.003	0.008	0.001	0.000
8-8	Th	22.3	79.8	0.21	56.7	3.4	0.028	0.010	0.034	–	0.000	1.52	0.52	1.04	0.009	0.005	0.005	0.001	0.002
8-9	F	23.5	71.2	0.30	–	4.2	0.038	0.011	0.029	–	0.000	1.53	0.42	0.99	0.009	0.004	0.006	0.001	0.000
8-10	Sat.	23.0	74.2	0.22	77.3	6.5	0.041	0.006	0.018	–	0.000	1.58	0.31	0.78	0.006	0.003	0.013	0.002	0.000
8-11	Sun.	22.7	88.1	0.13	–	4.8	0.019	0.005	0.015	0.025	0.000	1.47	0.20	0.48	0.004	0.003	0.007	0.000	0.000
8-12	M	24.1	66.0	0.33	40.3	1.4	0.030	0.008	0.024	0.008	0.000	1.52	0.51	1.00	0.007	0.003	0.004	0.000	0.000

(a) Global Irradiance, cal-cm^{-3}-min^{-1}.

TABLE 7. SUMMARY OF AIR QUALITY DATA – DAYTON SITE NO. 2

Date	Day	Pollutants – 1-Hour Max., ppm													Light Scattering, 10^{-4} M^{-1}
		O_3	NO	NO_x	SO_2	NH_3	CH_4	NMHC	CO	C_2H_4	C_2H_2	C_2H_6	PAN	HNO_3	
7-17	W	0.120	0.058	0.086	0.069	0.008	2.37	1.04	2.94	–	–	–	0.004	0.006	2.7
7-18	Th	0.119	0.039	0.113	0.079	0.008	2.19	0.79	3.37	–	–	–	0.004	0.015	8.9
7-19	F	0.104	0.040	0.081	0.067	0.017	2.06	2.24	2.88	–	–	–	0.006	0.005	12.0
7-23	T	0.079	0.015	0.053	0.028	0.010	1.88	0.78	1.73	–	–	–	0.002	0.000	9.9
7-24	W	0.097	0.047	0.092	0.015	0.003	1.69	0.58	2.26	0.072	0.013	–	0.001	0.000	8.2
7-25	Th	0.096	0.034	0.070	0.050	0.002	1.78	0.66	1.86	0.020	0.017	0.016	0.001	0.012	7.4
7-26	F	0.107	0.052	0.110	0.034	0.002	1.69	1.18	3.75	0.035	0.009	0.019	0.010	0.006	11.4
7-29	M	0.090	0.064	0.109	0.013	0.001	1.99	1.11	3.14	0.037	0.013	0.022	0.000	0.000	8.8
7-30	T	0.063	0.038	0.066	0.014	0.000	1.70	1.24	1.65	0.023	0.010	0.015	0.000	0.000	2.0
7-31	W	0.062	0.093	0.131	0.032	0.001	2.18	1.82	3.46	0.032	0.010	0.020	0.004	0.000	2.5
8-1	Th	0.133	0.108	0.149	0.032	0.000	1.73	1.06	2.50	0.019	0.014	0.011	0.005	0.000	3.9
8-2	F	0.104	0.021	0.052	0.024	0.000	1.73	0.82	2.45	0.019	0.010	0.014	0.005	0.000	4.1
8-5	M	0.057	0.030	0.075	0.018	0.000	1.64	0.72	0.74	0.018	0.007	0.004	0.004	0.000	2.2
8-6	T	0.095	0.011	0.043	–	0.000	1.56	0.71	1.39	0.011	0.007	0.010	0.003	0.000	4.8
8-7	W	0.075	0.054	0.084	–	0.000	1.88	0.70	1.68	0.015	0.007	0.016	0.003	0.000	5.6
8-8	Th	0.081	0.026	0.067	–	0.000	1.75	0.98	1.85	0.016	0.009	0.013	0.008	0.005	6.8
8-9	F	0.089	0.078	0.101	–	0.000	2.08	1.20	3.83	0.027	0.014	0.014	0.004	0.000	8.0
8-10	Sat.	0.061	0.013	0.033	–	0.000	1.75	0.51	1.25	0.011	0.006	0.020	0.008	0.000	10.8
8-11	Sun.	0.034	0.010	0.023	0.037	0.000	1.58	0.35	1.30	0.009	0.005	0.021	0.002	0.000	10.7
8-12	M	0.066	0.044	0.080	0.011	0.000	1.92	1.60	2.84	0.034	0.016	0.013	0.002	0.000	6.0

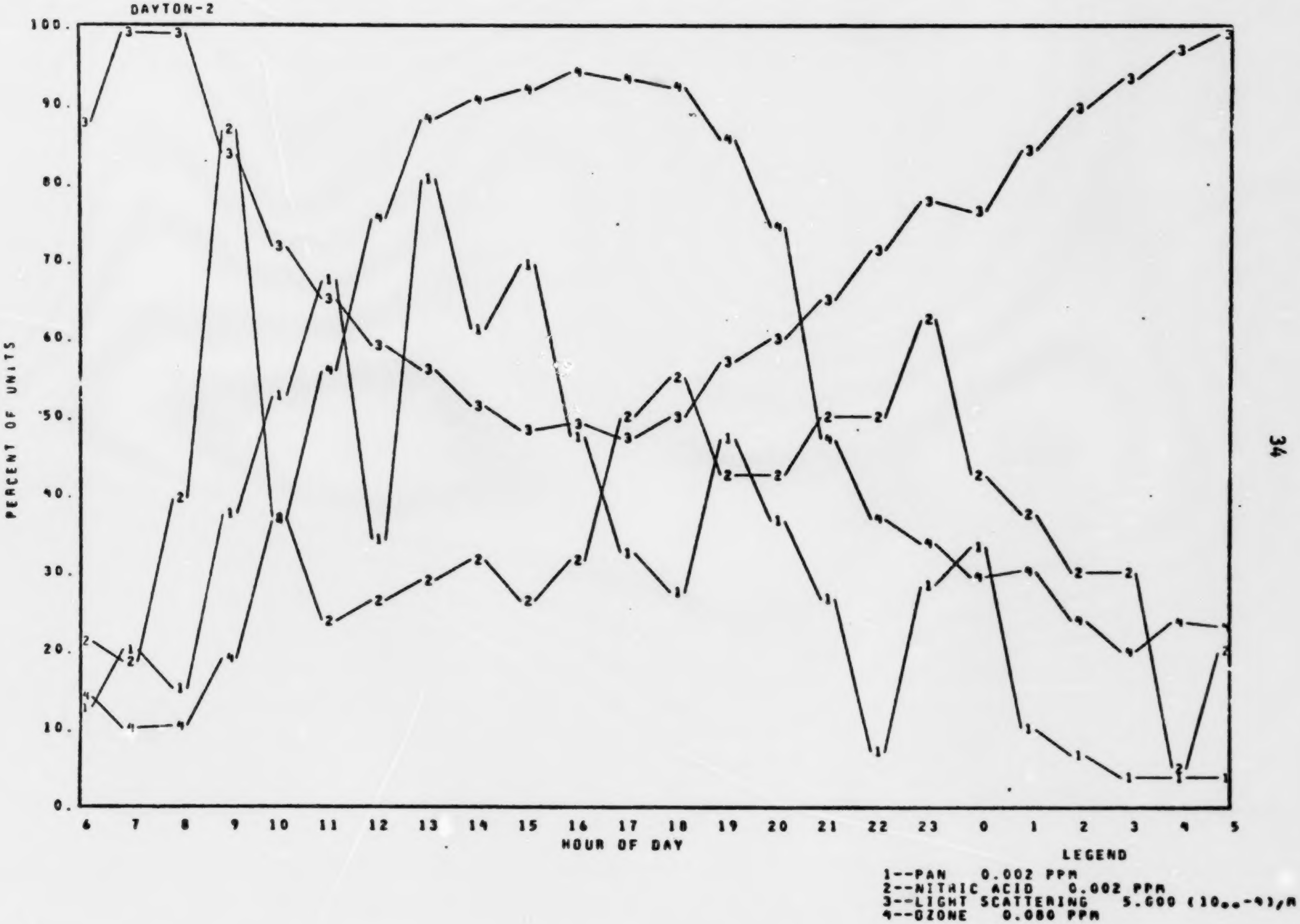
DAYTON-2
PERCENT OF UNITS
100.
90.
80.
70.
60.
50.
40.
30.
20.
10.
0.
6
7
8
9
10
11
12
13
14
15
16
17
18
19
20
21
22
23
0
1
2
3
4
5
HOUR OF DAY
LEGEND
1--PAN 0.002 PPM
2--NITRIC ACID 0.002 PPM
3--LIGHT SCATTERING 5.600 (10..-4)/M
4--OZONE 0.080 PPM

[illegible]

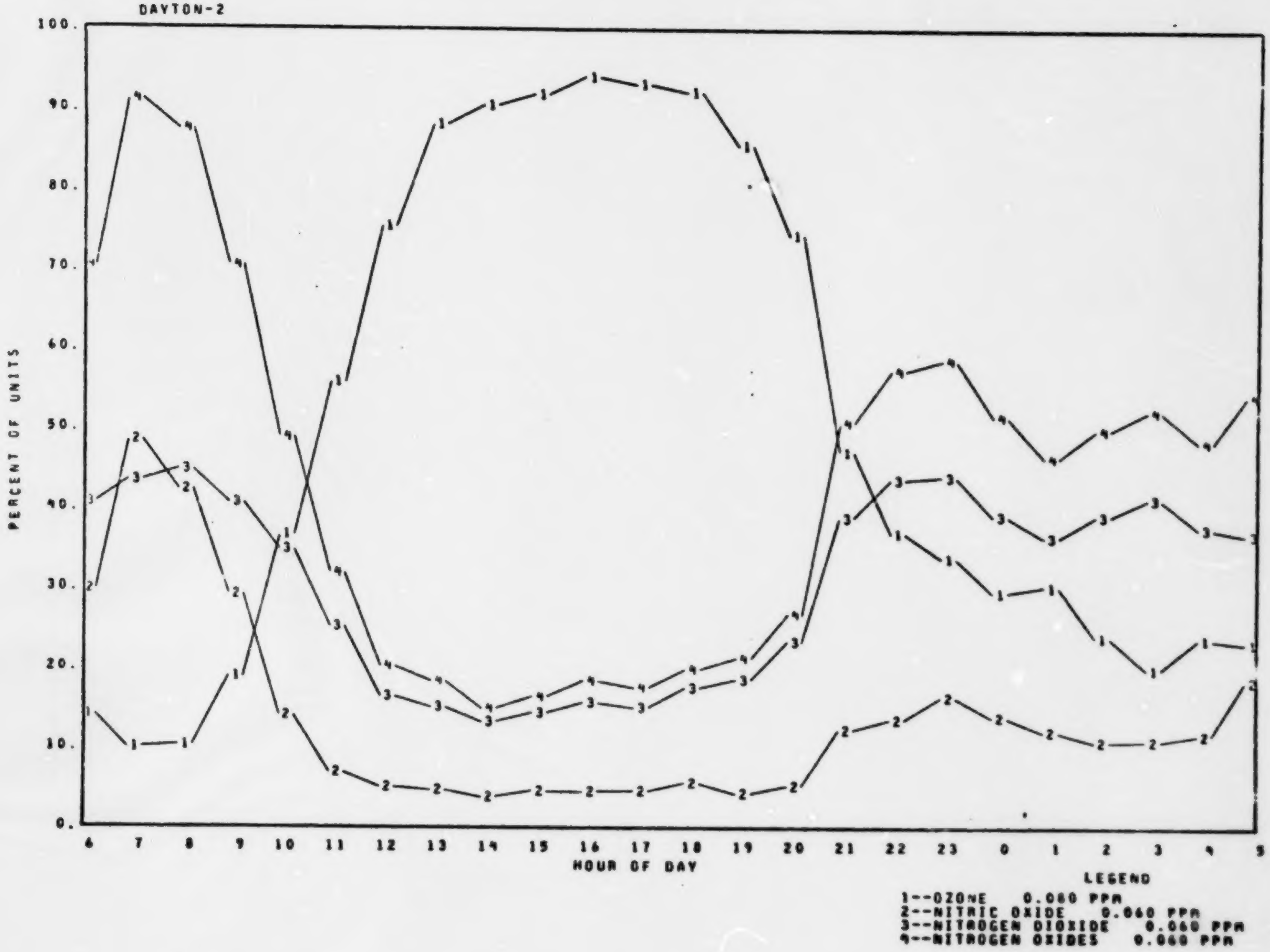

FIGURE 10 B. SITE 2 COMPOSITE PROFILES

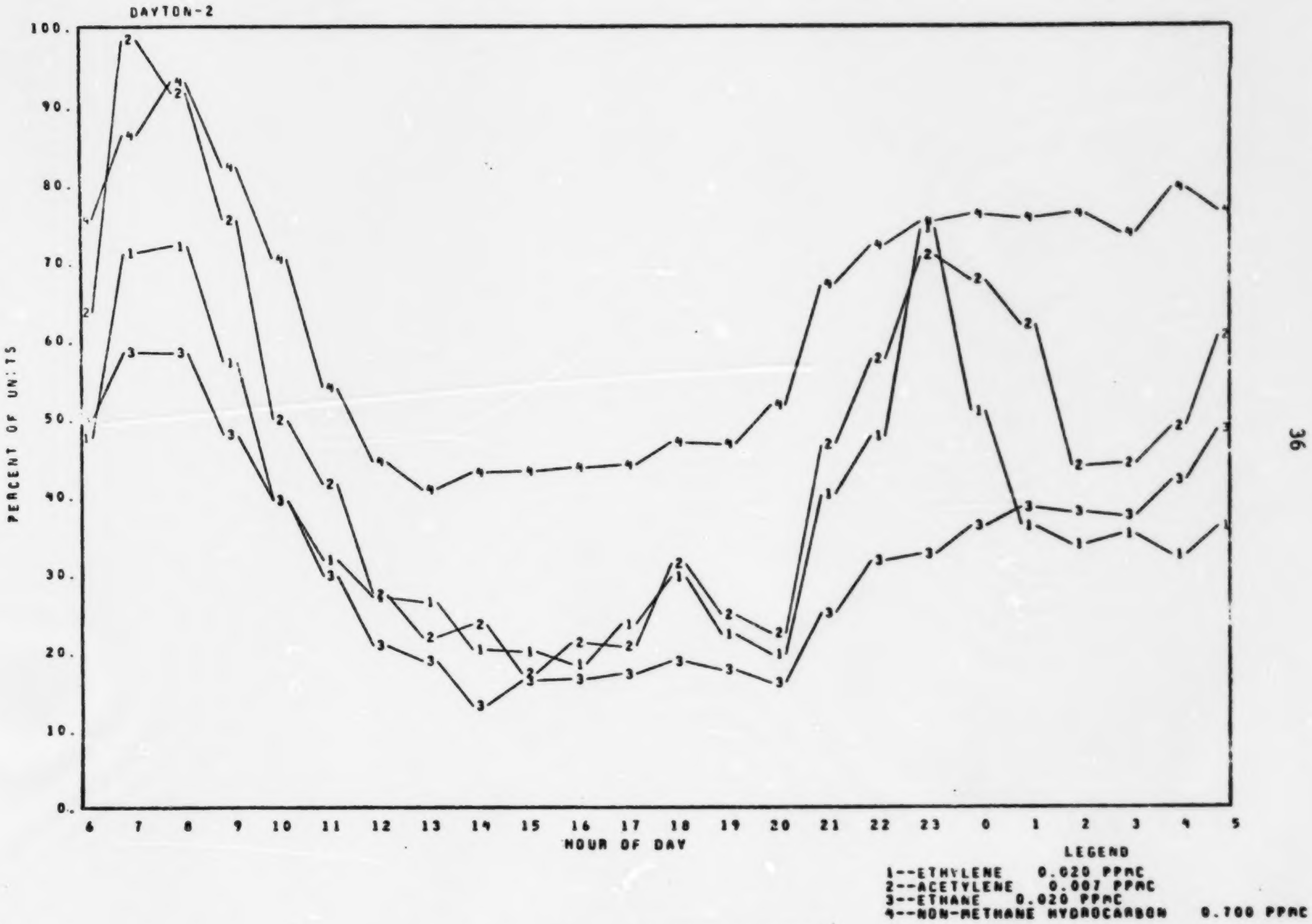

FIGURE 10 C. SITE 2 COMPOSITE PROFILES

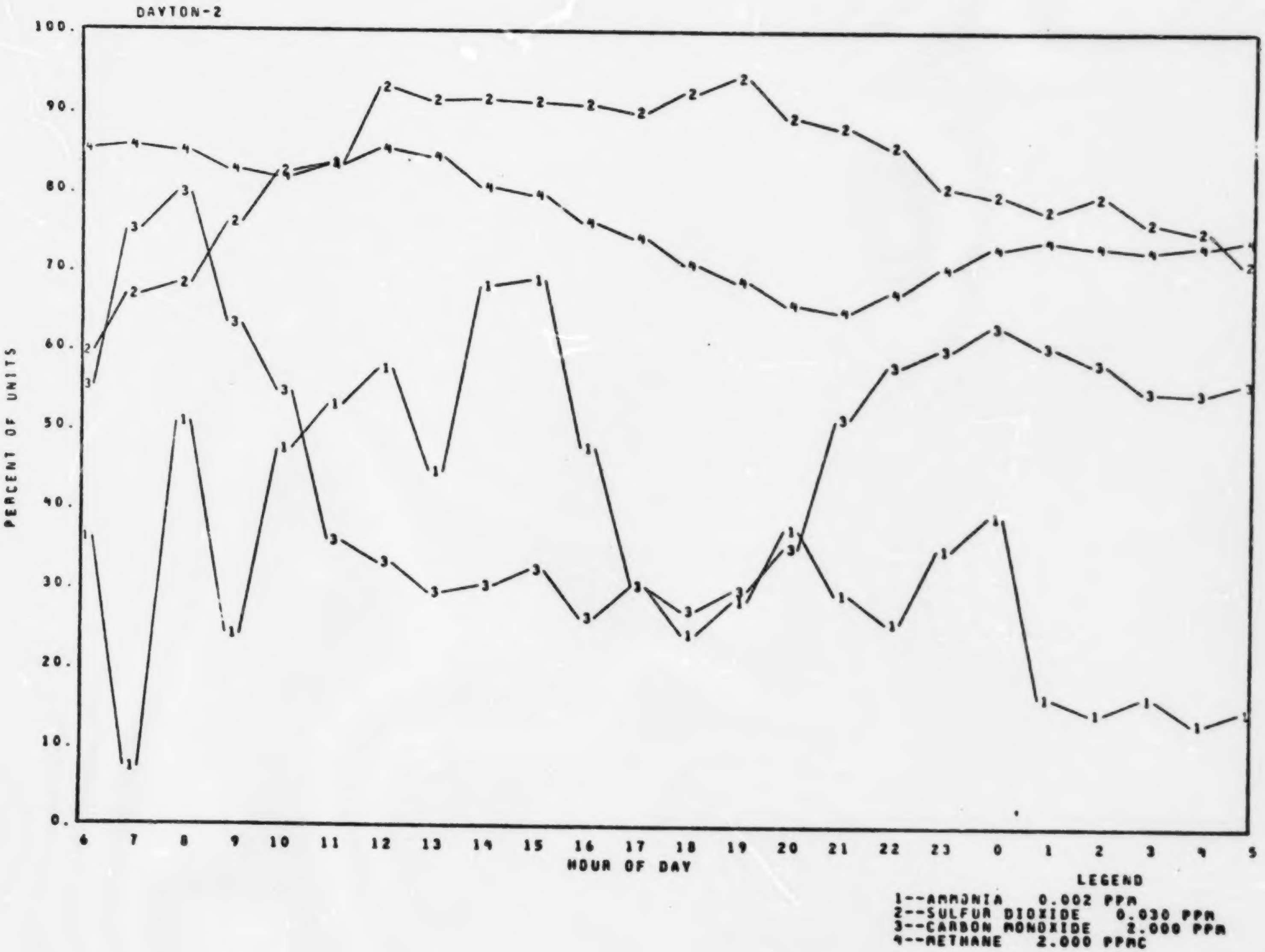

FIGURE 10 D. SITE 2 COMPOSITE PROFILES

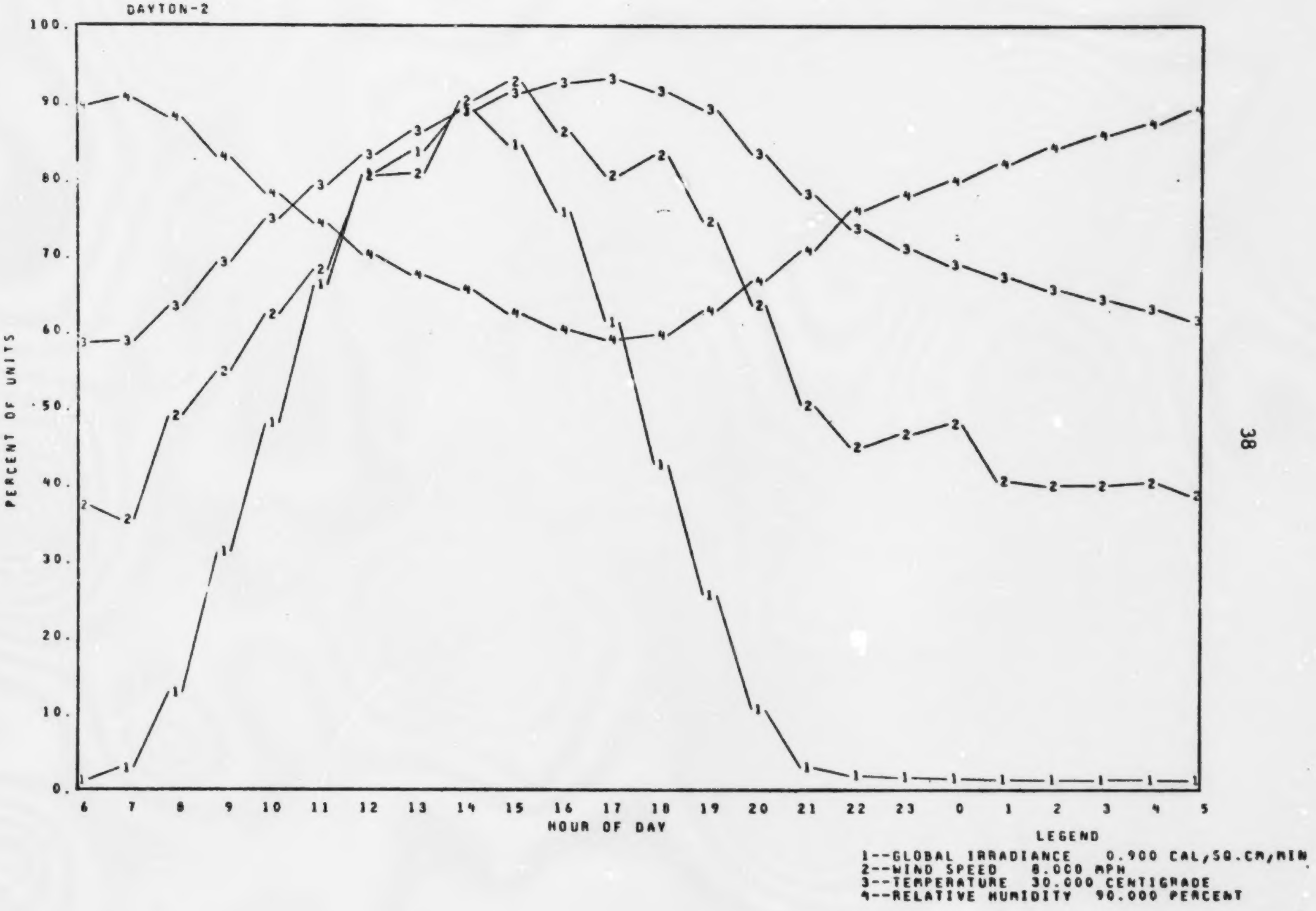

FIGURE 10 F. SITE 2 COMPOSITE PROFILES

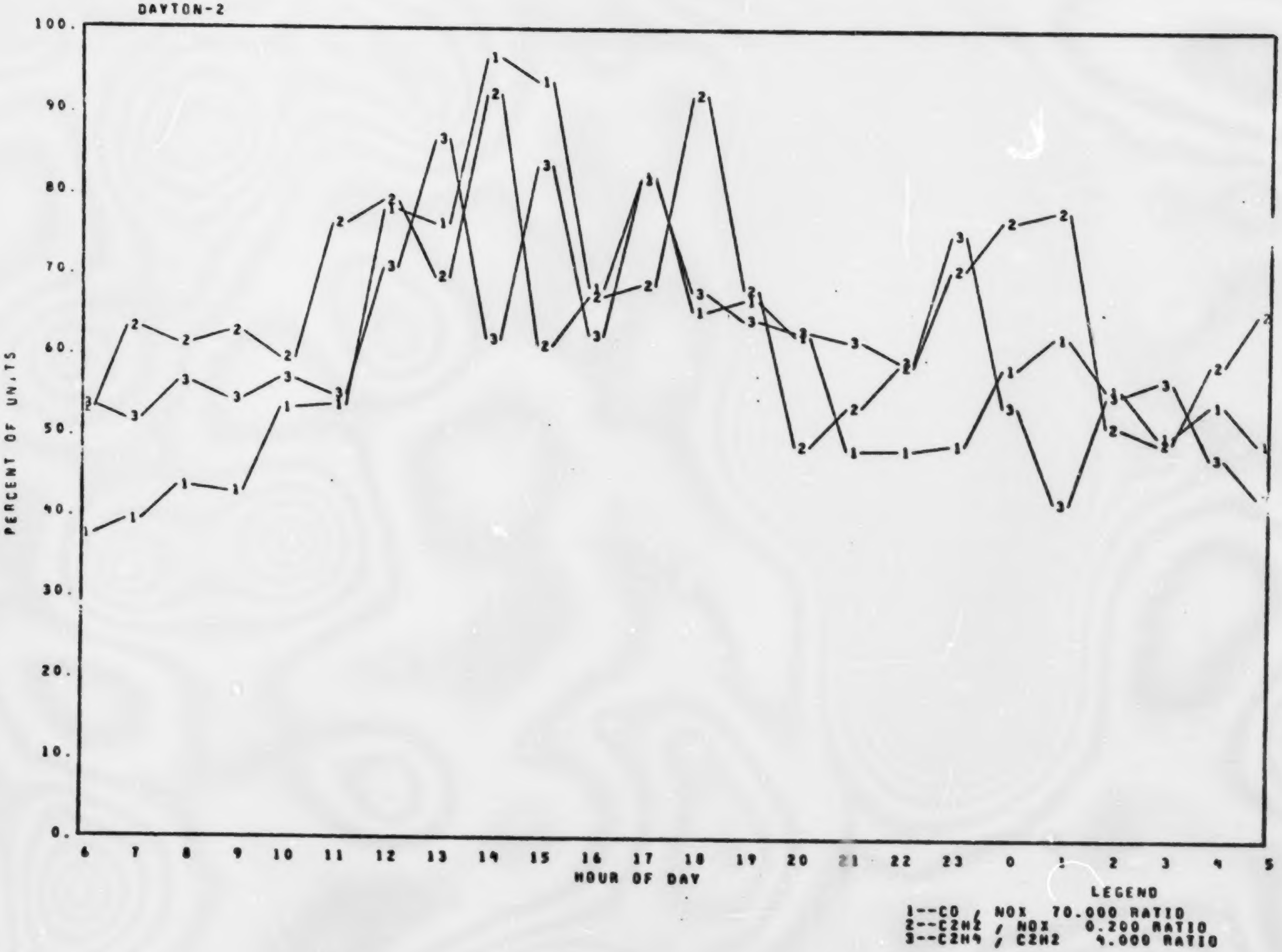

FIGURE 10 F. SITE 2 COMPOSITE PROFILES

TABLE 8. SUMMARY OF AIR QUALITY DATA - DAYTON SITE NO. 3

		Pollutants									
		24-Hour Average, ppm					1-Hour Max., ppm				
Date	Day	O_3	NO	NO_2	SO_2	HNO_3	O_3	NO	NO_x	SO_2	HNO_3
7-17	W	0.056	0.009	0.027	0.005	--	0.116	0.052	0.080	0.017	--
7-18	Th	0.069	0.004	0.024	0.013	0.006	0.117	0.030	0.064	0.037	0.015
7-19	F	0.033	0.006	0.022	0.002	0.002	0.074	0.021	0.043	0.007	0.005
7-20	Sat.	0.052	0.000	0.001	0.003	--	0.090	0.004	0.016	0.009	--
7-21	Sun.	0.053	0.003	0.008	0.006	--	0.090	0.037	0.067	0.017	--
7-22	M	0.066	0.004	0.019	0.014	--	0.108	0.018	0.047	0.050	--
7-23	T	0.039	0.006	0.017	0.000	0.000	0.071	0.031	0.061	0.002	0.000
7-24	W	0.049	0.000	0.002	0.000	0.000	0.077	0.006	0.008	0.002	0.000
7-25	Th	0.053	0.003	0.014	0.007	0.002	0.106	0.027	0.040	0.020	0.005
7-26	F	0.054	0.004	0.020	0.007	0.002	0.126	0.016	0.041	0.031	0.006
7-27	Sat.	0.050	0.004	0.021	0.004	--	0.121	0.018	0.062	0.010	--
7-28	Sun.	0.036	0.007	0.026	0.005	--	0.086	0.034	0.061	0.016	--
7-29	M	0.037	0.006	0.021	0.005	0.000	0.089	0.027	0.061	0.021	0.000
7-30	T	0.017	0.010	0.020	0.002	0.000	0.047	0.034	0.060	0.013	0.000
7-31	W	0.024	0.012	0.026	0.003	0.000	0.057	0.054	0.080	0.017	0.000
8-1	Th	0.060	0.005	0.019	0.008	0.006	0.134	0.016	0.037	0.029	0.020
8-2	F	0.050	0.006	0.027	0.015	0.010	0.118	0.017	0.050	0.066	0.045
8-3	Sat.	0.034	0.007	0.022	0.002	--	0.065	0.022	0.040	0.010	--
8-4	Sun.	0.021	0.004	0.012	0.002	--	0.046	0.021	0.033	0.010	--
8-5	M	0.025	0.007	0.013	0.004	0.000	0.042	0.036	0.040	0.015	0.000
8-6	T	0.058	0.001	0.006	0.008	0.003	0.116	0.018	0.039	0.032	0.010
8-7	W	0.046	0.004	0.017	0.008	0.000	0.091	0.014	0.043	0.036	0.000
8-8	Th	0.038	0.005	0.017	0.008	0.000	0.083	0.017	0.036	0.015	0.000
8-9	F	0.045	0.005	0.014	0.002	0.000	0.095	0.041	0.056	0.009	0.000
8-10	Sat.	0.058	0.001	0.010	0.007	0.000	0.089	0.005	0.021	0.054	0.000
8-11	Sun.	0.025	0.008	0.019	0.003	0.002	0.050	0.022	0.039	0.035	0.005
8-12	M	0.028	0.011	0.027	0.003	0.002	0.063	0.026	0.056	0.007	0.008

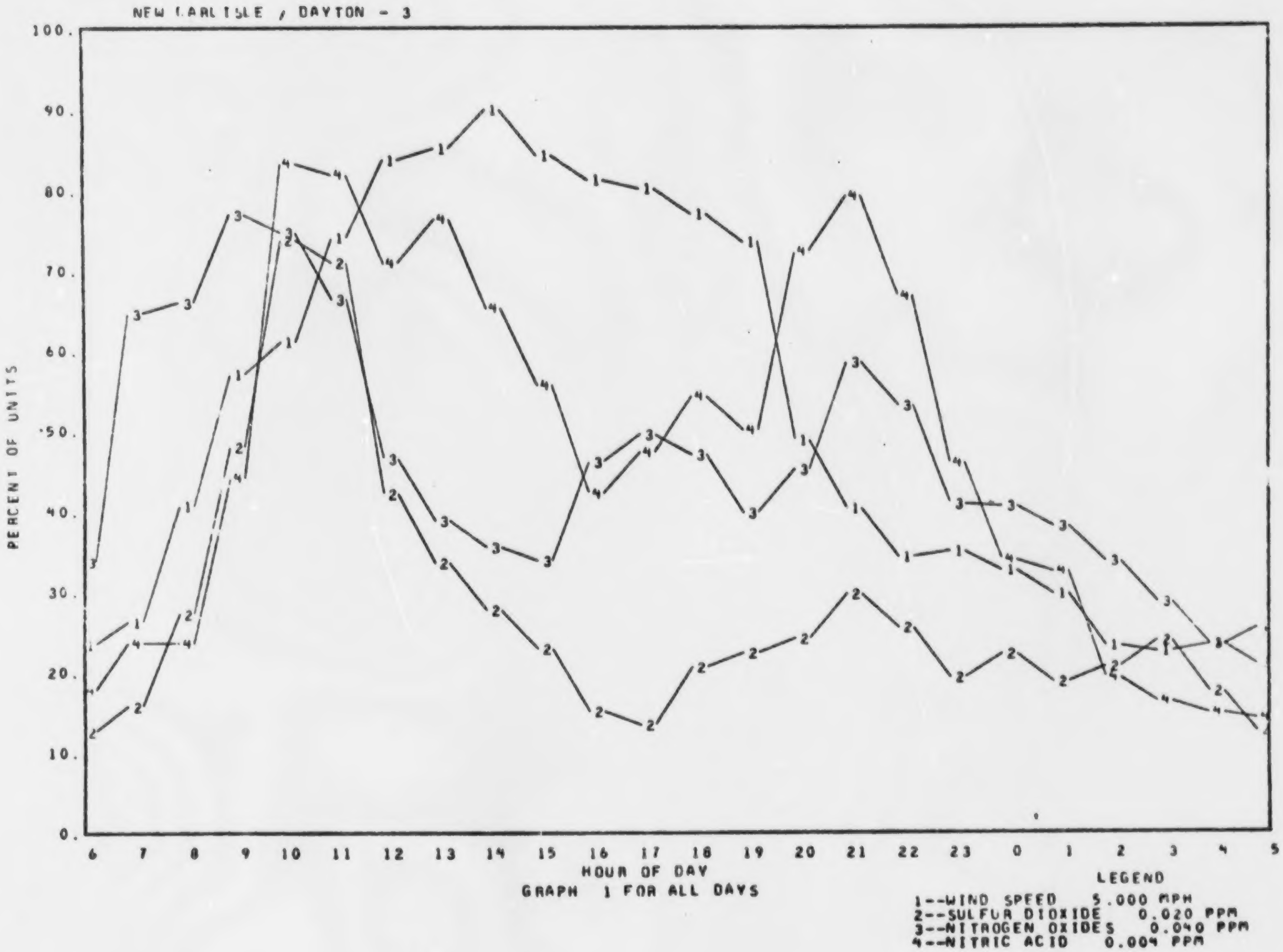

FIGURE 11 A. SITE 3 COMPOSITE PROFILES

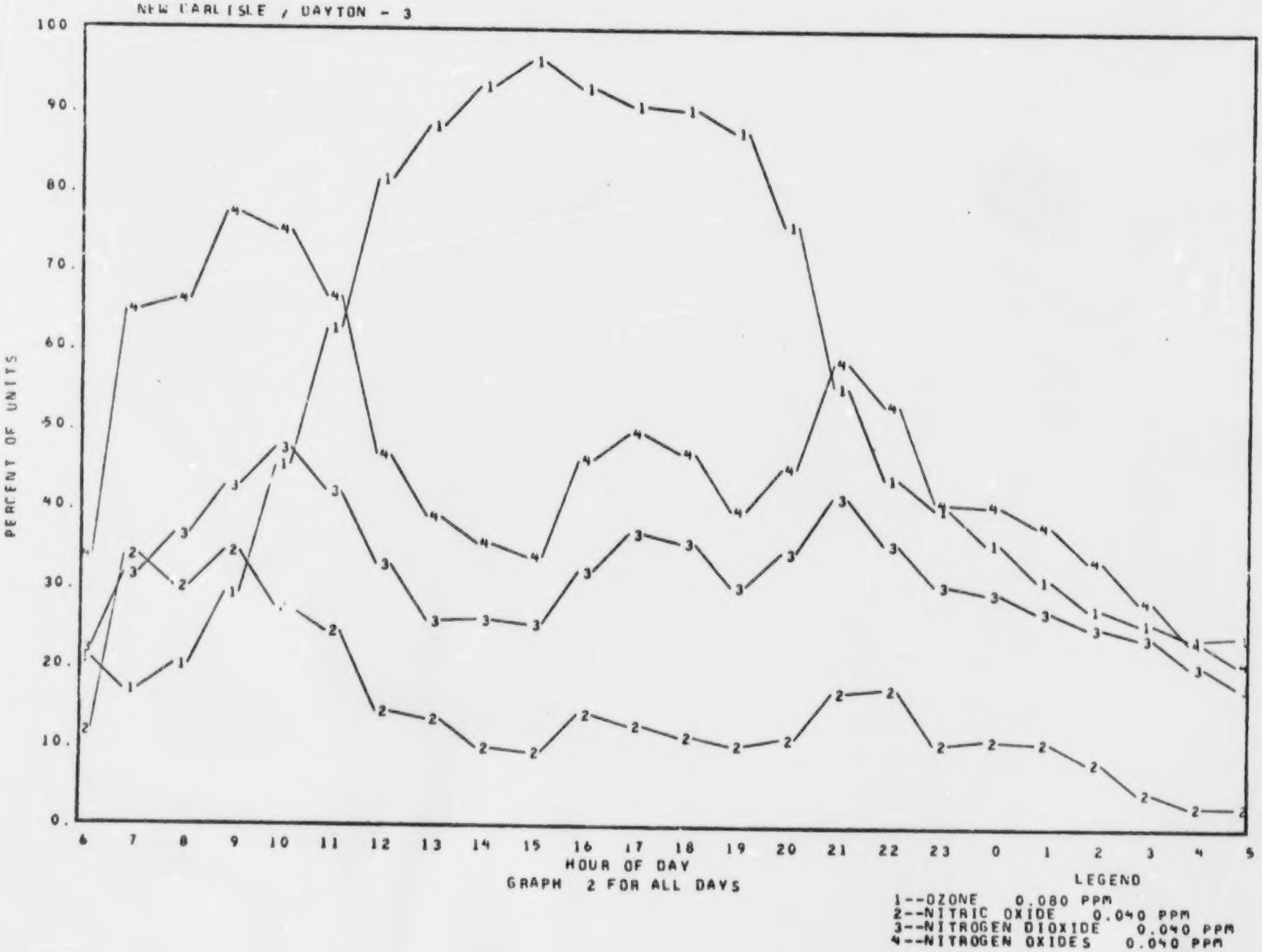

FIGURE 11 B. SITE 3 COMPOSITE PROFILES

TABLE 9 A. OZONE (PPM)

MIAMISBURG, OHIO

DATE	HOUR +	6 18	7 19	8 20	9 21	10 22	11 23	12 0	13 1	14 2	15 3	16 4	17 5	DAILY AVERAGE
JULY 17	(6-17)	0.000	0.000	0.000	0.008	0.024	0.032	0.024	-0.051	0.077	0.073	0.076	0.079	
JULY 17	(18-5)	0.079	0.068	0.076	0.039	0.000	0.000	0.000	0.008	0.000	0.003	0.000	0.003	0.029
JULY 18	(6-17)	0.003	0.005	0.000	0.003	0.010	0.034	0.068	0.079	0.076	0.081	0.079	0.079	
JULY 18	(18-5)	0.073	0.081	0.079	0.063	0.059	0.059	0.039	0.024	0.032	0.034	0.019	0.015	0.046
JULY 19	(6-17)	0.019	0.013	0.013	0.022	0.015	0.019	0.029	0.039	0.049	0.056	0.054	0.051	
JULY 19	(18-5)	0.046	0.044	0.034	0.041	0.032	0.024	0.013	0.005	0.005	0.000	0.000	0.000	0.026
JULY 20	(6-17)	0.000	0.000	0.000	0.019	0.032	0.044	0.054	0.063	0.079	0.083	0.081	0.063	
JULY 20	(18-5)	0.063	0.059	0.049	0.034	0.029	0.034	0.019	0.017	0.005	0.000	0.000	0.003	0.035
JULY 21	(6-17)	0.005	0.008	0.008	0.013	-0.018	0.024	0.046	0.056	0.066	0.073	0.081	0.081	
JULY 21	(18-5)	0.079	0.076	0.066	0.024	0.000	0.000	0.000	0.000	0.000	0.000	0.000	0.000	0.031
JULY 22	(6-17)	0.000	0.000	0.000	0.000	0.003	0.039	0.059	0.079	0.081	0.085	0.093	0.093	
JULY 22	(18-5)	0.081	0.066	0.056	0.029	0.005	0.003	0.005	0.005	0.000	0.003	0.008	0.005	0.033
JULY 23	(6-17)	0.019	0.019	0.024	0.022	0.037	0.032	0.039	0.041	0.046	0.034	0.044	0.049	
JULY 23	(18-5)	0.051	0.054	0.051	0.046	0.037	0.032	0.024	0.024	0.019	0.015	0.019	0.024	0.034
JULY 24	(6-17)	0.022	0.010	0.008	0.010	-0.026	0.041	0.046	0.063	0.066	0.073	0.063	0.073	
JULY 24	(18-5)	0.071	0.068	0.063	0.044	0.003	0.000	0.000	0.000	0.000	0.000	0.000	0.000	0.032
JULY 25	(6-17)	0.000	0.000	0.000	0.003	-0.026	0.049	0.059	0.066	0.071	0.081	0.079	0.079	
JULY 25	(18-5)	0.073	0.071	0.066	0.037	0.005	0.000	0.000	0.000	0.000	0.003	0.003	0.003	0.032
JULY 26	(6-17)	0.005	0.003	0.003	0.003	0.005	0.034	0.059	0.071	0.083	0.093	0.098	0.110	
JULY 26	(18-5)	0.108	0.088	0.086	0.049	0.000	0.000	0.000	0.000	0.000	0.000	0.000	0.000	0.037
JULY 27	(6-17)	0.000	0.000	0.000	0.003	-0.009	0.015	0.076	0.091	0.095	0.093	0.088	0.088	
JULY 27	(18-5)	0.086	0.086	0.063	0.039	0.029	0.003	0.003	0.000	0.000	0.000	0.000	0.000	0.037
JULY 28	(6-17)	0.000	0.000	0.000	0.003	0.019	0.041	0.056	0.054	0.051	0.056	0.059	0.059	
JULY 28	(18-5)	0.059	0.059	0.056	0.039	0.024	0.017	0.003	0.000	0.000	0.000	0.000	0.000	0.027
JULY 29	(6-17)	0.000	0.000	0.000	0.005	0.016	0.029	0.037	0.039	0.043	0.045	0.045	0.041	
JULY 29	(18-5)	0.047	0.067	0.055	0.047	0.013	0.011	0.015	0.019	0.008	0.000	0.000	0.000	0.024
JULY 30	(6-17)	0.000	0.000	0.000	0.010	0.019	0.029	0.032	0.039	0.046	0.049	0.046	0.046	
JULY 30	(18-5)	0.044	0.046	0.046	0.034	0.003	0.000	0.003	0.000	0.000	0.000	0.000	0.000	0.021
JULY 31	(6-17)	0.000	0.000	0.000	0.005	-0.020	0.034	0.044	0.049	0.054	0.054	0.054	0.056	
JULY 31	(18-5)	0.059	0.063	0.063	0.066	0.010	0.000	0.000	0.000	0.000	0.000	0.000	0.000	0.027

TABLE 9 B. OZONE (PPM)

MIAMISBURG, OHIO

DATE	HOUR →	6 18	7 19	8 20	9 21	10 22	11 23	12 0	13 1	14 2	15 3	16 4	17 5	DAILY AVERAGE
AUGUST 1	(6-17)	0.000	0.000	0.000	0.003	0.005	0.022	0.049	0.061	0.066	0.066	0.068	0.073	
AUGUST 1	(18-5)	0.088	0.127	0.108	0.073	0.054	0.051	0.049	0.049	0.044	0.044	0.034	0.027	0.048
AUGUST 2	(6-17)	0.027	0.010	0.008	0.019	0.010	0.019	0.032	0.041	0.054	0.079	0.079	0.063	
AUGUST 2	(18-5)	0.079	0.059	0.044	0.034	0.019	0.019	0.019	0.029	0.029	0.029	0.034	0.027	0.037
AUGUST 3	(6-17)	0.029	0.024	0.024	0.019	0.019	0.022	0.024	0.034	0.044	0.044	0.051	0.044	
AUGUST 3	(18-5)	0.044	0.041	0.034	0.019	0.027	0.024	0.019	0.015	0.015	0.017	0.010	0.008	0.027
AUGUST 4	(6-17)	0.038	0.005	0.015	0.015	0.019	0.029	0.029	0.029	0.029	0.029	0.032	0.034	
AUGUST 4	(18-5)	0.032	0.032	0.032	0.029	0.017	0.010	0.010	0.003	0.005	0.005	0.005	0.005	0.019
AUGUST 5	(6-17)	0.005	0.003	0.003	0.005	0.013	-0.022	0.032	0.037	0.039	0.041	0.041	0.039	
AUGUST 5	(18-5)	0.044	0.049	0.044	0.010	0.000	0.000	0.000	0.000	0.000	0.000	0.000	0.000	0.018
AUGUST 6	(6-17)	0.000	0.000	0.000	0.010	0.029	0.041	0.049	0.059	0.061	0.066	0.063	0.063	
AUGUST 6	(18-5)	0.066	0.063	0.061	0.039	0.034	0.024	0.015	0.005	0.005	0.005	0.005	0.003	0.033
AUGUST 7	(6-17)	0.003	0.000	0.000	0.003	-0.010	0.017	0.044	0.059	0.061	0.066	0.063	0.063	
AUGUST 7	(18-5)	0.063	0.049	0.029	0.024	0.034	0.019	0.008	0.005	0.000	0.010	0.017	0.015	0.028
AUGUST 8	(6-17)	0.005	0.000	0.008	0.015	0.010	0.015	0.017	0.029	0.034	0.049	0.049	0.063	
AUGUST 8	(18-5)	0.054	0.054	0.049	0.034	0.024	0.015	0.003	0.000	0.000	0.003	0.000	0.000	0.022
AUGUST 9	(6-17)	0.000	0.000	0.000	0.003	0.013	0.044	0.059	0.076	0.088	0.103	0.110	0.112	
AUGUST 9	(18-5)	0.108	0.103	0.071	0.056	0.056	0.039	0.010	0.008	0.010	0.003	0.005	0.005	0.045
AUGUST 10	(6-17)	0.003	0.000	0.000	0.010	0.015	0.024	0.032	0.037	0.039	0.046	0.041	0.041	
AUGUST 10	(18-5)	0.044	0.046	0.034	0.029	0.019	0.013	0.015	0.019	0.024	0.029	0.029	0.027	0.025
AUGUST 11	(6-17)	0.024	0.015	0.015	0.015	0.010	0.010	0.005	0.032	0.010	0.015	0.015	0.015	
AUGUST 11	(18-5)	0.015	0.017	0.017	0.015	0.010	0.013	0.010	0.008	0.005	0.003	0.000	0.003	0.012
AUGUST 12	(6-17)	0.005	0.005	0.008	0.013	0.015	0.022	0.029	0.034	0.041	0.044	0.044	0.041	
AUGUST 12	(18-5)	0.046	0.044	0.024	0.005	0.000	0.000	0.000	-1.000	-1.000	-1.000	-1.000	-1.000	0.022
20-DAY	(6-17)	0.007	0.004	0.004	0.009	0.015	0.029	0.039	0.050	0.055	0.061	0.061	0.063	
AVERAGES	(18-5)	0.063	0.063	0.055	0.039	0.021	0.016	0.011	0.011	0.010	0.009	0.009	0.008	0.030

TABLE 10 A. OZONE (PPM)

TIMBER LANE - DAYTON, OHIO

DATE	HOUR	6	7	8	9	10	11	12	13	14	15	16	17	DAILY AVERAGE
		18	19	20	21	22	23	0	1	2	3	4	5	
JULY 17	(6-17)	0.000	0.000	0.000	0.005	0.017	0.034	0.056	0.066	0.071	0.066	0.068	0.071	
JULY 17	(18-5)	0.063	0.061	0.049	0.039	0.015	0.000	0.000	0.003	0.003	0.005	0.000	0.000	0.029
JULY 18	(6-17)	0.000	0.000	0.000	0.005	0.032	0.044	0.063	0.068	0.068	0.058	0.071	0.066	
JULY 18	(18-5)	0.061	0.061	0.063	0.059	0.046	0.044	0.049	0.049	0.046	0.046	0.039	0.039	0.045
JULY 19	(6-17)	0.034	0.027	0.015	0.017	0.022	0.024	0.032	0.037	0.049	0.054	0.049	0.046	
JULY 19	(18-5)	0.049	0.046	0.034	0.013	0.041	0.039	0.019	0.005	0.005	0.003	0.003	0.000	0.028
JULY 20	(6-17)	0.000	0.000	0.013	-0.014	0.015	0.019	0.032	0.044	0.054	0.054	0.046	0.045	
JULY 20	(18-5)	0.044	0.039	0.037	0.029	0.024	0.022	0.015	0.008	0.000	0.008	0.010	0.005	0.025
JULY 21	(6-17)	0.003	0.003	0.003	-0.011	0.019	0.029	0.039	0.046	0.049	0.049	0.049	0.051	
JULY 21	(18-5)	0.051	0.049	0.034	0.010	0.000	0.000	0.000	0.000	0.000	0.000	0.000	0.000	0.021
JULY 22	(6-17)	0.000	0.000	0.000	0.003	0.005	0.017	0.044	0.054	0.059	0.059	0.068	0.073	
JULY 22	(18-5)	0.066	0.056	0.049	0.039	0.024	0.005	0.000	0.000	0.000	0.000	0.000	0.000	0.026
JULY 23	(6-17)	0.010	0.019	0.024	0.005	0.008	0.019	0.022	0.024	0.024	0.024	0.037	0.041	
JULY 23	(18-5)	0.041	0.037	0.032	0.027	0.024	0.017	0.015	0.010	0.015	0.017	0.019	0.019	0.022
JULY 24	(6-17)	0.013	0.005	0.005	0.019	0.027	0.034	0.037	0.041	0.044	0.051	0.041	0.041	
JULY 24	(18-5)	0.044	0.041	0.044	0.039	0.000	0.000	0.000	0.000	0.000	0.000	0.000	0.000	0.022
JULY 25	(6-17)	0.000	0.000	0.000	0.005	0.015	0.039	0.051	0.054	0.056	0.056	0.056	0.051	
JULY 25	(18-5)	0.051	0.049	0.037	0.044	0.003	0.000	0.000	0.000	0.000	0.000	0.000	0.000	0.024
JULY 26	(6-17)	0.003	0.000	-1.000	-1.000	-1.000	-1.000	-1.000	-1.000	-1.000	-1.000	-1.000	-1.000	
JULY 26	(18-5)	-1.000	-1.000	-1.000	-1.000	-1.000	-1.000	-1.000	-1.000	-1.000	-1.000	-1.000	-1.000	0.001
JULY 27	(6-17)	-1.000	-1.000	-1.000	-1.000	-1.000	-1.000	-1.000	-1.000	-1.000	-1.000	-1.000	-1.000	
JULY 27	(18-5)	-1.000	-1.000	-1.000	-1.000	-1.000	-1.000	-1.000	-1.000	-1.000	-1.000	-1.000	-1.000	I
JULY 28	(6-17)	-1.000	-1.000	-1.000	-1.000	-1.000	-1.000	-1.000	-1.000	-1.000	-1.000	-1.000	-1.000	
JULY 28	(18-5)	-1.000	-1.000	-1.000	-1.000	-1.000	-1.000	-1.000	-1.000	-1.000	-1.000	-1.000	-1.000	I
JULY 29	(6-17)	-1.000	-1.000	-1.000	-1.000	-1.000	-1.000	-1.000	-1.000	-1.000	-1.000	-1.000	-1.000	
JULY 29	(18-5)	-1.000	0.085	0.077	0.085	0.045	0.035	0.031	0.017	0.013	0.017	0.019	0.010	0.040
JULY 30	(6-17)	0.008	0.005	0.003	0.008	0.022	0.041	0.056	0.063	0.068	0.076	0.076	.071	
JULY 30	(18-5)	0.066	0.063	0.063	0.046	0.013	0.003	0.000	0.000	0.000	0.000	0.000	0.000	0.031
JULY 31	(6-17)	0.000	0.000	0.005	0.027	0.051	0.066	0.081	-0.083	-0.084	0.086	0.086	0.088	
JULY 31	(18-5)	0.093	0.095	0.083	0.059	0.015	0.000	0.000	0.000	0.000	0.000	0.000	0.000	0.038

Reproduced from best available copy.

TABLE 10 B. OZONE (PPM)

TIMBER LANE - DAYTON, OHIO

DATE	HOUR →	6 18	7 19	8 20	9 21	10 22	11 23	12 0	13 1	14 2	15 3	16 4	17 5	DAILY AVERAGE
AUGUST 1	(6-17)	0.000	0.000	0.003	0.003	0.019	0.061	0.095	0.098	0.095	0.100	0.105	0.105	
AUGUST 1	(18-5)	0.123	0.137	0.176	0.130	0.076	0.066	0.046	0.061	0.066	0.056	0.071	0.056	0.073
AUGUST 2	(6-17)	0.066	0.005	0.003	0.017	0.032	0.049	0.063	0.105	0.127	0.132	0.137	0.132	
AUGUST 2	(18-5)	0.127	0.098	0.063	0.049	0.010	0.003	0.015	0.032	0.044	0.034	0.029	0.049	0.059
AUGUST 3	(6-17)	0.032	0.046	0.029	0.041	0.034	0.044	0.049	0.063	0.076	0.083	0.091	0.079	
AUGUST 3	(18-5)	0.071	0.046	0.044	0.019	0.039	0.039	0.027	0.015	0.029	0.037	0.032	0.022	0.045
AUGUST 4	(6-17)	0.015	0.024	0.024	0.029	0.039	0.049	0.056	0.051	0.046	0.051	0.051	0.054	
AUGUST 4	(18-5)	0.054	0.054	0.051	0.041	0.015	0.013	0.008	0.008	0.010	0.013	0.013	0.010	0.033
AUGUST 5	(6-17)	0.038	0.000	0.003	0.008	0.024	0.041	0.056	0.061	0.065	0.066	-0.073	0.073	
AUGUST 5	(18-5)	0.081	0.081	0.068	0.034	0.000	0.000	0.000	0.010	0.027	0.010	0.003	0.003	0.031
AUGUST 6	(6-17)	0.000	0.000	0.000	0.003	0.034	0.066	0.073	0.083	0.093	0.100	0.112	0.103	
AUGUST 6	(18-5)	0.103	0.103	0.073	0.024	0.015	0.008	0.003	0.000	0.000	0.000	0.000	0.000	0.042
AUGUST 7	(6-17)	0.000	0.000	0.000	0.008	0.019	0.044	0.091	0.100	0.103	0.108	0.110	0.108	
AUGUST 7	(18-5)	0.098	0.086	0.029	0.019	0.039	0.032	0.010	0.008	0.005	0.003	0.008	0.003	0.043
AUGUST 8	(6-17)	0.005	0.003	0.003	0.005	0.015	0.024	0.049	0.071	0.103	0.100	0.083	0.088	
AUGUST 8	(18-5)	0.079	0.071	0.068	0.034	0.005	0.003	0.000	0.000	0.000	0.000	0.000	0.000	0.034
AUGUST 9	(6-17)	0.000	0.000	0.000	0.010	0.017	0.049	0.083	0.105	0.103	0.123	0.125	0.130	
AUGUST 9	(18-5)	0.132	0.088	0.093	0.059	0.059	0.034	0.038	0.013	0.015	0.010	0.010	0.003	0.053
AUGUST 10	(6-17)	0.033	0.003	0.003	0.013	0.019	0.034	0.059	0.075	0.081	0.053	0.083	0.063	
AUGUST 10	(18-5)	0.079	0.079	0.079	0.061	0.029	0.044	0.034	0.051	0.063	0.053	0.063	0.059	0.052
AUGUST 11	(6-17)	0.054	0.041	0.032	0.034	0.024	0.010	0.019	0.029	0.034	0.039	0.044	0.049	
AUGUST 11	(18-5)	0.049	0.046	0.037	0.015	0.015	0.010	0.038	0.033	0.005	0.010	0.008	0.017	0.025
AUGUST 12	(6-17)	0.027	0.029	0.019	0.024	0.037	0.049	0.066	0.071	0.073	0.079	0.081	0.095	
AUGUST 12	(18-5)	0.095	0.093	0.073	0.029	0.003	0.000	0.000	-1.000	-1.000	-1.000	-1.000	-1.000	0.050
20-DAY	(6-17)	0.012	0.007	0.006	0.012	0.024	0.041	0.059	0.068	0.074	0.079	0.081	0.080	
AVERAGES	(18-5)	0.080	0.075	0.066	0.046	0.024	0.018	0.012	0.014	0.017	0.016	0.015	0.014	0.039

TABLE 11 A. OZONE (PPM)

WAYNE TOWNSHIP - HUBER HEIGHTS, OHIO

DATE	HOUR	6 18	7 19	8 20	9 21	10 22	11 23	12 0	13 1	14 2	15 3	16 4	17 5	DAILY AVERAGE
JULY 17	(6-17)	0.015	0.005	-0.007	0.010	0.020	0.045	0.060	0.080	0.090	0.095	0.085	0.090	
JULY 17	(18-5)	-0.063	-0.077	0.070	0.060	0.040	0.005	0.005	0.015	0.015	0.015	0.015	0.020	0.043
JULY 18	(6-17)	0.015	0.000	0.005	0.005	0.030	0.070	0.090	0.100	0.100	0.095	0.100	0.100	
JULY 18	(18-5)	0.095	0.090	0.090	0.090	0.075	0.070	0.070	0.070	0.070	0.060	0.055	0.055	0.067
JULY 19	(6-17)	0.045	0.040	0.020	0.015	0.030	0.040	0.040	0.050	0.065	0.075	0.070	0.075	
JULY 19	(18-5)	0.070	0.065	0.055	0.020	0.040	0.065	0.050	0.030	0.005	0.000	0.000	0.000	0.040
JULY 20	(6-17)	0.030	0.000	0.025	0.020	0.020	0.025	0.040	0.055	0.065	0.055	0.070	0.070	
JULY 20	(18-5)	0.055	0.050	0.045	0.040	0.035	0.035	0.030	0.025	0.010	0.015	0.015	0.005	0.034
JULY 21	(6-17)	0.005	0.005	0.010	0.025	0.030	0.040	0.050	0.055	0.060	0.060	0.060	0.065	
JULY 21	(18-5)	0.065	0.065	0.060	0.035	0.030	0.030	0.020	0.005	0.015	0.025	0.010	0.010	0.032
JULY 22	(6-17)	0.010	0.005	0.000	0.005	0.030	0.030	0.055	0.065	0.075	0.055	0.080	0.090	
JULY 22	(18-5)	0.085	0.085	0.065	0.055	0.050	0.005	0.020	0.020	0.020	0.020	0.020	0.025	0.042
JULY 23	(6-17)	0.005	0.000	0.000	0.005	0.015	0.015	0.020	0.035	0.030	0.050	0.040	0.050	
JULY 23	(18-5)	0.055	0.055	0.050	0.040	0.035	0.030	0.025	0.015	0.015	0.015	0.015	0.020	0.025
JULY 24	(6-17)	0.015	0.005	0.005	0.015	0.040	0.040	0.045	0.050	0.060	0.060	0.055	0.067	
JULY 24	(18-5)	0.065	0.070	0.070	0.040	0.030	0.015	0.025	0.020	0.020	0.005	0.005	0.025	0.033
JULY 25	(6-17)	0.005	0.005	0.000	0.005	0.035	0.030	0.010	0.050	0.085	[illegible]	0.050	0.050	
JULY 25	(18-5)	0.100	0.085	0.085	0.075	0.050	0.045	0.040	0.050	0.035	0.030	0.025	0.030	0.032
JULY 26	(6-17)	0.010	0.017	0.005	0.010	0.015	0.040	0.075	0.090	0.105	0.110	0.115	0.120	
JULY 26	(18-5)	0.115	0.115	0.110	0.085	0.025	0.035	0.010	0.015	0.020	0.030	0.015	0.015	0.052
JULY 27	(6-17)	0.005	0.000	0.000	-0.020	0.040	0.020	0.110	0.125	0.130	0.120	0.110	0.105	
JULY 27	(18-5)	0.105	0.105	0.095	0.085	0.065	0.060	0.060	0.060	0.020	0.030	0.050	0.050	0.067
JULY 28	(6-17)	0.045	0.055	0.055	0.025	-0.050	0.075	0.095	0.100	0.095	0.095	0.100	0.100	
JULY 28	(18-5)	0.085	0.075	0.070	0.045	0.015	0.025	0.035	0.000	0.005	0.000	0.000	0.000	0.053
JULY 29	(6-17)	0.000	0.000	0.000	0.020	0.050	0.065	0.075	0.085	0.085	0.090	0.065	0.060	
JULY 29	(18-5)	0.075	0.070	0.065	0.065	0.040	0.030	0.030	0.020	0.010	0.000	0.000	0.000	0.042
JULY 30	(6-17)	0.000	0.000	0.000	0.000	0.010	0.030	0.040	0.050	0.055	0.060	0.060	0.055	
JULY 30	(18-5)	0.050	0.050	0.050	0.040	0.015	0.010	0.010	0.005	0.000	0.000	0.000	0.000	0.025
JULY 31	(6-17)	0.000	0.000	0.000	0.005	0.020	0.045	0.060	0.060	0.065	0.055	0.065	0.070	
JULY 31	(18-5)	0.080	0.075	0.055	0.020	0.010	0.015	0.010	0.000	0.015	0.005	0.015	0.000	0.031

TABLE 11 B. OZONE (PPM)

WAYNE TOWNSHIP - HUBER HEIGHTS, OHIO

DATE	HOUR	6	7	8	9	10	11	12	13	14	15	16	17	DAILY AVERAGE
	-	18	19	20	21	22	23	0	1	2	3	4	5	
AUGUST 1	(6-17)	0.000	0.000	0.000	0.013	0.032	0.054	0.082	-0.081	-0.081	-0.080	-0.079	0.079	
AUGUST 1	(18-5)	0.079	0.088	0.105	0.083	0.054	0.049	0.034	0.039	0.044	0.046	0.044	0.039	0.043
AUGUST 2	(6-17)	0.037	0.015	0.013	0.013	0.027	0.039	0.056	0.073	0.093	0.098	0.110	0.108	
AUGUST 2	(18-5)	0.103	0.079	0.049	0.039	0.027	0.022	0.022	0.027	0.034	0.032	0.029	0.032	0.049
AUGUST 3	(6-17)	0.032	0.039	0.034	0.029	0.024	0.032	0.039	0.049	0.059	0.053	0.068	0.063	
AUGUST 3	(18-5)	0.046	0.024	0.029	0.029	0.032	0.039	0.029	0.015	0.019	0.024	0.013	0.010	0.036
AUGUST 4	(6-17)	0.005	0.013	0.015	0.019	0.027	0.037	0.039	0.041	0.034	0.037	0.037	0.039	
AUGUST 4	(18-5)	0.039	0.039	0.034	0.032	0.010	0.000	0.005	0.000	0.005	0.006	0.003	0.005	0.022
AUGUST 5	(6-17)	0.033	0.000	0.000	0.000	0.015	0.029	0.037	0.044	0.044	0.046	0.049	0.054	
AUGUST 5	(18-5)	0.054	0.056	0.046	0.015	0.000	0.015	0.024	0.037	0.039	0.039	0.034	0.034	0.031
AUGUST 6	(6-17)	0.019	0.017	0.008	0.019	0.034	0.044	0.061	0.059	0.068	0.061	0.083	0.083	
AUGUST 6	(18-5)	0.091	0.088	0.071	0.051	0.029	0.037	0.019	0.019	0.029	0.029	0.015	0.015	0.045
AUGUST 7	(6-17)	0.015	0.010	-0.009	0.008	0.010	0.028	0.043	0.063	0.066	0.071	0.066	0.061	
AUGUST 7	(18-5)	0.076	0.061	0.049	0.046	0.039	0.032	0.039	0.039	0.027	0.010	0.024	0.022	0.041
AUGUST 8	(6-17)	0.022	0.013	0.005	0.013	0.022	0.022	0.032	0.046	0.054	0.063	0.073	0.073	
AUGUST 8	(18-5)	0.059	0.059	0.061	0.034	0.005	0.013	0.019	0.015	0.010	0.003	0.000	0.000	0.033
AUGUST 9	(6-17)	0.000	0.000	0.000	0.003	0.013	0.037	0.059	0.068	0.076	0.076	0.079	0.081	
AUGUST 9	(18-5)	0.083	0.068	0.063	0.061	0.046	0.039	0.024	0.019	0.022	0.019	0.010	0.010	0.040
AUGUST 10	(6-17)	0.008	0.003	0.005	0.008	0.015	0.032	0.041	0.049	0.056	0.053	0.063	0.059	
AUGUST 10	(18-5)	0.051	0.056	0.049	0.044	0.049	0.029	0.051	0.049	0.049	0.054	0.051	0.046	0.041
AUGUST 11	(6-17)	0.039	0.037	0.029	0.029	0.024	0.019	0.024	0.024	0.024	0.034	0.034	0.039	
AUGUST 11	(18-5)	0.037	0.034	0.034	0.024	0.019	0.015	0.019	0.015	0.015	0.010	0.010	0.013	0.025
AUGUST 12	(6-17)	0.017	0.019	-0.019	0.019	-0.026	-0.032	-0.038	-0.044	-0.050	0.056	0.051	0.059	
AUGUST 12	(18-5)	0.066	0.068	0.063	0.049	0.024	0.019	0.000	-1.000	-1.000	-1.000	-1.000	-1.000	0.040
20-DAY	(6-17)	0.013	0.009	0.006	0.011	0.024	0.040	0.054	0.062	0.068	0.071	0.072	0.074	
AVERAGES	(18-5)	0.073	0.070	0.065	0.049	0.031	0.028	0.026	0.026	0.025	0.021	0.019	0.018	0.040

Reproduced from best available copy.

TABLE 12. AVERAGE OF 3-HOUR INTEGRATED DATA

	Downtown Dayton (Site 1)			Huber Heights (Site 2)			New Carlisle (Site 3)		
	6-9	9-12	12-3	6-9	9-12	12-3	6-9	9-12	12-3
Ethylene, ppmC	0.037	0.017	0.014	0.012	0.008	0.005	0.020	0.022	0.037
Ethane, ppmC	0.016	0.010	0.007	0.011	0.007	0.003	0.007	0.011	0.008
Acetylene, ppmC	0.036	0.022	0.014	0.006	0.003	0.002	0.017	0.016	0.019
PAN, ppm	0.005	0.002	0.002	0.000	0.001	0.001	0.001	0.001	0.001
CO, ppm	3.12	2.20	1.75	1.36	0.92	0.63	1.54	1.48	1.68
Methane, ppmC	1.98	1.70	1.55	1.70	1.65	1.64	1.78	1.65	1.58
Non-Methane Hydrocarbon, ppmC	1.76	0.90	0.92	0.60	0.44	0.29	0.67	0.78	0.72

All aerosol collections during the Dayton study were taken at the Huber Heights station (Site No. 2). The daily concentrations of NO_3^-, $SO_4^=$, NH_4^+, CHN, and mass loading are listed in Table 13. The values in parentheses in the table are analyses of a second filter collected on the same day, and indicate the precision of the overall collection and analysis procedure.

The average composition of aerosols greater than 2.5 μm in diameter is shown in Table 14. These "dustfall" collections were made throughout the 20-day sampling period. The results are presented as percent by weight.

Several pertinent meteorological variables which are summarized on a daily basis by the Wright-Patterson Air Force Base weather station are presented in Table 15. The Air Stagnation Index shown in the table is keyed to afternoon ventilation, which in turn is the product of mixing height times transport wind.

TABLE 13. DAYTON AEROSOL DATA

			($\mu g/m^3$)						
Date	Filter	Stack	NO_3^-	$SO_4^=$	NH_4^+	H	N	C	Mass Loading
7-17	2D	2	0.48	13.4	2.8	2.0	3.2	13.4	79.1
7-18	3D	1	0.26	32.3	6.5	3.8	6.2	16.4	136.8
7-18	4D	2	0.30	33.8 (33.5)	6.7	4.1	6.4	17.0	134.7
7-19	6D	2	0.28	22.9	3.5	2.5	3.6	13.9	74.9
7-23	8D	2	0.19	31.0 (34.0)	8.8	2.8	7.5	9.6	69.6
7-24	10D	2	0.29	18.3	5.4	1.7	4.4	9.1	57.8
7-25	12D	2	0.33	36.4	6.6	3.5	5.5	10.3	106.8
7-26	14D	2	0.28	57.1 (59.3)	8.5	4.8	7.2	11.3	141.4
7-29	16D	2	0.38	12.3	2.5	1.7	2.6	13.6	132.5
7-30	18D	2	0.54	4.4	0.7	0.8	1.1	11.5	117.6
7-31	20D	2	0.68	6.1	0.8	1.0	1.2	12.8	101.0
8- 1	22D	2	0.31	19.3	4.0	2.6	3.9	11.5	88.3
8- 2	24D	2	0.21	15.6	2.7	2.2	2.5	7.8	72.0
8- 2	25D	1	0.23	14.2	2.7	1.8	2.5	7.6	74.5
8- 5	26D	2	0.29	7.1	1.1	1.1	1.3	6.7	30.7
8- 6	28D	2	0.37	19.1	3.7	2.0	3.6	9.1	75.1
8- 7	31D	1	0.21	18.9	3.9	1.8	3.4	7.6	66.9
8- 8	33D	1	0.22	10.0	3.0	2.2	2.8	7.4	56.7
8- 9	35D	1	0.17	20.0	4.5	1.7	4.0	8.0	--
8-10	37D	1	0.19	30.8	4.8	3.1	3.8	6.1	77.3
8-12	42D	2	0.24	< 1.0	0.9	1.1	1.4	8.4	40.3

TABLE 14. LARGE PARTICLE (>2.5 μm) COMPOSITION

Component	Concentration, weight percent
NO_3^-	7.7
$SO_4^=$	8.0
NH_4^+	1.2
H	1.5
C	9.6
N	2.1

TABLE 15. DAYTON METEOROLOGICAL FACTORS

Date	Air Stagnation Index	Mixing Height, meters	Mean Wind Direction	Transport Wind, meters/Sec	Afternoon[(a)] Ventilation, meters^2/Sec	Inversion Spread, F	Surface Wind Direction	Surface Wind Speed
7-17-74	Poor	2000	100°	2	4,100	10	84°	1
7-18-74	Moderate	1700	250°	4.5	7,650	7	175°	3
7-19-74	Good	1200	325°	8.5	10,200	1	300°	5
7-22-74	Good	1400	165°	4	9,600	15	80°	3
7-23-74	Moderate	1200	240°	6	7,200	0	130°	3
7-24-74	Good	1800	45°	5	9,000	2	20°	5
7-25-74	Poor	1360	110°	3.5	4,460	7	70°	5
7-26-75	Poor	2000	165°	2.5	5,000	6	160°	7
7-29-74	Good	1700	255°	8	13,600	7	180°	3
7-30-74	Good	2500	250°	4	10,000	8	165°	3
7-31-74	Good	2600	265°	6.5	16,900	10	200°	6
8-1-74								
8-2-74	Good	1900	215°	7.5	14,250	9	180°	4
8-5-74	Good	2200	325°	8.5	18,700	6	290°	4
8-6-74	Moderate	1600	55°	4.5	7,200	8	74°	-
8-7-74	Poor	1400	170°	3.5	4,900	5	85°	5
8-8-74	Moderate	1400	210°	4.5	6,300	0	130°	3
8-9-74	Poor	1900	280°	3	5,700	6	220°	4
8-12-17	Good	1400	295°	7	9,800	1	270°	7

(a) Afternoon Ventilation Key

Less than 4000 - Poor
4000 to 6000 - Poor to Moderate
6000 to 8000 - Moderate to Good
Greater than 8000 - Good

DISCUSSION

A prodigious volume of data was collected during the course of the Dayton field study. On a broad scale, EPA will ultimately combine these data with the results of the other research groups studying oxidant transport in the Ohio Valley, to form a clearer picture of oxidant and precursor relationships and movement on a regional scale. In the remaining sections of this report it will be our task to describe and interpret our data from the Dayton area in terms of the generation and transport of ozone. There are obviously a great many ways to treat a data base of this kind, and a great many questions concerning both ozone transport and other aspects of atmospheric chemistry which might be answered through use of these data. However, it is our objective here to investigate primarily oxidant transport, so that other uses of the data collected in this study will have to await future data analysis investigations. Unfortunately, time constraints prohibit us from treating these data in as many ways and in as much detail as we would like. However, since the data will be analyzed again in conjunction with the entire Ohio Valley study, most of the important information will ultimately be extracted from the data.

Our discussion of the program results will commence with a general description of the entire data base along with a discussion of some descriptors of the data. We will then present a statistical analysis of the ozone data over the entire study period, followed by a discussion of the meteorology during the study period and its influence on ozone generation and transport. Finally, we will investigate in detail several of the individual days during the study in which transport conditions appear to be important.

Overview of the Dayton Field-Study Results

In this discussion of the Dayton results, we will first review the trends in the air-quality data at the three main ground stations, then describe the results of the aerosol collections from the Huber Heights

(No. 2) site, and finally consider the relationships exhibited by the gas-phase data from site to site. Obviously, the data presented here were collected over only a limited number of days during the summer of 1974. Any generalizations of our results to other seasons or other years must be regarded with some degree of skepticism.

Air-Quality Data

The air-quality data from our three main monitoring stations, downtown Dayton, Huber Heights, and New Carlisle, will be discussed in that order. Because of the large quantity of data involved, we will necessarily discuss only the averaged data in this section of the report. The usual *caveats* for dealing with average data apply to this discussion. With sufficient caution however, it is possible to derive an understanding of the general trends in the air quality by using composited data.

Downtown Dayton (Site No. 1). The average Site 1 air-quality data has been tabulated earlier in Table 5 and profiled in Figure 9. The average 3-hour integrated data were also presented in Table 12. The behavior of the Site 1 air-quality data appears to follow the generally accepted pattern of urban photochemical smog, with some minor exceptions. Referring to the average profiles in Figure 9, a large increase in NO is observed between 6-9 a.m., with a rapid decrease to a low concentration which is maintained during the later morning and afternoon hours. The C_2 hydrocarbons, non-methane hydrocarbons, and CO are also at their maximum during this 6-9 a.m. interval, as seen in Table 12. Nitrogen dioxide rises very slowly to a peak at 10 a.m. and then drops off to a fairly constant value throughout the remainder of the day. The C_2 hydrocarbons, CO, and NMHC generally decrease through the later morning and early afternoon hours. Interestingly, while the concentrations of C_2 hydrocarbons decrease during the day, the ratios of C_2H_4/C_2H_2 and C_2H_4/C_2H_6, which have been used in the past to indicate the extent of photochemical reaction of the air mass, remain relatively constant. This seems to indicate that our ground site was, on the average, monitoring either fresh hydrocarbon emissions or emissions of a relatively constant age. The ozone concentration begins to increase rapidly at approximately 8 a.m. as the NO drops and NO_2 rises slowly. Ozone reaches an initial peak, or more correctly a plateau, between 1-3 p.m., begins to drop off, and then rises sharply to its highest value at approximately 6 p.m. This second late afternoon peak is a most intriguing feature of these data. At this time of day the ultraviolet intensity of the sunlight reaching the lower atmosphere has dropped drastically from its midafternoon peak, so that the generation of significant quantities of ozone at this time of day is unlikely. One explanation for this late ozone peak is advection or transport from another location. This possibility will be discussed in detail later in this report.

The sulfur dioxide profile exhibits a sharp increase between 9-11 a.m. with the maximum occurring at about noon. Throughout the remainder of the day SO_2 gradually decreases. Nitric acid rises rapidly to a peak at about 11 a.m. and then fluctuates in a downward trend throughout the remainder of the day.

Huber Heights (Site No. 2). The trends in the average gas-phase data from Site 2 are similar to those discussed for Site 1. Referring to the profile in Figure 10, we note that NO peaks at 7 a.m. and then drops off to rather low afternoon values. Nitrogen dioxide reaches a morning peak at 8 a.m., about 1 hour after the NO maximum, and then also drops off to low midday levels. Both NO and NO_2 increase again late in the evening between 8-11 p.m. We have observed this phenomenon in several other urban areas(2,3) and believe that it is due to inhibited vertical mixing caused by the low-level nighttime inversion layer. This conclusion is supported by the meteorological data discussed later in this report. The C_2 hydrocarbons, NMHC and CO all exhibit profiles very similar to NO, with a morning peak due largely to rush-hour traffic occurring at approximately 8 a.m., and a secondary peak during the late evening hours due to trapping of the gaseous species below the inversion.

The ozone curve begins to rise rapidly between 8-9 a.m. as NO falls off. A broad ozone maximum is maintained between 1-6 p.m. at a level just slightly below the ozone standard of 0.08 ppm. After about 8 p.m. the ozone concentration falls rapidly as NO, which is continuously emitted into the atmosphere, reacts with the O_3 to produce NO_2. It is important to note that, while O_3 and NO are reacting with and destroying one another below the inversion layer, there are no strong sinks for O_3 above the inversion. Presumably this O_3 is diluted during the night and possibly advected to another area. In any case, since we are aware of no rapid destruction mechanisms for O_3 above the nighttime inversion, this O_3 very likely persists through the night.

The PAN profile shows rapid fluctuations and very little consistent trend. This is understandable since the average PAN levels are approaching the sensitivity limit of our detector. PAN does appear to increase in concentration starting at about 8 a.m. and remains at its higher levels throughout the afternoon. The nighttime concentrations are generally lower than the afternoon levels.

The average nitric acid concentrations at Site 2 were also extremely low and approaching the limit of sensitivity of our instrument. The average HNO_3 profile peaks at 9 a.m. and then fluctuates, apparently randomly, throughout the remainder of the day.

Light scattering as measured by an integrating nephelometer reached peak values between about 5-8 a.m.

The concentration of ammonia measured at Site 2 was extremely low during our study period in Dayton. Indeed, the levels were frequently below the lower limit of detection of our instrument. Thus, much of the NH_3 signal may well be instrument noise, and extreme caution must be exercised in discussing the ammonia values.

The composite sulfur dioxide profile rises gradually from a 6 a.m. minimum to a maximum at noon. Throughout the remainder of the afternoon the concentration remains relatively constant, with a very gradual decrease beginning at approximately 7 p.m. This pattern is very similar to that reported for SO_2 at Site 1, in terms of both concentration and time dependence.

The average profiles of solar intensity, wind speed, temperature, and relative humidity are shown in Figure 10 E for the Huber Heights site. Wind direction was also measured and is included in Appendix B on an individual daily basis. An average wind direction profile has not been computed for the study period since the wind direction variable is not amenable to arithmetical averaging. Vector averaging of wind speed and direction will be discussed later in the report. A detailed discussion of the meteorology during the study will also be presented later in the report.

New Carlisle (Site No. 3). The trends in the average gas-phase data from Site 3 are shown as profiles in Figure 11. Wind speed is also profiled in the figure. As at Site 2, wind direction was monitored and the data are included in Appendix C. The SO_2 levels at Site 3 average somewhat less than at Site 1 or 2. A maximum appears in the profile between 10-11 a.m. with a sharp drop thereafter. The average nitric acid concentration was low and somewhat variable, with major peaks occurring between 10-11 a.m. and again at 9 p.m. The late morning peak in HNO_3 occurs at all three sites and is a most interesting feature of these data. The evening HNO_3 peaks occur at the same time as an increase in both SO_2 and NO_x and may be associated with the emission or transport of these species.

Both NO and NO_2 show morning increases, with NO peaking between 7-9 a.m. and NO_2 reaching its maximum at about 10 a.m. Emissions of NO increase again between 4-6 p.m. Since O_3 is still present at this time however, the increase in NO emissions is evidenced largely by an increase in the NO_2 concentration. Later in the evening, between 8-11 p.m., we note another increase in the NO and NO_2 concentration. This increase occurs at about the same time at all three sites and probably reflects the formation of the low nighttime inversion.

The average ozone concentration begins to rise rapidly at 9 a.m. as NO begins to decrease. The actual O_3 maximum occurs at 3 p.m., although a broad plateau is maintained throughout the afternoon until 7 p.m.; thereafter, O_3 decreases steadily.

The 3-hour integrated bag data, shown earlier in Table 12, reveal that, unlike the other two sites, ethylene increases during the day at Site 3 while ethane, acetylene, CO, and NMHC remain relatively constant. It is difficult to rationalize this ethylene behavior except to note that the increase during the afternoon is based on only 7 sampling days due to a variety of problems with the sampling bags, the gas chromatograph, and an ethylene leak from the nitric acid monitor. Because of the limited number of days for which valid afternoon ethylene data are available at Site 3, we are probably well advised not to draw any major conclusions from the apparent afternoon increase in ethylene. The concentrations of C_2H_6, C_2H_2, PAN, CO CH_4, and NMHC appear on the average to remain relatively constant throughout the day at Site 3. The ratios of C_2H_6/C_2H_2, and C_2H_2/CO are very similar for Sites 1 and 3. The Site 2 ratios are somewhat different, although relatively constant throughout the day, for these rather inert gases.

In general, the concentrations of the C_2 hydrocarbons, CO, and NMHC are highest at Site 1 and lowest at Site 2, with Site 3 exhibiting intermediate levels of these species. This trend is consistent with the location of these sites in terms of proximity to sources, traffic density, etc.

Aerosol Composition

The average particulate mass loading during our Dayton field study was approximately 87 $\mu g/m^3$ as determined by high-volume sampling. It was pointed out earlier that high-purity quartz-fiber filters were employed for high-volume sampling. It must also be emphasized that all aerosol collections were carried out at Site 2. Referring to Table 13, we note that carbon makes up on the average about 12 percent of the total aerosol mass, hydrogen about 2.5 percent, and nitrogen roughly 4.3 percent These three elements alone comprise almost 19 percent of the average aerosol mass. It is assumed that water, oxygen, sulfur, and metals account for most of the remaining mass. Of the ionic species determined specifically, ammonium at 4.0 $\mu g/m^3$ accounts for 4.6 percent of the mass, nitrate at

0.31 μg/m^3 makes up about 0.4 percent, and sulfate at 20.2 μg/m^3 contributes about 23.3 percent of the total aerosol mass.

Table 16 gives the comparison between the average total aerosol analysis and the composite large particle (diameter >2.5 μm) analysis. Both ammonium and sulfate are seen to be associated with smaller particles while nitrate is predominately in the large-particle-size range. This is consistent with our findings(2) in St. Louis, Missouri, and the Los Angeles basin. We have previously discussed the fact that, since quartz filters do not remove gaseous HNO_3 from the air, the concentration and distribution of particulate nitrate reported here may differ considerably from the findings of other studies in which total (gaseous and particulate) nitrate was collected on the filter medium. For a detailed discussion of these effects and interactions the reader is referred to previous Battelle-Columbus reports(2,4).

A comparison of the total aerosol composition and the large particle composition for Dayton, St. Louis, and West Covina, California, is shown in Table 17. There are many similarities among the aerosol data from these three areas but also several obvious differences. For example, there appears to be almost twice as much ammonium and nitrate, on a weight-percent basis, in the large particle collections from Dayton than from either of the other two cities. On the other hand, the total aerosol nitrate from Dayton is less than either St. Louis or West Covina, with West Covina yielding considerably more total nitrate than either of the other two regions.

The sulfate and ammonium data for each sampling day at Site 2 were shown earlier in Table 13. A plot of these results is shown as Figure 12. The correlation coefficient derived from the regression plot of these two aerosol constituents is approximately 0.91. Since the size distribution data indicate that these two substances are both present predominately in the small-particle-size range, and since they are so well correlated, it is reasonable to suggest that they may be associated chemically. The slope of the regression plot implies a 1:1 molar ratio so that if these species are chemically associated, it must be in a form such as $(NH_4)HSO_4$. Charlson et al.(5) have reported detecting the

TABLE 16. DAYTON AEROSOL COMPOSITION (WEIGHT PERCENT)

	NH_4^+	NO_3^-	$SO_4^=$	C	H	N
Average Total Aerosol Composition	4.6	0.4	23.3	12.0	2.5	4.3
Large Particle (>2.5 μm) Composition	1.2	7.7	8.0	9.6	1.5	2.1

TABLE 17. AEROSOL COMPOSITION (WEIGHT PERCENT)

	NH_4^+	NO_2^-	NO_3^-	C	H	N
St. Louis, Missouri						
Average Total Aerosol	4.7	—	0.62	19.0	3.6	4.6
Large Particles (>2.5 μm)	0.55	0.001	2.6	14.6	1.8	1.5
West Covina, California						
Average Total Aerosol	4.7	—	1.7	19.4	3.8	5.3
Large Particles (>2.5 μm)	0.63	0.001	4.8	12.6	1.8	2.2
Dayton, Ohio						
Average Total Aerosol	4.6	—	0.40	12.0	2.5	4.3
Large Particles (>2.5 μm)	1.2	—	7.7	9.6	1.5	2.1

```
DAYTON AEROSOL DATA
```

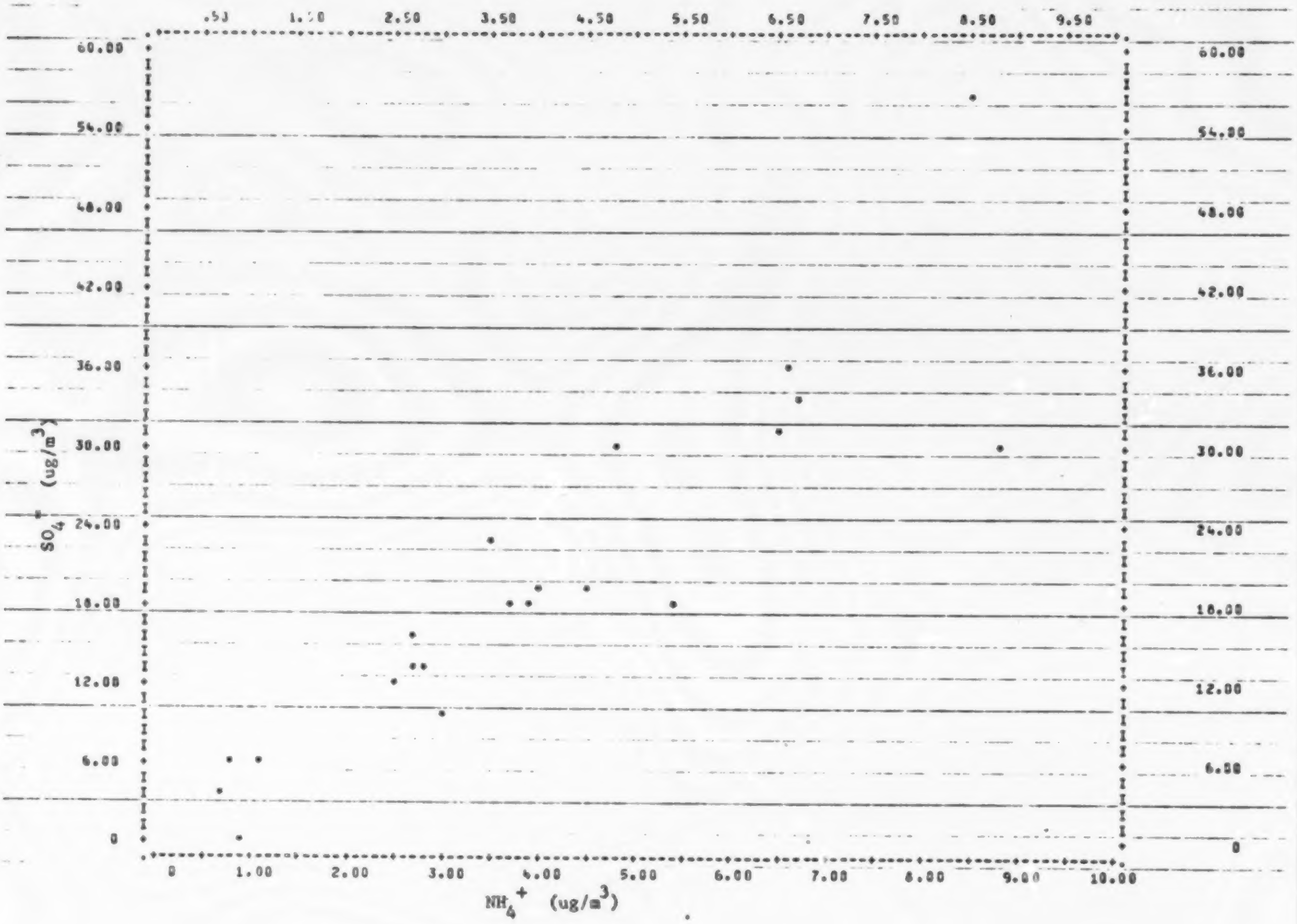

```
DAYTON AEROSOL DATA

STATISTICS..
   CORRELATION (R)-        .90876      R SQUARED       -       .82585      SIGNIFICANCE R -          .00001
   STD ERR OF EST -       5.62955      INTERCEPT (A)   -       .14828      STD ERROR OF A -         2.44281
   SIGNIFICANCE A -        .47612      SLOPE (B)       -      5.00459      STD ERROR OF B -          .52723
   SIGNIFICANCE B -        .00001
   PLOTTED VALUES -      21            EXCLUDED VALUES-       0            MISSING VALUES -        0
```

FIGURE 12. DAYTON REGRESSION: SULFATE VERSUS AMMONIUM

half-neutralized acid, $(NH_4)HSO_4$, in St. Louis. Since $(NH_4)HSO_4$ will readily react with NH_3 to form $(NH_4)_2SO_4$, the half-neutralized acid could only be the dominant form of sulfate when the ammonia concentration is too low to completely neutralize the acid. This is consistent with our NH_3 results which indicated extremely low NH_3 concentrations. It may well be that the low levels of NH_3 in the Dayton region limit the neutralization of sulfuric acid aerosols such that the major product is $(NH_4)HSO_4$.

One of the initial objectives of this program involved assessing the fate of nitrogen oxides in the Dayton area. However, as mentioned earlier, shifting research priorities and conflicting siting criteria have turned the program in the direction of an ozone/precursor transport study. The selection of Dayton as the study site was ideal from the standpoint of oxidant transport but troublesome in terms of a nitrogen oxides study due to the very low concentrations of NO_x and nitrogen reaction products found in the Dayton area. The levels are frequently so low as to approach the instrument sensitivity limits. For this reason, calculations of nitrogen oxides losses and nitrogen balances are probably meaningless. Nevertheless, it is possible to assess the aerosol nitrogen balance in order to determine whether a substantial fraction of nitrogeneous aerosol may be unaccounted for. Table 18 displays the daily aerosol nitrogen balance during the Dayton field study. Ammonium and nitrate accounted for an average of 79 percent of the total nitrogen collected on the quartz filters, with daily extremes of 54 and 97 percent. The fact that only 21 percent of the total aerosol nitrogen is not accounted for by ammonium and nitrate strengthens our belief that unsuspected nitrogen-containing aerosols are not playing any significant role in the fate of the nitrogen oxides in Dayton. The Dayton aerosol nitrogen balance compares quite favorably to similar nitrogen balances computed from aerosol collections from previous Battelle-Columbus studies. A list of study regions and particulate nitrogen accountability are shown in Table 19.

TABLE 18. DAYTON FILTER NITROGEN BALANCE

Date	Filter	NH_4^+-N, mg	NO_3^--N, mg	Σ NH_4^+-N+NO_3^--N mg	Total N mg	$100 \times \frac{\Sigma\ NH_4^+\text{-N}+NO_3^-\text{-N}}{\text{Total}}$ Percent
7-17-74	2	2.4	0.12	2.52	3.7	68
7-18-74	1	5.8	0.07	5.87	7.2	82
7-18-74	2	5.7	0.07	5.77	7.1	81
7-19-74	2	3.1	0.07	3.17	4.2	75
7-23-74	2	7.8	0.05	7.85	8.6	91
7-24-74	2	4.6	0.07	4.67	4.9	95
7-25-74	2	5.8	0.98	5.88	6.3	93
7-26-74	2	7.5	0.07	7.57	8.3	91
7-29-74	2	2.2	0.10	2.30	3.1	74
7-30-74	2	0.6	0.14	0.74	1.3	57
7-31-74	2	0.7	0.18	0.88	1.5	59
8- 1-74	2	3.6	0.08	3.68	4.6	80
8- 2-74	2	2.4	0.05	2.45	3.0	82
8- 2-74	1	2.5	0.06	2.56	3.1	83
8- 5-74	2	0.9	0.07	0.97	1.6	61
8- 6-74	2	3.3	0.10	3.40	4.3	79
8- 7-74	1	3.6	0.06	3.66	4.2	87
8- 8-74	1	2.8	0.06	2.86	3.5	82
8- 9-74	1	4.2	0.04	4.24	4.9	86
8-10-74	1	4.5	0.05	4.55	4.7	97
8-12-74	2	0.8	0.06	0.86	1.6	54
		$\overline{3.6}$	$\overline{0.08}$	$\overline{3.64}$	$\overline{4.4}$	$\overline{79\%}$

TABLE 19. AEROSOL NITROGEN BALANCE

City	Average Aerosol Nitrogen Accounted for as NH_4^+ and NO_3^-, percent
St. Louis, Missouri	82.5
West Covina, California	73.6
Columbus, Ohio	73.6
New York, New York	75.8
Pomona, California	70.7
Dayton, Ohio	79.0

Pollutant Directionality and Frequency

It is important in attempting to understand the mechanism and extent of pollutant transport to determine whether the concentration of any given pollutant is correlated with wind direction. If ozone or ozone precursors are found to be associated with particular wind directions, one might conclude that either ozone or its precursors are being transported into the area. In order to investigate whether any of the gaseous pollutants monitored during the program had a strong directional association, we employed a modified wind rose computer program to generate "pollutant roses". The pollutant rose is similar to the traditional wind rose, which shows the association between wind speed frequencies and wind direction. The pollutant rose displays the frequency of specified concentration ranges for a given pollutant as a function of wind direction. In the figures that follow, the percentage of the time that the wind blew from a given direction is shown numerically at the extreme of each wind direction stem. The width of the rectangles which make up the stems of the rose denote the concentration range, the wider rectangles indicating higher concentrations. The length of each of these rectangles indicates the fraction of the time that the pollutant occurred in a given concentration range for any particular wind direction component. Since wind direction was monitored at both Sites 2 and 3, two sets of wind and pollutant roses are available, one from each of these sites. The Site 2 roses will be discussed first, beginning with the standard wind rose.

The Site 2 wind rose is shown in Figure 13. It is immediately obvious from this figure that the wind direction frequency during the study period was rather different from that suggested for July and August by the 30-year wind direction averages. As discussed in the section on site location, the long-term meteorological data were used in selecting sites which would hopefully be parallel to the prevailing wind direction. As judged by Figure 13, the usually dominant southwesterly summer winds were not exactly dominant during our study period. The individual daily wind direction plots reveal that, for a great many study days, the wind was from the easterly directions early in the morning and slowly shifted

FIGURE 13. WIND ROSE - DAYTON - 2

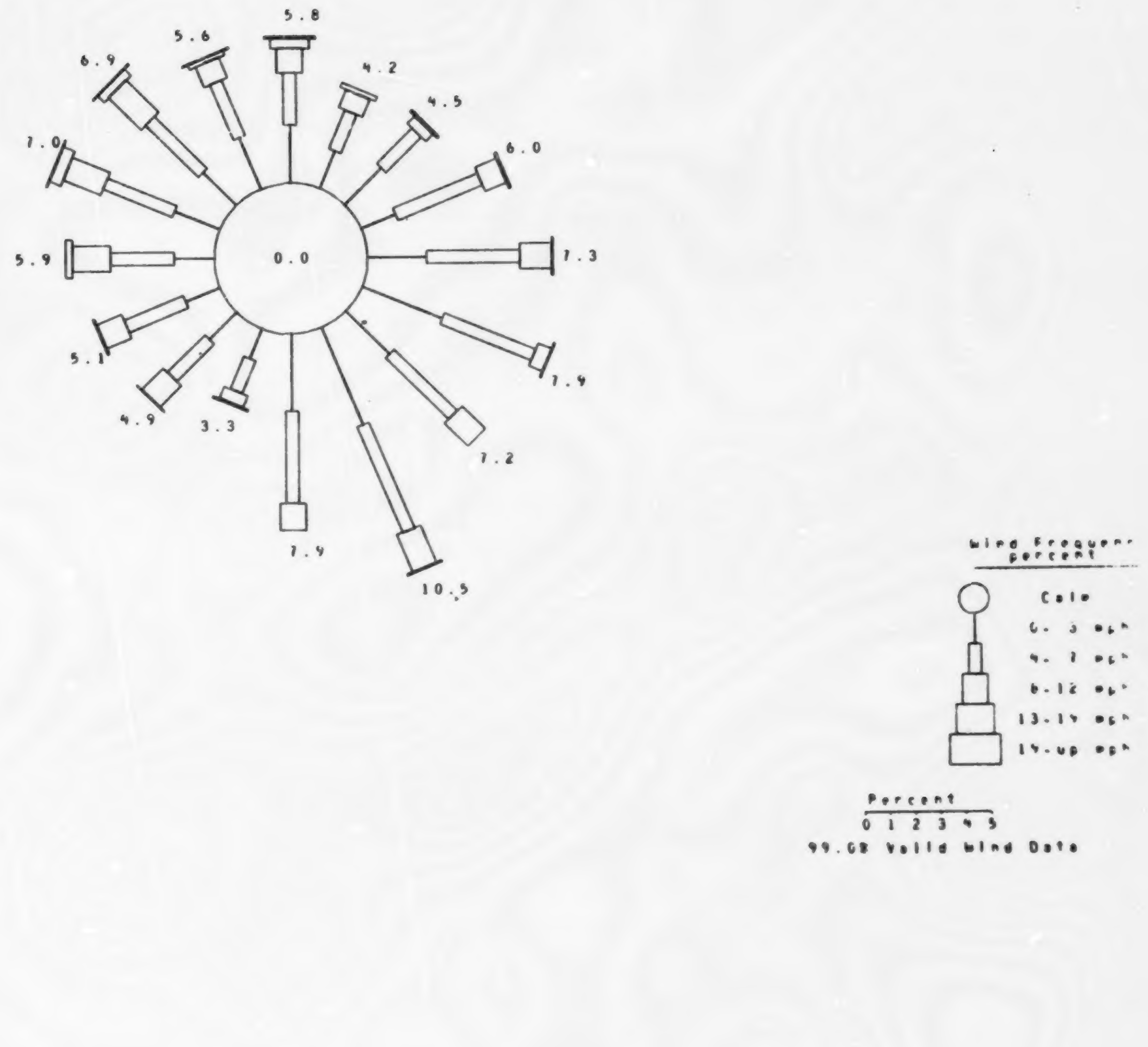

through the south during the morning hours to ultimately come from the west-to-northwest by late morning or early afternoon. Later in the afternoon or during the evening hours the pattern would reverse itself such that the wind was from the east again by morning. It can be seen from the figure that the wind came from the direction of Columbus (east to east-northeast) much more frequently than from the direction of Dayton and Cincinnati (south-southwest). More important to transport considerations than the mean wind direction however, is the mean wind velocity, computed from the vector addition of wind speed and wind direction. This variable will be discussed later in this report.

The pollutant roses from Site 2 are normalized such that all stems are of equal length, with the values at the stem extremes indicating directional frequency. The normalization process presents a clearer picture of the concentration ranges by preventing them from appearing compressed on wind direction stems of low frequency. The sulfur dioxide rose of Figure 14 shows that the highest levels of SO_2 occurred when the wind was from the east-northeast, the west-southwest, and the north-northwest. Since the first two directions are aimed at major urban areas (Columbus and Dayton/Cincinnati), transport may be occurring. However, this evidence is tenuous at best. The figure certainly reveals no strong directionality associated with SO_2.

The nitrogen oxides rose in Figure 15 presents a stronger case for directionality, with wind directions from 45° to about 225° showing a much greater frequency of elevated NO_x concentrations than westerly or northerly wind direction. Indeed, a line drawn through the center of the rose along the 45°-225° path separates the NO_x frequencies rather well, with higher NO_x levels expected more frequently when the wind direction is greater than 45° and less than 225°. The easterly and southwesterly directions are particularly interesting due to the major urban areas located in those directions.

The ammonia rose is shown in Figure 16. While a strong directional trend is observed, it is important to note that measurable NH_3 levels only occurred on a few days during the study. For the

FIGURE 14. POLLUTANT ROSE - DAYTON - 2 SULFUR DIOXIDE

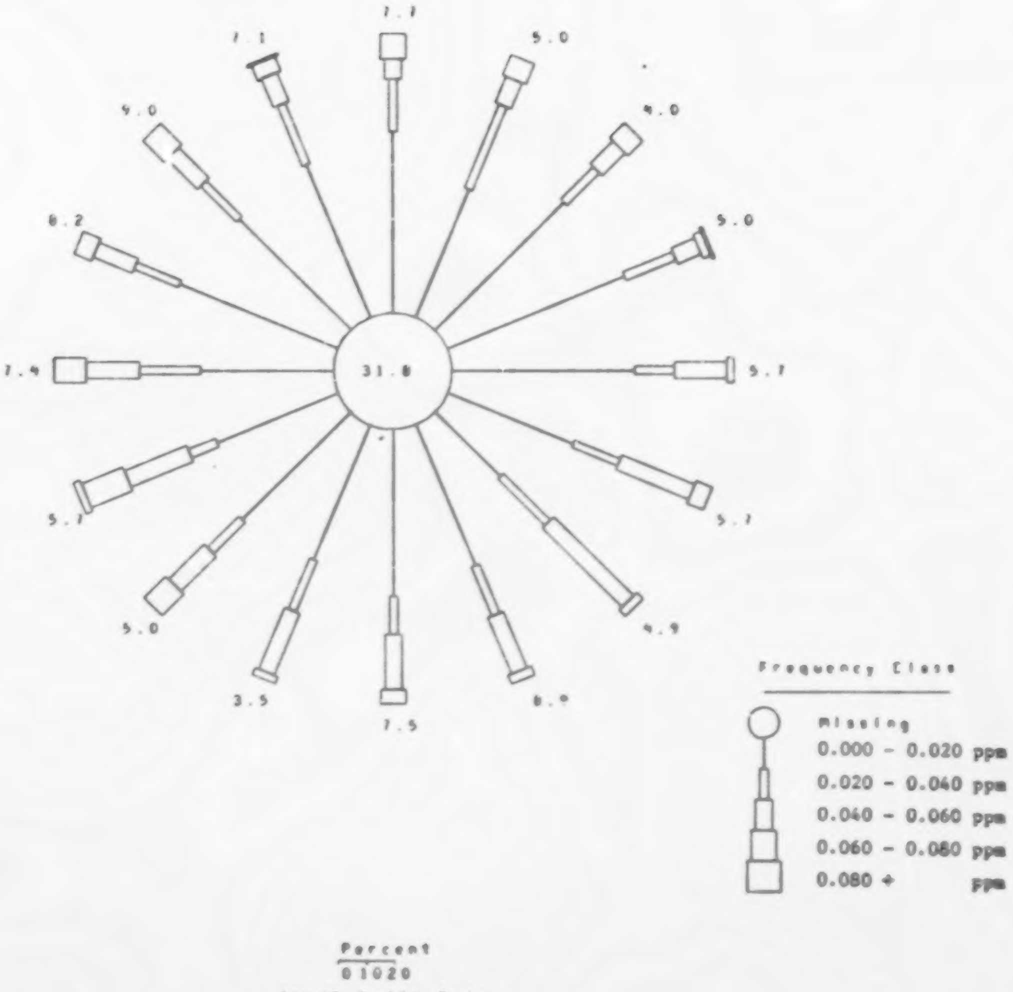

FIGURE 15. POLLUTANT ROSE - DAYTON - 2 NITROGEN OXIDES

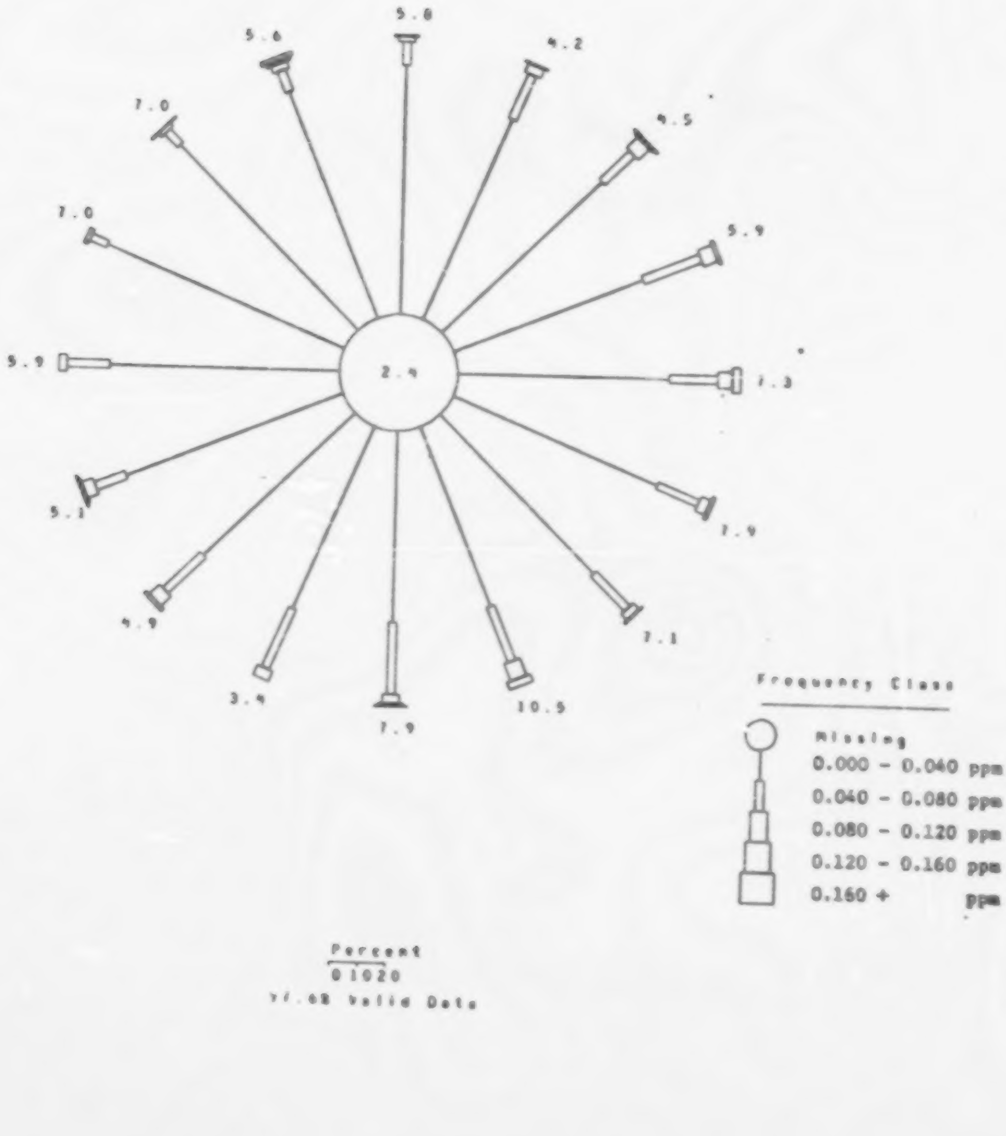

FIGURE 16. POLLUTANT ROSE - DAYTON - 2 AMMONIA

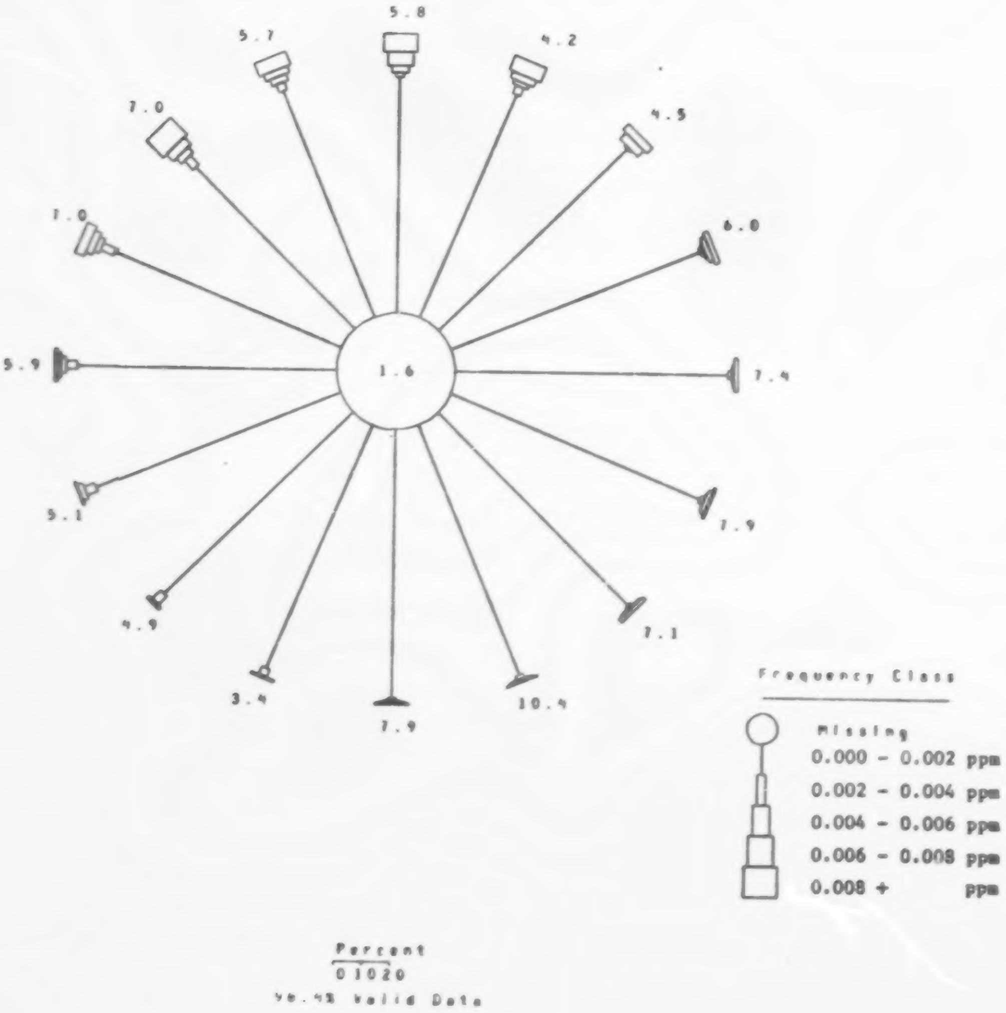

most part the ammonia levels were below the detection limits of our technique. Thus the concentrations and directional patterns of NH_3 must be regarded with skepticism.

The methane rose in Figure 17 is expected to be rather insensitive to wind direction since the major portion of methane is natural in origin and ubiquitous in nature. However, it does appear that higher levels of CH_4 are associated with winds from the southerly to westerly directions. This may well be due to the increased traffic density and greater number of stationary sources of hydrocarbons located in Dayton, just a few miles from Site 2. Automobiles especially are known to emit substantial quantities of methane and may be responsible for the directional component of methane. The same reasoning can be used to explain the directionality of NMHC shown in Figure 18. Again, the southerly to westerly wind directions show higher frequencies of elevated NMHC levels. The most likely explanation is the urban complex located just a few miles away in that general direction.

The pollutant rose for carbon monoxide, shown in Figure 19, is similar to the NO_x rose in that most of the elevated values occur when the wind direction is between 45° and approximately 240°.

The most important pollutant rose in terms of the objective of this study is the ozone rose shown in Figure 20. Close scrutiny of this figure leads to the conclusion that elevated ozone can occur from any wind direction. Nevertheless, while no wind direction can be considered dominant, winds from the general southwesterly direction lead to the highest levels of ozone even though the winds came from that direction very infrequently. Winds from the westerly and northwesterly directions also lead to higher ozone concentrations than most other wind directions. Higher ozone associated with southwesterly winds may be explained by the movement of ozone and its precursors from the urban complex located in that direction; recall that the hydrocarbons, NO_x, and CO all exhibited higher concentrations when the wind was from that direction. Elevated ozone when the winds are from the west and northwest is somewhat more difficult to explain however, and will be reserved for the discussion of meteorological interactions.

FIGURE 17. POLLUTANT ROSE - DAYTON - 2 METHANE

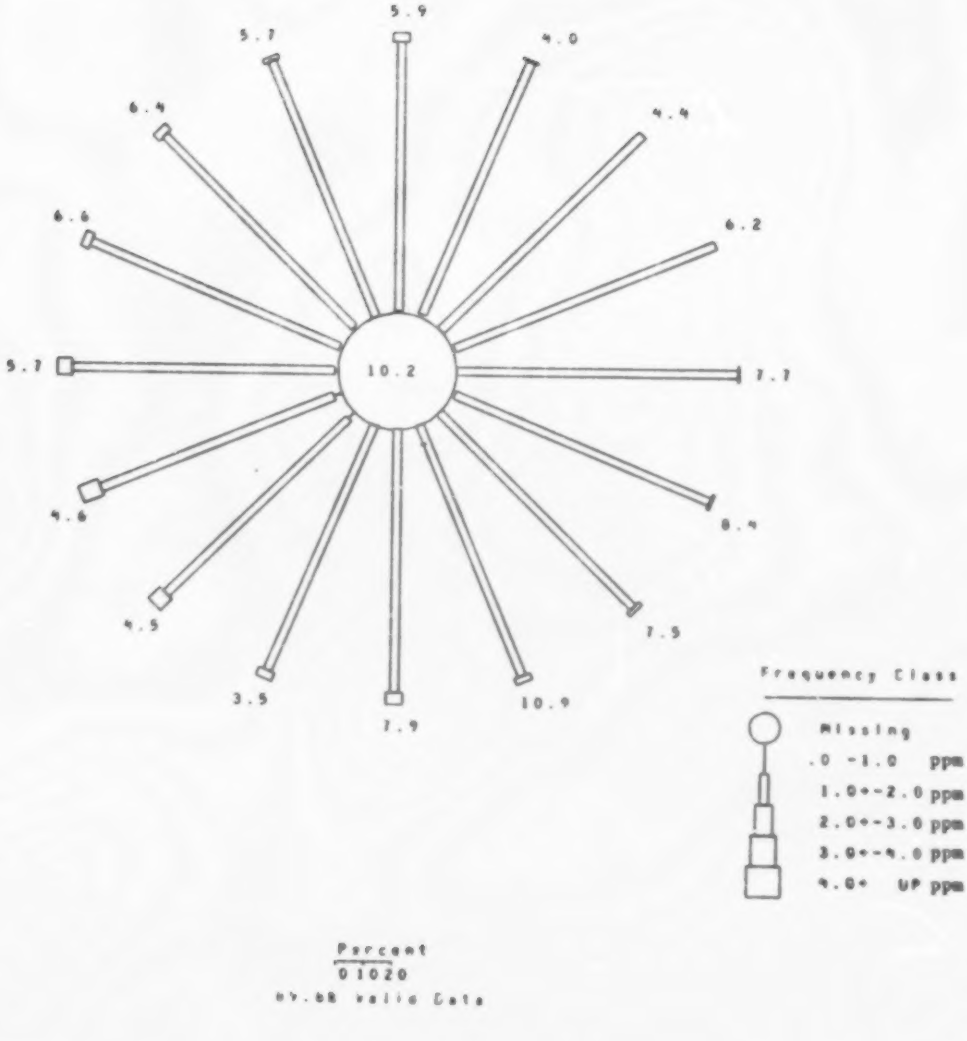

FIGURE 18. POLLUTANT ROSE - DAYTON - 2 NON-METHANE HYDROCARBON

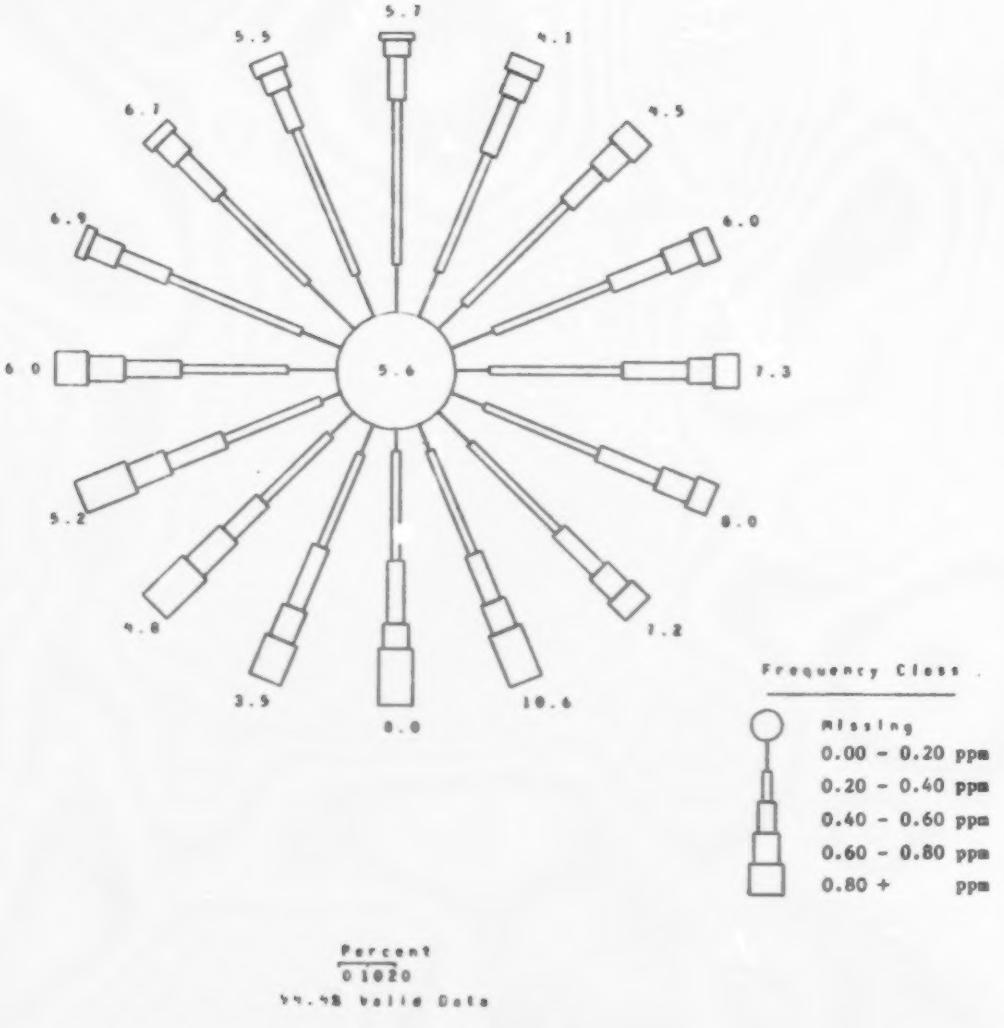

FIGURE 19. POLLUTANT ROSE - DAYTON - 2 CARBON MONOXIDE

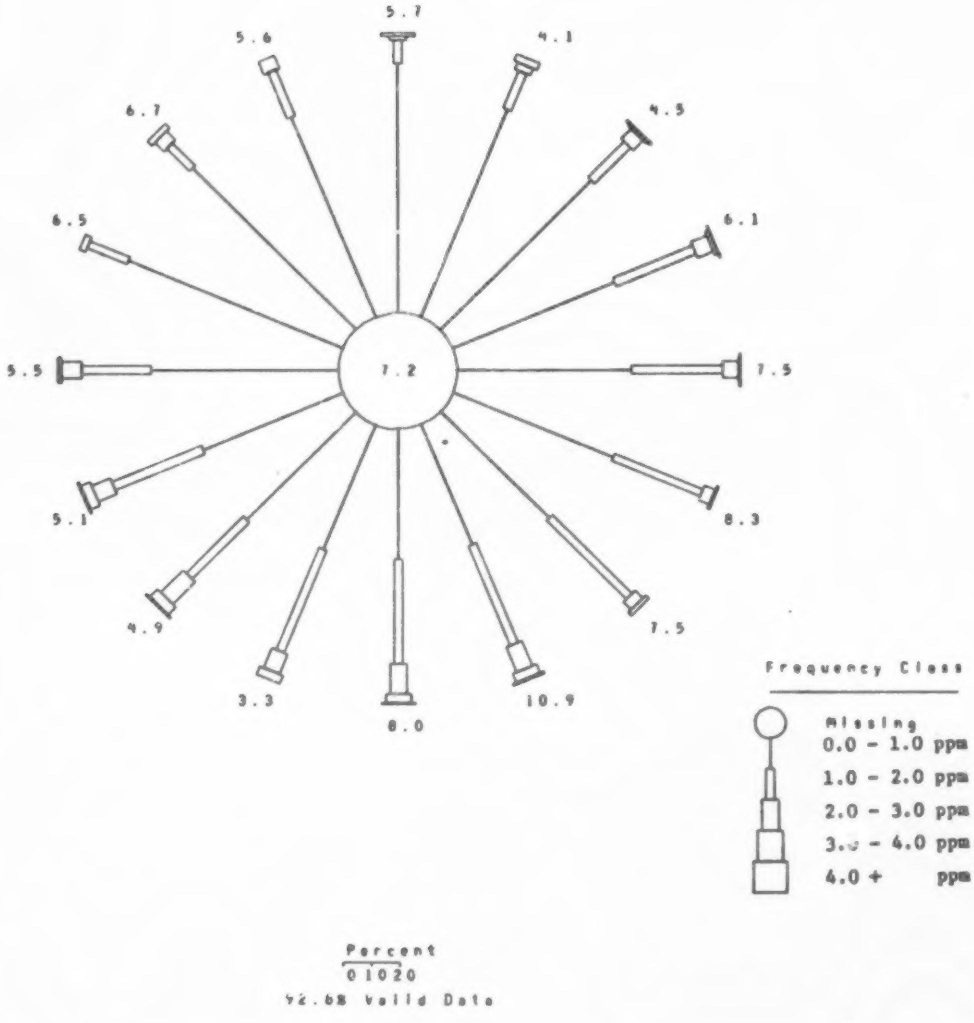

FIGURE 20. POLLUTANT ROSE - DAYTON - 2 OZONE

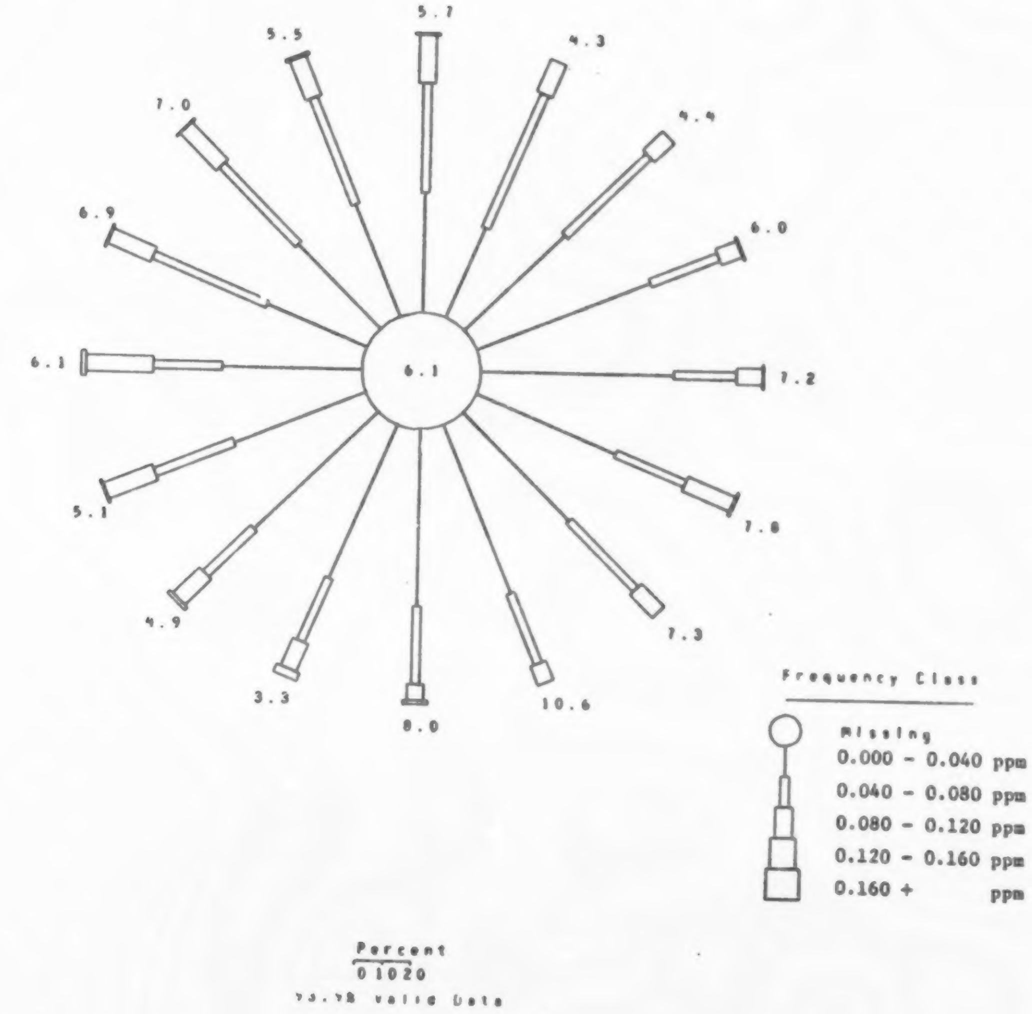

Wind and pollution roses from Site 3 are in the same format as those just discussed. The New Carlisle wind rose, shown in Figure 21, is somewhat different from the Huber Heights rose in that westerly winds and northeasterly winds occurred with greater frequency at Site 3. These changes took place at the expense of northerly and southeasterly winds. It is necessary to note that the normally "prevailing" southwest winds occurred with the same low frequency at Site 3 as at Site 2. The differences in wind direction frequencies between the two sites are no doubt caused by differences in local topography. Since Site 2 was located on a level plain free from obstructions and was also located midway between the other two major stations, its wind data are considered to be more representative of the three-site area and will be used in subsequent discussions involving wind data.

The pollution rose representing SO_2 at New Carlisle is given in Figure 22. The southerly directions, from southeast to southwest, obviously dominate. We attribute this directional association to the multitude of stationary emissons sources of SO_2 located in the areas around Springfield and Dayton, southeast and southwest of the New Carlisle site.

The NO_x rose for Site 3 is shown in Figure 23. The elevated concentrations with the wind from the southwest can possibly be attributed to the urban emissions from Dayton, 20 miles to the southwest.

The New Carlisle ozone rose is shown in Figure 24. It is obvious from this figure, as from the Site 2 ozone rose, that no strong directionality can be associated with elevated levels of ozone. Ozone levels above the Federal standard are seen to occur from virtually every wind direction. One must be cautious however of reading too much from any of these pollutant roses. All of the roses show only the association of a pollutant with the current wind direction. However, the time history and trajectory of the air parcel are likely to be more important influences on pollutant concentrations than the simple wind direction. Vector averaging and trajectory analysis will be employed later in this report to investigate the sources of high O_3 air masses.

FIGURE 21. WIND ROSE - NEW CARLISLE / DAYTON - 3

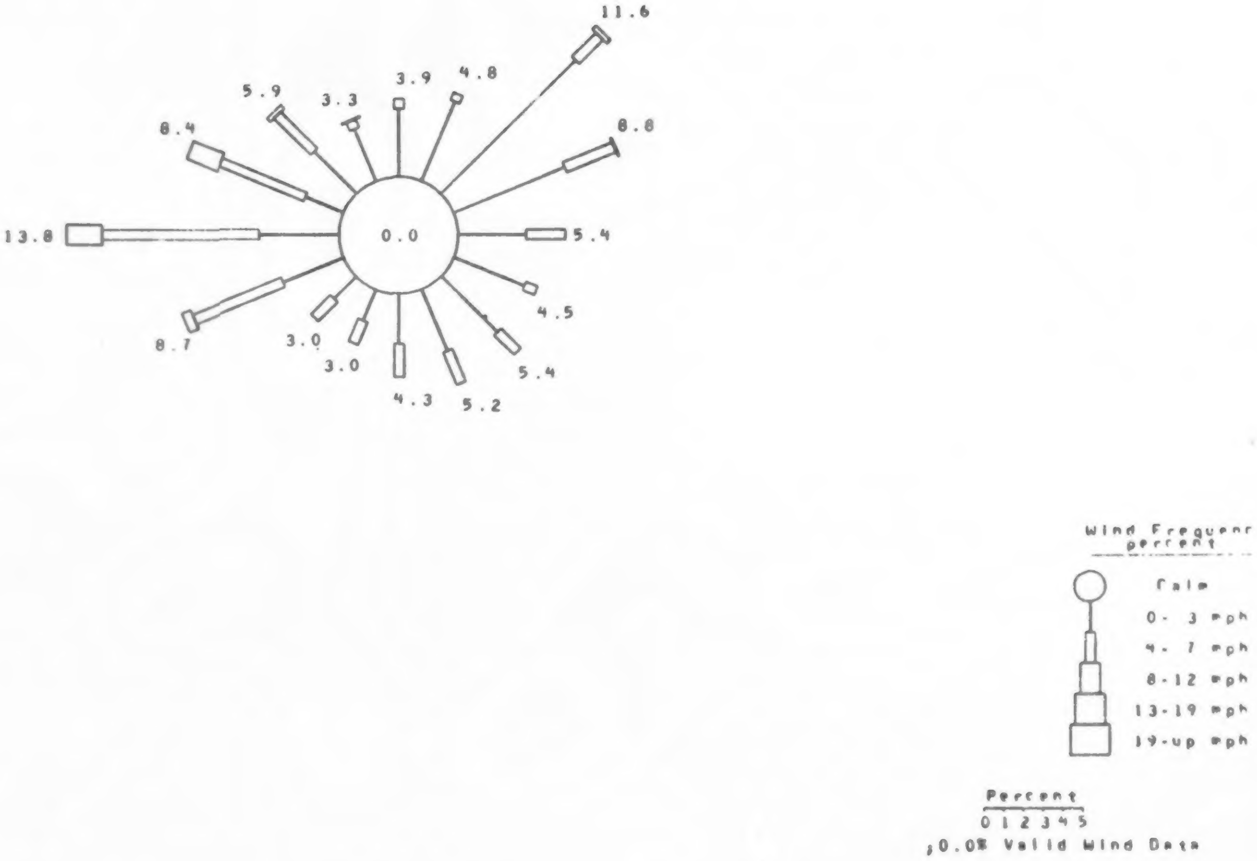

FIGURE 22. POLLUTANT ROSE - NEW CARLISLE / DAYTON - 3 SULFUR DIOXIDE

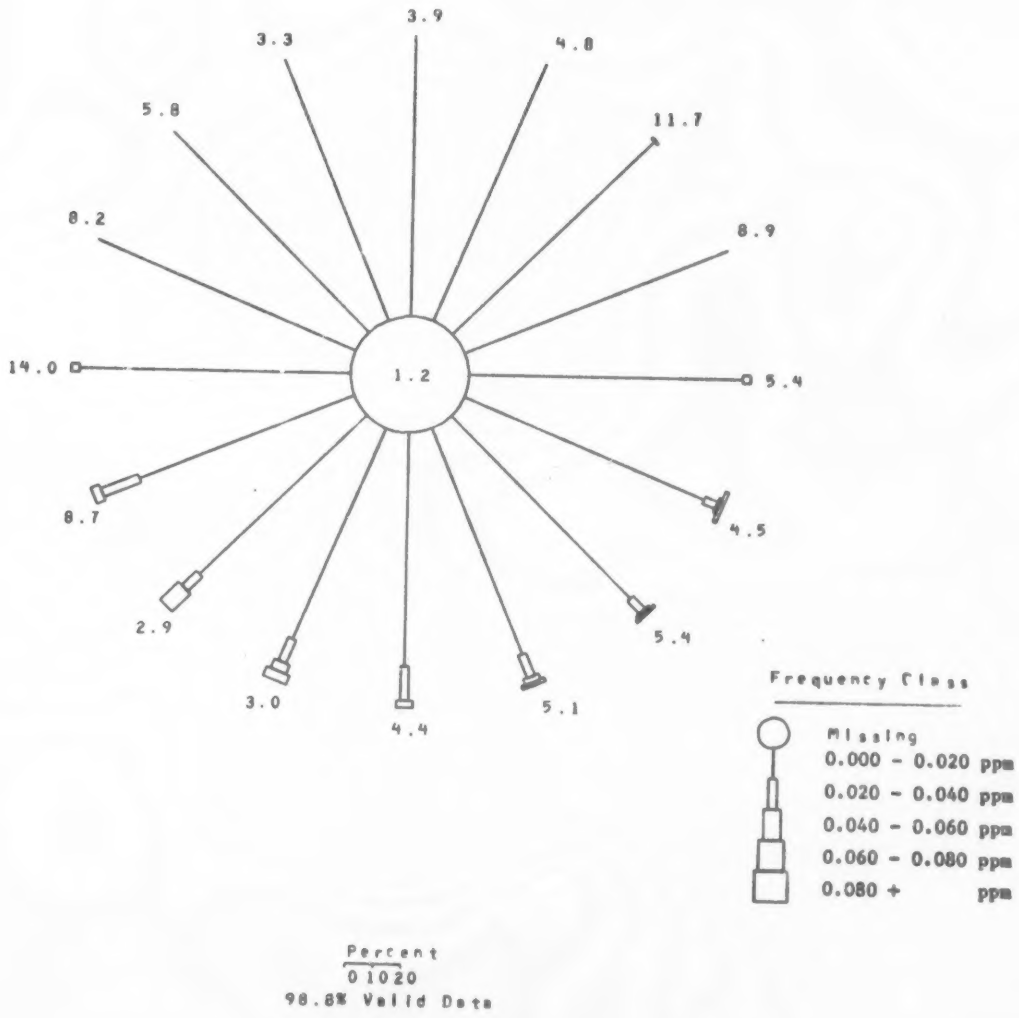

FIGURE 23. POLLUTANT ROSE - NEW CARLISLE / DAYTON - 3   NITROGEN OXIDES

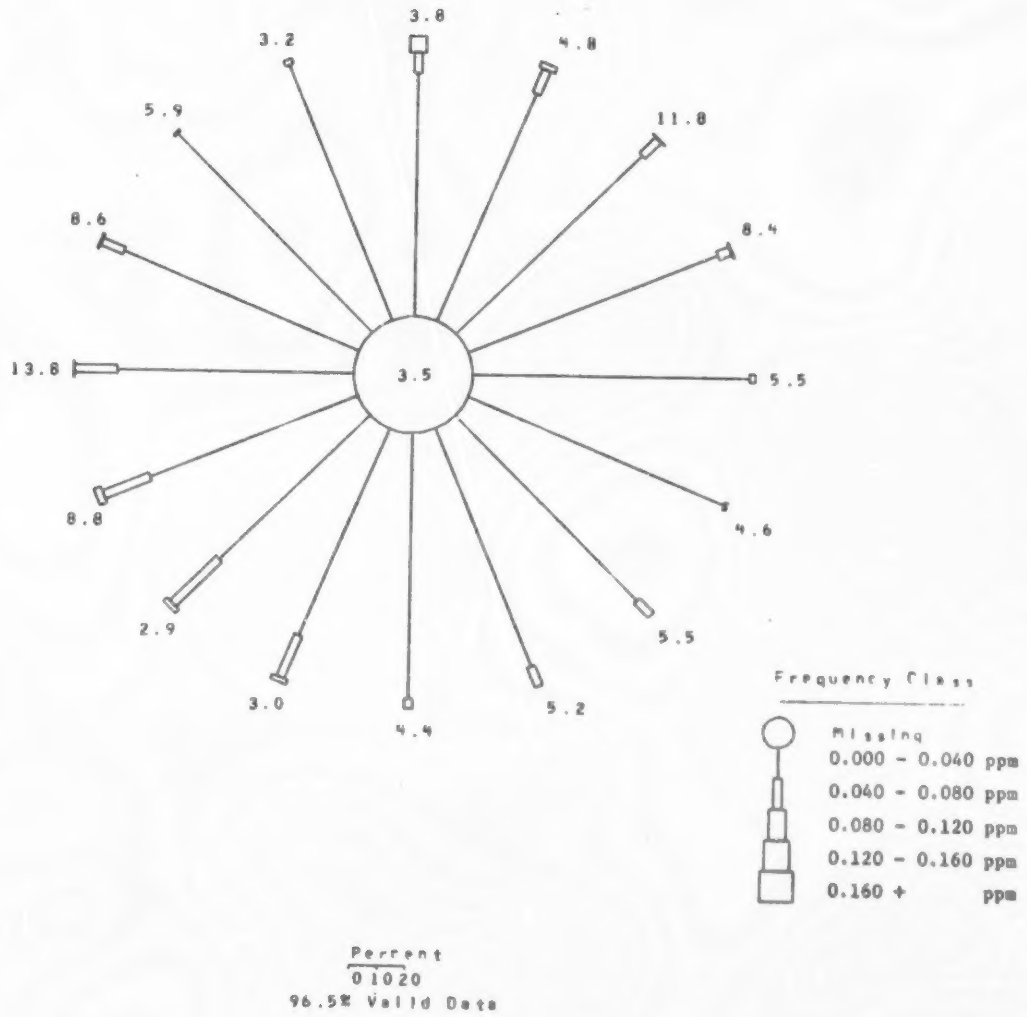

FIGURE 24. POLLUTANT ROSE - NEW CARLISLE / DAYTON - 3 OZONE

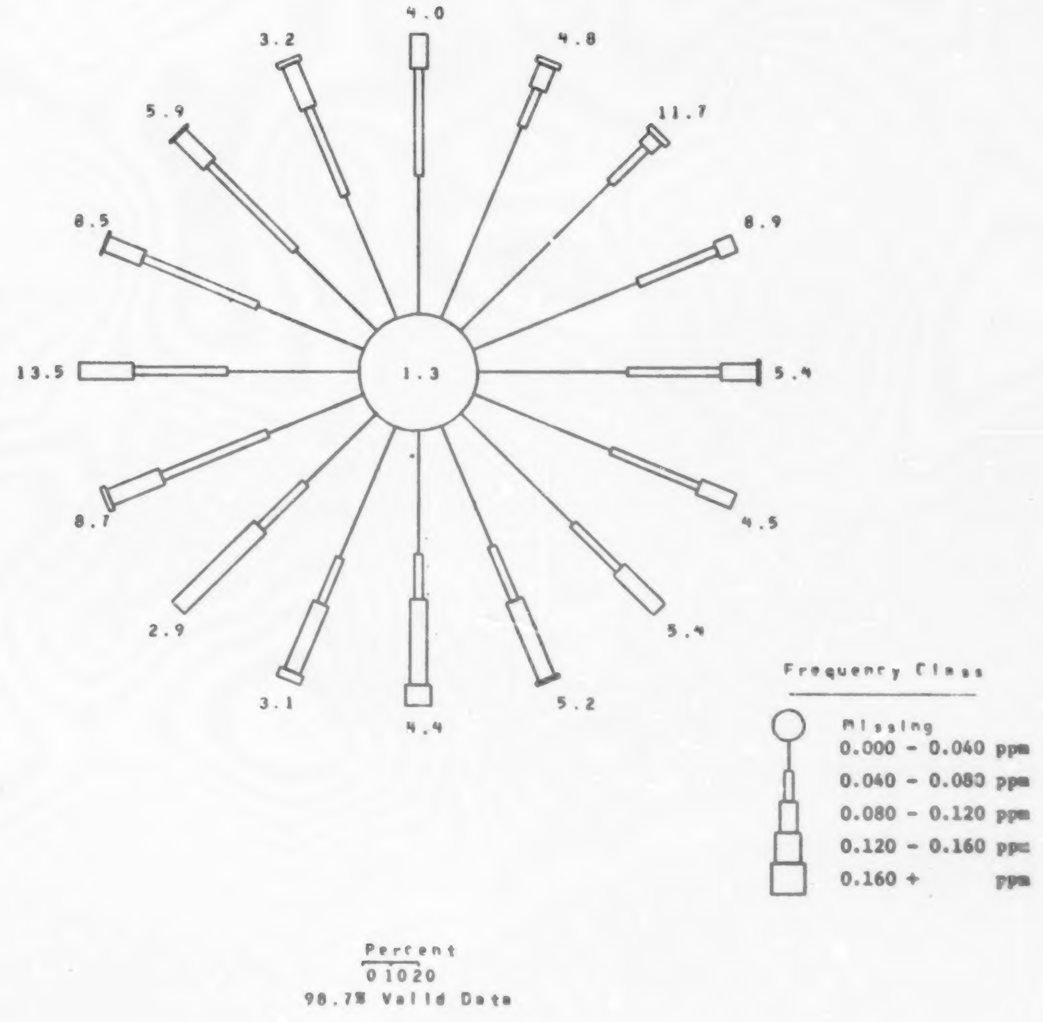

The large volume of data collected during this field study makes it difficult to gain a feeling for the frequency and spatial distribution of the pertinent pollutants. In order to give the reader a better understanding of the ozone patterns in Dayton, we refer you to Table 20, where O_3 frequency is shown for each of four separate sites for each day of the study. Twenty-seven days of ozone data are tabulated for each of the four most widely separated sites; namely, Miamisburg (M), downtown Dayton (1), Huber Heights (2), and New Carlisle (3). The "X" markings indicate that O_3 on that day exceeded the specified concentration for at least 1 hour at the given site. Shown in the extreme right column of the table are the 6 a.m. to 2 p.m. average wind direction vectors for each day, computed by averaging the vector sums of wind speed and direction at 10-minute intervals throughout the 8-hour period. It is clear from this table that most of the high O_3 values (>0.10 ppm) were recorded at Sites 2 and 3 when the average air mass movement was from either the south-to-southwest direction (July 17,18; August 1,2) or from the east (July 25,26; August 6). Since Dayton and the urban complex between Dayton and Cincinnati lie to the south and southwest, and Columbus lies in the easterly direction, there is good reason to suspect that contaminated air from these urban complexes may be contributing to the elevated O_3 levels at these sites.

The individual daily ozone distributions will be discussed later in this report. However, a few brief comments based on Table 20 are in order at this time. It is apparent from the table that days of elevated ozone levels above the Federal standard occur in groups which might be thought of as ozone "episodes". There are four rather clearly defined intervals during which O_3 exceeded the 0.08 ppm standard at more than one site for more than one day. Exceedence of the 0.10 ppm O_3 value occurred during three distinct periods with occasional exceedences on other days. Site 3 had the greatest number of days with at least 1 hour above 0.08 ppm at 17, and the greatest number above 0.1 ppm at 9. Site 2 was next at 14 and 8; the Miamisburg site followed at 10 and 3, and downtown Dayton had the fewest days of

TABLE 20. DAYTON AREA OZONE LEVELS

	[O$_3$] >0.08 ppm				[O$_3$] >0.10 ppm				
Date Site(b)	M	1	2	3	M	1	2	3	6 a.m.-2 p.m. Wind Vector, Degrees
7-17		XXX	XXX	XXX			XXX	XXX	158
7-18	XXX		XXX	XXX			XXX	XXX	243
7-19			XXX				XXX		306
7-20(a)	XXX			XXX					——
7-21(a)	XXX			XXX					——
7-22	XXX			XXX				XXX	——
7-23									284
7-24			XXX						45
7-25	XXX		XXX	XXX				XXX	99
7-26	XXX	XXX	XXX	XXX	XXX		XXX	XXX	108
7-27(a)	XXX	XXX	XXX	XXX		XXX	XXX	XXX	——
7-28(a)			XXX	XXX			XXX		——
7-29			XXX	XXX					276
7-30									325
7-31									304
8-1	XXX	XXX	XXX	XXX	XXX	XXX	XXX	XXX	225
8-2	XXX	XXX	XXX	XXX			XXX	XXX	241
8-3(a)									——
8-4(a)									——
8-5									328
8-6			XXX	XXX				XXX	106
8-7				XXX					132
8-8			XXX	XXX					176
8-9	XXX	XXX	XXX	XXX	XXX				18
8-10(a)				XXX					131
8-11(a)									190
8-12									301

(a) Weekend

(b) M = Miamisburg
1 = Downtown Dayton
2 = Huber Heights
3 = New Carlisle

elevated ozone at 6 and 2. There were 8 days during the study period in which none of these four sites reported maximum 1-hour ozone values in excess of 0.08 ppm. Of these 8 days, two were on a weekend for which wind vector data are not available, five of the remaining 6 days had wind vectors from the west and northwest, and the last day experienced heavy rain and overcast skys throughout the day and would not be expected to generate high levels of ozone. These results suggest that the Dayton area will generally experience periods of low ozone when air mass movement into the area is from the west and northwest. This finding is entirely consistent with the hypothesis that part of Dayton's ozone problems result from transport of O_3 or its precursors into the area from other urban environments, since there are no major urban complexes located to the northwest of Dayton within short range transport distance.

One of the most interesting sites in terms of transport considerations is the Miamisburg station. Since it is located between Dayton and the Cincinnati complex it should serve as an indication of the effect of Cincinnati on the Dayton region. For example, using data from only Sites 1-3, it is difficult to determine whether high ozone on days of southwesterly winds is coming from Dayton itself or from further south in the Cincinnati area. The Miamisburg site located between the two cities should help to clarify this situation. From the distributions in Table 20, it appears that on August 1 and 2 there is a high probability that O_3 and/or precursors from Cincinnati served as the source of the high ozone values since all four sites, including Miamisburg, reported elevated O_3 during this period of southwesterly winds. In contrast, on August 9 during a period of northerly winds, Miamisburg was the only station reporting O_3 in excess of 0.10 ppm. We suspect that this elevated O_3 level was caused by the movement of polluted Dayton air south toward Miamisburg. A more detailed site-to-site discussion of O_3, categorized as to wind direction, will be presented later in this report. Prior to that however, we will discuss the correlation of the hourly ozone data among our six ground-level stations.

Site-to-site correlations of ozone data collected during the Dayton field study are presented in Table 21. Shown in the table along with the correlation coefficients are the slopes and intercepts for each regression line. The regression of perhaps the greatest interest is between Site 2 and Huber Heights (EPA). These sites were located side by side within 20 meters of one another with one O_3 instrument being operated by EPA and the other by Battelle-Columbus in our main mobile laboratory. Since these two instruments were located so close together they should, presumably, exhibit a high degree of agreement. The correlation coefficient between these two units is indeed excellent at 0.94, the highest coefficient among any of the sites. The slope of the regression line, 1.05, reveals only a 5 percent discrepancy between the two instruments, which is about the limit of accuracy attributed to the calibration procedure for ozone chemiluminescent instruments. A negative intercept of only one ppb further confirms the excellent agreement between these two independently operated monitors. In general, all of the correlation coefficients are greater than 0.75 and there is only one intercept greater than 5 ppb. The slopes varied from 0.53 to 1.07, with downtown Dayton and Miamisburg showing generally lower levels of ozone than the other four stations. Presumably these two sites have lower average ozone readings because of the higher nitric oxide emissions in their vicinity(6), nitric oxide serving as a strong inhibitor of O_3 formation.

A Statistical View of the Dayton Field-Study Results

Linear Regression Analysis

The results from our three main stations in the Dayton area can be readily compared by means of regression techniques. A number of regressions were run on the data from each site to check whether major differences in the gas-phase relationships are observed from site to site. The results of regression analyses on the data from Sites 1-3 are shown in Tables 22-24. The first two columns in these regression tables show

TABLE 21. SIX SITE OZONE CORRELATIONS

Site vs Site	Correlation Coefficient	Slope	Intercept, ppm
Miamisburg vs Site 1	0.87	0.95	0.002
Miamisburg vs Timberlane	0.85	0.64	0.005
Miamisburg vs Site 2	0.86	0.74	0.000
Miamisburg vs Huber Heights (EPA)	0.88	0.84	-0.003
Miamisburg vs Site 3	0.86	0.76	-0.003
Site 1 vs Timberlane	0.76	0.53	0.008
Site 1 vs Site 2	0.86	0.68	0.002
Site 1 vs Huber Heights (EPA)	0.86	0.75	0.000
Site 1 vs Site 3	0.86	0.70	-0.001
Timberlane vs Site 2	0.77	0.88	0.004
Timberlane vs Huber Heights (EPA)	0.84	1.07	-0.003
Timberlane vs Site 3	0.78	0.90	0.000
Site 2 vs Huber Heights (EPA)	0.94	1.05	-0.001
Site 2 vs Site 3	0.88	0.89	0.002
Huber Heights (EPA) vs Site 3	0.90	0.83	0.004

TABLE 22. SITE 1 REGRESSIONS (3-HOUR AVERAGE EXCEPT AS MARKED)

Y	X	R	M
SO_2 (a)	NO_x (a)	-0.26	-0.08
O_3 (a)	NO_x (a)	-0.42	-0.22
CO	NO_x	0.76	18.2
C_2H_2	NO_x	0.51	0.17
O_3	C_2H_4/C_2H_2	-0.03	-0.94
C_2H_4/C_2H_2	C_2H_2/NO_x	-0.50	-0.94
C_2H_4	C_2H_2	0.80	0.79
C_2H_6	C_2H_2	0.61	0.24
C_2H_2	NMHC	0.54	0.008
CO	NMHC	0.91	1.11
C_2H_2	CO	0.67	0.009
C_2H_4	CO	0.95	0.012
C_2H_6	NMHC	0.68	0.004

(a) Hourly averages.

TABLE 23. SITE 2 REGRESSIONS (HOURLY AVERAGES)

Y	X	R	M
CO	NO_x	0.77	19.5
CO	NMHC	0.74	1.49
CO	C_2H_4	0.66	50.6
CO	C_2H_2	0.66	13.0
NO_x	SO_2	-0.16	-0.21
NO_x	NMHC	0.63	0.05
O_3	NO_x	-0.57	-0.79
O_3	C_2H_4/C_2H_2	0.12	2.65
NMHC	C_2H_2	0.62	55.4
C_2H_4	C_2H_2	0.72	1.84
C_2H_6	C_2H_2	0.60	1.08
C_2H_6	NMHC	0.55	0.011
C_2H_2	NO_x	0.64	0.078

TABLE 24. SITE 3 REGRESSIONS (3-HOUR AVERAGES EXCEPT AS MARKED)

Y	X	R	M
SO_2(a)	NO_x(a)	0.18	0.64
O_3(a)	NO_x(a)	0.24	0.39
CO	NO_x	0.10	4.4
C_2H_2	NO_x	0.04	0.03
O_3	C_2H_4/C_2H_2	0.36	15.9
C_2H_4/C_2H_2	C_2H_2/NO_x	-0.24	-0.14
C_2H_4	C_2H_2	0.55	0.52
C_2H_6	C_2H_2	0.01	0.006
C_2H_2	NMHC	0.21	0.008
CO	NMHC	0.66	1.04
C_2H_2	CO	0.55	0.010
C_2H_4	CO	0.56	0.020
C_2H_6	NMHC	0.14	0.003

(a) Hourly averages.

the Y and X coordinate variables, while the third column lists the correlation coefficient (R) and the final column tabulates the slope of the regression line. Tables 22 and 24 for Sites 1 and 3 consist primarily of 3-hour integrated data from the Teflon bag samples collected three times a day. The Site 2 data in Table 23 are 1-hour averages for 24 hours per day. There is consequently a much larger volume of data from Site 2 and the results include both day and nighttime hours. Since the data from Sites 1 and 3 were collected only between 6 a.m. and 3 p.m., the results from the three sites are not completely comparable and must be interpreted with caution.

It is apparent from the regression tables that some variables show no relationship to one another at any of the three sites. For example, the correlation coefficients for SO_2 vs NO_x and O_3 vs C_2H_4/C_2H_2 are negligible at all three sites. The coefficients for O_3 vs NO_x, while not high, actually change signs for different sites. This likely reflects the ambiguous nature of the term "NO_x". If NO_x at a given site is composed largely of NO_2 than a positive correlation between NO_x and ozone is expected since NO_2 is a direct precursor to ozone; if however the NO_x is made up primarily of NO, then a negative correlation is expected due to the rapid reaction between NO and O_3. We have discussed the meaning of this behavior in terms of a kinetic mechanism in a previous report(2).

The regressions involving CO and the hydrocarbon variables are often in considerable disagreement among the three sites. The correlations between C_2H_4 and C_2H_2 for example are all reasonably high but the slopes differ by more than a factor of three. The ratio C_2H_4/C_2H_2 has often been used to describe the "age" or extent of photochemical reaction of an air mass, since acetylene is relatively unreactive and ethylene moderately reactive in photochemical smog. The ratios of these two hydrocarbons as derived from the slopes of the regression lines are about 0.8, 1.8, and 0.5 for Sites 1-3 respectively. Taken at face value, these ratios imply that the average air mass at Site 2 is the least reacted of the three and that Site 3 has experienced the greatest degree of reaction. This assumes of course that the initial emissions ratio of the ethylene and acetylene observed at all three sites is the same. Kopczynski, Lonneman and coworkers(7,8) have reported the ethylene to acetylene ratio in urban areas to average about 1.2, with nonurban ratios of approximately 2.0. This implies that our Site 2 has a pronounced nonurban characteristic, in agreement with our knowledge of the source distribution and air mass movement during our Dayton study period. The C_2H_2 vs CO correlations were reasonably high at all three sites, with the C_2H_2/CO ratios varying from 0.009 at Site 1 to 0.008 at Site 2 and 0.010 at Site 3. Kopczynski et al.(7) have reported this ratio as approximately 0.02 for urban sites and 0.01 at nonurban locations. They have also measured a ratio of 0.013 for roadway samples in St. Louis. Since C_2H_2 must come largely from auto exhaust, our lower ratios suggest other nonautomotive contributions to the CO level at each site.

Essentially the same C_2H_4/CO ratio was found at both Sites 2 and 3, the ratio averaging 0.020, in reasonable agreement with both the urban (0.025) and nonurban (0.022) ratios which have been reported(7). The correlations were fairly strong at both sites. The highest correlation determined in the study was between C_2H_4 and CO at Site 1 in downtown Dayton. The ratio from the slope of the Site 1 regression line is 0.012, considerably lower than either of our other two sites or the urban, nonurban, or roadway samples mentioned above. At the present time we have no explanation as to why this ratio is lower than at our other sites.

The remaining regression results, while interesting, are not particularly relevant to the oxidant transport problem and will not be discussed further at this time.

Interpretation of Maximum Ozone Concentrations by Means of Regression Integrals

One method which has frequently been used to model the formation of ozone in photochemical smog is to relate maximum daily ozone formation to the daily variation in species suspected of leading to O_3 production. In this regard the 6-9 a.m. average of non-methane hydrocarbons and nitrogen oxides have often been employed to predict the subsequent maximum hourly average ozone concentration. Such approaches neglect meteorology and air mass movement however, and do not take into account the distribution of the "precursor" variables over the time period prior to maximum ozone formation.

Realizing that 20 days is a very small data base on which to construct a model, nevertheless we believe that it is important to apply new mathematical techniques to atmospheric data to minimize the shortcomings of the models used in the past and we have therefore applied the technique of regression integrals to our Dayton results. Since, to the best of our knowledge, this technique has not been employed previously for investigating atmospheric data, we will describe the procedure in some detail prior to discussing the results.

The method of regression integrals was developed by R. A. Fisher(9) as a means of analyzing weather-yield problems. He reasoned that it was not only total rainfall or other summary statistics which help determine crop yields, but also the distribution of such variables throughout the growing season. In essence, the method he developed allows yield to be regressed on distribution variables. This method is pertinent also for analyzing maximum ozone concentrations. Maximum ozone formation is influenced not only by summary variables, such as the 6-9 a.m. average of non-methane hydrocarbons, but also by the distribution of such variables over a suitable period prior to maximum ozone formation.

In order to compare a single ozone value to a sequence of values of another variable, the first step is to fit a curve to the sequence of values by means of orthonormal polynomials. For example, letting H(t) denote the level of non-methane hydrocarbons at time t, we may represent H(t) by

$$H(t) = \rho_0 f_0 + \rho_1 f_1(t) + \ldots + \rho_k f_k(t), \tag{1}$$

where f_0, f_1 ..., f_k are orthonormal polynomials of degrees 0 through k respectively. Then ρ_0, ρ_1, ..., ρ_k are the non-methane hydrocarbon distribution constants determined by the method of least squares. In practice, a good fit is often obtained for small k.

Letting M denote maximum ozone concentration, the following multiple regression equation may be developed:

$$M = c + \alpha_0 \rho_0 + \alpha_1 \rho_1 + \ldots \alpha_k \rho_k \quad . \tag{2}$$

In this relationship, ρ_0, ..., ρ_k are the independent variables, whose values at any observation set are those obtained from the curve fitting procedure.

By using the orthonormality of f_0, ..., f_k, the following relation can be obtained from (2):

$$M = c + \alpha_0 \sum_t H(t)\ f_0(t) + \ldots + \alpha_k \sum_t H(t)\ f_k(t) \quad . \tag{3}$$

Rewriting Equation (3), we obtain

$$M = c + \sum_t a(t)\ H(t), \tag{4}$$

where $a(t) = \alpha_0 f_0(t) + \alpha_1 f_1(t) + \ldots + \alpha_k f_k(t)$. Equation (4) leads to the following observation: at hour t, a unit increase in H(t) will lead to a change in maximum ozone of a(t). Determining the values α_0, ..., α_k from (2) allows the computation of a(t). The term "regression integral" comes from the continuous analog of Equation (4):

$$M = c + \int a(t)\ H(t)\ dt,$$

where the integral is evaluated over the time interval during which the variable H(t) is observed. In essence the method permits us to determine the effect on maximum O_3 of a unit change in any predictor variable (e.g., NMHC or wind direction) at any time prior to the ozone maximum.

Eight hourly averages from 6 a.m. through 1 p.m. for the entire 20-day period were used to determine distribution coefficients. From the results of the curve fitting, it was determined that only second order polynomials were necessary. Variables used for predictors included non-methane hydrocarbons, nitric oxide, nitrogen dioxide, and wind direction. It was decided to test this method using maximum ozone values from Site 3 and predictor values from Site 2. It was thought that this procedure might yield some information about transport of ozone and precursors from Site 2 to Site 3. However, since the ozone data from the two sites are highly correlated ($R = 0.9$), ozone values from either site could be used. Stepwise multiple regressions were run with each set of distribution parameters as predictors. The stepwise method chooses the variable on the first step which best explains maximum ozone by itself. On the next step, the "best" variable to use with the first is chosen, and so on. The word "best" is in quotations since the method is only an approximation to the optimum solution. The results of these regression analyses are presented in Table 25.

In Table 25, α_0, α_1, and α_2 are, respectively, the regression coefficients of the constant, linear, and quadratic components of the 6 a.m. to 1 p.m. distribution for each variable. The entries in the "significance to enter" column show the significance level of the coefficient of the variable brought into the regression at each step. Examination of Table 25 shows that the wind direction and nitrogen dioxide distributions have the most significant impact on maximum ozone.

The orthonormal polynomials f_0, f_1, and f_2 used in the above calculations are given by

$$\begin{aligned} f_0(t) &= .3540 \\ f_1(t) &= .1543t \\ f_2(t) &= .07715t^2 - .4050 \,, \end{aligned}$$

where t is measured from the midpoint of the observation interval. Since the observation interval is compressed by averaging the 6 a.m. to 1 p.m. values, the length of the observation interval is 7 hours. Hence the 6 a.m. average corresponds to $t = -3.5$, the 1 p.m. average to $t = 3.5$,

TABLE 25. STEPWISE REGRESSION INTEGRALS

	Significance to Enter	R	Significance of Regression
A. Maximum Ozone vs Nitric Oxide			
Step 1. $\alpha_1 = -.3114$	.214	.290	.214
Step 2. $\alpha_1 = -.2885$, $\alpha_2 = .0781$	.883	.292	.468
Step 3. $\alpha_1 = -.0043$, $\alpha_2 = .2140$, $\alpha_0 = .2544$	.785	.300	.670
B. Maximum Ozone vs Nitrogen Dioxide			
Step 1. $\alpha_0 = .7238$	.005	.602	.005
Step 2. $\alpha_0 = .8830$, $\alpha_2 = .4746$	.479	.618	.017
Step 3. significance too low to include			
C. Maximum Ozone vs Wind Direction			
Step 1. $\alpha_0 = -.6384 \times 10^{-4}$	.011	.554	.011
Step 2. $\alpha_0 = -.6574 \times 10^{-4}$, $\alpha_1 = .1151 \times 10^{-3}$	.174	.616	.017
Step 3. $\alpha_0 = -.7162 \times 10^{-4}$, $\alpha_1 = .1093 \times 10^{-3}$, $\alpha_2 = -.5149 \times 10^{-3}$	.258	.666	.026
D. Maximum Ozone vs Non-Methane Hydrocarbons			
Step 1. $\alpha_2 = -.0866$	.045	.453	.045
Step 2. $\alpha_2 = -.0912$, $\alpha_1 = -.0061$	.673	.462	.130
Step 3. $\alpha_2 = -.1200$, $\alpha_1 = -.0298$, $\alpha_0 = -.0255$	.358	.505	.182

and values intermediate are linearly interpolated between these extremes. Using the regression coefficients from Table 25 and the orthonormal polynomials, a(t), the "impact function" which describes the effect of a unit increase of a predictor variable on maximum ozone, can now be computed. Figure 25 shows the three impact functions for wind direction corresponding to Steps 1 through 3 in Table 25 C. Figure 25 A shows the case when the 6 a.m. to 1 p.m. distribution of wind direction is fit by a constant. This is an illustrative case, worth discussion in detail, as it helps clarify the significance of the impact function.

In fitting the distributions by the constant polynomial f_0, the distribution constants ρ_0 are simply multiples of the overall average of wind direction over the entire 6 a.m. to 1 p.m. period. Hence, a regression of maximum ozone against the distribution variable ρ_0 is identical to a regression against the overall average of wind direction, except for a scalar multiple of the independent variable. The impact function $a(t) = \alpha_0 f_0 = 1/8 \beta$, where β is the slope of the linear regression of maximum ozone on the overall average terms. Since in a regression equation, the slope equals the change in the depending variable given a unit increase in the predictor variable, it can be seen that $a(t) = 1/8 \beta$ equals the change in maximum ozone due to a unit increase in wind direction during the t^{-th} hour (hence the physical significance of the factor 1/8, as there are 8 hourly averages). Since the impact function is negative, increasing wind direction (in the range 0°-360°) tends to decrease maximum ozone. This is in agreement with findings, discussed earlier, that low levels of ozone are associated with westerly and northwesterly wind directions. Quantitatively, an increase of 90° over the entire period of observation will cause a decrease of .016 ppm in predicted maximum ozone. Hence, it can be seen that much information can be gained simply by a further study of maximum ozone vs wind direction averaged over the entire period. This observation is reinforced by the fact that the α_1 and α_2 terms in the maximum ozone vs wind direction analysis are less significant than the α_0 term.

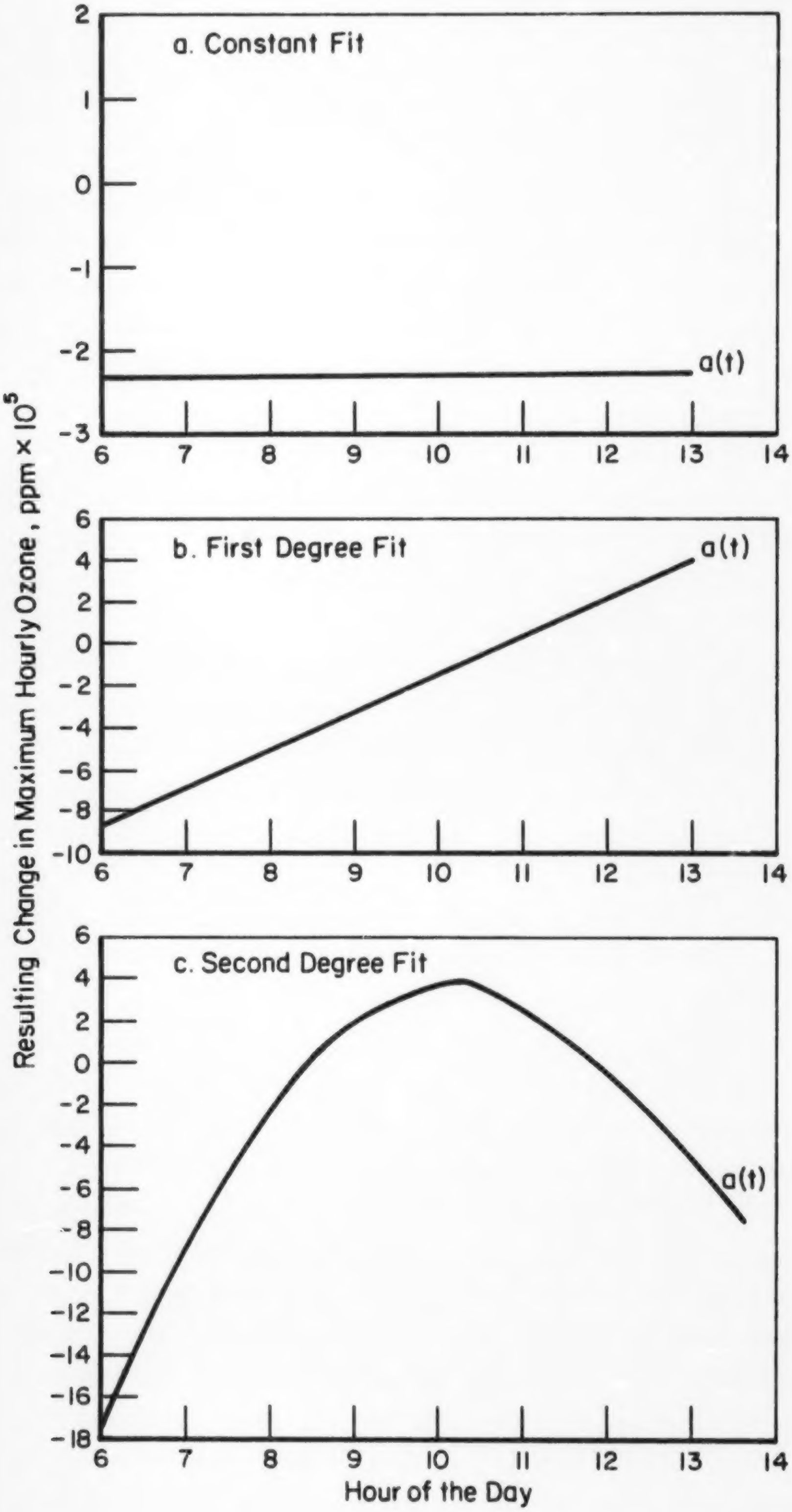

FIGURE 25. IMPACT FUNCTIONS - WIND DIRECTION ON MAXIMUM HOURLY OZONE

The impact function in Figure 25 B is constructed from both the α_0 and α_1 terms. This may be considered a "refinement" of Figure 25 A, subject to this qualification: since the significance level of α_1 is .174, there is a risk involved that there is more noise than structure in this refinement. This impact function shows a strong negative impact of increasing wind direction in the early morning hours. This could signify, for example, that a pattern is begun in the early morning hours and that shifting this pattern can have an impact in terms of transport of ozone and precursors much later on. In fact, certain patterns do seem to exist in the Dayton area, and are discussed more fully later in the report.

Figure 25 C shows the impact function obtained when the 6 a.m. to 1 p.m. averages of wind direction are fit by orthonormal polynomials up to the second degree. Again, this is a refinement of Figure 25 B, if the additional information obtained from the quadratic term is reliable. With a significance of .258, inferences obtained from this figure must be treated with caution.

Figure 26 A shows the impact function for non-methane hydrocarbons. Only the impact function for Step 1 is shown for this variable since the significance is low for the constant and linear components of the fit. The impact function shows that there is a positive impact on maximum ozone from increases in non-methane hydrocarbon in the midmorning hours. Many researchers have used the 6 a.m. to 9 a.m. average of non-methane hydrocarbons as a primary statistic in making inferences about maximum ozone. While the impact function shows a lag time, it is not entirely consistent with this view. It would appear from our data that the maximum sensitivity of peak ozone to NMHC occurs somewhat later in the morning between approximately 8-11 a.m. During this time, an increase in 1 ppmC NMHC predicts an increase of about 0.075 ppm maximum hourly ozone. A study of this kind using regression integrals should be performed on a larger data base to get a statistically more reliable idea of the relationship between maximum ozone and non-methane hydrocarbons.

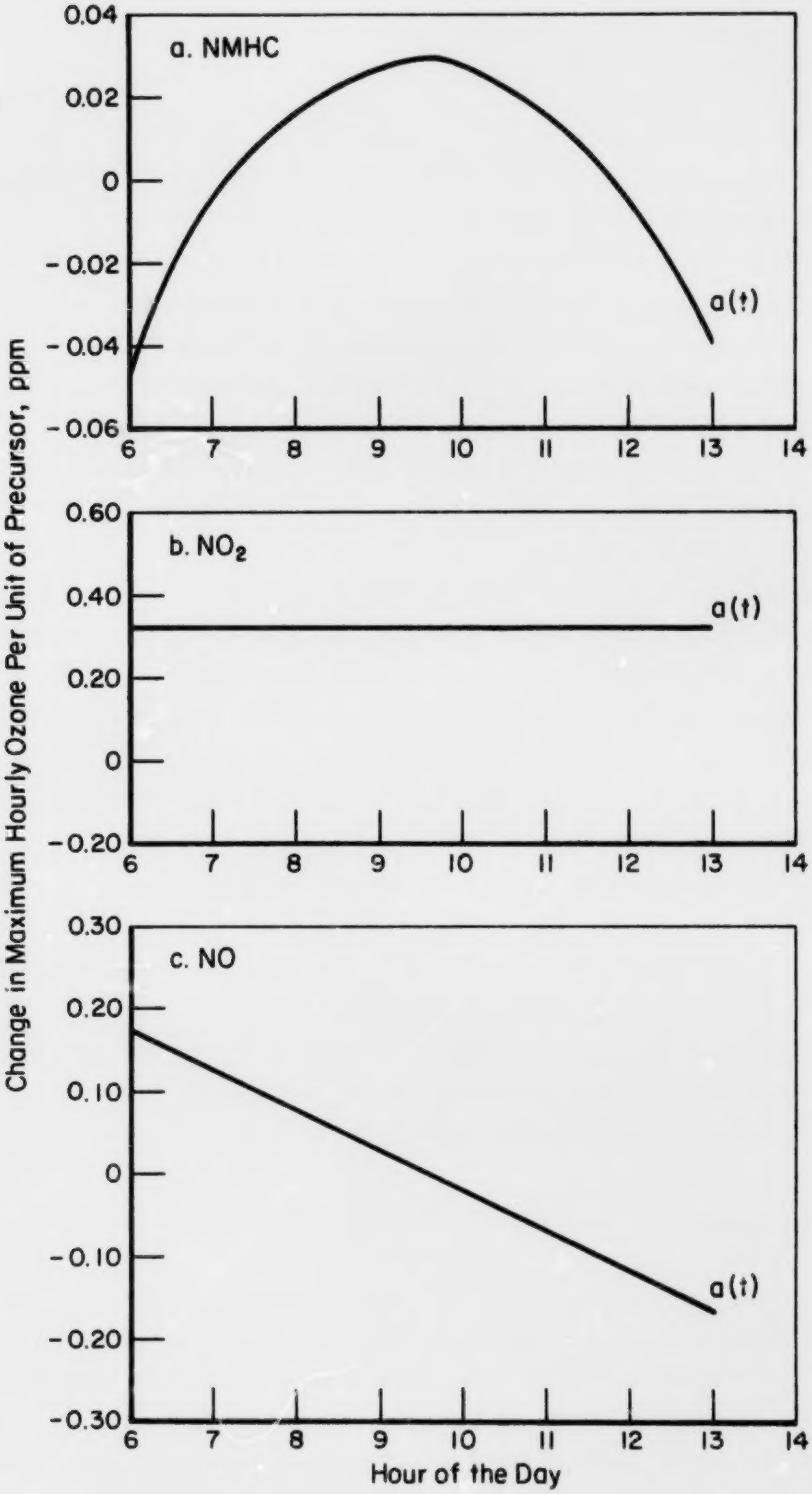

FIGURE 26. IMPACT FUNCTIONS - PRECURSORS ON MAXIMUM HOURLY OZONE

Figure 26 B shows the relationship between maximum ozone and NO_2. The only significant term in the regression integral is α_0, so the impact function is a constant. Increasing NO_2 increases maximum ozone.

Figure 26 C is the graph of the impact function of NO on maximum ozone. This impact function is less significant than the others. However, even here there is a plausible explanation for its shape. The amount of NO present early can be a guide to the NO_x level. Hence more NO implies more maximum ozone. However, later on, increasing NO tends to destroy ozone, thereby having a negative impact.

The next step in the regression integral analysis is a multivariate analysis. Using distribution parameters up to the second degree for all four variables, a multiple regression integral was formed. The results of this analysis are presented in Table 26. Using the four variables, wind direction, NMHC, NO_2, and NO, a multiple correlation coefficient of 0.86 was obtained. Thus, approximately 75 percent of the variance in our Dayton maximum ozone concentrations is explained by the regression integral. A plot of the measured maximum ozone values versus the values predicted by the regression integral is given in Figure 27. It is apparent that the predicative ability is reasonably good.

This regression integral analysis must be considered a preliminary study on a relatively small data base. However, it appears that many useful observations have been made possible by this analysis. It remains for a future study to perform this kind of analysis on a more appropriately sized data base.

Graphical Analysis of Ozone Directionality

Another means of investigating the relationship between ozone concentration and air mass movement is through the use of plots of ozone, classified according to wind direction, at the different monitoring sites. Such a graphical study of the effect of wind direction on maximum hourly average ozone is shown in Figure 28. The values plotted are the maximum hourly average ozone readings for each day versus the 6 a.m. to 2 p.m.

TABLE 26. MULTIPLE STEPWISE REGRESSION INTEGRAL MAXIMUM OZONE vs WIND DIRECTION, NO, NO_2, AND NON-METHANE HYDROCARBONS

	Variable Entered	Significance to Enter	Multiple R	Overall Significance
Step 1.	α_0 (NO_2)	.031	.602	.005
Step 2.	α_0 (Wind Dir)	.069	.692	.004
Step 3.	α_2 (Wind Dir)	.244	.722	.067
Step 4.	α_0 (NMHC)	.164	.763	.008
Step 5.	α_2 (NO)	.068	.820	.004
Step 6.	α_2 (NMHC)	.113	.856	.004

Step 6. Summary	Significance
α_0 (NO_2) = .7041	.031
α_0 (Wind Dir) = $-.2740 \times 10^{-4}$	.216
α_2 (Wind Dir) = -2591×10^{-3}	.031
α_0 (NMHC) = $-.2755 \times 10^{-1}$	.051
α_2 (NO) = .7637	.025
α_2 (NMHC) = $-.6043 \times 10^{-1}$	.113
CONSTANT = $.9443 \times 10^{-1}$	0.0

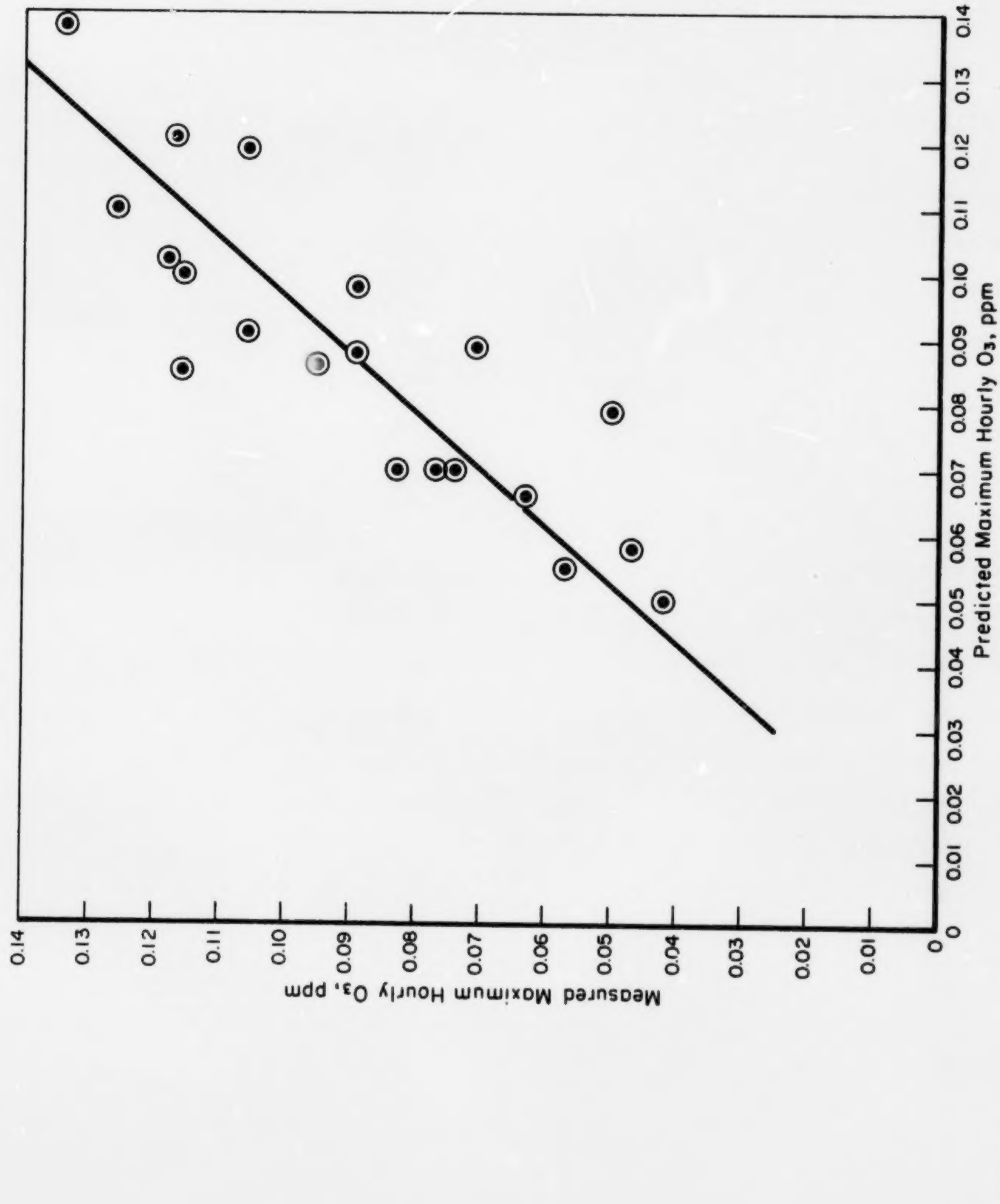
Predicted Maximum Hourly O_3, ppm
Measured Maximum Hourly O_3, ppm
0
0.01
0.02
0.03
0.04
0.05
0.06
0.07
0.08
0.09
0.10
0.11
0.12
0.13
0.14

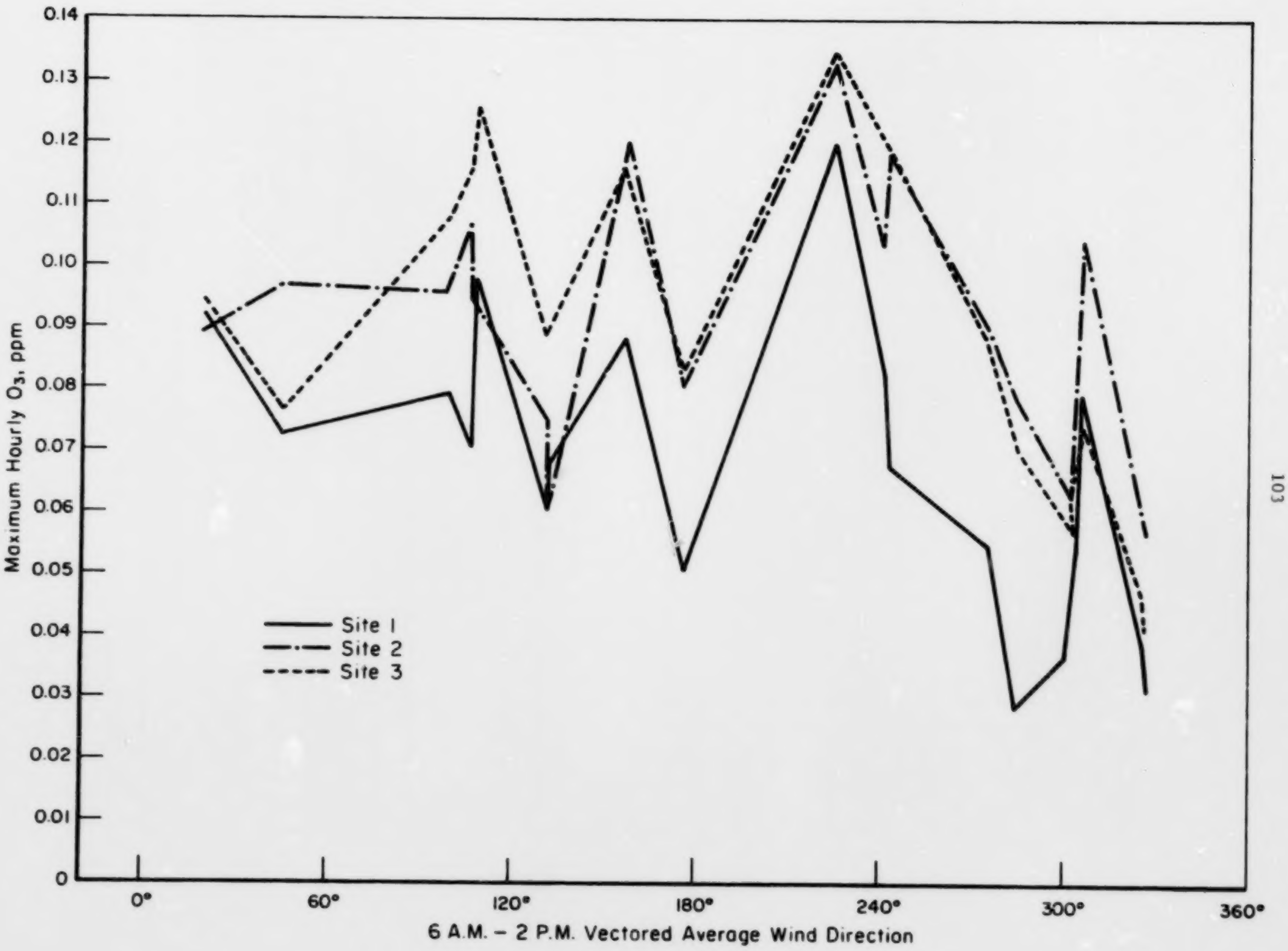

FIGURE 28. MAXIMUM HOURLY OZONE vs WIND DIRECTION

wind direction component of the corresponding daily wind velocity averages. All the data are plotted on this figure with the exception of August 11 which was rainy and overcast throughout the day. No other attempt was made to filter the data. Although not very definitive, the graph does confirm the fact that the trends in ozone concentration are similar at all three sites. It also suggests that higher maximum ozone occurs when the direction of air mass movement is less than about 240° and lower ozone at greater than 240°. A peak seems to occur at between 220°-240°. Since this is the direction of the Cincinnati urban complex, the high ozone levels may well be an indication of pollutant transport.

The information from Figure 28 was useful in making a decision to classify wind direction readings into four sectors: 60°-150°, 150°-240° 240°-330°, and 330°-60°. Using these sectors, composite ozone plots were generated. The 6 a.m. through 2 p.m. wind velocity averages were vector averaged, and the wind direction component was used to determine with which sector to tag each day. For all days tagged with Section 1, a computation was made of the ozone averages for each hour at a given site. A composite ozone graph was then plotted. This procedure was repeated for Sectors 2 through 4; then for each site, these four curves, appropriately labeled, were plotted on the same graph for comparison. This was done for all six sites.

Another set of graphs was made differing from the above set only in the specifications of the wind direction sectors. For this second set, the four wind direction sectors were chosen at 75°-345°, and 345°-75°. There were two motivating factors for making this 15° shift of the wind direction sectors. One was that the sector 165°-255° is symmetric about 210°, the approximate angle along which the sites lie, and the other was to test the sensitivity of the graphs to selection of sectors.

To complete this graphical analysis of ozone vs wind direction two more sets of graphs were made. These sets differ from the first two only in that wind direction is vector averaged over the 6 a.m. to 11 a.m. averages rather than from 6 a.m. to 2 p.m. Again, this is a kind of sensitivity analysis, and also was motivated by the dominating influence of early morning wind shown in the regression integral analysis.

In general, the sensitivity of the composited ozone profiles to the 15° shift in wind direction sectors and the use of 6 a.m.-11 a.m. wind direction data were very low. Only very minor differences could be discerned among the four different sets of plots. For this reason we will only discuss the first set of plots described above, where the 6 a.m. to 2 p.m. wind direction component of the average wind vector was used, and each day was classified according to wind direction as follows:

Sector 1 - wind from 60°-150°
Sector 2 - wind from 150°-240°
Sector 3 - wind from 240°-330°
Sector 4 - wind from 330°-60°.

A map of the region showing this sector breakdown is included as Figure 29. The Columbus area lies within Sector 1 while the Cincinnati urban complex is situated in Sector 2.

The wind direction classified average ozone profiles are presented for each of our five spatially separated ground stations in Figures 30 A-E.

The results from the Miamisburg site are shown first in Figure 30 A. It is apparent from this figure that higher ozone levels at Miamisburg are associated primarily with wind from Sector 4 (330°-60°). Since wind from Sector 4 blows across the city of Dayton prior to arriving at Miamisburg, we can surmise that the much higher O_3 levels when the wind is from that direction result from movement of ozone and/or precursors from Dayton to Miamisburg. We might expect that if Dayton were having a major influence on the O_3 levels of the communities and monitoring stations surrounding it then the wind direction dependence would vary from site to site (since Dayton is located between the sites). If, on the other hand O_3 were moving into the Dayton area en mass from some source outside the region, then the wind direction dependence of the ozone concentration should be similar at each site. Obviously both of these processes involve pollutant transport. Transport from Dayton to its surrounding communities can be thought of as short range, while movement of pollutants from Columbus or Cincinnati into the Dayton area

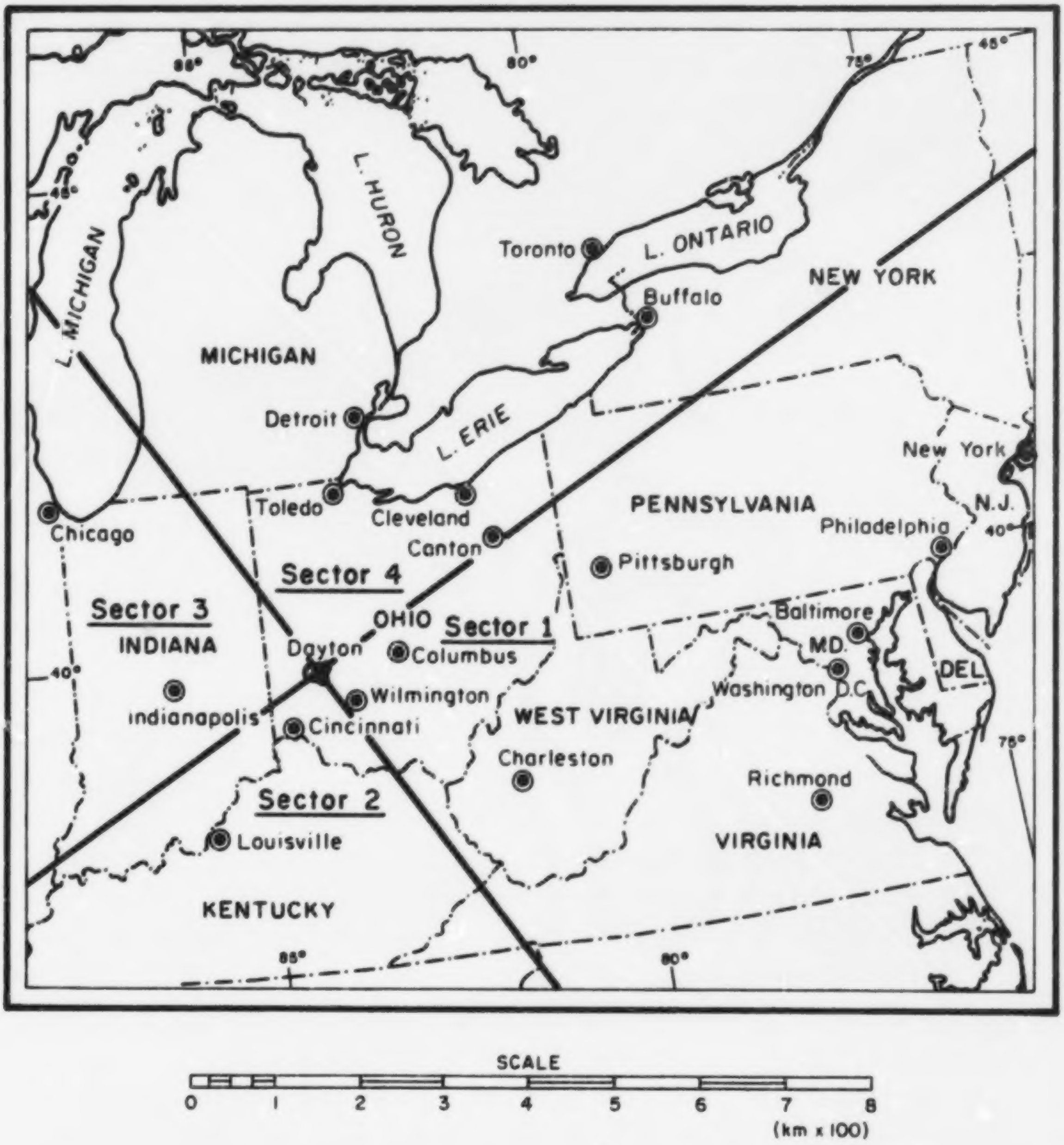
L. MICHIGAN
L. HURON
L. ONTARIO
L. ERIE
MICHIGAN
NEW YORK
PENNSYLVANIA
OHIO
INDIANA
WEST VIRGINIA
VIRGINIA
KENTUCKY
MD.
DEL
N.J.
Toronto
Buffalo
Detroit
Toledo
Cleveland
Canton
Chicago
Pittsburgh
New York
Philadelphia
Baltimore
Washington D.C.
Dayton
Columbus
Wilmington
Cincinnati
Indianapolis
Charleston
Richmond
Louisville
Sector 1
Sector 2
Sector 3
Sector 4
85°
80°
75°
45°
40°
SCALE
0
1
2
3
4
5
6
7
8
(km x 100)

FIGURE 29. STUDY AREA DIVIDED INTO WIND SECTORS

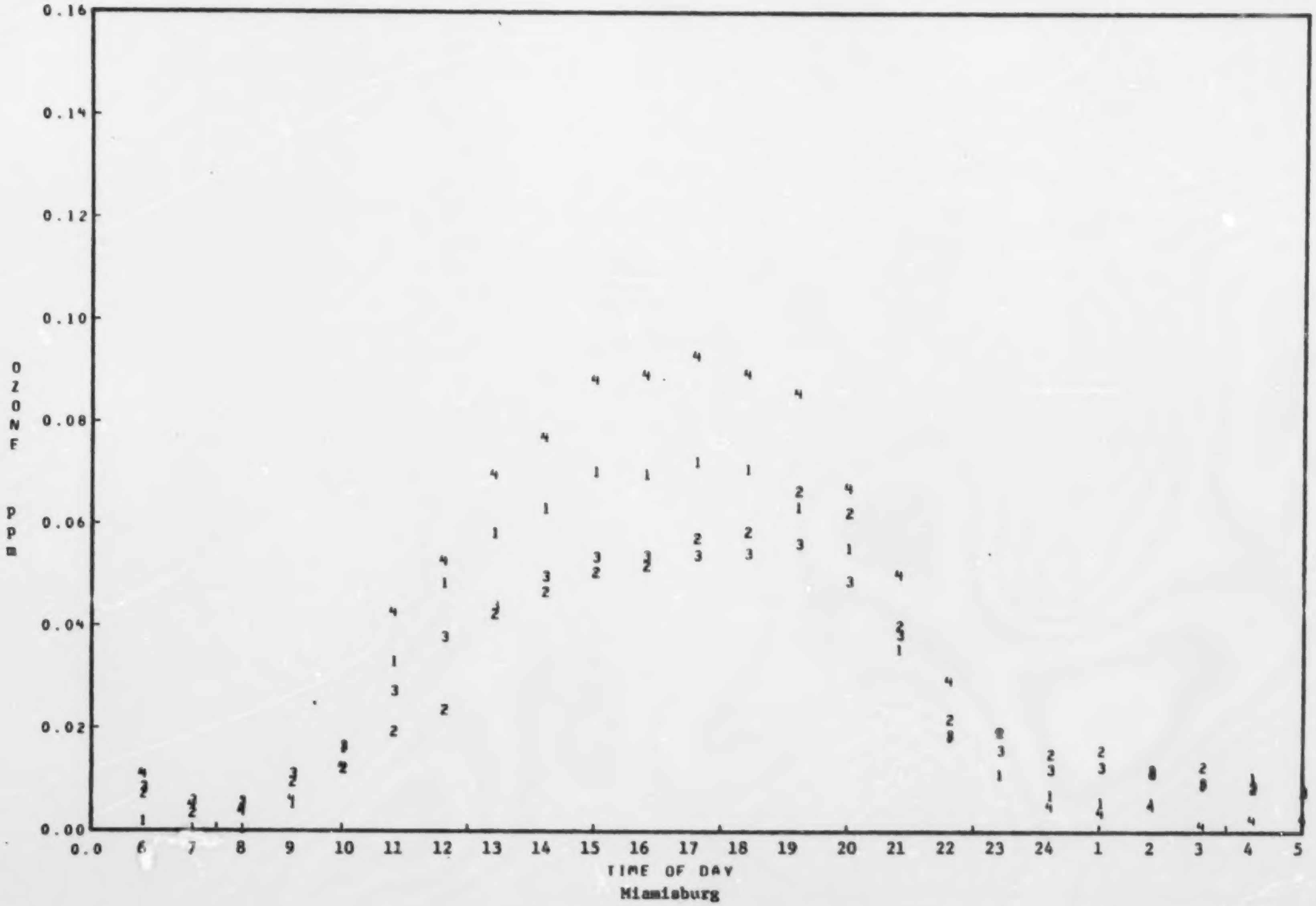

FIGURE 30 A. OZONE PROFILES BY WIND DIRECTION

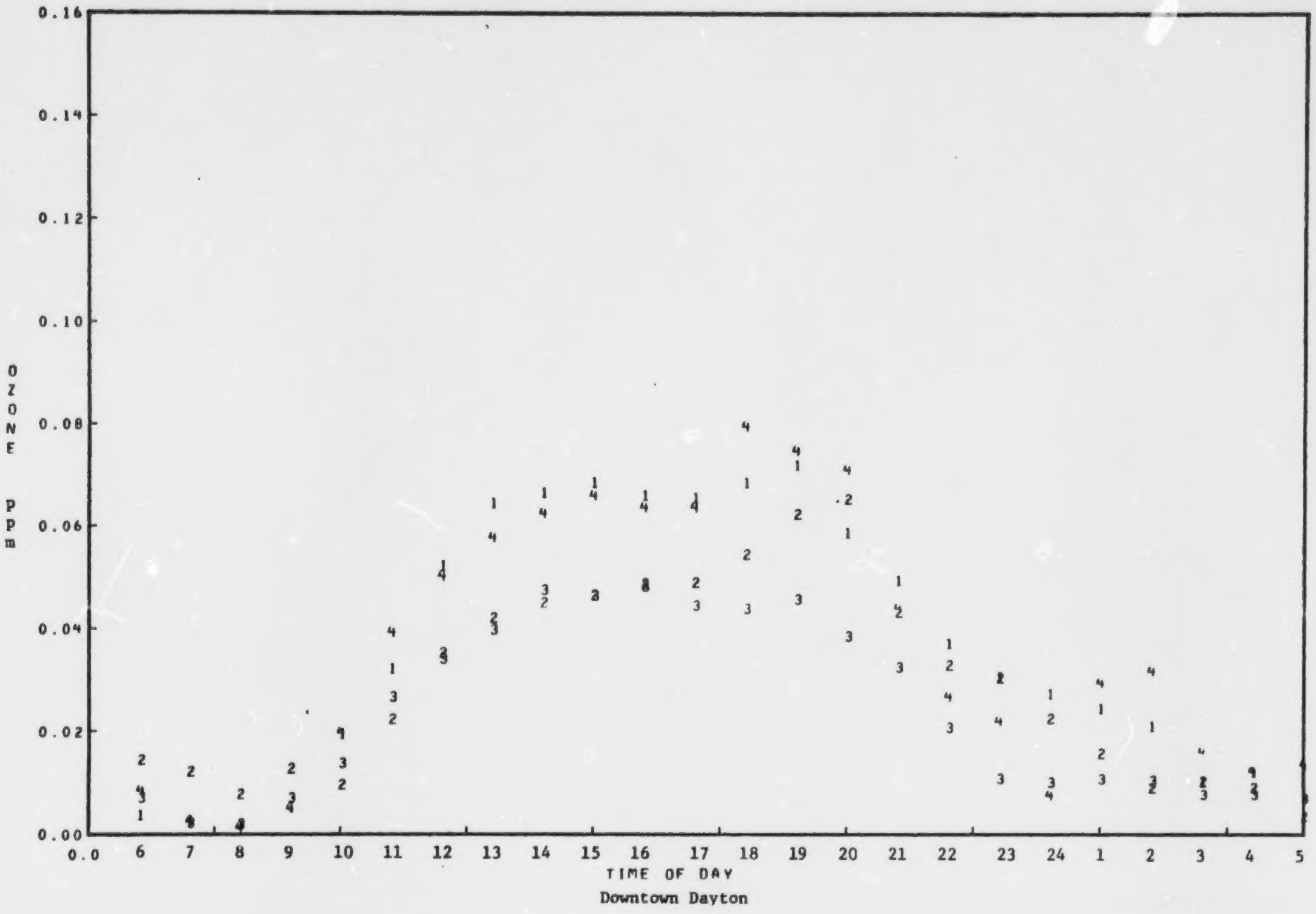

FIGURE 30 B. OZONE PROFILES BY WIND DIRECTION

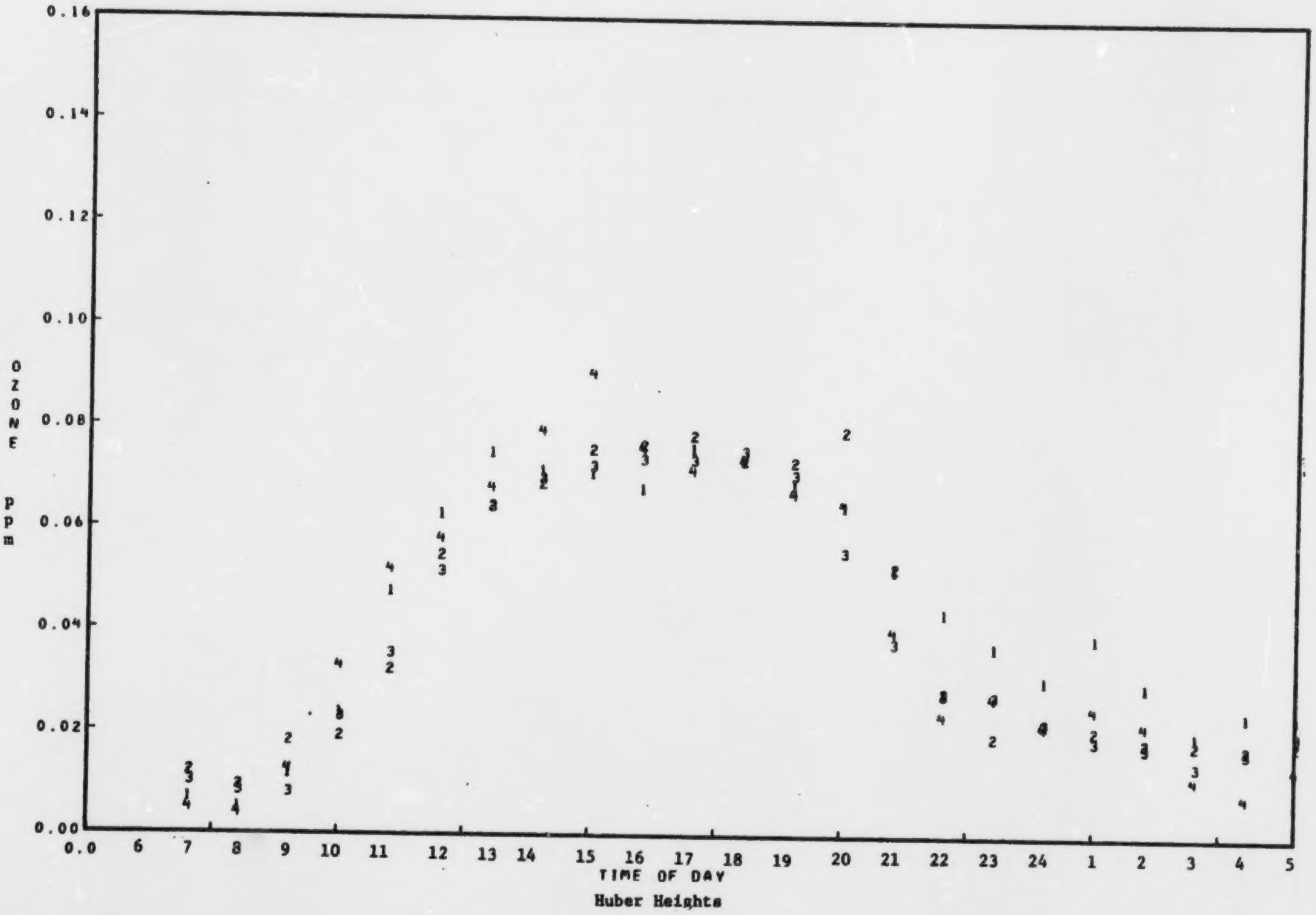

FIGURE 30 D. OZONE PROFILES BY WIND DIRECTION

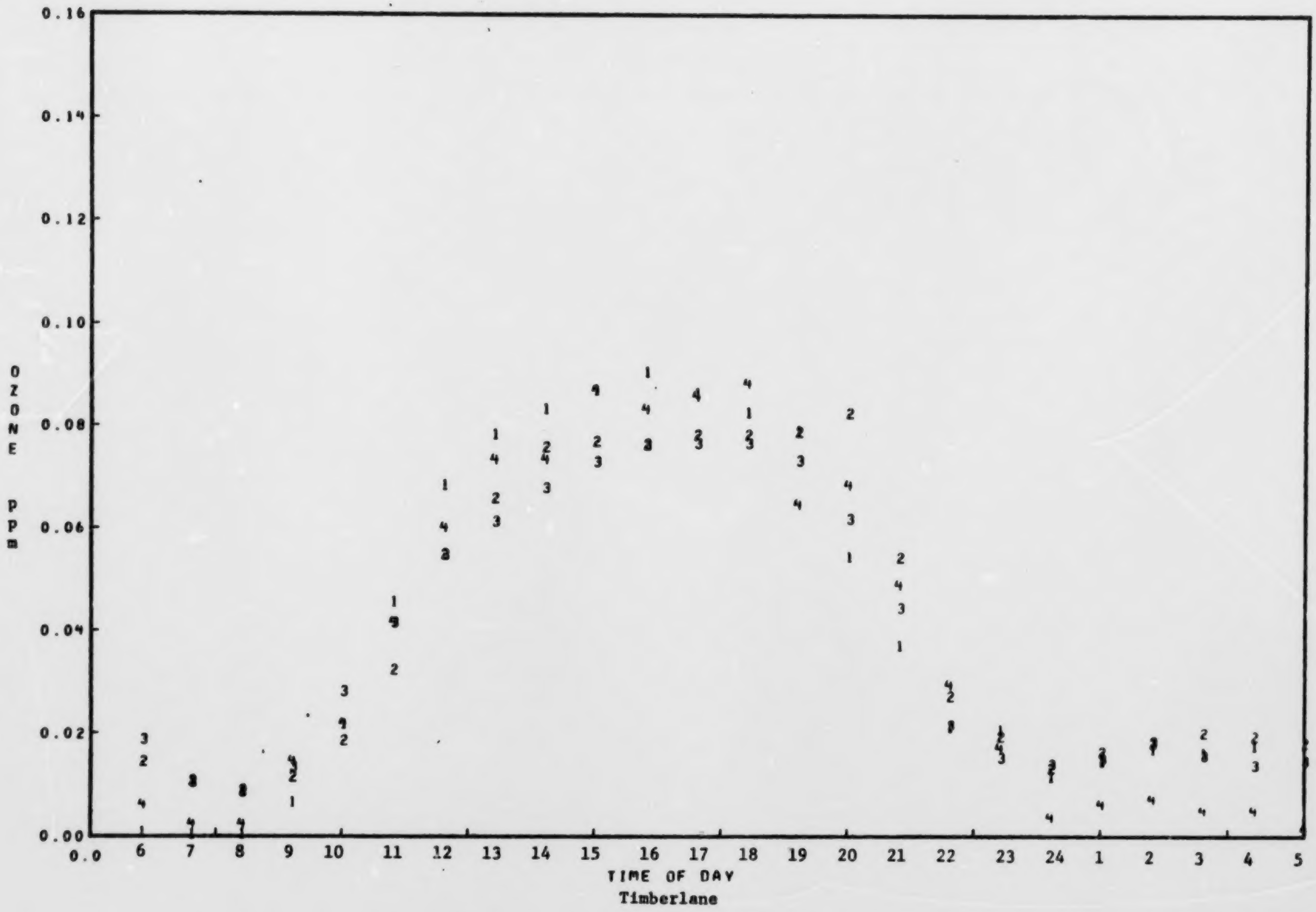

FIGURE 30 C. OZONE PROFILES BY WIND DIRECTION

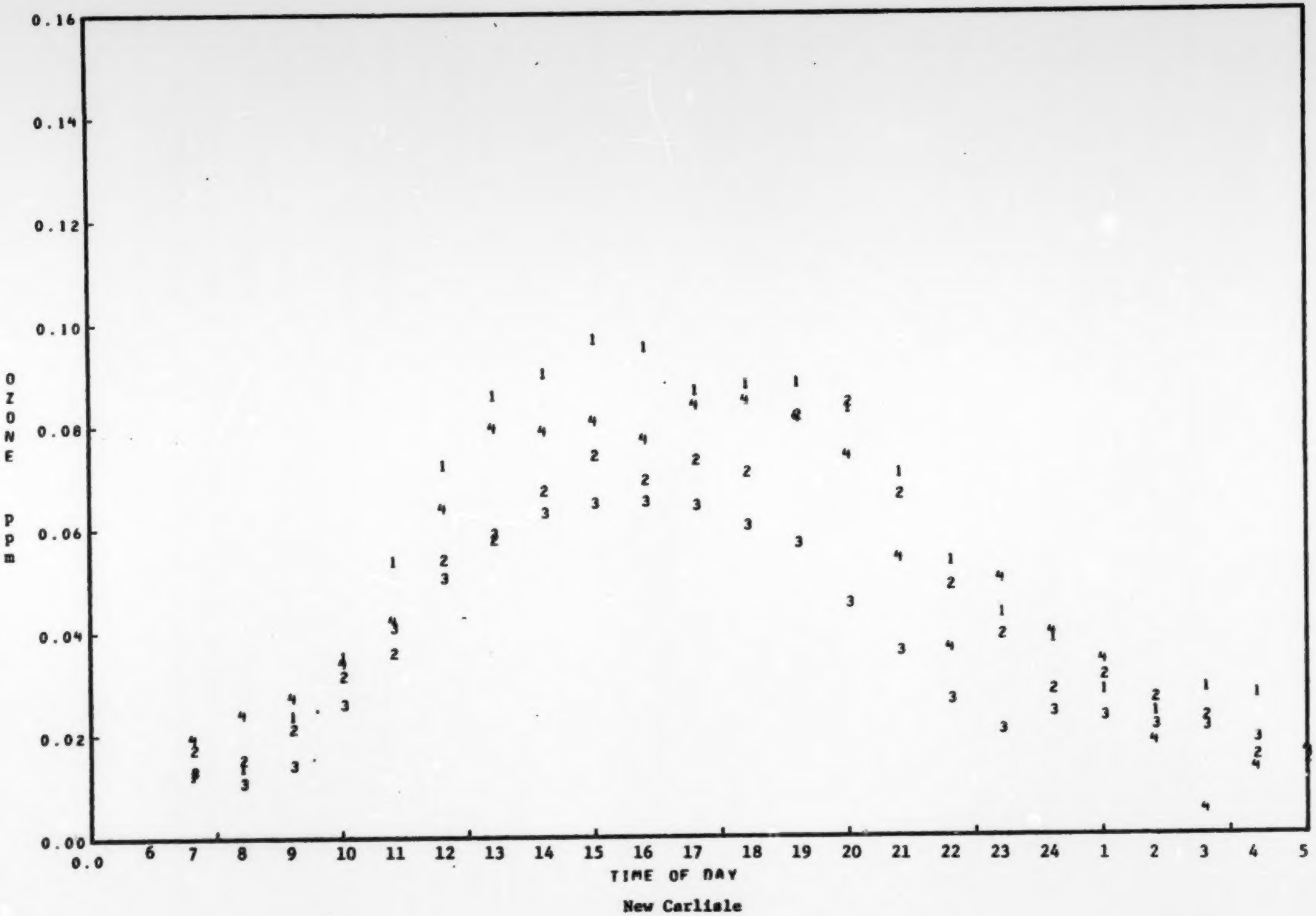

FIGURE 30 E. OZONE PROFILES BY WIND DIRECTION

is transport on a somewhat larger scale. In addition, long-range transport, transport over hundreds of miles, may also be occurring. Unfortunately, if all of these processes are important under certain conditions, as we believe they are, and in addition local generation of ozone occurs (either from natural or anthropogenic sources), then we should expect a mixture of effects which will tend to obscure the sources of ozone. Our results suggest that each of these sources of ozone can be important in the Dayton area, depending on the prevailing meteorological conditions.

Returning to Figure 30 A, we observe that wind from Sector 1 yields the second highest average ozone profile. Sector 1 includes winds from Columbus and also, to some extent, winds which pass over Dayton prior to arriving in Miamisburg. Winds from Sectors 2 and 3 both yield relatively low ozone values during most of the day. However, the Sector 2 profile differs from the other three in general shape. The Sector 2 profile increases during the late morning and afternoon hours and does not peak until seven o'clock in the evening. This phenomenon can be explained by ozone and precursors which were generated in the Cincinnati area early in the day arriving in Miamisburg near sundown. Thus there is evidence in this figure for pollutant transport southwestward (from Dayton to Miamisburg) and northeastward (Cincinnati to Miamisburg).

The composite ozone profiles from the downtown Dayton station (Figure 30 B) show that up until approximately 5:00 p.m., winds from Sectors 1 and 4 gave similar high levels of O_3 while Sectors 2 and 3 yielded low ozone. Since our monitoring station was located toward the southwest corner of the Dayton urban area, winds from the north and east will pass over much of Dayton before arriving at our monitoring stations within the city, and are therefore likely to contain higher concentrations of ozone and other pollutants than winds from the other two sectors, at least during the early part of the day. During the late afternoon and evening there has been sufficient time for pollutants from Columbus, Cincinnati, etc., to reach Dayton, and the wind direction pattern set up earlier in the day could vary. In fact, we note in Figure 30 B that only the Sector 3 ozone profile appears "normal", i.e., reaches a peak in midafternoon and decreases thereafter. Sector 2 ozone shows the greatest effect, with average O_3 rising sharply after 5 p.m. and reaching its maximum at 8 p.m. Such elevated ozone values so late in the evening certainly indicate transport, most probably from the Cincinnati area.

The composited ozone profiles from the Timberlane station are shown in Figure 30 C. The main point to be made from the Timberlane data is that the directionality is becoming much less pronounced. Although Sectors 1 and 4 still yield higher average levels of O_3, the differences among the four sectors has been sharply reduced.

This trend toward nondirectionality continues at the Huber Heights site shown in Figure 30 D, where O_3 is almost equivalent from any of the four wind direction sectors. It would appear that this site is so located that the ozone sources from the four sectors are relatively equally distributed around it. Such a uniform distribution would explain the nondirectional nature of the ozone profiles. The nondirectionality of O_3 at Site 2 was discussed earlier in relation to the Site 2 "ozone rose".

The ozone distribution classified according to wind direction for our New Carlisle station is shown in Figure 30 E. While wind from Sector 3 continues to yield low concentrations of ozone, the Sector 1 wind direction becomes the most important in terms of ozone yield. The ozone profiles from wind direction Sectors 1, 2, and 4 all show dual peaks, suggesting the possibility of transport. Both Columbus and the smaller city of Springfield, Ohio, lie to the east of New Carlisle and could be responsible for the secondary ozone peak from Sector 1. The high evening O_3 associated with Sector 2 could be due to transport from either Dayton or Cincinnati. The reason for the smaller and earlier secondary peak with Sector 4 winds is unknown at this time.

In order to summarize this graphical analysis of the Dayton ozone data, it is instructive to view the data in a slightly different format. In this regard, we have replotted the ozone data in order to compare two sites on each graph, with each different graph representing a single wind direction sector. The first four plots, Figures 31 A-D, show the composite O_3 profiles for both Miamisburg and New Carlisle

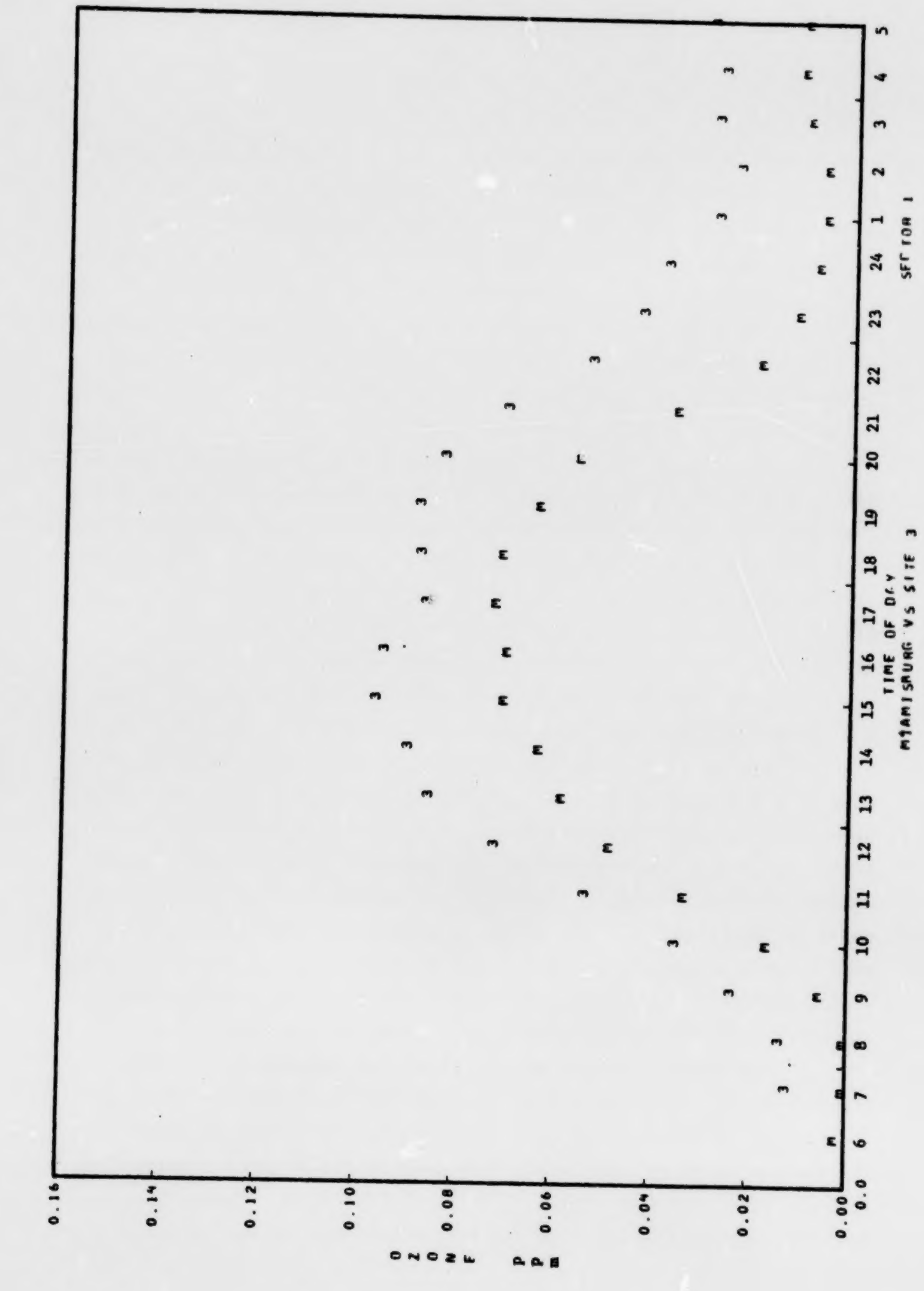

FIGURE 31 A. SITE-TO-SITE OZONE PROFILES BY WIND SECTOR

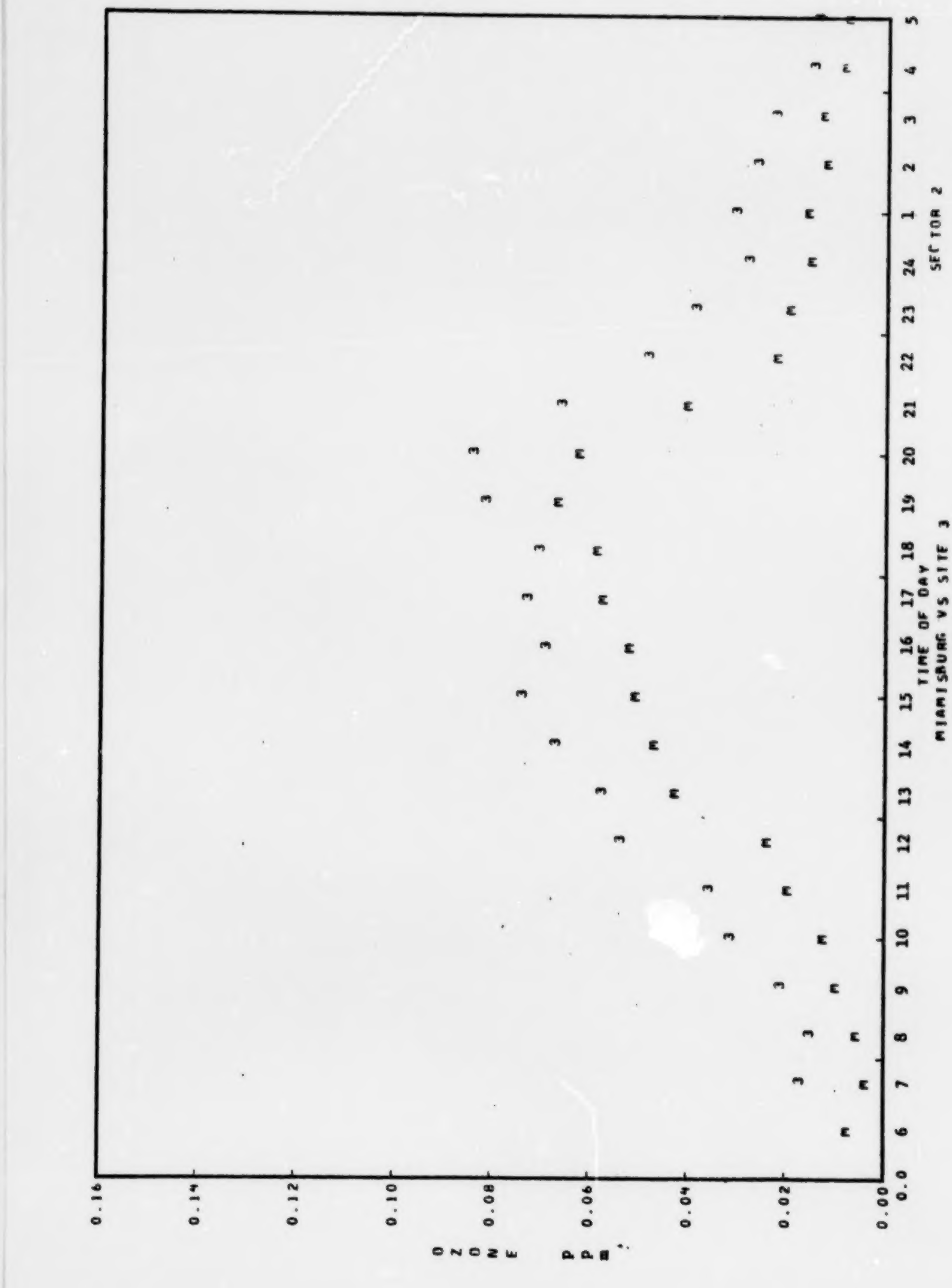

FIGURE 31 B. SITE-TO-SITE OZONE PROFILES BY WIND SECTOR

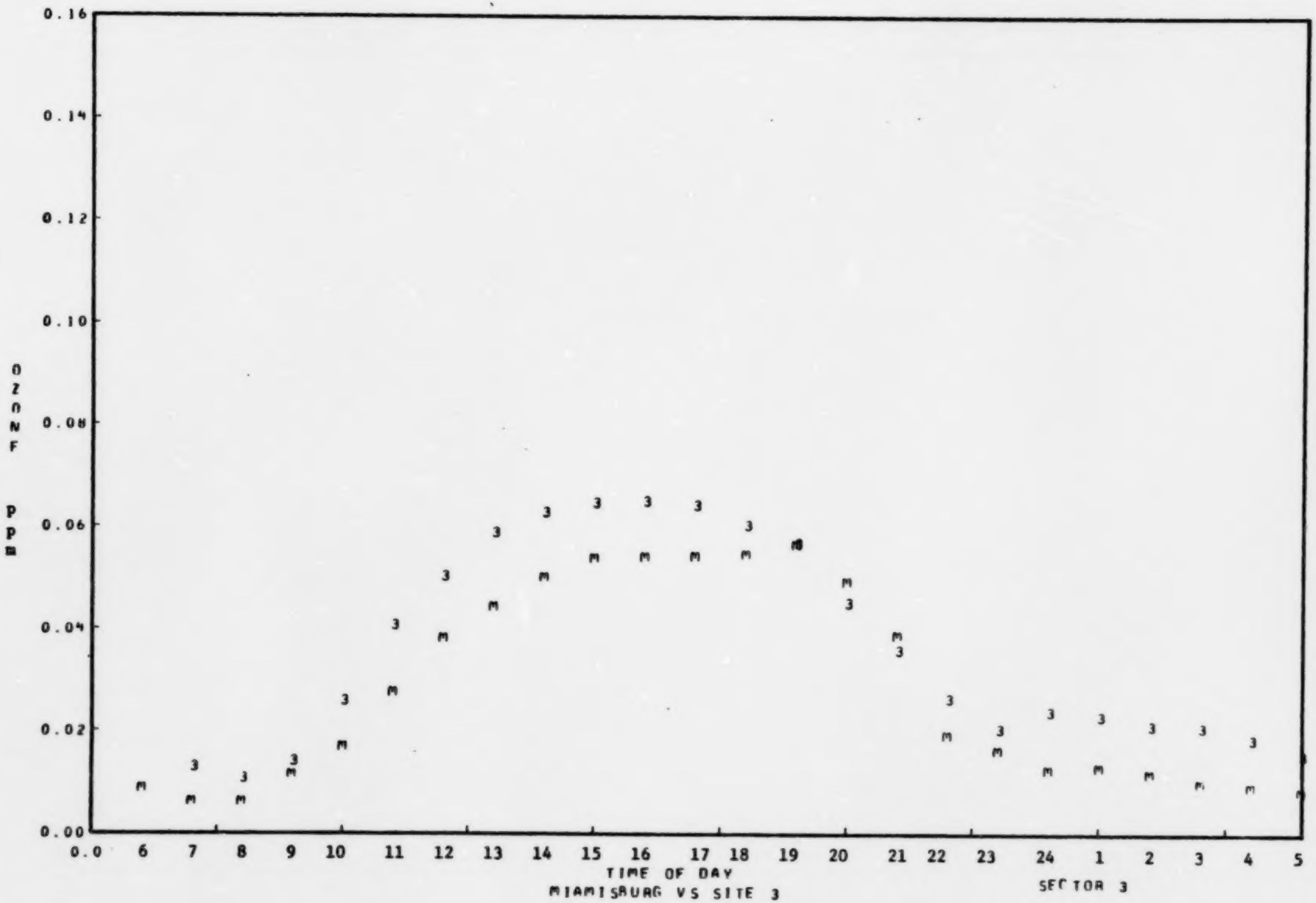

FIGURE 31 C. SITE-TO-SITE OZONE PROFILES BY WIND SECTOR

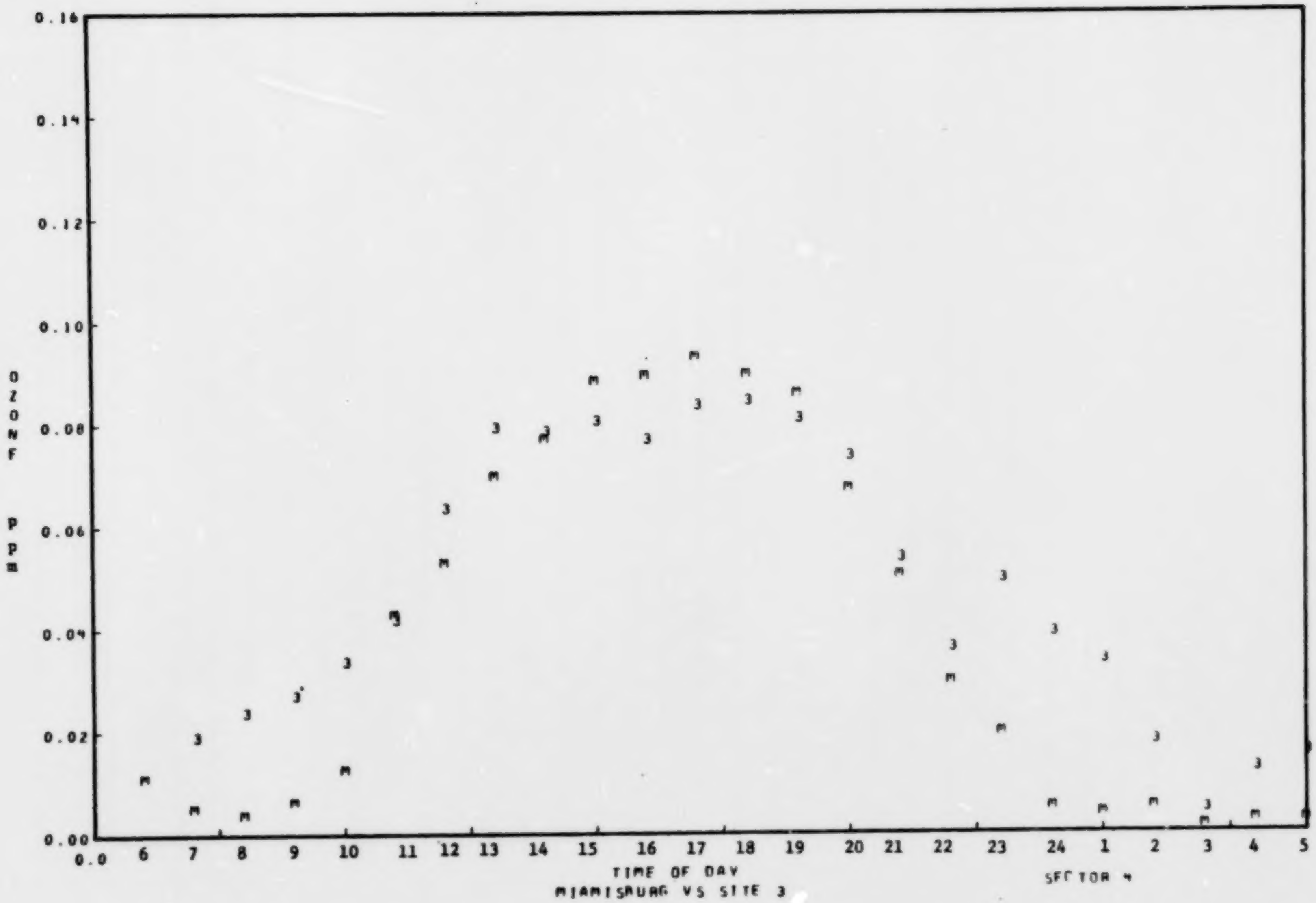

FIGURE 31 D. SITE-TO-SITE OZONE PROFILES BY WIND SECTOR

for each of the four wind direction sectors respectively. The Miamisburg and New Carlisle sites were selected because they are the furthest apart physically and they are situated on opposite sides of the city of Dayton; hence their ozone profiles might be expected to show the most pronounced differences in terms of wind direction dependence.

Figure 31 A displays the composite ozone profiles for Miamisburg (M) and Site 3 (3) when the wind direction component of the averaged 6 a.m.-2 p.m. wind vectors is from Sector 1 (60°-150°). It is clear that Site 3 exhibits higher ozone than Miamisburg at all hours of the day when the average air mass movement is from Sector 1. We suspect that Miamisburg experiences lower levels of O_3 than New Carlisle because of the much greater emission of nitric oxide in the Miamisburg area. The continuously emitted NO reacts rapidly with O_3 to lower the average concentration of O_3. This explanation is partially confirmed by the observation that O_3 drops essentially to zero at night and in the early morning in Miamisburg but remains near 20 ppb in New Carlisle during this same period. There is obviously a stronger O_3 sink in Miamisburg than in New Carlisle, and this sink is most probably reaction with NO. The Miamisburg profile exhibits a broad ozone maximum during the afternoon. The Site 3 profile on the other hand, shows a definite secondary ozone peak occurring at approximately 7 p.m. With winds from Sector 1 and this secondary O_3 peak occurring so late in the evening, we must suspect transport of ozone or its precursors from the Columbus area as the source of the second maximum. Since both the first and second O_3 maxima are above the Federal ozone standard, the source of ozone in both cases is extremely important. With average wind speeds of 4-5 mph, the 6-9 a.m. Columbus air mass should arrive in the vicinity of Site 3 at approximately 7 p.m. We suggest that transport of the polluted early morning Columbus air mass, with ozone generation occurring enroute, may well be the source of the evening O_3 peak. Specific instances of this type of air mass movement will be discussed in detail as part of the review of individual study days later in this report.

The plot of Miamisburg and New Carlisle ozone profiles associated with Sector 2 wind directions is shown in Figure 31 B. Once again the

New Carlisle O_3 values are always higher than Miamisburg. The important feature of this plot however, is the fact that ozone peaks so late in the evening at both sites. The maximum ozone occurs in Miamisburg at approximately 7 p.m. and in New Carlisle an hour later at 8 p.m. This kind of behavior, where sites both upwind and downwind of Dayton are affected, strongly suggests that ozone is moving into the region from some outside source. Since the wind is from Sector 2, the Cincinnati urban complex is indicated. The fact that the O_3 maximum reached New Carlisle approximately an hour after Miamisburg further suggests discrete air mass movement.

The ozone profiles for wind from Sector 3 are shown in Figure 31 C. The only noteworthy features of these plots are that Site 3 again records higher ozone than Miamisburg and that ozone at both sites is lower than when the wind is from the other three wind direction sectors. This, of course, is in agreement with the results of the statistical and graphical analyses presented earlier.

Figure 31 D shows the ozone profiles for wind from Sector 4. The most obvious difference between this figure and the other three just presented is the reversal of the two sites during the afternoon in terms of ozone concentrations. With winds from the northerly direction, the Miamisburg site experiences higher peak levels of ozone than New Carlisle. This no doubt reflects the fact that Dayton air can affect Miamisburg when the wind is from the north. It is very likely that this reversal is due to short-range transport. It must be noted that only when the winds are from Sector 4 does the composite ozone at Miamisburg exceed the Federal standard.

A second series of plots of the type just discussed are presented in Figures 32 A-D and will be mentioned only briefly. This second set of graphs compares the Huber Heights and New Carlisle ozone profiles for the four different wind sectors. The Sector 1 plot of Figure 32 A shows Site 3 ozone higher than Site 2. The New Carlisle profile, and to a less extent the Huber Heights curve, shows a secondary

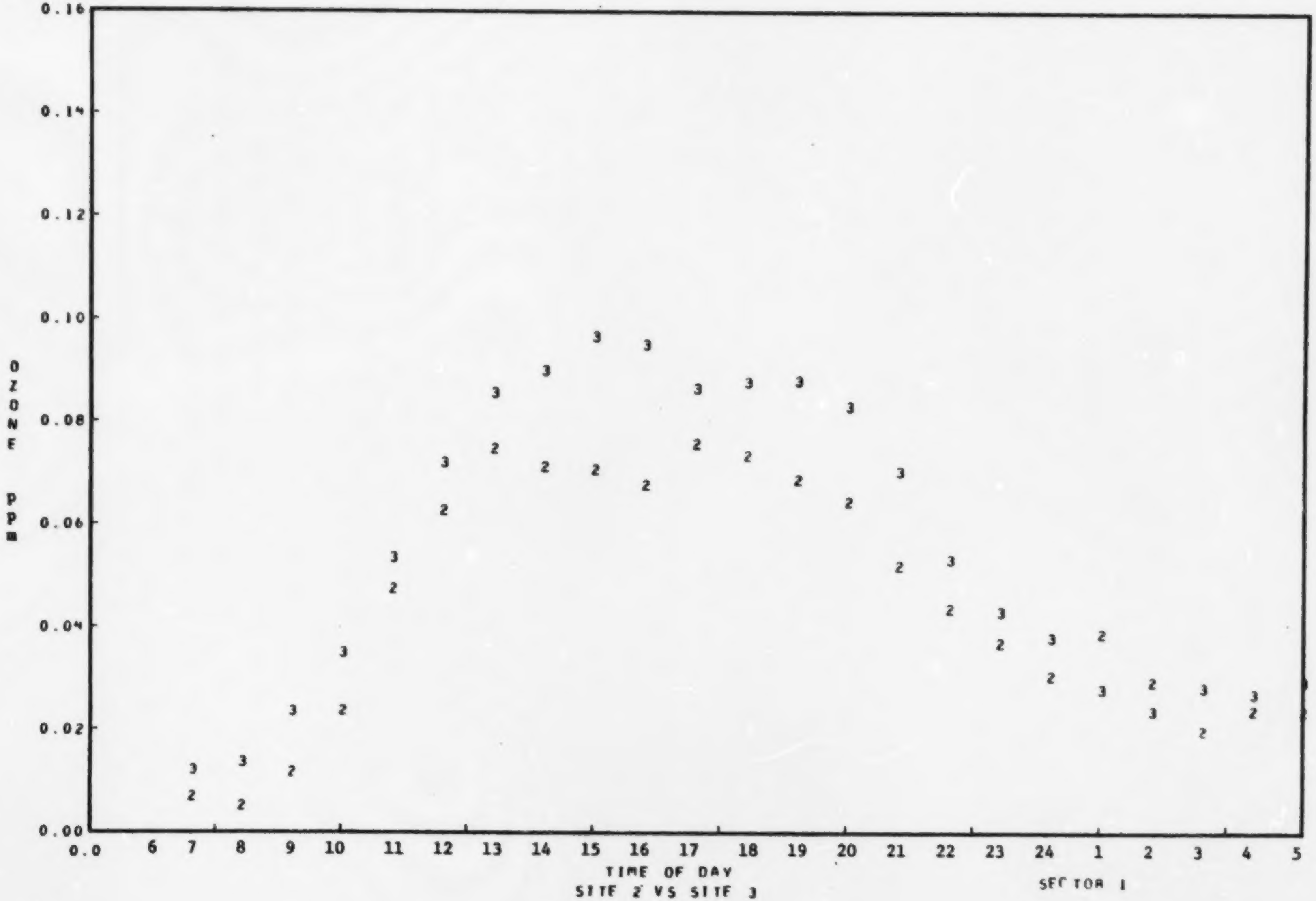

FIGURE 32 A. SITE-TO-SITE OZONE PROFILES BY WIND SECTOR

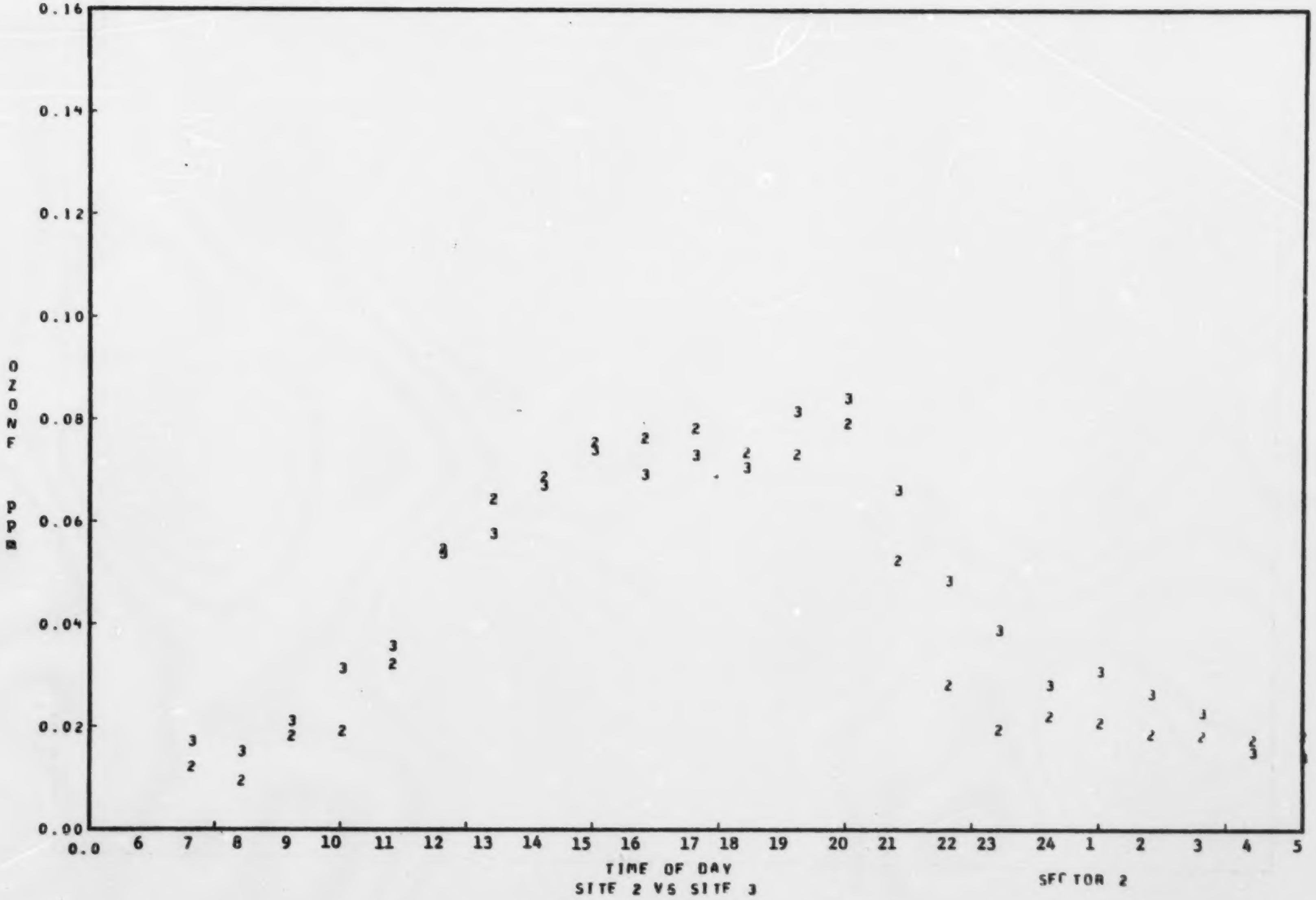

FIGURE 32 B. SITE-TO-SITE OZONE PROFILES BY WIND SECTOR

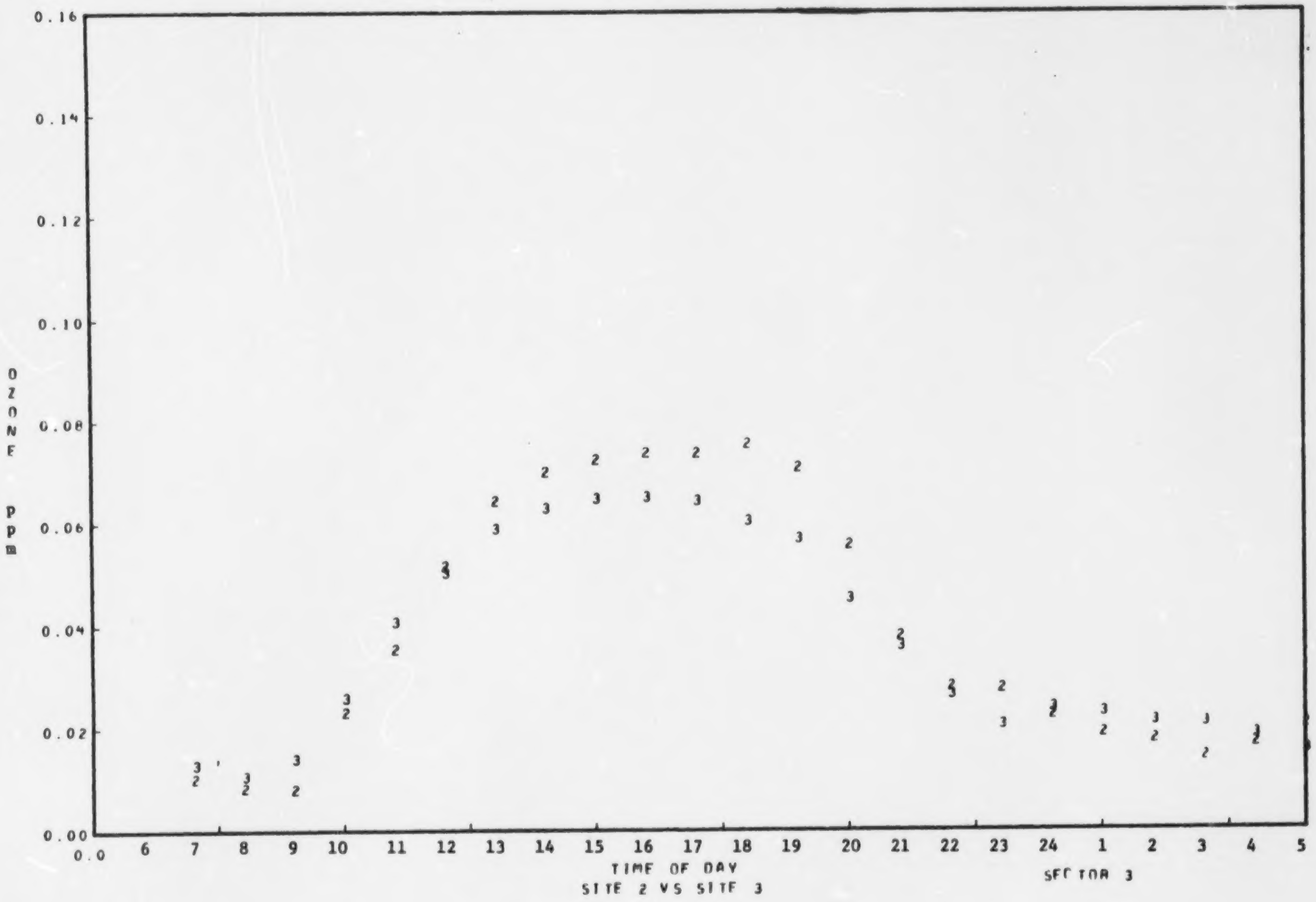

FIGURE 32 C. SITE-TO-SITE OZONE PROFILES BY WIND SECTOR

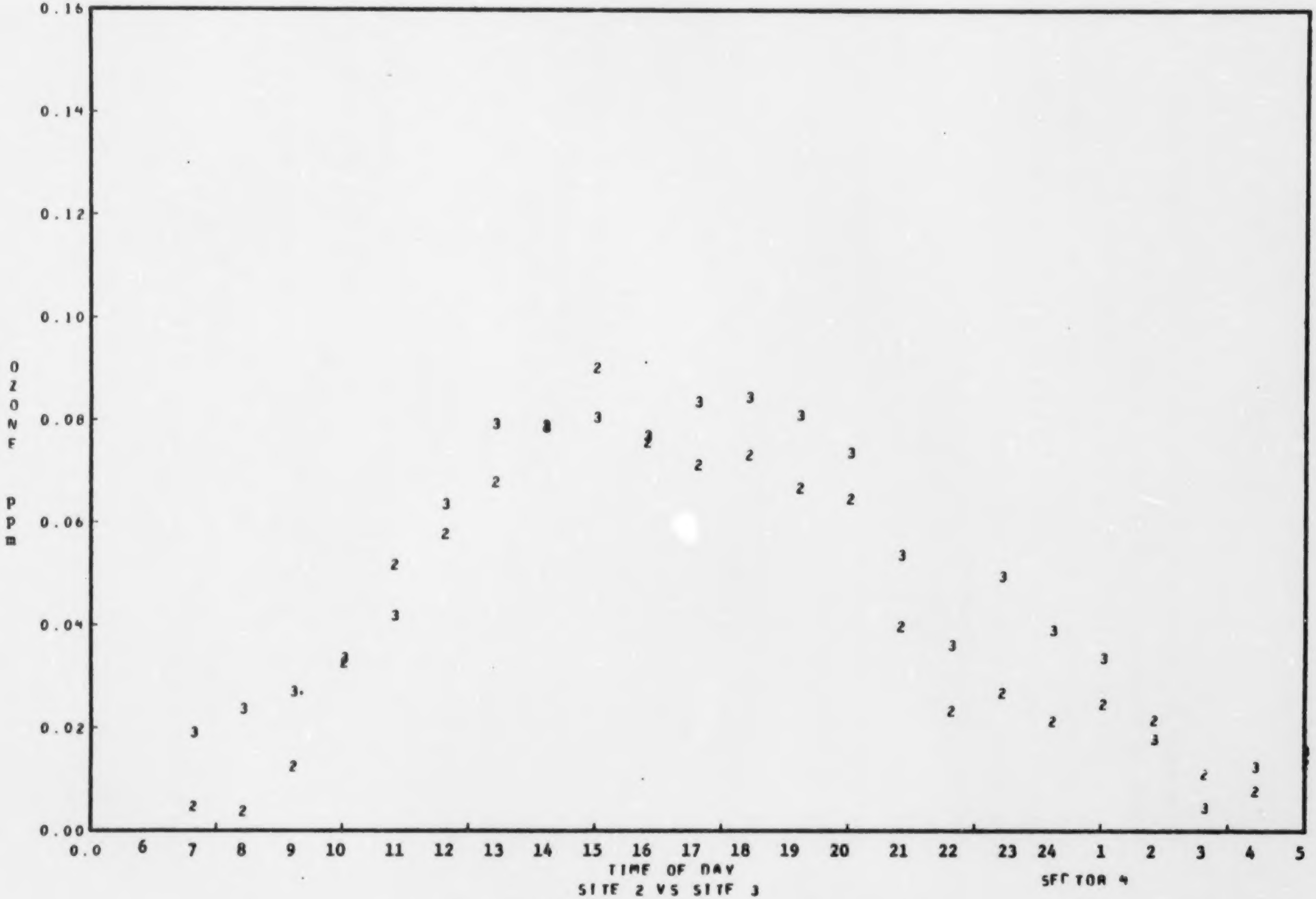

FIGURE 32 D. SITE TO SITE OZONE PROFILES BY WIND SECTOR

ozone peak during the evening hours which we have mentioned earlier in regard to pollutant transport from the Columbus area.

When the wind is from the sourtherly direction, as in Figure 32 B, the two ozone profiles are quite similar, with both showing peak ozone values occurring at about eight o'clock at night. As we have pointed out previously, such behavior suggests transport of ozone from a moderately distant source, presumably the Cincinnati area.

The ozone profiles associated with winds from Sectors 3 and 4, are shown in Figures 32 C and D. Aside from Sector 3 winds being associated with generally lower levels of O_3 than other wind directions, these two figures offer little new information.

Analysis of the Dayton Ozone Data by an Interaction Method

Another method used to study the ozone distribution is the Automatic Interaction Detector (AID) program developed by Morgan and Sonquist(10). This computer program uses a binary splitting algorithm which successively divides the data into two groups such that the error sum of squares of the dependent variable is minimized at each split. The result of this procedure is summarized in a binary tree in which each node in the tree represents a set of observations with a particular combination of values of the predictor variables. The AID method is an empirical means of searching for structure in data, with the advantages that no prior assumptions need be made, and in particular that interactions may exist among the predictor variables. In fact, one of AID's strong points is its ability to point out interactions in the data.

Figure 33 shows the result of an AID analysis with ozone at Site 3 as dependent variable. The predictor variables used for this particular run are listed in Table 27. Variables which were left out were deleted because of missing data. Certain variables were lagged for up to 9 hours so that current ozone could be compared to past values of these predictors. In particular, this treatment was accorded to wind velocity. Due to the unique construction of this variable, it will be discussed in more detail later.

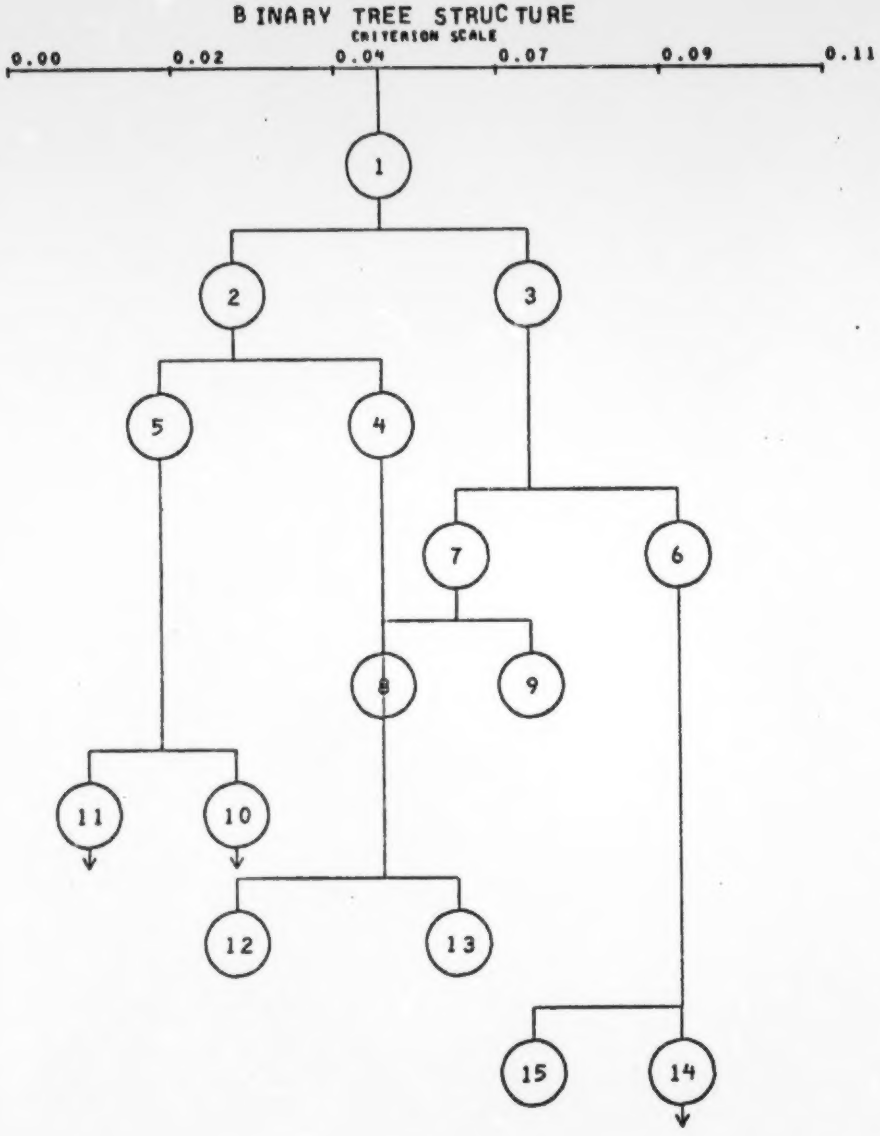

```
                     SUMMARY TABLE

                  ---TOTAL GROUP---

               CRITERION  -OZONE3

           TOTAI GROUP N =       378
           MEAN          =      0.05
           STD. DEV.     =      0.03

 PARENT   1    SPLITTING VARIABLE - TEMP
 MEAN=   0.03 S.D.=   0.02  N= 229 | MEAN=   0.07 S.D.=   0.02  N= 149
 PREDICTOR VALUES --  0  1  3  5  7 | PREDICTOR VALUES -- 37 38 39 40 41
  8  9 10 11 12 13 14 15 16 17 18 1 | 42 43 44 45 46 47 48 49 50 51 52 53
  20 21 22 23 24 25 26 27 28 29 30 - |  54 55 56 61 62 63

 PARENT   2    SPLITTING VARIABLE - WV3
 MEAN=   0.02 S.D.=   0.02  N= 157 | MEAN=   0.05 S.D.=   0.02  N=  72
 PREDICTOR VALUES --  0  1  2  3  8 | PREDICTOR VALUES --  9 11 18 19 26
 10 16 17 24 25 28 32 33 40 41 42 4 | 27 34 35 50 58 59 60
  48 49 51 56 57                    |

 PARENT   3    SPLITTING VARIABLE - WV5
 MEAN=   0.06 S.D.=   0.02  N=  77 | MEAN=   0.09 S.D.=   0.02  N=  72
 PREDICTOR VALUES --  0  8 10 11 26 | PREDICTOR VALUES --  1  9 17 18 19
 32 35 40 41 42 44 49 50 51 52 53 5 | 24 25 27 28 33 34 43 48 56 57
  59 60 63                          |

 PARENT   7    SPLITTING VARIABLE - TEMP
 MEAN=   0.05 S.D.=   0.02  N=  37 | MEAN=   0.07 S.D.=   0.02  N=  40
 PREDICTOR VALUES -- 37 38 39 40 41 | PREDICTOR VALUES -- 44 45 46 47 48
 42 43                              | 50 51 52 54 61 62 63
                                    |
 FINAL GROUP                        | FINAL GROUP

 PARENT   5    SPLITTING VARIABLE - NO2
 MEAN=   0.01 S.D.=   0.01  N=  91 | MEAN=   0.03 S.D.=   0.01  N=  86
 PREDICTOR VALUES -- 19 20 21 22 23 | PREDICTOR VALUES --  0  1  2  3  4
 24 25 26 27 28 29 30 31 32 33 34 35 |  5  6  7  8  9 10 11 12 13 14 15 16
  36 37 38 39 42 43 49 63           |  17 18

 PARENT   4    SPLITTING VARIABLF - TEMP
 MEAN=   0.03 S.D.=   0.01  N=  33 | MEAN=   0.06 S.D.=   0.02  N=  39
 PREDICTOR VALUES --  5  8  9 10 14 | PREDICTOR VALUES -- 26 27 28 29 30
 15 16 17 18 19 20 21 22 23 24 25   | 31 32 33 34 35 36
                                    |
 FINAL GROUP                        | FINAL GROUP

 PARENT   6    SPLITTING VARIABLE - WV7
 MEAN=   0.07 S.D.=   0.01  N=  14 | MEAN=   0.09 S.D.=   0.02  N=  58
 PREDICTOR VALUES --  8 11 16 26 40 | PREDICTOR VALUES --  0  1  9 10 17
 41 42 49 51                        | 18 19 24 25 28 32 33 34 35 48 56 58
                                    |
 FINAL GROUP                        |
```

FIGURE 33. AUTOMATIC INTERACTION DETECTOR - DAYTON OZONE STUDY - SITE 3

02/27/79
13.44.53
BATTELLE-COLUMBUS

PAGE 1 OF 2

FIGURE 33. DAYTON OZONE STUDY - SITE 3
...CONTINUED...

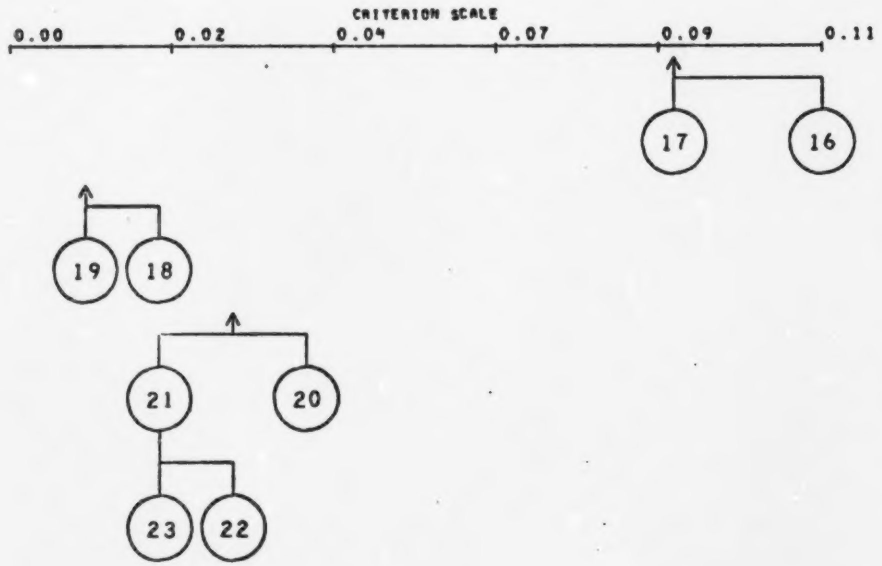

SUMMARY CONTINUED	
PARENT 14 SPLITTING VARIABLE - WV	
MEAN= 0.09 S.D.= 0.01 N= 46 PREDICTOR VALUES -- 0 1 9 10 11 16 17 18 19 26 27 28 35 41 43 50 5 56 63 FINAL GROUP	MEAN= 0.11 S.D.= 0.01 N= 12 PREDICTOR VALUES -- 8 24 25 34 44 51 57 FINAL GROUP
PARENT 11 SPLITTING VARIABLE - WV6	
MEAN= 0.01 S.D.= 0.01 N= 54 PREDICTOR VALUES -- 1 2 3 8 16 18 19 24 49 50 51 56 57 59 60 FINAL GROUP	MEAN= 0.02 S.D.= 0.01 N= 37 PREDICTOR VALUES -- 0 9 10 17 25 26 32 33 34 40 42 58 FINAL GROUP
PARENT 10 SPLITTING VARIABLE - WV7	
MEAN= 0.02 S.D.= 0.01 N= 47 PREDICTOR VALUES -- 1 11 16 18 25 26 27 32 33 34 42 43 44 48 49 50 56 60	MEAN= 0.04 S.D.= 0.01 N= 19 PREDICTOR VALUES -- 8 9 17 19 24 35 41 51 57 59 FINAL GROUP
PARENT 21 SPLITTING VARIABLE - WV5	
MEAN= 0.02 S.D.= 0.01 N= 23 PREDICTOR VALUES -- 17 18 19 26 27 28 32 33 41 43 49 FINAL GROUP	MEAN= 0.03 S.D.= 0.01 N= 24 PREDICTOR VALUES -- 10 25 34 40 44 48 50 56 57 59 60 61 FINAL GROUP

TABLE 27. VARIABLES USED IN AID ANALYSIS

Variable Name	Coded Name	Type
Global Irradiance	Global	Monotone
Wind Velocity	WV	Free
Temperature	Temp	Monotone
Relative Humidity	RH	Monotone
Nitric Oxide	NO	Monotone
Nitrogen Dioxide	NO_2	Monotone
Nitrogen Oxides	NO_x	Monotone
Non-Methane Hydrocarbons	NMHC	Monotone
Carbon Monoxide	CO	Monotone
Light Scattering	LC	Monotone
PAN	PAN	Monotone
Time	Time	Free
Wind Speed Site 3	WSS3	Monotone
Nitrogen Dioxide Site 3	NO_2S3	Monotone
Nitric Oxide Site 3	NOS3	Monotone
Nitrogen Oxides Site 3	NO_xS3	Monotone
Wind Velocity, Lagged 1 hour	WV1	Free
Wind Velocity, Lagged 2 hours	WV2	Free
Wind Velocity, Lagged 9 hours	WV9	Free
Nitrogen Oxides, Lagged 1 hour	NO_x1	Monotone
Nitrogen Oxides, Lagged 9 hours	NO_x9	Monotone
Non-Methane Hydrocarbons, Lagged 1 hour	NMHC1	Monotone
Non-Methane Hydrocarbons, Lagged 9 hours	NHHC9	Monotone

First, in order that the output from the AID run be understood, a detailed description of the output through the first split will be given. The criterion scale on the left is in terms of the dependent variable, ozone. After some cases (hourly averages) were deleted due to missing data, 378 cases remained. This information, together with information about the mean and variance of ozone in the total group, is summarized at the top of the tabular information on the right side of the figure. Group 1, the total group, is placed at its mean on the criterion scale.

Group 1 is then split into Groups 2 and 3, which are placed at their respective group means on the criterion scale. The information pertaining to this split is found immediately to the right in the tabular information. The heading reads "Parent 1 Splitting Variable - Temp". Hence, the variable which best splits the observations into two groups such that the error sum of squares of ozone is minimized is temperature. The variable Time was a close competitor, and it is of interest that temperature was more significant. The time variable was included in the analysis expressly to segregate the high midafternoon ozone readings from the lower background ozone, so that variables affecting the high ozone values could be studied in a separate part of the tree. Temperature essentially takes over this role and actually does a better job of separating high from low ozone. As seen in the tabular information, Group 2 contains 229 observations whose ozone mean is .03 and Group 3 contains 149 observations whose ozone mean is .07. The standard deviation in both groups is .02. The predictor values list shows what coded values of the predictor variable, in this case temperature, are associated with each group. Coded values 0 through 36 are associated with Group 2 and coded values 37 through 63 are associated with Group 3 (an asterisk terminating a list indicates there there are more items in the list, but that available space has been exhausted). All variables are coded into integral values in the range of 0 through 63. Some variables have a natural representation, such as time of day, namely 1 through 24. However, most variables are treated in the following manner: the maximum value among the observations is coded as 63, the minimum as 0, and values intermediate are linearly interpolated between these values. Hence, a coded value of 32 is approximately halfway between the minimum and maximum of the observed values of a variable.

Returning to the first split on temperature, the approximate splitting value can now be computed. The minimum temperature in these observations was 13 C, the maximum 33 C. Hence the splitting value is approximately

$$\left[\frac{36.5}{63} \times (33-13)\right] + 13 = 24.6 \text{ C} \quad .$$

Ozone readings associated with temperatures higher than this are significantly higher than ozone readings associated with lower temperatures and this information is reflected in the AID tree.

The remaining splits in the tree can be analyzed in a similar fashion, and an interpretation given to various paths of the tree. Before this can be done, however, it must be noted that wind velocity is coded differently from the other variables. This is necessary, of course, since wind velocity is a vector and the one dimensional ordering used in determining codes in the above procedure no longer applies. Figure 34 illustrates the method of coding used for wind velocity and more importantly, graphically displays the result of splitting the high O_3 group according to wind velocity. The basic figure is constructed in the following way: concentric circles are drawn with radial increments of 2 mph up to a maximum of 16 mph, and the plane is then divided into octants. This creates 64 sections which are numbered from 0 through 63 as shown. For example, the coded value 19 is assigned to all wind velocity vectors whose wind speed component is between 6 and 8 mph and whose wind direction component is between 90° and 135°.

Figure 34 also reveals how Group 3 was split on wind velocity to obtain Groups 6 and 7. Recall that Group 3 observations have higher ozone and temperature readings than Group 2. Group 3 readings are thus at least roughly comparable to the maximum ozone readings. It is, therefore, of interest to compare the AID partition of Group 3 with results from

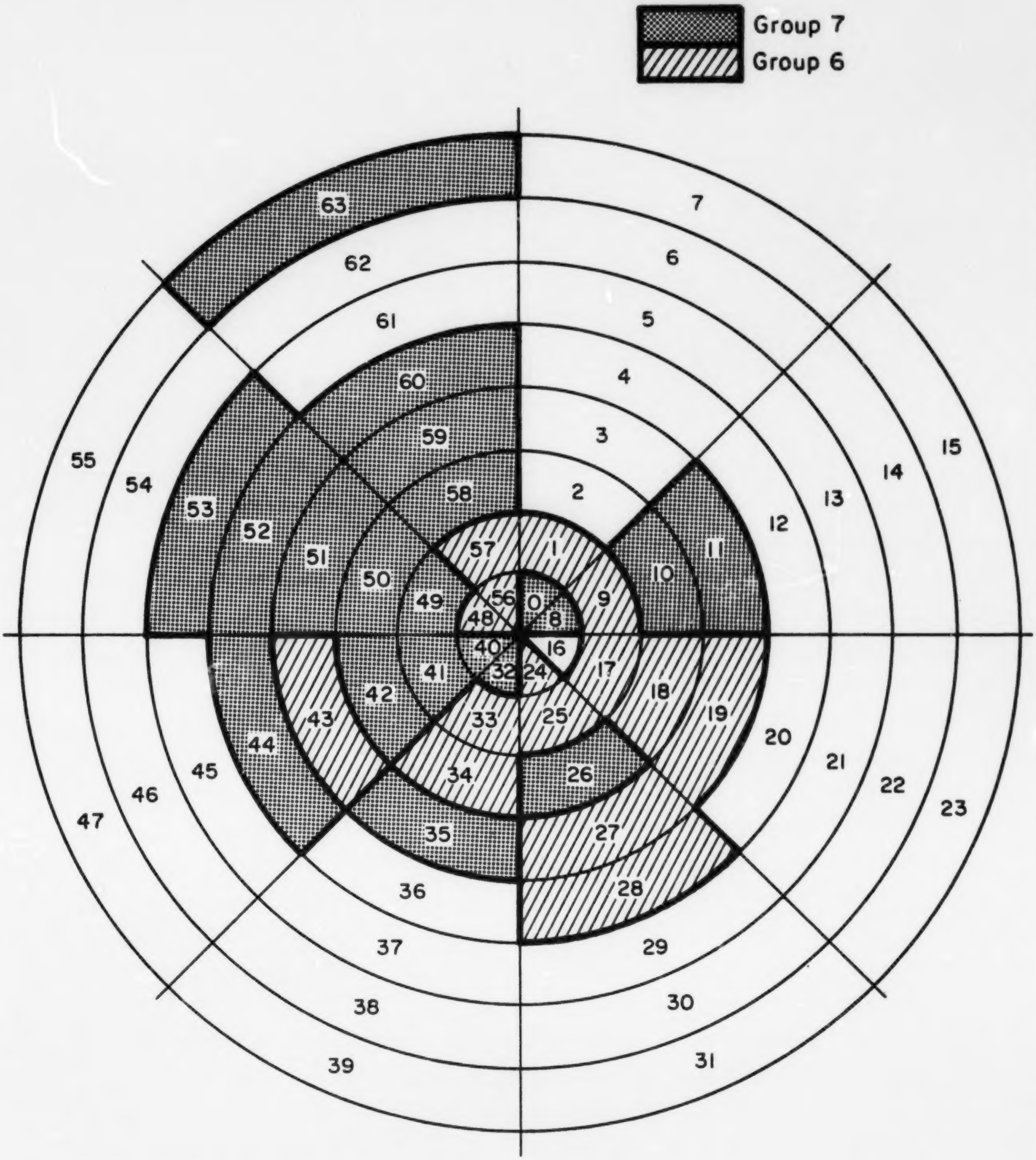
Group 7
Group 6
0
1
2
3
4
5
6
7
8
9
10
11
12
13
14
15
16
17
18
19
20
21
22
23
24
25
26
27
28
29
30
31
32
33
34
35
36
37
38
39
40
41
42
43
44
45
46
47
48
49
50
51
52
53
54
55
56
57
58
59
60
61
62
63

FIGURE 34. AID PARTITION OF OZONE RESULTS BY WIND VECTOR

previous analyses of maximum ozone. The split occurs on wind velocity lagged 5 hours. Observations in the hatched areas belong to Group 6 (higher O_3), those in the dotted areas to Group 7 (lower O_3). The entire "scenario" of this split is consistent with earlier results. First, the fact that there is such a large lag in wind velocity agrees with results of the regression integral analysis. Consistent with the graphical analysis, wind direction from the 60°-240° half plane leads to higher ozone values than wind directions opposite. There is little evidence in this split that indicates much significance for wind speed.

The Effect of Meteorological Variables on Dayton Ozone

During the study period in Dayton, the eastern United States experienced a progression of fronts and anticyclonic (high-pressure) areas typical of summertime conditions. Between July 17 and August 12, five cold fronts moved through Dayton in a direction from west to east, and one cold front moved across the area from north to south.

This 27-day period was generally dominated by the fair weather associated with the high-pressure areas. In the July portion of the period, there was only 0.17 inches of rain and of the 2.26 inches of rain in the August portion, 1.15 inches fell on August 3. Eighteen of the 27 days experienced more than 50 percent of the possible sunshine and 11 days had 90 percent or more.

Haze and morning fog were quite frequent throughout the period. The Local Climatological Data records issued by the National Oceanic and Atmospheric Administration list the weather observations made at 3-hour intervals. During the study period, there were 80 of these 3-hour intervals in both July and August. The following table lists the number of occurrences of various types of weather during this 80-interval period. On several occasions more than one type of weather was observed (e.g., rain showers and haze) and each type has been listed.

Twice a day, at 7 a.m. and 7 p.m. EST, the National Weather Service station at the Dayton Municipal Airport launches balloon-borne

TABLE 28. WEATHER FREQUENCY DURING DAYTON STUDY

Weather Type	3-Hour Observations July Occurrences	 August Occurrences
Haze	31	24
Fog	4	4
Ground fog	3	13
Rain showers	1	5
Rain	0	1
No precipitation or obstructions to visibility	41	33

radiosondes as part of NWS's synoptic upper air network. As part of the meteorological analysis of the Dayton study period, the temperature soundings from these radiosonde ascents were plotted and examined for the 20 days during which the sampling program was operating. These temperature plots were made for all standard and significant levels between the surface and 500 mb (approximately 5850 meters) to identify temperature inversions or stable layers that would limit mixing. They were also compared with the temperature data taken during the airplane soundings made during the study, and they supplied additional information regarding the temperature structure above the top of the airplane soundings.

Good agreement was found between the two types of soundings even though there was 3 to 4 hours' difference between the radiosonde launches and the airplane soundings. Temperatures were generally within 2 C and the temperature lapse rates in the comparable layers were very similar.

During the 20 sampling days there were 13 morning soundings on which there was a surface-based temperature inversion with an increase of temperature with height of 3 C or more within the lowest 500 m. Six morning soundings had weaker surface inversions and one had no inversion. These surface inversions are related to the nocturnal cooling of the surface that accompanies clear nighttime skies with little resistance to the radiational cooling of the surface.

Most soundings, both morning and evening, measured upper-level temperature inversions indicative of either subsiding conditions in a high-pressure area or a frontal layer. Of the 40 soundings made on sampling days, 14 morning and 14 evening soundings had elevated inversions between 900 mb (about 1000 meters) and 500 mb. Most of these inversions (20) had their bases between 850 mb (about 1500 meters) and 700 mb (about 3200 meters).

Thus, most of the Dayton study period was characterized by the presence of an elevated inversion limiting mixing of pollutants to the lowest 3000 meters of the atmosphere. During the night, nocturnal surface inversions put an even lower height limit (500 m) on dispersion. These surface inversions also created a nighttime layer between 500 m and

3000 m in which any pollutants placed there by vertical or horizontal transport were protected from turbulent forces outside the layer. Within this layer, temperature lapse rates were adiabatic or subadiabatic so that mixing processes might be expected to distribute ozone and other pollutants uniformly throughout the elevated layer between the two inversions. If the ozone were uniformly mixed through the layer, then the soundings through the layer would note no change with altitude of the values of ozone mixing ratio* or ozone measured in parts per million.

Ozone-Meteorology Relationships

Several meteorological parameters were examined to determine their relationship to ozone concentrations. In some cases good agreement was found; in others there was no consistent agreement or there were too few examples to draw any firm conclusions.

Figure 35 displays the average station pressure (measured in inches of mercury) as recorded at the Dayton National Weather Service Station, the Dayton mixing height, the transport wind, the afternoon ventilation, and the daily ozone peaks (Site 3) for the study period. The mixing height and ventilation values are given for only the weekday portion of the sampling period.

---

* Ozone mixing ratio is a term used in upper atmospheric ozone studies and is defined as mixing ratio, $r_3 \equiv \frac{\text{mass of ozone}}{\text{mass of air}}$, in a given volume. It can be expressed in micrograms/gram or parts per million by mass (ppmm). It is related to the surface ozone unit of parts per million by volume (ppmv) by the ratio of the molecular weight of ozone (48) to the mean molecular weight of air (28.97).

$$\begin{aligned} r_3(\mu g\ g^{-1}) &= O_3 \text{ concentration (ppmm)} \\ &= \frac{48}{28.97} O_3 \text{ concentration (ppmv)} \\ &= 1.657\ O_3 \text{ concentration (ppmv)} . \end{aligned}$$

The ozone mixing ratio remains constant when the air undergoes adiabatic changes (with no saturation). A gram of air may contain x grams of ozone. During the unsaturated adiabatic motion of the density and temperature of the air may vary but the original gram of air retains its x grams of ozone.

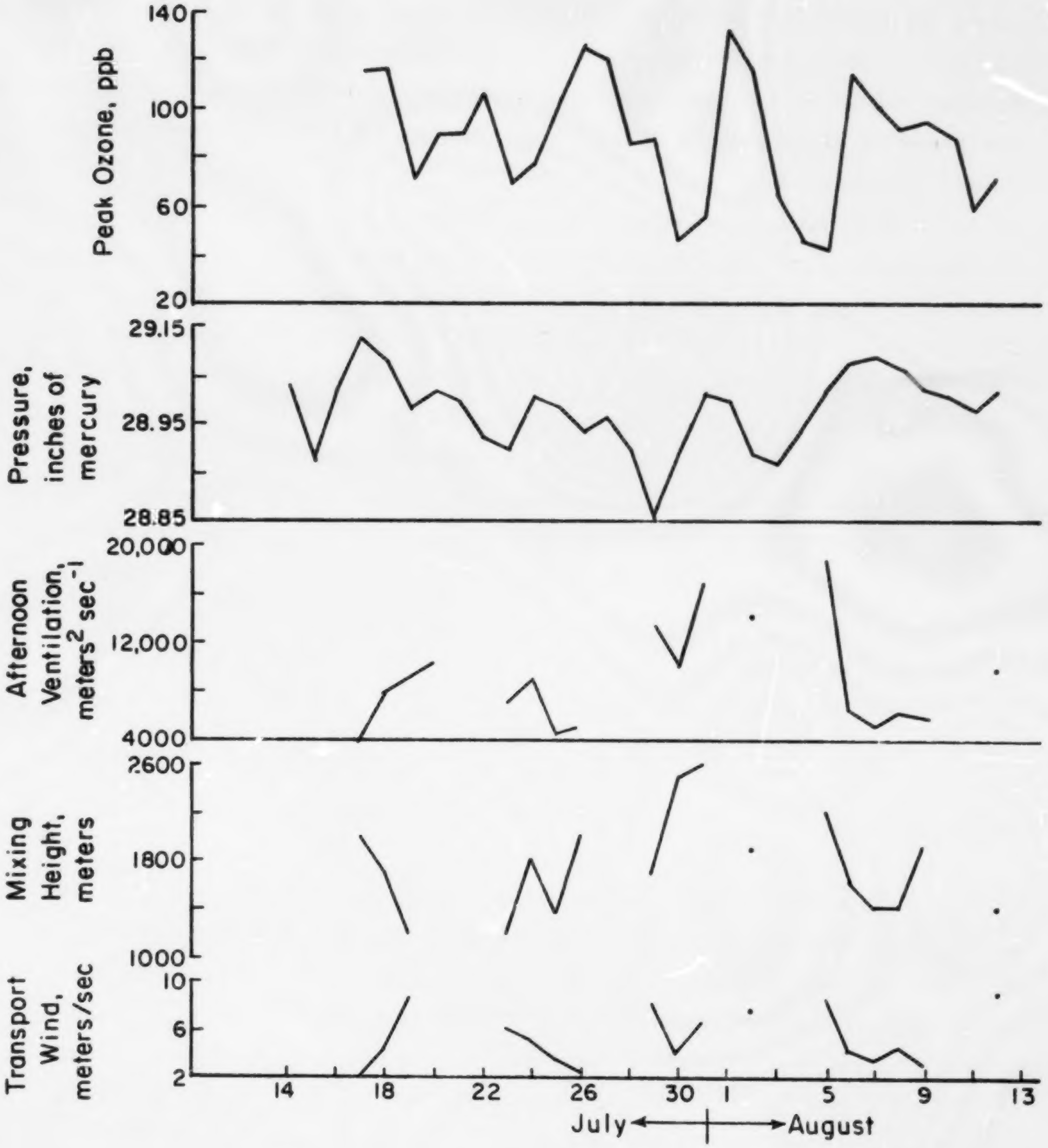

FIGURE 35. VARIATIONS OF PEAK OZONE AND SELECTED METEOROLOGICAL PARAMETERS DURING THE DAYTON STUDY PERIOD

In general there is a strong correspondence between maximum daily ozone and barometric pressure. Higher levels of ozone occur during periods of high pressure and lower ozone during low-pressure periods. Of the five minimum points on the peak-ozone curve, three occurred on the same day that the pressure minimized, one lagged the pressure by 1 day and the other lagged by 2 days.

For uniform creation of ozone it would be expected that low mixing height, low transport winds and low afternoon ventilation would be related to high ozone concentrations. As seen in Figure 35 the four week-day periods for which sampling was done in Dayton do not consistently match the relationships listed above. Among the three air pollution meteorology parameters, the expected mixing height-peak ozone relationship appeared only once out of four cases while the expected transport wind speed-peak ozone relationship appeared three times out of four. The afternoon ventilation which is the product of the transport wind speed and the mixing height also showed the expected relationship with peak ozone on three of the four weeks. It can be concluded that other factors such as solar radiation, variations in ozone precursor emissions, wind direction, and horizontal advection of ozone must also be taken into account in explaining the daily ozone variations.

Ozone and Haze

During periods of atmospheric stagnation, visibility decreases and weather station hourly observations report haze. Airplanes taking off rise through a layer of haze before reaching the clear air. It has been suggested that since haze often serves as an indicator of stagnation, it may also be an indicator of high ozone. If so, haze observations made at official weather stations could be used to estimate the areal extent of the high ozone.

Following up this suggestion, observations of haze made at the Dayton National Weather Service station at 1300 and 1600 hours were compared with the ozone readings made at Site 2. For the haze readings at 1300 the ozone readings ranged from 0.052 to 0.114 ppm, while the 1600 range was from 0.056 to 0.119 ppm. From this sample there appeared to be no correlation between high ozone and observations of haze.

On the possibility that the haze was occasionally caused by moisture in the air rather than stagnant pollutants, a further examination of the data was made. Combining the readings at 1300 and 1600 and selecting an arbitrary dewpoint temperature level of 64 F*, it was found that when haze was reported and the dewpoint was 64 F or below, the ozone readings at Station 2 ranged from 0.063 to 0.119. When the dewpoint temperature was 65 F or above and haze was reported, the range of ozone concentrations at this station was from 0.052 to 0.083. The correlation when dewpoint is used to separate dry and moist haze is better than when haze alone was used as an indicator of ozone. This relationship is worth further study in making estimates of the pervasiveness of an ozone layer.

Haze and Trajectories

An additional observation regarding haze was made during this study utilizing a set of 3000' trajectories** prepared by computer for this study period. These trajectories shown in Appendix F, advance the air parcels in 12-hour time steps ending at 1200 Greenwich, England, Mean Time (GMT) (0800 EDT) and 0000 GMT (2000 EDT of the preceding day). One set of trajectories was prepared for air arriving at Wilmington, Ohio, which is about 30 miles from Dayton. For our study it was assumed that the air parcels arriving at Dayton had followed horizontal trajectories parallel to the Wilmington trajectories.

---

* The dewpoint temperature, 64 F, was chosen because it was the median dewpoint temperature for all the haze measurements at the hours of 1300 and 1600 during the study period.

** Trajectories courtesy of Research Triangle Institute.

The first days of high ozone readings at Dayton were July 17 (peak = 0.120 ppm) and July 18 (peak = 0.119). The 17th was not a haze day at Dayton but the 18th exhibited haze from 0700 hours through the remainder of the day. In tracing back the air arriving in the Dayton vicinity at 2000 on the 17th, at 0800 on the 18th and at 2000 on the 18th it was found that the air parcels, 12 hours before their arrival in Dayton, were located in areas where haze was reported by the National Weather Service. For the trajectories ending at 2000 on the 17th and 0800 on the 18th the air was in central Kentucky 12 hours earlier. For the air reaching Dayton at 2000 on the 18th the trajectory can be traced back for 48 hours to a point near the junction of Missouri, Illinois, and Kentucky. At each 12-hour step along this trajectory haze was reported.

For all three of these trajectories there was a point at which the air parcel performed looping or doubling back indicating slow movement or stagnation. For the air parcels arriving at Dayton at 2000 on the 17th and 0800 on the 18th, the loops were performed over central Kentucky in the vicinity of the Cincinnati metropolitan area. However, for the air arriving in Dayton at 2000 on the 18th the loop encompassed the area in southern Illinois and southeastern Missouri, where there is no large urban area. After leaving the Missouri-Illinois area, this air parcel passed north of Evansville, Indiana, and probably touched only the edge of the Cincinnati area as it entered Dayton from the west.

On July 19 in Dayton the peak ozone was again high at the Dayton-2 station and haze was reported through most of the day. The air arriving at 0800 had been in the vicinity of Indianapolis 12 hours earlier and haze was reported there at that time. By 2000 hours the trajectory had shifted to a northwest direction as a cold front passed over Dayton and the ozone concentration curve took a dip.

An interesting observation which we cannot explain at this time is that in each instance where the Dayton air could be traced back to an area where the trajectory performed a loop, the region of the loop was 500 to 1000 kilometers southwest of the center of the high-pressure area.

There was one day during the study when an area reporting haze served as the source of an air parcel exhibiting high O_3 upon arrival in Dayton but which exhibited no looping in its trajectory. On August 6 the peak ozone at Station 2 was 0.095 ppm. At 0800 on the 6th the air parcel which appeared in the Dayton area at 2000 hours was located near Arkon, Ohio, in an area where haze and fog reports predominated. This trajectory experienced no tight loop but followed a clockwise path around the high-pressure center.

Consideration of the trajectories indicates that haze observations sometimes, but not always, accompany high ozone. Indeed, the leading edge of the haze area may be a better indicator of high ozone since the haze observed along the trajectory ending at Dayton on July 18 was not in the center of the haze area but at its edge.

Vertical Temperature Structure and Surface Ozone

Advantage was taken of the twice-daily temperature soundings made regularly by the Dayton National Weather Service station to study possible relationships between temperature or dewpoint structure and the variations in surface ozone. Among the limited number of cases considered, the following joint occurrences were rather consistent:

(1) On mornings when a strong temperature inversion is present at the surface (3 C increase of temperature within the first 500 meters above the surface--Figure 36 A), the surface ozone will drop below 0.02 ppm for at least 1 or 2 hours. When there is no temperature inversion or the inversion is weaker, the ozone will generally remain above 0.02 ppm throughout the night and morning.

(2) When the morning sounding records a dry layer just above the surface (Figure 36 B) the peak surface ozone value for the day will be high.

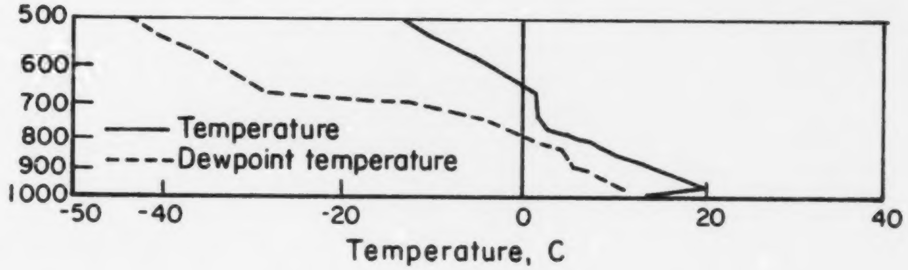

A - July 31

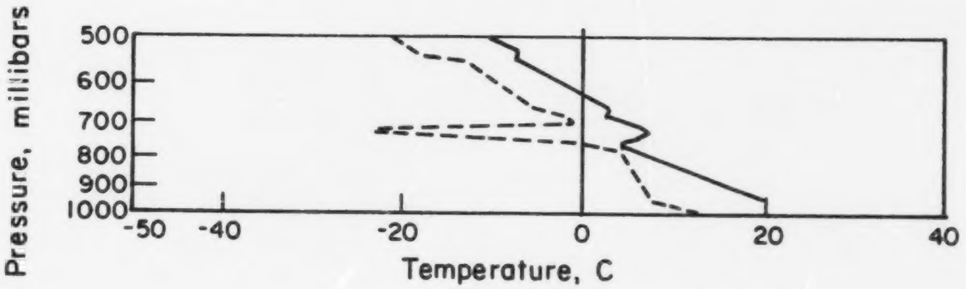

B - August 1

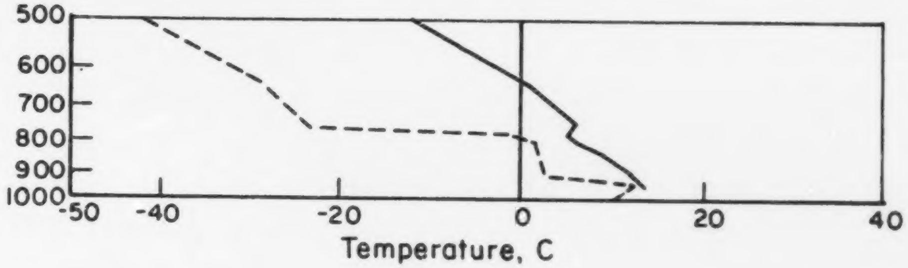

C - August 5

FIGURE 36. EXAMPLES OF DAYTON NWS SOUNDINGS OF TEMPERATURE AND DEWPOINT

(3) When the morning sounding records relatively dry air in the layer from 700 mb to 500 mb (Figure 36 C), the peak surface ozone value will be low.

The latter two relationships became apparent when the peak ozone values observed at Site 2 on weekdays were separated into concentrations of 0.10 ppm and above, 0.07 to 0.10 ppm, and 0.07 ppm and below. It was noted that the highest afternoon peak-ozone readings followed mornings when there was a marked increase of temperature and a marked decrease of dewpoint temperature in the layer above the surface (between 1000 and 900 mb) as depicted in Figure 36 B. When the morning sounding shows a uniform temperature decrease (Figure 36 A) or an increase of dewpoint with height (Figure 36 C) the peak ozone was generally below 0.07 ppm.

Figure 36 A and C also show the dry layer between 700 mb (about 3000 m) and 500 mb (about 5800 meters) that typically preceded a day of lower peak ozone. Temperature-dewpoint differences of 15 C or more were the demarcation for these dry layers.

The first relationship between morning temperature inversions and low morning ozone values can be explained by the suppression of mixing and diffusion that occurs within the inversion layer. Ozone can be destroyed by chemical and physical interactions within the layer. Possible replacement of surface ozone by ozone in the reservoir above the inversion is prevented because of the poor mixing conditions within the inversion.

Airplane and Balloon Soundings

Results of the vertical soundings of temperature and ozone made to 5000 feet during airplane flights are presented elsewhere in this report (Figures 49 and 50). To gain additional information concerning the conditions on these days, the National Weather Service (NWS) Dayton temperature soundings made on the days of the airplane soundings have been combined with the airplane sounding results in Figures 37 through 44.

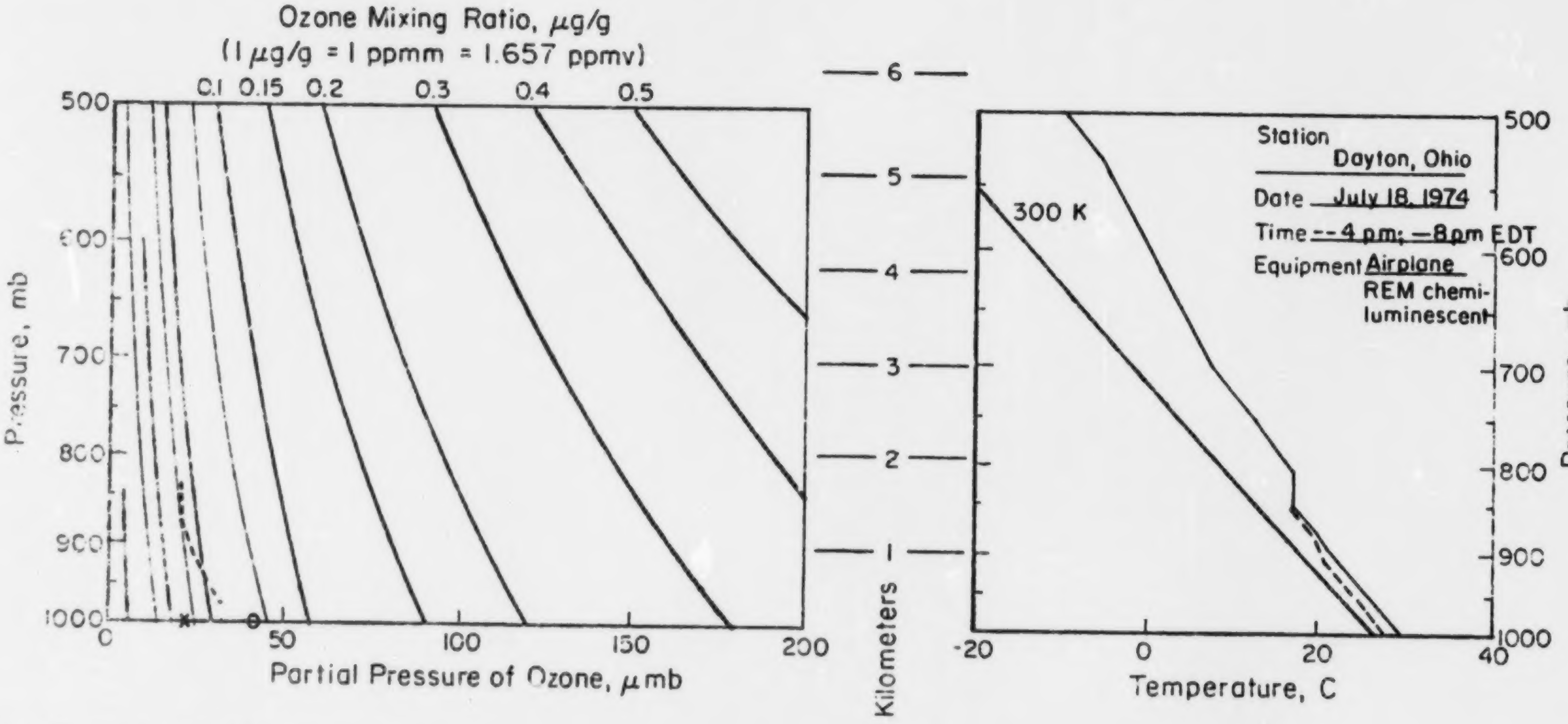

x = O_3 concentration at downtown site at time of Airplane Sounding

o = Maximum surface O_3 concentration in Dayton Area at time of Airplane Sounding

LOWER TROPOSPHERE OZONAGRAM

FIGURE 37. AFTERNOON SOUNDINGS FOR JULY 18 -- AIRPLANE, 4 PM; NWS BALLOON, 8 PM

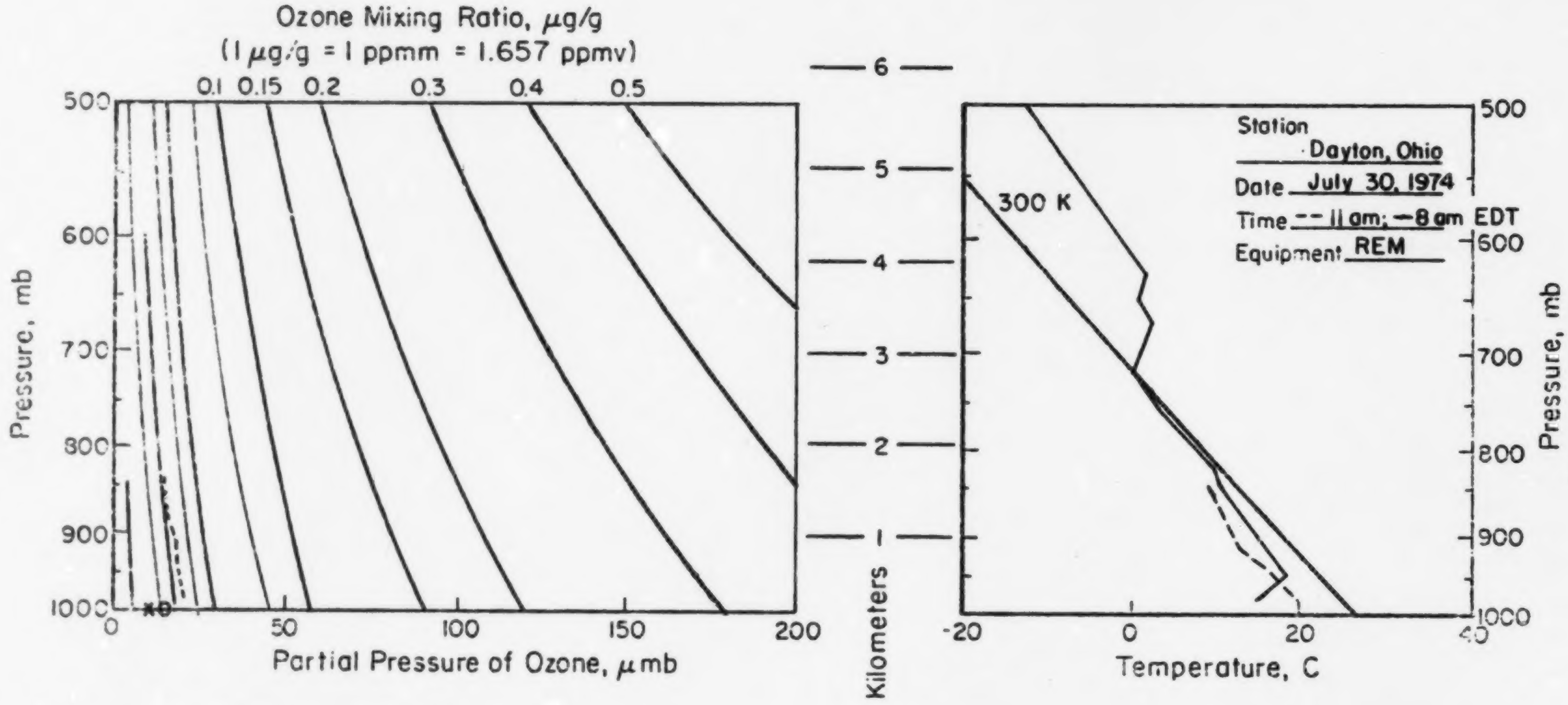

x = O_3 concentration at downtown site at time of Airplane Sounding

o = Maximum surface O_3 concentration in Dayton Area at time of Airplane Sounding

LOWER TROPOSPHERE OZONAGRAM

FIGURE 38. MORNING SOUNDINGS FOR JULY 30 -- AIRPLANE, 11 AM; NWS BALLOON, 8 AM

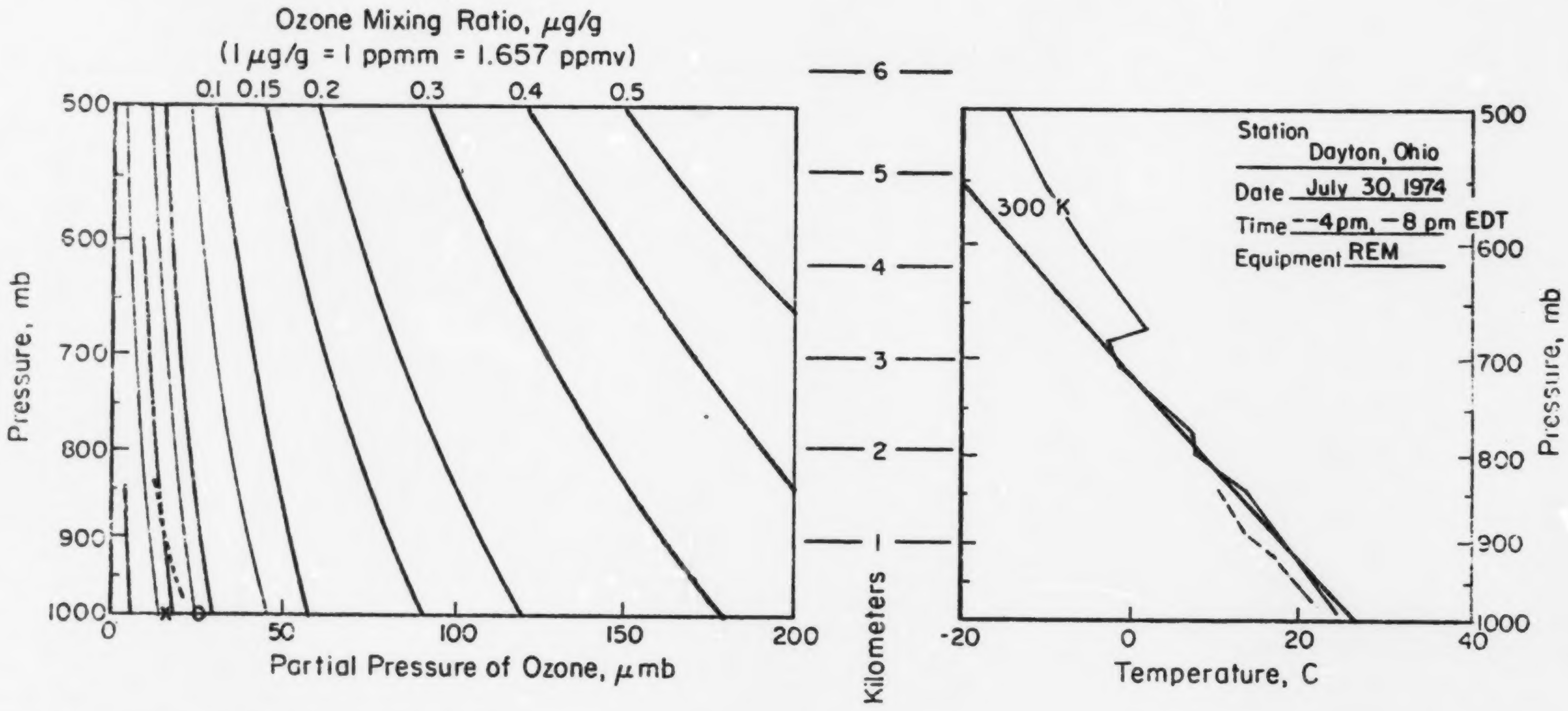

x = O_3 concentration at downtown site at time of Airplane Sounding

o = Maximum surface O_3 concentration in Dayton Area at time of Airplane Sounding

LOWER TROPOSPHERE OZONAGRAM

FIGURE 39. AFTERNOON SOUNDINGS FOR JULY 30 -- AIRPLANE, 4 PM; NWS BALLOON, 8 PM

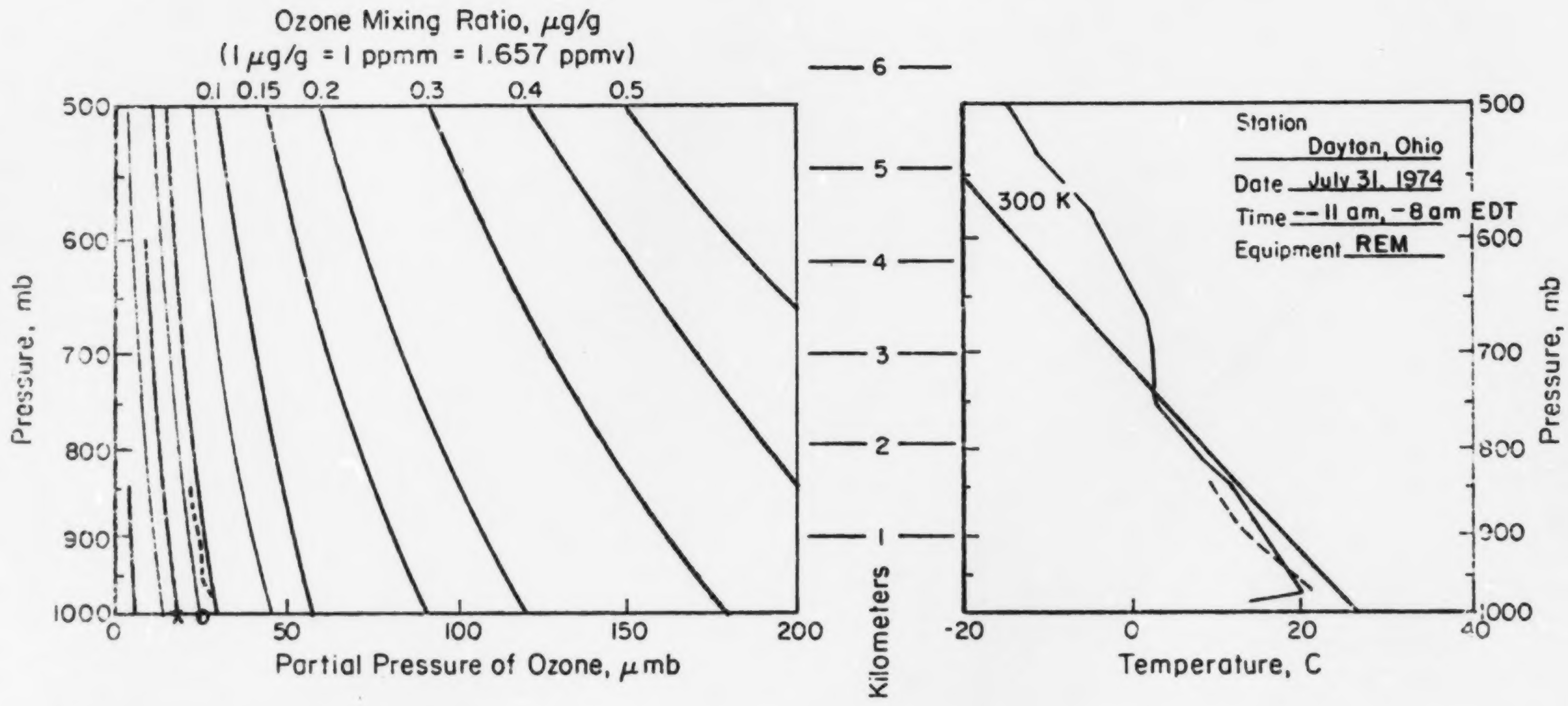

x = O_3 concentration at downtown site at time of Airplane Sounding

o = Maximum surface O_3 concentration in Dayton Area at time of Airplane Sounding

LOWER TROPOSPHERE OZONAGRAM

FIGURE 40. MORNING SOUNDINGS FOR JULY 31 -- AIRPLANE, 11 AM; NWS BALLOON, 8 AM

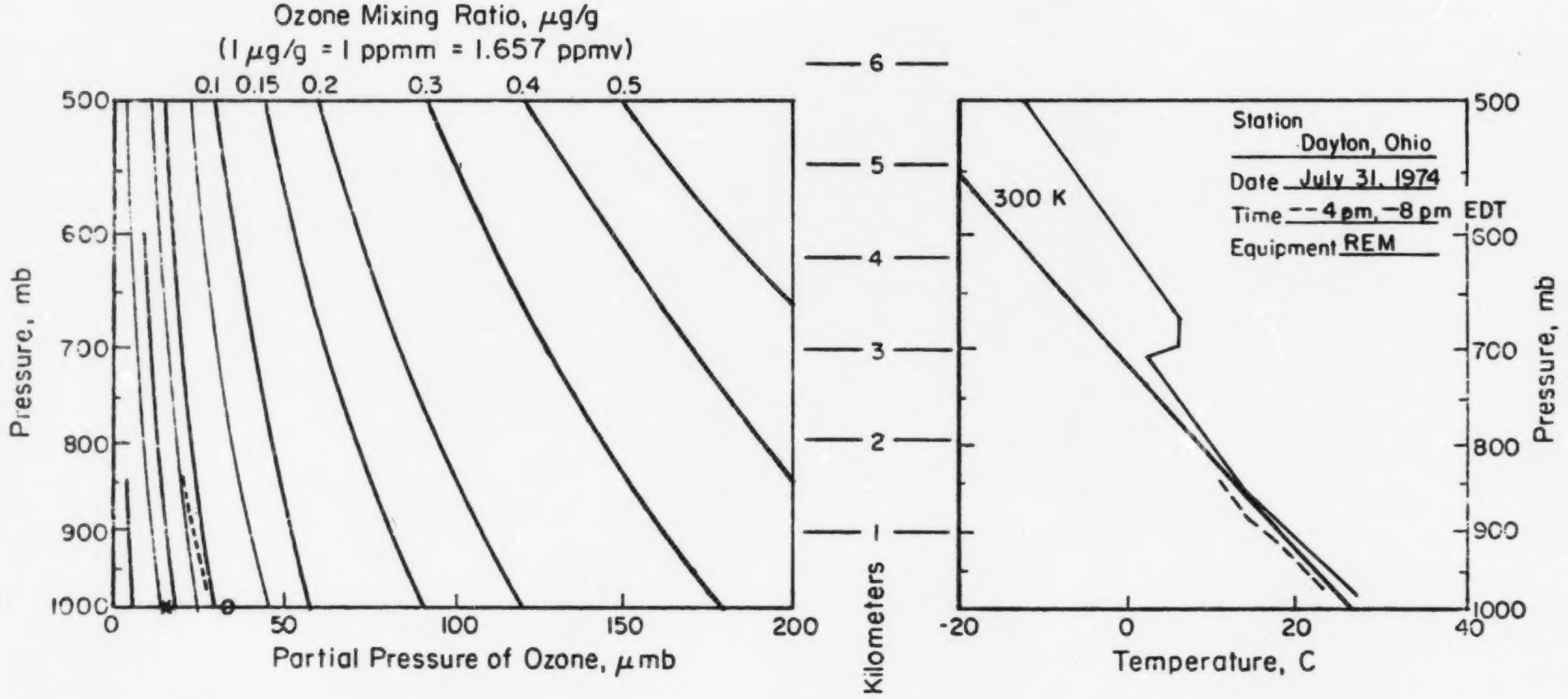

x = O_3 concentration at downtown site at time of Airplane Sounding

o = Maximum surface O_3 concentration in Dayton Area at time of Airplane Sounding

LOWER TROPOSPHERE OZONAGRAM

FIGURE 41. AFTERNOON SOUNDINGS FOR JULY 31 -- AIRPLANE, 4 PM; NWS BALLOON, 8 PM

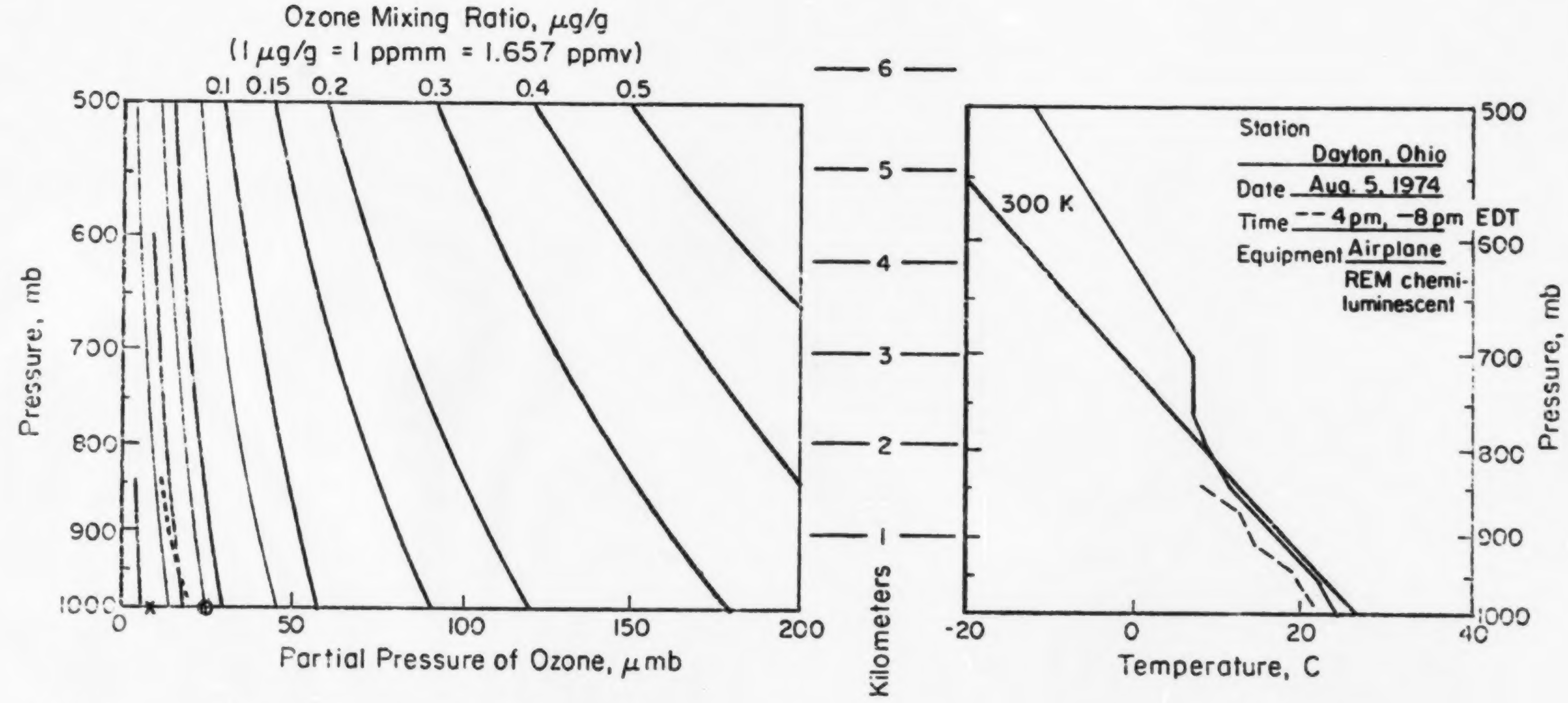

x = O_3 concentration at downtown site at time of Airplane Sounding

o = Maximum surface O_3 concentration in Dayton Area at time of Airplane Sounding

LOWER TROPOSPHERE OZONAGRAM

FIGURE 42. AFTERNOON SOUNDINGS FOR AUGUST 5 --AIRPLANE, 4 PM; NWS BALLOON, 8 PM

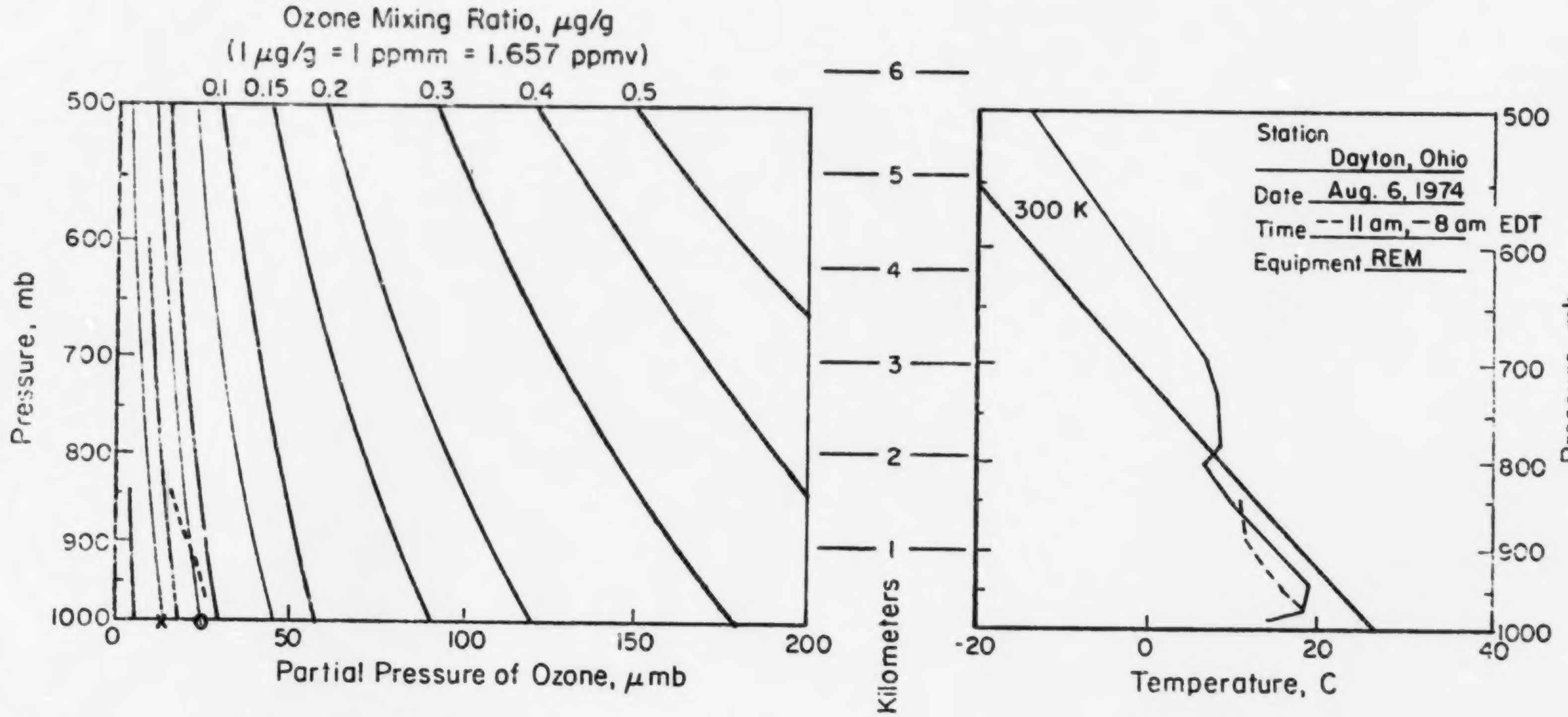

x = O_3 concentration at downtown site at time of Airplane Sounding

o = Maximum surface O_3 concentration in Dayton Area at time of Airplane Sounding

LOWER TROPOSPHERE OZONAGRAM

FIGURE 43. MORNING SOUNDINGS FOR AUGUST 6 -- AIRPLANE, 11 AM; NWS BALLOON, 8 AM

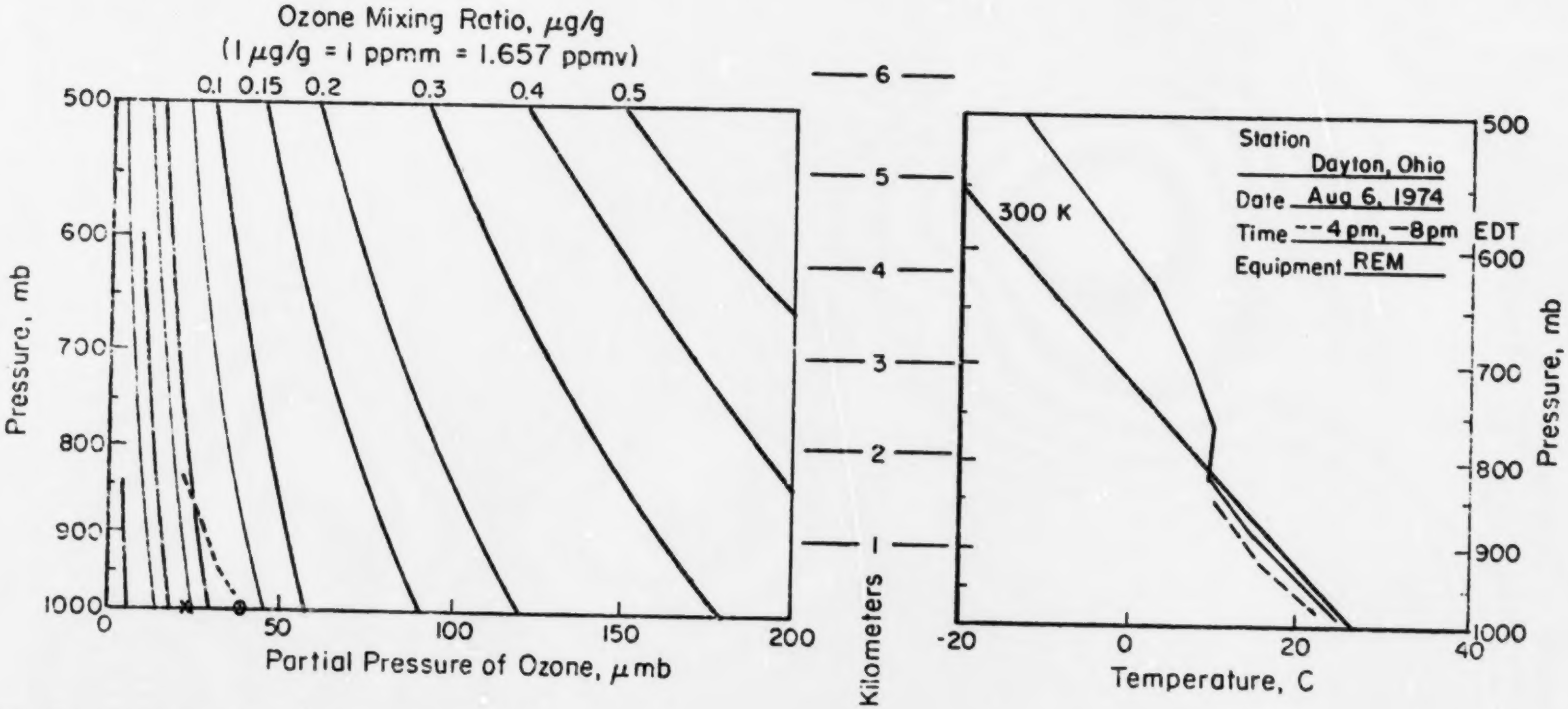

x = O_3 concentration at downtown site at time of Airplane Sounding

o = Maximum surface O_3 concentration in Dayton Area at time of Airplane Sounding

LOWER TROPOSPHERE OZONAGRAM

FIGURE 44. AFTERNOON SOUNDINGS FOR AUGUST 6 -- AIRPLANE, 4 PM; NWS BALLOON, 8 PM

Morning airplane soundings (approximately 12 noon EDT) have been combined with 1200 GMT (8 a.m. EDT) balloon soundings and afternoon airplane data (approximately 4 p.m. EDT) have been plotted with the 0000 GMT (8 p.m. EDT) balloon data. The ozone values have been converted to ozone mixing ratios (equivalent to ozone concentration in parts per million by mass--ppmm) in order to be consistent with the units on the ozonagram, a diagram adapted from upper atmospheric ozone studies(11). Ozone mixing ratio lines on the ozone portion of the ozonagram are the lines curving upward from right to left. On the temperature portion of the diagram the line sloping upward from right to left is a dry adiabat. Temperature lapse rates paralleling this line would represent adiabatic condition.

In a well-mixed layer the ozone mixing ratio would be constant with height. A decrease of ozone mixing ratio with height would indicate the diffusion of ozone or its precursors from the surface or from a lower elevation where ozone concentrations were higher. However, under stagnant conditions with only minimal advection of the air mass, diffusive mixing would also eventually lead to a uniform distribution of ozone, a constant mixing ratio (or parts per million value) throughout the layer. Examination of upper atmospheric ozone soundings(12) has shown that relative maxima of ozone can be found in layers beneath tropospheric subsidence inversions.

July 18, 1974. On the afternoon of July 18, as shown in Figure 37, the base of the subsidence inversion occurred at 5000 feet, thus, the mixing ratio of 0.042 μg/g (70 ppb) at 5000 feet represents the maximum "background" concentration for this layer. This relative maximum is very likely due to contributions from mature ozone created at the surface or in the layer itself and from stratospheric ozone that has entered the troposphere and then been transported downward.

From 1000 feet up to 4000 feet on this afternoon, the ozone mixing ratio decreased with height similar to the model of ozone diffusion moving down the gradient from higher concentrations to lower concentrations. Since the surface concentration, as measured in downtown Dayton below the point at which the sounding was made, was lower than the concentration at

1000 feet, the source of higher ozone could not have been in downtown Dayton. However, Dayton may have served as the source of precursors which have generated ozone as they diffuse upward. Also, concentrations at other locations in the Dayton area at this time were great enough to serve as sources for the diffusive mixing of ozone into the layer above the ground. Once carried upward into the layer the surface ozone joins the ozone already there and spreads out horizontally.

Other Soundings. On the later days during which soundings were made (Figures 38 through 44), the base of the temperature inversion or stable layer was considerably above 5000 feet, ranging from 800 to 700 mb. In all of these cases there may be a relative ozone maximum between the top of the airplane sounding and the base of the subsidence inversion.

On each of the ozonagram plots it can be seen that there is a relatively uniform decrease of ozone concentration with height between 1000 feet and 4000 feet; however, the rate of this decrease varies markedly. There is little change of ozone with height on July 30 (Figure 39), but on August 6 (Figure 44), the rate of decrease with height is quite rapid. This pattern of ozone decrease with height is uniform for both morning and afternoon soundings. One would expect this pattern in the afternoon when the ozone is being created in the surface layer and mixed upward; however, this mechanism would not be operating in the morning. Surface ozone observations taken at the time of the morning soundings (12 noon) show no concentrations as high as those at 1000 feet. Very likely, the early morning ozone precursors which are difussing upward are generating ozone, with the ground level O_3 formation being somewhat inhibited by continuous NO emissions at the surface.

Three airplane soundings were made between noon on August 5 and the evening of August 6. Comparison of the ozone profiles from these soundings shows that the ozone concentration at each level between 1000 feet and 5000 feet increased during each successive period. There was also a marked increase in the 1000-foot to 5000-foot ozone gradient from August 5 to August 6 indicating that the low level ozone source was greater on the 6th than on the 5th and/or that the rate of vertical mixing was different on the second day.

Tracing the air which arrived over Dayton on the 6th backward by means of the trajectories shows that a clockwise path was followed from Lake Michigan across northeastern Ohio, and then a movement westward terminating in Dayton. The air could have passed over Milwaukee, Detroit, Cleveland-Akron, and Columbus before it reached Dayton. There was considerable opportunity for urban sources to contribute ozone or ozone precursors to the air mass. The increase in ozone through the entire layer from the 5th to the 6th could be the result of a different path on the 2 days or of a greater effect of photochemical processes on the part of the anticyclonic air mass arriving over Dayton on the second day. The successive increases of ozone throughout the layer supports a theory of a center or several centers of high O_3 concentration in a regional ozone layer. At the bottom of this mobile pervasive layer there is a diurnal cycle of ozone creation and ozone destruction. This cycle is controlled by the combination of the emission of new precursors, the incoming solar radiation, horizontal transport, and vertical mixing during the daylight hours. At night the nitric oxide concentration increases at the surface as the solar radiation is cut off and the clear skies of the anticyclone promote surface temperature inversions with their inhibition of mixing. As a result of this decrease in mixing, the nitric oxide is trapped within the nocturnal inversion where it can remove ozone by chemical reaction. Moreover, the inversion prevents the downward transport of ozone from the above-surface layer.

Contribution of Upper Atmospheric Ozone on August 5 and 6, 1974. During this August 5 to 6 period the base of the subsidence inversion or elevated stable layer remained between 750 and 800 mb. There might have been a relative ozone maxima between 5000 feet and the base of the stable layer during these 2 days. If so, it is possible that during the day, when the solar heating caused a warming of the layer beneath the subsidence inversion, ozone from this relative maximum was mixed downward increasing the general ozone"background" of the layer. Even if this possibility were true, the surface ozone peaks during the day still must have been caused by surface sources, not upper atmospheric ozone, becuase of the marked surface-to-5000' ozone gradients.

Summarizing the meteorological hypotheses resulting from the examination of the soundings, a decrease of ozone mixing ratio with height in the layer from the surface to 5000 feet indicates that surface sources are the prime factors in determining peak afternoon ozone concentration at the surface. A constant mixing ratio from 1000 feet up to the subsidence inversion indicates good mixing within this layer; this ozone concentration can probably be thought of as the "background" ozone associated with the high-pressure system. Within this widespread "background" ozone layer, horizontal advection can transport high ozone/precursor pockets or plumes from localized sources (cities). These phenomena will be considered further in the following sections of this report.

Description of Selected Study Days

Due to the vast amount of data collected during the Dayton field study it would be quite impossible to discuss each day of the study in detail in a report of this nature. We have therefore opted for summarizing the study data in the various formats already presented, and then selecting a few pertinent study days to discuss in detail. The individual days chosen for discussion will include all of the aircraft sampling days, and, in addition, several other days which exhibited interesting ozone patterns.

To facilitate comparison of the ground level ozone concentrations at the six ground stations, we have plotted the ozone profiles from each site on a single graph for each day of the study. These plots are quite instructive and are included in Figure 45 A-U. Because of the compression of the ordinate axis however, some important detail is lost in these plots so that the ozone profiles for certain days will be replotted later in this section in a manner which better exposes small site-to-site variations. The first of the ground station comparison plots, shown in Figure 45 A, displays the 20-day composited-ozone profiles for each site. While these averaged profiles are relatively featureless and will not be discussed in any detail, they do show that quantitative differences exist in the average afternoon O_3 plateaus for the six sites.

In order to attempt to explain the ozone patterns which we observed in Dayton, we will digress for a moment to present a working hypothesis which we shall test on the Dayton field data.

Model of Urban and Rural Ozone Patterns

The basic precepts of our hypothesis are simple and most have been discussed elsewhere. A brief description of the model follows.

Ozone is generated in the troposphere by a series of chemical reactions involving hydrocarbons, nitrogen oxides, and sunlight. Since all of these ingredients are present in "background" tropospheric air, some ozone is produced in pristine air with no help from mankind. In

Reproduced from best available copy.

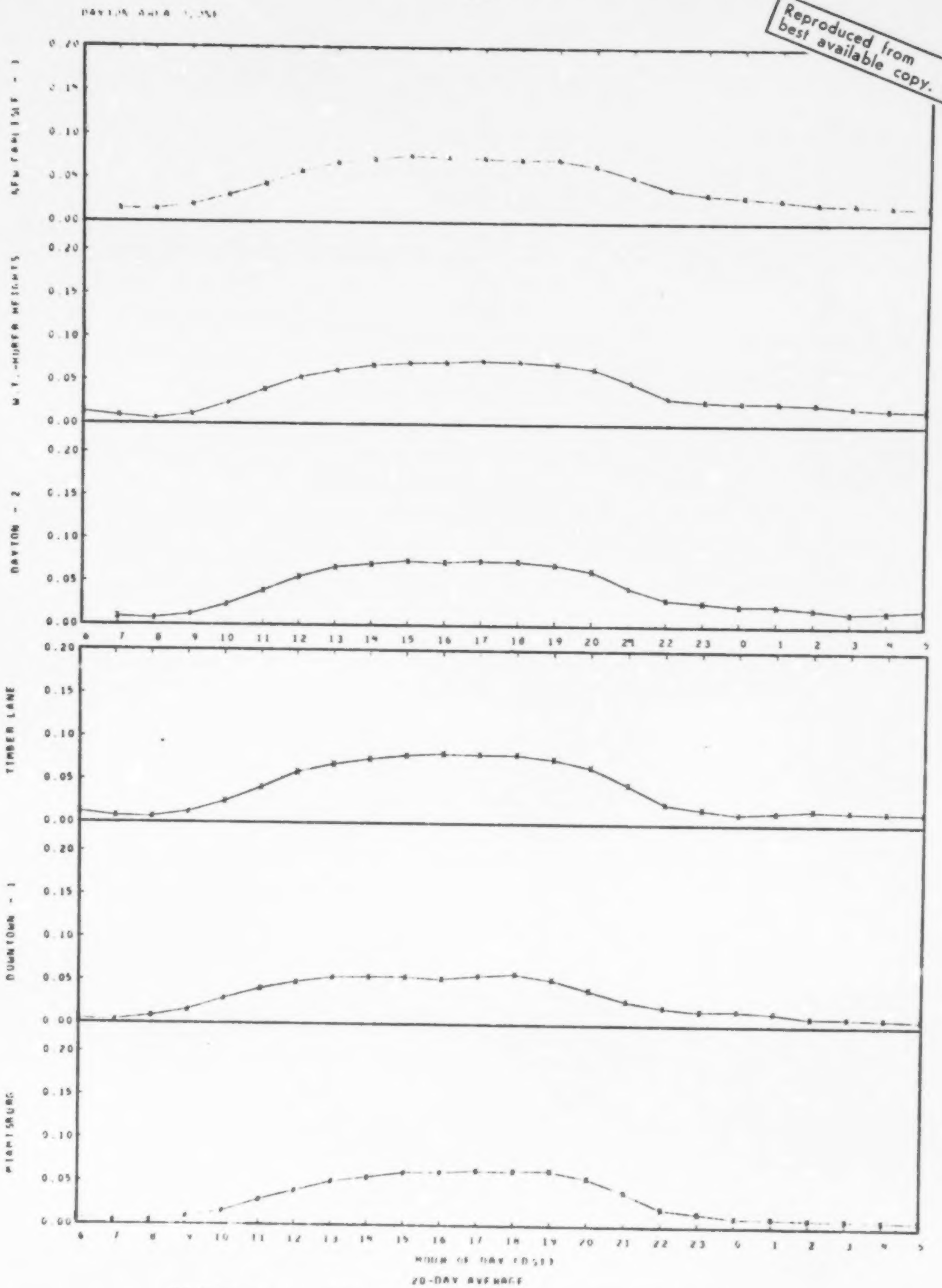

FIGURE 45 A. SIX SITE PROFILES OF OZONE (IN ppm)

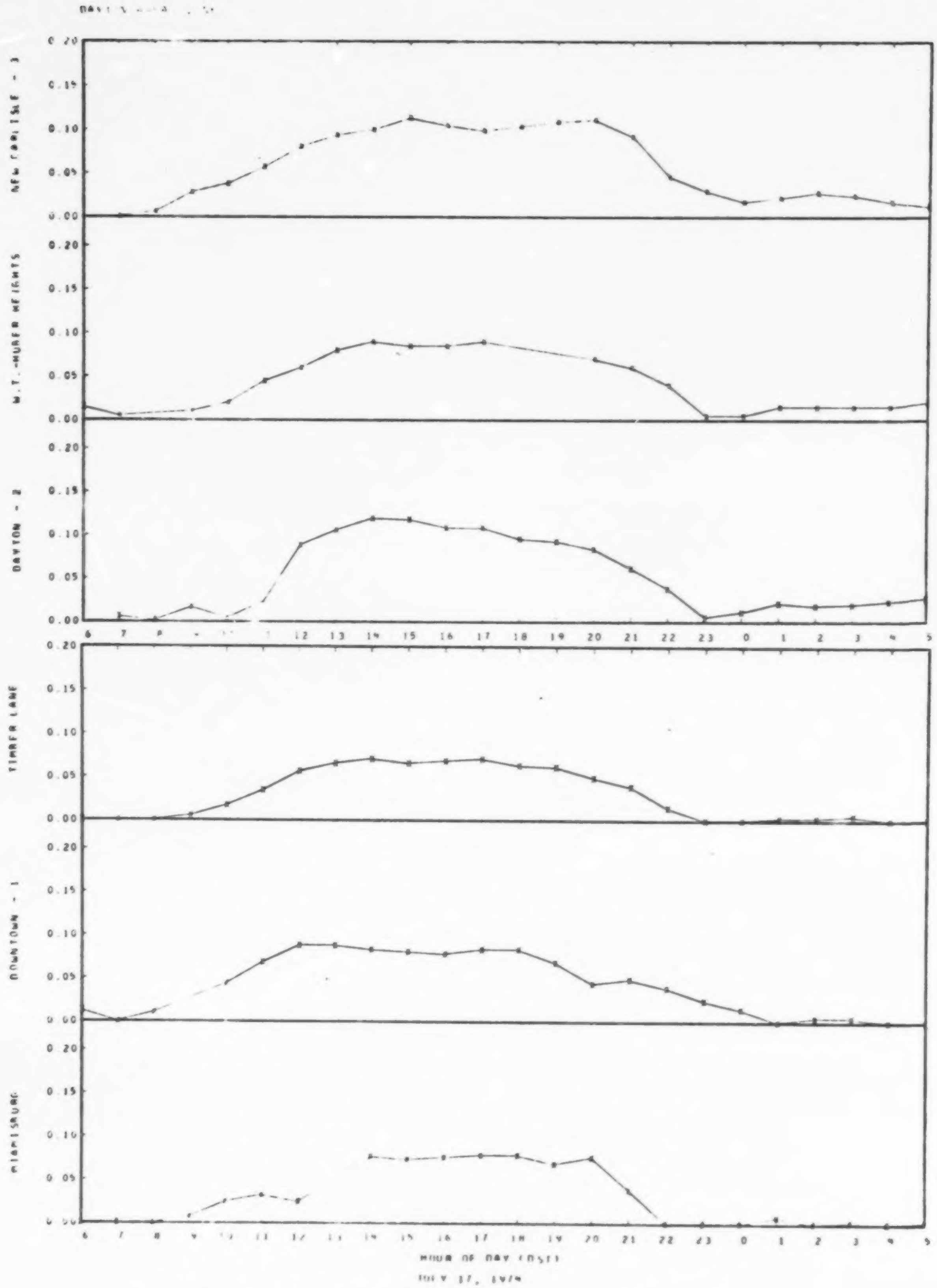

FIGURE 45 B. SIX SITE PROFILES OF OZONE (IN ppm)

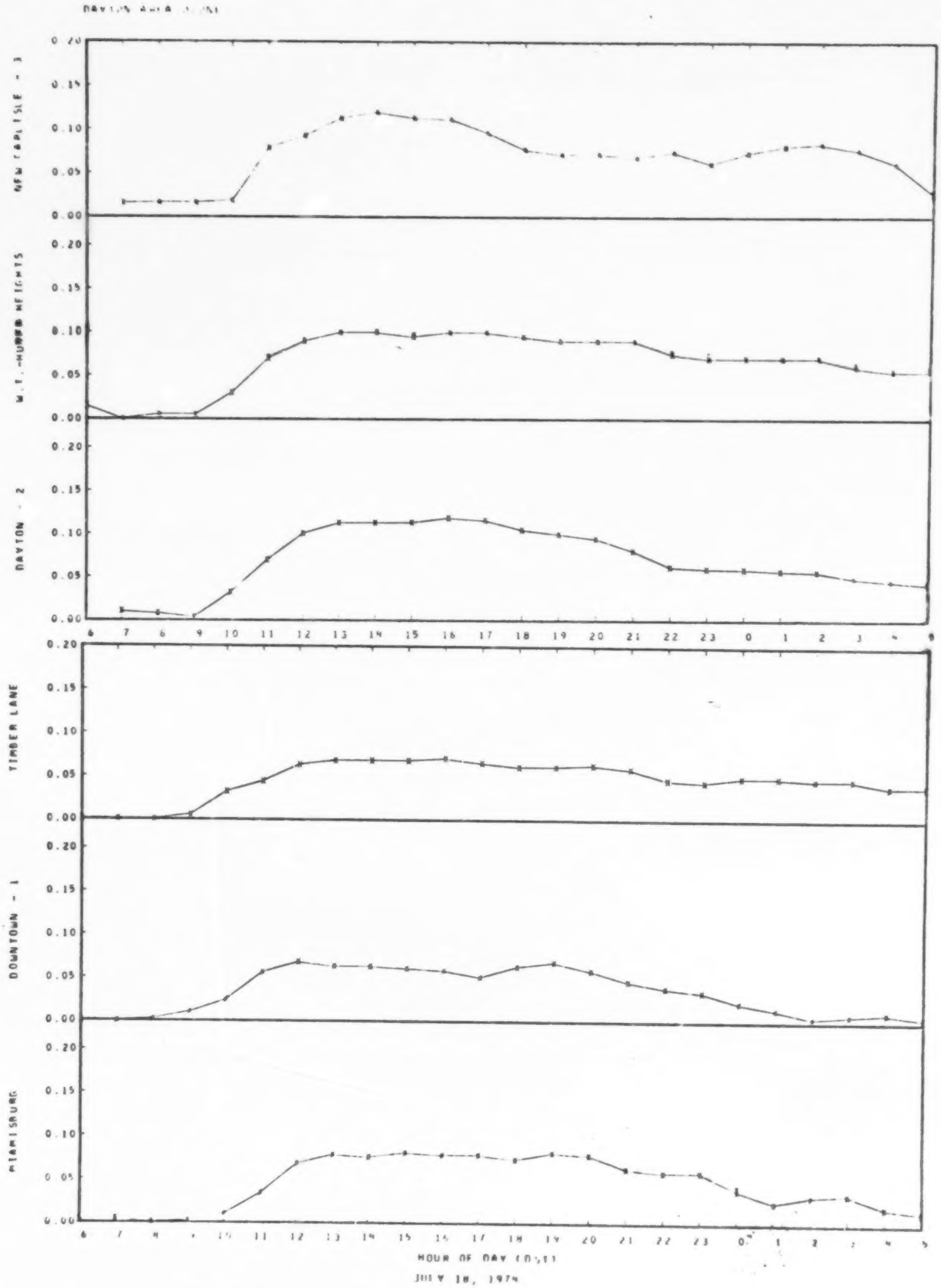

FIGURE 45 C. SIX SITE PROFILES OF OZONE (IN ppm)

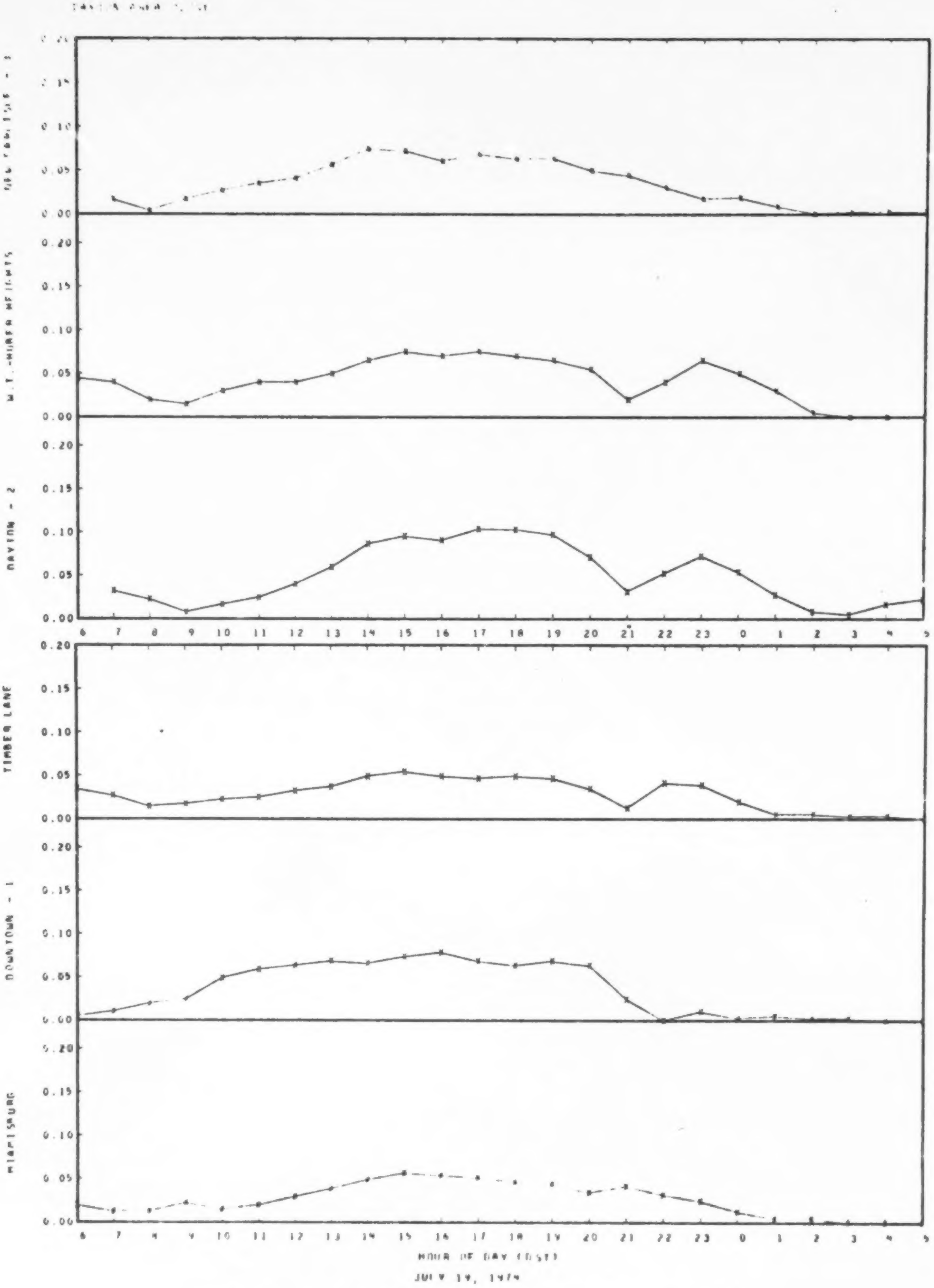

FIGURE 45 D. SIX SITE PROFILES OF OZONE (IN ppm)

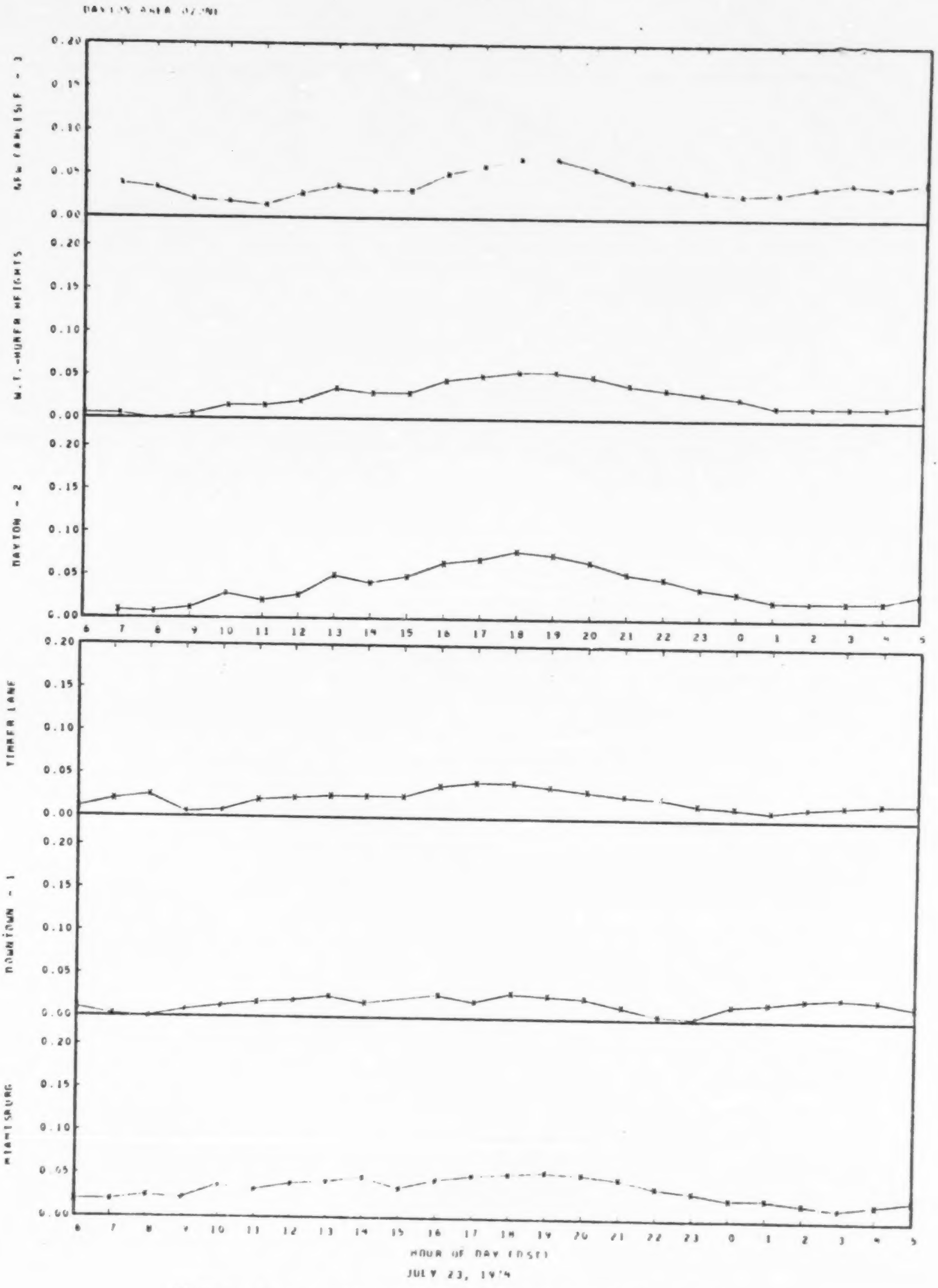

FIGURE 45 E. SIX SITE PROFILES OF OZONE (IN ppm)

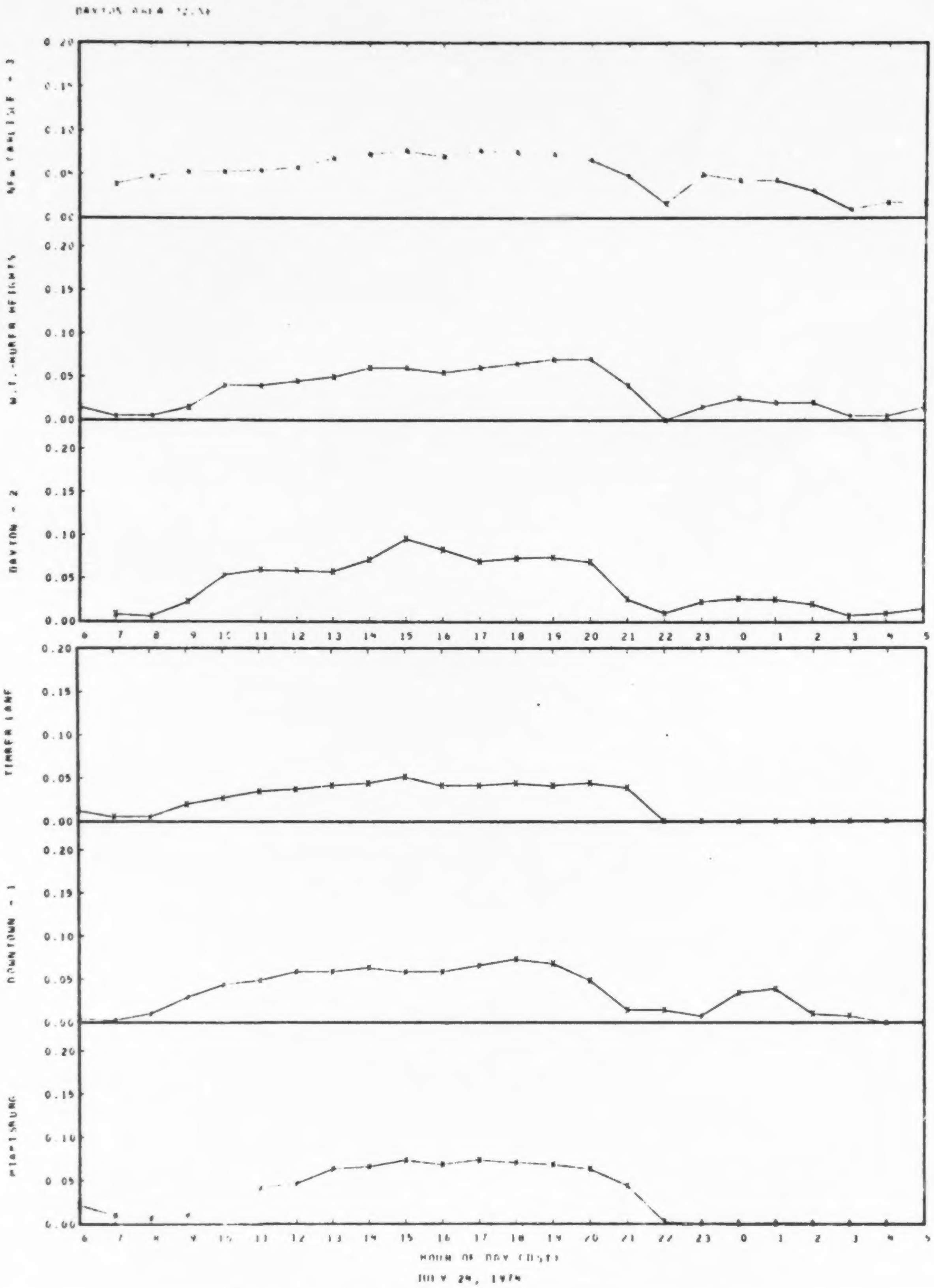

FIGURE 45 F. SIX SITE PROFILES OF OZONE (IN ppm)

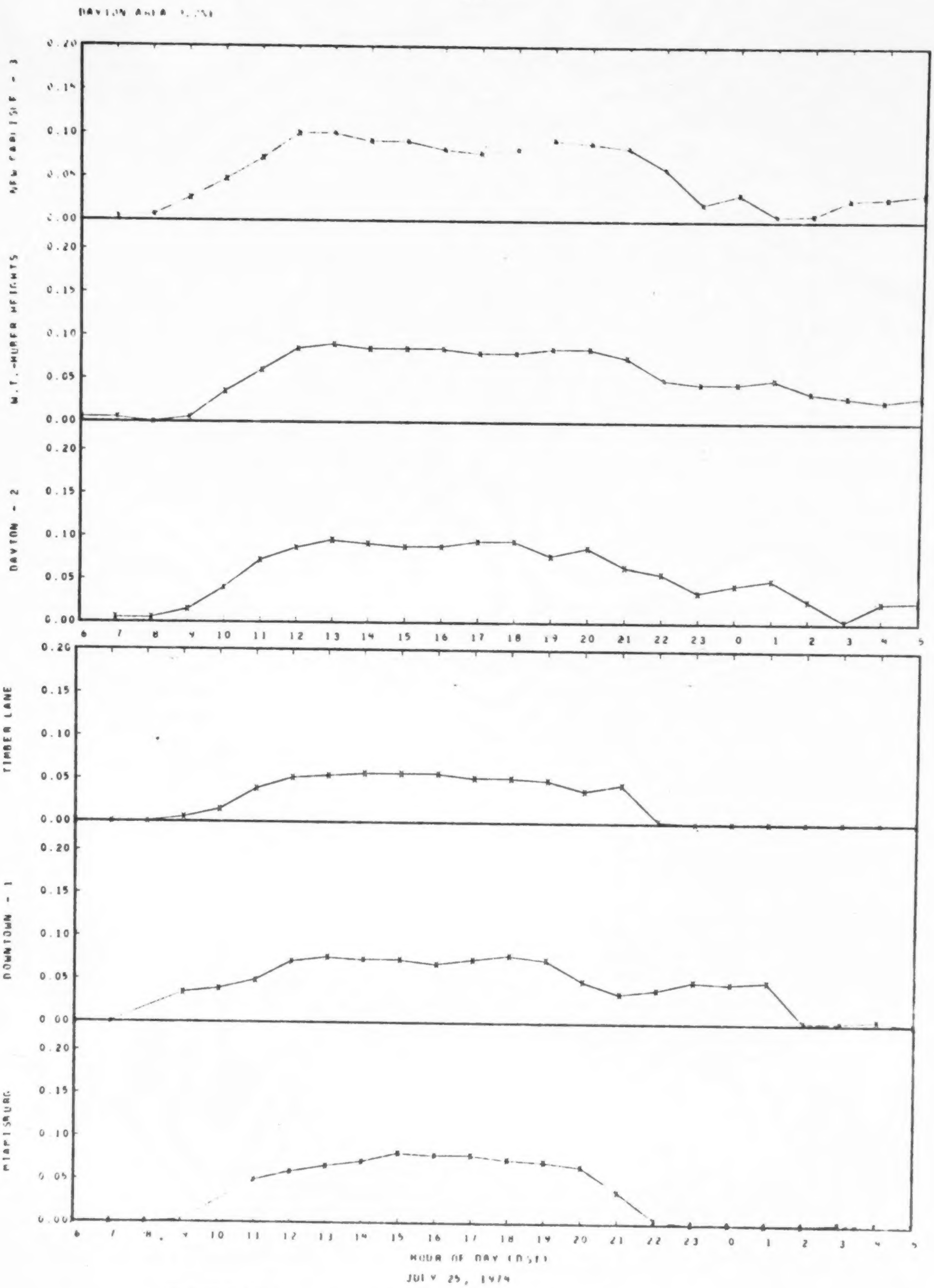

FIGURE 45 G. SIX SITE PROFILES OF OZONE (IN ppm)

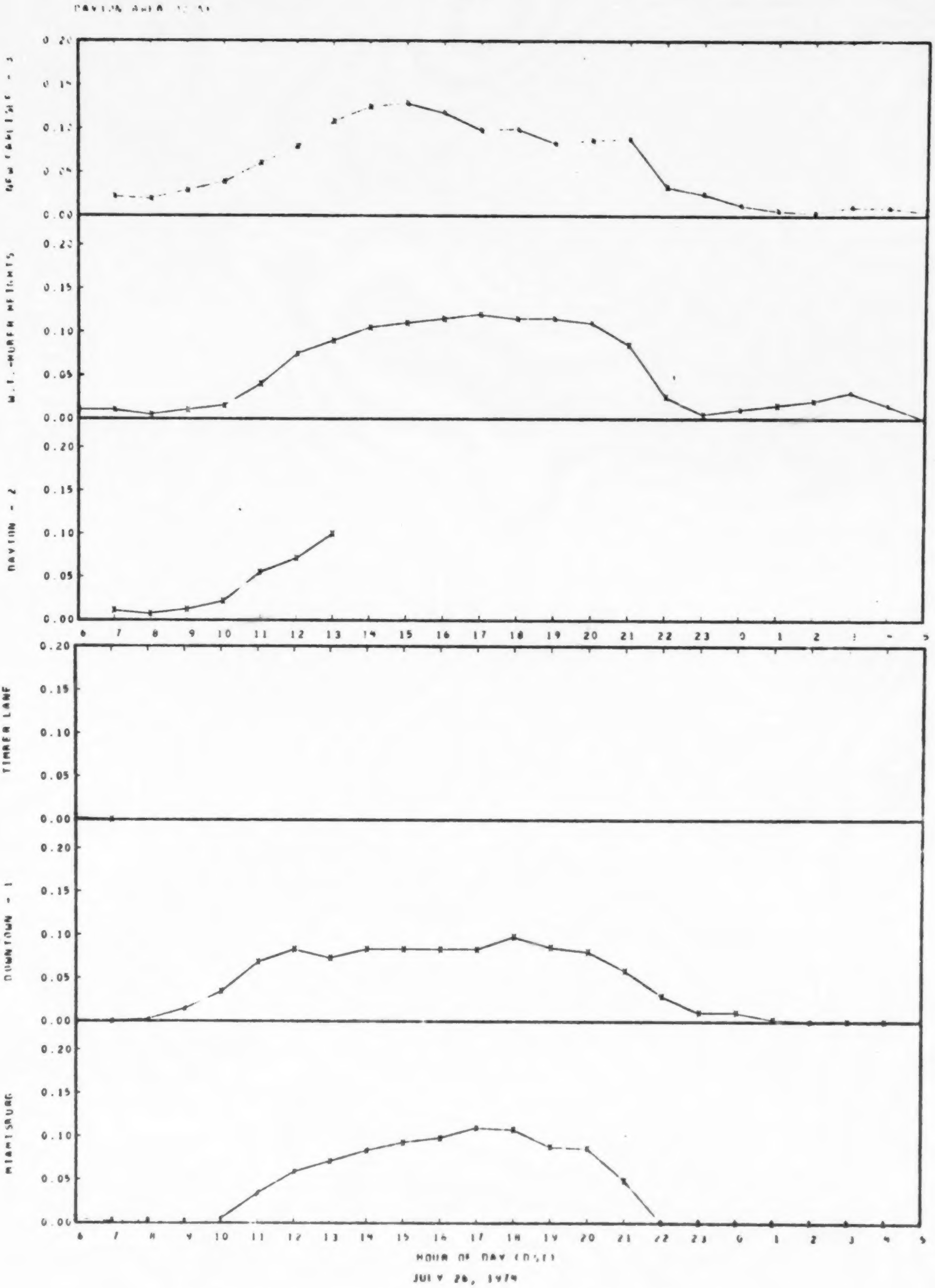

FIGURE 45 H. SIX SITE PROFILES OF OZONE (IN ppm)

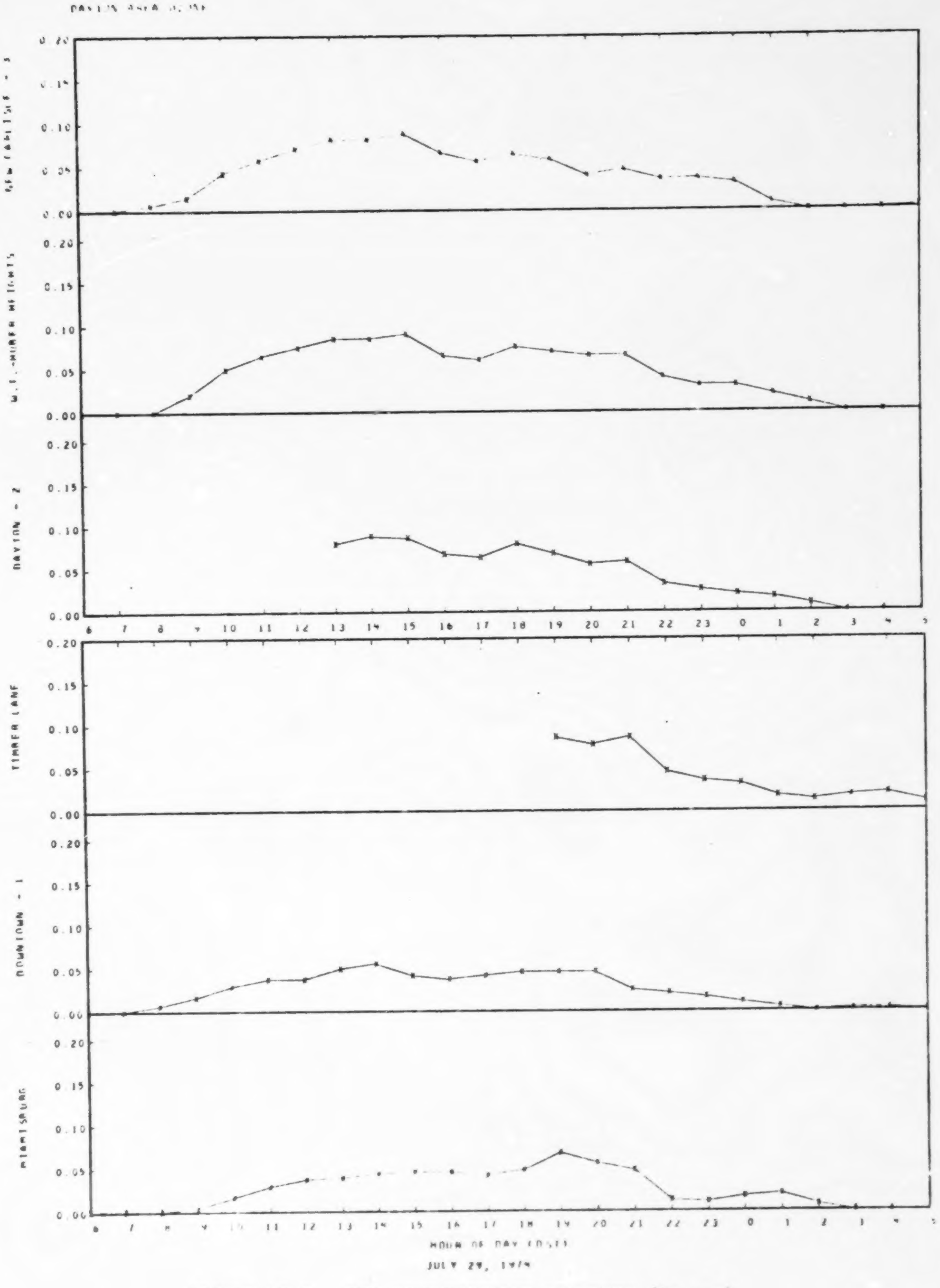

FIGURE 45 I. SIX SITE PROFILES OF OZONE (IN ppm)

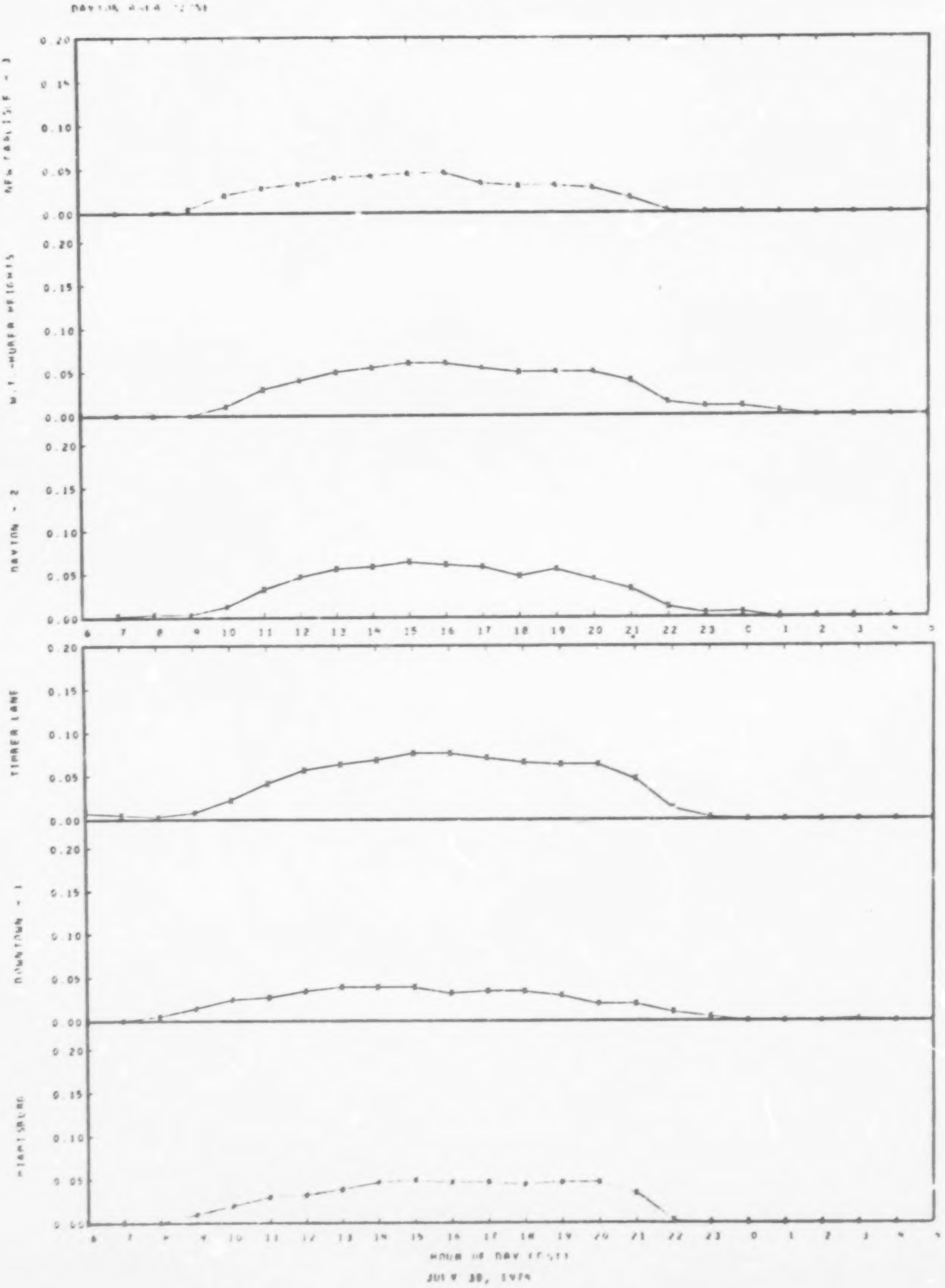

FIGURE 45 J. SIX SITE PROFILES OF OZONE (IN ppm)

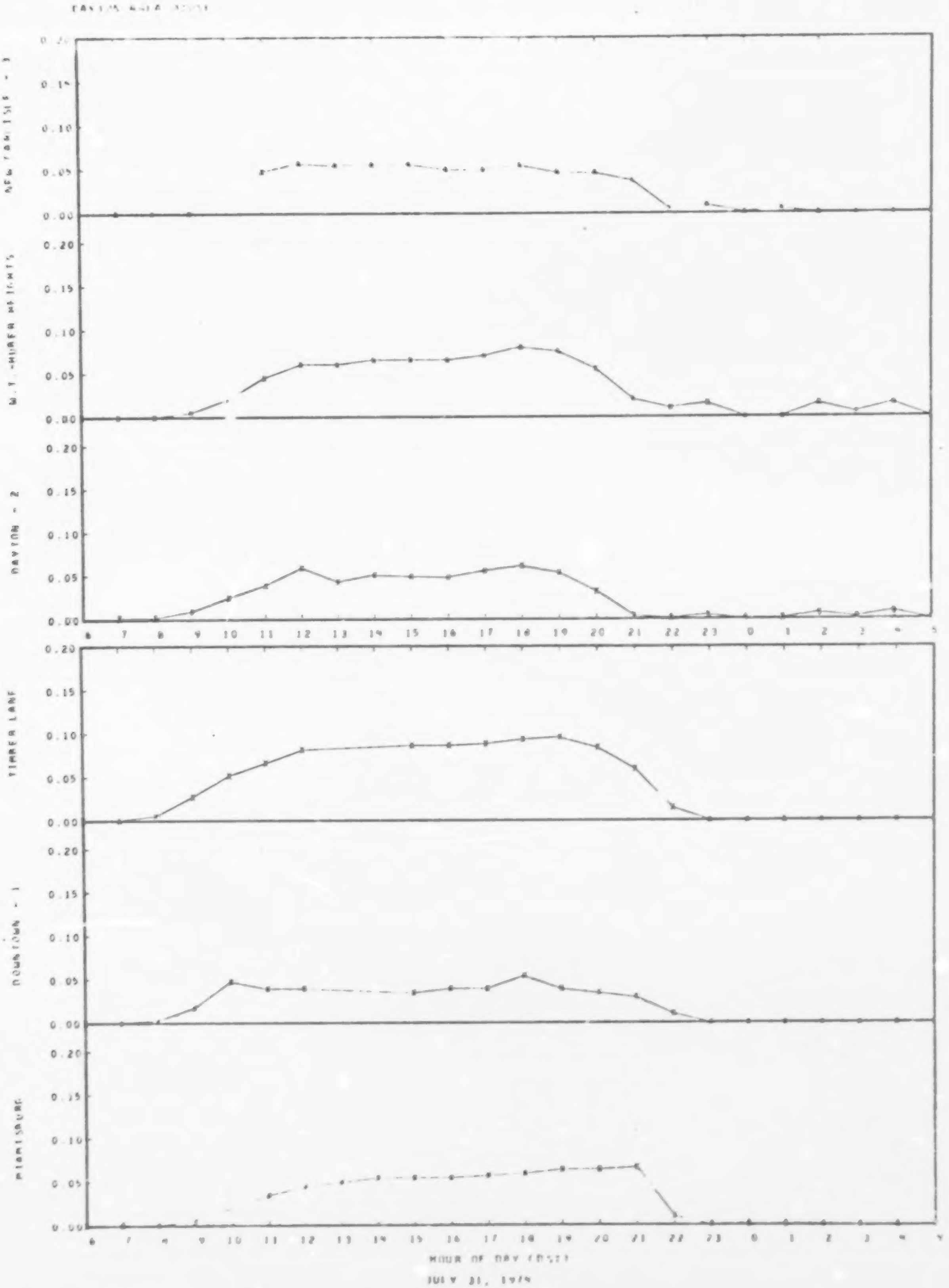

FIGURE 45 K. SIX SITE PROFILES OF OZONE (IN ppm)

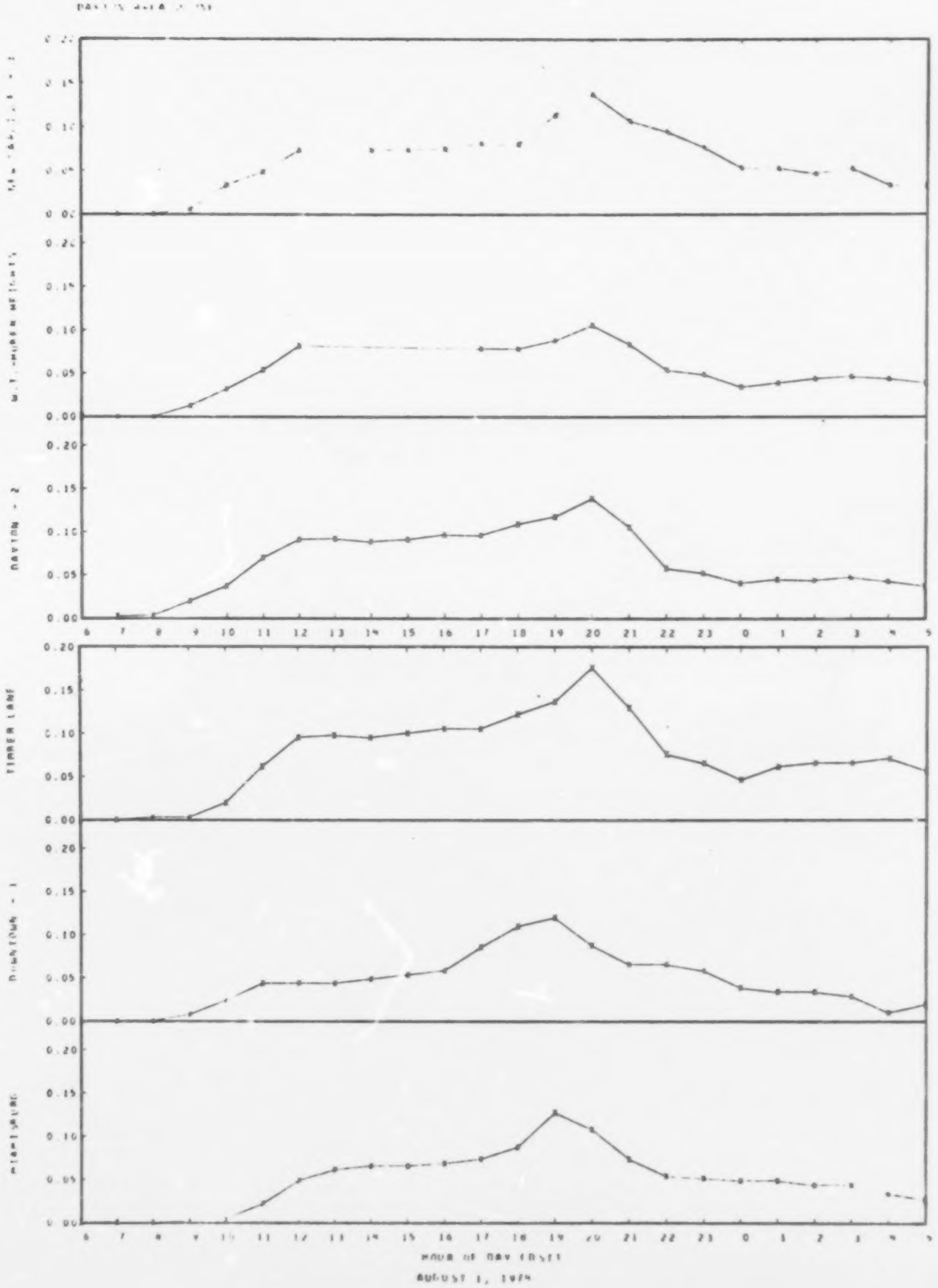

FIGURE 45 L. SIX SITE PROFILES OF OZONE (IN ppm)

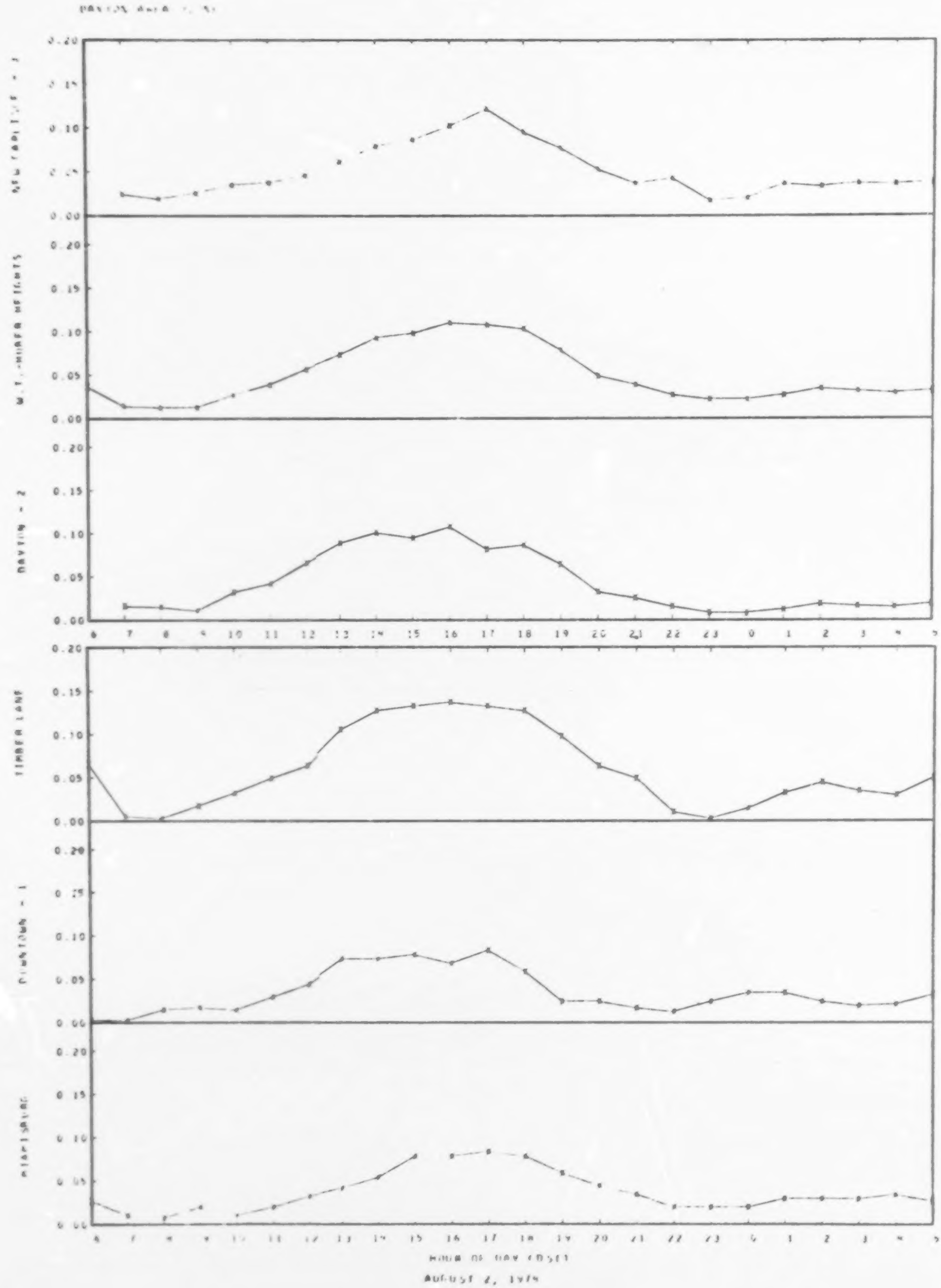

FIGURE 45 M. SIX SITE PROFILES OF OZONE (IN ppm)

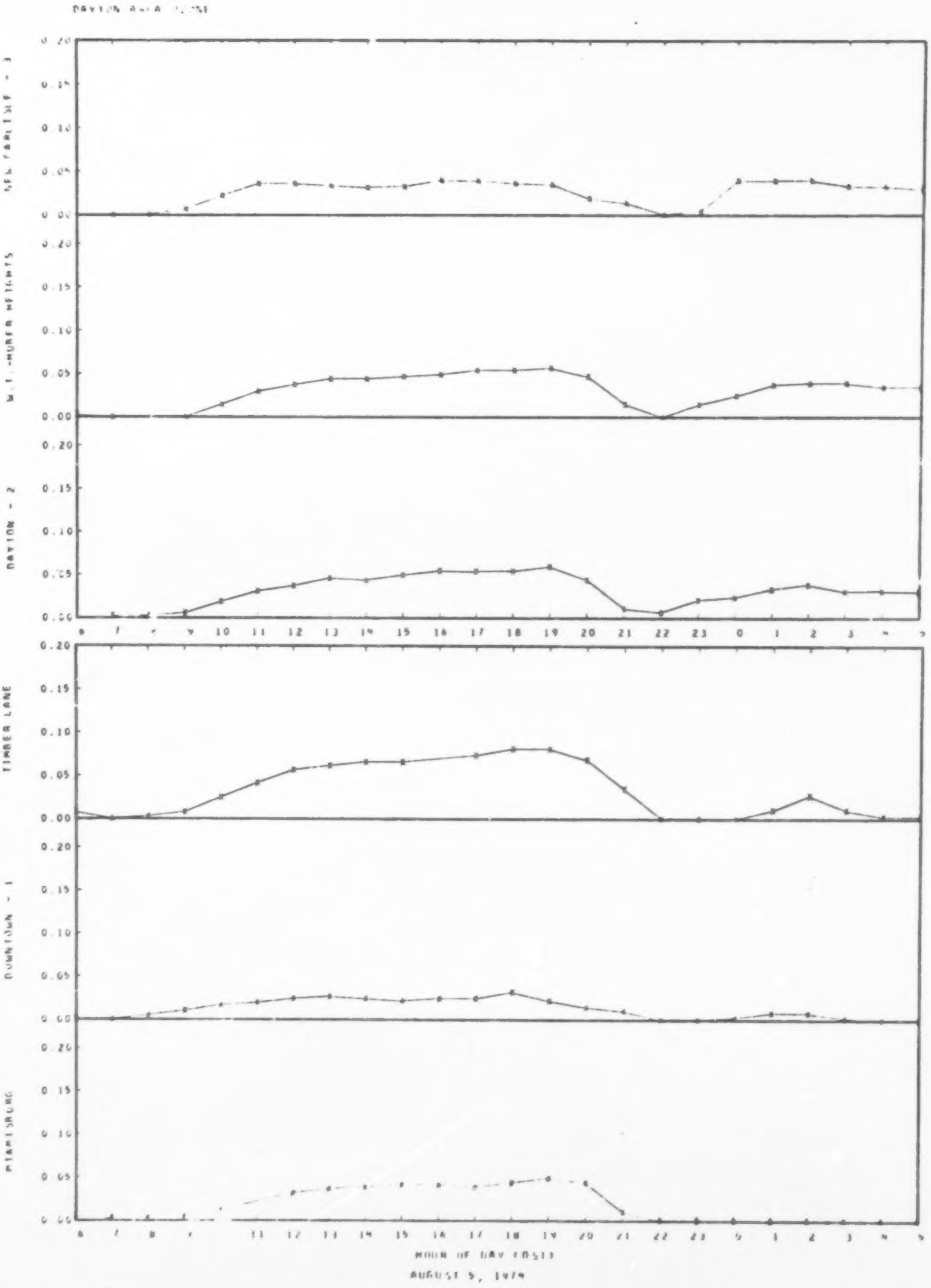

FIGURE 45 N. SIX SITE PROFILES OF OZONE (IN ppm)

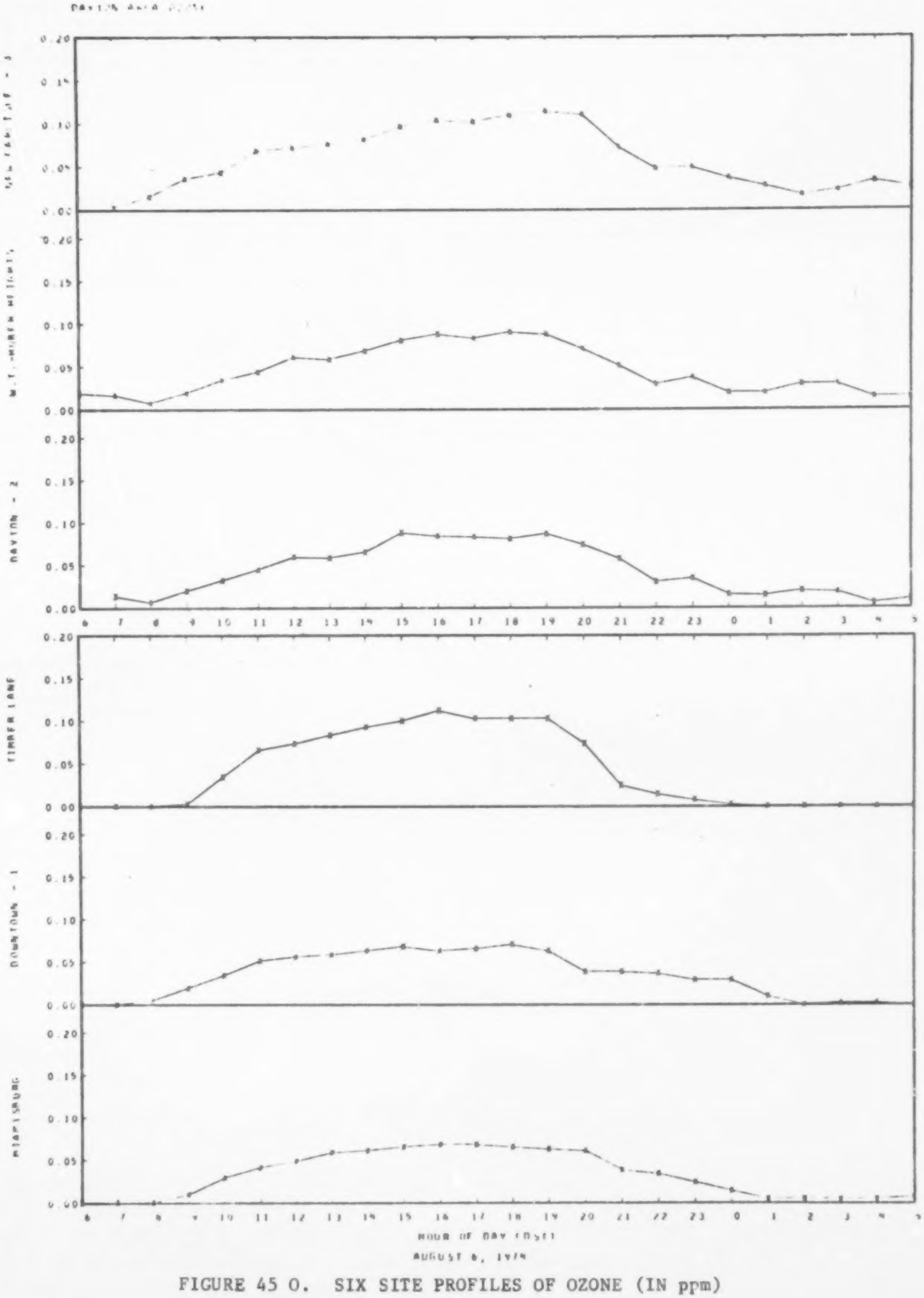

FIGURE 45 O. SIX SITE PROFILES OF OZONE (IN ppm)

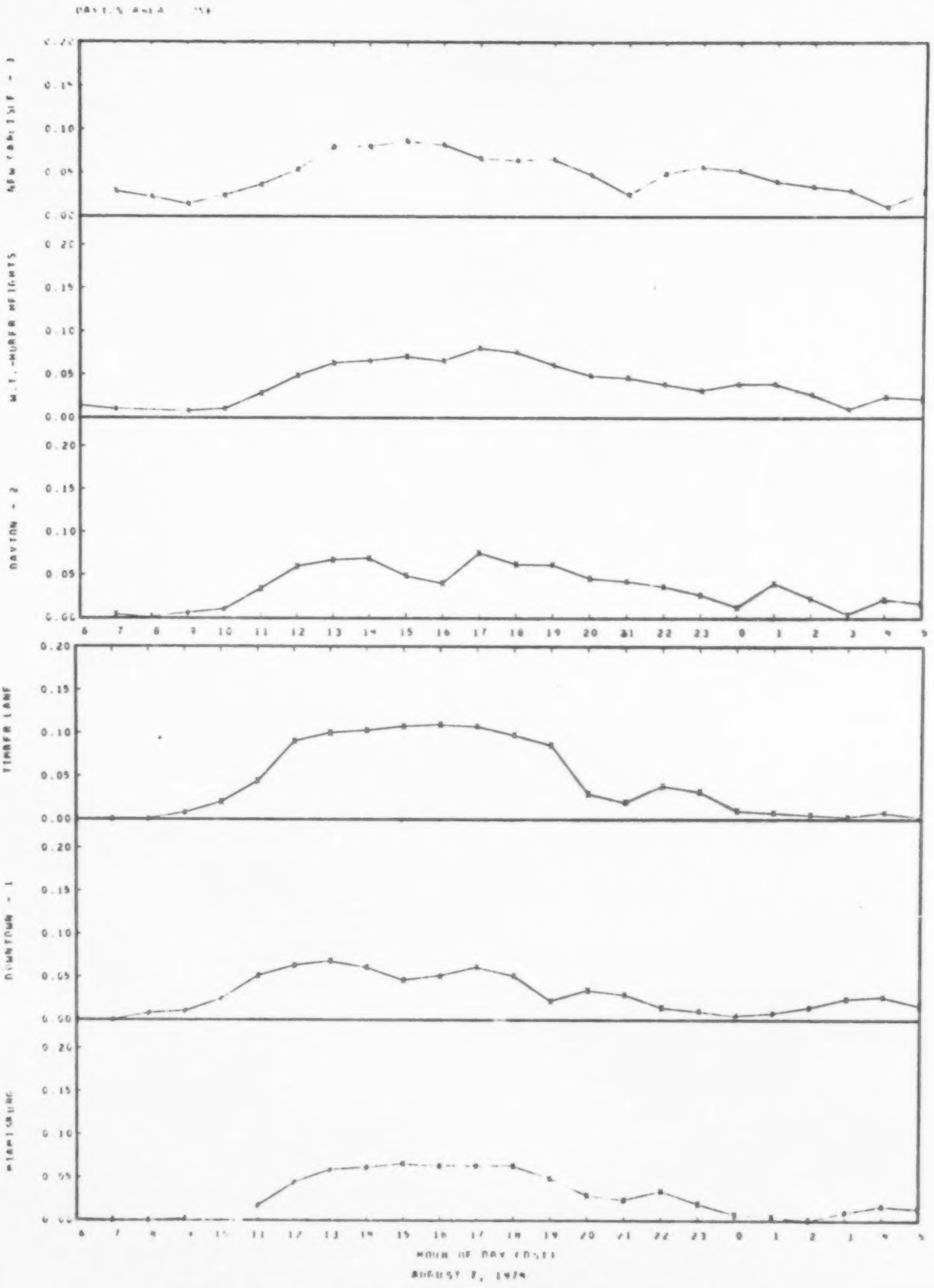

FIGURE 45 P. SIX SITE PROFILES OF OZONE (IN ppm)

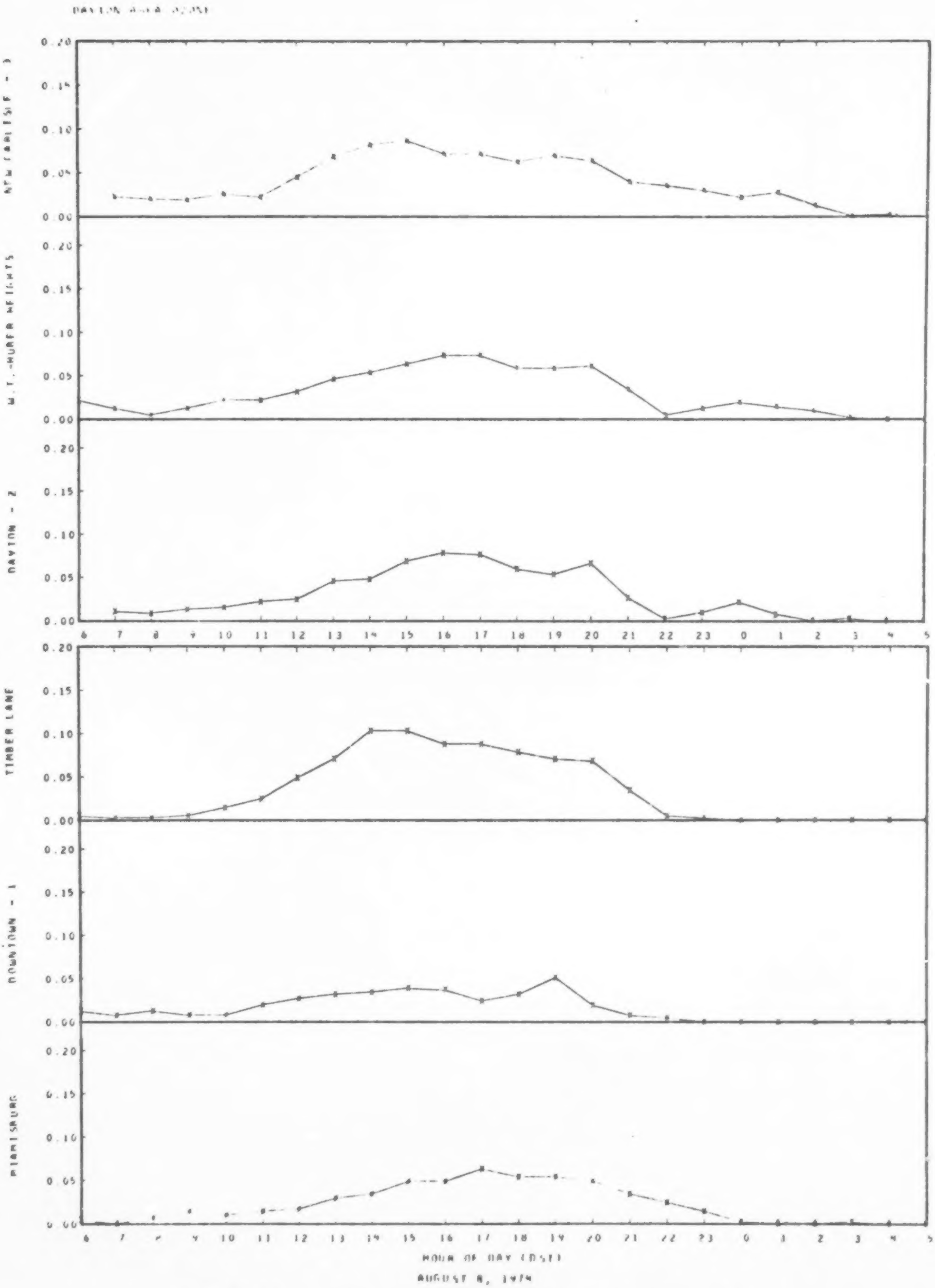

FIGURE 45 Q. SIX SITE PROFILES OF OZONE (IN ppm)

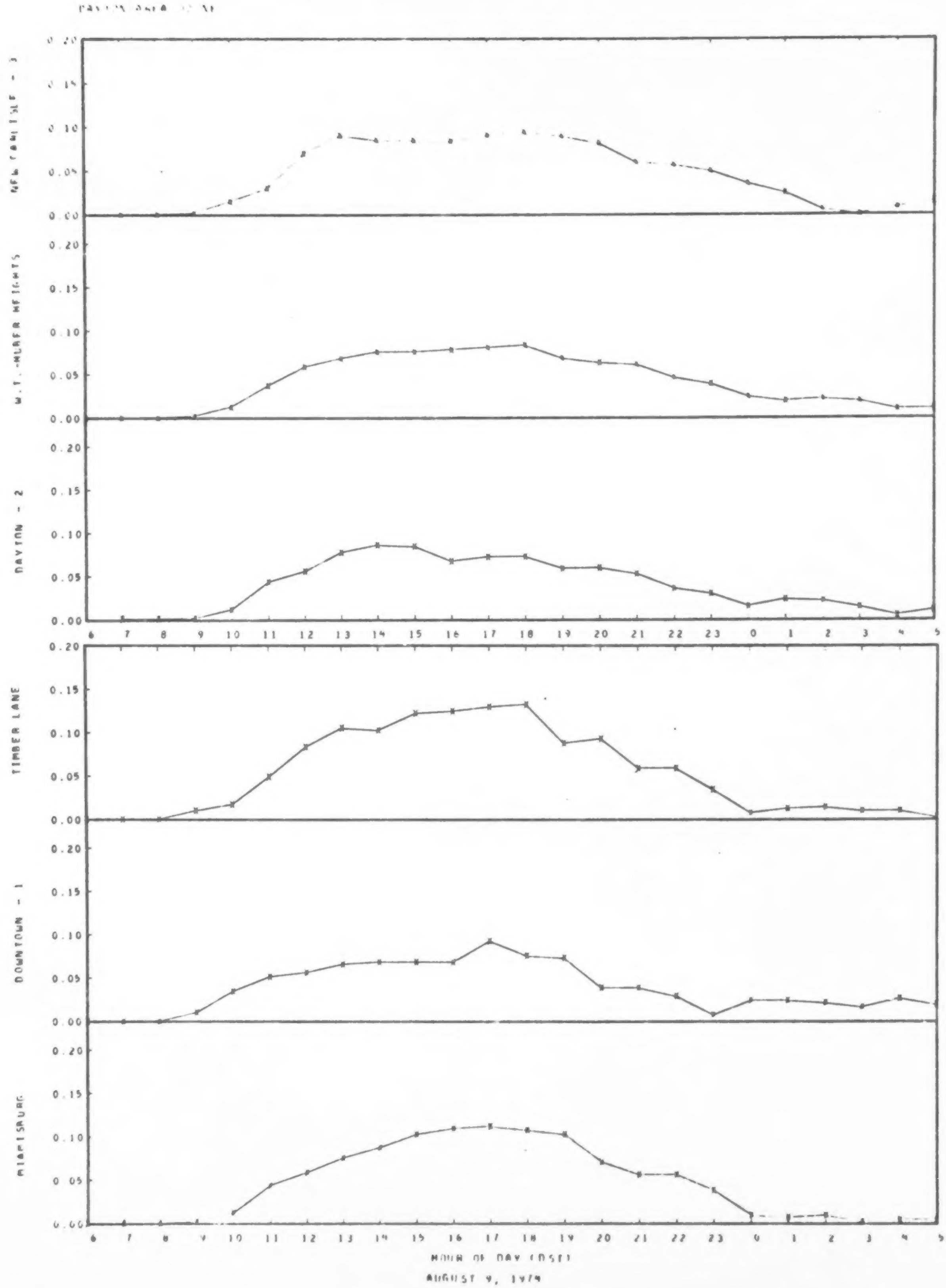

FIGURE 45 R. SIX SITE PROFILES OF OZONE (IN ppm)

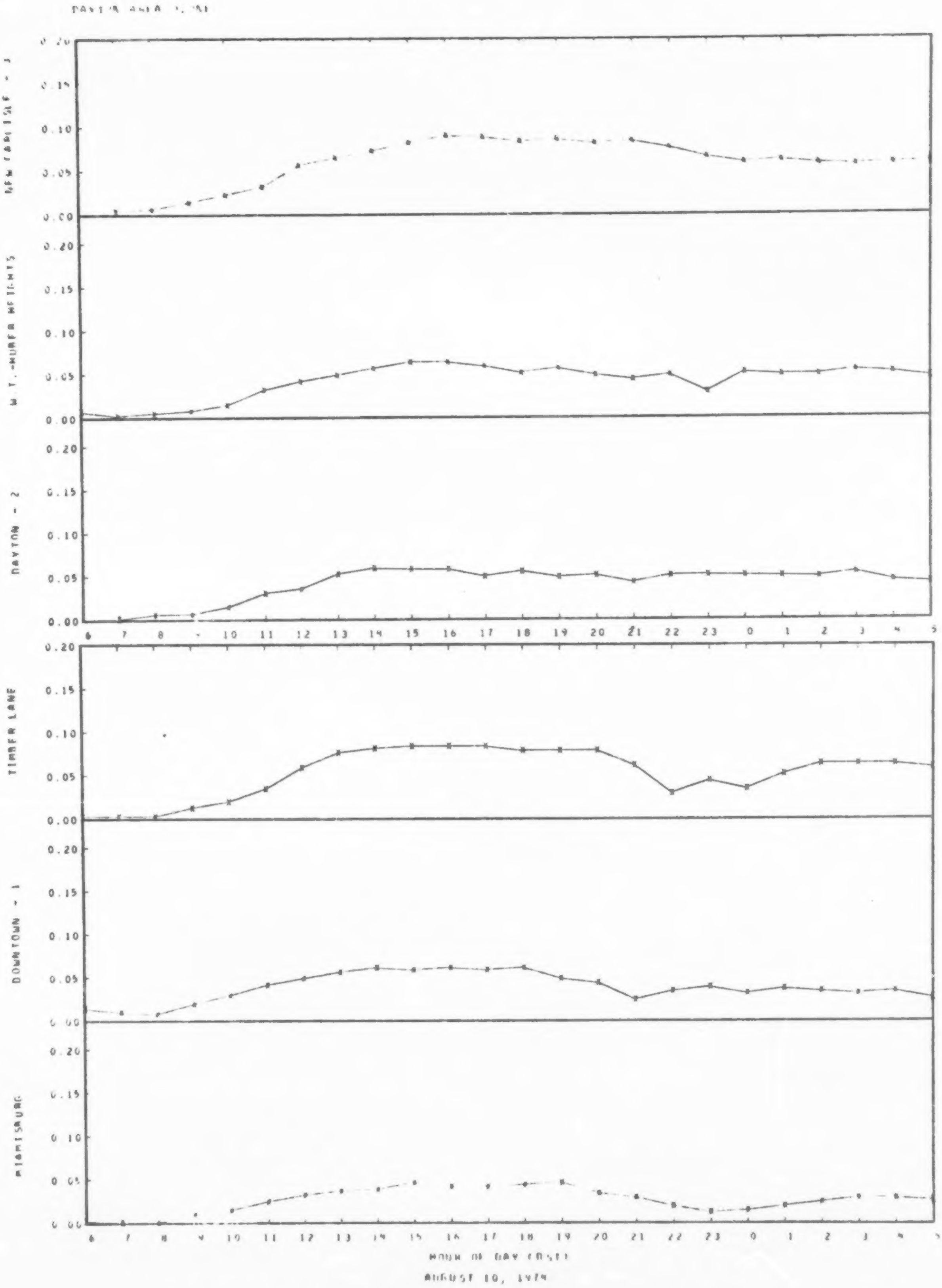

FIGURE 45 S. SIX SITE PROFILES OF OZONE (IN ppm)

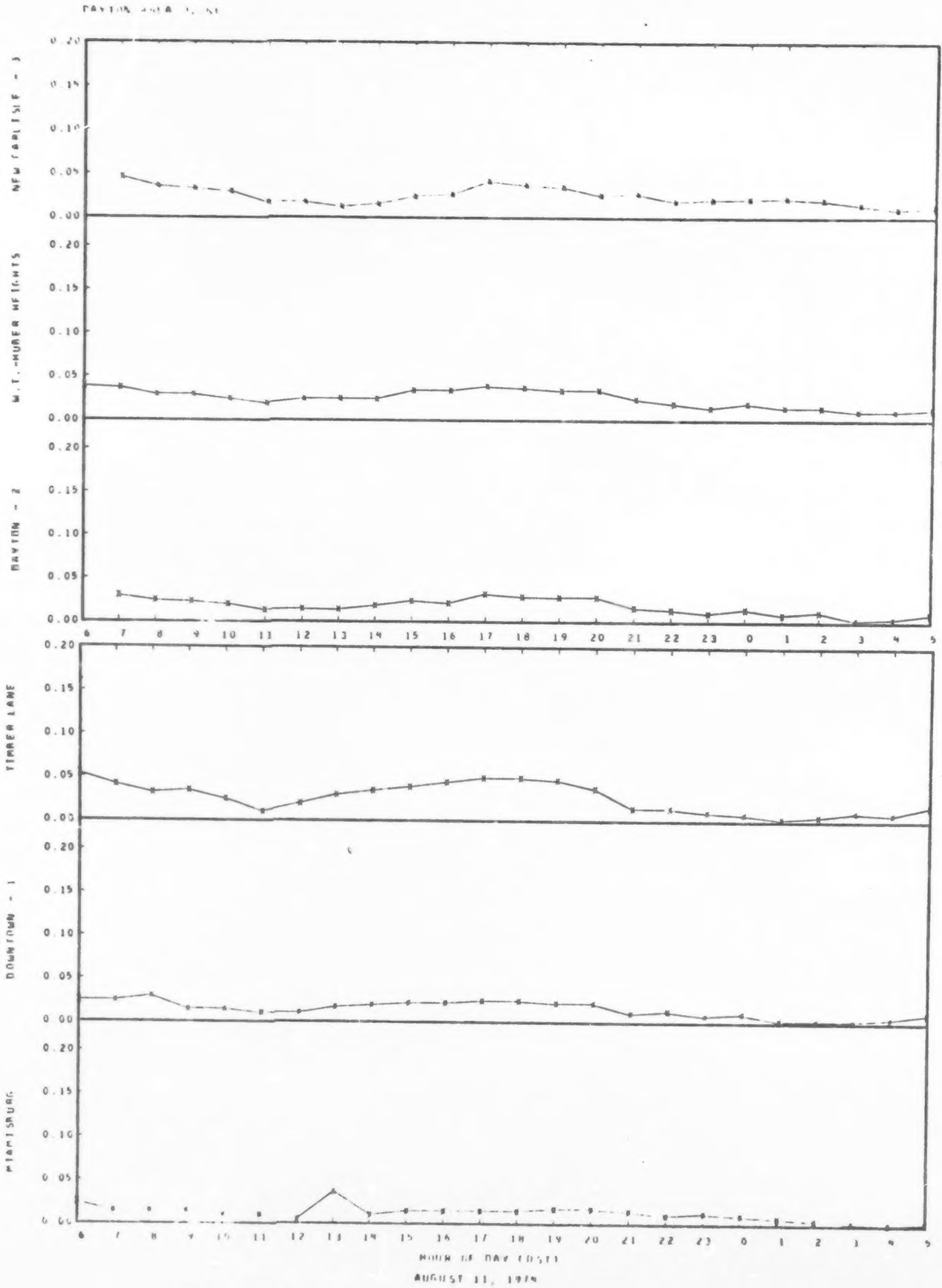

FIGURE 45 T. SIX SITE PROFILES OF OZONE (IN ppm)

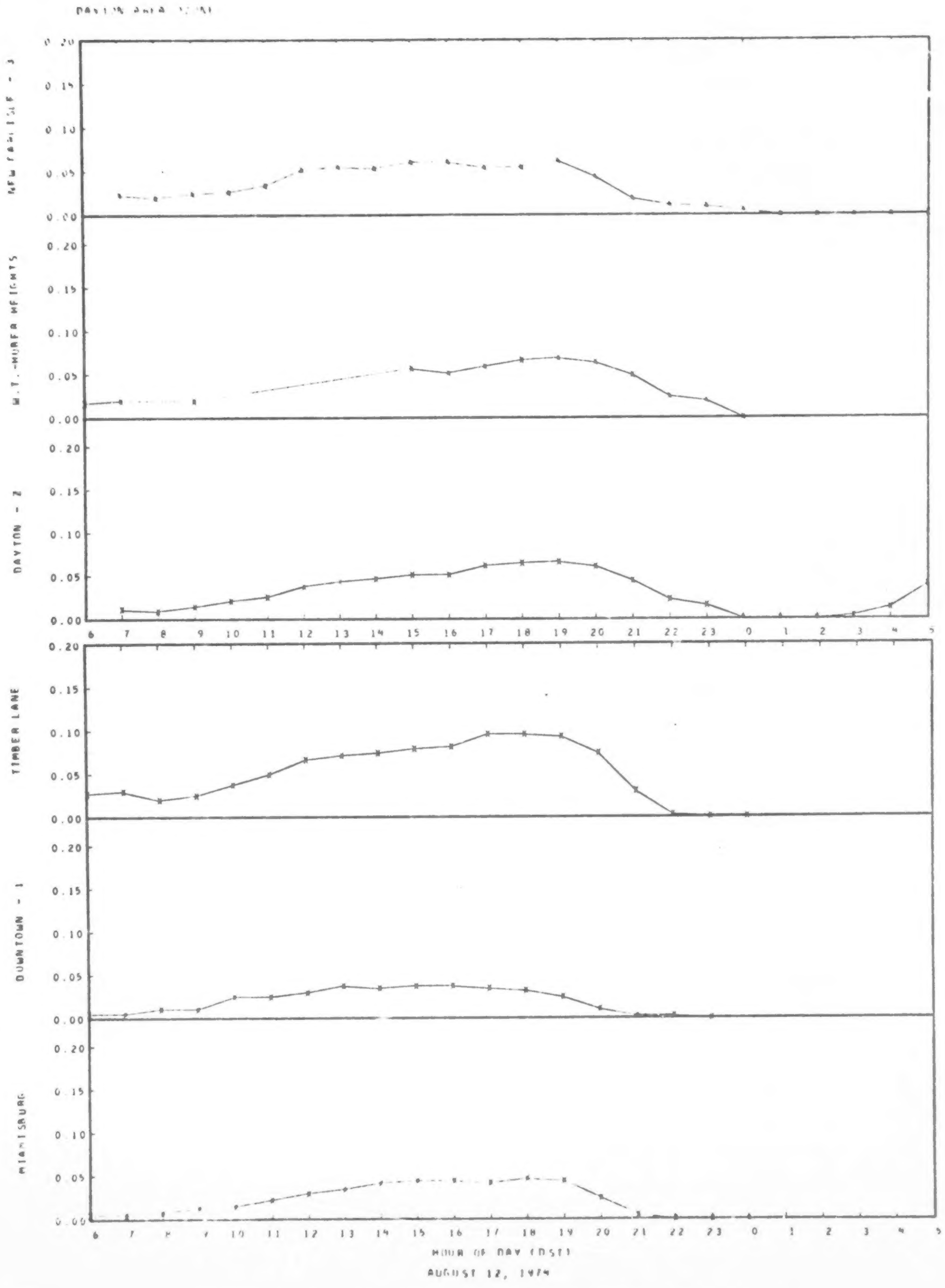

FIGURE 45 U. SIX SITE PROFILES OF OZONE (IN ppm)

addition, movement of stratospheric ozone downward through breaks in the tropopause yields tropospheric ozone. These two sources together account for a natural background O_3 level of perhaps 20-30 ppb. Substantially higher levels of O_3 found in the troposphere are normally related to increased concentration of hydrocarbon and/or nitrogen oxide ingredients (precursors) from anthropogenic activities. The ozone concentration produced from the precursor species by a complex free-radical mechanism can be equated, as a first approximation, to the product of the ultraviolet sunlight intensity and the ratio of nitrogen dioxide to nitric oxide:

$$[O_3] = K \frac{[NO_2]}{[NO]} ,$$

where K is proportional to U.V. intensity. Most hydrocarbons can react, with varying degrees of rapidity, to convert NO to NO_2 and thereby increase the level of ozone. On the other hand, when NO is emitted into an air mass the O_3 concentration will diminish (the NO_2/NO ratio decreases) due to the rapid reaction between NO and O_3. At night when there is no sunlight to regenerate O_3, the O_3-NO reaction can proceed essentially to completion until one of the two reactants is virtually exhausted. Surfaces, such as the earth's surface, also serve as a sink for removal of O_3 from the atmosphere. While this mechanism of ozone formation and removal is a gross simplification of the chemistry involved, it is adequate for the purposes of this discussion and further detail would only obscure our arguments.

Meteorology can greatly influence the ozone concentation by affecting (1) the concentration of ozone precursors, (2) the sunlight intensity, (3) the reaction time of an air mass, (4) the trajectory of an air mass, and (5) the transport of stratospheric O_3 to ground level. We suggest that under proper meteorological conditions elevated levels of tropospheric ozone can exist over very widespread areas. One condition which fosters this type of ozone formation is the trapping of precursors (both natural and anthropogenic) below the subsidence inversion generally associated with high-pressure systems. Precursor concentrations can build up below the subsidence inversion during the multiday lifetime of the high-pressure system. Indeed we saw earlier that it was possible to track haze associated with a high-pressure system over hundreds of miles.

We suggest that, in an area such as the Ohio Valley, this effect can be observed on a regional basis. The pervasive precursor emissions sources essentially blanket the region with hydrocarbon and nitrogen oxide precursors and ultimately with ozone (after suitable reaction time). Thus we can envision ozone and ozone precursors spread over very large areas and reacting over periods of several days or longer, acting as a kind of generalized ozone source or reservoir. Superimposed on this region-wide ozone blanket will be local "hot spots" in the spatial O_3 distribution caused by local emissions sources such as cities. Within an urban center and for some distance downwind of the urban area we suggest that ozone is depleted due to chemical scavenging by primary pollutants (e.g., NO). The "sheath" of NO-rich air (i.e., the urban plume) should extend downwind of the city to a point where the reaction time of the air mass has permitted conversion of the NO to NO_2; from that point the urban plume will be enriched in O_3, forming what we term a "hot spot". This O_3-enriched air mass can be transported through the region-wide O_3 blanket to rural areas and to other urban areas. Under appropriate meteorological conditions elevated O_3 levels would exist throughout the region, with even higher concentration pockets of ozone moving through the area. Under certain conditions, even stratospheric ozone could be transported to the ground and cause elevated ozone levels. The important point is that we believe no one particular O_3 source, be it urban transport, natural emissions, stratospheric transport, etc., can account for the ozone patterns observed in this and other studies. We suggest that only the interaction and superposition of these various sources can fully explain rural and urban ozone patterns.

At night, when the driving force of the photochemical reactions is eliminated we expect the O_3 concentration in an urban area to drop rapidly due to O_3 scavenging by the continuous NO emissions. Thus, below the nighttime inversion in the vicinity of NO sources (as in a city), the concentration of O_3 should go almost to zero. Above the inversion, where little NO has penetrated, high levels of O_3 are expected to remain throughout the night. With the breakup of the inversion the next day this ozone trapped aloft can be returned to the ground by turbulent mixing, perhaps after being transported during the night by the winds aloft.

In rural areas the O_3 behavior is somewhat different. The much lower nighttime rural NO emissions will often not exhaust the O_3 blanket, so that in some areas ozone may persist throughout the night. Even here however, reaction with the earth's surface and the low levels of NO will create a depletion of O_3 near the ground so that a gradient will be set up below the inversion.

The basic features of this model will be used shortly in examining our field study results. However, first we would like to discuss how they can be used to answer the question of higher weekend versus weekday ozone levels in some cities.

The question of elevated ozone in cities during weekends, when primary pollutant emissions are much lower than on weekdays, has been raised by several researchers(13,14). Referring to Table 20, our Dayton results also show high weekend O_3, with all stations exceeding the Federal standard during at least one weekend, and several exceeding 0.10 ppm. The traditional view of O_3 behavior would suggest that lower weekend emissions should result in lower weekend ozone concentrations within urban areas, in conflict with the experimental evidence in Dayton and many other cities. Our "model" accounts for the higher weekend O_3 quite simply. During weekdays the regional ozone blanket or reservoir continually supplies the city and the surrounding area with O_3. However, primary pollutant O_3 scavengers such as NO suppress the O_3 levels within the city to levels lower than the surrounding countryside. During weekends the ozone reservior still supplies the city, but the emission of scavengers is less, so that the ozone concentration is not suppressed to as great an extent as on weekdays. Thus the center-city monitoring station observes higher weekend ozone.

The model just described appears consistent with most of the ozone data we have examined and satisfactorily explains the following observations:

(1) High rural O_3 levels
(2) Differences between rural and urban nighttime ozone patterns
(3) Lower center-city O_3 levels
(4) Nondirectionality, with respect to wind direction, of moderate O_3 levels
(5) Weekend versus weekday urban ozone behavior.

The remainder of this report will be devoted to testing this model on individual days of our Dayton field data. First however, we would like to confirm the lower center-city O_3 concentration predicted by the model. Figure 46 shows this pattern quite clearly. The 20-day average ozone from all six ground stations is plotted versus time of day in the figure. The urban and industrialized areas of downtown Dayton and Miamisburg exhibit substantially lower average ozone than the other sites. As predicted, the nighttime ozone levels at these two stations also drop to lower values than the other sites. These features of the average O_3 patterns are entirely consistent with the model.

July 18, 1974

July 18, 1974, was a hot, sunny day in Dayton, with a heavy morning haze. The center of a high-pressure area had passed through Ohio on the previous day as indicated on the NWS map in Appendix E. Referring back to Table 20, our calculated 6 a.m.-2 p.m. wind direction component of the average wind vector was 243°. Computer-calculated air mass trajectories* show air mass movement into Dayton from the southwesterly

---

* We would like to express our appreciation to Mr. Jim Worth of Research Triangle Institute for making these trajectories available to us.

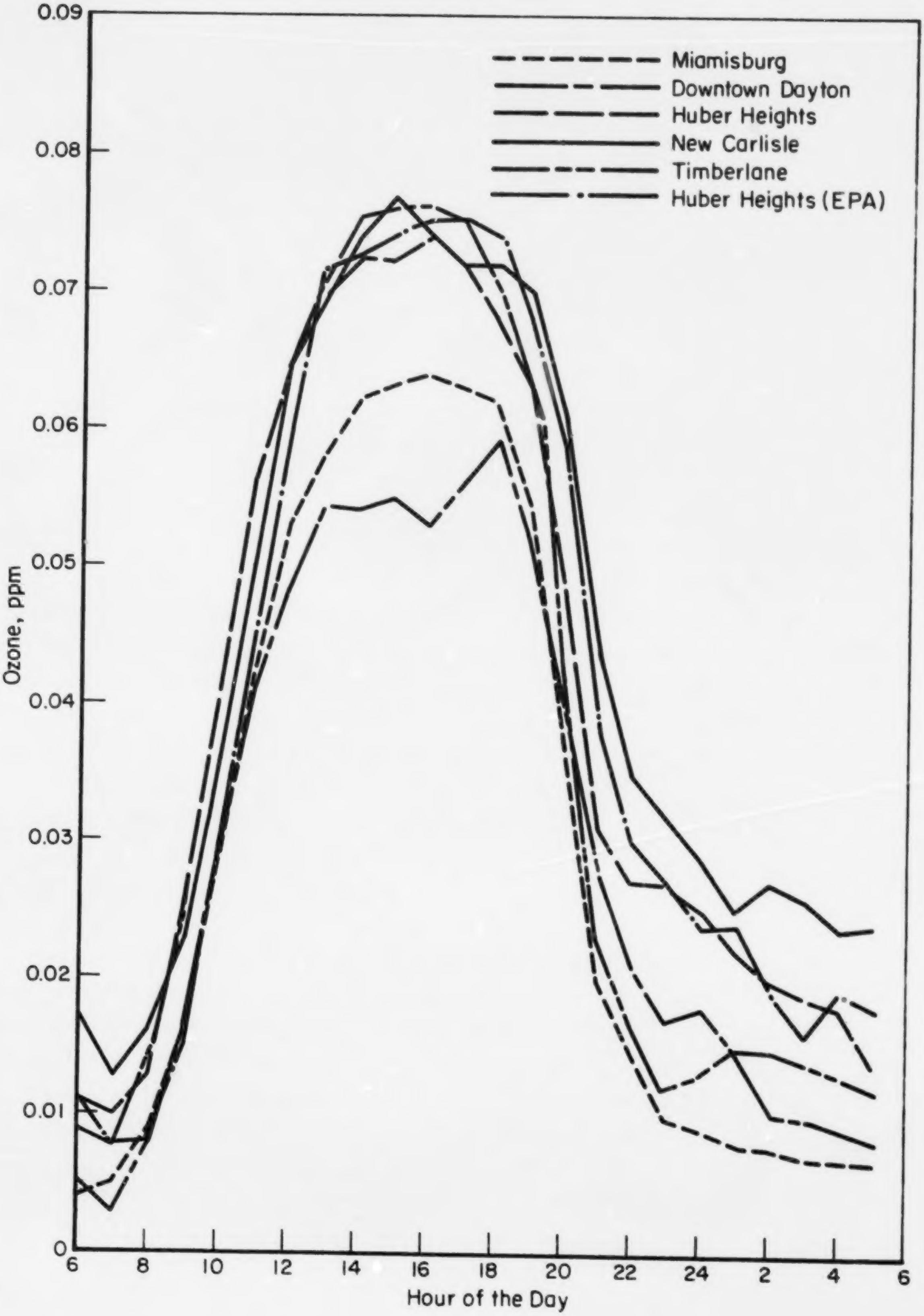

FIGURE 46. 20-DAY AVERAGE DAYTON AREA OZONE PROFILES

direction for at least the previous 12 hours. These trajectories are shown in Appendix F. As seen in Table 20, the O_3 levels exceeded 0.10 ppm at Sites 2 and 3 during this day, and also exceeded the Federal standard of 0.08 ppm at Miamisburg. The ozone profiles from all six sites for this day were shown earlier in Figure 45 C. An expanded version of this plot is shown in Figure 47. The ozone concentrations at the four sites represented in the figure all reach an initial maximum between noon and 2 p.m., with the exception of Site 2 which peaks at about 4 p.m. Miamisburg, downtown Dayton and, to some extent, Huber Heights, show a second maximum occurring at approximately 7 p.m., long after the photochemical processes generating ozone have subsided. A third, very pronounced ozone maximum occurs at the New Carlisle site at about 1 a.m., reaching a level in excess of the 0.08 ppm ozone standard. These late evening and nighttime increases in ozone concentration cannot be caused by photochemical reactions occurring at these late hours; such ozone must be transported into the area. The transported ozone may have originated in another urban area, perhaps Cincinnati on this day because of the air mass trajectories, or it may be part of the area-wide ozone reservoir. Our airplane observations may help to elucidate this question.

The morning and afternoon airplane flight patterns are plotted in Figures 48 A and B. The airplane flight routines were described earlier in this report. Ozone concentrations are marked throughout the flight path in ppb units. The results of the analysis of the airplane bag samples collected at the extremes of each flight loop are reported in Table 29. On this second day of the field program we were plagued with problems including a malfunctioning gas chromatograph and a tendency to overfill, and thus explode, our Teflon sampling bags. The bag data from this first aircraft sampling flight are therefore somewhat sparse.

The morning ozone distribution from Figure 48A reveals a range of O_3 concentration at the 1000-foot level from 0.090 to 0.138 ppm. It must be emphasized however, that the morning flights took place during the period when ground-level ozone concentrations were increasing rapidly. Since there is usually a time difference of 2 hours between the short

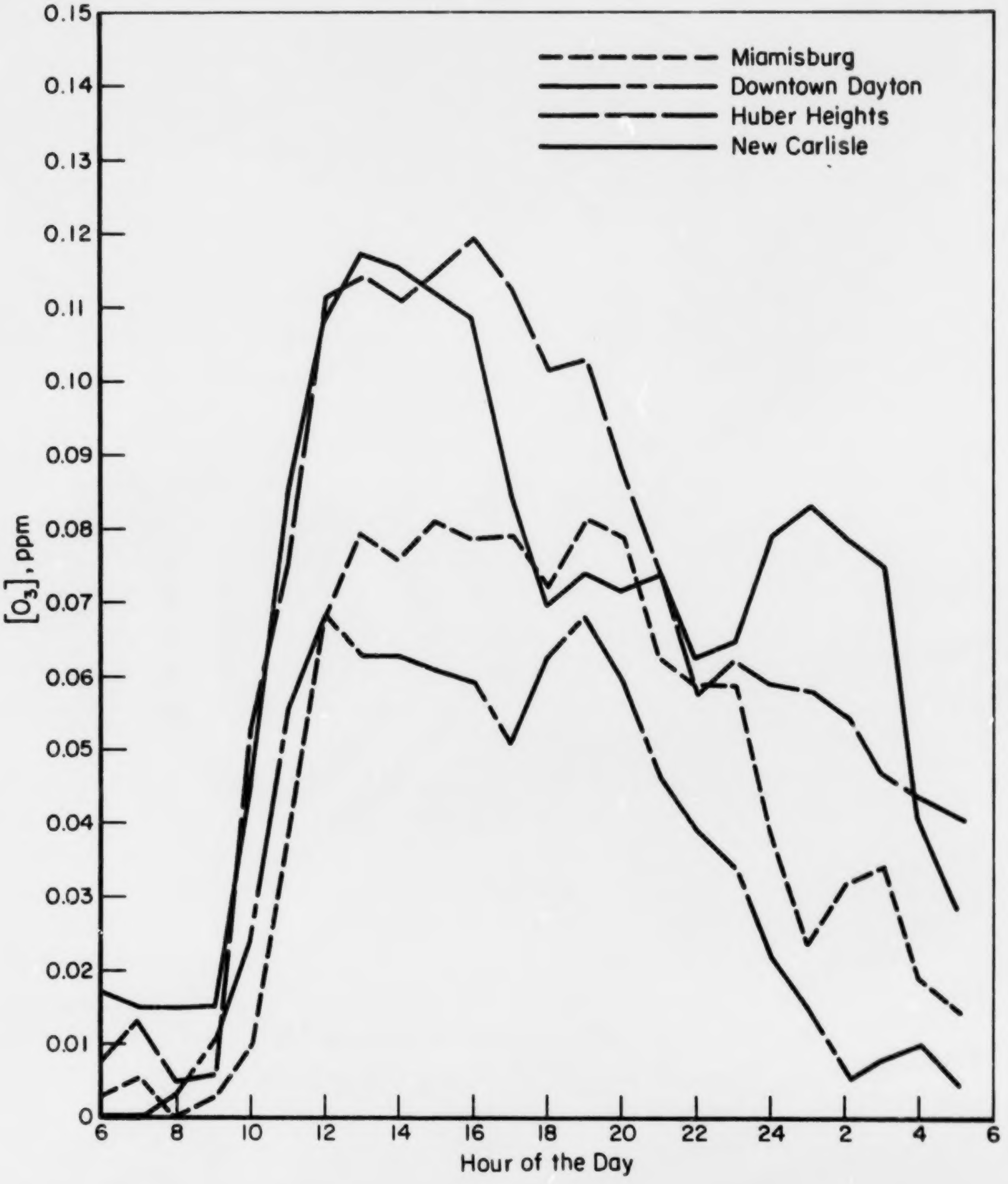

FIGURE 47. DAYTON AREA OZONE PROFILES - JULY 18, 1974

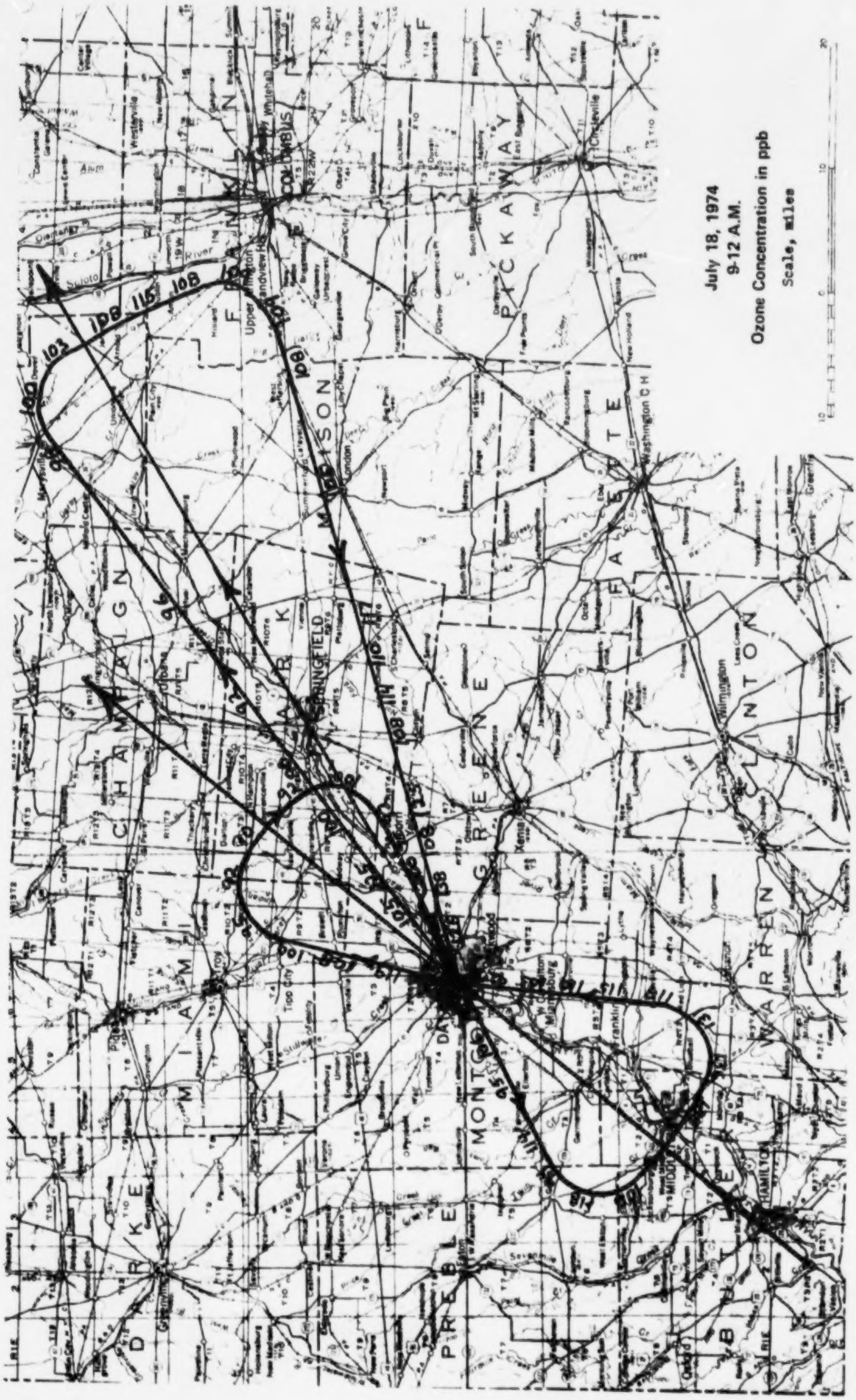
July 18, 1974
9-12 A.M.
Ozone Concentration in ppb
Scale, miles
0
10
20
COLUMBUS
SPRINGFIELD
DAYTON
HAMILTON
Washington C H
Wilmington
Xenia
Marysville
Upper Sandusky
London
PICKAWAY
MADISON
CHAMPAIGN
CLARK
GREENE
MONTGOMERY
MIAMI
DARKE
PREBLE
BUTLER
WARREN
CLINTON
FAYETTE
FRANKLIN
103
108
115
108
100
96
117
110
119
108
115
138

FIGURE 48 A. AIRCRAFT OZONE RESULTS

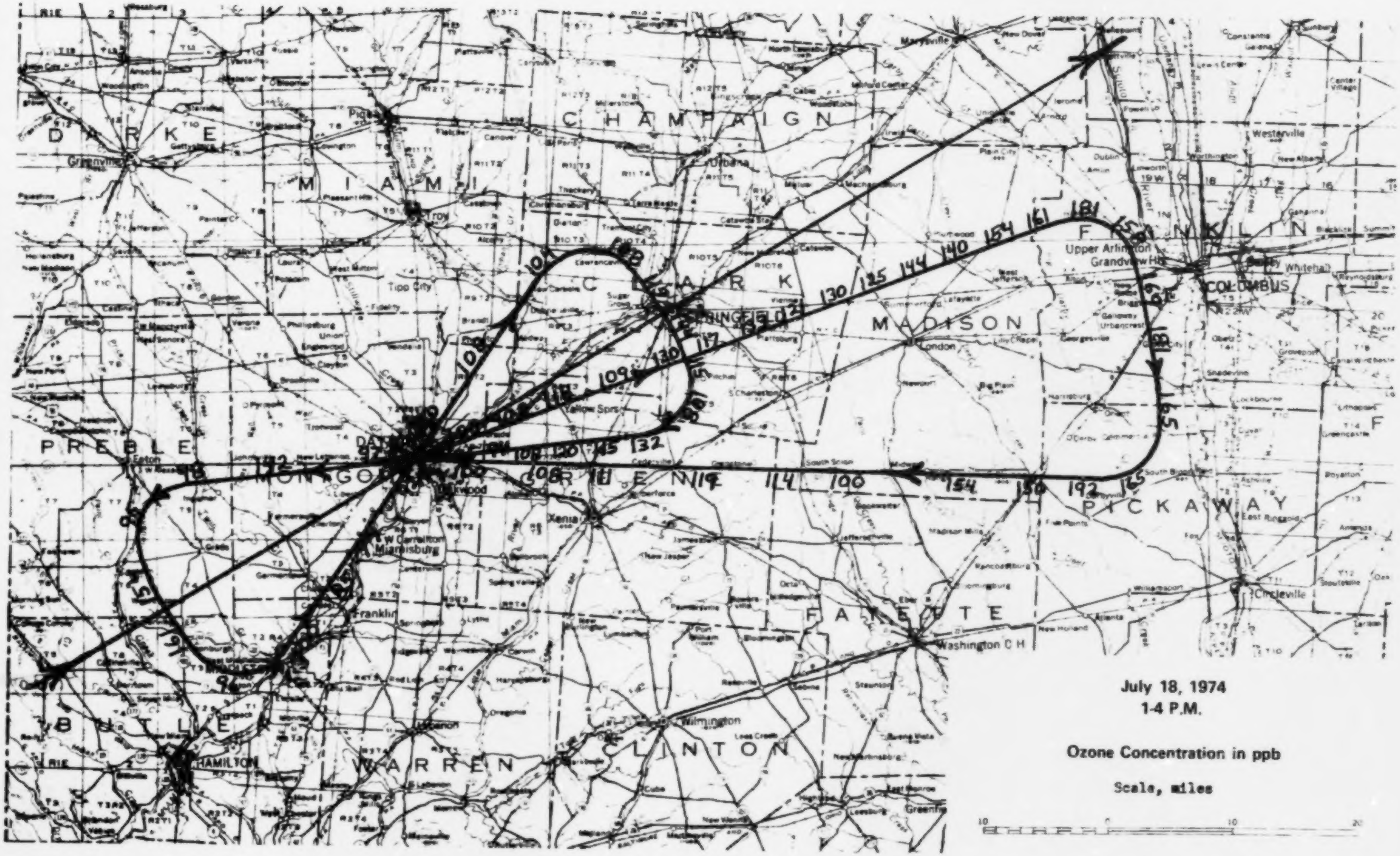
DARKE
MIAMI
CHAMPAIGN
CLARK
MADISON
FRANKLIN
COLUMBUS
SPRINGFIELD
PREBLE
MONTGOMERY
GREENE
PICKAWAY
FAYETTE
BUTLER
WARREN
CLINTON
HAMILTON
Washington C H
Upper Arlington
Grandview Hts
10
0
10
20

July 18, 1974
1-4 P.M.

Ozone Concentration in ppb

Scale, miles

FIGURE 48 B. AIRCRAFT OZONE RESULTS

TABLE 29. AIRPLANE BAG SAMPLE RESULTS
JULY 18, 1974

	20 Miles Upwind	20 Miles Downwind	60 Miles Downwind
I. 9:00-12:00 a.m.			
Ethylene (ppmC)	--	--	--
Ethane (ppmC)	--	--	--
Acetylene (ppmC)	--	--	--
PAN (ppm)	--	--	0.000
CO (ppm)	--	2.15	1.80
CH_4 (ppm)	--	1.50	1.70
NMHC (ppmC)	--	0.80	1.10
II. 1:00-4:00 p.m.			
Ethylene (ppmC)	--	--	--
Ethane (ppmC)	--	--	--
Acetylene (ppmC)	--	--	--
PAN (ppm)	0.000	0.001	0.003
CO (ppm)	0.80	0.85	1.10
CH_4 (ppm)	2.0	2.05	1.60
NMHC (ppmC)	1.20	1.70	1.30

upwind loop (flown first) and the long downwind (flown last), significant changes in O_3 concentration may have occurred. The fact that these plots contain both spatial and, of necessity, temporal O_3 distributions requires that they be interpreted with caution.

The arrows in the figure point in the direction toward which the wind was blowing. The morning profile for July 18 shows high ozone values widely distributed both upwind and downwind of Dayton. The O_3 concentration is as high or higher 20 miles upwind of Dayton as it is 20 and 60 miles downwind of the city. A "hot spot" possibly associated with Dayton's plume is observed 5-10 miles downwind of the city, where O_3 reaches 0.12-0.14 ppm. Another hot spot is apparent 20 miles upwind of the city in the vicinity of Hamilton and Middletown. This may represent a Cincinnati air mass with high O_3 and precursors moving toward Dayton through the pervasive ozone blanket. It may even be the remnants of the previous day's Cincinnati O_3 which was maintained within and above the nighttime inversion. Since our aircraft did not have the capability for night flights we were unable to test this possibility.

The airplane bag data from the morning of the 18th, shown in Table 29, is sparse and contains no elucidating information.

The afternoon ozone profiles at the 1000-foot level are plotted in Figure 48 B. Whereas the aircraft data revealed higher concentrations of O_3 aloft as opposed to the ground stations during the morning, the afternoon concentrations above Huber Heights and New Carlisle are roughly comparable to the ground station values. With wind speeds averaging 8 mph during the day (see Site 2 hourly wind speed data in Appendix), the 6-9 a.m. Dayton air mass should be arriving in Columbus toward the end of our afternoon flight period. Indeed the 60-mile downwind loop, which is flown between 3-4 p.m., indicates very high concentrations (0.15-0.20 ppm) of O_3 approaching Columbus. Columbus air-quality data* (Appendix G) show O_3 peaking in Columbus on this day between 4-5 p.m. (EDT) at 0.135 ppm. It is highly probable that this O_3 originated in Dayton.

---

* Columbus data courtesy of Mr. Fred Booth, Ohio Environmental Protection Agency.

The ozone levels moving into Dayton during the afternoon are also quite high, with values 20 miles out approaching 0.16 ppm. If this air mass is moving toward Dayton at an average speed of about 5 mph, the high O_3 air mass would reach Dayton between 6-8 p.m., and could therefore account for the secondary ozone peaks observed at several of the ground stations at this time.

The afternoon airplane profiles show that the lowest O_3 concentrations were found along the Dayton-Miamisburg corridor. Since this is a high-density NO emission area, this observation is consistent with the model.

Further aspects of the aircraft data are the vertical temperature and O_3 distributions shown in Figures 49 and 50. The temperature appears to decrease with altitude at approximately the adiabatic lapse rate, so that vertical mixing is unhindered, at least to 5000 feet. The mixing height and afternoon ventilation reported in Table 15 were 1700 meters and 7550 meters^2/sec. This mixing height is consistent with the passage of a high-pressure system through the region, since the subsidence inversion associated with high-pressure systems is frequently found at such altitudes.

The vertical O_3 profile for the afternoon of July 18 (approximately 5:00 p.m.) is shown in Figure 50. As in all of the vertical O_3 data we collected over downtown Dayton, the levels aloft were higher than the ground-station readings. We believe this is due to inhibition and scavenging of O_3 by primary pollutants such as NO which originate at the surface. As ozone moves into the downtown area it is partially removed by reaction with primary pollutants near the surface. Thus a dynamic balance is set up, with ozone being removed near the surface and being diluted by mixing at higher altitudes. Our data indicate that this balance creates an ozone maximum on this day somewhere between the surface and 1000 feet. It is interesting to note that the concentration of O_3 increases slightly between 4000-5000 feet. Since the subsidence inversion base is often located near the 5000 foot level, this may indicate O_3 accumulation just below the inversion base. From the shape of the O_3 profile we might suggest that the concentration of O_3 in the regional

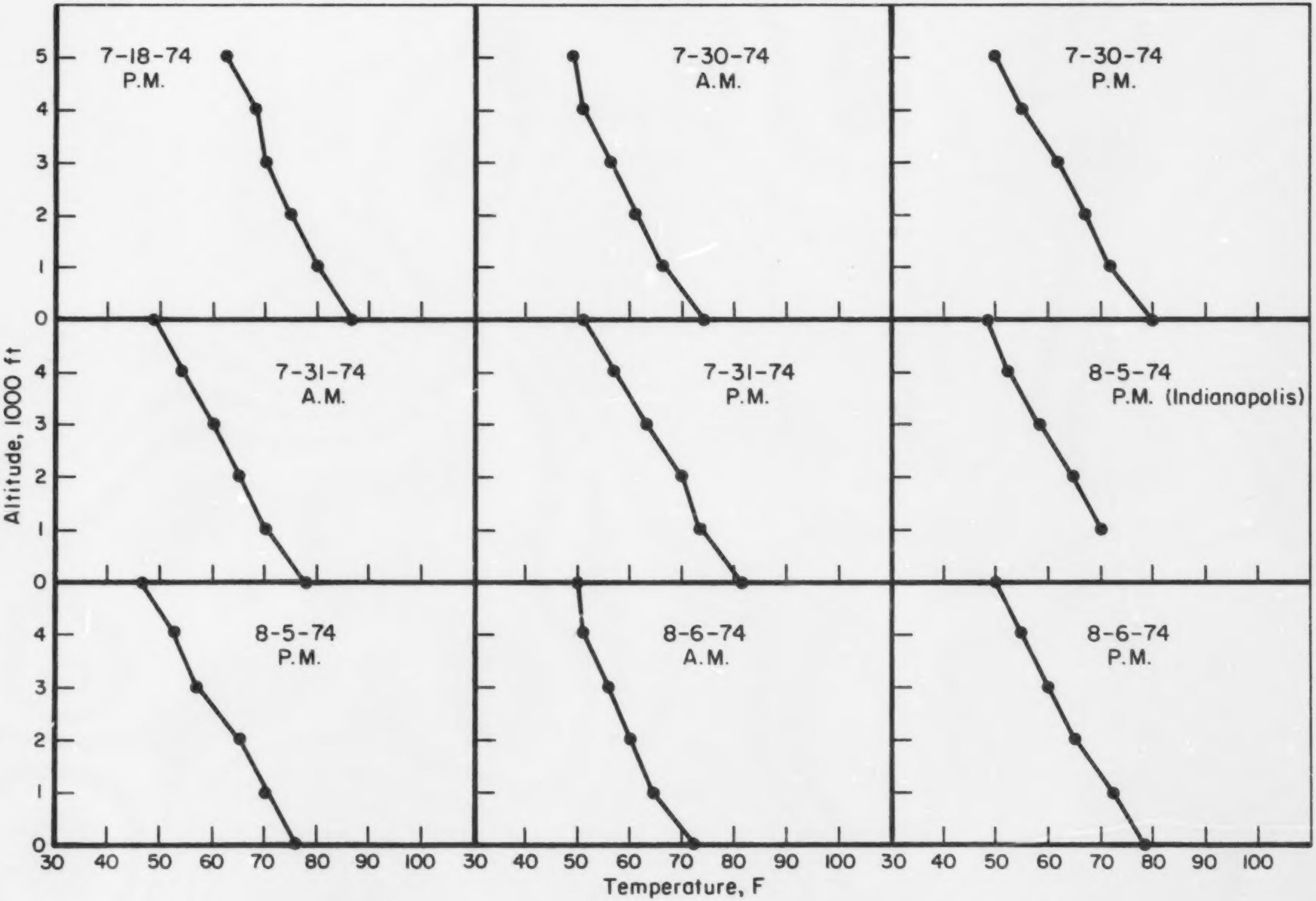

FIGURE 40. VERTICAL TEMPERATURE PROFILES

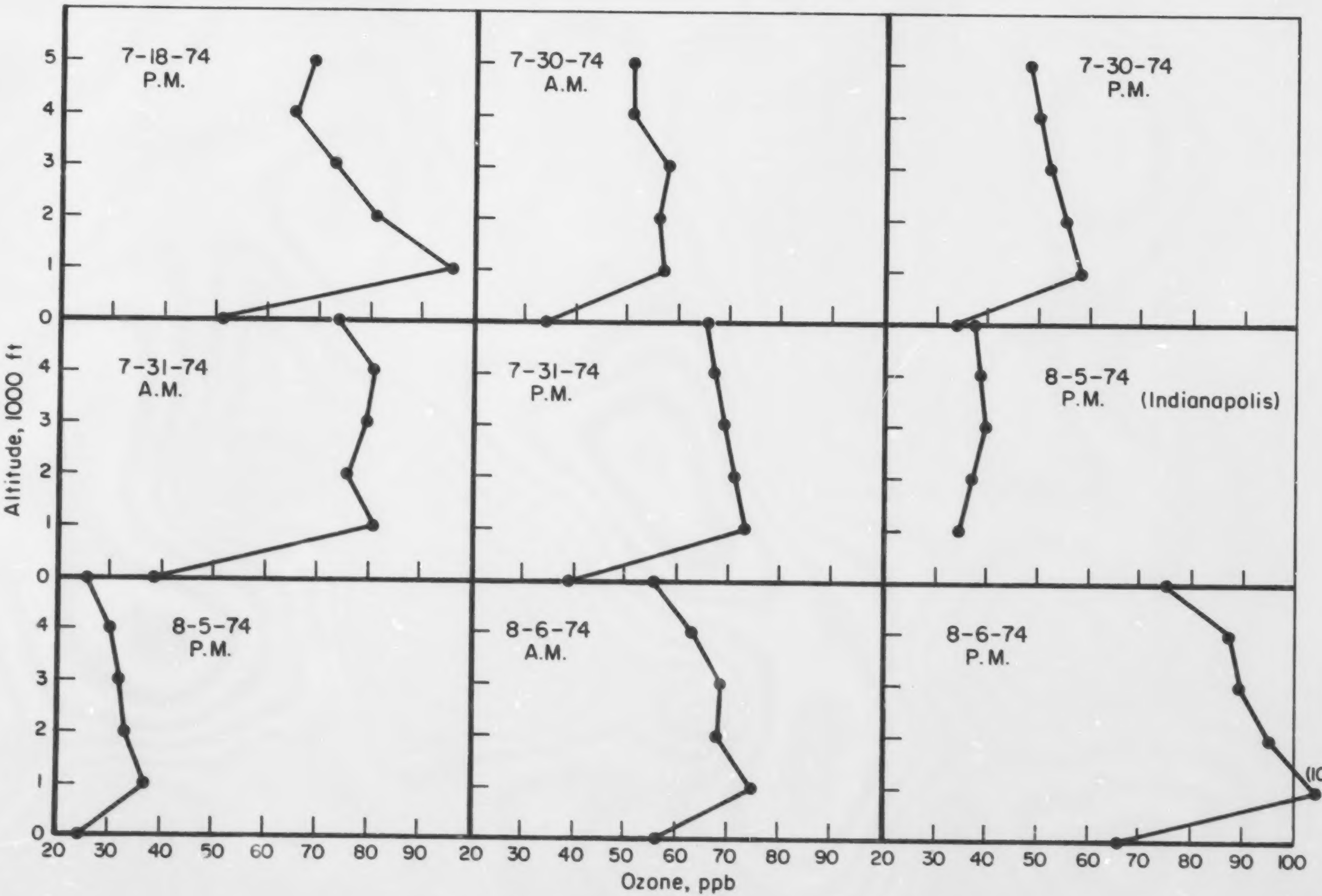

FIGURE 50. VERTICAL OZONE PROFILES, DOWNTOWN DAYTON

"blanket" of polluted air is between 60-70 ppb (the value between 4000-5000 feet). This ozone has been forming below the subsidence inversion of the high-pressure system for several days and should be well mixed. The increasing O_3 as the airplane descends from 4000 to 1000 feet is likely a result of "hot spot" transport (high O_3 air from Cincinnati moving into Dayton) as discussed earlier. It may also be partly due to the reaction of Dayton emissions as they diffuse upward. During the vertical diffusion process, NO is converted to NO_2 by the normal photochemical smog reactions, with the consequent generation of O_3. We therefore envision a sheath of O_3-depleted air within and extending to some distance downwind of the urban center. As the urban precursors diffuse upward and move downwind, the photochemical processes operate on the primary pollutants to ultimately generate ozone after some induction period. This ozone becomes Dayton's own "hot spot" superimposed on the more widespread O_3 blanket. These phenomena will be discussed further when we consider some of the other specific sampling days.

The integrated and continuous data for hydrocarbons, nitrogen oxides, SO_2, CO, HNO_3, PAN, etc., at the three main ground stations are reported in the Appendices. The CO, NO_x, NMHC, and light-scattering profiles all show a concentration increase beginning at approximately 7 p.m., which probably is related to the increased stability conditions associated with the incipient formation of a nighttime near-surface inversion. With this exception, there are no other unusual or elucidating features which appear in this large volume of ground-station data. For this reason a discussion of these data will not be presented at this time. The interested reader is referred to the Appendix for tabulations and profiles of these data.

July 25, 1974

July 25, 1974, was a warm hazy Thursday in Dayton. As noted in Table 20, it was also the start of a 4-day episode of elevated ozone concentrations. The average air mass movement between 6 a.m. and 2 p.m.

on this day was from almost due east (99° in Table 20). Computerized trajectory analyses (Appendix F) indicate that this air mass had passed over Lake Erie, through Cleveland, through the Columbus area, and then west to Dayton. This same air mass pattern appeared in both the 8 a.m. and 8 p.m. trajectory analysis and was probably operative throughout the day. A large high-pressure system dominated the meteorology throughout the Ohio Valley on this day. The meteorological summary in Table 15 indicates a mixing height of only 1360 meters and an afternoon ventilation of 4460 m^2/sec. This is rated as poor to moderate ventilation.

As shown in Figure 51, the maximum hourly ozone reading in downtown Dayton occurred at 6 p.m. Secondary maxima above the Federal standard also occurred at Site 2 and Site 3 between 7 and 8 p.m. The highest level of ozone was observed at Site 3 at noon, when the concentration reached 0.106 ppm.

A special flight was carried out as a separate study for EPA on this day. As a result, our normal flight patterns were not flown and we have no hydrocarbon or vertical O_3 profile data. Nevertheless, we were able to record O_3 at the 1000-foot level during the patterns which were flown. These patterns are shown in Figures 52 A and B for morning and afternoon flights respectively. The morning pattern shown in Figure 52 A consisted of flying from Columbus to the Dayton airport and then a short flight 5 miles downwind of downtown Dayton. During the flight from Columbus to the Dayton airport, the ozone concentration varied from 0.065-0.114 ppm. The ozone concentration fluctuated rather rapidly on this flight as if we were passing through pockets of O_3. Without vertical ozone profiles it is rather difficult to explain this behavior. However, the following explanation appears consistent with our model. The regional ozone reservoir which moves into the area with the high-pressure system contains moderate to high concentrations of ozone well mixed up to the base of the subsidence inversion. During the nighttime near-surface inversion some fraction of the O_3 close to the surface will be removed by both chemical and physical processes. During the morning breakup of this surface inversion, turbulent mixing of the

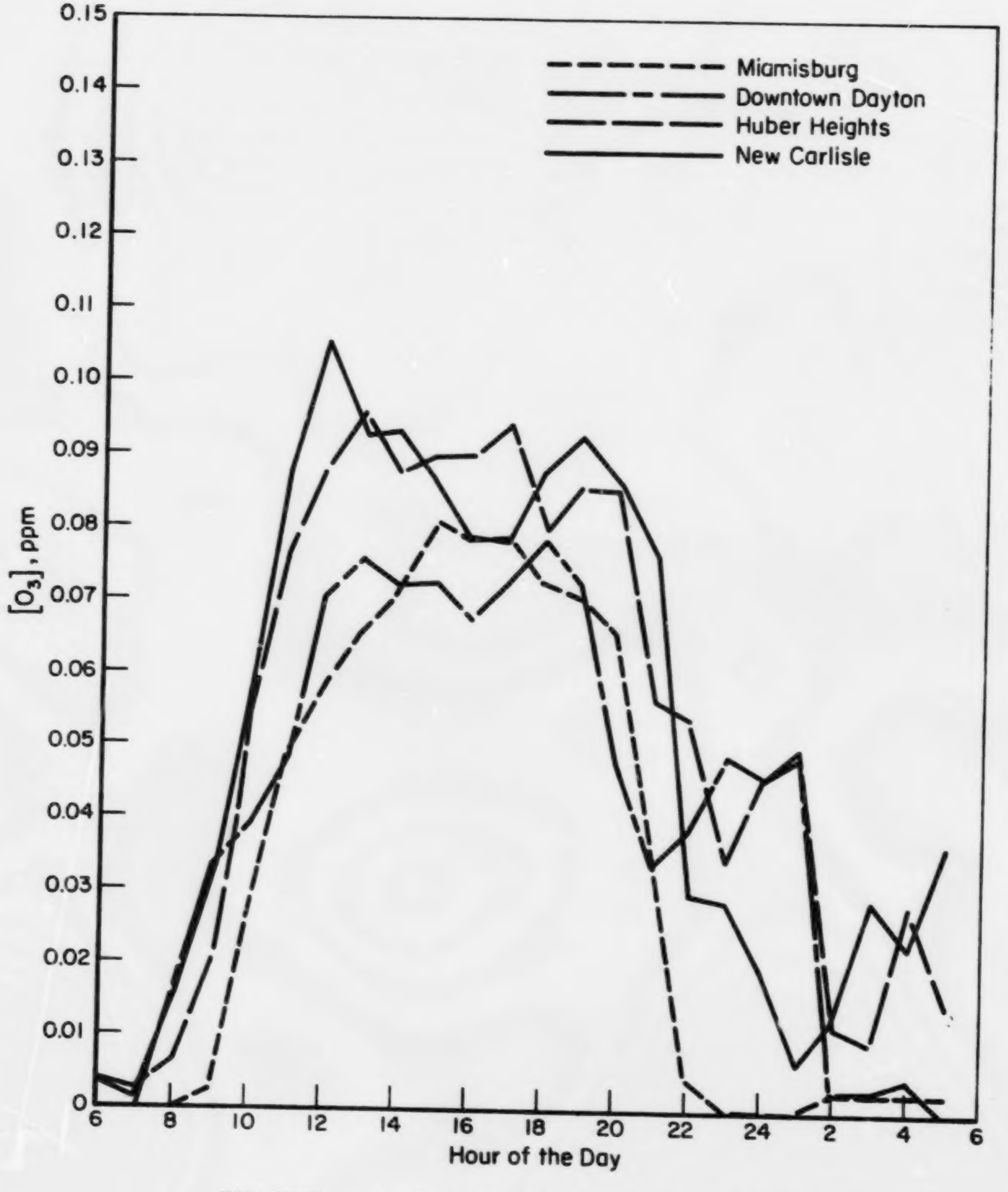

FIGURE 51. DAYTON AREA OZONE PROFILES - JULY 25, 1974

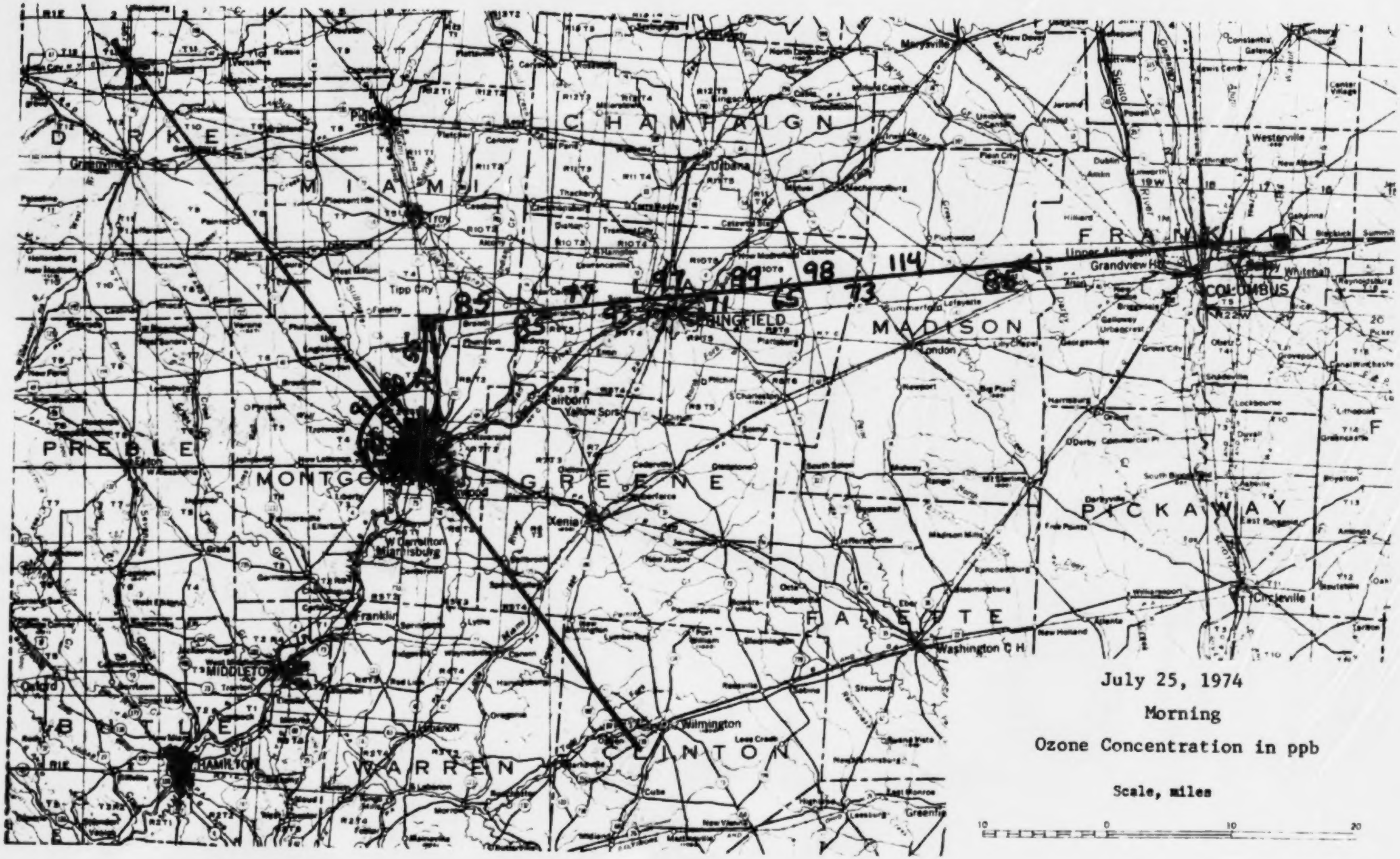
CHAMPAIGN
DARKE
MIAMI
PREBLE
MONTGOMERY
GREENE
MADISON
FRANKLIN
PICKAWAY
FAYETTE
CLINTON
WARREN
BUTLER
SPRINGFIELD
COLUMBUS
Grandview Hts
Upper Arlington
Whitehall
Westerville
Tipp City
Troy
Piqua
Urbana
Marysville
London
Fairborn
Yellow Springs
Xenia
Miamisburg
Franklin
MIDDLETOWN
HAMILTON
Wilmington
Washington C H
Circleville
85
85
47
97
93
99
98
114
73
65
86
10
0
10
20

July 25, 1974

Morning

Ozone Concentration in ppb

Scale, miles

FIGURE 52 A. AIRCRAFT OZONE RESULTS

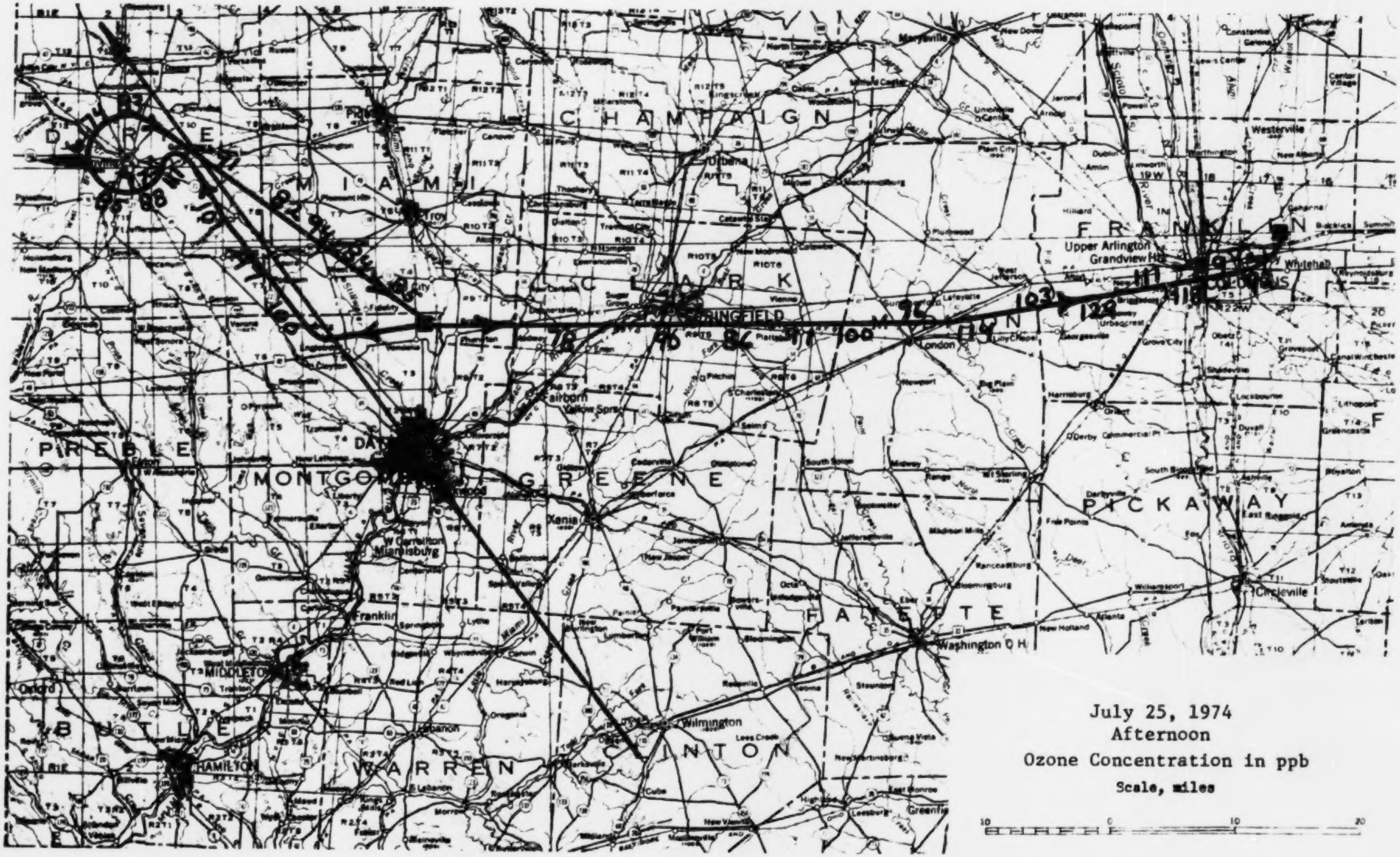
CHAMPAIGN
MIAMI
DARKE
CLARK
FRANKLIN
PREBLE
MONTGOMERY
GREENE
PICKAWAY
FAYETTE
BUTLER
WARREN
CLINTON
SPRINGFIELD
Upper Arlington
Grandview Hts
Whitehall
COLUMBUS
Fairborn
Xenia
Miamisburg
Franklin
MIDDLETOWN
HAMILTON
Wilmington
Washington C H
Circleville
London
Westerville
78
86
100
95
119
103
122
111
118
82
88
100
10
0
10
20

July 25, 1974
Afternoon
Ozone Concentration in ppb
Scale, miles

FIGURE 52 B. AIRCRAFT OZONE RESULTS

depleted surface layer and the O_3-enriched air at higher altitudes could cause this effect of ozone pockets.

The ozone concentrations along the arc 5 miles downwind of downtown Dayton are slightly lower, on the average, than the values observed between Columbus and Dayton, and they also fluctuate dramatically. These effects may be caused by turbulent mixing of air from the Dayton urban plume, which is rich in O_3 scavengers during the morning hours, with the ozone-rich air above the city. At the same time, pockets of precursors released in the urban area may be reacting at different rates as they move downwind, thereby creating O_3 pockets.

During the afternoon of the 25th a flight was made from the Dayton airport in a loop around the town of Greenville, Ohio. The aircraft then returned to the Dayton airport and from there back to Columbus. The ozone concentrations just downwind of Greenville were somewhat lower on average than those recorded anywhere else along the flight path. This may well be due to a sheath of NO and other primary pollutants around the city which react with O_3.

Since this special flight was conducted early in the afternoon, we cannot be sure that the ozone concentrations between Dayton and Columbus had stabilized; neither can we be certain of the position and trajectory of the Columbus air mass, since we were unable to map the horizontal O_3 distribution in any detail on this day. Nevertheless, our calculation of the average direction of air mass movement, along with the computer-generated trajectories, suggest that an air mass which had passed over Columbus early in the day is aimed at the Dayton area by early afternoon. At this point we can only speculate that the Columbus air masses eventually pass through Dayton and are responsible for the second and third ozone peaks occurring in the late evening at several of the Dayton ground stations (see Figure 51).

July 30 and 31, 1974

The meteorology of the study region on July 30, 1974, was dominated by a large low-pressure system centered over the southern end of Hudson Bay in Canada (surface meteorological charts included in Appendix E). On July 31, 1974, a high-pressure system moved into the area from the southwest. The ventilation on these 2 days was good, as noted in Table 15. Air mass movement on both of these days was from the northwest (Table 20), with the computerized trajectory analyses (Appendix F) indicating that the air masses had passed over Iowa, central Illinois, and Indiana during the 2 preceding days.

The ozone concentrations at our ground stations never exceeded 0.08 ppm on an hourly average basis on either of these 2 days. Even the 1000-foot ozone concentrations only exceeded the 0.08 ppm standard during the afternoon of July 31. Since the ozone concentrations on these 2 days are not unusual or of special interest, we will simply present the aircraft data along with a very brief description thereof. The specific ground-station data, meteorology, and trajectory outputs are included in the various appendices and should be consulted for more detail.

The aircraft flight patterns and ozone distributions are given in Figures 53 A and B for the morning and afternoon of July 30, and Figures 54 A and B for July 31. The integrated aircraft bag sample results are presented in Tables 30 and 31 for the 30th and 31st respectively. Vertical temperature and ozone profiles for these days are shown in Figures 49 and 50.

The July 30 results from Figures 50 and 53 A and B indicate relatively uniform concentrations of ozone between 1000 and 5000 feet over downtown Dayton. With some allowance for temporal variations in ozone concentration, the ozone moving into Dayton at the 1000-foot level is rather similar to the ozone concentration downwind of the city. This is also the case on July 31 (Figures 50 and 54 A and B). The nearly constant concentration of O_3 with altitude, along with the horizontal distribution, givesstrong indication of a pervasive region-wide ozone

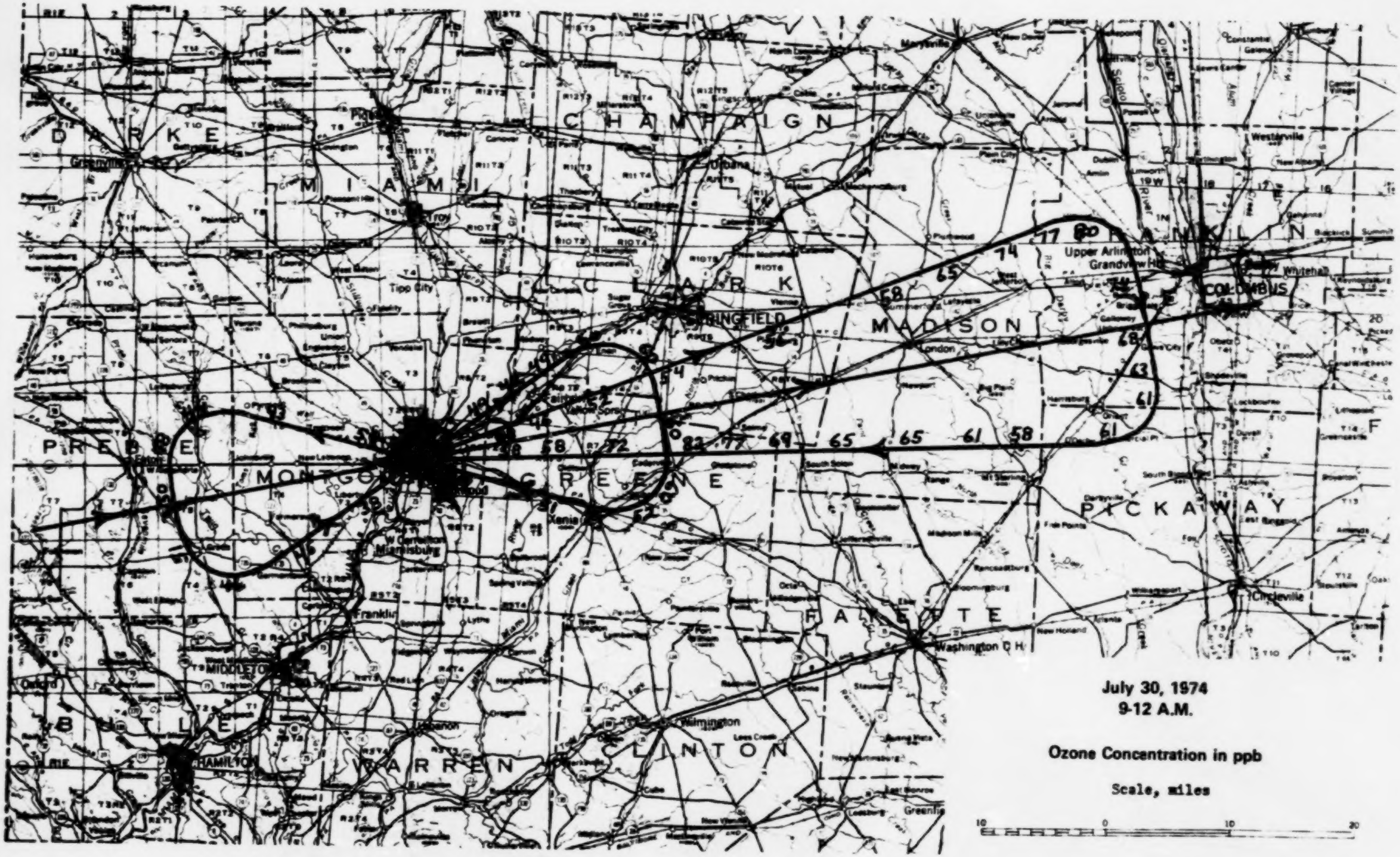
DARKE
MIAMI
CHAMPAIGN
CLARK
MADISON
FRANKLIN
PREBLE
MONTGOMERY
GREENE
PICKAWAY
FAYETTE
BUTLER
WARREN
CLINTON
Greenville
Piqua
Troy
Tipp City
Urbana
Springfield
London
Upper Arlington
Grandview Hts
Columbus
Whitehall
Xenia
Miamisburg
Franklin
Middletown
Hamilton
Lebanon
Wilmington
Washington C H
Circleville
Westerville
Scioto River
80
77
74
65
58
56
54
63
68
61
58
61
65
65
69
77
82
72
58
52
0
10
20

July 30, 1974
9-12 A.M.

Ozone Concentration in ppb

Scale, miles

FIGURE 53 A. AIRCRAFT OZONE RESULTS

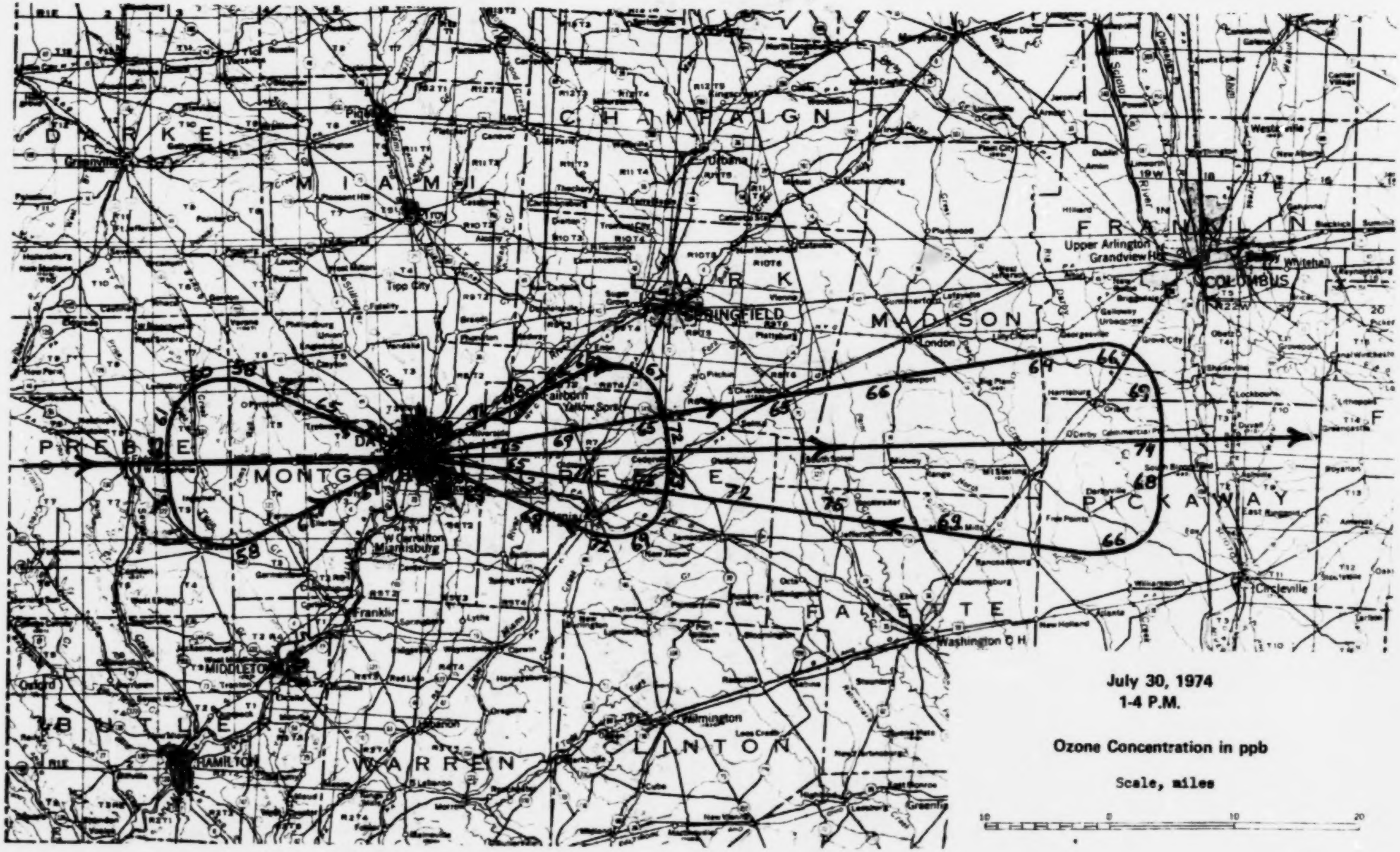
DARKE
MIAMI
CHAMPAIGN
CLARK
MADISON
FRANKLIN
PREBLE
MONTGOMERY
GREENE
PICKAWAY
FAYETTE
BUTLER
WARREN
CLINTON
Springfield
Columbus
Upper Arlington
Grandview Hts
Fairborn
Yellow Springs
Tipp City
Miamisburg
West Carrollton
Franklin
Middletown
Hamilton
Wilmington
Washington C H
Circleville
London
58
65
61
69
58
48
67
65
69
65
55
72
72
75
69
65
66
69
66
69
74
68
66
July 30, 1974
1-4 P.M.
Ozone Concentration in ppb
Scale, miles
10
0
10
20

FIGURE 53 B. AIRCRAFT OZONE RESULTS

TABLE 30. AIRPLANE BAG SAMPLE RESULTS
JULY 30, 1974

	20 Miles Upwind	20 Miles Downwind	60 Miles Downwind
I. 9:00-12:00 a.m.			
Ethylene (ppmC)	0.028	0.003	0.003
Ethane (ppmC)	0.000	0.002	0.002
Acetylene (ppmC)	0.021	0.005	0.005
PAN (ppm)	0.000	0.000	0.000
CO (ppm)	1.35	0.80	0.50
CH_4 (ppm)	1.35	1.45	1.45
NMHC (ppmC)	0.45	0.45	0.55
II. 1:00-4:00 p.m.			
Ethylene (ppmC)	0.015	0.007	0.006
Ethane (ppmC)	0.004	0.006	0.005
Acetylene (ppmC)	0.005	0.031	0.000
PAN (ppm)	0.000	0.000	0.000
CO (ppm)	0.55	0.70	1.00
CH_4 (ppm)	1.45	1.34	1.45
NMHC (ppmC)	0.40	0.44	0.50

TABLE 31. AIRPLANE BAG SAMPLE RESULTS
JULY 31, 1974

	20 Miles Upwind	20 Miles Downwind	60 Miles Downwind
I. 9:00-12:00 a.m.			
Ethylene (ppmC)	0.008	0.004	--
Ethane (ppmC)	--	--	--
Acetylene (ppmC)	0.012	0.009	--
PAN (ppm)	0.000	0.000	--
CO (ppm)	0.60	0.35	--
CH_4 (ppm)	1.45	1.45	--
NMHC (ppmC)	0.50	0.35	--
II. 1:00-4:00 p.m.			
Ethylene (ppmC)	0.005	0.006	0.000
Ethane (ppmC)	0.004	0.004	0.000
Acetylene (ppmC)	0.014	0.024	0.000
PAN (ppm)	0.000	0.000	0.000
CO (ppm)	0.50	0.80	--
CH_4 (ppm)	1.45	1.45	1.45
NMHC (ppmC)	0.30	0.30	0.35

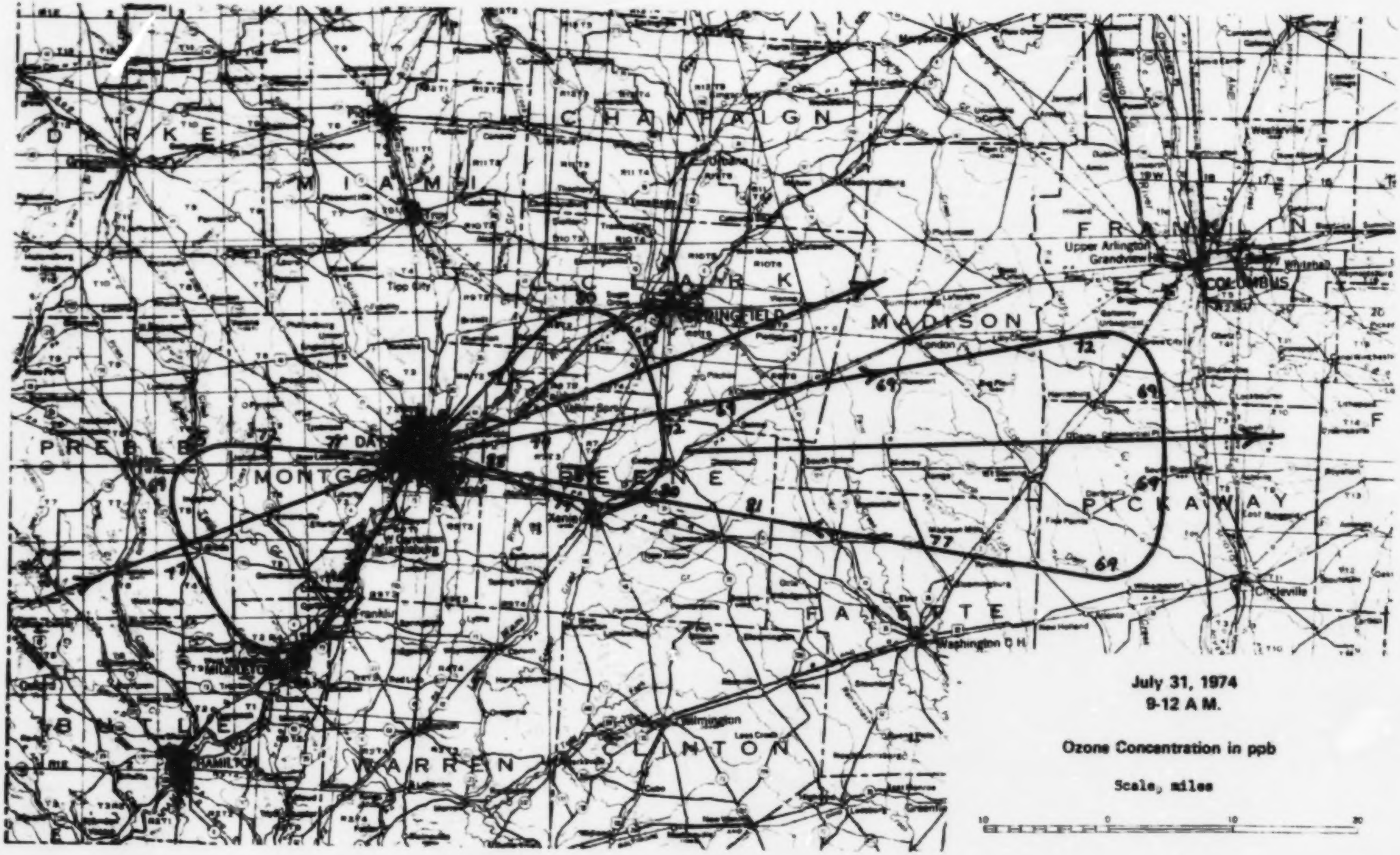
DARKE
MIAMI
CHAMPAIGN
CLARK
SPRINGFIELD
MADISON
FRANKLIN
Upper Arlington
Grandview
COLUMBUS
PREBLE
MONTGOMERY
GREENE
PICKAWAY
Circleville
FAYETTE
Washington C H
BUTLER
HAMILTON
MIDDLETOWN
WARREN
CLINTON
Wilmington
Tipp City
72
77
77
77
80
85
81
69
69
72
69
69
69
77
10
0
10
20

July 31, 1974
9-12 A M.

Ozone Concentration in ppb

Scale, miles

FIGURE 54 A. AIRCRAFT OZONE RESULTS

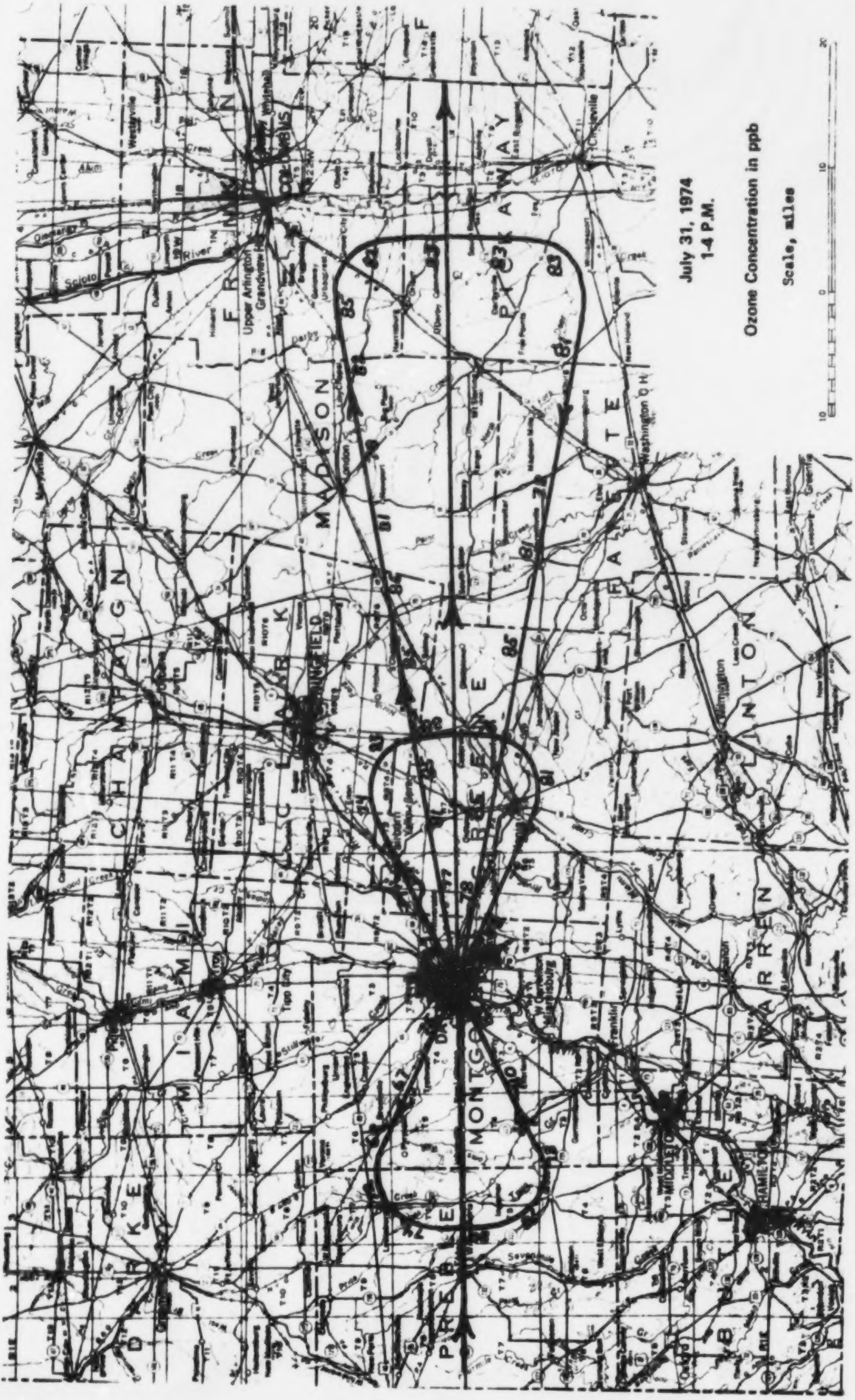

July 31, 1974
1-4 P.M.

Ozone Concentration in ppb

Scale, miles
10
0
10
20
CHAMPAIGN
CLARK
MADISON
FRANKLIN
PICKAWAY
FAYETTE
CLINTON
GREENE
MIAMI
MONTGOMERY
PREBLE
DARKE
WARREN
BUTLER
Springfield
Columbus
Washington C.H.
Hamilton
Middletown

FIGURE 54 B. AIRCRAFT OZONE RESULTS

blanket, even under these rather different meteorological conditions. Scrutiny of the 1000-5000-foot ozone profiles for these 2 days reveals O_3 on July 31 averaging approximately 20 ppb higher than on July 30. We suggest that this additional regional ozone is associated with the high-pressure system which moved into the Ohio area on July 31.

August 1, 1974

In terms of ozone origin and transport, one of the most intriguing days of the Dayton field program was Thursday, August 1, 1974. The following is an excerpt of an article in a local newspaper:

> "Photochemical oxidant reached the highest level in three years in Dayton last night, and the Regional Air Pollution Control Agency asked for a voluntary reduction on all traffic in the downtown area today.
>
> "The photochemical oxidants passed the Alert Level of 200 last night . . . persons with respiratory problems should stay in air-conditioned rooms today and should avoid being active if possible."

August 1 was a hot and sunny day in Dayton. The meteorology was dominated by a high-pressure system which was centered over West Virginia at 8 a.m. and which reached Western Pennsylvania by 8 p.m. (surface meteorological maps included in Appendix E). The wind averaged between 4 and 20 mph throughout the day, with the 6 a.m.-2 p.m. wind direction vector given in Table 20 indicating winds from the southwest (225°). The computer-generated trajectories in Appendix F show that the air mass arriving in Dayton on the morning of August 1 had passed over north-central Illinois and south-central Indiana during the previous 36 hours prior to moving into Dayton from the west-southwest. By 8 a.m. however, the air arriving in Dayton was coming from the south-southwest and had passed over the Cincinnati urban complex within the previous 12 hours.

The ozone data for August 1 from four of our ground stations are summarized in Table 20. This is the only day of the entire study period in which all four stations experienced ozone concentrations in excess of 0.1 ppm. Even more intriguing are the concentration-time profiles for these four sites, shown in Figure 55. At each site the maximum hourly ozone concentration was observed between 7 and 8 o'clock at night, long after the ultraviolet intensity of the sunlight had fallen off. All of the sites recorded an hourly ozone maximum exceeding 0.12 ppm. Since the ozone concentration rises rapidly and ultimately peaks well after the photochemical ozone generation processes have been curtailed by lack of ultraviolet light, these high ozone concentrations must have been transported into the Dayton area.

The very slow movement of the high-pressure cell mentioned earlier suggest rather stable atmospheric conditions existing on this day. Ample confirmation of this stability during the morning is gained from the downtown Dayton ground-station data. The 6-9 a.m. integrated Teflon bag samples (Appendix D) showed 7.7 ppmC NMHC, 8.8 ppm CO, 0.101 ppmC of C_2H_4, 0.070 ppmC of C_2H_2, and 0.034 ppmC of C_2H_6. In addition, the continuous Site 1 data (Appendix A) show 0.4 ppm NO at 8 a.m. These extraordinary concentrations of primary pollutants surpass by far the levels observed on any other day of the field program.

The pollutant profiles from Sites 2 and 3 were not as dramatic as the downtown observations but do reveal some interesting features. The NO and NO_2 profiles exhibit the usual early morning peaks (6-9 a.m.) at both sites and then decrease to low levels by midafternoon. However, the NO_2 concentration then rises quite rapidly to a secondary peak between 6 and 8 p.m., corresponding quite closely to the rise in O_3. Since the O_3 concentration was rising simultaneously with the NO_2, it is likely that the NO_2 is a result of transport into the area rather than the reaction of O_3 with locally emitted NO.

The combination of the meteorology and the pollutant profiles for August 1 suggest quite strongly that the high ozone values observed in Dayton resulted from transport into the area. Certainly the ozone associated with the passage of the high-pressure system contributed to the ozone episode on this day; however, we believe the trajectories and

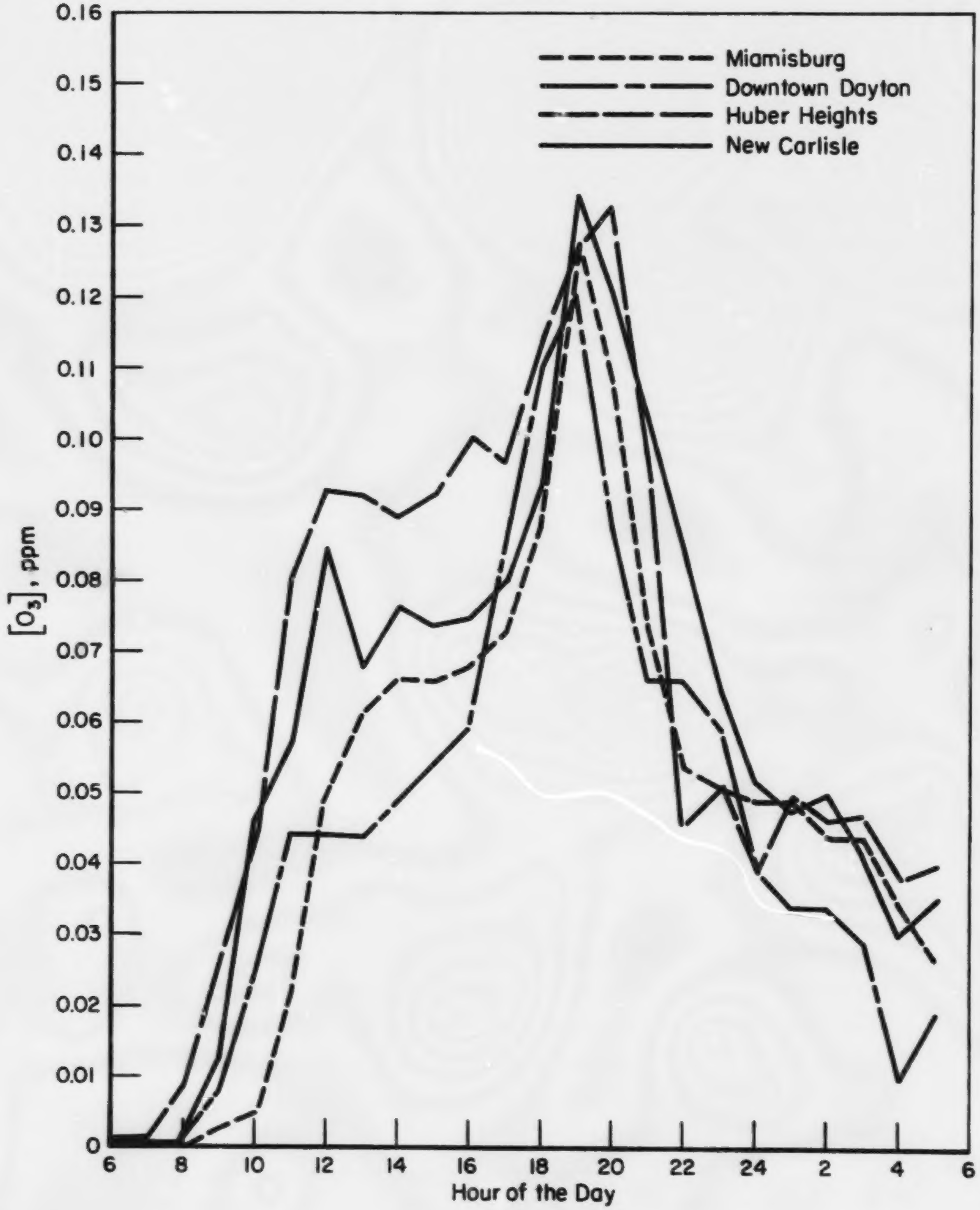

FIGURE 55. DAYTON AREA OZONE PROFILES - AUGUST 1, 1974

the chemical data show that the very high peak ozone levels observed in the evening resulted from medium-range transport from the Cincinnati urban complex to the Dayton area. It is interesting to note that the Columbus area just 60 miles to the east did not even exceed the 0.08 ppm oxidant standard on this day (Columbus data in Appendix G). Columbus, it should be noted, has no major urban complex located southwest of it along the wind trajectory for this day.

August 5, 1974

The ozone levels on Monday, August 5, 1974, were moderate to low at all of our ground stations. In fact, not one of the ground stations indicated in Table 20 exhibited an hourly average ozone concentration in excess of 0.08 ppm. Nevertheless, we chose to include a brief discussion of this sampling day for two reasons: (1) a special airplane flight was undertaken on this day and (2) the ozone levels increased rather sharply at several stations during the middle of the night.

The meteorology of the study region was influenced on this day primarily by a high-pressure system centered over Missouri, Iowa, and western Illinois, as seen in the surface weather map in Appendix E. At both Sites 2 and 3, winds were from the northwest throughout the day until 7-8 p.m. At this time the wind direction changed suddenly to the northeast direction (winds from the northeast). The 6 a.m.-2 p.m. wind direction component of the wind vector, from Table 20, suggests air mass movement from 328° during this time period. The computerized trajectory analysis indicates that the wind had shifted to the northwest, with the 8 p.m. Dayton air mass having been positioned over northeastern Indiana 12 hours earlier.

The ozone profiles from the six ground stations for August 5 are shown in Figure 45 N. At many of the stations the ozone concentration appears to decrease beginning at approximately 7 p.m., the same time that the wind direction shifted. Starting at about 10 p.m., the ozone concentration begins to rise again at most of the ground stations. At Huber Heights and New Carlisle the concentration remains fairly constant throughout the remainder of the night. The detailed chemical and meteorological data given in the Appendix for this particular day show a sharp drop in wind speed and a very rapid increase in NO, C_2H_4, C_2H_2, C_2H_6, and NMHC during the time period between 7-11 p.m. It appears that between about 7-10 p.m. the Dayton area experienced a period of calm, with very low winds and high stability. This period of calm coincides with the change in wind direction. The buildup of the primary pollutants during this period is another indication of rather stable atmospheric conditions. It is apparent from the Site 2 gas-phase data that the sharp drop in O_3 during this period corresponds with the increase in primary pollutants. From the NO, NO_2, and O_3 profiles from Site 2 it appears that the removal of O_3 during this interval can be accounted for largely in terms of the reaction of NO with O_3 to form NO_2. Between 11 p.m. and midnight the winds pick up, the concentrations of the primary pollutants drop sharply, and the ozone concentration rises. At Sites 1 and 3 the O_3 concentration begins to decrease even before NO and NO_2 start to increase, suggesting that chemical removal alone cannot account for the drop in ozone at these two sites. Apparently as the wind direction shifts during this 7-11 p.m. period some relatively clean air is transported into the Dayton area from the north and the O_3 levels begin to drop. As the wind speed decreases and conditions stabilize, the buildup of primary emissions such as NO react with O_3 to reduce the level even further. At Site 1 for example, the maximum NO concentration for the day occurred at midnight and exceeded 0.1 ppm. As the wind increased again after 11 p.m., the primary pollutants were dispersed and the O_3 level at the nonurban sites increased as ozone-containing air from the northeast was transported into the area. The O_3 level at Sites 2 and 3 remained relatively constant throughout the rest of the night at approximately 40-50 ppb. In terms of our model of O_3 behavior, this 40-50 ppb level is probably the O_3 concentration associated with the passing high-pressure system, and thus comprises the pervasive regional ozone blanket we described earlier. We may think of this as the "background" ozone peculiar to this high-pressure system. In the following discussion we will describe the results of our aircraft sampling, which give some indication of the spatial extent of this O_3 blanket.

A special airplane mission was flown on this day in an attempt to define the horizontal extent of the ozone blanket. A secondary objective of this special flight was to coordinate our study with an ozone monitoring program(15) being carried out in Indianapolis simultaneously with our study in Dayton. Unfortunately, at least from the viewpoint of our study objectives, high levels of ozone did not develop on this day. Nevertheless, the airplane profiles are instructive and are shown in Figures 56 A and B. The plane left Columbus at approximately 9 a.m. and flew directly to Indianapolis, passing just north of Dayton. This flight path is shown in Figure 56 A. Both morning and afternoon flights were carried out at 1000 feet. In general the ozone concentration fluctuated between 35-40 ppb over the entire 200+ mile flight path.

On the return trip, shown in Figure 56 B, the plane conducted a vertical spiral over downtown Indianapolis, then returned to 1000 feet and started toward Dayton. Teflon bag samples were collected (1) 5 miles downwind (east) of Indianapolis, (2) midway between Indianapolis and Dayton, and (3) 5 miles upwind (west) of Dayton. A vertical spiral over Dayton was followed by the transfer of the Teflon sampling bags at the Dayton airport and a return trip to Columbus. The O_3 concentrations on the return trip were somewhat higher than the morning flight, averaging about 45 ppb between Indianapolis and Dayton, and near 60 ppb between Dayton and Columbus. It is interesting to note the low ozone levels over Indianapolis and on the outskirts of Dayton, due very likely to the scavenging of O_3 by primary pollutants such as NO. The ozone values between Indianapolis and Columbus are just slightly higher than the values found at our Dayton stations later at night, as we discussed earlier. We suggest that the morning and late night ozone values represent the "background" ozone associated with and moving with this particular high-pressure system. The source of the ozone is likely the photochemical

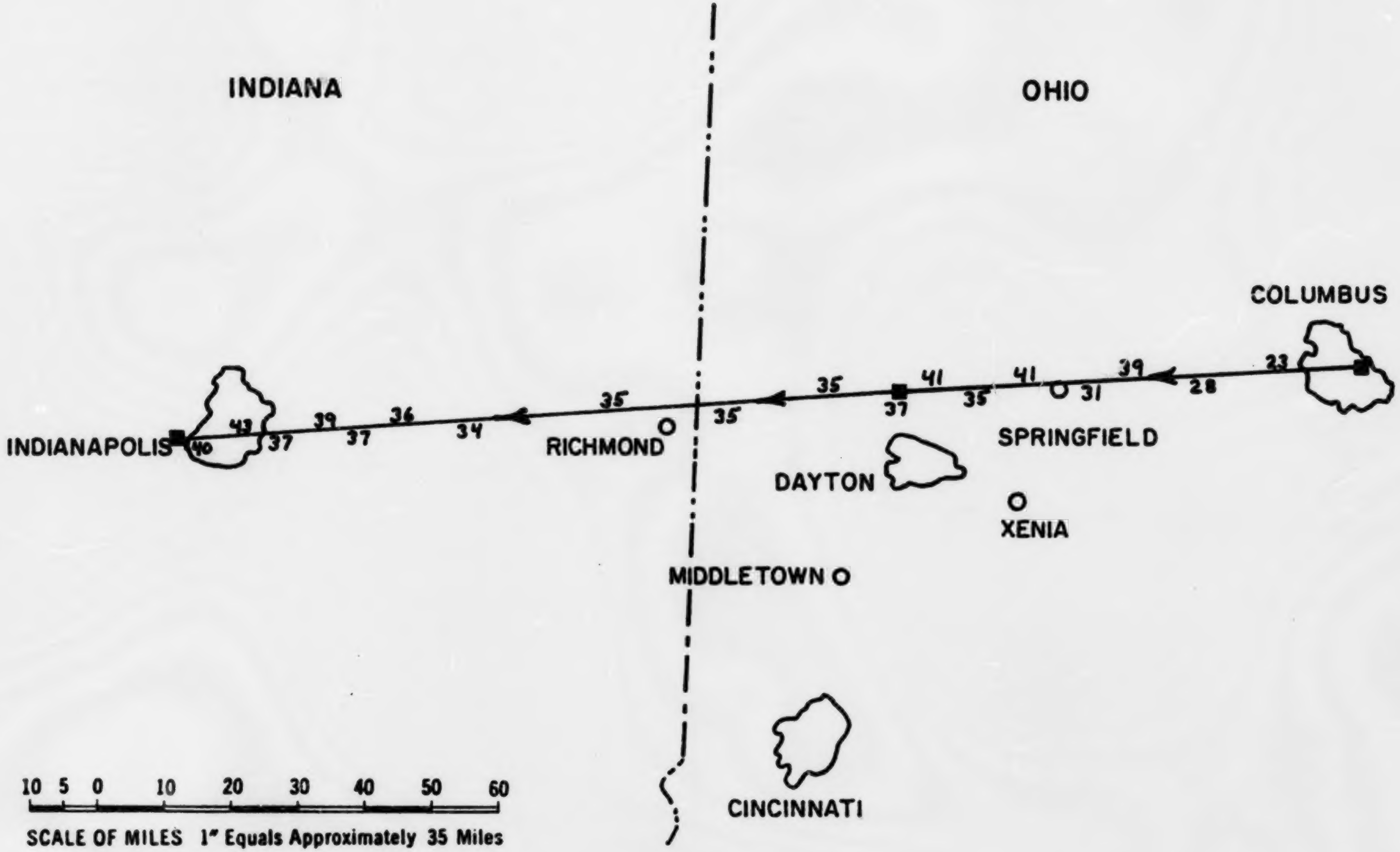
INDIANA
OHIO
COLUMBUS
23
28
39
31
41
35
41
37
35
SPRINGFIELD
DAYTON
XENIA
35
35
RICHMOND
34
36
37
39
37
43
40
INDIANAPOLIS
MIDDLETOWN
CINCINNATI
10 5 0 10 20 30 40 50 60
SCALE OF MILES 1" Equals Approximately 35 Miles

FIGURE 56 A. MORNING OZONE CONCENTRATION IN ppb - AUGUST 5, 1974

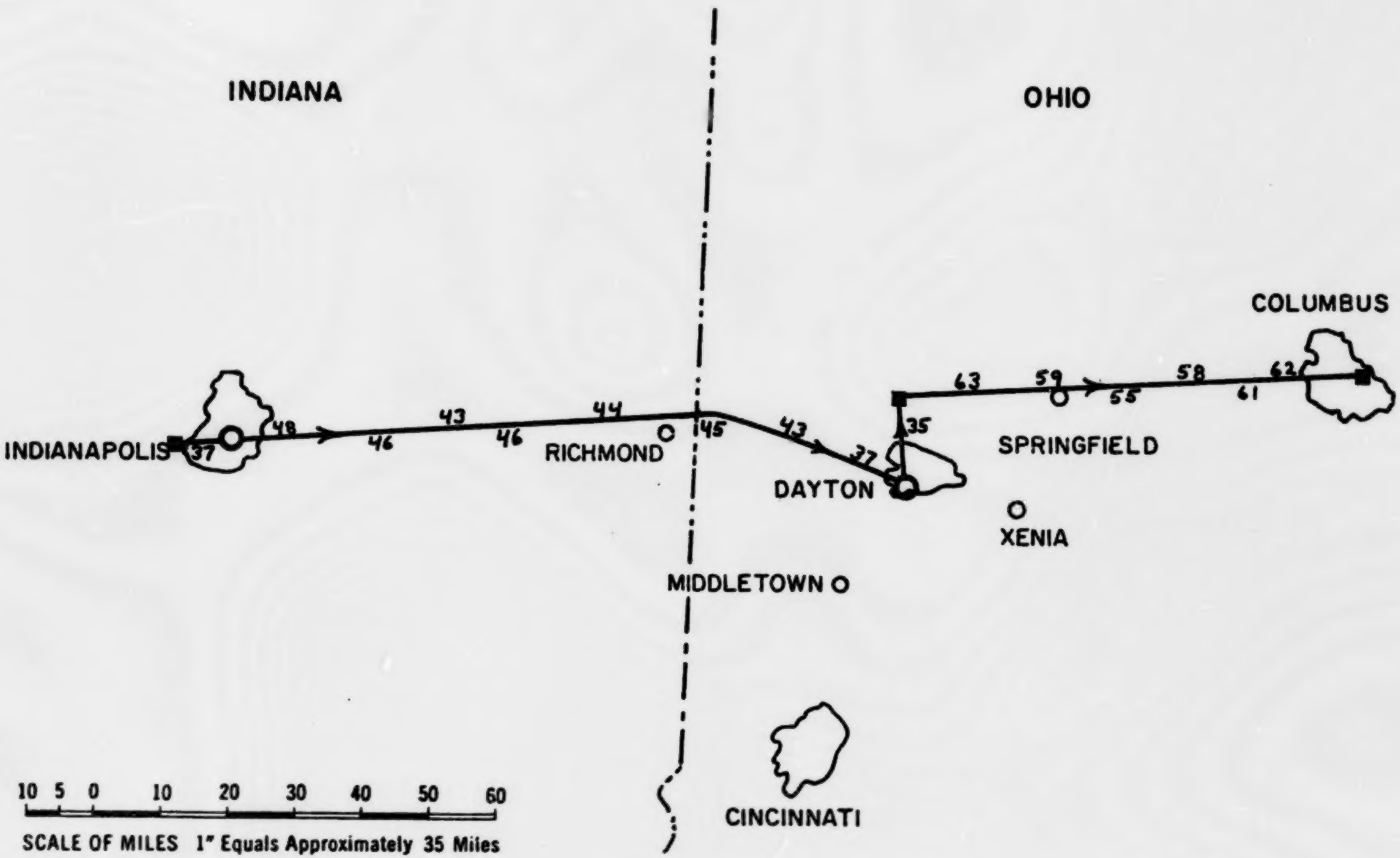
INDIANA
OHIO
COLUMBUS
INDIANAPOLIS
37
48
46
43
46
44
RICHMOND
45
43
37
DAYTON
35
63
59
55
58
61
62
SPRINGFIELD
XENIA
MIDDLETOWN
CINCINNATI
10 5 0 10 20 30 40 50 60
SCALE OF MILES 1" Equals Approximately 35 Miles

FIGURE 56 B. AFTERNOON OZONE CONCENTRATION IN ppb - AUGUST 5, 1974

reaction of natural and anthropogenic precursors trapped below the subsidence inversion. These precursors may have resulted from emission days earlier and hundreds of miles away; they have traveled with the high-pressure system and been exposed to a number of days of irradiation. Injection of fresh precursors each day and the ultimate reaction of even the low reactivity hydrocarbons under these conditions has led to the buildup of an ozone layer which travels with the high-pressure system. Most of the ozone remains above the surface inversion each night and therefore is present the following day. Irradiation of the air mass on each succeeding day can build up the ozone concentration, with very strong O_3 increases in the vicinity of local sources (e.g., downwind of urban areas). The ozone generated in these "hot spots" is superimposed on the regional ozone associated with the high-pressure system.

Based on the evening and nighttime ground-station ozone profiles, we suggested earlier that the level of O_3 associated with this high-pressure system could be as high as 40-50 ppb. The concentrations and uniform distribution of O_3 found in the rural areas between Dayton and Indianapolis in the morning are consistent with a value closer to 40 ppb. The higher ozone concentrations observed during the afternoon flight no doubt result from the localized photochemical generation of O_3 superimposed on the regional ozone blanket.

The vertical temperature profiles over Indianapolis and Dayton are shown in Figure 49. There is no indication of inhibited mixing up to the 5000-foot level. This is consistent with the good afternoon ventilation and almost 7000-foot mixing height reported for Dayton in Table 15, and shown in Figure 42.

The vertical ozone profiles for Indianapolis and Dayton are given in Figure 50. The vertical ozone distribution over Indianapolis is almost constant between 1000 and 5000 feet, with a very slight increase at the 3000 foot level. This vertical ozone profile is consistent with a regional O_3 concentration of close to 40 ppb. The ozone profile over downtown Dayton on the afternoon of August 5 exhibits the same decrease in ozone between 1000 feet and the ground that we observed on all of our flights over the downtown area. Ozone reaches a maximum at the 1000-foot level over Dayton and thereafter drops off slowly with increasing altitude up to 5000 feet. This behavior is somewhat different than the O_3 pattern over Indianapolis. The reason for this inconsistency is not clear at this time.

The integrated bag data from the airplane flight on this day are shown in Table 32. There are two unusual features of these data. First, the relatively higher levels of CO and C_2H_2 found midway between Dayton and Indianapolis are surprising in light of the fact that the NMHC value at the midpoint of the flight is lower than either the Indianapolis or Dayton value. We have no reason to doubt these results but the trend is unusual. The second disconcerting result in Table 32 is the ethylene concentration. The ethylene concentrations from all three bag samples are considerably higher than we found in any of our other airplane samples and are inconsistent with the acetylene and NMHC concentrations. We must suspect that some ethylene contamination occurred during this special flight. None of the other aircraft bag data from other flight days gives indication of such contamination, so that the source of the suspected error is undefined. However, the C_2H_4 results on this day are sufficiently suspicious as to warrant extreme caution in interpretation.

August 6, 1974

Tuesday, August 6, can be generally characterized as warm and hazy. The meteorology was dominated by a large high-pressure system centered over Pennsylvania, as seen in the surface weather maps for this day in Appendix E. Average wind speed for the day was approximately 5 mph. The wind was steady from almost due east the entire day at both Sites 2 and 3. Afternoon ventilation was moderate to good at 7200 m^2/sec. The transport wind was reported (Table 15) at 9 miles/hour. The trajectories for the day shown in Appendix F indicate that the air masses followed a clockwise path, passing in the vicinity of Detroit, Cleveland, Akron, and Columbus before arriving in Dayton. Thus, any or all of these urban areas

TABLE 32. AIRPLANE BAG SAMPLE RESULTS
AUGUST 5, 1974 - AFTERNOON

	5 Miles Downwind of Indianapolis	Midway Between Indianapolis and Dayton	5 Miles Upwind of Dayton
Ethylene (ppmC)	0.034	0.023	0.023
Ethane (ppmC)	0.002	0.003	0.002
Acetylene (ppmC)	0.004	0.007	0.000
PAN (ppm)	0.003	0.003	0.000
CO (ppm)	0.90	1.00	0.45
CH_4 (ppm)	1.50	1.48	1.52
NMHC (ppmC)	0.68	0.45	0.60

may have contributed to the pollutant levels in the air reaching Dayton on this day.

As seen from the six-site composite profiled in Figure 45 O, the ozone patterns exhibited substantial differences from site to site. Ozone peaked at Miamisburg at 4-5 p.m. at 0.068 ppm. At Site 1 the O_3 peak was bimodal, with maxima occurring at 3 and 6 p.m. at about 0.070 ppm. Timberlane O_3 peaked at 4 p.m. at 0.112 ppm with a broad plateau at 0.103 ppm until 7 p.m. The ozone profile at Site 2 showed several fluctuations, with a peak at noon of 0.062 ppm, a sharp peak at 3 p.m. at 0.095 ppm, a broad peak between 5 and 8 p.m. at 0.085 ppm, and a small peak at 11 p.m. of about 0.040 ppm. The EPA monitor at Site 2 showed a similar pattern. Site 3 ozone reached a plateau at 0.103 ppm between 3 and 5 p.m. and then peaked at 0.116 at 6-7 p.m.

With the wind from the east and the unusual bimodal O_3 profiles at most sites, we must consider transport of O_3 and/or precursors from Columbus to Dayton as a real possibility. With winds of about 6 miles per hour (averaged over the 6 a.m.-6 p.m. period), the 6-9 a.m. Columbus air mass should reach Dayton between 4 and 7 p.m. This does indeed correspond with the broad maximum in the O_3 profile exhibited at several of the sites.

Ozone profiles from Sites 1-3 are shown along with the solar intensity profile (from Site 2) in Figure 57 A. It is obvious from this figure that at the time of the second major ozone peak at about 6 p.m., the driving force for ozone formation, ultraviolet radiation, has dropped drastically and is falling sharply at 6 p.m. The curve shown in the figure is for total solar irradiance; the ultraviolet portion of this curve is dropping even more rapidly due to the more rapid loss of U.V. radiation at larger zenith angles (i.e., as the sun sets U.V. intensity drops faster than the total intensity). If we make certain approximations in relating our measured sunlight intensity to NO_2 photolysis rates, then we can calculate a "predicted" ozone concentration based on the assumption of photostationarity. A "predicted" ozone profile based on this calculation is shown in Figure 57 B. In carrying out this very rough

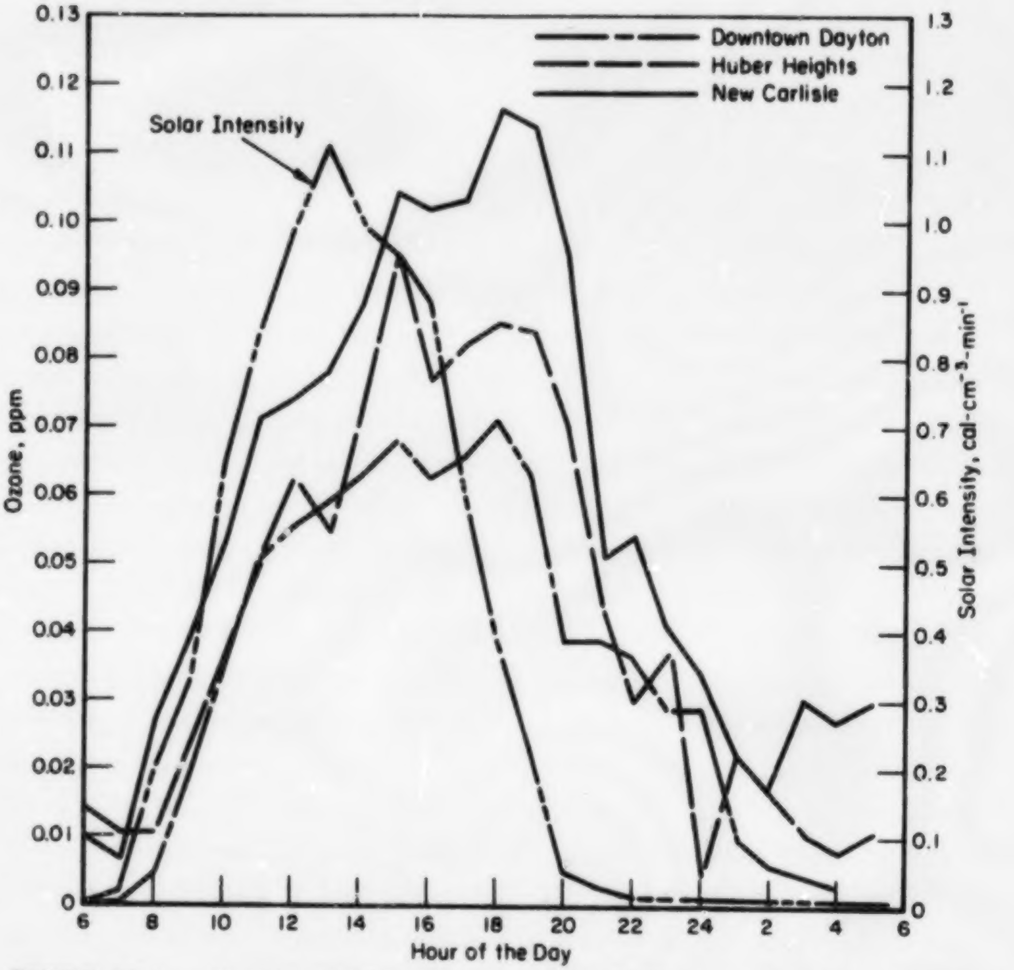

FIGURE 57 A. DAYTON AREA OZONE AND SOLAR INTENSITY PROFILE - AUGUST 6, 1974

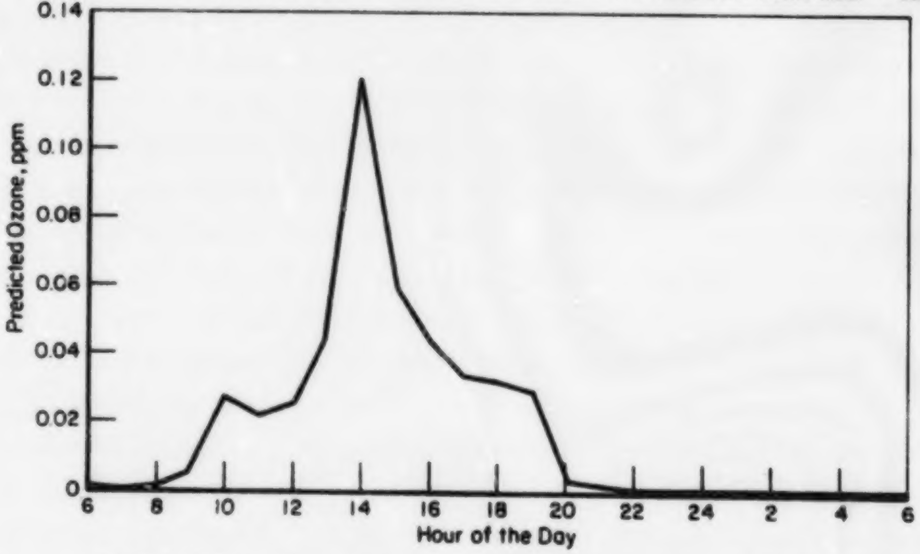

FIGURE 57 B. "PREDICTED" DAYTON AREA OZONE - AUGUST 6, 1974

calculation we have used Site 1 data for NO and NO_2 since the concentrations at Site 1 were high enough to ensure valid measurements. Even at Site 1 however, the NO concentration became so low in the afternoon (1-2 p.m.) that we suspect inaccuracies in the data due to instrument insensitivity. Such measurement inaccuracies may well be the cause of the sharp peak at about 2 p.m. in Figure 57 B. Except for the sharp 2 p.m. peak, the patterns of this "predicted" O_3 profile and the actual Site 1 ozone profile are qualitatively similar up until about 3 p.m. After 3 p.m. however, the curves differ markedly. The predicted ozone concentration drops rapidly as the solar intensity decreases; indeed the predicted O_3 is actually an overestimate since it is based on total intensity rather than U.V. intensity which if falling even more sharply at this time of day. In direct contradiction, the actual measured O_3 at Site 1, as well as Sites 2 and 3, begins to increase at 4 p.m. and reaches a fairly broad peak at 6 p.m. It is our intention to demonstrate that this second, late afternoon, ozone peak arises from transport of the 6-9 a.m. Columbus air mass which has been reacting and generating ozone on its route from Columbus.

The vertical soundings for ozone and temperature carried out at approximately noon and 4 p.m. over downtown Dayton are shown in Tables 49 and 50. No inversion conditions are indicated from the vertical temperature profile. The ozone concentration essentially decreases with height above 1000 feet. The ozone concentration above downtown Dayton was 75 ppb at the 1000-foot level and decreased slowly with height up to 5000 feet. In contrast, the ground level ozone concentration in downtown Dayton (Site 1) at noon was approximately 56 ppb, considerably lower than the concentration at 1000 feet. It appears that the continuous emission of ozone scavengers, primarily nitric oxide, at the surface causes the ozone concentration to maximize at some distance above the surface. Since ozone is in excess, we should expect that the scavenging effect near the surface is probably confined to a few hundred feet above ground, so that the true ozone maximum with respect to altitude is probably between ground level and 1000 feet. This theory that ozone concentrations above ground level are higher than ground level values due to scavenging by near-surface emissions is to some extent substantiated by the fact that the Site 3 ozone concentration at noon was the same as the 1000-foot concentration. The NO emissions in the vicinity of Site 3 are minimal compared to Site 1, so the near-surface scavenging effect should also be minimal. This appears to be the case, since the O_3 concentrations at Site 3 are similar.

The 4 p.m. sounding above the downtown area was similar to the noon profile in that the temperature readings give no indication of inversion conditions and the ozone concentration dropped continuously above 1000 feet. Again the surface ozone concentration in the downtown area was much less than the concentration at 1000 feet (105 ppb versus 63 ppb at ground level), and even up to 5000 feet the concentration remained higher than ground level. Again at Site 3, away from major emissions sources or heavy traffic, the ground ozone concentration was virtually the same as the 1000-foot concentration (102 ppb versus 105 ppb).

The upwind and downwind patterns flown by the aircraft are shown as Figures 58 A and B for morning (9-12 a.m.) and afternoon (1-4 p.m.) flights respectively. The morning ozone levels were generally low, varying between 50 and 75 ppb on the 20-mile upwind loop (the first loop and therefore the earliest in the day), 45 to 59 ppb during the 20-mile downwind loop, and between about 60 to 90 ppb on the 60-mile downwind loop. In general, the 20-mile downwind loop showed the lowest ozone concentration and the 60-mile downwind loop showed the highest. This is consistent with the idea that the city's emissions form a "scavenger shadow" which retards O_3 formation in the urban plume at short distances downwind of the city. The long downwind loop is probably higher than the other two since it is the last loop run in the morning and the irradiation time has consequently been the longest. The morning integrated data from the airplane bag collections are shown in Table 33. Non-methane hydrocarbon and CO levels from the short downwind loop are definitely higher than either of the other two loops, in agreement with the picture of an emissions shadow. Indeed, this 20-mile downwind arc is at just about the position where the 7-8 a.m. Dayton air mass should reside, and we should therefore expect a peak in primary pollutants at this point.

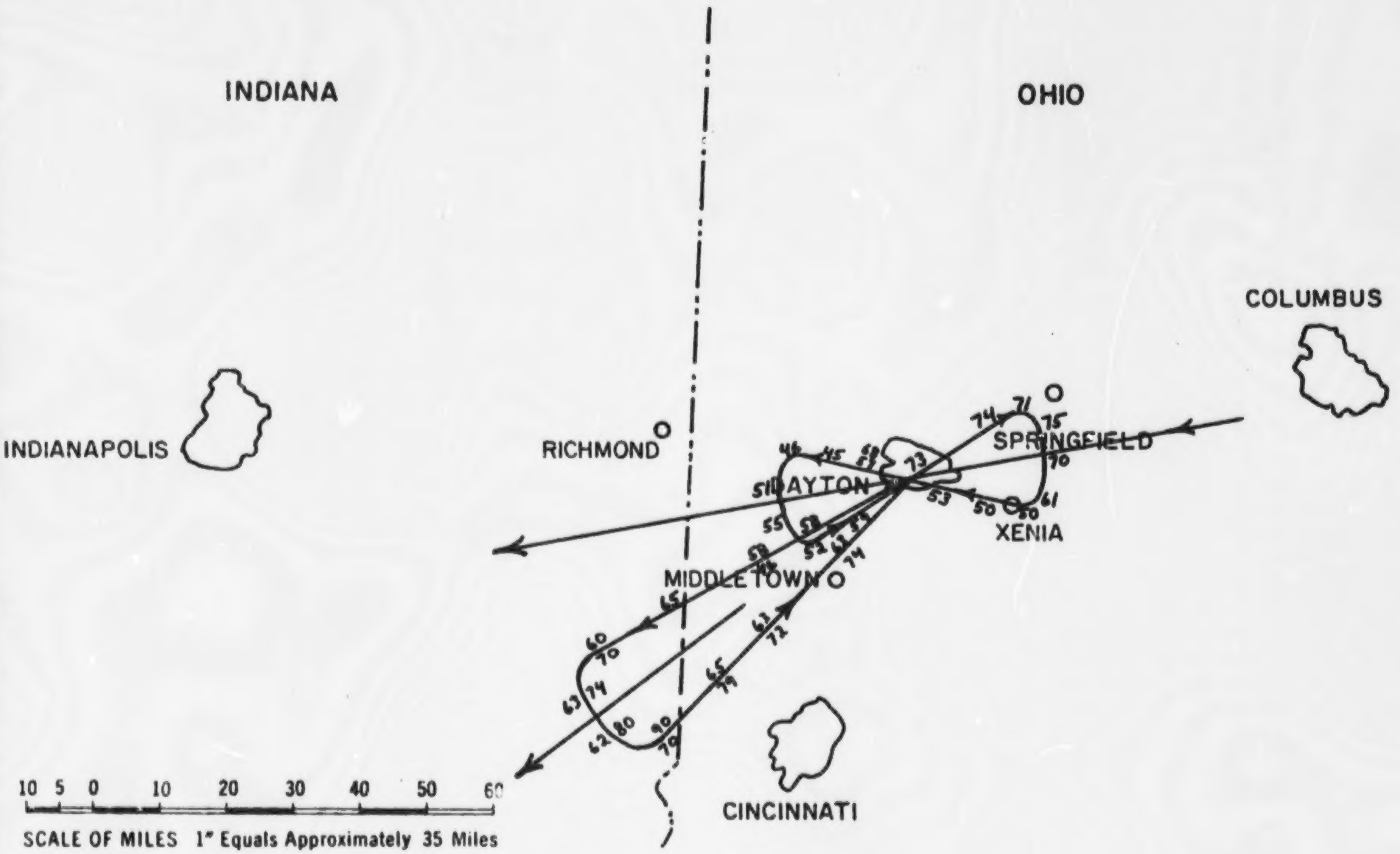
INDIANA
OHIO
COLUMBUS
INDIANAPOLIS
RICHMOND
SPRINGFIELD
DAYTON
XENIA
MIDDLETOWN
CINCINNATI
74
71
75
70
61
50
53
73
46
45
51
55
53
65
60
70
74
63
62
80
90
79
72
10 5 0 10 20 30 40 50 60
SCALE OF MILES 1" Equals Approximately 35 Miles

FIGURE 58 A. AUGUST 6, 1974 - 9-12 A.M.
OZONE CONCENTRATION IN ppb

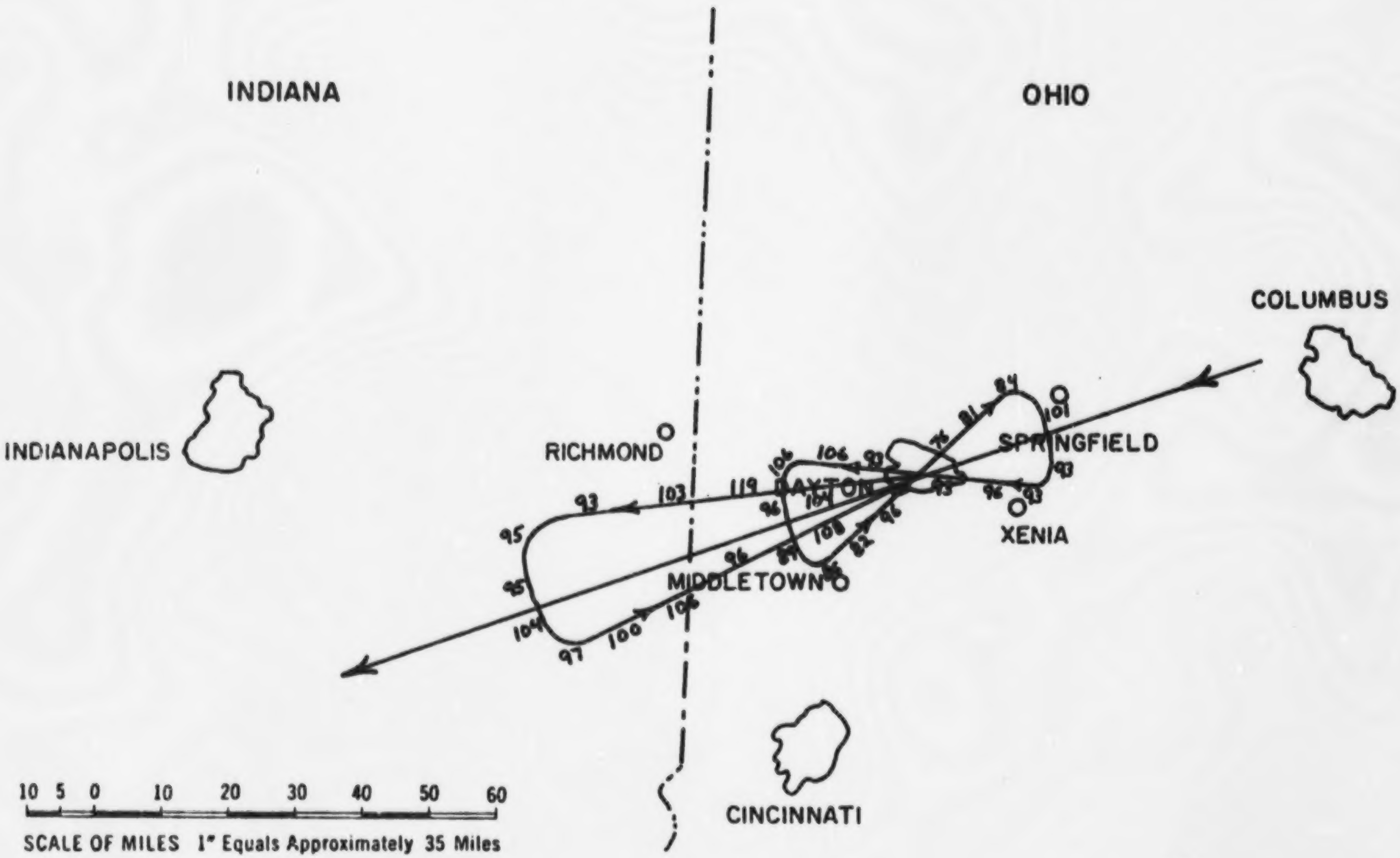
INDIANA
OHIO
COLUMBUS
INDIANAPOLIS
RICHMOND
SPRINGFIELD
XENIA
DAYTON
MIDDLETOWN
CINCINNATI
84
81
75
101
93
93
96
93
106
106
93
119
103
93
95
95
104
97
100
106
96
104
96
108
84
82
96
10 5 0 10 20 30 40 50 60
SCALE OF MILES 1" Equals Approximately 35 Miles

FIGURE 58 B. AUGUST 6, 1974 - 1-4 P.M.
OZONE CONCENTRATION IN ppb

TABLE 33. AIRPLANE BAG SAMPLE RESULTS AUGUST 6, 1974

		20 Miles Upwind	20 Miles Downwind	60 Miles Downwind
I.	9:00-12:00 a.m.			
	Ethylene (ppmC)	0.002	0.002	0.002
	Ethane (ppmC)	0.002	0.002	0.001
	Acetylene (ppmC)	0.000	0.004	0.000
	PAN (ppm)	0.000	0.002	0.000
	CO (ppm)	0.60	5.2	0.50
	CH_4 (ppm)	1.45	1.45	1.45
	NMHC (ppmC)	0.45	0.6	0.45
II.	1:00-4:00 p.m.			
	Ethylene (ppmC)	0.009	0.005	0.007
	Ethane (ppmC)	0.005	0.002	0.002
	Acetylene (ppmC)	0.009	0.004	0.009
	PAN (ppm)	0.000	0.000	0.003
	CO (ppm)	0.80	0.59	0.85
	CH_4 (ppm)	1.44	1.50	1.43
	NMHC (ppmC)	0.29	0.42	0.25

The CO value of 5.2 ppm for the 20-mile downwind arc is unusually high however, and might be indicative of some abnormal circumstance. In both the 20-mile upwind and 60-mile downwind arcs, the concentration of acetylene was below our detection limits. The C_2H_4/C_2H_2 ratio of 0.5 found 20 miles downwind is approximately one half the usual ratio for auto exhaust. If we make the usual assumption that auto exhaust is the dominant source of both C_2H_4 and C_2H_2, then the 0.5 ratio is indicative of ethylene removal from the air mass. Very likely this removal is occurring through smog reactions, since this air mass has experienced several hours of irradiation by late morning.

The afternoon airplane flight results for August 6 are shown in Figure 58 B. It is interesting to note that the O_3 concentration exceeded 0.1 ppm at at least one point on each of the three loops. The lowest O_3 values are seen on the northeast leg of the upwind loop. This is the first leg of the first loop flown in the afternoon, so the ozone concentrations represent the values at approximately 1:00 p.m. Since O_3 was still rising sharply at all ground stations at this time, the low values are not too surprising. The O_3 concentration at the point 20 miles directly upwind of Dayton is approximately 0.1 ppm. Very simple calculations employing the wind direction, which was essentially constant all day, and wind speed indicate that the early portions of the 6-9 a.m. Columbus air mass have reached this point 20 miles upwind of Dayton between 1-2 p.m. Thus the high O_3 levels upwind of the city may be explained by the transport of 6-9 a.m. Columbus precursors which have reacted enroute to form ozone.

A clearer picture of this transport phenomenon can be gained from Figure 59 which shows the ozone concentration at 1000 feet along the path from about 15 miles north of Dayton to Columbus (this is the path flown from Dayton to the Columbus home base each night). The airplane profile shows an ozone maximum to be just east, and upwind of, Springfield, Ohio. The aircraft was not flying along the wind vector from Columbus to Dayton but rather was flying initially somewhat north of that vector. Therefore the true position of the O_3 maximum is somewhat

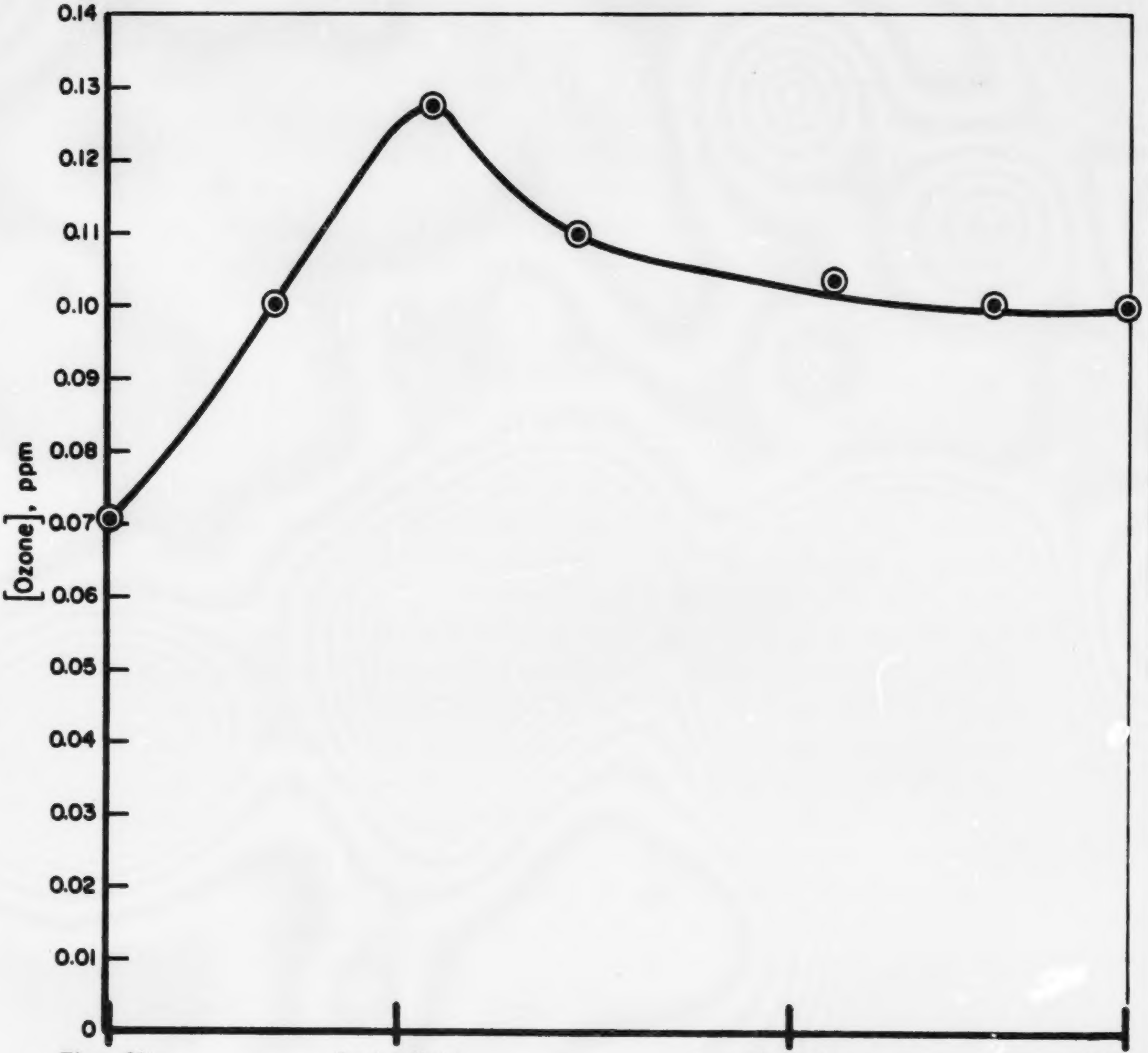

FIGURE 59. OZONE AT 1000 FEET BETWEEN DAYTON AIRPORT AND COLUMBUS

uncertain since the aircraft may have cut into the Columbus plume to the east and upwind of the true maximum. In any case, a simplified calculation of the origin of the 6-7 p.m. Dayton air mass indicates that it was positioned over the Columbus area during the 6-9 a.m. interval. The high precursor concentrations which would be picked up over Columbus at this time, and the long irradiation time, may well explain the high O_3 concentrations observed at all Dayton sites between 6 and 7 p.m. on this date.

Much smaller O_3 peaks in Dayton between 10 and 11 p.m. may also represent transport of O_3 from Columbus. In this case however, we may be dealing with transport of O_3 itself, that is, the movement of the ozone-rich air which forms over Columbus during midafternoon, as opposed to precursor transport. Evidence for this mechanism is still unclear, however.

August 7 and 9, 1974

August 7 and August 9 have been singled out for discussion because aircraft ozone data are available on both of these days. The ventilation on these days is classified as poor to moderate (Table 15) with mixing heights between 4000 and 6000 feet. The wind direction component of our 6 a.m.-2 p.m. wind vector indicates air mass movement from the southeast on August 7. The trajectory analysis in Appendix F indicates that the air arriving in Dayton in the morning has passed southeast over Lake Erie, over Cleveland, down into West Virginia and then across and up into the Dayton vicinity during the previous 48-60 hours. The evening trajectory shows air mass movement from the south, generally from the direction of the Cincinnati urban complex.

As noted in Table 20, the only ground station which exceeded the 0.08 ppm ozone standard on August 7 was Site 3 in New Carlisle. The ozone concentration at the 1000-foot level along the special flight pattern run on this day is shown in Figure 60. The August 7 special flight was a first attempt to cross-check our aircraft monitoring system with that being flown by Research Triangle Institute (RTI) out of Wilmington, Ohio. Because of a technical problem with the sampling system aboard the EPA C-45 aircraft being flown by RTI, this first attempt at a comparison flight had to be aborted. The ozone data recorded by our aircraft during the initial segments of the aborted flight are displayed in Figure 60. Dashed lines in the figure indicate the plane was flying through a rain storm. It is clear from this figure and Table 20 that the concentration of O_3 at 1000 feet in the vicinity of Dayton is again considerably higher than the ground station concentrations. It must be emphasized that the initial leg of the flight, from Columbus to Wilmington, was flown early in the morning during the initial increase in ozone concentration. The remaining segments of the flight were conducted several hours later after making preparation on the ground in Wilmington. Thus the relatively low O_3 values on the Columbus-to-Wilmington leg of the trip result primarily from a lack of extensive photochemical generation of O_3 so early in the day.

The average air mass movement between 6 a.m. and 2 p.m. on August 9 was from the north-northeast according to our wind vector data (Table 20). However, the trajectory analyses in Appendix F reveal that the air arriving in Dayton during the day had actually been located in Tennessee 2 days earlier and had passed through Kentucky and over the Cincinnati area prior to looping around Dayton to the west and returning to Dayton from the north. The fact that the air mass had passed over Lexington, Kentucky, and Cincinnati before arriving in Dayton may explain the relatively high ozone concentrations observed at all four Dayton-area ground stations listed in Table 20. All exceeded 0.08 ppm for at least 1 hour and the Miamisburg station showed ozone concentrations in excess of 0.1 ppm.

The aircraft ozone data for two comparison flights on this day are shown in Figures 61 A and B. The flight from Columbus to the Dayton airport took place much earlier than the other flights and so is not directly comparable in terms of ozone concentration.

Both comparison loops flown on August 9 show very high ozone concentrations at the 1000 foot level, especially to the southeast of the city of Dayton. This is consistent with the finding that Miamisburg

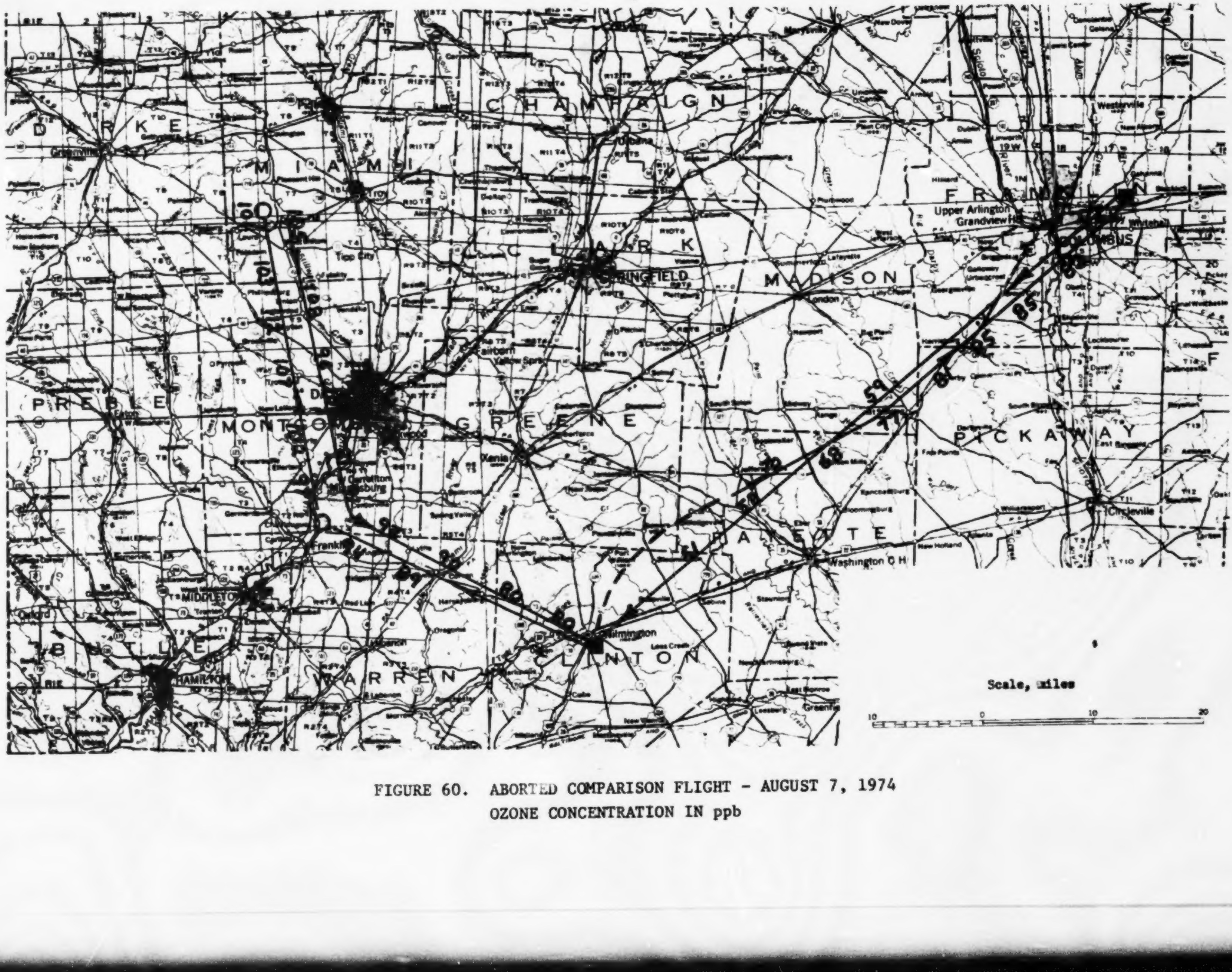
DARKE
MIAMI
CHAMPAIGN
CLARK
MADISON
FRANKLIN
PICKAWAY
PREBLE
MONTGOMERY
GREENE
FAYETTE
BUTLER
WARREN
CLINTON
Springfield
Columbus
Upper Arlington
Grandview Hts
Whitehall
Xenia
Wilmington
Washington C H
Circleville
Hamilton
Middletown
Tipp City
London
Westerville
Scale, miles
10
0
10
20

FIGURE 60. ABORTED COMPARISON FLIGHT - AUGUST 7, 1974
OZONE CONCENTRATION IN ppb

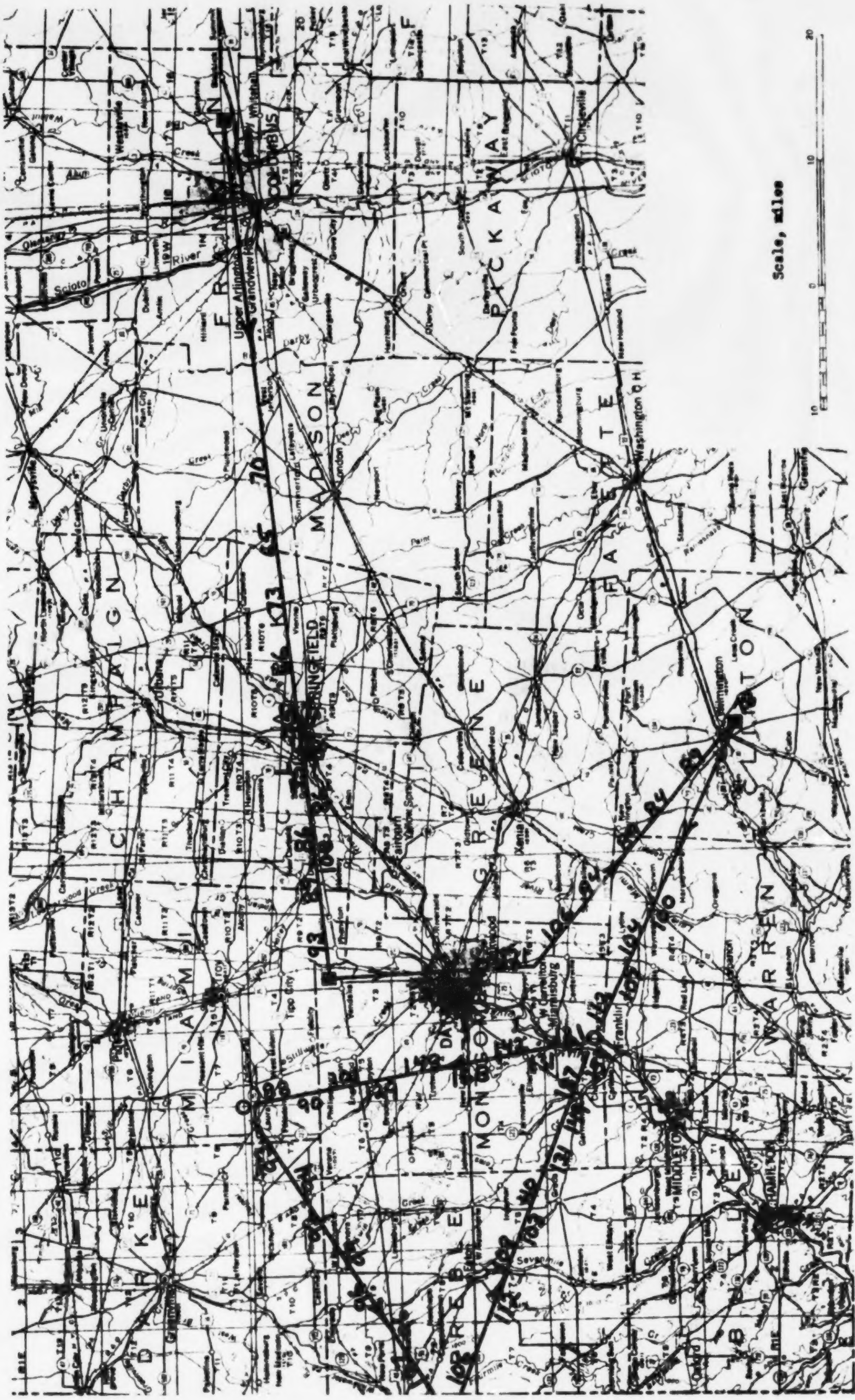
COLUMBUS
Upper Arlington
Grandview Hts
Scioto River
FRANKLIN
PICKAWAY
Circleville
MADISON
London
Washington C.H.
FAYETTE
CHAMPAIGN
Urbana
SPRINGFIELD
GREENE
Xenia
CLINTON
Wilmington
MIAMI
Troy
Tipp City
DAYTON
MONTGOMERY
Miamisburg
Franklin
WARREN
DARKE
Greenville
PREBLE
BUTLER
MIDDLETOWN
HAMILTON
70
65
93
84
89
Scale, miles
10
0
10
20

FIGURE 61 A. FIRST LOOP - COMPARISON FLIGHT - AUGUST 9, 1974
OZONE CONCENTRATION IN ppb

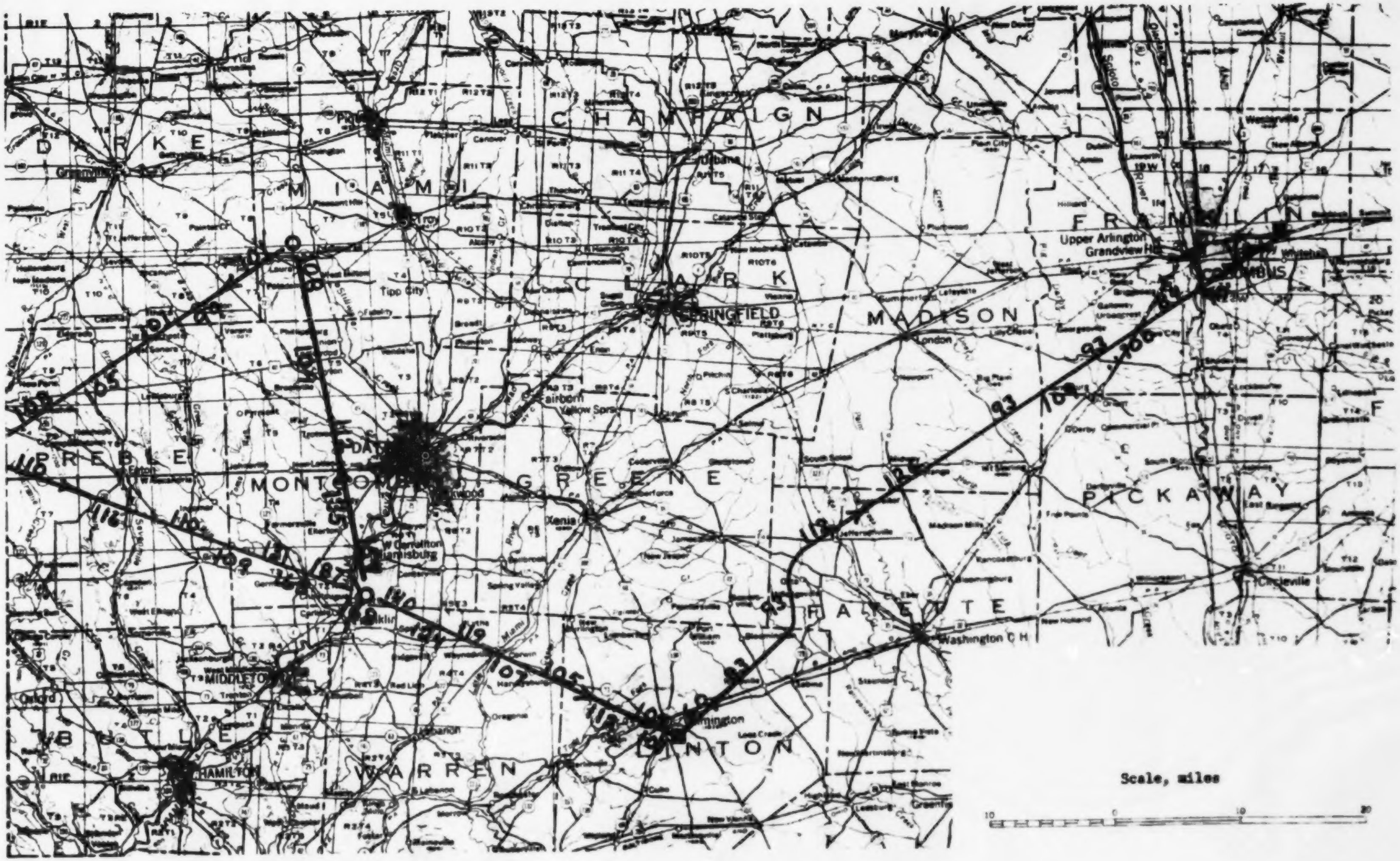
DARKE
MIAMI
CHAMPAIGN
CLARK
SPRINGFIELD
MADISON
FRANKLIN
COLUMBUS
Upper Arlington
Grandview Hts
PICKAWAY
Circleville
PREBLE
MONTGOMERY
GREENE
Xenia
Fairborn
Tipp City
Troy
London
FAYETTE
Washington C H
CLINTON
WARREN
BUTLER
HAMILTON
MIDDLETOWN
Miamisburg
Scale, miles
10
0
10
20

FIGURE 61 B. SECOND LOOP - COMPARISON FLIGHT - AUGUST 9, 1974
OZONE CONCENTRATION IN ppb

recorded the highest O_3 concentration of all the ground stations on this day. It is very likely, judging from the northeast (from the NE) airflow patterns indicated by the Dayton wind vector and computerized trajectory analysis, that these high ozone levels to the southwest of Dayton, both on the ground and aloft, result from the movement of the high ozone/precursor-containing Dayton air mass toward the southwest. Consistent with the strong local emissions of NO in this region southwest of Dayton, the O_3 levels at the Miamisburg ground station, while high, are still much lower than the concentrations observed at 1000 feet.

In summary, the combination of the ground and aircraft ozone data, along with the wind direction and trajectory results, provide rather strong evidence for the transport of Dayton ozone and/or reacting precursors southwest through the populated Miami River Valley on August 9. In terms of our model, we are observing the movement of an ozone "hot spot" which originated from local urban sources and is superimposed on the regional ozone blanket which has been transported over much longer distances.

Intercomparability of Data. The cross-comparison test between the Battelle and RTI aircraft was carried out to ensure data comparability. The flight path and our Battelle ozone data were shown earlier in Figures 61 A and B for loops one and two respectively. The triangular pattern flown by the two aircraft is shown in Figure 62. A formation flight was precluded by the different cruising speeds of the two aircraft, so the triangular pattern shown in the figure was flown twice by each aircraft. Plots of the ozone data recorded during the two flight loops are presented in Figures 63 and 64. Since ozone concentrations had to be plotted versus position along the flight path there is a temporal difference between the data shown at each point. The time differences notwithstanding, there is good agreement between the RTI and Battelle ozone data, with differences generally less than 10 percent. This fact, combined with the excellent agreement obtained between the Battelle and EPA ozone instruments located at Huber Heights, provides confidence in the general intercomparability of the ozone data collected during the Ohio Valley ozone study.

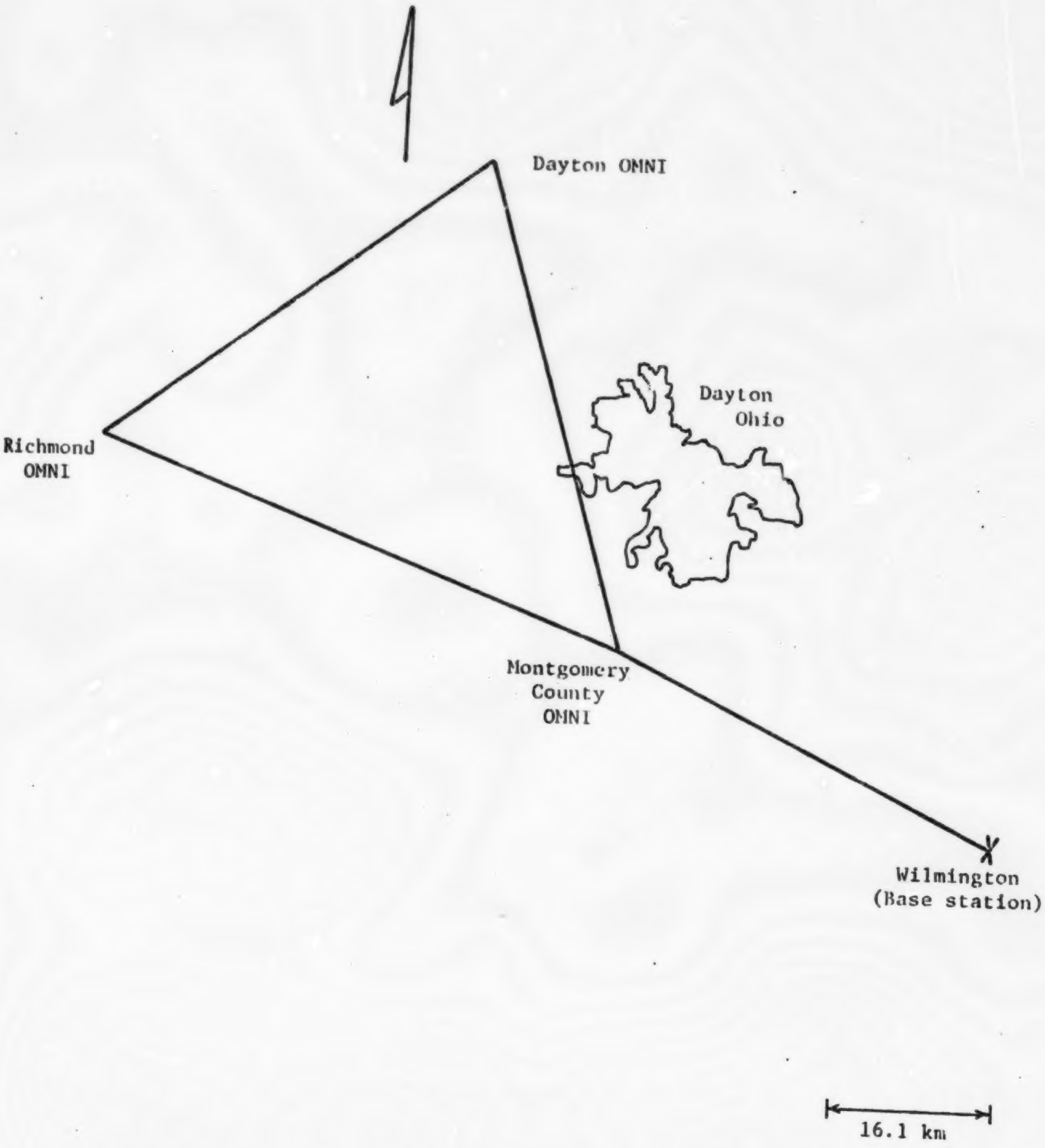
Dayton OMNI
Dayton
Ohio
Richmond
OMNI
Montgomery
County
OMNI
Wilmington
(Base station)
16.1 km

FIGURE 62. BATTELLE-RTI COMPARISON FLIGHT PATTERN

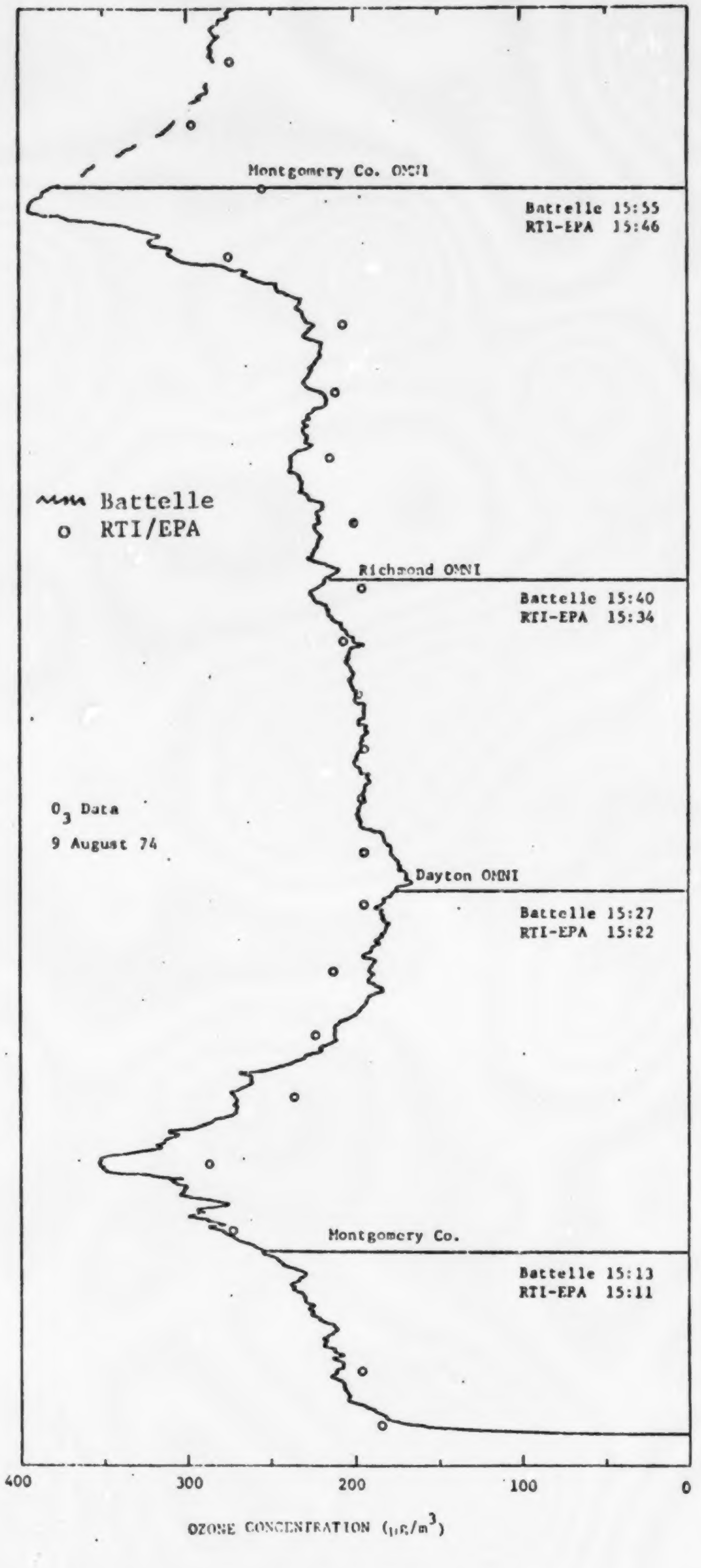

FIGURE 63. DATA FROM RTI/BATTELLE COMPARISON FLIGHT

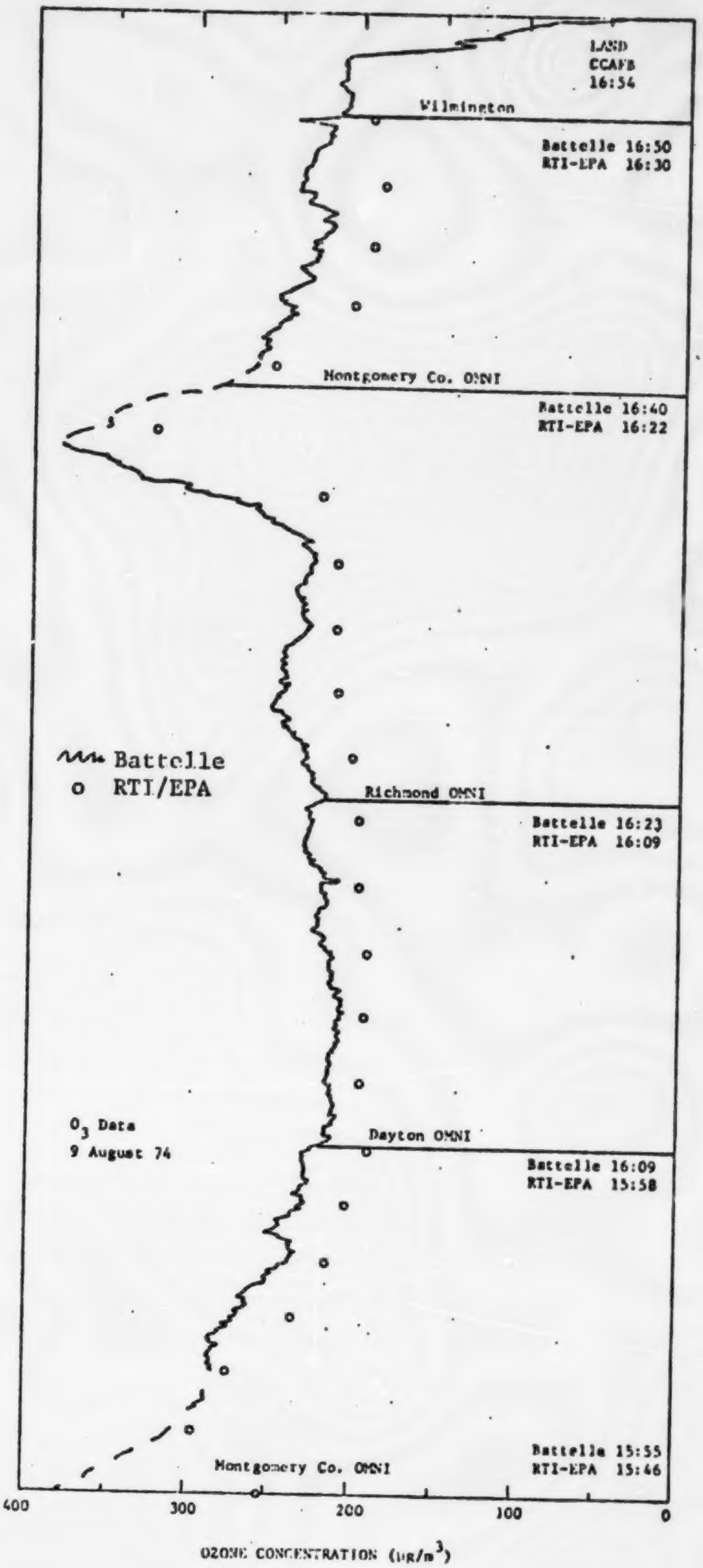

FIGURE 64. DATA FROM RTI/BATTELLE COMPARISON FLIGHT

Another cross-comparison of data was initiated on August 9 between EPA and Battelle to ensure intercomparability of the field-study data for hydrocarbons and carbon monoxide. EPA investigators prepared and analyzed three Teflon bag samples containing ethylene, acetylene, and carbon monoxide. These bags were then transported by automobile from Wilmington to the Battelle mobile laboratory in Dayton. A comparison of the EPA and Battelle determination on the three samples is shown in Table 34. In general the acetylene data are in good agreement and the CO results, while variable, show reasonable agreement. The ethylene values differ by approximately 20 percent. This may represent a real difference in calibration or it may be the result of loss of ethylene due to photochemical reaction during the few hours which elapsed between the EPA analysis and the Battelle analysis. The fact that cross-comparisons of EPA and Battelle calibration sources yielded excellent agreement gives some credence to this latter explaination. However, at this time we cannot unambiguously define the cause of the ethylene differences.

CONCLUSION

The results of this study indicate that several factors affect ozone formation and transport and that the interaction and superposition of several different sources of ozone is often necessary to explain ozone behavior.

One important source of ozone appears to be long-range transport of ozone and ozone precursors trapped below the subsidence inversion associated with high-pressure systems. This ozone is very likely partly natural and partly anthropogenic in origin. Demonstration of such a source of ozone would render the current oxidant control strategies untenable, since almost all natural and man-made precursors will generate ozone under the conditions likely to be encountered in a long-distance transport situation. One important implication of long-range transport is that the classification of organic emissions based on the maximum amount of O_3 generated in a short

TABLE 34. BATTELLE-EPA CROSS CALIBRATION(a)

	C_2H_4, ppbC	C_2H_2, ppbC	CO, ppm
Sample No. 1			
EPA	104.2	43.7	2.46
Battelle(b)	85	47	2.6
Sample No. 2			
EPA	170.5	22.6	1.55
Battelle(b)	133	26	1.6
Sample No. 3			
EPA	51.2	80.2	2.46
Battelle(b)	42	86	3.0

(a) Teflon bag samples prepared and analyzed by William Lonneman of EPA.

(b) Average of two determinations.

smog-chamber irradiation is no longer viable. Instead we must consider the ozone dosage over long-term irradiation periods such as might be encountered in long-range transport. It is no longer just the maximum concentration of O_3 which can be generated in an urban area that we are concerned with, but rather the total dosage formed within a moving air mass over its entire trajectory. Thus it may be desirable to reclassify precursors in terms of oxidant dosage over long irradiation times rather than on the basis of O_3 maxima during a 6-hour experiment. Such a classification would likely result in a "total reactive hydrocarbon" or possibly just a NMHC standard rather than the current complex reactivity rating systems.

The use of O_3 dosage over long irradiation periods as a control criterion impacts another method which has been employed for de facto control of oxidant over the past few years. This refers to the policy of using the nitric oxide inhibition of ozone formation for control. As organic emissions from motor vehicles have been reduced, the nitrogen oxides emissions have often been permitted to increase, thus helping to reduce O_3 formation in the local emission area. However, theoretical and laboratory studies predict that the O_3 dosage along the air mass trajectory will likely be increased by such a policy, to the detriment of populations located downwind of high-density vehicular emissions.

The implications of long distance transport are obviously far-reaching. For this reason alone, the sources of ozone and particularly the long-distance transport phenomenon must be carefully documented by further detailed research. Our work will continue in this area in the coming year.

REFERENCES

1. Holzworth, G. C., J. Applied Meteor., 6, 1039 (1967).

2. Spicer, C. W., "The Fate of Nitorgen Oxides in the Atmosphere", Battelle-Columbus Report to CRC (CAPA-9-71) and EPA (Contract No. 68-02-0799), September, 1974.

3. Miller, D. F., Schwartz, W. E., Jones, P. E., Joseph, D. W., Spicer, C. W., Riggle, C. J., and Levy, A., "Haze Formation: Its Nature and Origin - 1973", Battelle-Columbus Report to EPA and CRC, June, 1973.

4. Spicer, C. W., Gemma, J. L., Joseph, D. W., and Levy, A., "The Fate of Nitrogen Oxides in Urban Atmospheres", paper presented at 168th National Meeting of The American Chemical Society, Atlantic City (1974).

5. Charlson, R. J., Vanderpol, A. H., Covert, D. S., Waggoner, A. P., and Ahliquist, N. C., Atmos. Environ., 8, 1257 (1974).

6. Hoffman, A. J. and Morita, C. B., "Dayton Air Pollutant Emission Inventory", PB 206, 242, U.S. Dept. of Health, Education, and Welfare (1968).

7. Kopczynski, S. L., Lonneman, W. A., Winfield, T., and Seila, R., J. Air Poll. Control Assoc., 25, 251 (1975).

8. Lonneman, W. A., Kopcyznski, S. L., Darley, P. E., and Sutterfield, F. D., Environ. Sci. and Tech., 8, 229 (1974).

9. Fisher, R. A., Phil. Tran. of Roy. Soc. London, Series B, 213, 89 (1924).

10. Sonquist, J. A. and Morgan, J. N., "The Detection of Interaction Effects", Monograph No. 35, University of Mighigan (1964).

11. Godson, W. D., Quart. J. Roy. Meteor. Soc., 88, 220 (1962).

12. See for example, Hering, W. S. and Borden, T. R., "Environ. Research Paper No. 133", Air Force Cambridge Research Laboratories, Bedford, Mass., 1967.

13. Elkus, B. and Wilson, K., information presented at Berkeley UC-ARB Conference on "Chemical and Physical Interactions of SO_x, NO_x, and Photochemical Oxidant: Current Status and Priorities in Research", Berkeley, Calif., March, 1974.

14. Cleveland, W. S., Kleiner, B., and Warner, J. L., "Using Robust Statistical Methods in Analyzing Air Pollution Data with Applications to New York-New Jersey Photochemistry", presented at 67th Annual Meeting of Air Poll. Control Assoc., Denver, June, 1974.

15. "Interim Report for the Indianapolis Summer Ozone Study", report by the Indianapolis Center for Advanced Research and the IUPUI Computing Services Dept., September, 1974.

APPENDICES

(Appendices A-D are available through the National Technical Information Service)

APPENDIX E

NATIONAL WEATHER SERVICE SURFACE WEATHER MAPS

Reproduced from
best available copy.

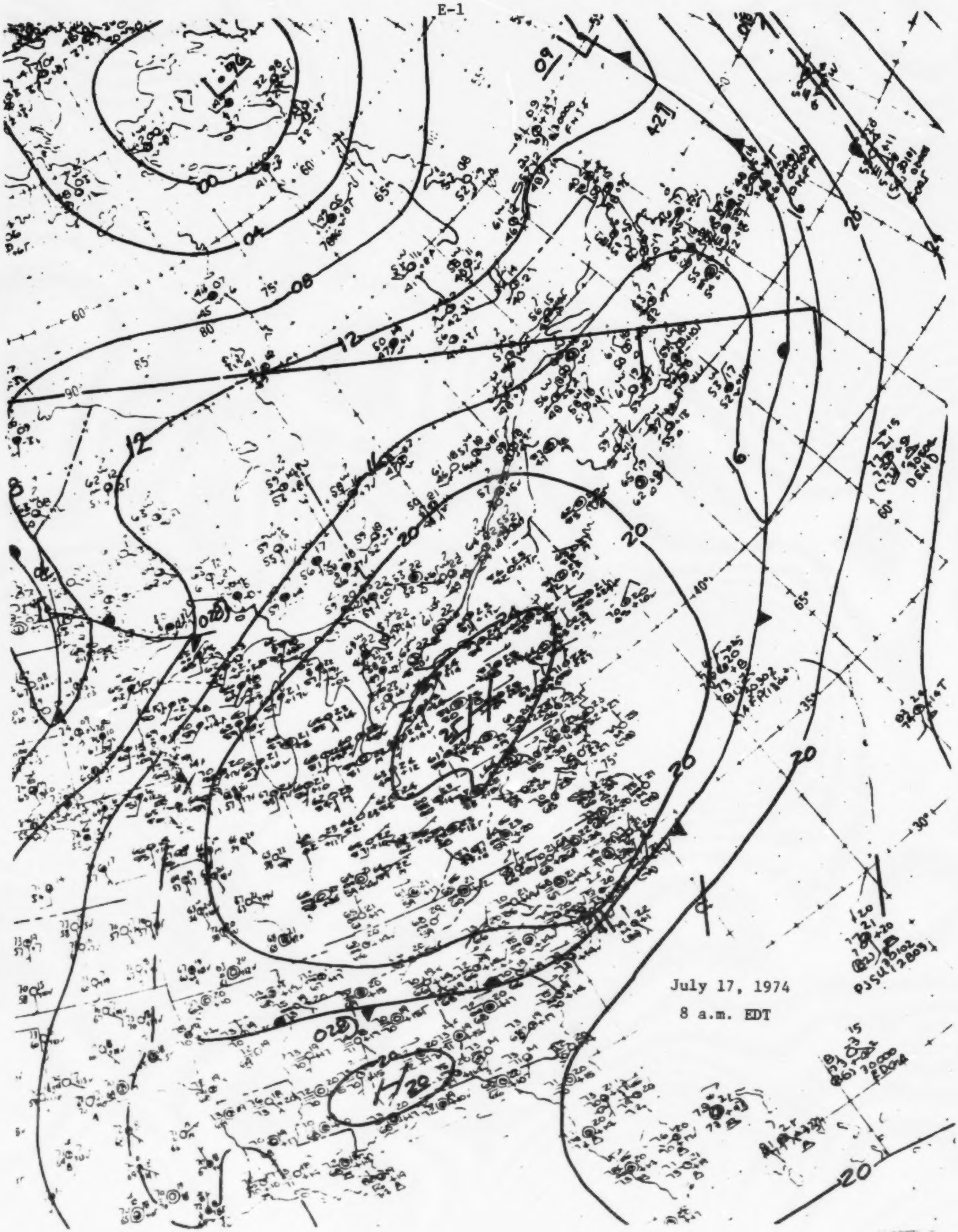
00
04
08
12
16
20
24
60°
75°
80°
85°
90°
65°
40°
35°
30°
1020
1028

July 17, 1974

8 a.m. EDT

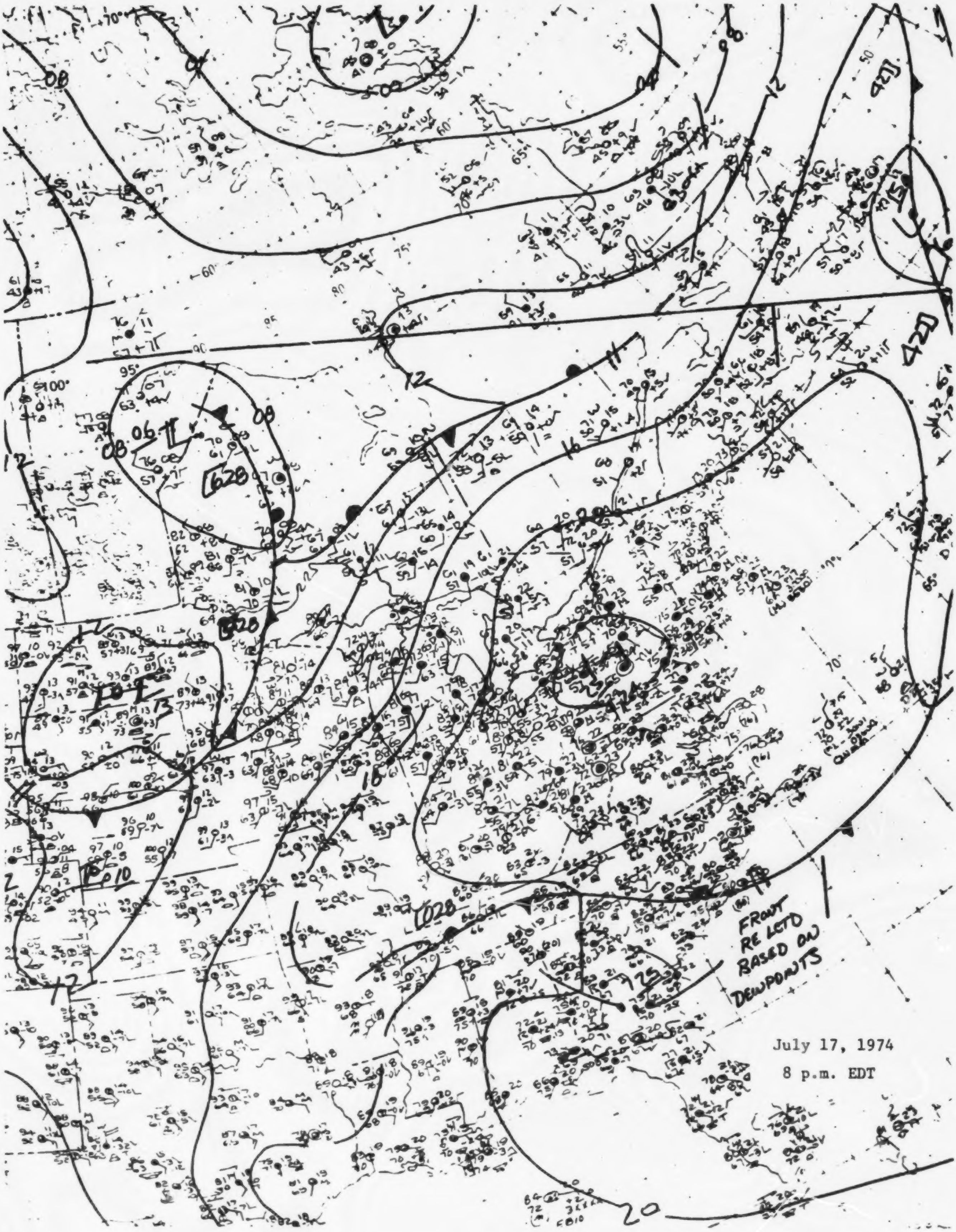

FRONT RE LCTD BASED ON DEWPOINTS

July 17, 1974

8 p.m. EDT

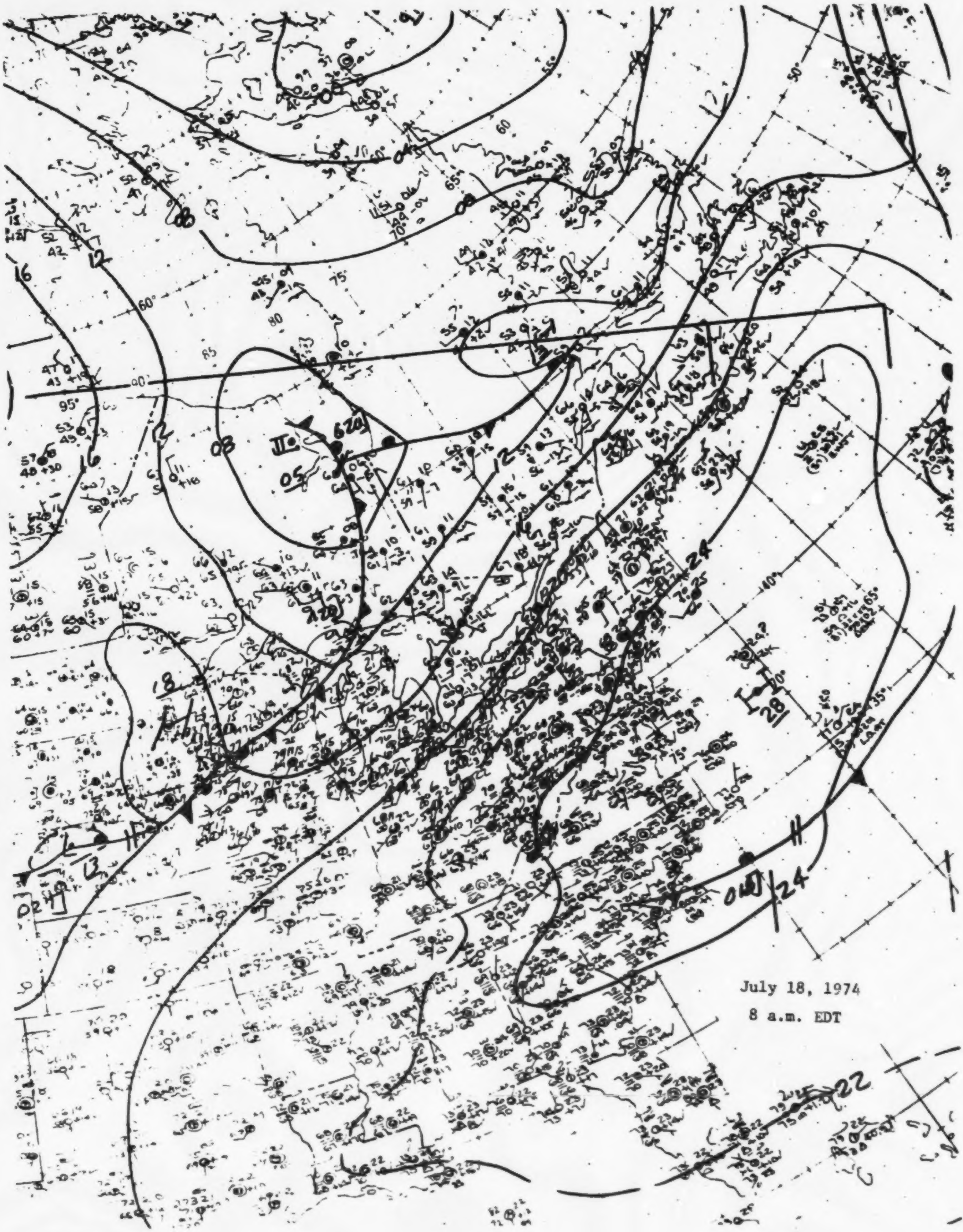

July 18, 1974

8 a.m. EDT

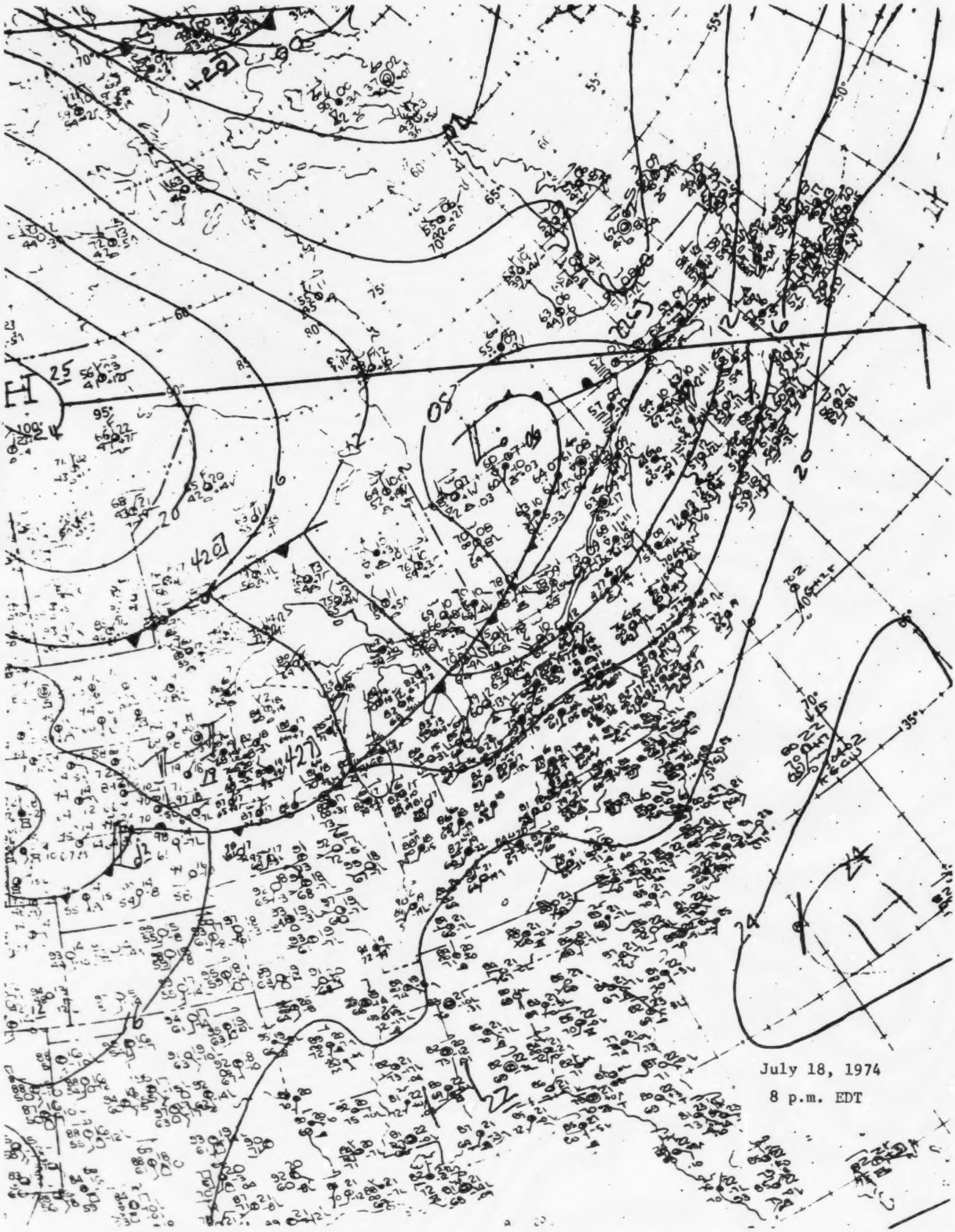

July 18, 1974

8 p.m. EDT

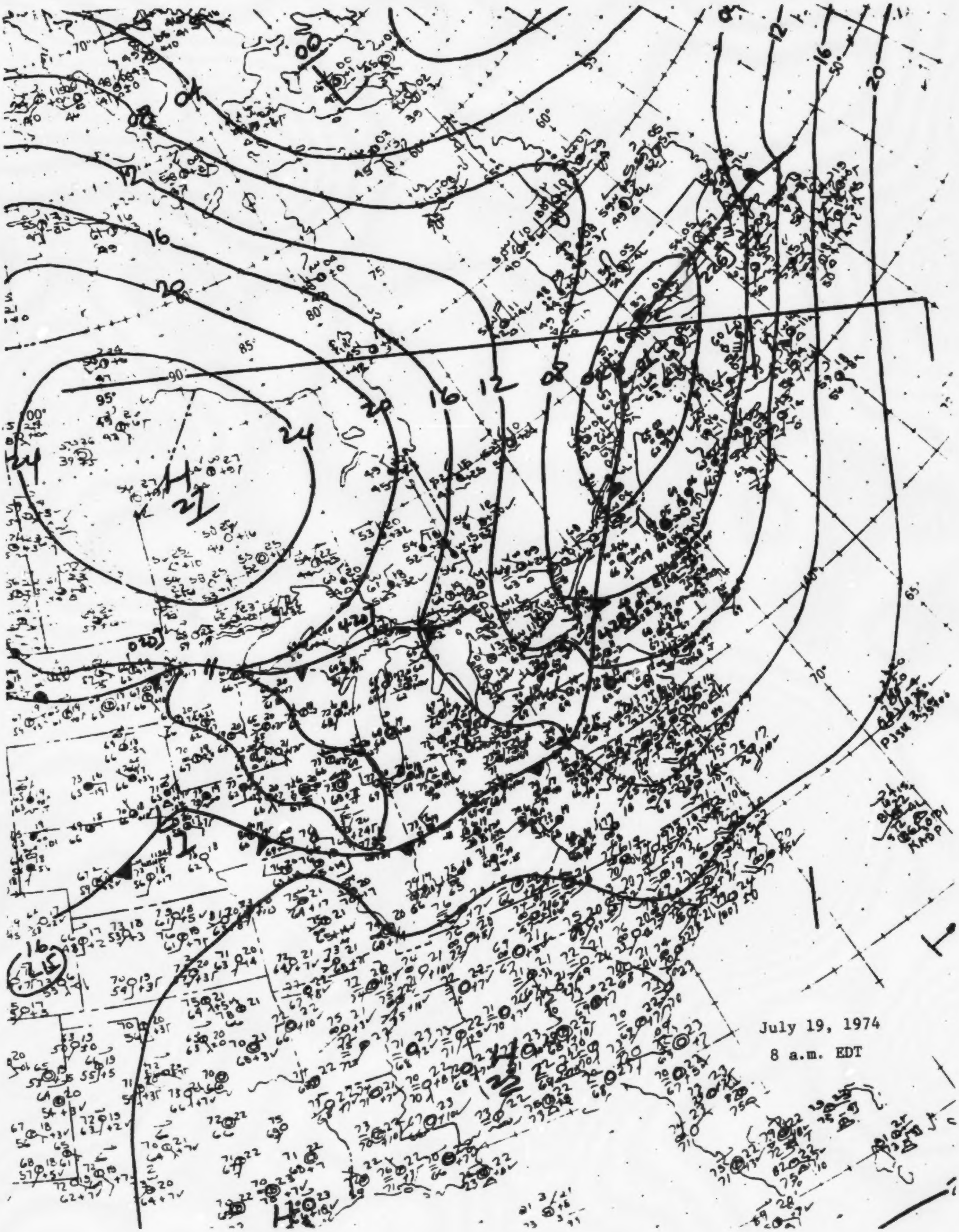

July 19, 1974

8 a.m. EDT

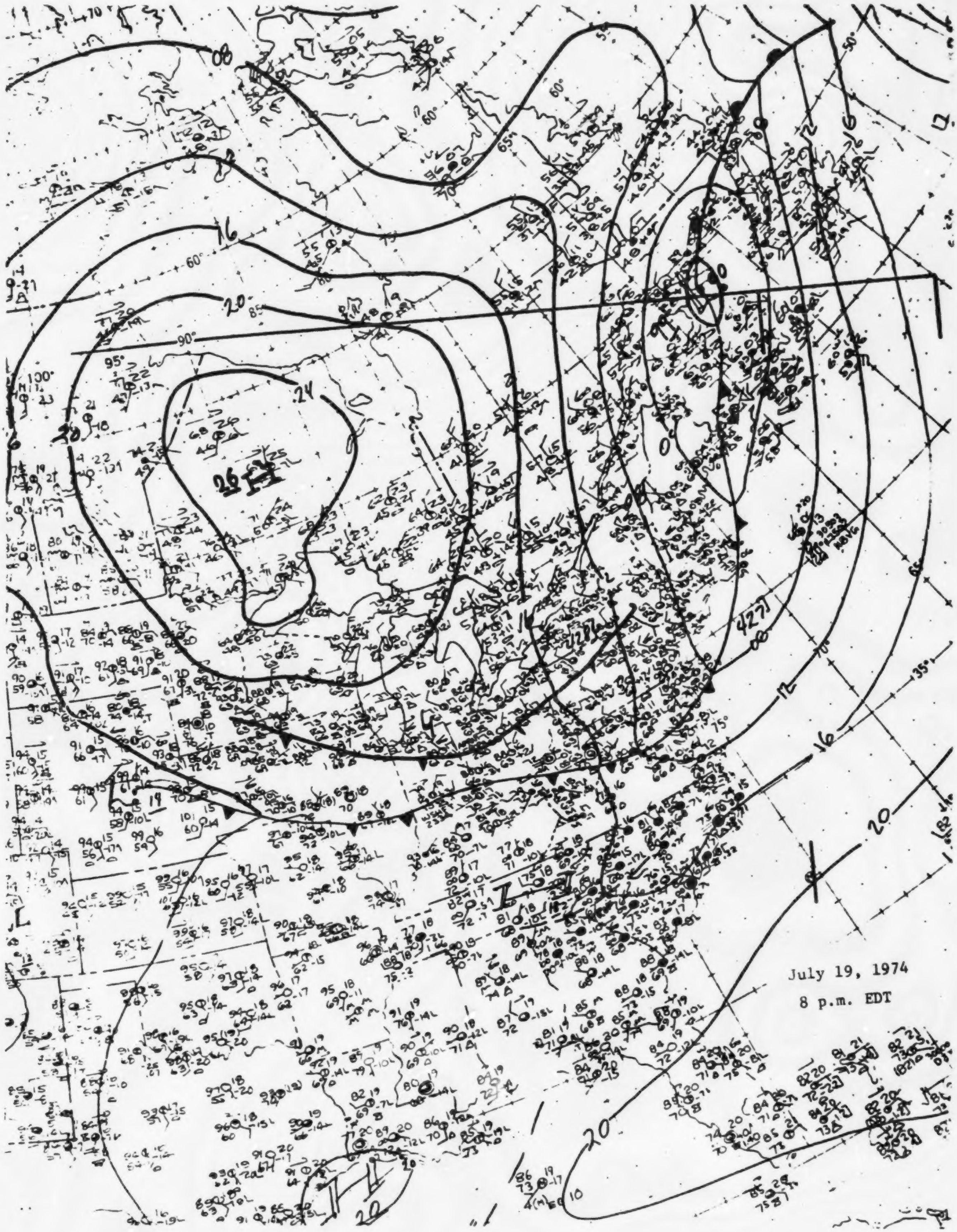

July 19, 1974

8 p.m. EDT

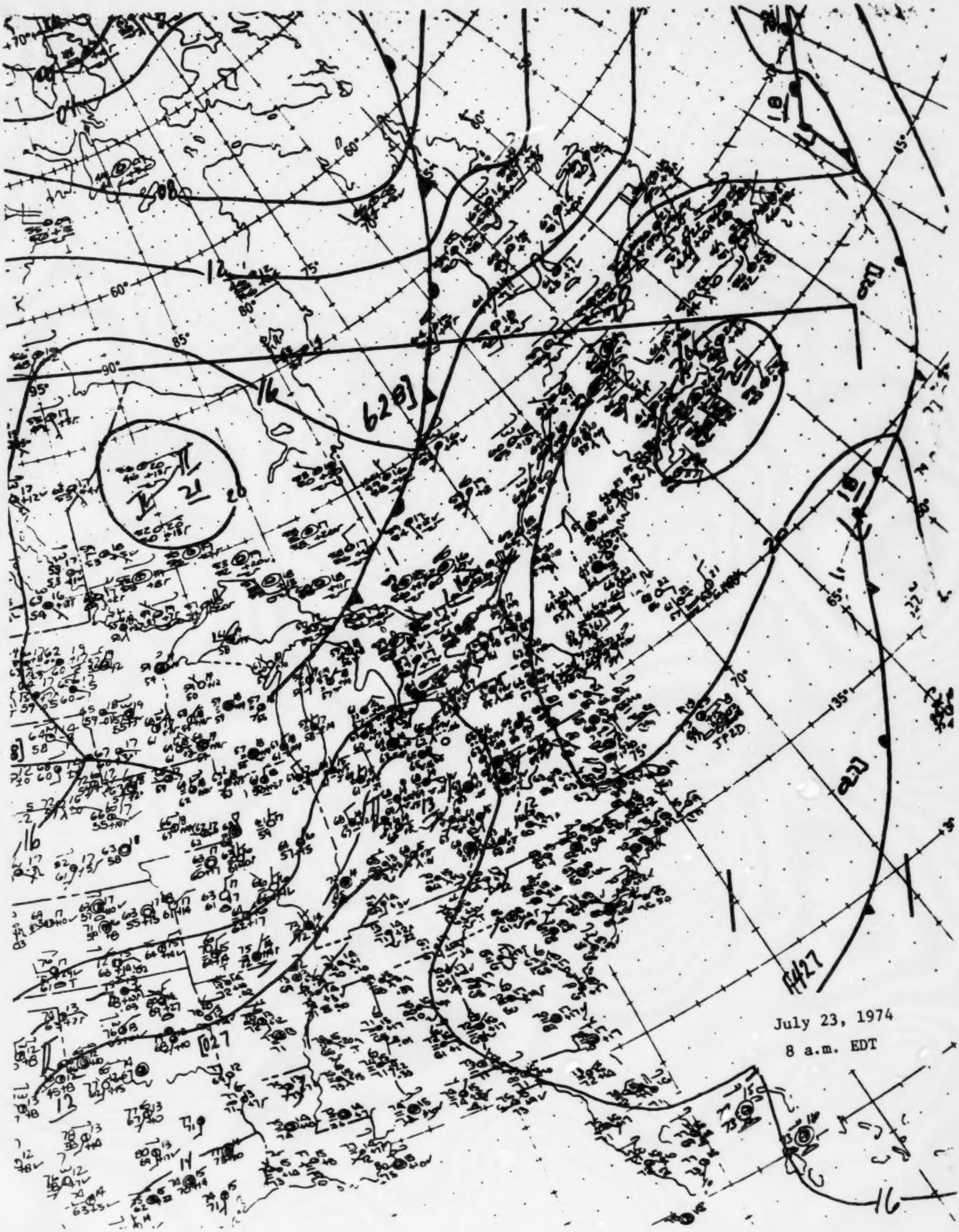

July 23, 1974
8 a.m. EDT

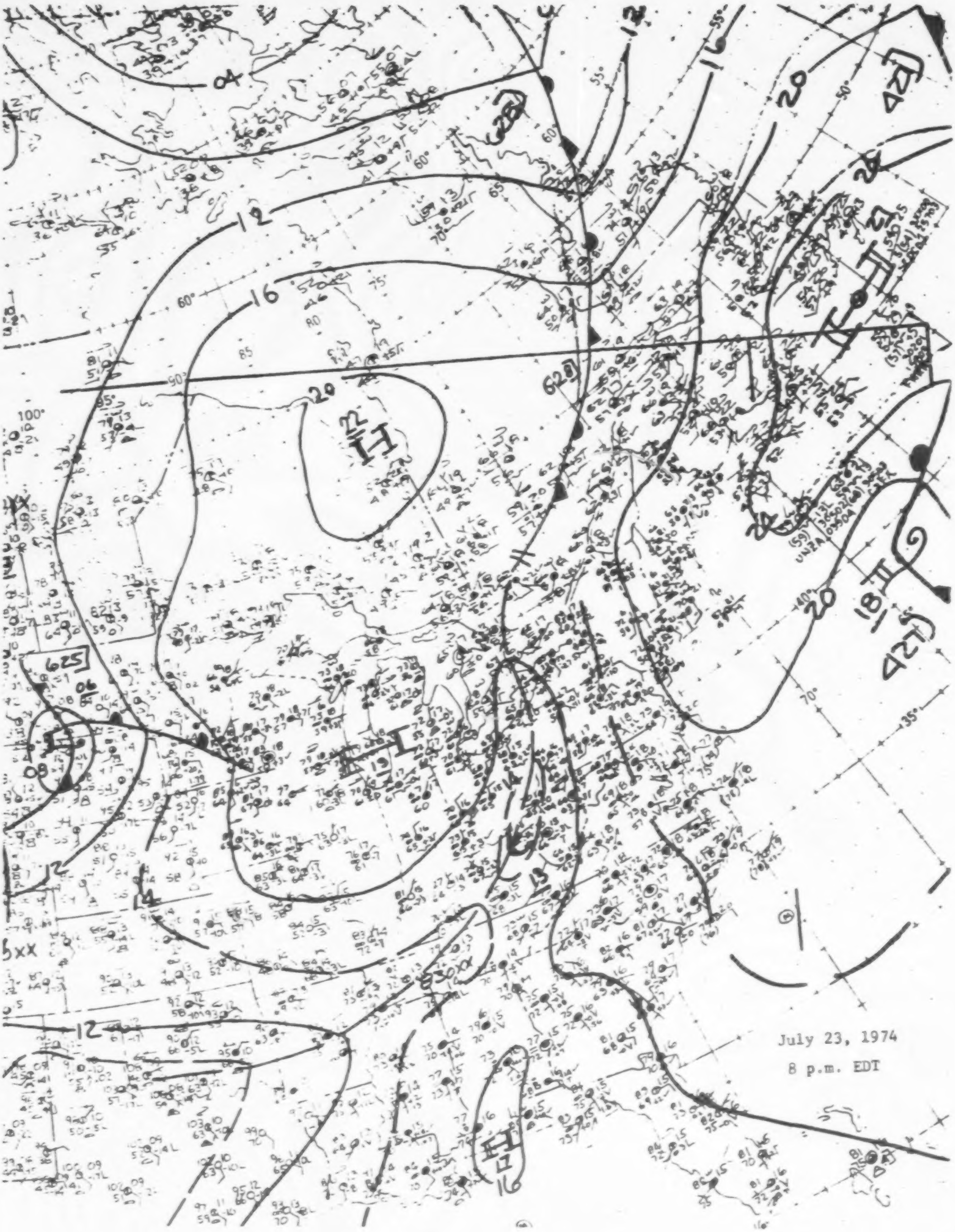

July 23, 1974

8 p.m. EDT

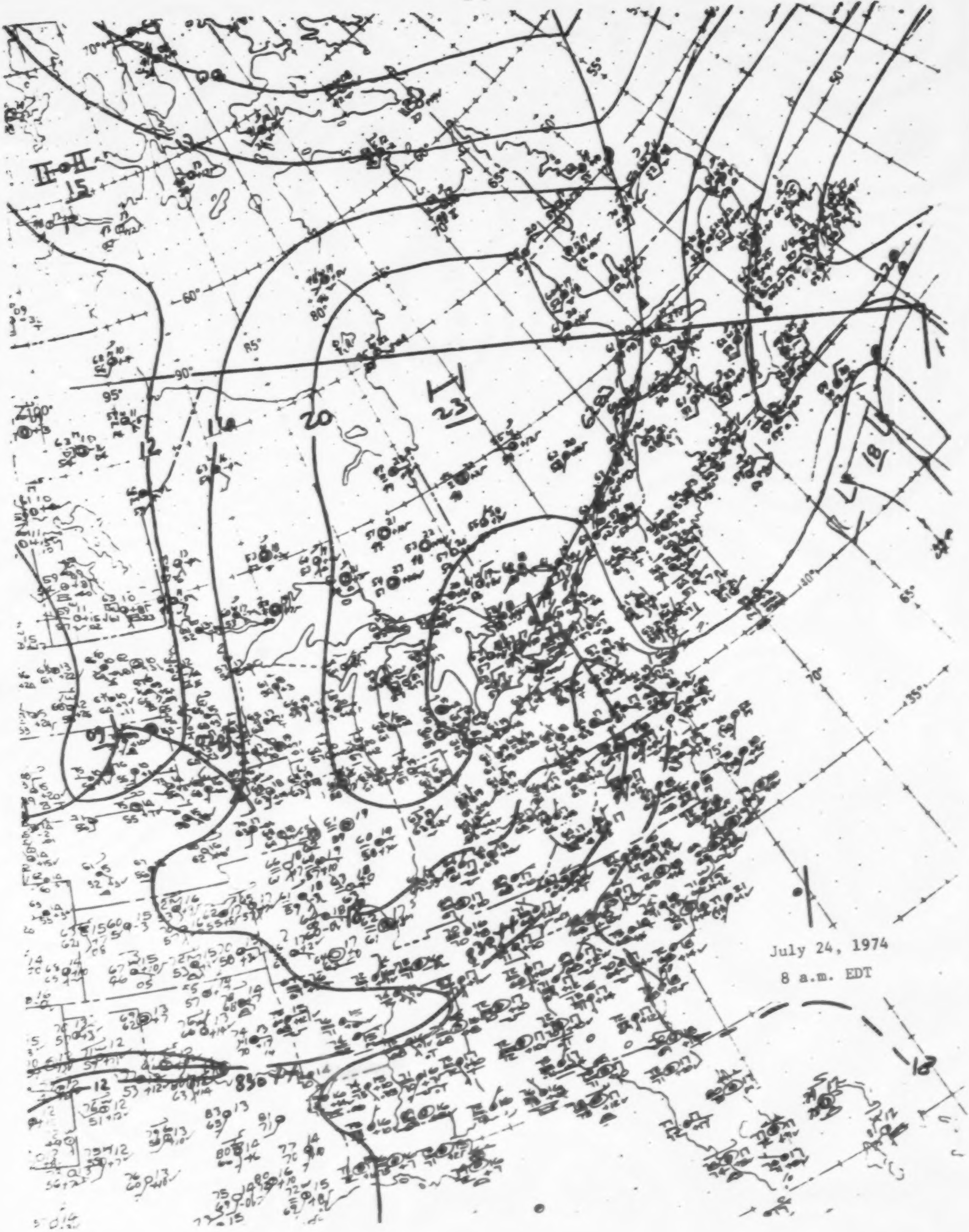

July 24, 1974

8 a.m. EDT

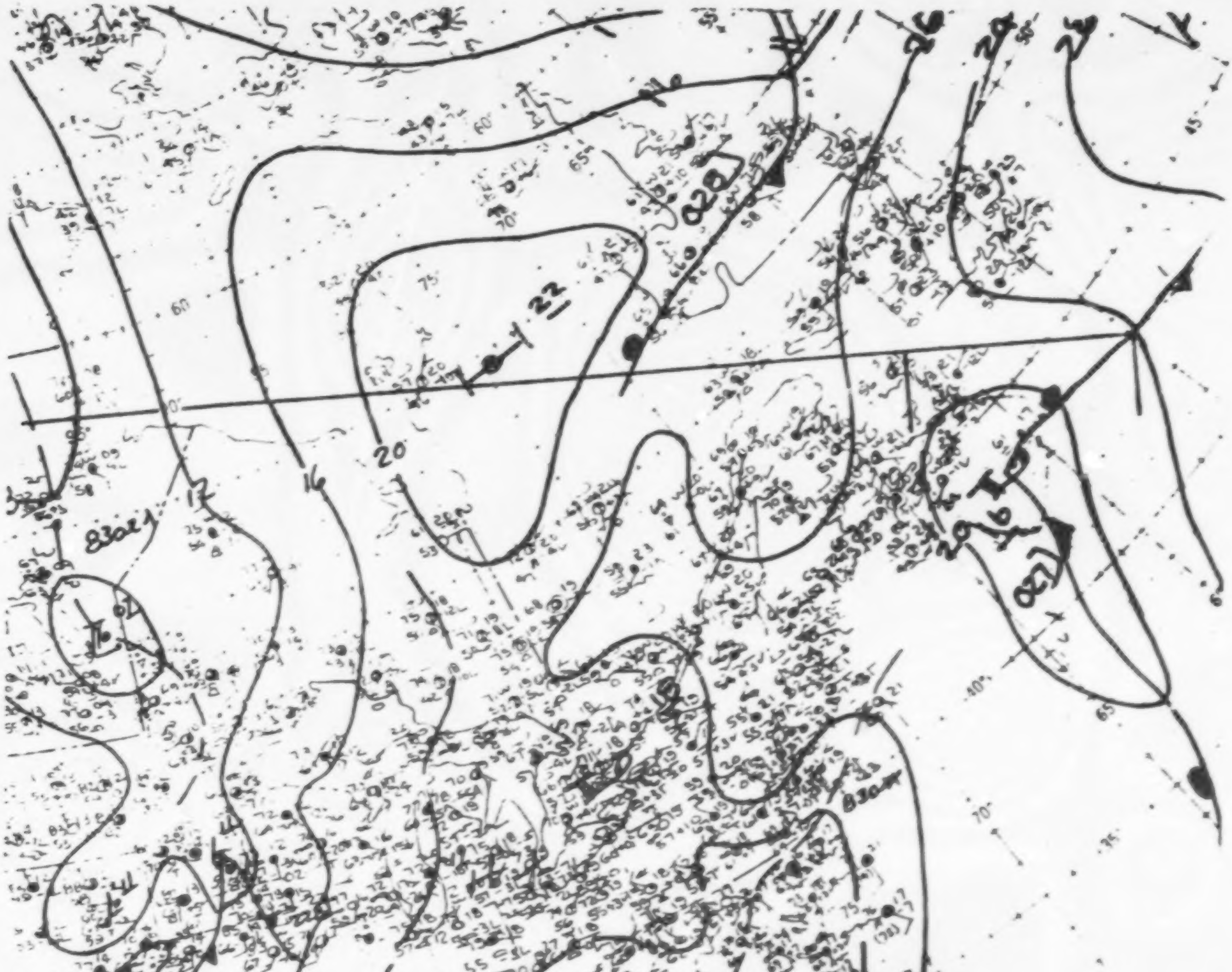

July 24, 1974

8 p.m. EDT

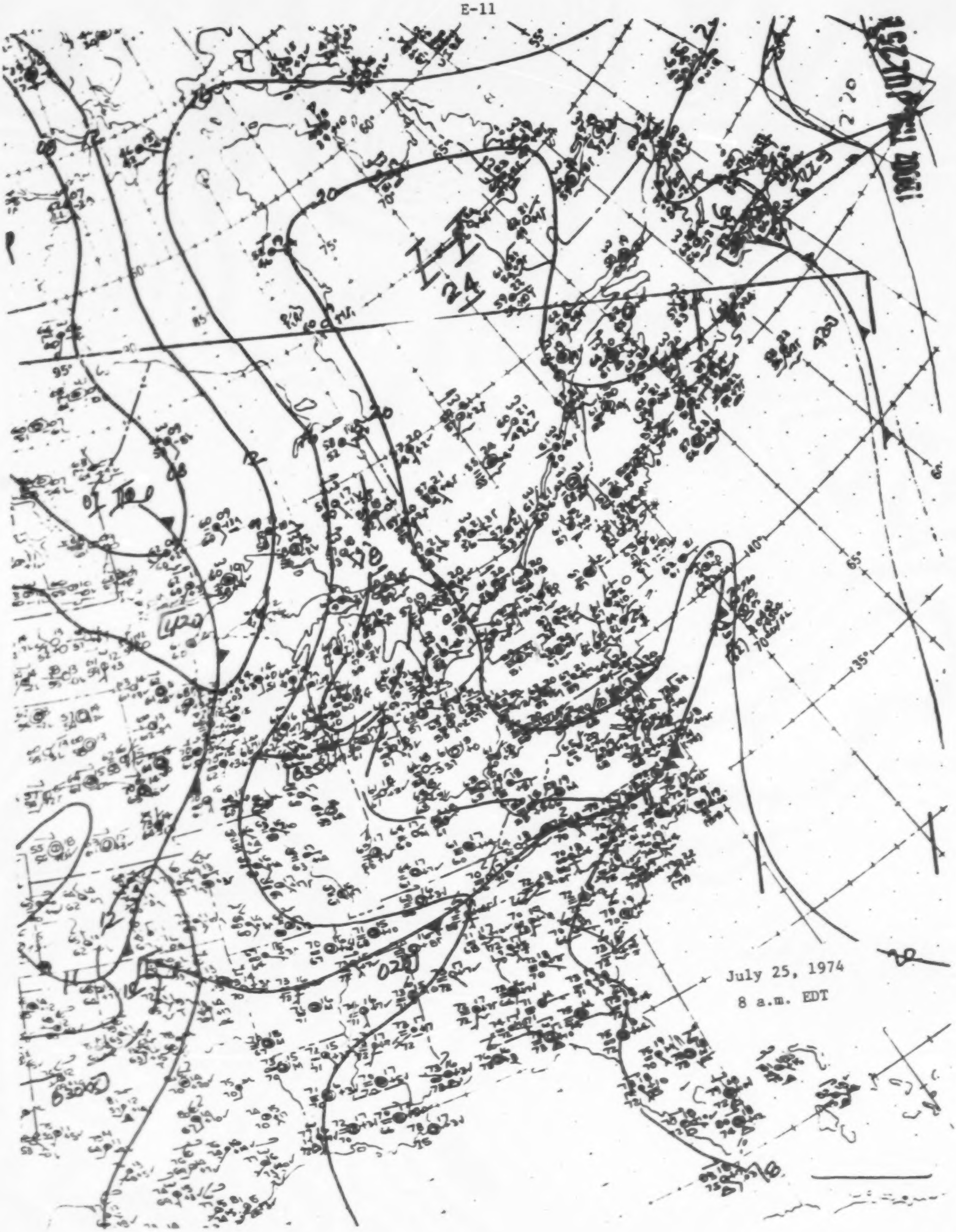

July 25, 1974
8 a.m. EDT

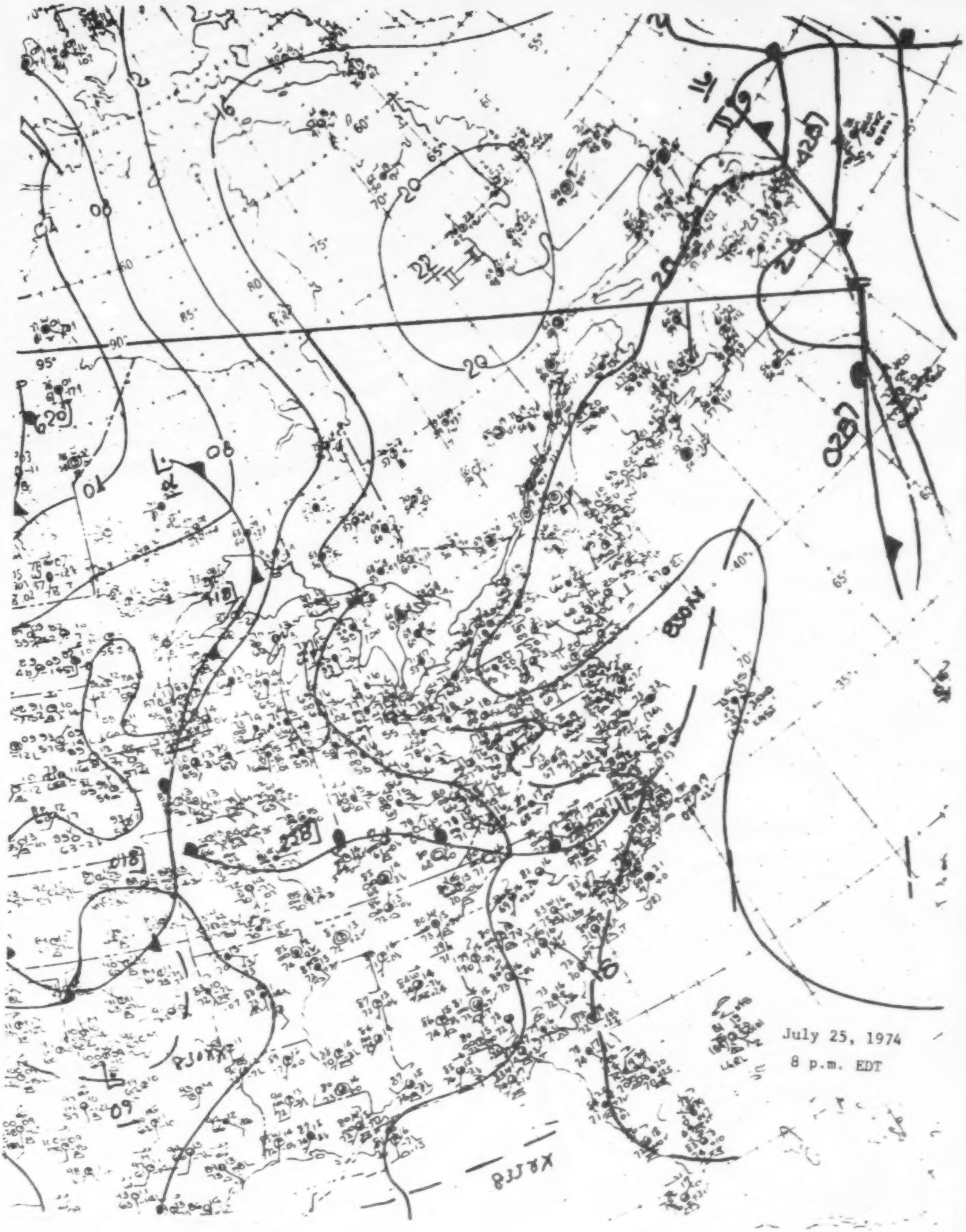

July 25, 1974
8 p.m. EDT

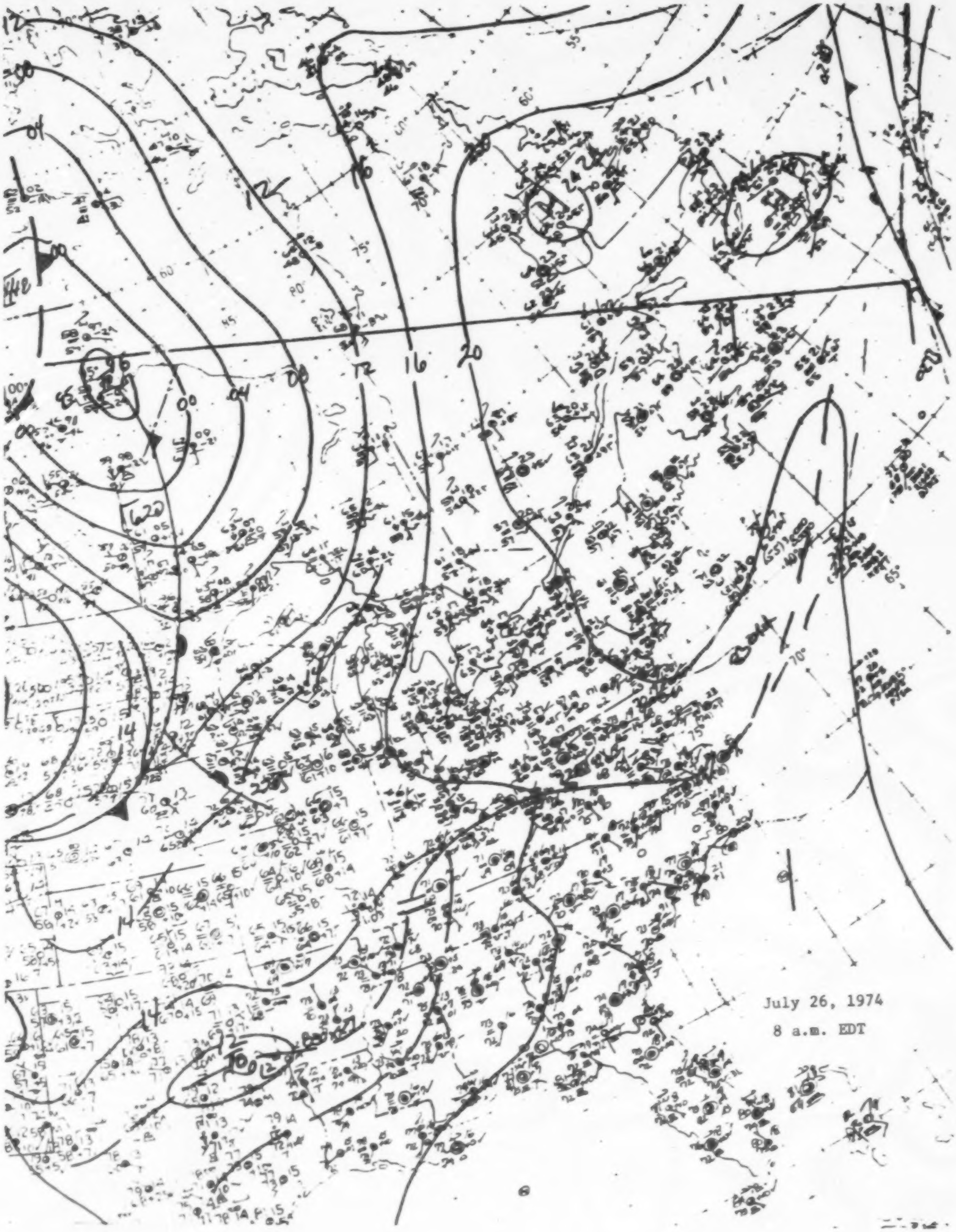
12
08
04
00
08
12
16
20
1022
14
14
1012

July 26, 1974

8 a.m. EDT

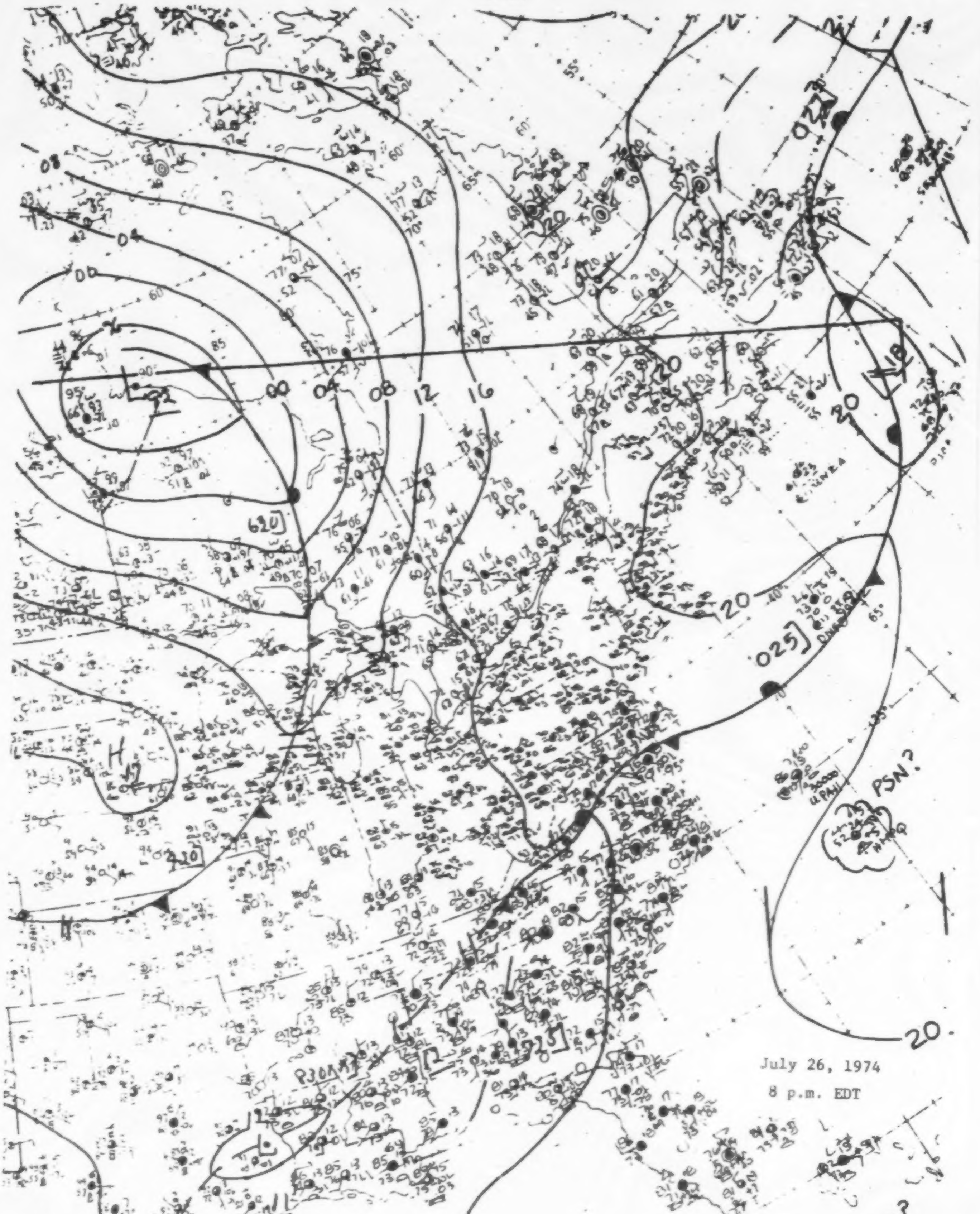
08
04
00
00
04
08
12
16
20
20
20
20
620
025
022
PSN?
?MB?

July 26, 1974

8 p.m. EDT

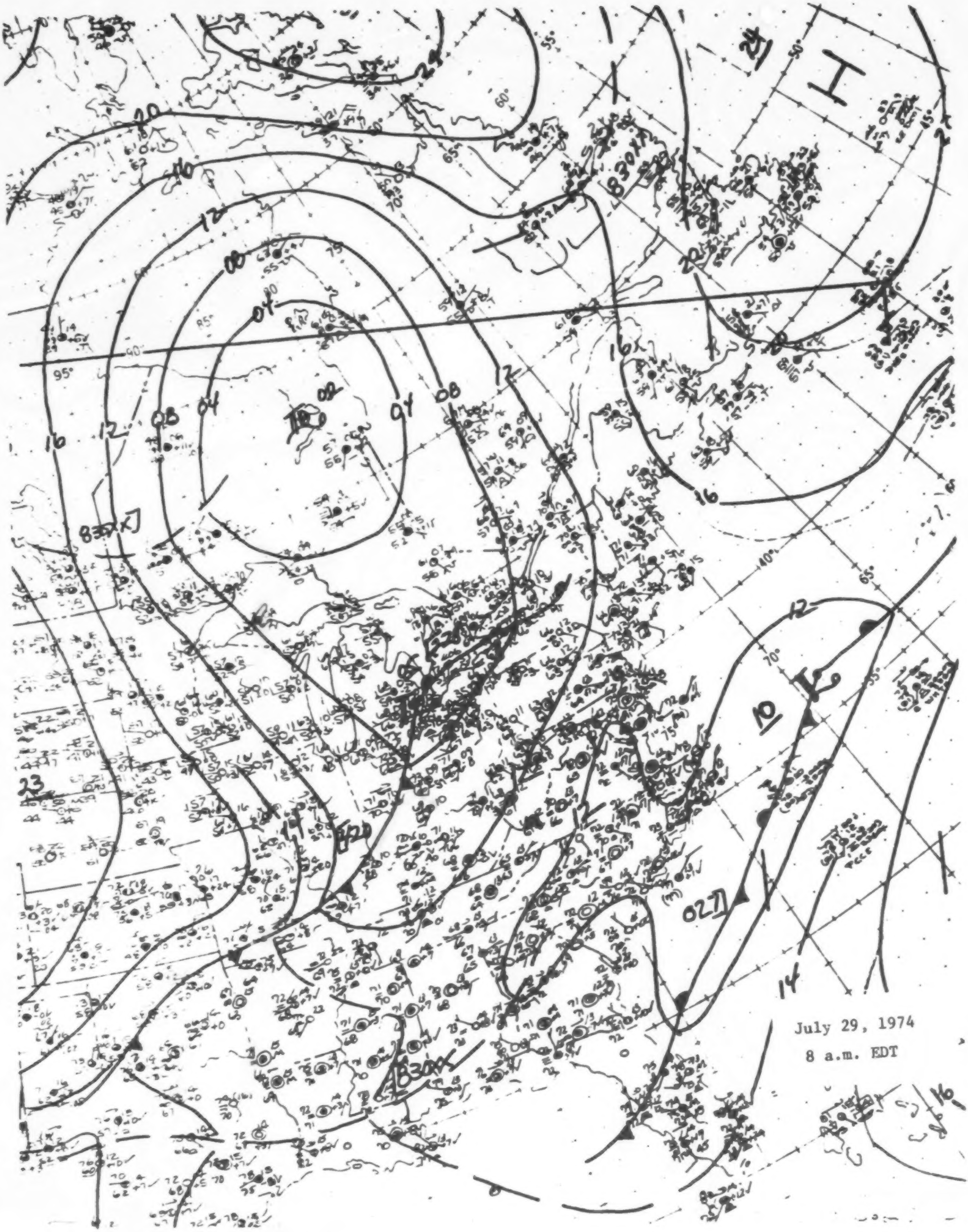
H
L
L
24
20
16
12
08
04
02
04
08
12
16
14
10
12
14
16
23
95°
90°
85°
80°
75°
70°
65°
60°
55°
50°
45°
40°
830XX
835XX
820
827
830XX
830XX

July 29, 1974

8 a.m. EDT

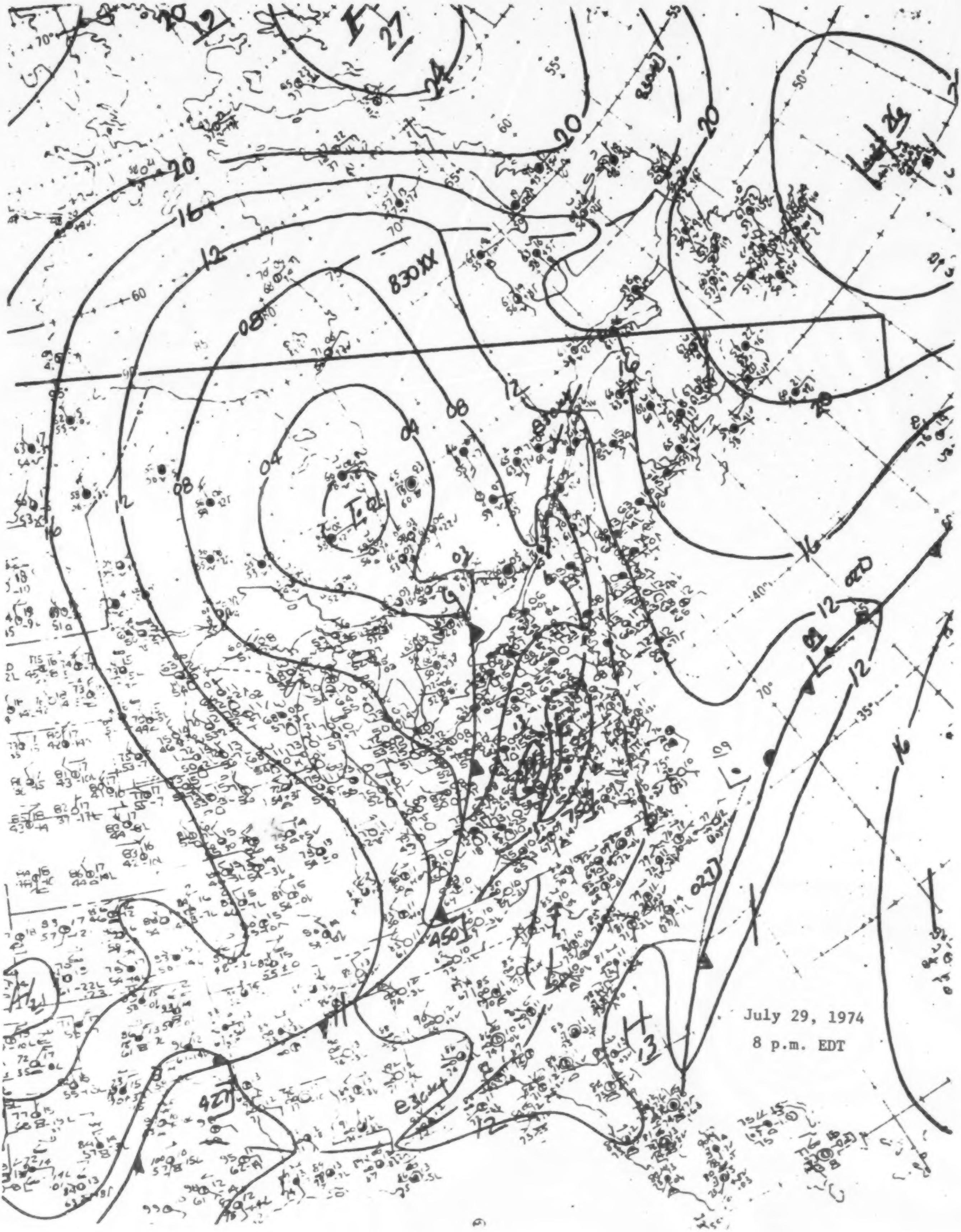

July 29, 1974
8 p.m. EDT

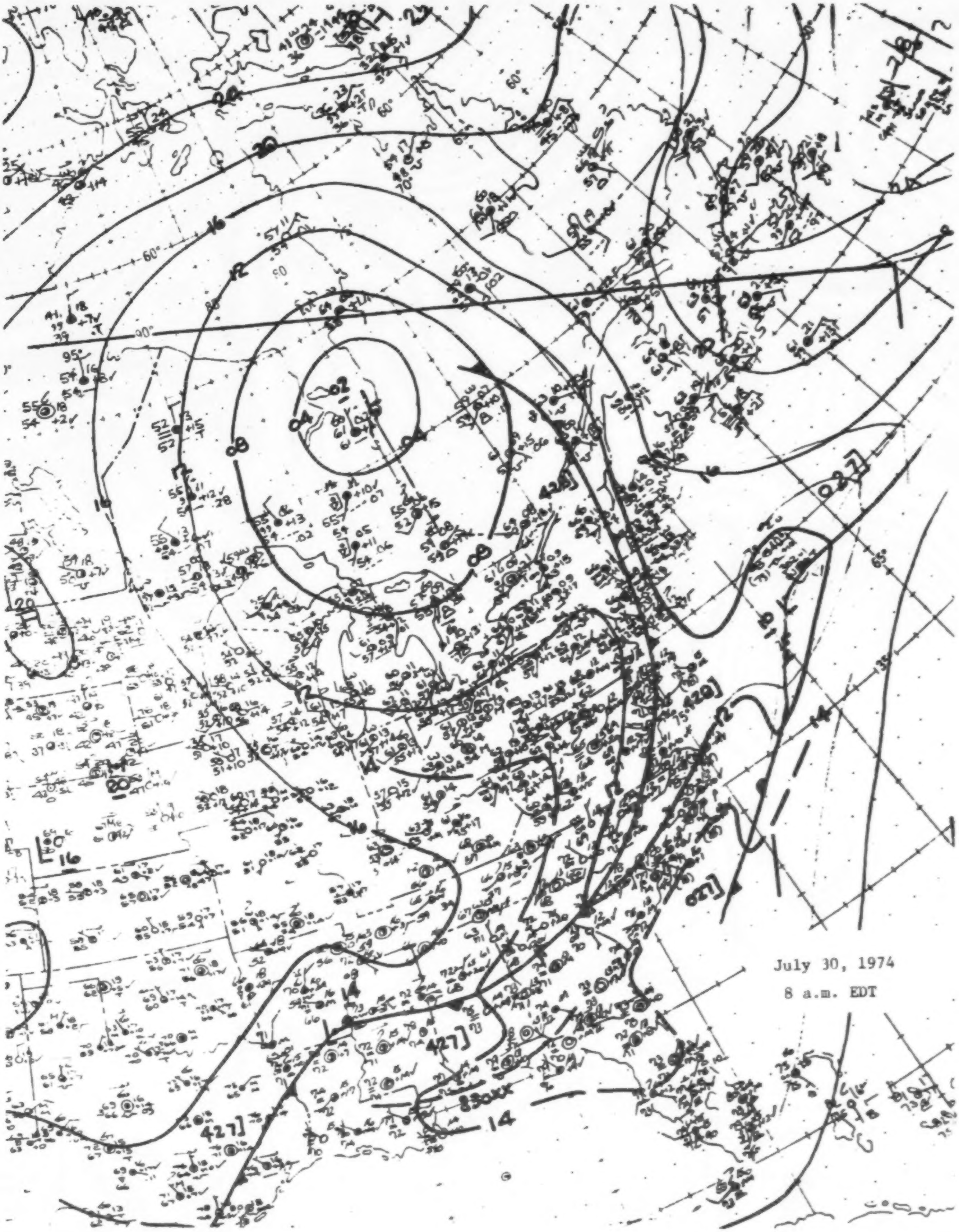

July 30, 1974

8 a.m. EDT

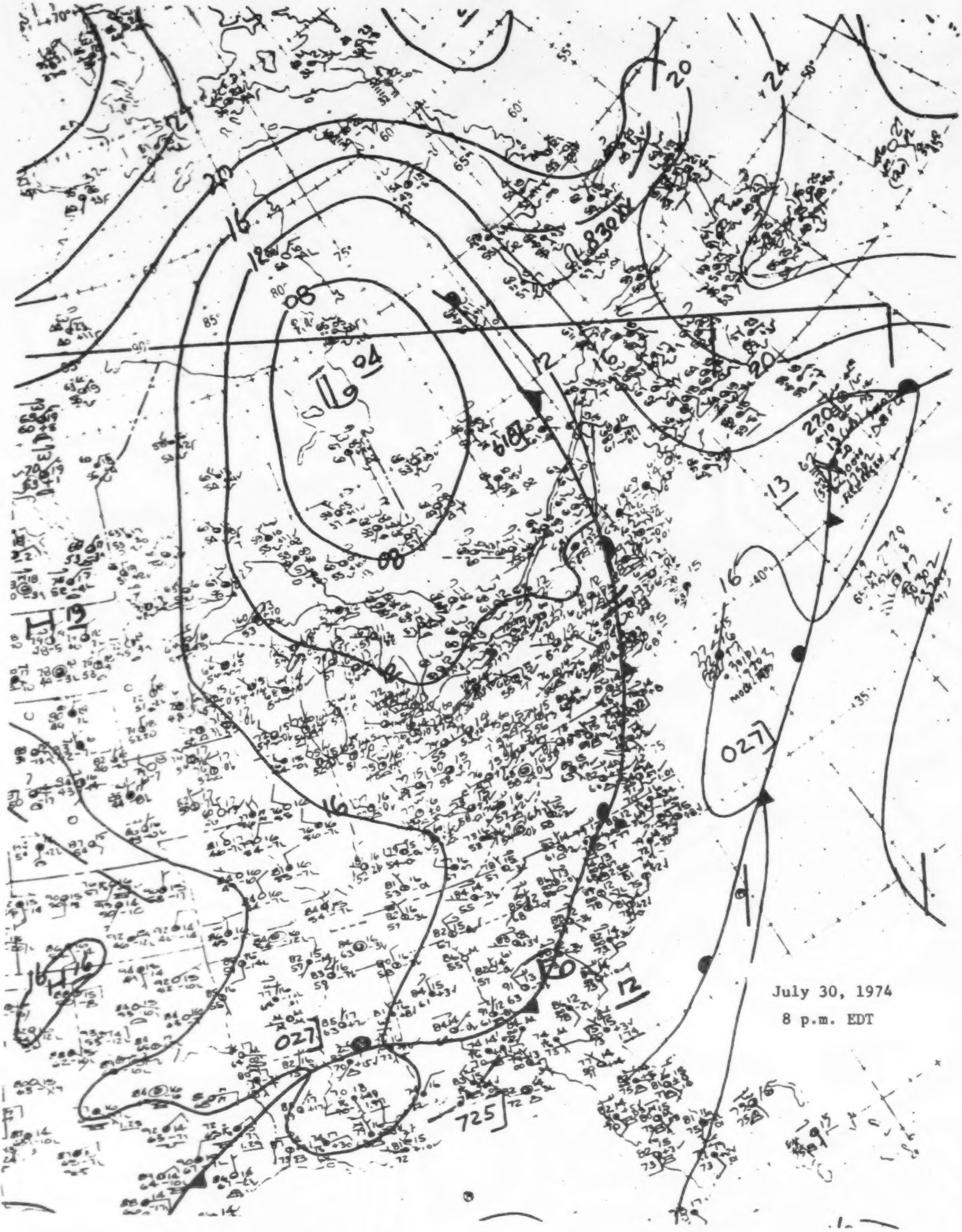
08
04
L
12
16
20
24
H
19
027
725
13
16
027
12
830

July 30, 1974
8 p.m. EDT

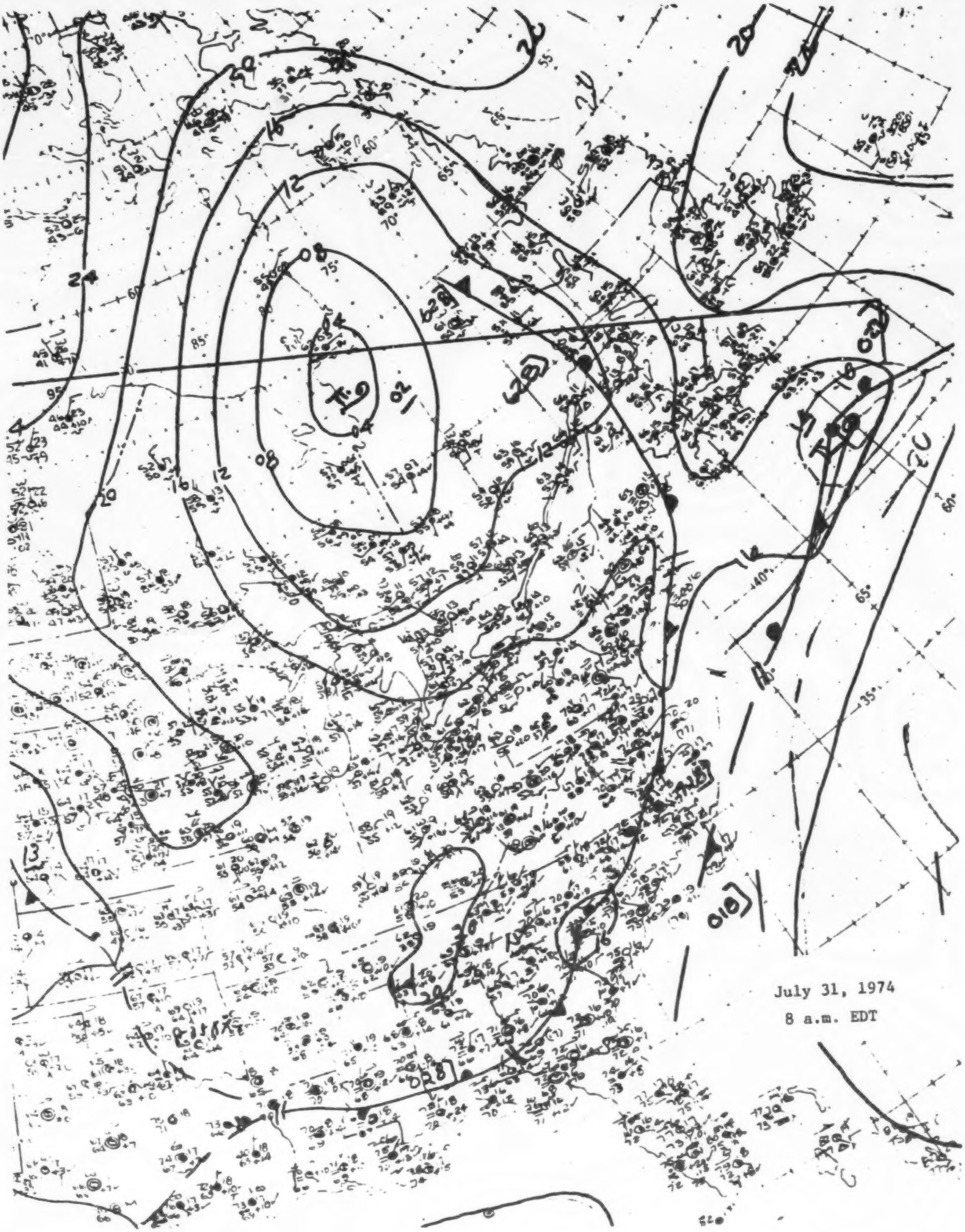

July 31, 1974

8 a.m. EDT

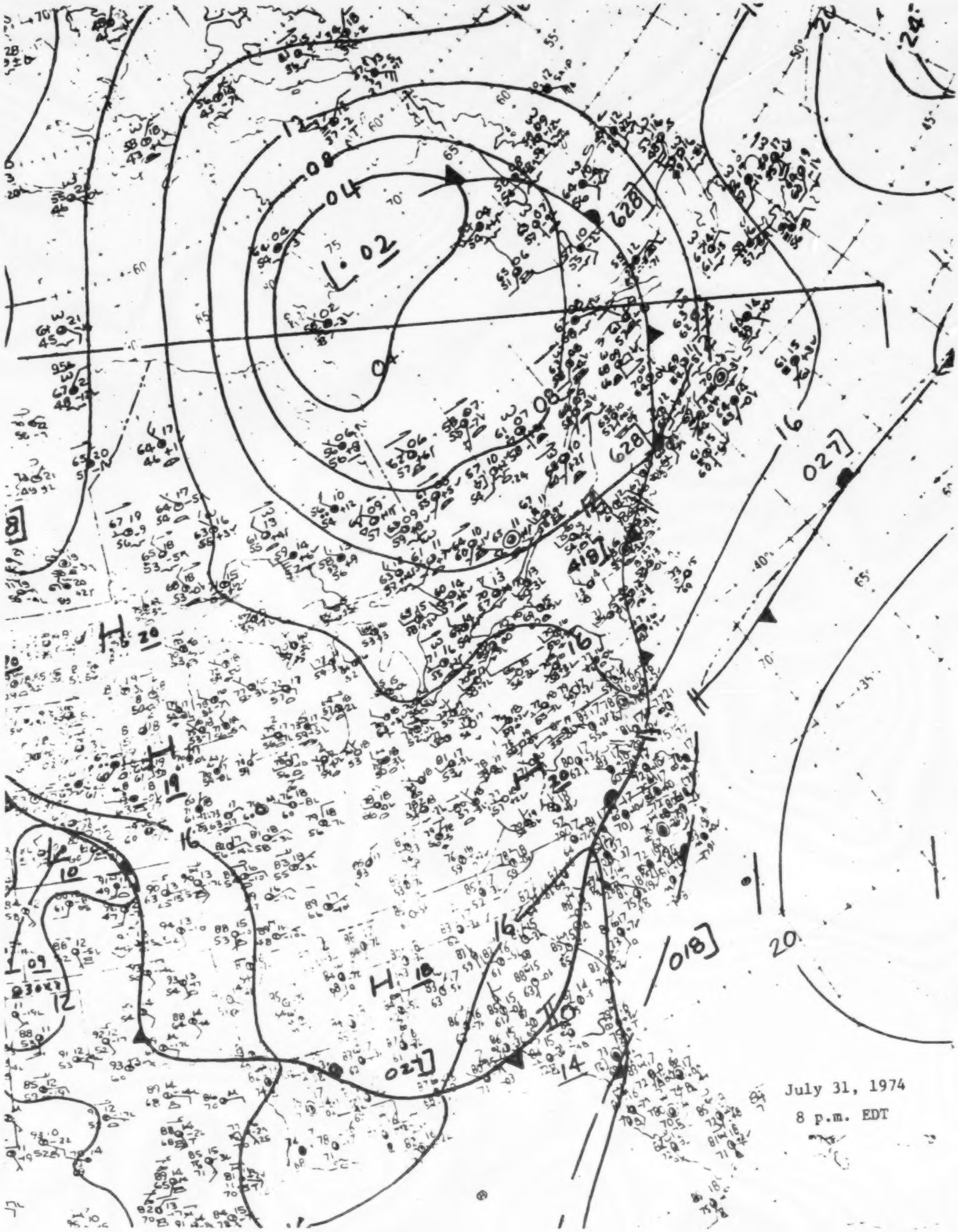
L 02
H 20
H 19
H 18
12
08
04
16
20
10
09
14
027]
018]
628]
418]

July 31, 1974

8 p.m. EDT

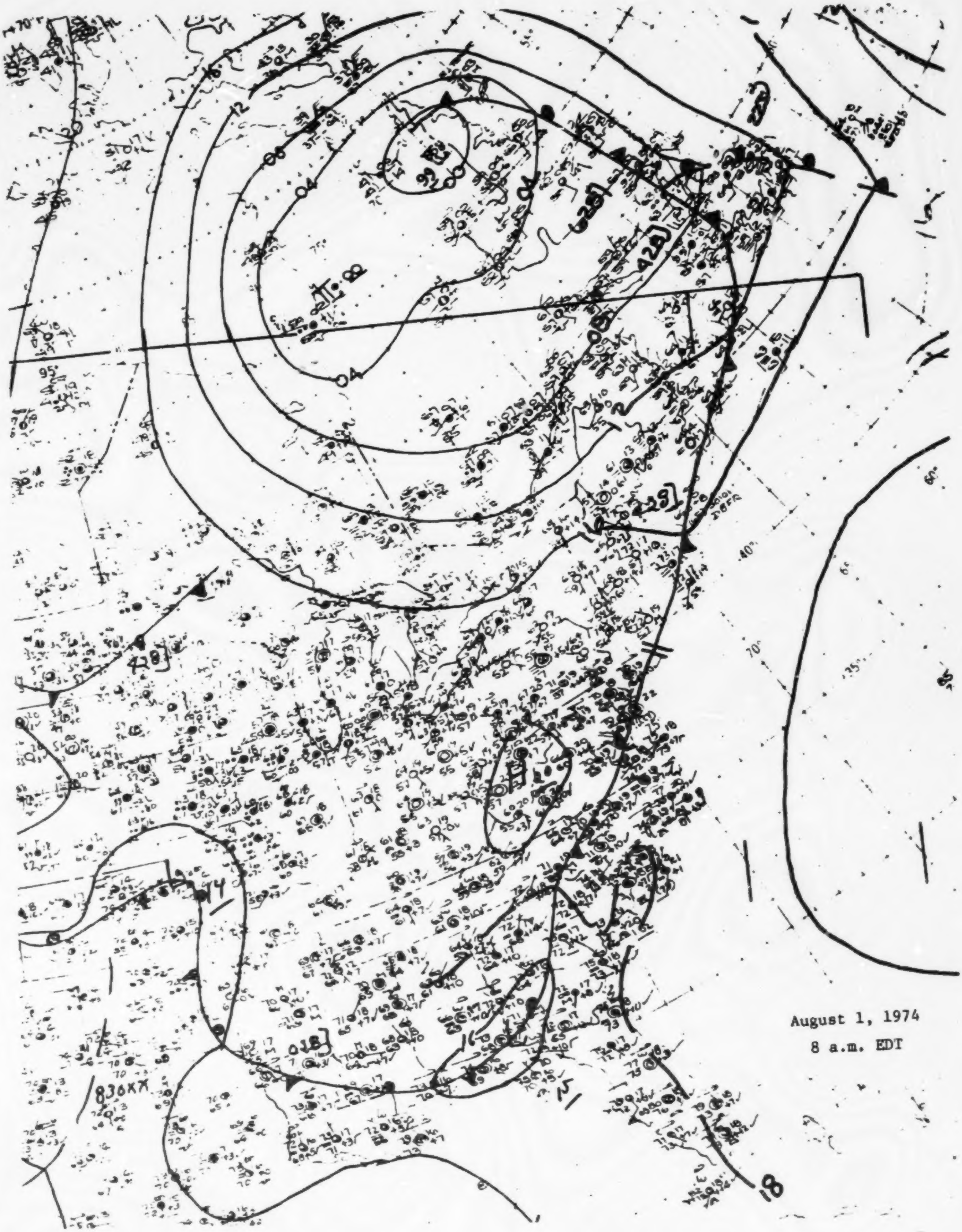

August 1, 1974
8 a.m. EDT

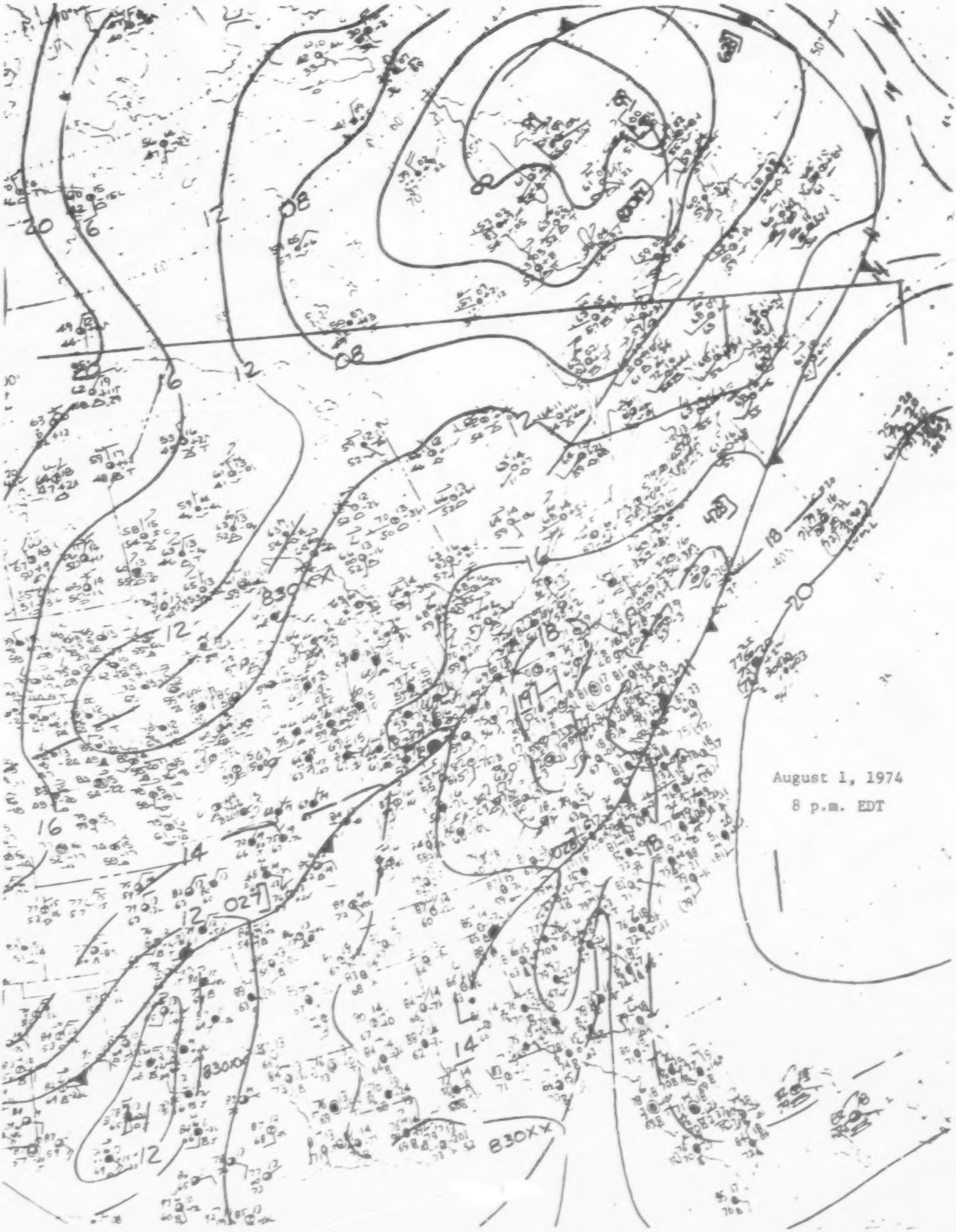

August 1, 1974
8 p.m. EDT

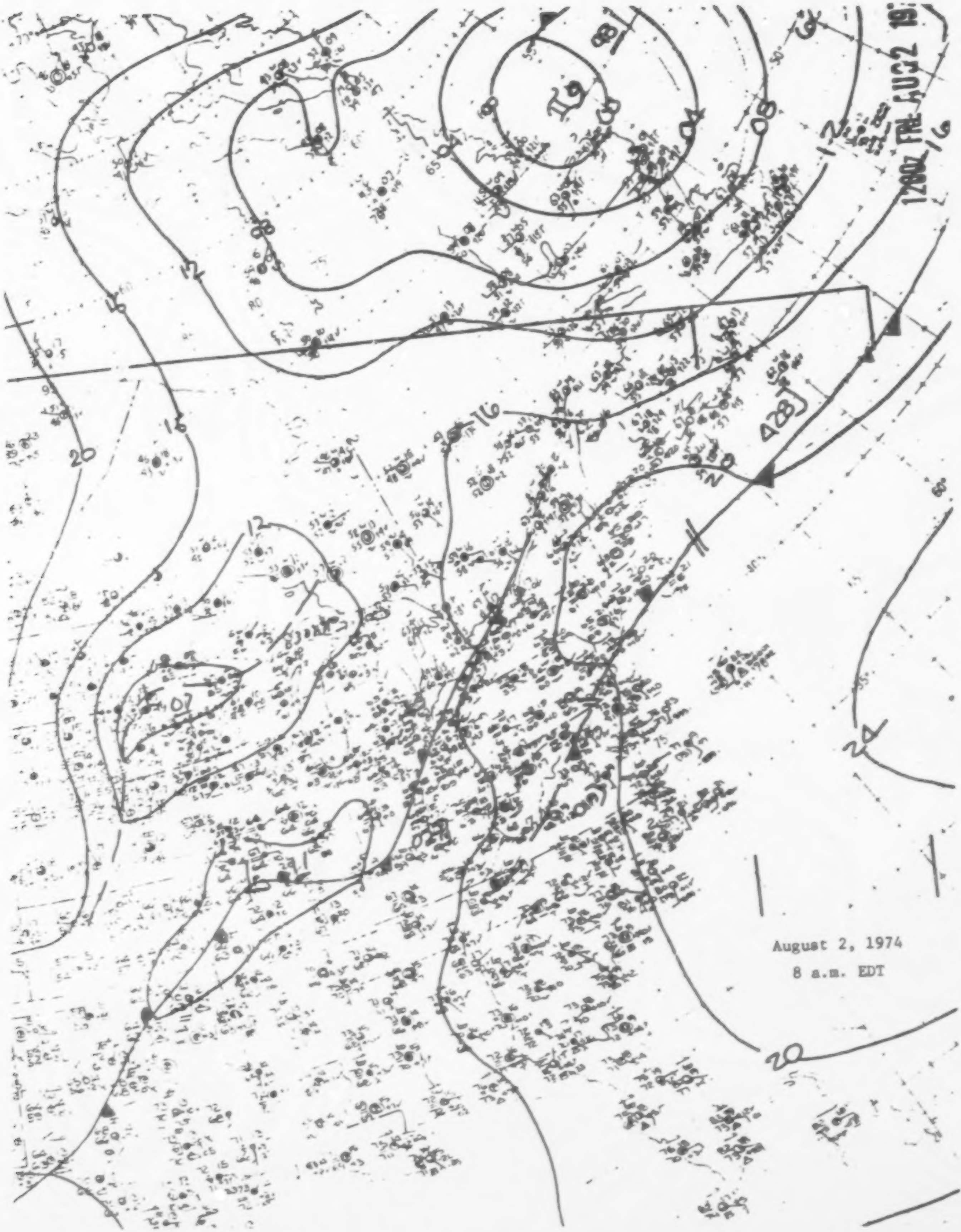
1200Z FRI AUG 2 19

August 2, 1974
8 a.m. EDT

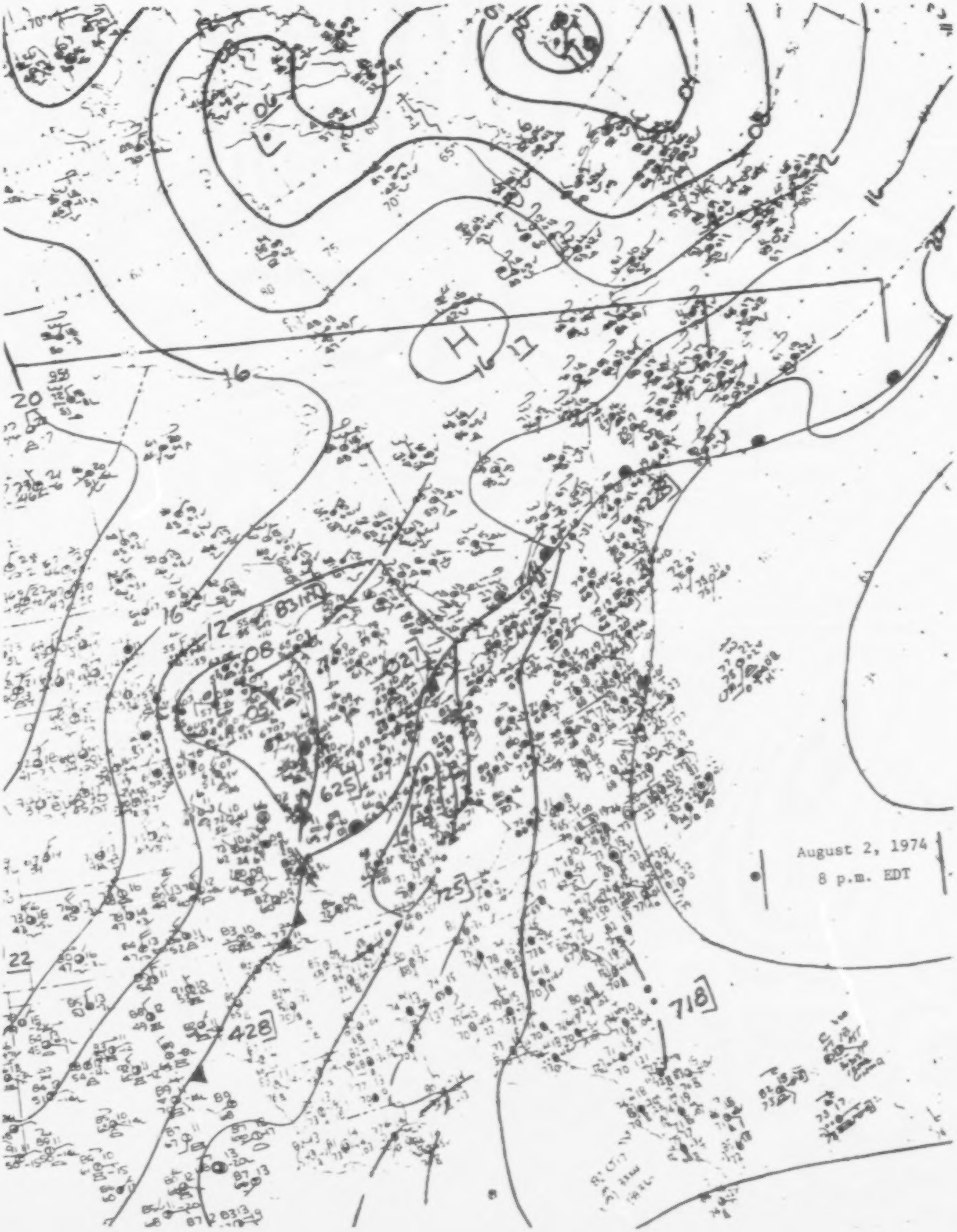
H
16
12
08
20
22
428
625
725
718

August 2, 1974
8 p.m. EDT

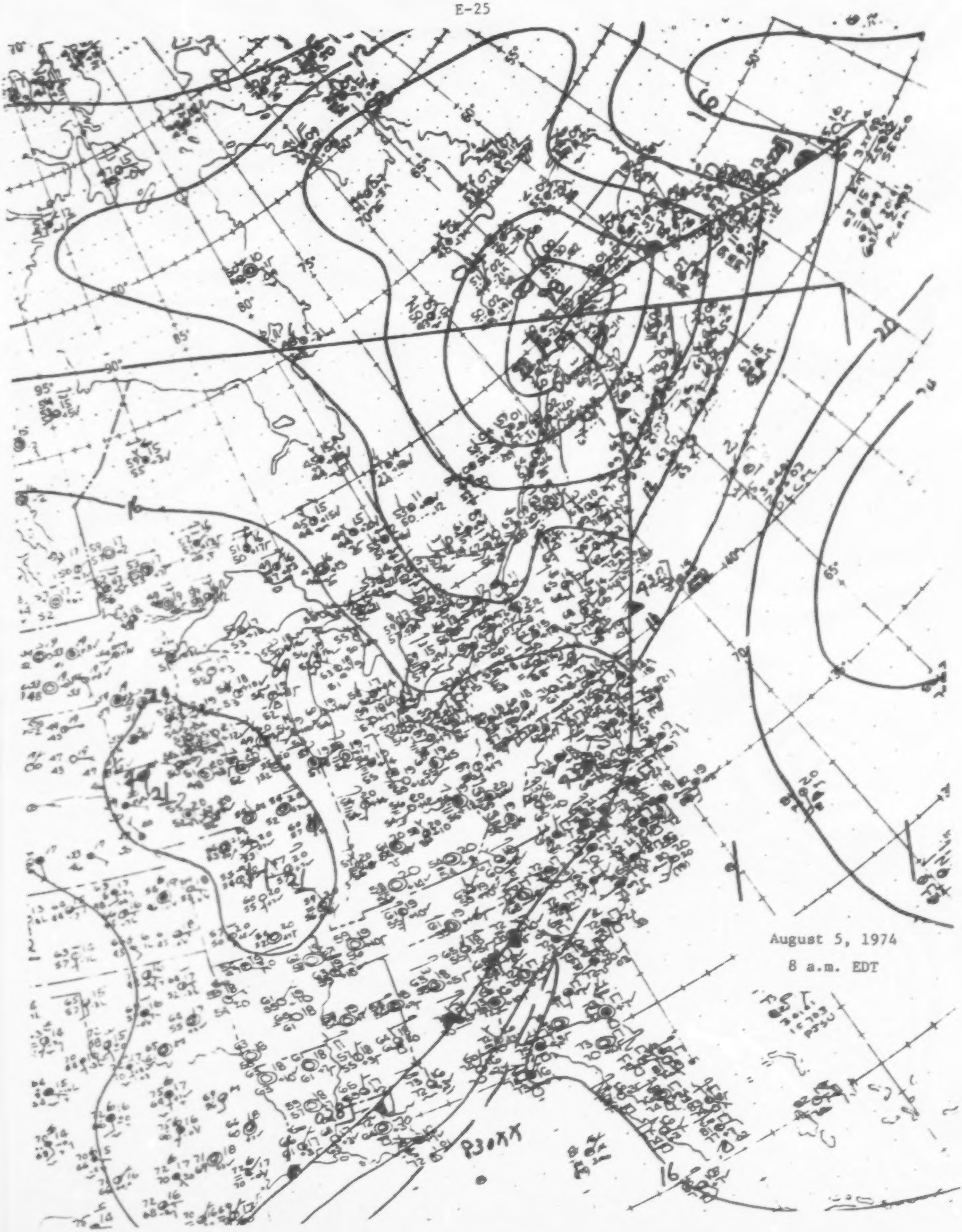
70°
75°
80°
85°
90°
95°
65°
70
16
20
P30XX

August 5, 1974

8 a.m. EDT

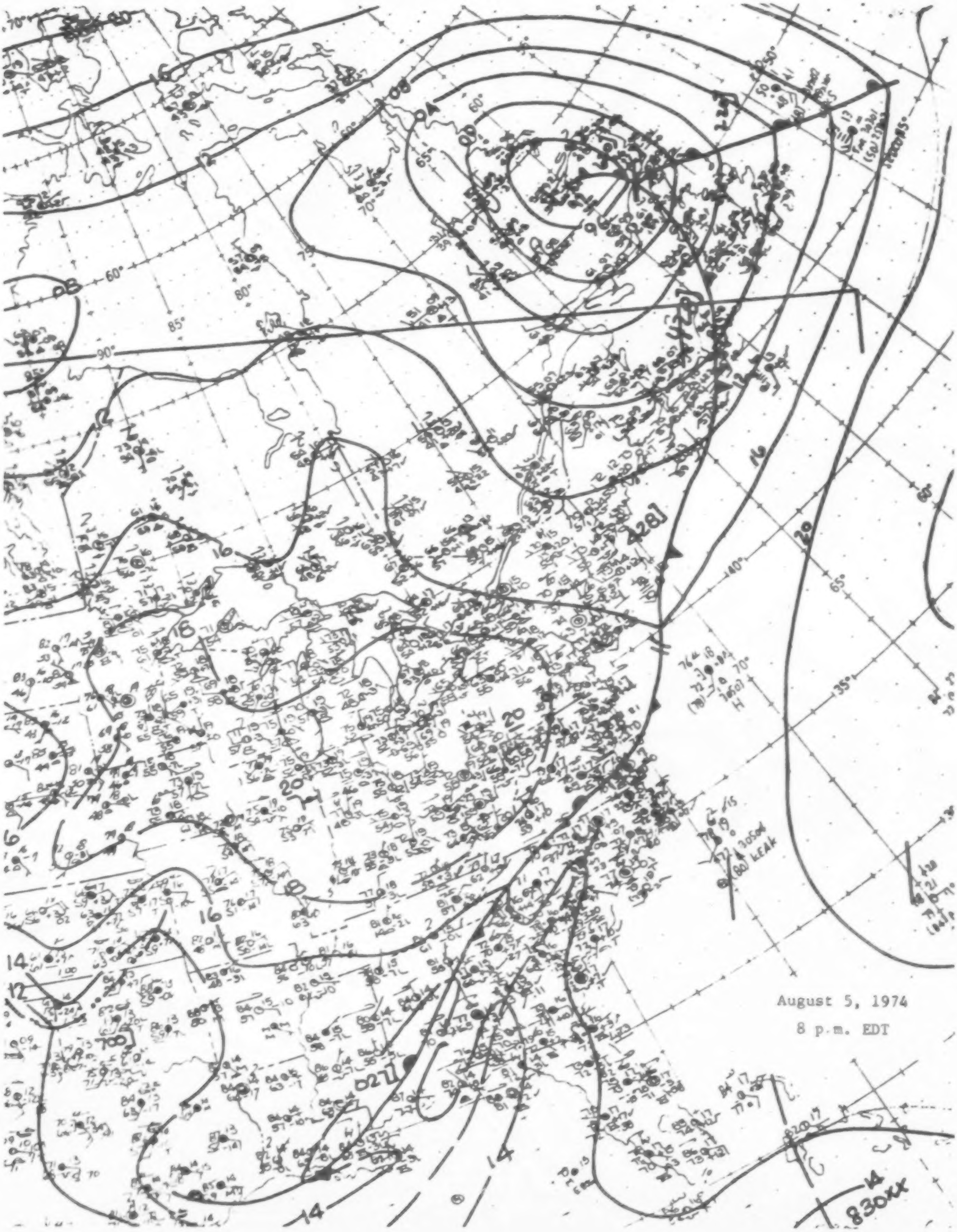

August 5, 1974

8 p.m. EDT

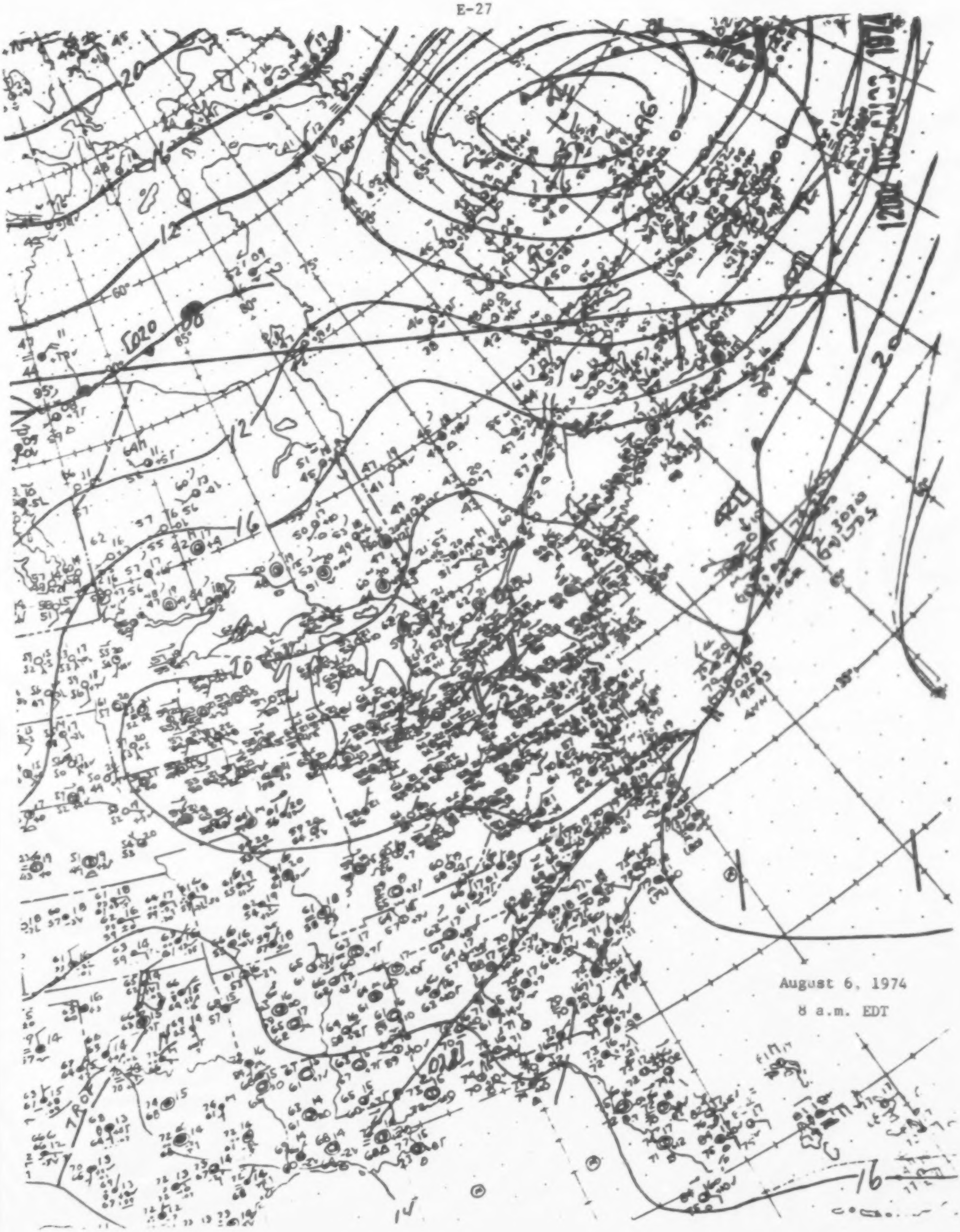

August 6, 1974

8 a.m. EDT

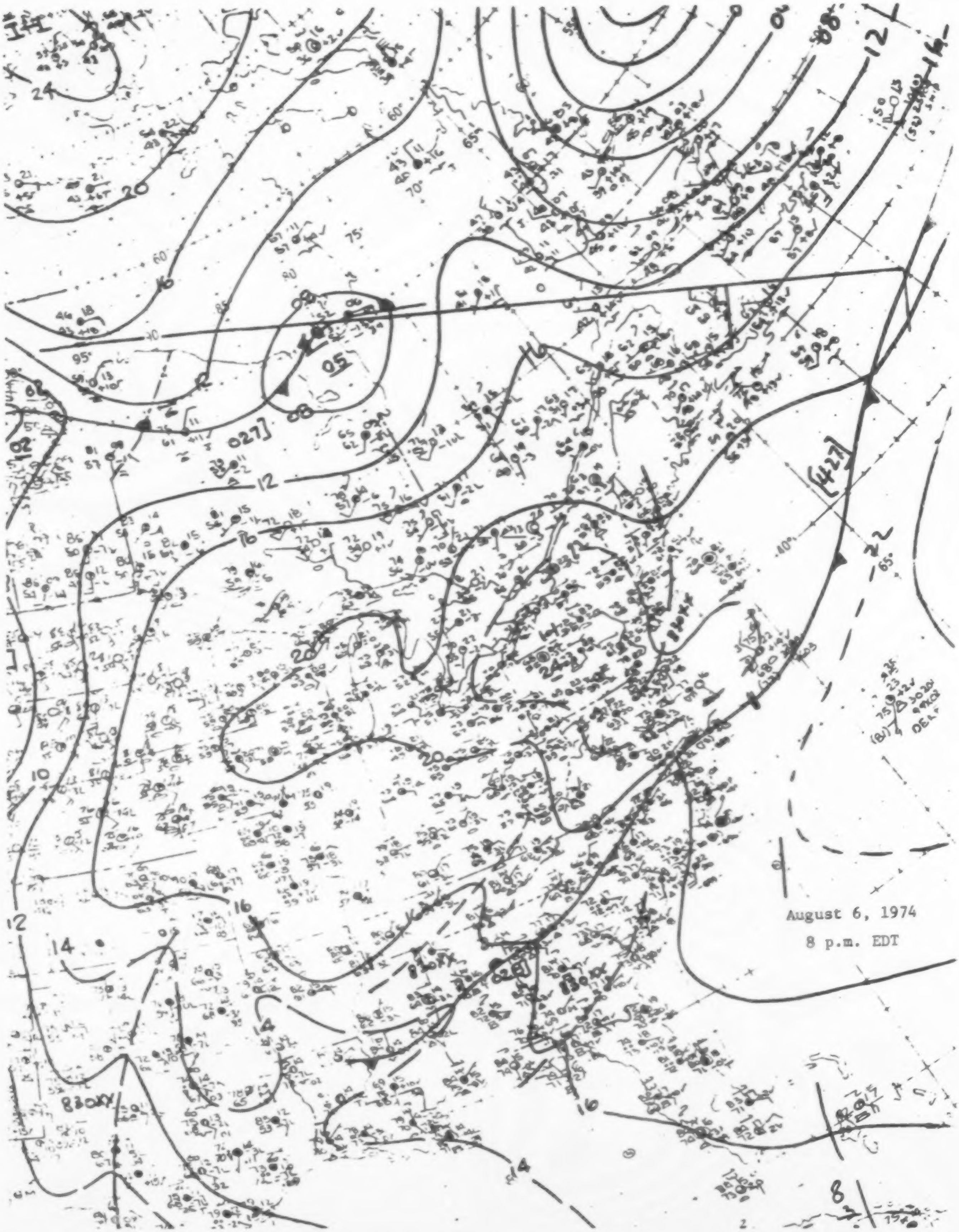
24
20
16
12
08
04
05
10
14
16
20
24
427
027
12
8

August 6, 1974
8 p.m. EDT

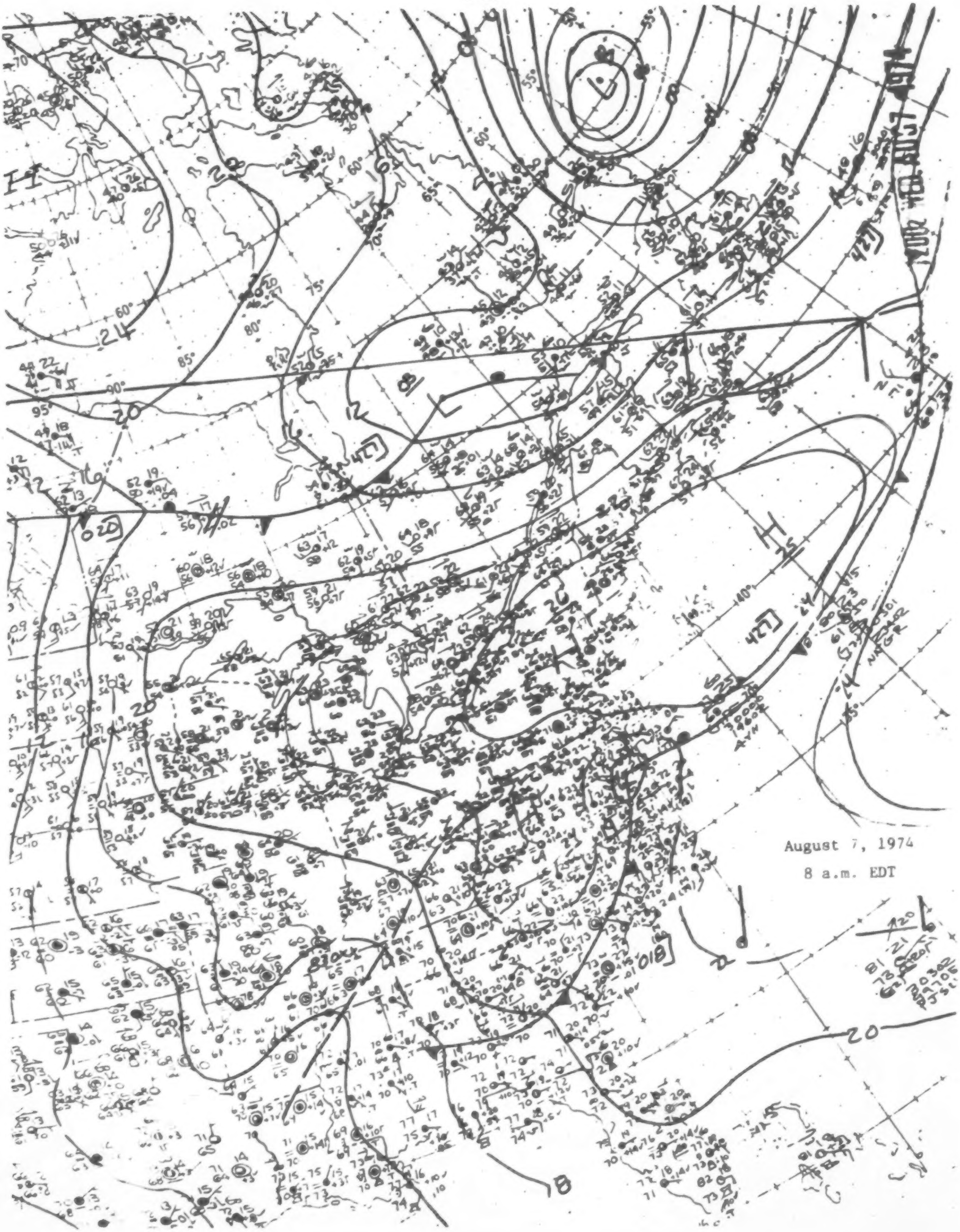

August 7, 1974

8 a.m. EDT

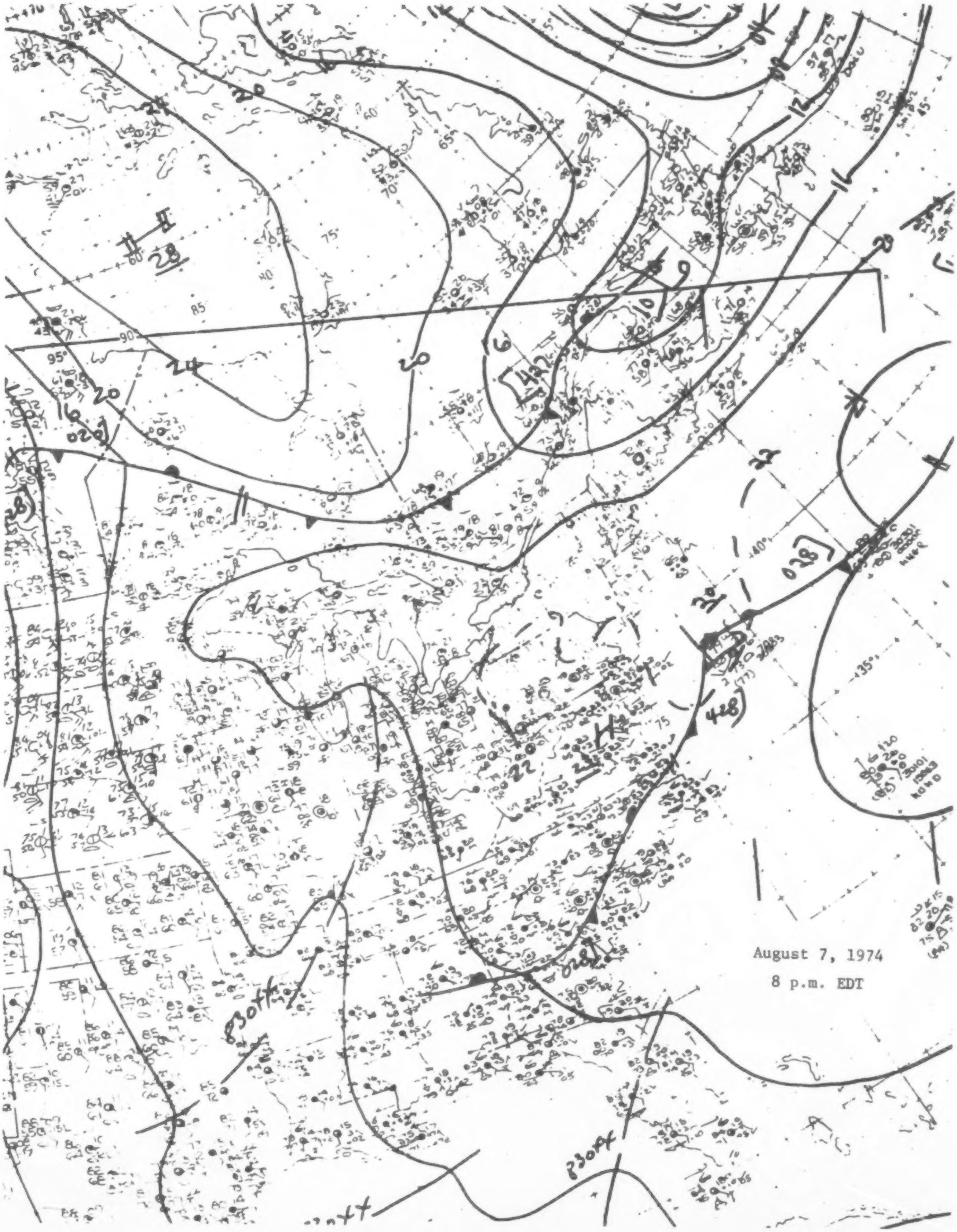

August 7, 1974

8 p.m. EDT

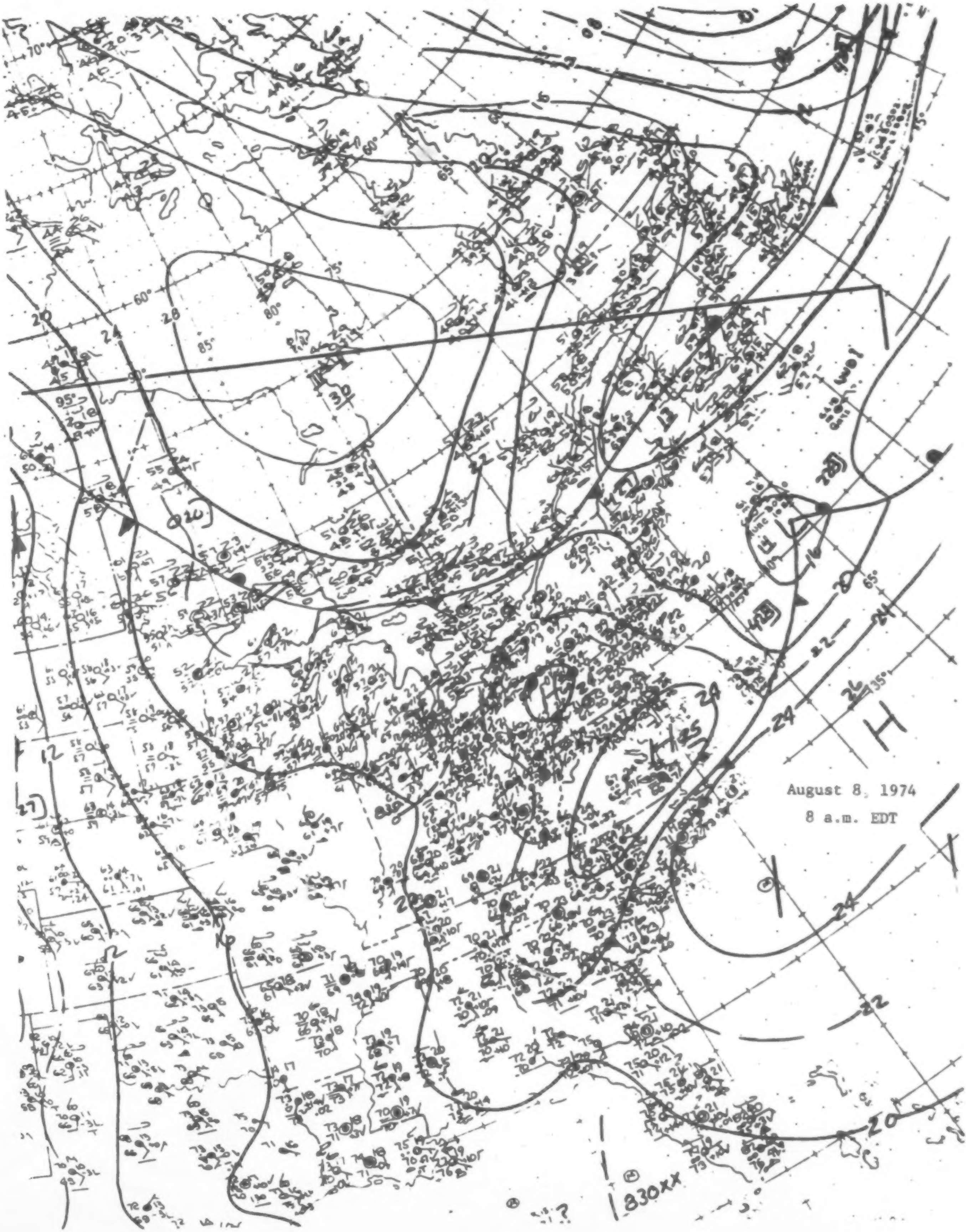

August 8, 1974
8 a.m. EDT

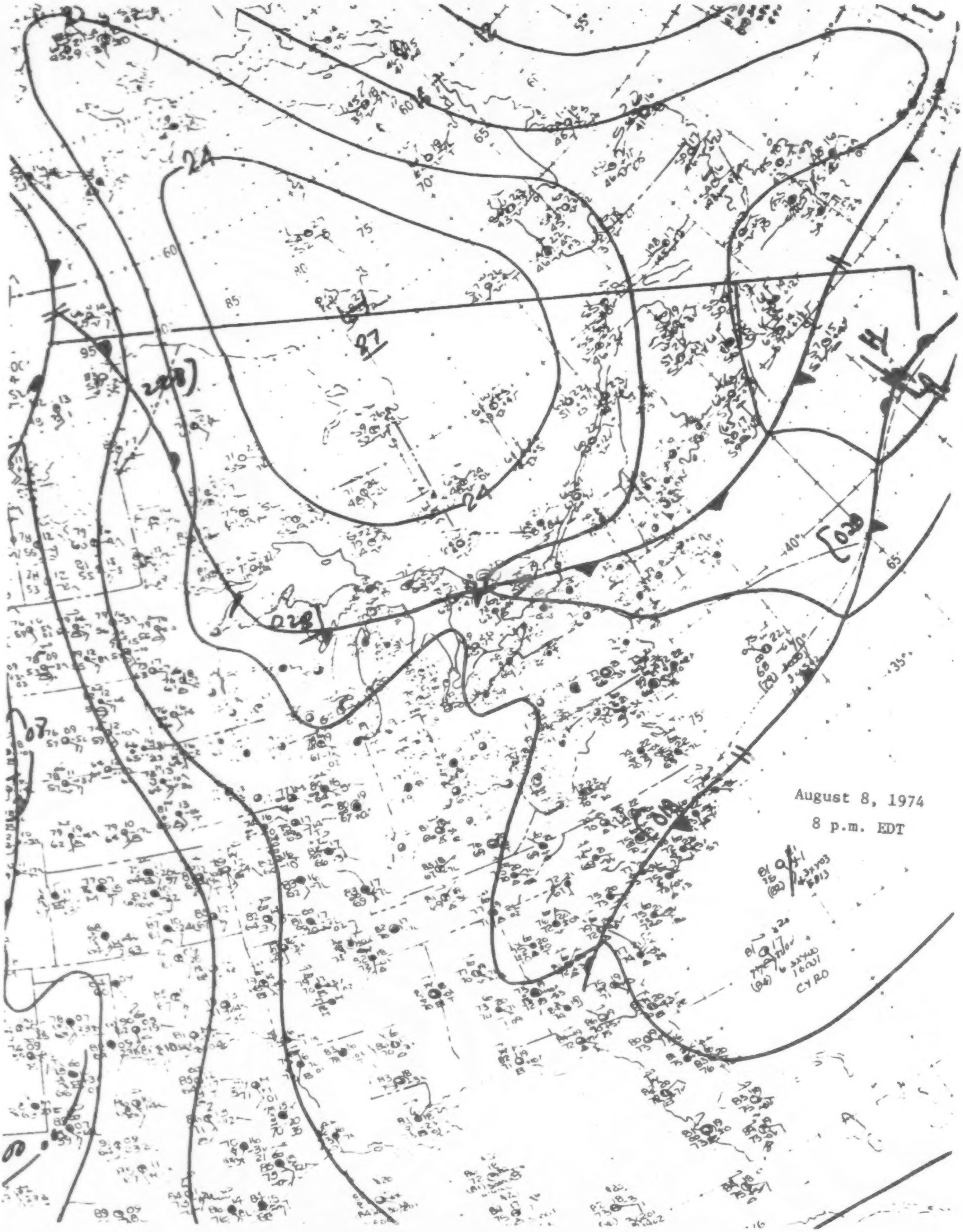
24
27
24
028
028
H
75
85
95
60
65
70
55
40°
35°

August 8, 1974
8 p.m. EDT

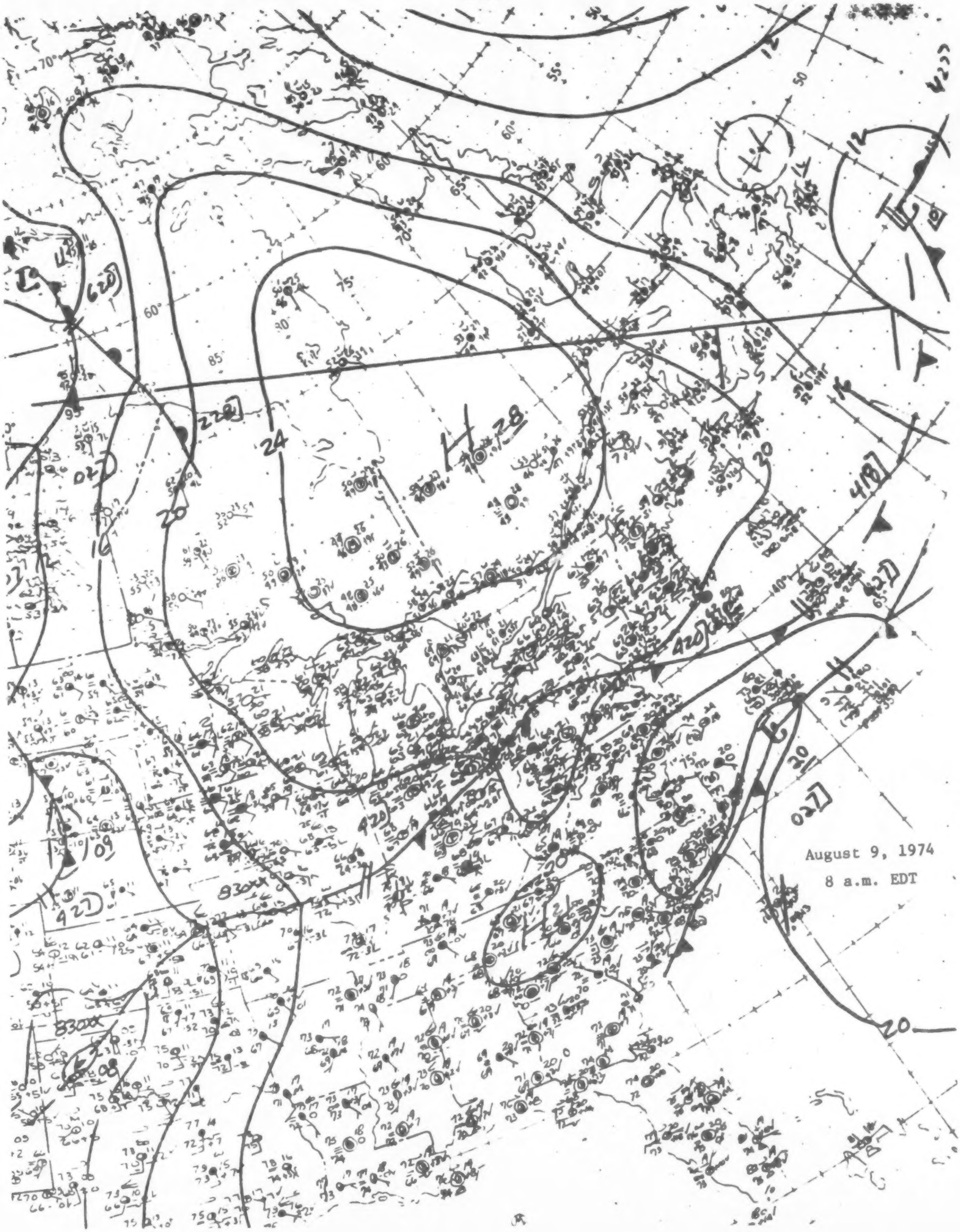
H
L
L
L
H
24
20
16
12
28
30
60°
85
75°
70°
50
95
4[8]
[02]
[22]
[62]
[42]
[83]

August 9, 1974
8 a.m. EDT

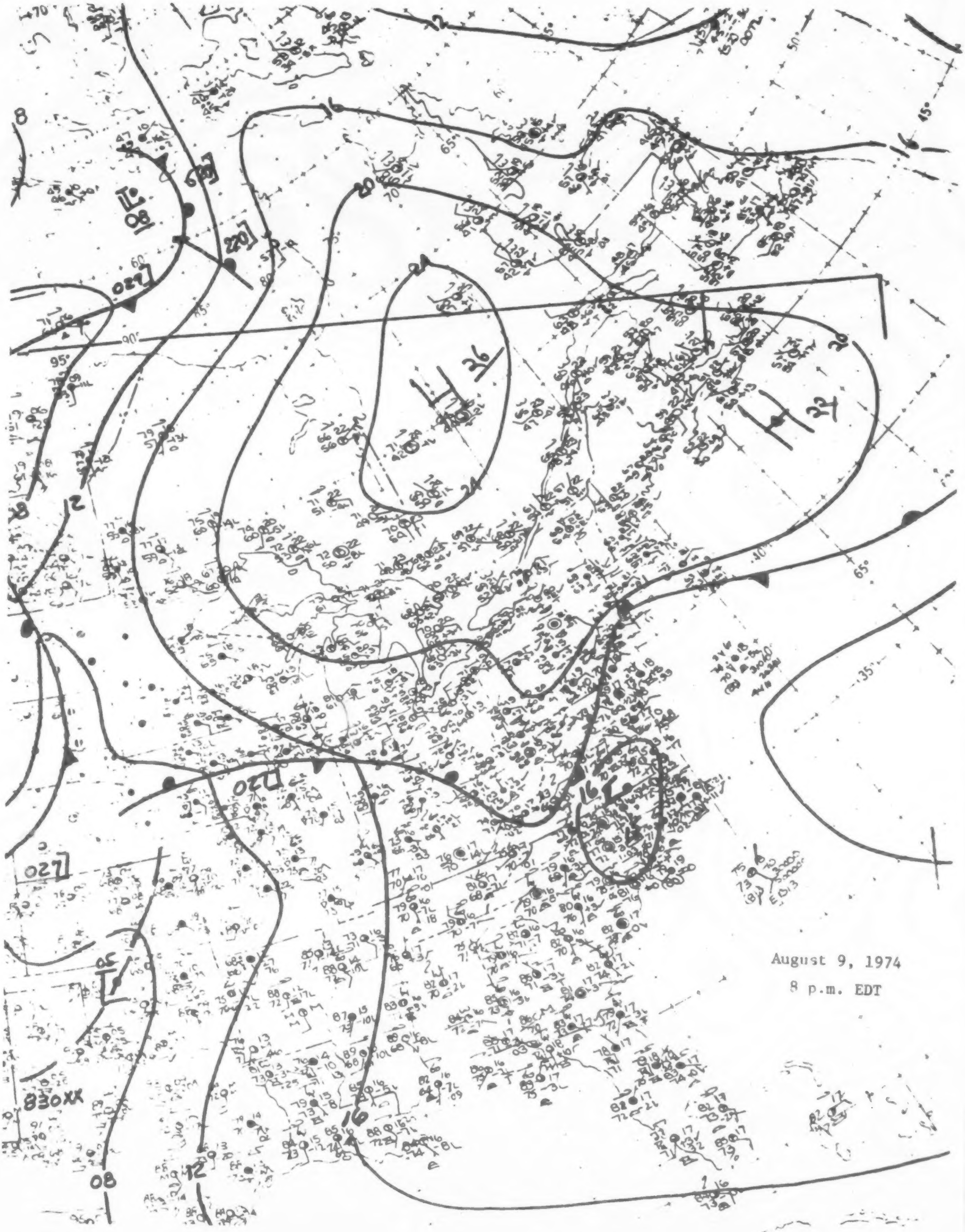

August 9, 1974
8 p.m. EDT

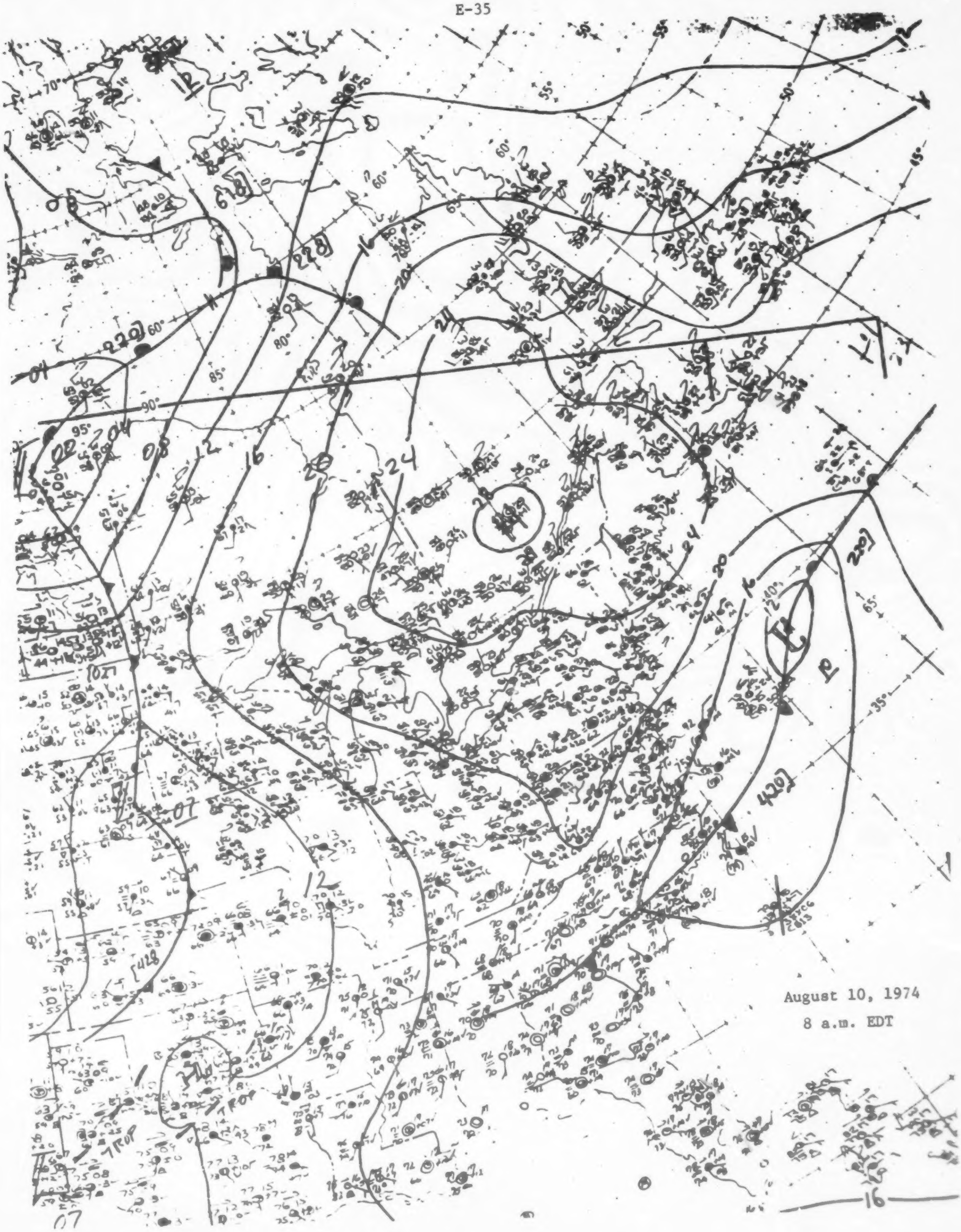

August 10, 1974
8 a.m. EDT

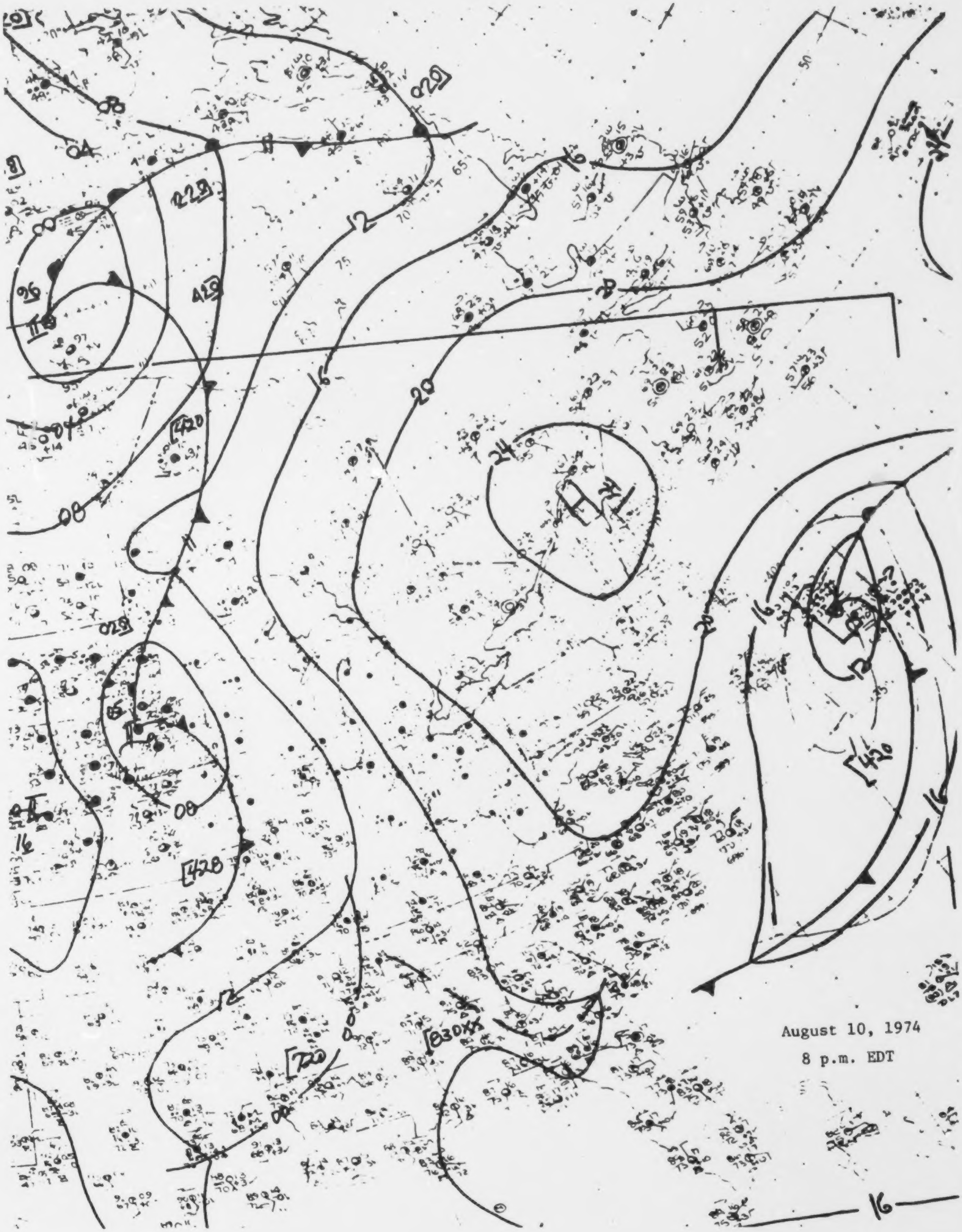
1029
1022
1020
1024
1016
1012
1008
1004
1000
996
1028
1020
1030
1016
H
L

August 10, 1974
8 p.m. EDT

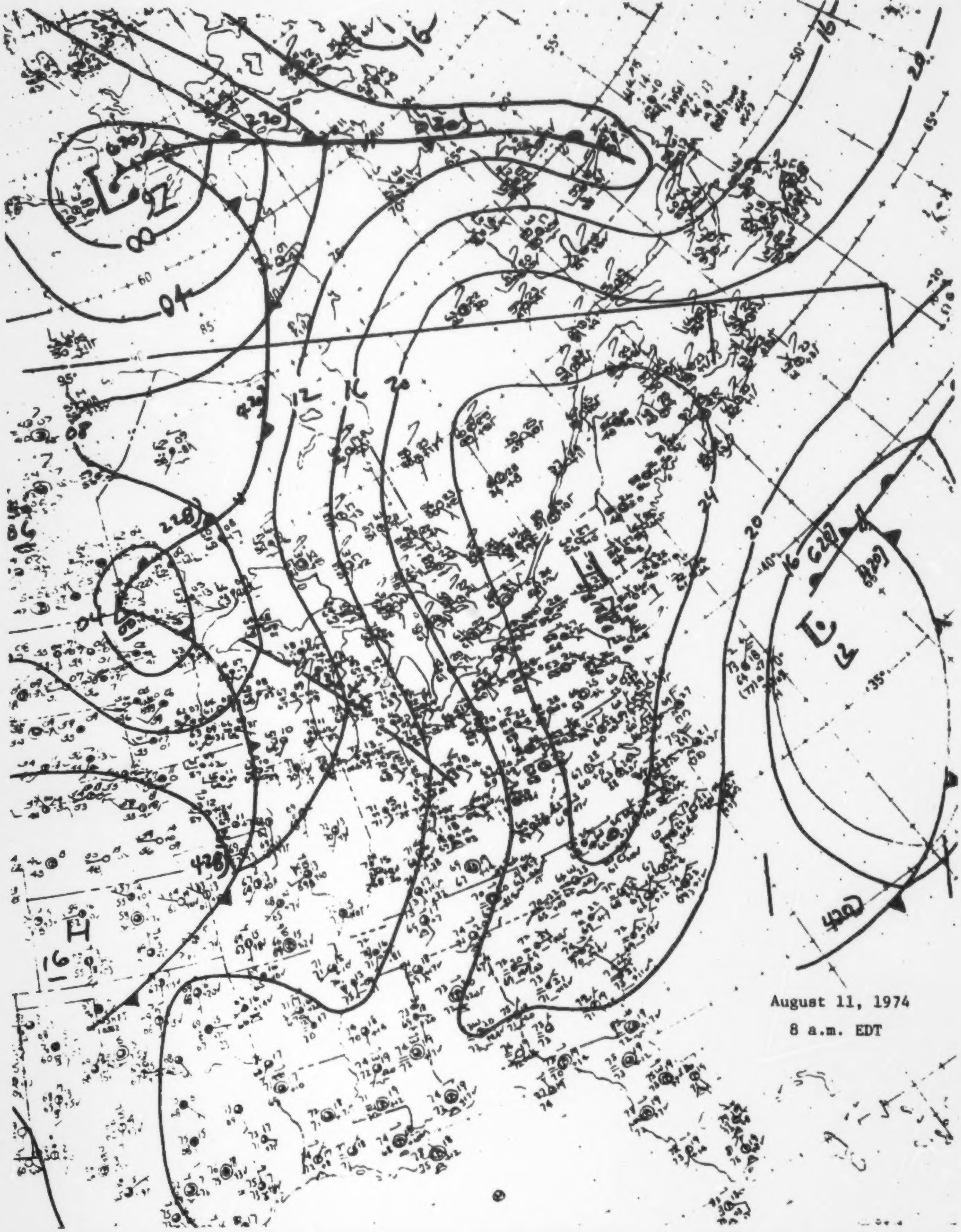

L
92
00
04
08
12
16
20
24
20
16
L
12
H
16
420
428

August 11, 1974
8 a.m. EDT

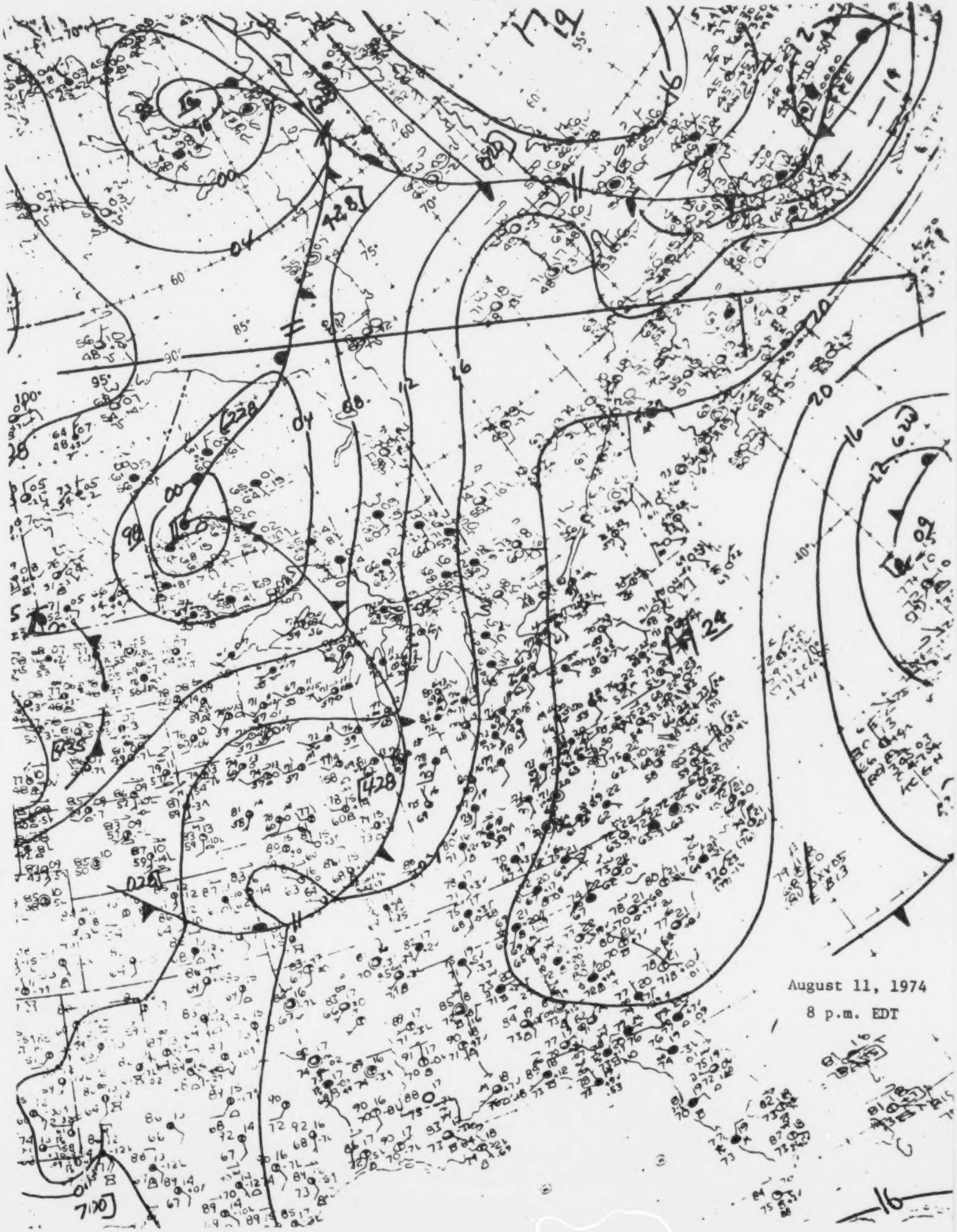

August 11, 1974

8 p.m. EDT

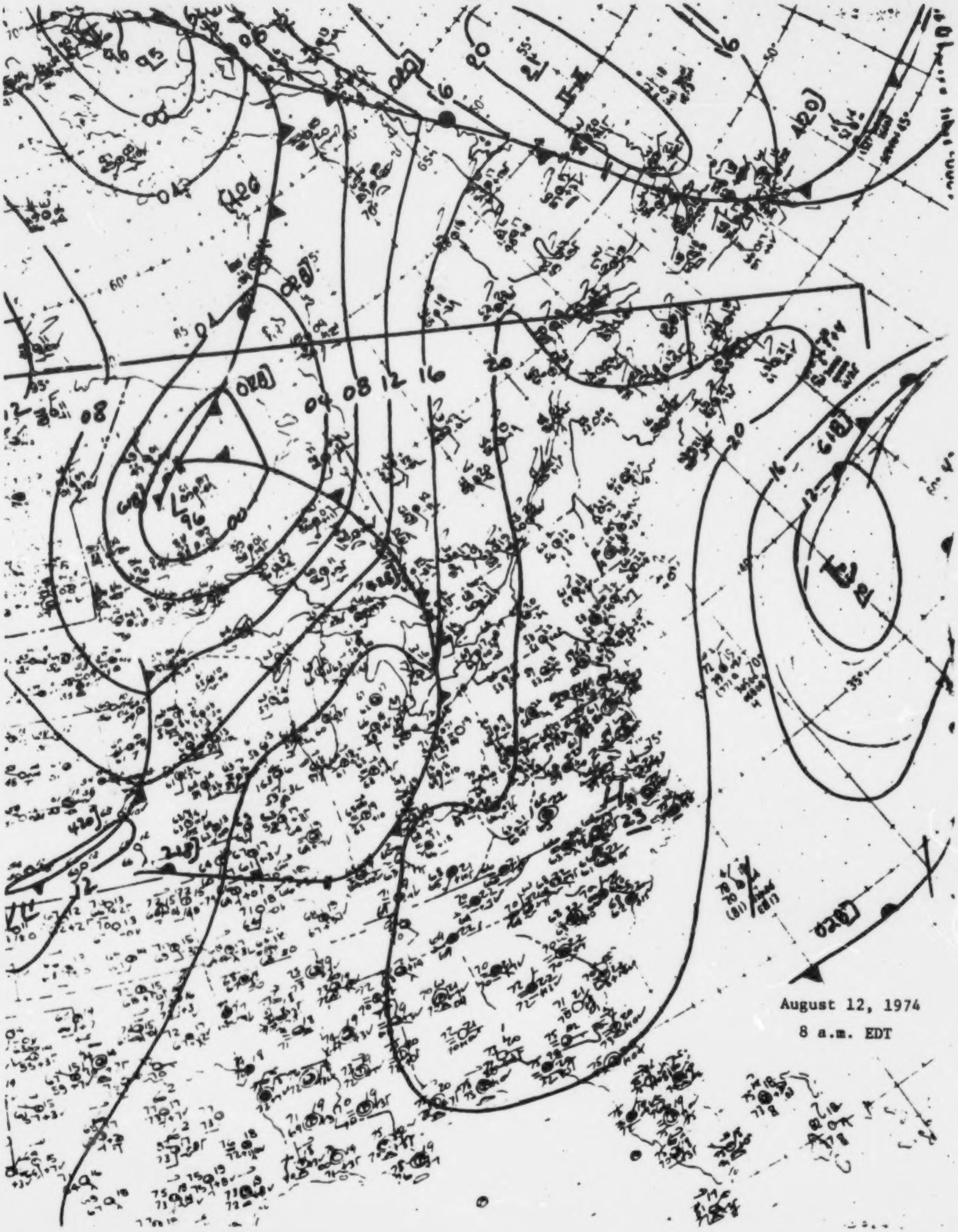

August 12, 1974
8 a.m. EDT

Reproduced from
best available copy.

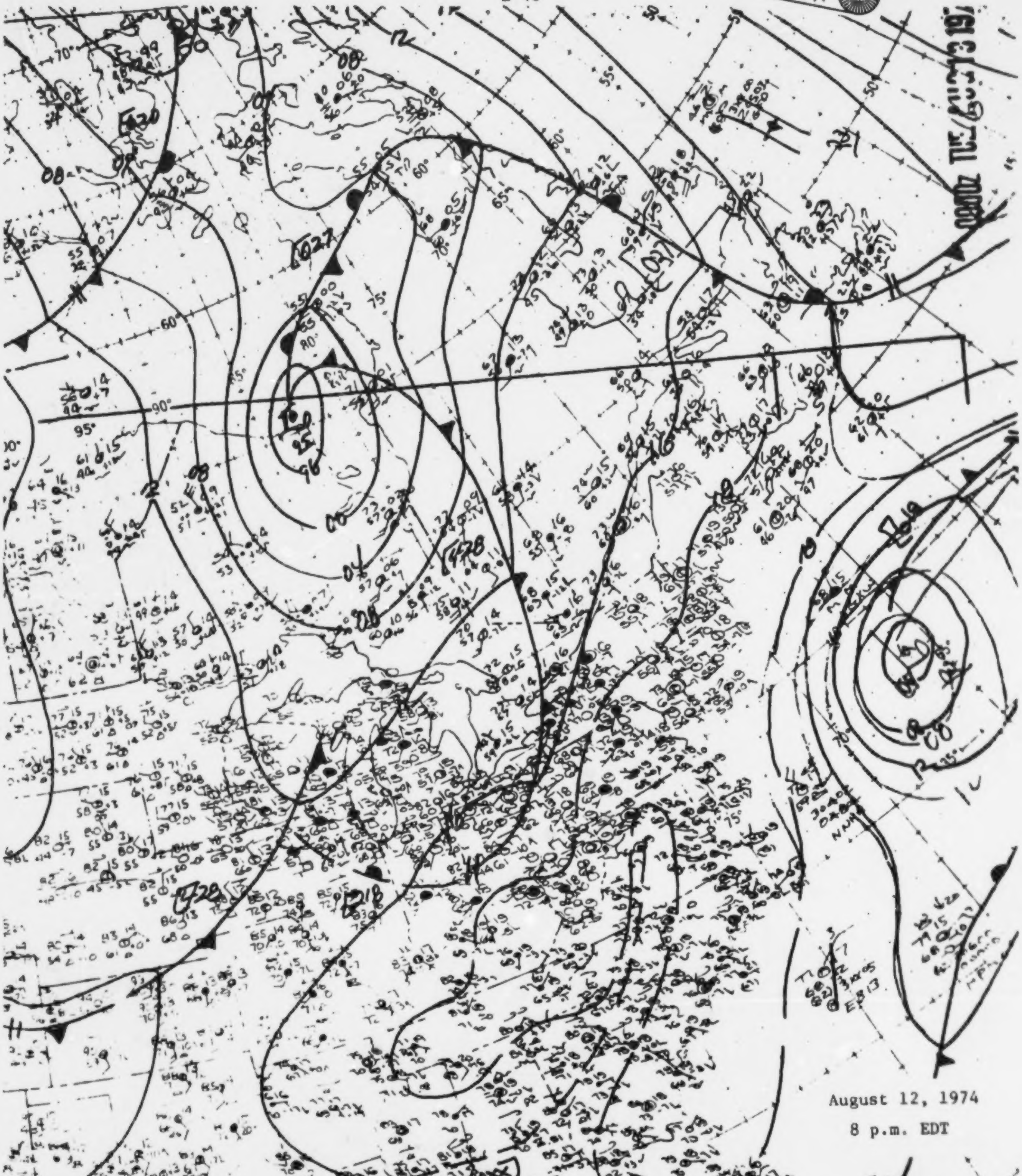

August 12, 1974
8 p.m. EDT

APPENDIX F

AIR PARCEL TRAJECTORIES*
3000 FEET MSL

---

* Twelve-hour positions prior to arrival are indicated by a triangle for those parcels arriving at 2000 Eastern Daylight Time and by a square for those arriving at 0800 Eastern Daylight Time. Since the soundings were taken at 0000 GMT (2000 EDT) and 1200 GMT (0800 EDT), the 8 a.m. EDT trajectory for a given day is shown by the squares on the plot for that day, while the 8 p.m. trajectory for a given day is shown by the triangles on the plot for the next subsequent day. Dates are shown in the lower left-hand corner of each plot.

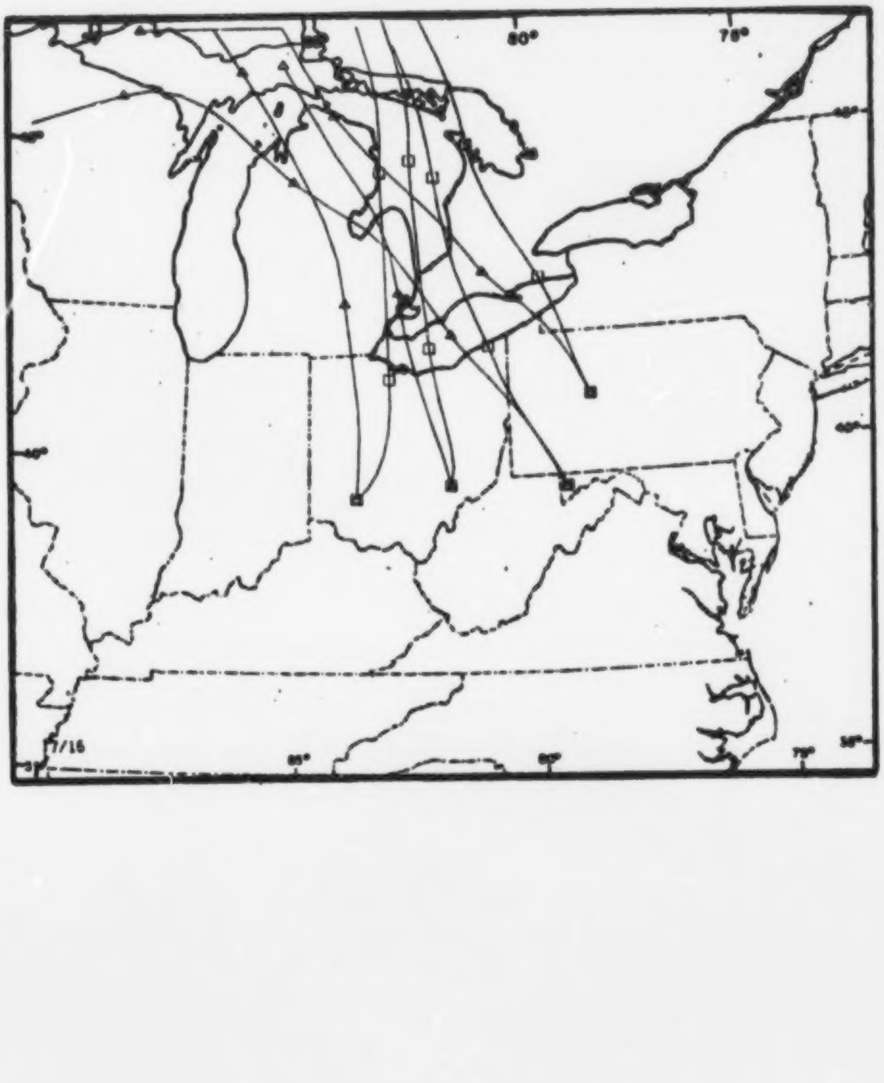
80°
75°
45°
40°
35°
85°
80°
75°
7/16

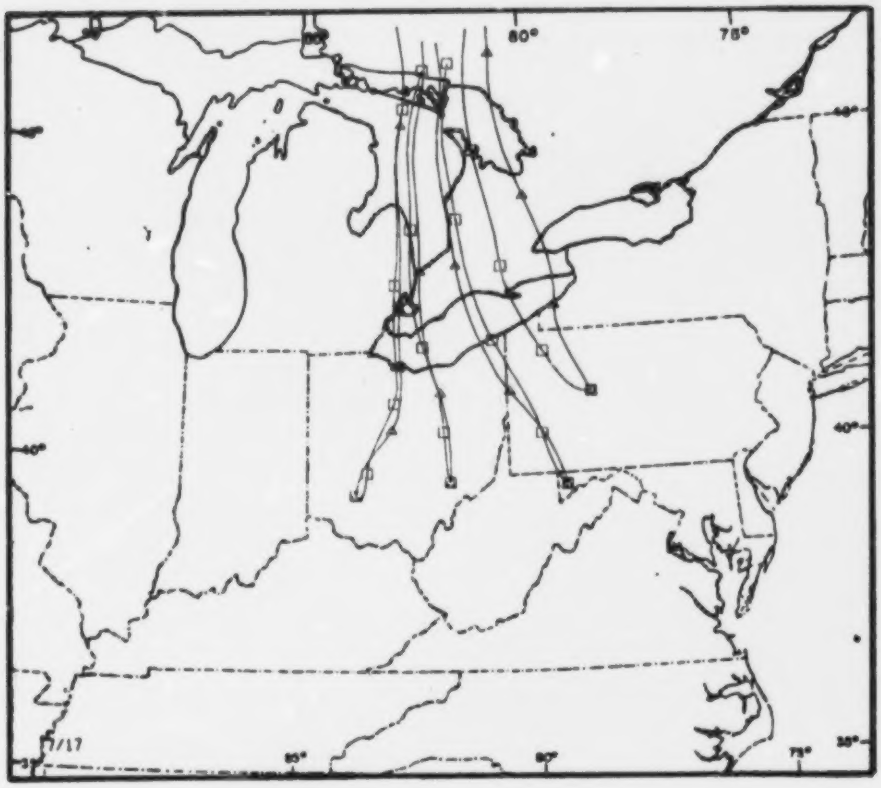
80°
75°
45°
40°
7/17
85°
80°
75°
35°

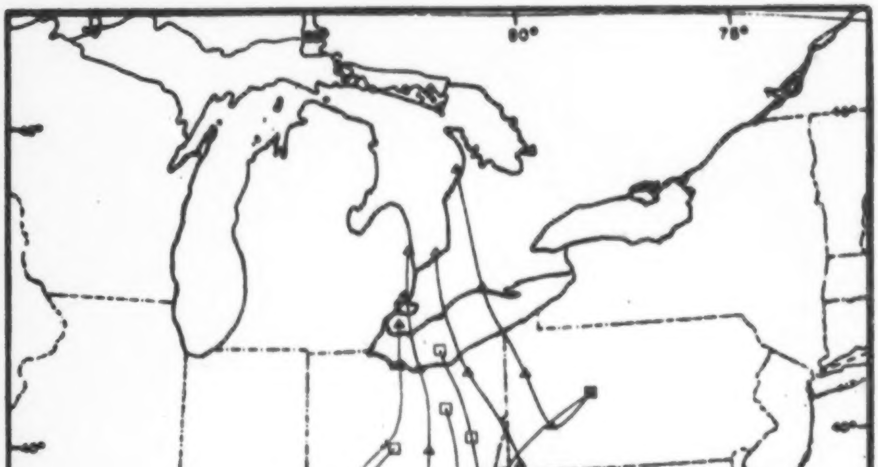
80°
75°
7/18
85°
80°
75°
35°

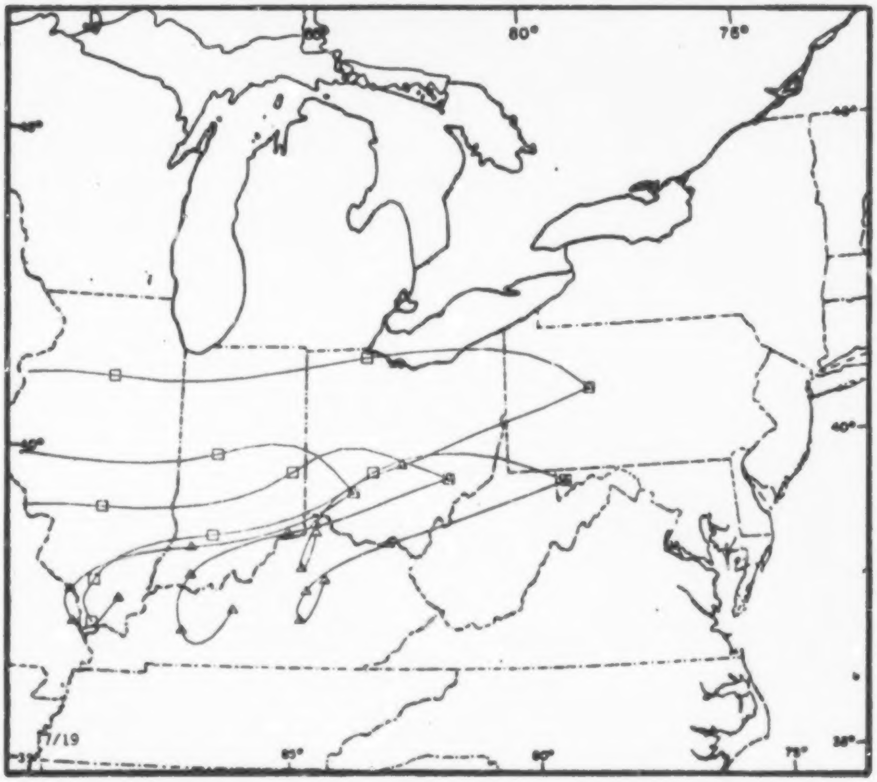
80°
75°
40°
40°
85°
80°
75°
35°
7/19

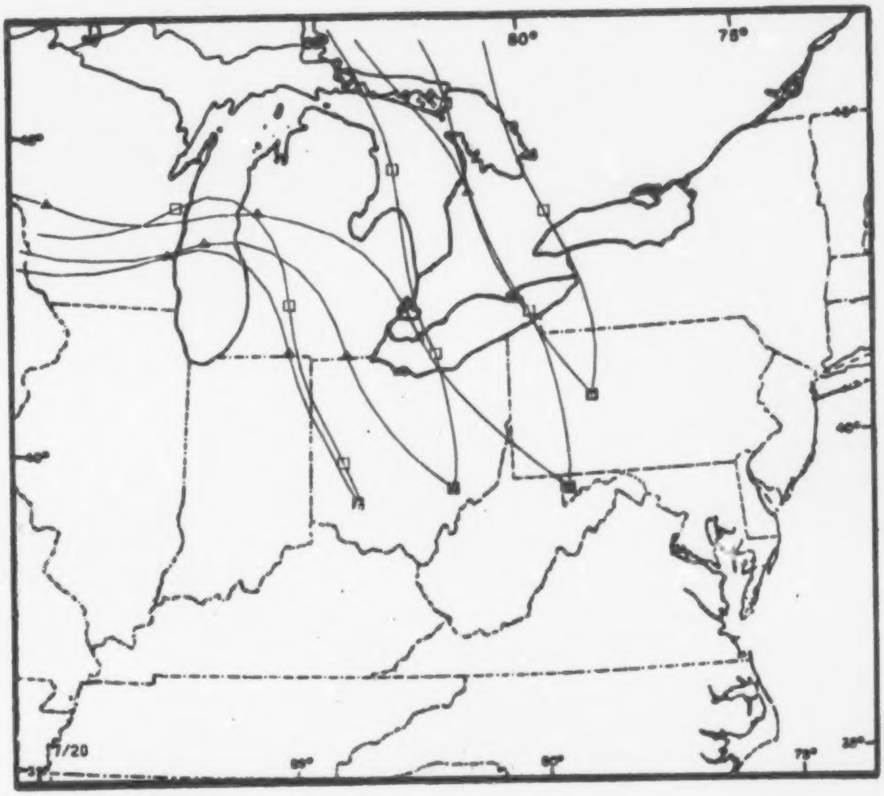
80°
75°
45°
40°
7/20
85°
80°
75°
35°

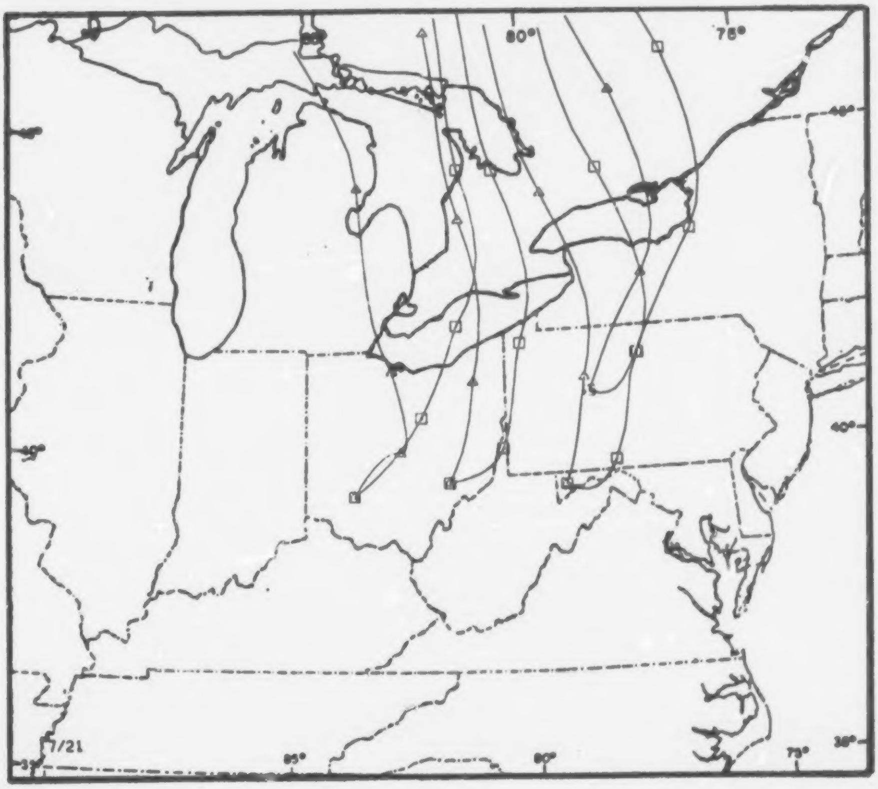
80°
75°
45°
45°
40°
40°
7/21
85°
80°
75°
35°

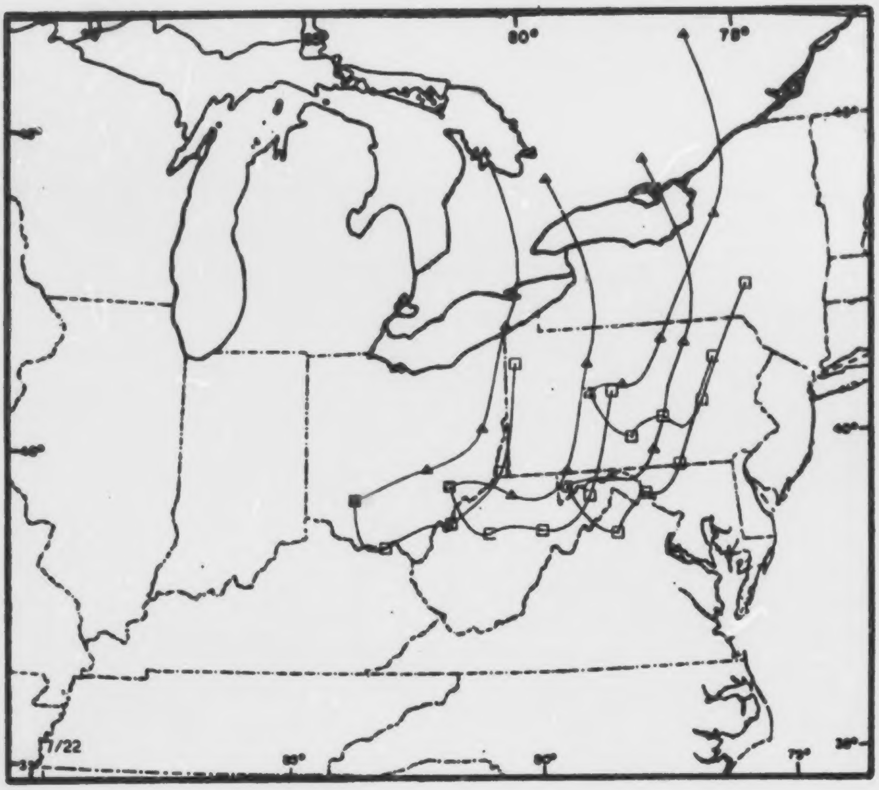
80°
75°
45°
40°
35°
7/22
85°
80°
75°

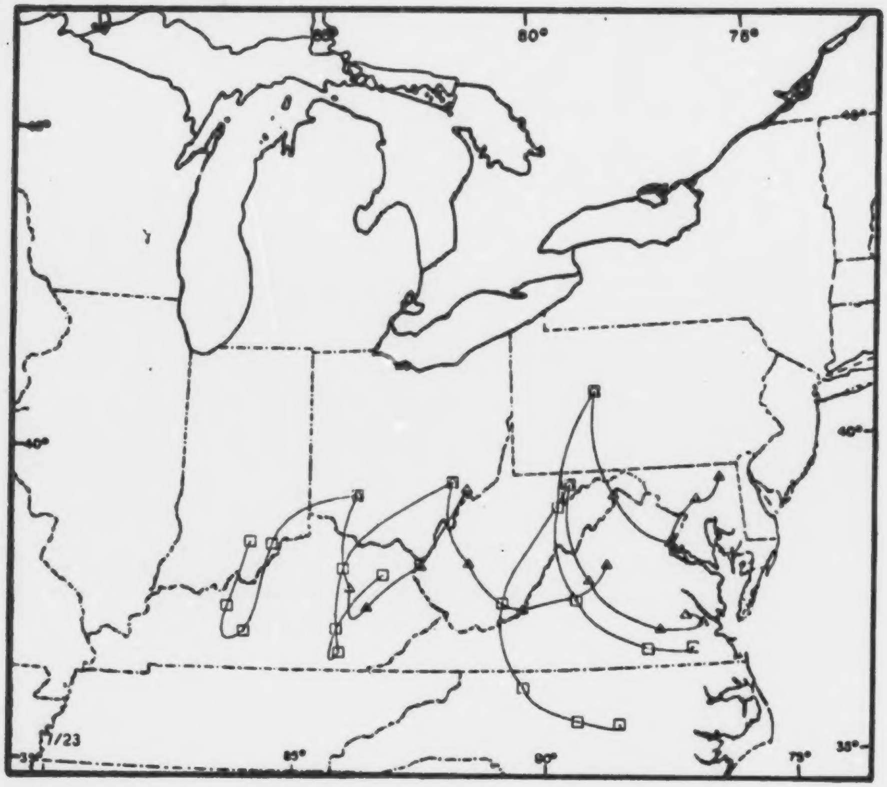
80°
75°
45°
45°
40°
40°
7/23
35°
85°
80°
75°
35°

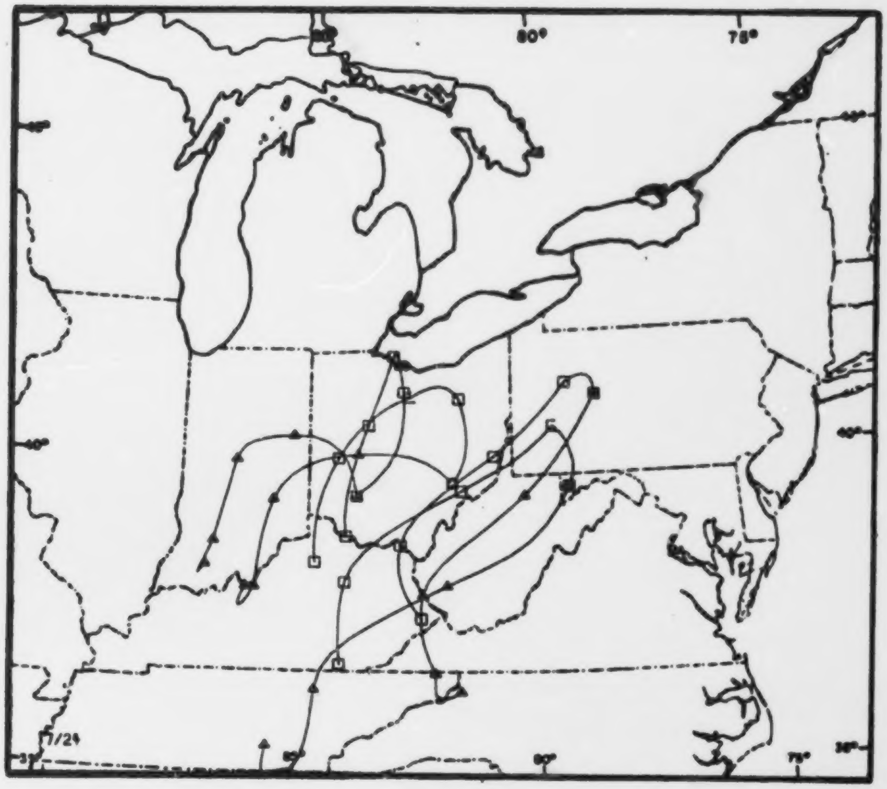
80°
75°
7/24
80°
75°

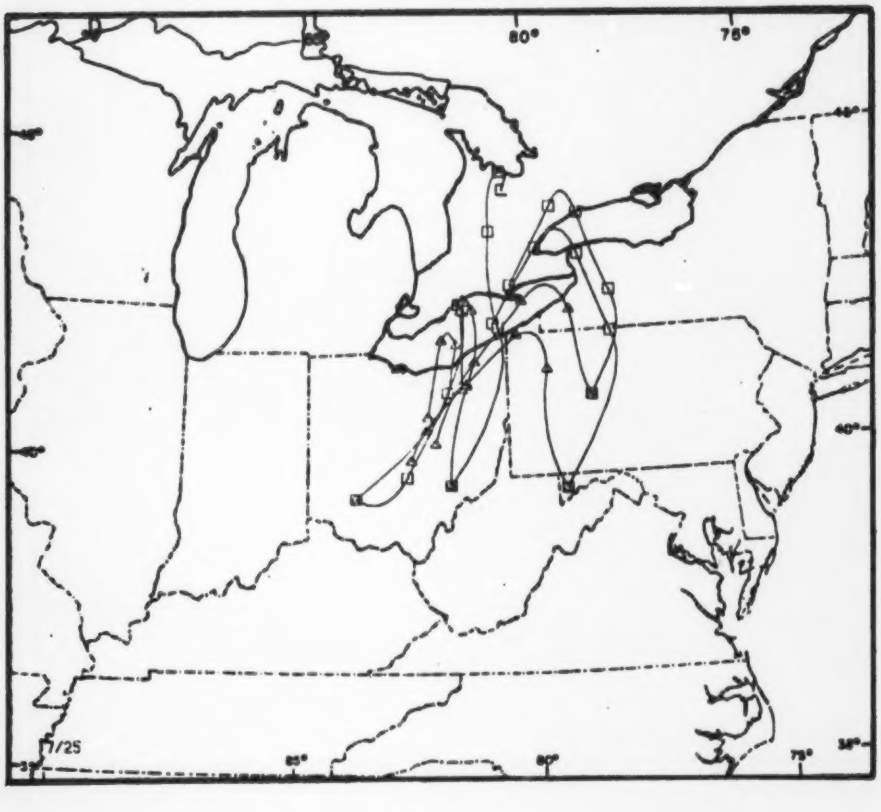
80°
75°
45°
40°
7/25
35°
85°
80°
75°
35°

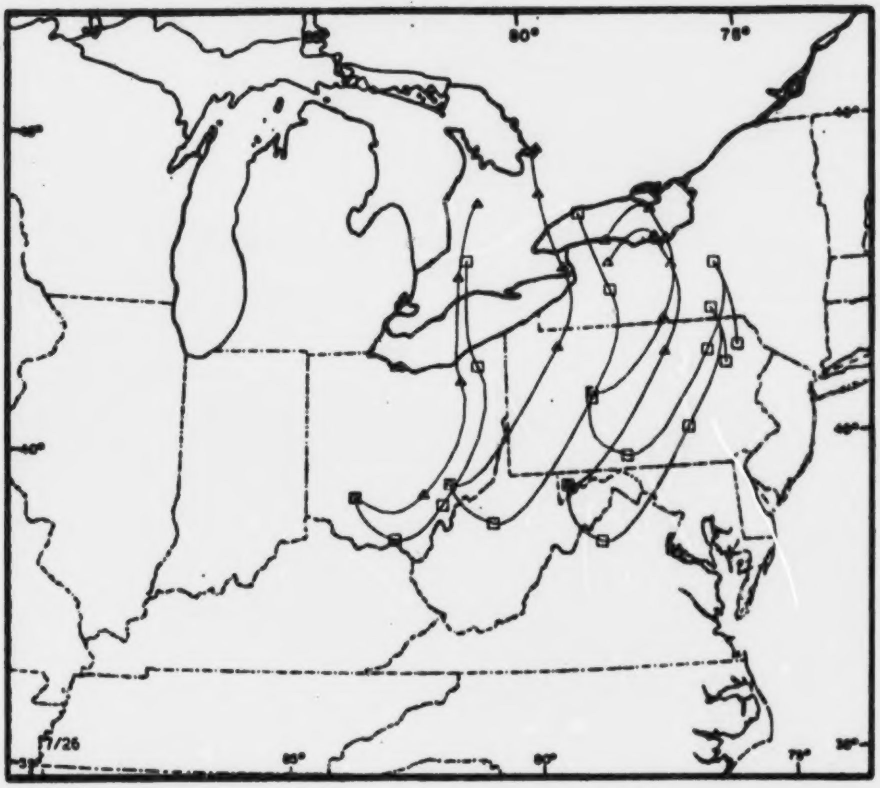
80°
75°
45°
40°
45°
40°
11/26
35°
85°
80°
75°
35°

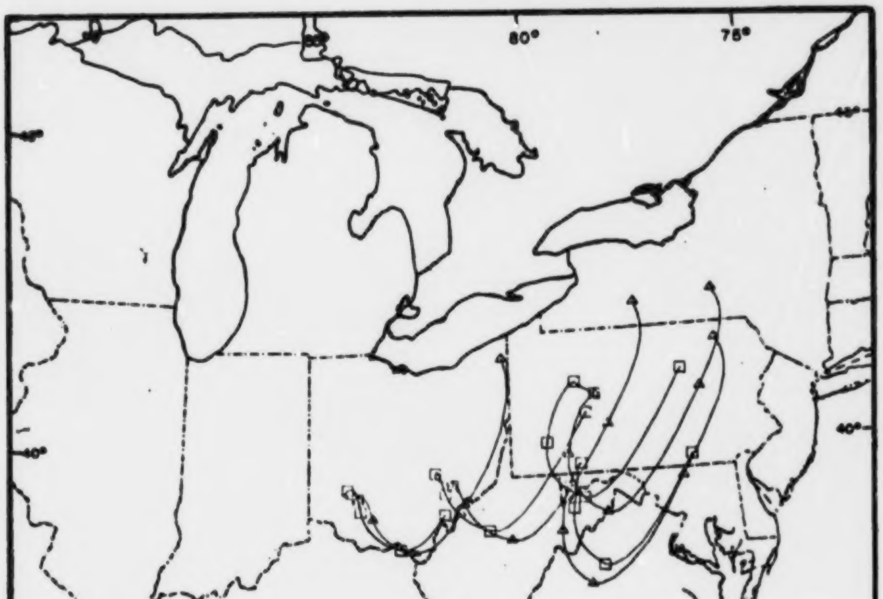
80°
75°
45°
40°
40°
45°
40°
35°
7/27
85°
80°
75°
35°

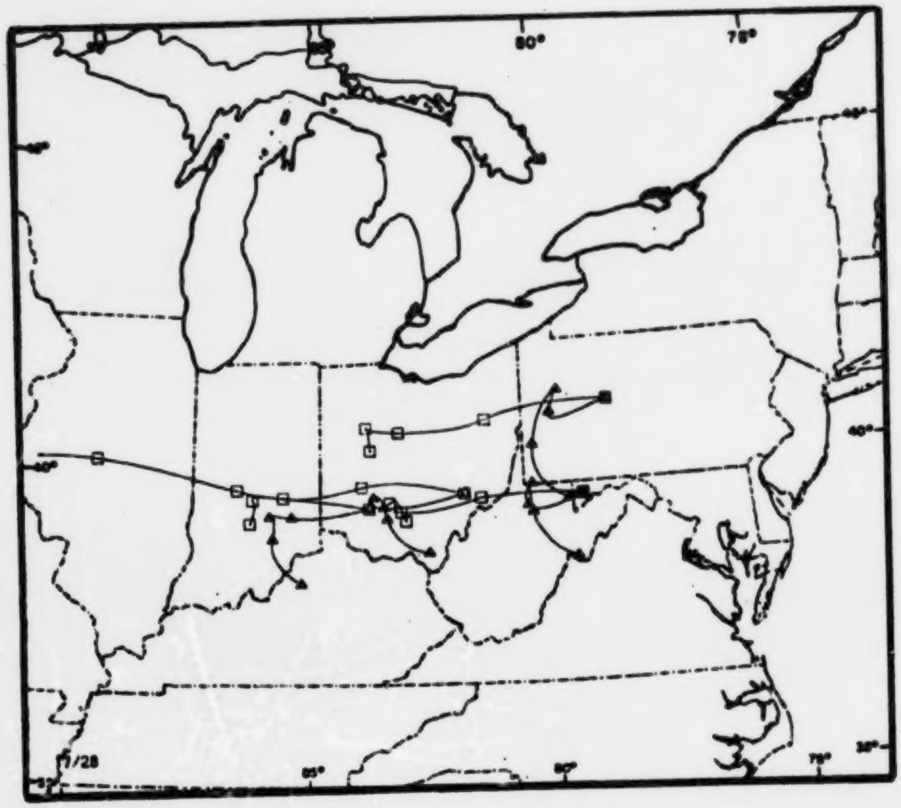
80°
75°
45°
40°
40°
7/28
85°
80°
75°
35°

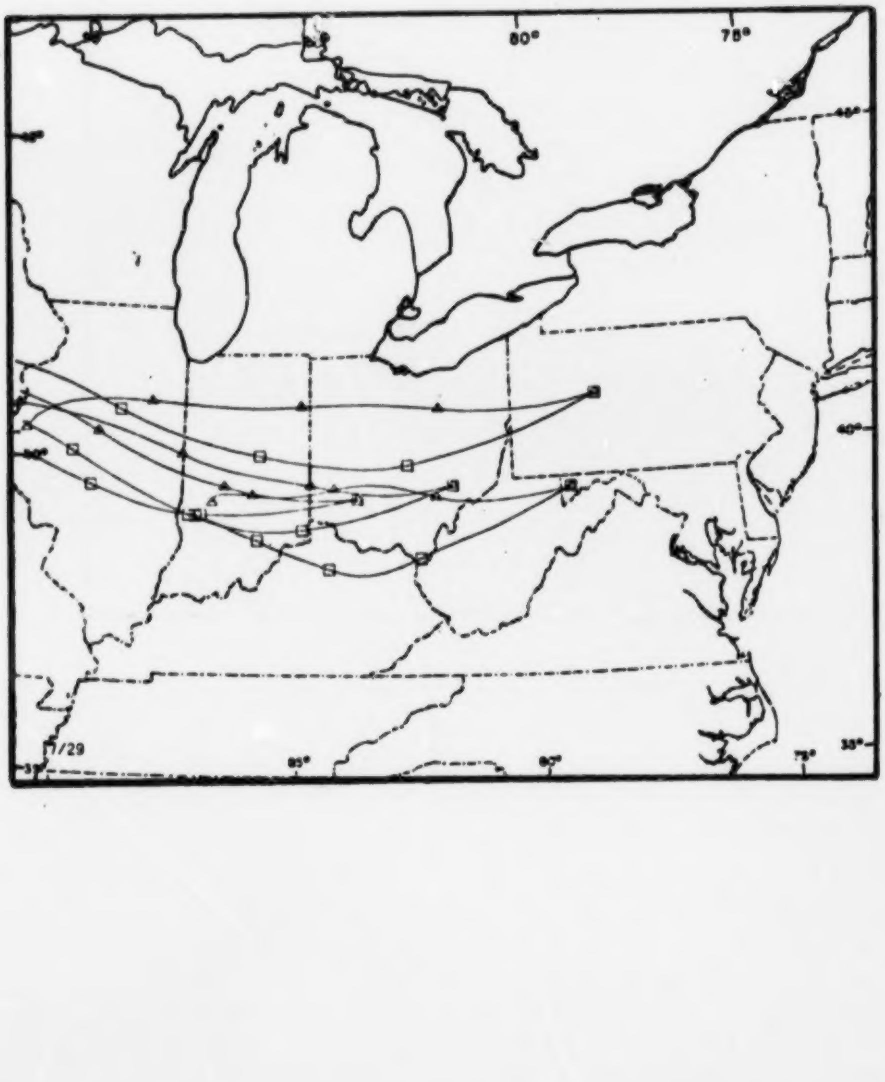
80°
75°
45°
40°
45°
40°
7/29
35°
85°
80°
75°
35°

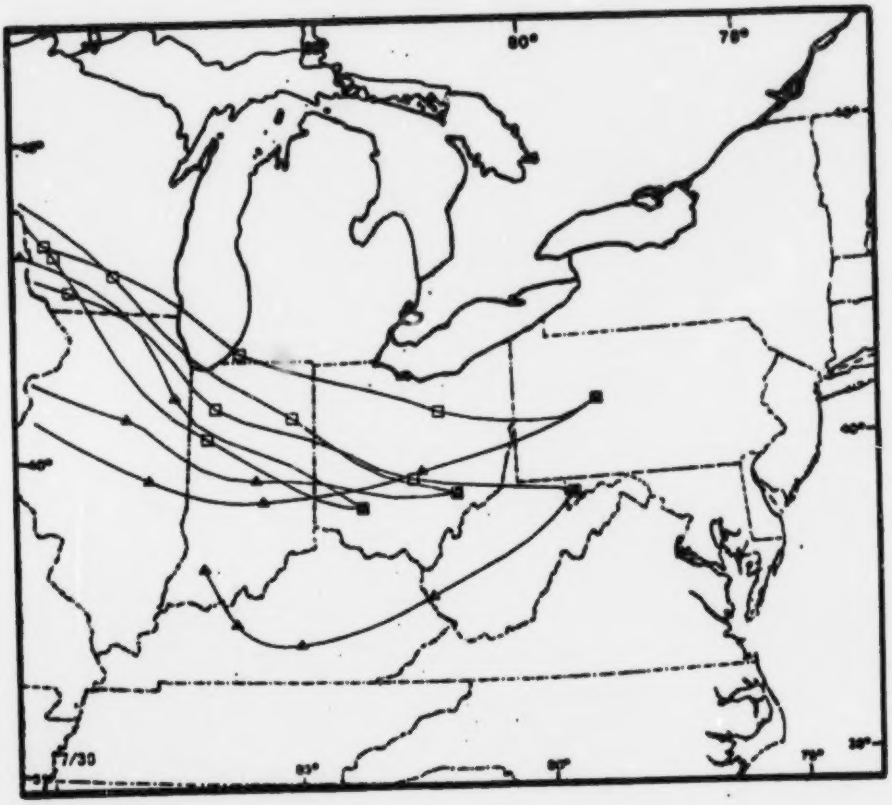
80°
75°
45°
40°
40°
35°
7/30
85°
80°
75°
35°

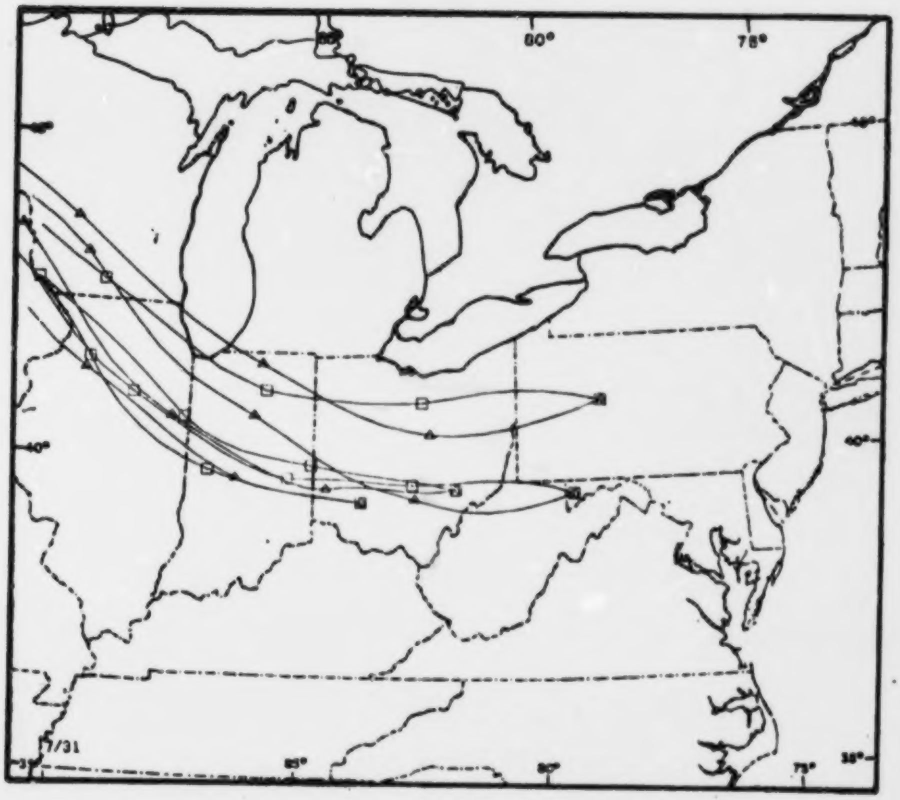
80°
75°
40°
40°
7/31
85°
80°
75°
35°

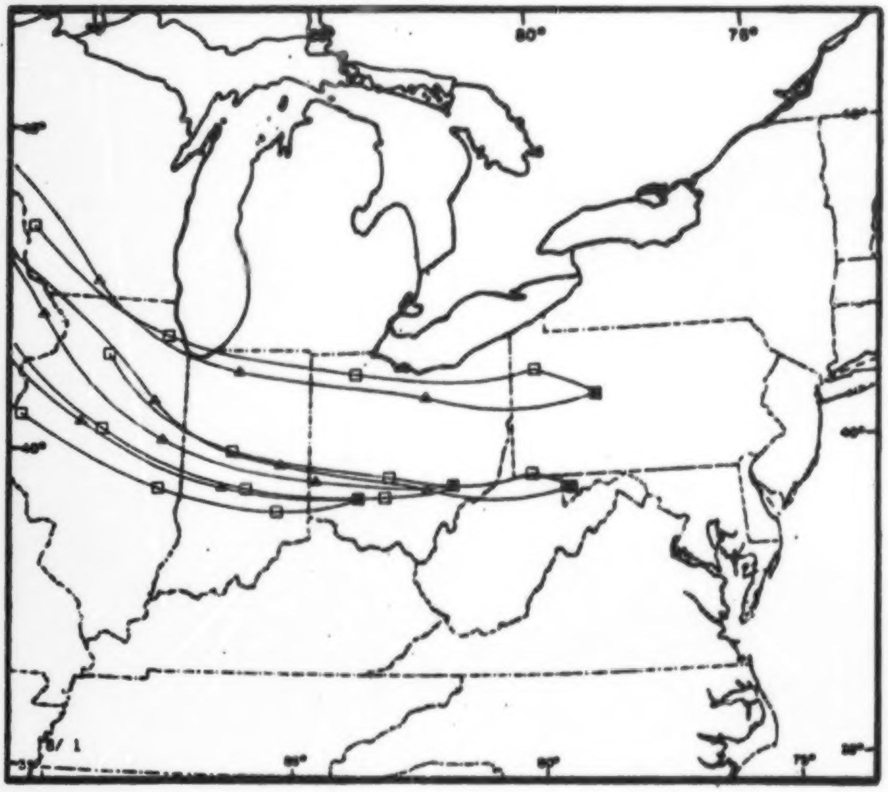
80°
75°
8/ 1
85°
80°
75°

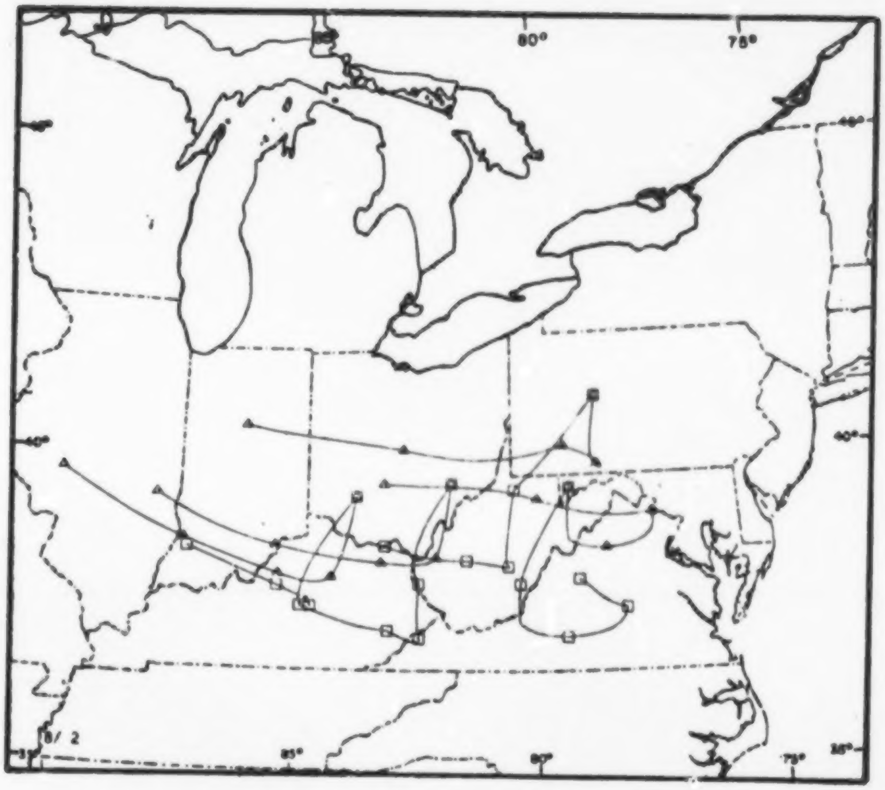
80°
75°
45°
45°
40°
40°
8/ 2
35°
85°
80°
75°
35°

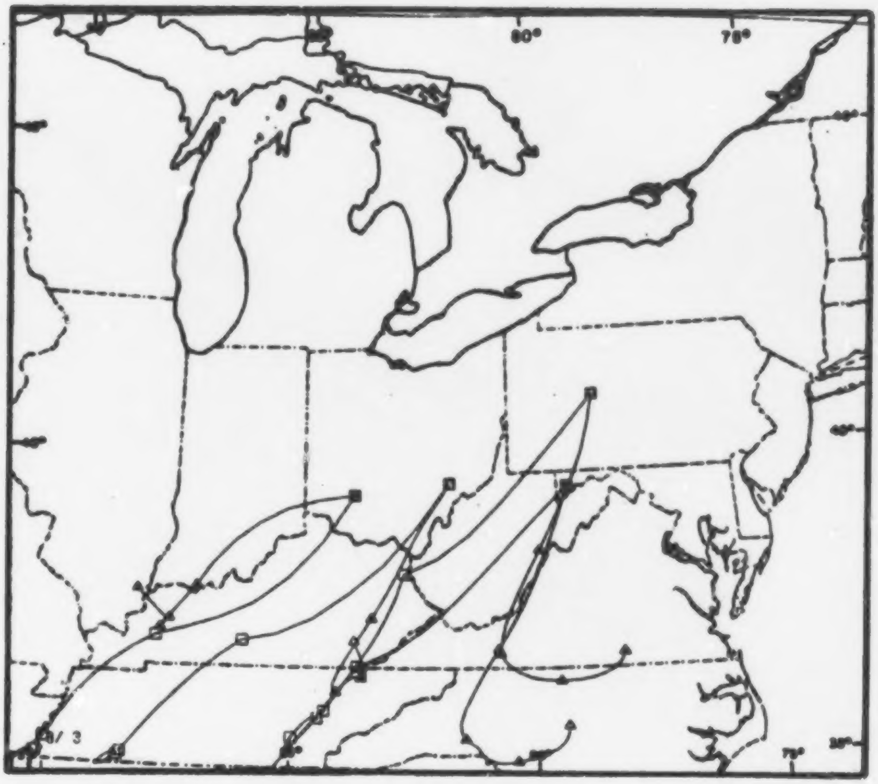
80°
75°
75°
35°

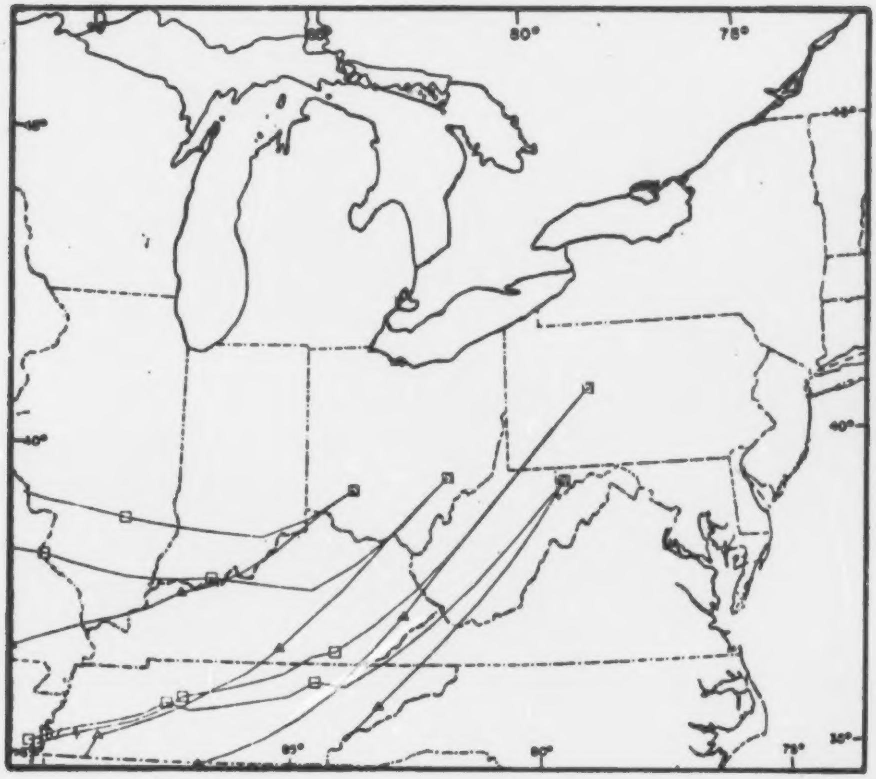
80°
75°
45°
45°
40°
40°
85°
80°
75°
35°

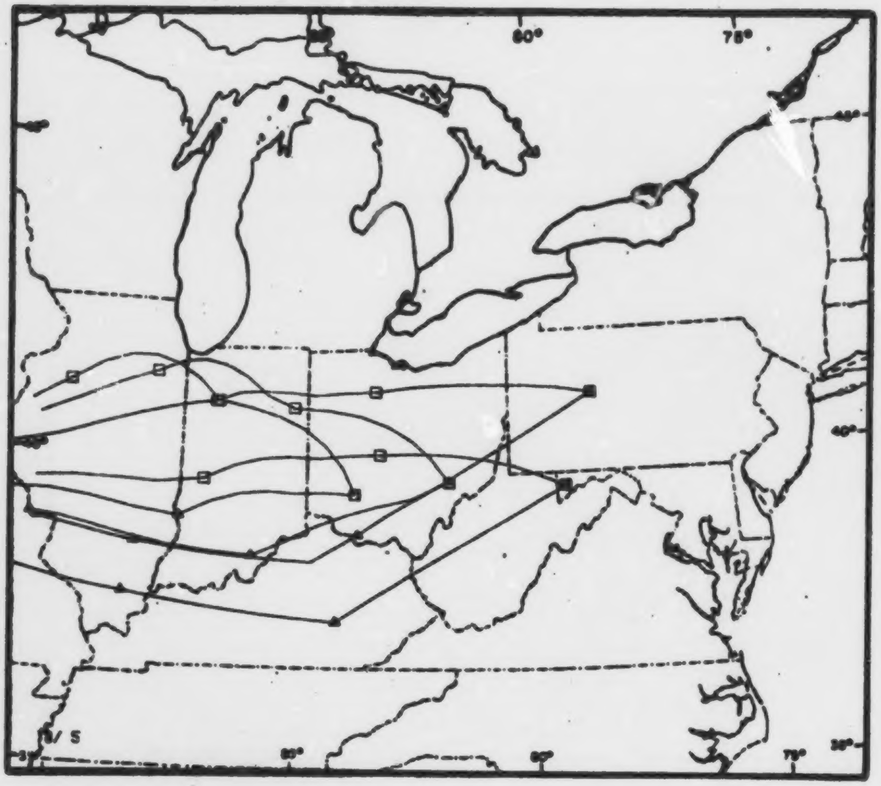
80°
75°
40°
40°
8/ 5
35°
85°
80°
75°
35°

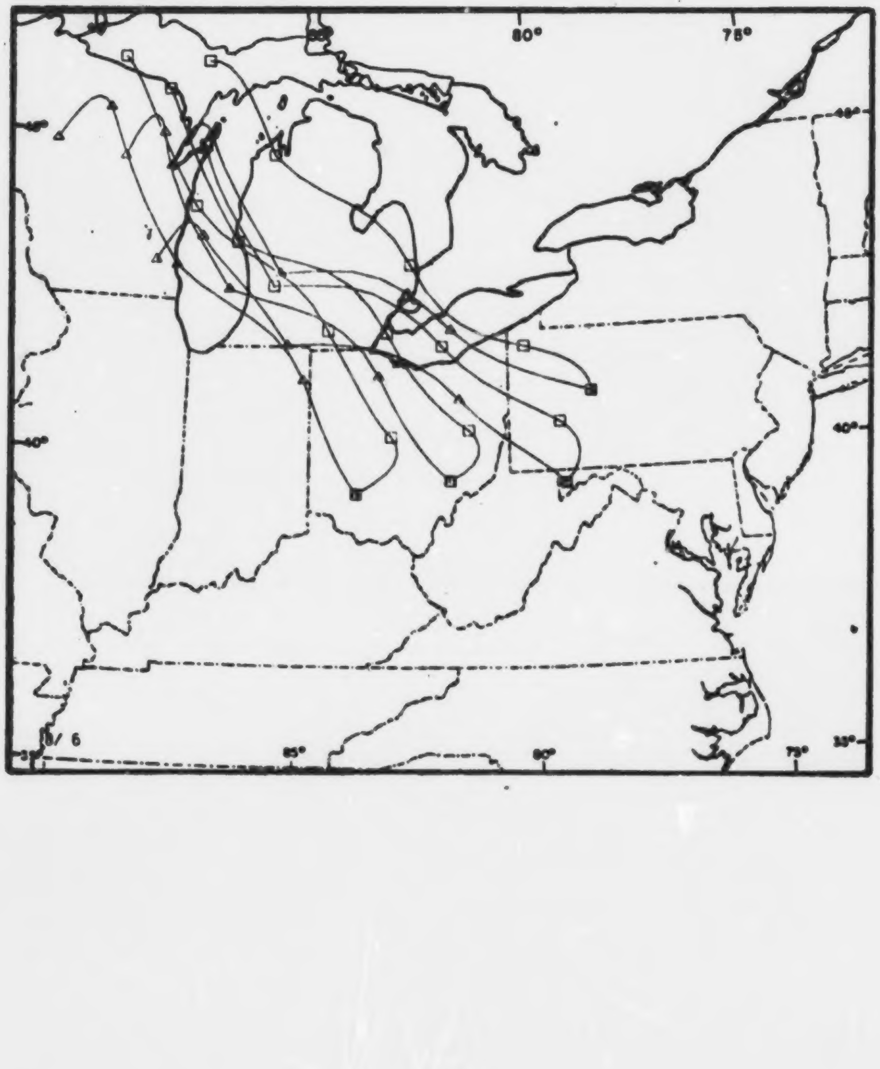
80°
75°
45°
40°
8/ 6
85°
80°
75°
35°
40°

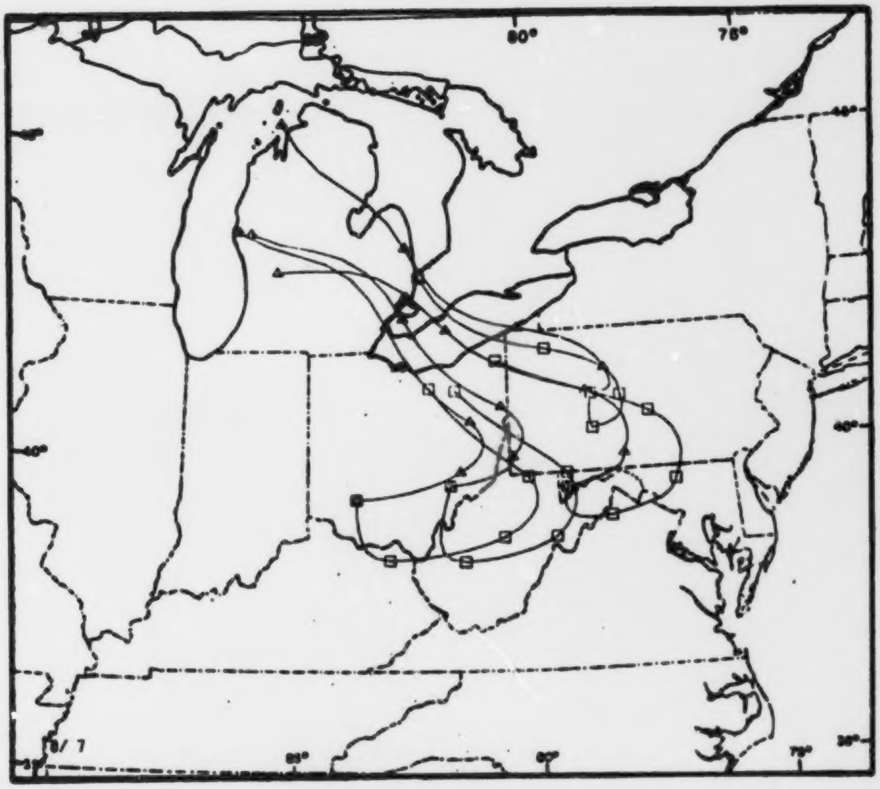
80°
75°
45°
45°
40°
40°
8/ 7
85°
80°
75°
35°

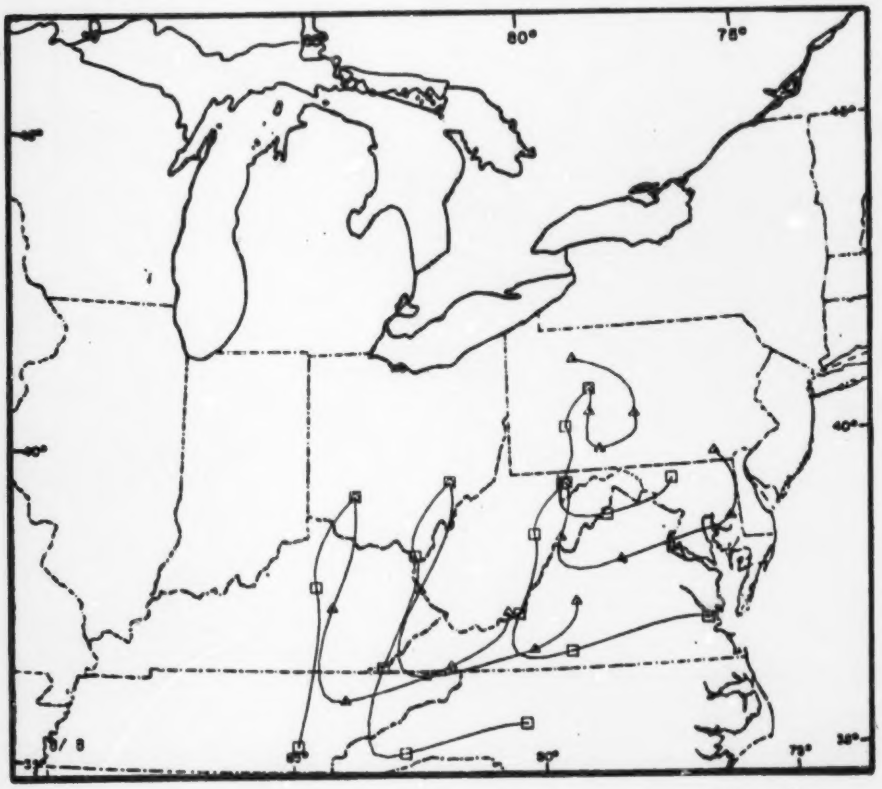
80°
75°
45°
40°
45°
40°
8/ 8
35°
85°
80°
75°
35°

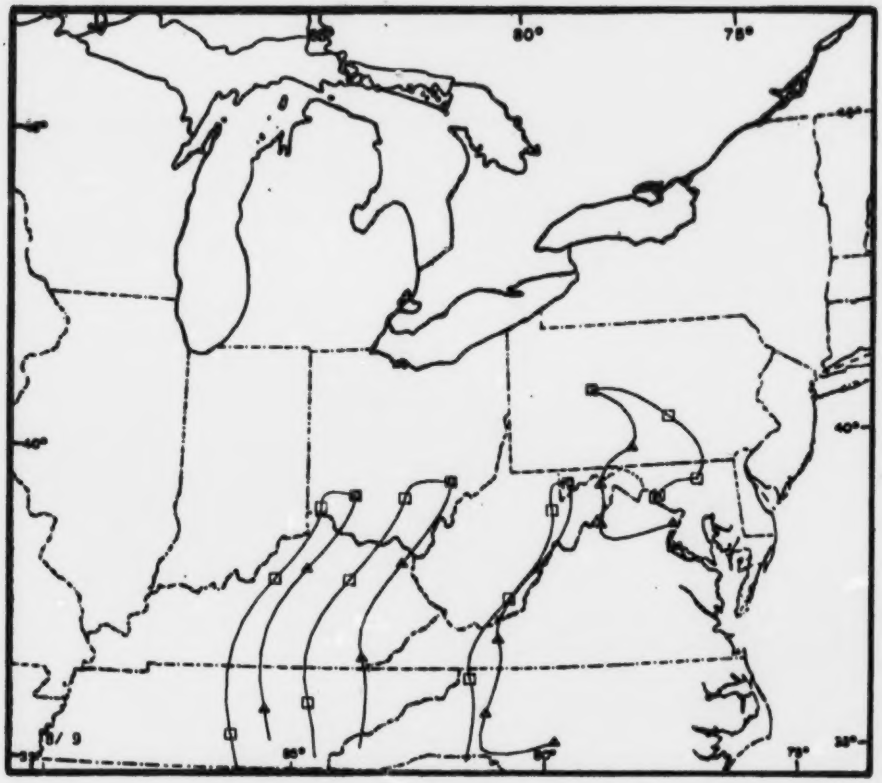
80°
75°
45°
40°
85°
35°
75°
8/ 9

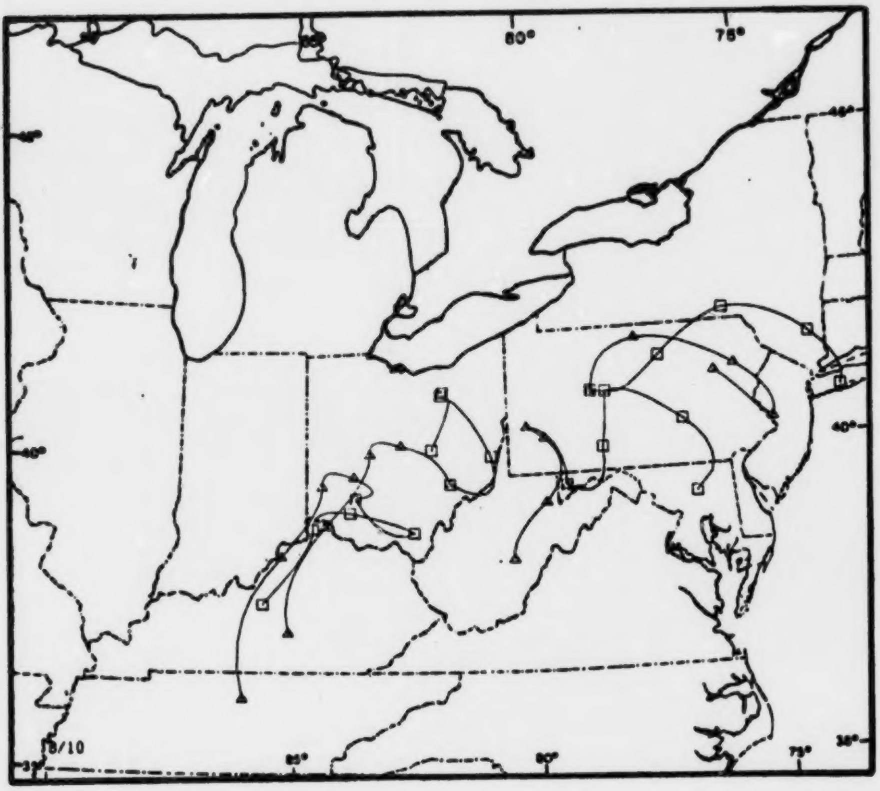
85°
80°
75°
45°
45°
40°
40°
8/10
35°
85°
80°
75°
35°

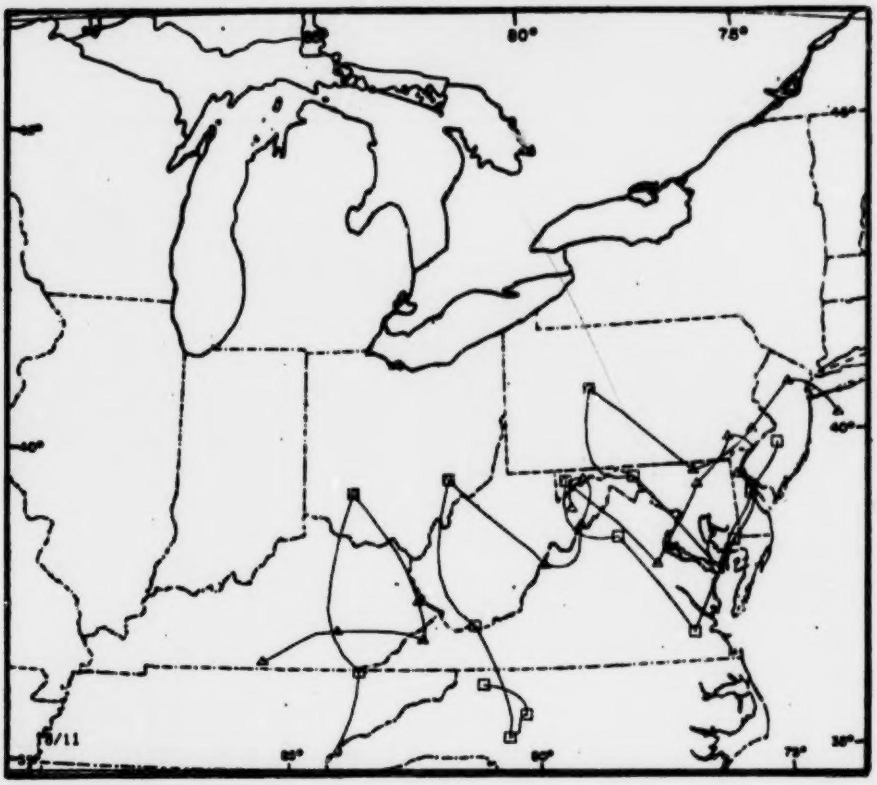
80°
75°
45°
40°
8/11
85°
80°
75°
35°

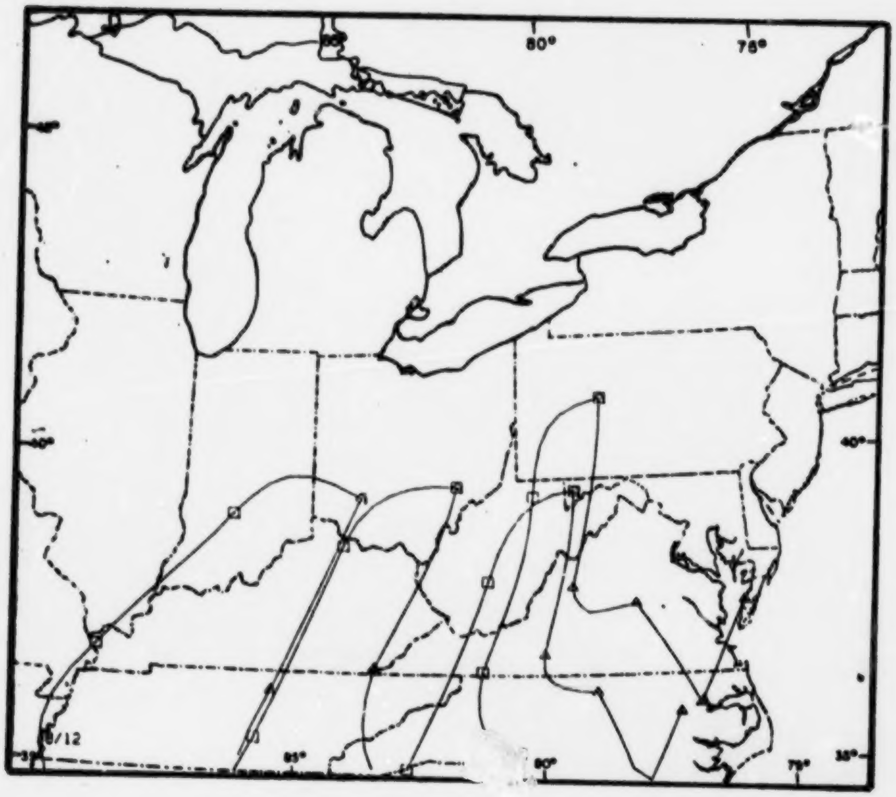
80°
75°
40°
40°
8/12
35°
85°
80°
75°
35°

APPENDIX G

OZONE DATA FROM COLUMBUS, OHIO

Less than 24-hour sampling interval

1 THE OHIO EPA
Agency

COLUMBUS
City Name

2750 Maple Canyon Road
Site Address

Special Studies
Project

ENVIRONMENTAL PROTECTION AGENCY
National Aerometric Data Bank
Research Triangle Park, N. C. 27711

SAROAD Hourly Data Form

OZONE
Parameter observed

Hourly
Time interval of obs.

CHEMILUMINESCENE
Method

PPM
Units of obs.

Area: 3 6 1 4 6 0
Site: 0 8 1
Agency: A
Project: 0 5
Time: 1 7 4
Month: 0 7
Parameter code: 4 4 2 0 1
Method: 1 1
Units: 0 7
DP: 3

Day	St	Hr	Rdg 1	Rdg 2	Rdg 3	Rdg 4	Rdg 5	Rdg 6	Rdg 7	Rdg 8	Rdg 9	Rdg 10	Rdg 11	Rdg 12
19 20	21	22	33 34 35 36	37 38 39 40	41 42 43 44	45 46 47 48	49 50 51 52	53 54 55 56	57 58 59 60	61 62 63 64	65 66 67 68	69 70 71 72	73 74 75 76	77 78 79 80
16	1	2	0040	0045	9999	9999	0050	0050	0050	0045	0040	0035	0035	0035
17	0	0	0030	0025	0020	0020	0020	0015	0000	0000	0005	0020	0045	0065
17	1	2	0070	0070	0080	0085	0095	0075	0065	0050	0025	0010	0010	0010
18	0	0	0000	0000	0000	0000	0000	0000	0000	0000	0005	0035	0050	0070
18	1	2	9999	9999	0110	0135	0135	0115	0100	0075	0075	0075	0080	0015
19	0	0	0015	0075	0070	0060	0050	0040	0035	0015	0020	0025	0030	0055
19	1	2	0070	0075	0070	0060	0070	0075	0075	0045	0075	0070	0065	0060
20	0	0	0045	0020	0010	0030	0065	0035	0015	0015	0015	0020	0035	0035
20	1	2	0045	0055	0065	0065	0065	0050	0045	0040	0035	0020	0015	0015
21	0	0	0015	0015	0010	0010	0085	0005	0005	0010	0015	0020	0035	0030
21	1	2	0065	0065	0065	0065	0070	0070	0070	0075	0075	0050	0010	0010
22	0	0	0000	0020	0015	0030	0020	0020	0015	0005	0015	0030	0060	0065
22	1	2	0075	0075	0085	0090	0085	0070	0060	0070	0050	0030	0035	0020
23	0	0	0015	0015	0045	0045	0035	0030	0020	0025	0010	0015	0030	0035
23	1	2	0045	0040	0035	0035	0045	0050	0050	0050	0040	0045	0040	0040
24	0	0	0035	0025	0030	0025	0015	0020	0015	0010	0015	0025	0040	0055
24	1	2	0065	0065	0070	0010	0070	0070	0075	0020	0060	0050	0045	0045
25	0	0	0040	0035	0045	0030	0035	0010	0005	0000	0015	0030	0045	0065
25	1	2	0090	0030	0090	0075	0030	0070	0065	0060	0055	0040	0030	0020
26	0	0	010	010	010	020	015	010	005	000	000	025	[illegible]	[illegible]
26	1	2	025	025	100	105	110	100	095	075	045	020	[illegible]	[illegible]
27	0	0	005	000	000	000	000	000	000	000	010	[illegible]	[illegible]	[illegible]
27	1	2	105	110	100	095	085	085	085	075	[illegible]	040	[illegible]	[illegible]
28	0	0	000	005	010	010	010	005	005	010	015	[illegible]	[illegible]	[illegible]
28	1	2	085	100	105	090	085	085	075	070	055	[illegible]	040	[illegible]
29	0	0	[illegible]	040	035	040	035	025	010	005	010	[illegible]	[illegible]	[illegible]
29	1	2	070	025	025	050	060	055	055	055	040	[illegible]	[illegible]	[illegible]
30	0	0	015	015	015	015	020	015	005	000	010	[illegible]	[illegible]	[illegible]
30	1	2	045	045	045	050	050	050	050	040	010	[illegible]	[illegible]	[illegible]
31	0	0	005	000	000	000	000	000	000	000	[illegible]	[illegible]	[illegible]	[illegible]
31	1	2	035	050	055	035	050	[illegible]	[illegible]	045	[illegible]	[illegible]	[illegible]	[illegible]

OMB No. 158-R0012
Approval Expires 3/[illegible]/76

Less than 24-hour sampling interval

[1] THE OHIO EPA
Agency

COLUMBUS
City Name

5[illegible]50 Maple Canyon Road
Site Address

Special Studies
Project

ENVIRONMENTAL PROTECTION AGENCY
National Aerometric Data Bank
Research Triangle Park, N. C. 27711

SAROAD Hourly Data Form

OZONE
Parameter observed

CHEMILUMINESCENE
Method

Hourly
Time interval of obs.

PPM
Units of obs.

Area: 3 6 1 4 6
Site: 0 0 8 1
Agency: A
Project: 0 5
Time: 1
7 4
Month: 0 8
Parameter code: 4 4 2 0 1
Method: 1 1
Units: 0 7
DP: 3

Day	St	Hr	Rdg 1	Rdg 2	Rdg 3	Rdg 4	Rdg 5	Rdg 6	Rdg 7	Rdg 8	Rdg 9	Rdg 10	Rdg 11	Rdg 12
19 20	21	22	33 34 35 36	37 38 39 40	41 42 43 44	45 46 47 48	49 50 51 52	53 54 55 56	57 58 59 60	61 62 63 64	65 66 67 68	69 70 71 72	73 74 75 76	77 78 79 80
01	0	0	000	000	000	000	000	000	000	0[illegible]0	00[illegible]	025	040	0[illegible][illegible]
01	1	2	060	075	075	075	070	070	065	0[illegible]0	045	[illegible]2[illegible]	02[illegible]	03[illegible]
0[illegible]	0	0	025	035	020	015	020	020	015	9999	9999	9999	9999	9999
0[illegible]	1	2	9999	9999	9999	9999	060	055	050	080	055	060	055	02[illegible]
0[illegible]	0	0	020	025	025	025	030	025	020	025	025	025	025	025
0[illegible]	1	2	9999	9999	045	045	035	030	030	010	020	025	005	005
0[illegible]	0	0	010	015	010	020	025	025	015	010	015	020	025	03[illegible]
0[illegible]	1	2	040	040	045	040	035	030	035	035	025	015	005	015
0[illegible]	0	0	015	015	015	015	015	040	005	005	005	010	025	030
0[illegible]	1	2	035	040	045	050	055	055	055	050	030	010	015	025
0[illegible]	0	0	0[illegible]5	025	025	025	015	010	005	005	010	040	045	050
[illegible]		2	060	065	065	075	080	080	080	070	050	025	010	00[illegible]
0[illegible]	0	0	015	020	030	040	035	025	015	005	010	025	040	045
0[illegible]	1	2	060	040	060	060	060	055	050	030	030	030	020	010
0[illegible]	0	0	005	000	000	020	030	035	020	010	010	010	025	030
0[illegible]	1	2	045	065	070	075	080	065	050	040	025	040	010	020
[illegible]	0	0												
[illegible]	1	2												
[illegible]	0	0												
[illegible]	1	2												
[illegible]	0	0												
[illegible]	1	2												
1[illegible]	0	0												
1[illegible]	1	2												
1[illegible]	0	0												
1[illegible]	1	2												
1[illegible]	0	0												
1[illegible]	1	2												
15	0	0												
15	1	2												
16	0	0												

OMB No. 15[illegible]
Approval Expires 6/[illegible]/76

TECHNICAL REPORT DATA

(Please read Instructions on the reverse before completing)

1. REPORT NO. EPA-600/3-76-018- a	2.	3. RECIPIENT'S ACCESSION NO.
4. TITLE AND SUBTITLE THE TRANSPORT OF OXIDANT BEYOND URBAN AREAS		5. REPORT DATE February 1976 6. PERFORMING ORGANIZATION CODE
7. AUTHOR(S) Chester W. Spicer, James L. Gemma, Darrell W. Joseph, Phillip R. Stricksel, & Gerald F. Ward		8. PERFORMING ORGANIZATION REPORT NO.
9. PERFORMING ORGANIZATION NAME AND ADDRESS Battelle, Columbus Laboratories 505 King Avenue Columbus, Ohio 43201		10. PROGRAM ELEMENT NO. PE 1A1008 21AKC-03 11. CONTRACT/GRANT NO. EPA 68-02-1714
12. SPONSORING AGENCY NAME AND ADDRESS Environmental Sciences Research Laboratory Office of Research and Development U.S. Environmental Protection Agency Research Triangle Park, NC 27711		13. TYPE OF REPORT AND PERIOD COVERED Final Report 14. SPONSORING AGENCY CODE EPA-ORD

15. SUPPLEMENTARY NOTES

16. ABSTRACT

The 1974 investigation of oxidants in the mid-western United States involved several research groups situated in various points in the Ohio Valley. The Battelle Laboratory group was positioned in Dayton Ohio.

The data collection was carried out over a 20-day period between July 17 and August 12, 1974. Interpretations of the results are discussed in terms of statistical, graphical, chemical, and meteorological analyses of the data. The data suggest that no single source of ozone, be it urban transport, natural, emissions, stratospheric, etc. can account for the ozone patterns observed in this and other studies.

17. KEY WORDS AND DOCUMENT ANALYSIS

a. DESCRIPTORS	b. IDENTIFIERS/OPEN ENDED TERMS	c. COSATI Field/Group
*Air Pollution		13B
*Field tests		14B
Measurement	Ohio Valley	14G
*Ozone	Dayton, Ohio	07B
Transport properties		12A
*Analysis (Mathematics)		

PRICES SUBJECT TO CHANGE

18. DISTRIBUTION STATEMENT RELEASE TO PUBLIC	19. SECURITY CLASS *(This Report)* UNCLASSIFIED	21. NO. OF PAGES 224
	20. SECURITY CLASS *(This page)* UNCLASSIFIED	22. PRICE 7.75 - 2.25

EPA Form 2220-1 (9-73)